# NUMERICAL AND PHYSICAL MODELLING OF UNDERGROUND EXCAVATIONS IN DISCONTINUOUS ROCK

by

IAN JAMES STEWART B.Sc.(Eng.)

A thesis submitted to the University of London (Imperial College of Science and Technology) for the Degree of Doctor of Philosophy in the Faculty of Engineering.

July, 1981.

ABSTRACT

The subject addressed in this thesis is the study of large scale displacement behaviour in the hangingwalls and crowns of underground excavations constructed in discontinuous, hard rock.

. The research involved two different but complementary approaches. Firstly, numerical techniques which permitted large scale translations and rotations were developed and utilized. The applicability of the dynamic relaxation method to underground excavation design was assessed and this technique was used for comparison purposes throughout the study.

An alternative relaxation technique was developed to overcome some limitations and disadvantages of the dynamic relaxation model. The inherent advantages of this new technique for underground excavation design applications are discussed. A number of numerical examples have been presented to illustrate the accuracy and potential of the method for analysing complex rock engineering problems.

A method for analysing large problem geometries was developed and successfully implemented. This enabled parametric studies to be performed, highlighting some of the pertinent characteristics and mechanisms to be considered in mine design.

The second portion of the work concerned the design and construction of a biaxial loading apparatus for studying the behaviour of openings located in discontinua. The apparatus was shown to adequately satisfy the design requirements. Experimental model studies were performed using this device and provided results for comparison with similar studies analysed using the developed numerical model.

The mode of failure and load distributing mechanisms generated for both sets of model studies were in close agreement, although there was generally a large discrepancy in the magnitudes of the measured and predicted displacements. This was

due to the inability of the numerical model to simulate tensile slabbing and fracturing phenomena, effects which may be important considerations in the design of structures in jointed rock masses.

ACKNOWLEDGEMENTS

The author is grateful for the interest of the many people who assisted in the completion of this thesis.

In particular, the author would like to thank:

Professor E.T. Brown for supervision of and enthusiasm for this work, for general advice and guidance throughout the work programme, and for critical assessment of the draft of the thesis.

Dr. J.W. Bray for the interest taken in the work, for unpublished information on a number of topics, and for enlightening discussions covering the broad field of rock engineering.

Dr. B.H.G. Brady for his initial supervision of this work and for stimulating the author's interest in numerical methods applied to mine design.

The technical staff of the Mineral Resources Engineering workshop and laboratory, Messrs. J. Sullivan, B. Lydall, F. Coombe who helped construct and operate the biaxial loading apparatus.

The staff and students of the Rock Mechanics Section for their discussion of problems and for providing a pleasant working environment.

Mr. B. Holt and members of his section for their assistance with photography and in the production of the thesis.

His parents, for their continued interest and encouragement in his education.

Miss P. O'Connell who patiently typed the thesis, and Miss M. Knox for assisting with labels.

The companies supporting the underground excavation design

in tabular orebodies project at Imperial College who provided the financial assistance. The author thanks the management of these companies for providing information on their operations.

CONTENTS


Page

ABSTRACT

ACKNOWLEDGEMENTS

LIST OF FIGURES

LIST OF TABLES

NOTATION

CHAPTER 1 INTRODUCTION 1

CHAPTER 2 NUMERICAL METHODS FOR DISCONTINUA 9

2.1. Methods available for the analysis of discontinuous rock masses.

2.2. Relaxation methods

2.2.1. General
2.2.2. Example of the relaxation process.

2.3. Assessment of the dynamic relaxation method.

2.3.1. General description of the method.
2.3.2. Dynamic relaxation as applied to discontinuous rock problems.
2.3.3. Computational Notes.
2.3.4. Results for an underground excavation design problem.

2.4. An alternative numerical model for the analysis of underground excavations in discontinuous rock masses.

2.4.1. Description of the method.
2.4.2. Fortran implementation.
2.4.3. Problem areas.

CHAPTER 3 VALIDATION AND EXTENSIONS OF THE STATIC RELAXATION METHOD 62

3.1. General discussion.

3.2. Validation Tests.

Page

3.2.1. Sixteen rectangular block test.
3.2.2. Continuum validation.
3.2.3. Comparison with dynamic relaxation.
3.2.4. Comparison with deformable block program.
3.2.5. Loading of a jointed foundation.
3.2.6. Block toppling model.
3.2.7. Collapse analysis of masonary arches.
3.2.8. Simultaneous versus successive relaxation.

3.3. Summary

CHAPTER 4 APPLICATIONS TO MINE DESIGN 115

4.1. General.

4.2. Changes to data structures.

4.3. Application of modified program to mine design.

4.3.1. Example Runs
4.3.2. Summary

CHAPTER 5 DEVELOPMENT OF A PHYSICAL MODELLING TECHNIQUE 158

5.1. Introduction.

5.2. Scope of the experimental programme.

5.3. Design requirements.

5.4. Review of previous work.

5.5. Design philosophy for the loading apparatus.

5.6. Model loading apparatus.

5.6.1. Loading mechanism.
5.6.2. Loading platens.
5.6.3. Reaction frame.
5.6.4. Hydraulic circuit.
5.6.5. Housing frame.

5.7. Calibration and preliminary testing of the biaxial loading apparatus.

5.7.1. Proving ring test.
5.7.2. Loading of a strain-gauged continuous plate.

Page

5.7.3. Differential boundary displacement test.
5.7.4. Stiffness test.
5.7.5. Static friction test.
5.7.6. Preliminary tests.

5.8. Buckling stability calculations.

5.9. Instrumentation of the model.

5.9.1. The equipment.
5.9.2. Experimental procedure and interpretation.
5.9.3. Camera calibration.
5.9.4. Error analysis.
5.9.5. Other instrumentation.

5.10. Modelling material

5.10.1. Requirements of modelling material.
5.10.2. Properties of modelling material.
5.10.3. Relationship to prototype.

5.11. Conclusions.

CHAPTER 6 RESULTS OF PHYSICAL AND NUMERICAL MODEL STUDIES 242

6.1. Objectives and general discussion.

6.2. Testing procedure.

6.3. Results of physical and numerical model studies.

6.3.1. Model I - continuous horizontal joints and discontinuous vertical joints.
6.3.2. Model II - continuous vertical joints and discontinuous horizontal joints.
6.3.3. Model III - continuous joints at 45 degrees to horizontal, discontinuous orthogonal joints (Pv > Ph).
6.3.4. Model IV - continuous joints at 45 degrees to horizontal, discontinuous orthogonal joints (Ph > Pv).
6.3.5. Model V - continuous joints at 60 degrees to horizontal, discontinuous orthogonal joints (Pv > Ph).

Page

6.3.6. Model VI - continuous jointing at 30 degrees to horizontal, discontinuous orthogonal joints (Pv > Ph).
6.3.7. Model VII - continuous joints at 60 degrees to horizontal, discontinuous orthogonal joints. Two openings 75 mm apart. (Pv > Ph).
6.3.8. Model VIII - continuous joints at 60 degrees to horizontal, discontinuous orthogonal joints. Two openings 50 mm apart. (Pv > Ph).
6.3.9. Summary.

CHAPTER 7 SUMMARY AND CONCLUSIONS 377

REFERENCES 380

APPENDIX I A. Rigid block displacement transformation. 386
B. Calculation of rigid block displacements.

APPENDIX II Derivation of simultaneous equations for static relaxation method. 389

APPENDIX III Representing a continuum by the rigid block model. 394

APPENDIX IV A. Summary of photogrammetric process. 398
B. Listing of PROGRAM GIRDER.

APPENDIX V Preparation of modelling material. 404

APPENDIX VI A. Listing of PROGRAM TEST. 406
B. Listing of PROGRAM RBM.

APPENDIX VII User information, input specifications and listings for static relaxation programs. 429
A. Baseline static relaxation program.
B. Modified static relaxation program for large problem geometries.

## LIST OF FIGURES


| Figure No. | Description |
|---|---|
| 1.1 | Rock discontinuities influencing hangingwall behaviour. |
| 1.2 | Modes of deformation possible in discontinua (after Brown, 1968). |
| 2.1 | Three block relaxation example. |
| 2.2 | Calculation cycle for dynamic relaxation (after Cundall, 1976). |
| 2.3 | Complete dynamic relaxation calculation cycle. |
| 2.4 | Normal and shear interactions in dynamic relaxation program. |
| 2.5 | Block bouncing due to time-step greater than critical. |
| 2.6 | Isometric view of underground excavation design problem. |
| 2.7 | Consolidation for mine design problem. |
| 2.8 | Block extraction for mine design problem. |
| 2.9 | Normal and shear interactions for static relaxation model. |
| 2.10 | The representation of interfaces between blocks. |
| 2.11 | Realistic characteristics for rock joints. |
| 2.12 | Contacts between block corners and edges. |
| 2.13 | Block displacement to equilibrium position. |
| 2.14 | Static relaxation calculation procedure. |
| 3.1 | Force distribution from a 'forwards' relaxation path. |
| 3.2 | Force distribution when relaxation path reversed. |
| 3.3 | Block geometry for elastic continuum validation. |
| 3.4 | Modified block geometry for elastic continuum validation. |

| Figure No. | Description |
|---|---|
| 3.5 | Block geometry for infinite strip load problem. |
| 3.6 | Block geometry for comparison with dynamic relaxation - first case. |
| 3.7 | Block geometry for comparison with dynamic relaxation - second case. |
| 3.8 | Comparison of static relaxation and dynamic relaxation rates of convergence. |
| 3.9 | Block geometry for comparison with deformable block program. |
| 3.10 | Block geometry for foundation loading problem. |
| 3.11 | Total strip loading of $P_c$ = 250.0 applied, tan $\phi$ = .364. |
| 3.12 | Total strip loading of $P_c$ = 20.0 applied, tan $\phi$ = .05. |
| 3.13 | Modified block geometry for foundation loading problem, for total strip loading of $P_c$ = 400.0. |
| 3.14 | 13 block geometry for toppling simulation. |
| 3.15 | Inter-block forces from static relaxation and limiting equilibrium. |
| 3.16 | 16 block geometry for toppling simulation. |
| 3.17 | Masonary arch geometry and results under self weight loading. |
| 3.18 | Collapse analysis of masonary arch. |
| 3.19 | Approximate line of thrust obtained from limit analysis. |
| 3.20 | Block geometry to compare simultaneous and successive relaxation. |
| 3.21 | Total displacement plot with successive relaxation. |
| 3.22 | Maximum resultant out-of-balance forces versus number of cycles for successive and simultaneous relaxation. |
| 4.1 | Occupation of CDC 6600 core by the program. |
| 4.2 | Structure of file LUN. |

| Figure No. | Description |
|---|---|
| 4.3 | Two different brick arrangements. |
| 4.4 | Schematic of records in array AO. |
| 4.5 | Consolidation with static relaxation. |
| 4.6 | Mass blasting with static relaxation. |
| 4.7 | Consolidation with dynamic relaxation. |
| 4.8 | Mass blasting with dynamic relaxation. |
| 4.9 | Base friction model study. |
| 4.10 | Open stoping simulation. |
| 4.11 | Up-dip cut-and-fill mining. |
| 4.12 | Down-dip cut-and-fill mining. |
| 4.13a | Mass blasting under full external loading. |
| b | Mass blasting under partial external loading. |
| 4.14 | Simultaneous mass blasting of two openings under external loading. |
| 4.15 | Mass blasting of secondary opening subsequent to primary - external loading. |
| 4.16 | Crown pillar under external loading. |
| 4.17a | Singular joint set in hangingwall. |
| b | Competent zone in hangingwall. |
| 5.1 | Overall view of loading apparatus. |
| 5.2 | Hydraulic cylinder loading arrangement. |
| 5.3 | Loading platen units. |
| 5.4 | Specifications of mounting brackets. |
| 5.5 | Layout of hydraulic circuit. |
| 5.6 | Proving ring test. |
| 5.7 | Strain gauge rosettes on continuous aluminium block. |
| 5.8 | Numerical uniaxial test results. |
| 5.9 | Strain gauge rosettes on discontinuous aluminium block. |

| Figure No. | Description |
|---|---|
| 5.10 | Three column differential boundary test. |
| 5.11 | Typical failure specimen from three column test. |
| 5.12 | Stiffness test results. |
| 5.13 | Failed connecting bolts. |
| 5.14 | Double shear test. |
| 5.15 | Failure mode for 100 mm dia. circular tunnel under vertical uniaxial load. |
| 5.16 | Failure mode for two rectangular openings under vertical uniaxial load. |
| 5.17 | Sinar monorail camera. |
| 5.18 | Pye measuring microscope. |
| 5.19 | Photogrammetric control set-up. |
| 5.20 | Theodolite arrangement. |
| 5.21 | Camera calibration set-up. |
| 5.22 | Plot of residuals. |
| 5.23 | Uniaxial compressive strength versus plaster-water ratio (after Eissa, 1974). |
| 5.24 | Uniaxial compressive strength versus curing time (after Eissa, 1974). |
| 5.25 | Perspex moulds. |
| 5.26 | Urethane rubber moulds. |
| 5.27 | Typical plaster failures. |
| 5.28 | Typical stress-strain curve for plaster. |
| 6.1 | Geometrical configurations modelled. |
| 6.2 | Preliminary loading of model. |
| 6.3 | Initial loading for Model I. |
| 6.4 | Model I - Pv/Ph = 4.5. |
| 6.5 | Model I - Pv/Ph = 9.0. |
| 6.6 | Model I - photogrammetric displacements for Pv/Ph = 4.5. |

| Figure No. | Description |
|---|---|
| 6.7 | Model I - photogrammetric displacements for Pv/Ph = 9.0. |
| 6.8 | Model I - block geometry for numerical simulation. |
| 6.9 | Model I - numerical results after initial loading. |
| 6.10 | Schematic block geometry and normal force magnitudes after initial loading. |
| 6.11 | Model I - numerical results for Pv/Ph = 4.5. |
| 6.12 | Schematic block geometry and normal force magnitudes for Pv/Ph = 4.5. |
| 6.13 | Model I - numerical results for Pv/Ph = 9.0. |
| 6.14 | Schematic block geometry and normal force magnitudes for Pv/Ph = 9.0. |
| 6.15 | Force distribution with variable stiffnesses. |
| 6.16 | Results for normal stiffness test. |
| 6.17 | Initial loading for Model II. |
| 6.18 | Model II - sliding along vertical joints. |
| 6.19 | Model II - photogrammetric displacements. |
| 6.20 | Model IIA - symmetrical sliding zones. |
| 6.21 | Model II - block geometry and results for numerical simulation with initial loading. |
| 6.22 | Model II - numerical results for increased vertical loading (Pv/Ph = 2.5). |
| 6.23 | Model II - alternative block geometry modelled numerically and initial results. |
| 6.24 | Model II - alternative block geometry numerical results for Pv/Ph = 2.5. |
| 6.25 | Initial loading for Model III. |
| 6.26 | Model III - Pv/Ph = 4.8. |
| 6.27 | Model III - Pv/Ph = 6.3. |
| 6.28 | Model III - photogrammetric displacements for Pv/Ph = 4.8. |

| Figure No. | Description |
|---|---|
| 6.29 | Model III - numerical block geometry and results after initial loading. |
| 6.30 | Model III - numerical results for Pv/Ph = 4.8. |
| 6.31 | Schematic block geometry and normal force magnitudes for Pv/Ph = 4.8. |
| 6.32 | Model IV - Pv/Ph = 0.34. |
| 6.33 | Model IV - Pv/Ph = 0.21. |
| 6.34 | Model IV - photogrammetric displacements for Pv/Ph = 0.34. |
| 6.35 | Model IV - numerical results for Pv/Ph = 0.34. |
| 6.36 | Schematic block geometry and normal force magnitudes for Pv/Ph = 0.34. |
| 6.37 | Initial loading for Model V. |
| 6.38 | Model V - Pv/Ph = 5.2. |
| 6.39 | Model V - photogrammetric displacements for Pv/Ph = 5.2. |
| 6.40 | Model V - Pv/Ph = 6.5. |
| 6.41 | Model V - numerical block geometry and results after initial loading. |
| 6.42 | Model V - numerical results for Pv/Ph = 5.2. |
| 6.43 | Schematic block geometry and normal force magnitudes for Pv/Ph = 5.2. |
| 6.44 | Initial loading for Model VI. |
| 6.45 | Model VI - Pv/Ph = 6.2. |
| 6.46 | Model VI - photogrammetric displacements for Pv/Ph = 6.2. |
| 6.47 | Model VI - numerical block geometry and results after initial loading. |
| 6.48 | Model VI - numerical results for Pv/Ph = 6.2. |
| 6.49 | Schematic block geometry and normal force magnitudes for Pv/Ph = 6.2. |
| 6.50 | Model VI - numerical results for Pv/Ph = 6.2 and Kn/Ks = 10. |

| Figure No. | Description |
|---|---|
| 6.51 | Model VI - results obtained with dynamic relaxation for Pv/Ph = 6.2. |
| 6.52 | Initial loading for Model VII. |
| 6.53 | Model VII - Pv/Ph = 4.4. |
| 6.54 | Model VII - photogrammetric displacements for Pv/Ph = 4.4. |
| 6.55 | Model VII - Pv/Ph = 5.2. |
| 6.56 | Model VII - numerical block geometry and results after initial loading. |
| 6.57 | Model VII - numerical results for Pv/Ph = 4.4. |
| 6.58 | Schematic block geometry and normal force magnitudes for Pv/Ph = 4.4. |
| 6.59 | Initial loading for Model VIII. |
| 6.60 | Model VIII - Pv/Ph = 4.2. |
| 6.61 | Model VIII - photogrammetric displacements for Pv/Ph = 4.2. |
| 6.62 | Model VIII - Pv/Ph = 5.0. |
| 6.63 | Model VIII - numerical block geometry and results after initial loading. |
| 6.64 | Model VIII - numerical results for Pv/Ph = 4.2. |
| 6.65 | Schematic block geometry and normal force magnitudes for Pv/Ph = 4.2. |

## LIST OF TABLES


| Table No. | Description |
|---|---|
| 2.1 | Relaxation table for three block example. |
| 3.1 | Comparison of forces calculated using static relaxation method and closed form solution, around circular hole in an infinite plate. |
| 3.2 | Comparison of displacements calculated using static relaxation method and closed form solution, around circular hole in an infinite plate. |
| 3.3 | Comparison of forces calculated using static relaxation method, and closed form solution, around circular hole in infinite plate. Severe variation in boundary conditions. |
| 3.4 | Comparison of displacements calculated using static relaxation method and closed form solution, around circular hole in an infinite plate. Severe variation in boundary conditions. |
| 3.5 | Comparison of forces calculated using static relaxation method and closed form solution, for infinite vertical line load in a semi-infinite mass. |
| 3.6 | Comparison of normal forces calculated using static relaxation and dynamic relaxation rigid block methods - first case. |
| 3.7 | Comparison of normal and tangential forces calculated using static and dynamic relaxation rigid block methods - second case. |
| 3.8 | Comparison of normal forces calculated using static relaxation and deformable block methods. Self weight only. |
| 3.9 | Comparison of normal and tangential forces calculated using static relaxation, dynamic relaxation and deformable block methods. Loads of 50 times block weight applied to top blocks. |
| 3.10 | Comparison of normal and tangential forces calculated using static relaxation and deformable block methods. Loads of 500 times block weight applied to top blocks. |

| Table No. | Description |
|---|---|
| 3.11 | Comparison of x and y displacements calculated using static relaxation, dynamic relaxation and deformable block methods. Loads of 50 times block weight applied to top blocks. |
| 3.12 | Comparison of inter-block contact force magnitudes using limiting equilibrium and static relaxation method, for 13 toppling block model. |
| 3.13 | Comparison of inter-block forces using limiting equilibrium and static relaxation method, for 16 toppling block model. |
| 4.1 | Mass blasting results. |
| 4.2 | Mass blasting results with dynamic relaxation. |
| 4.3 | Open stoping results. |
| 4.4 | Up-dip cut-and-fill results. |
| 4.5 | Down-dip cut-and-fill results. |
| 4.6 | Mass blasting under external loading. |
| 4.7 | Simultaneous mass blasting under external loading. |
| 4.8 | Mass blasting of secondary opening subsequent to primary opening. |
| 5.1 | Actual strains for four uniaxial tests. No PTFE tape on platens. |
| 5.2 | Actual strains for two uniaxial tests. PTFE tape on platens. |
| 5.3 | Numerical uniaxial strains. |
| 5.4 | Comparison between experimental and numerical strains for hydrostatic biaxial test, P = 6.86 MPa. |
| 5.5 | Strain distribution in discontinuous plate for applied uniaxial pressure of 4 MPa. |
| 5.6 | Results of camera calibration tests. |
| 6.1 | Summary of model testing programme. |
| 6.2 | Numerical and photogrammetric displacements for Model I. |
| 6.3 | Measured normal stiffnesses. |

| Table No. | Description |
|---|---|
| 6.4 | Measured shear stiffnesses. |
| 6.5 | Numerical and photogrammetric displacements for Model III. |
| 6.6 | Numerical and photogrammetric displacements for Model IV. |
| 6.7 | Numerical and photogrammetric displacements for Model V. |
| 6.8 | Numerical and photogrammetric displacements for Model VI. |
| 6.9 | Numerical and photogrammetric displacements for Model VII. |
| 6.10 | Numerical and photogrammetric displacements for Model VIII. |

# NOTATION

## ENGLISH

| Symbol | Quantity Represented |
|---|---|
| $a$ | length of radius vector (two dimensions) |
| $[a_{ij}]$ | matrix of stiffness coefficients |
| $b$ | length of triangular block edge |
| $c$ | cohesion |
| $D_a$ | actual displacement |
| $D_e$ | elastic displacement |
| $D_n$ | numerical displacement |
| $D_p$ | photogrammetric displacement |
| $E$ | Young's Modulus |
| $F$ | friction coefficient |
| $F_{cr}$ | critical buckling load |
| $F_h$ | horizontal load |
| $F_n$ | normal force |
| $F_s$ | shear force |
| $F_v$ | vertical load |
| $g_y$ | gravity in Y-direction |
| $H$ | block height |
| $I$ | moment of inertia of cross-section |
| $K$ | vertical to horizontal load ratio |
| $K_n$ | normal joint stiffness |
| $K_s$ | shear joint stiffness |
| $L$ | block width or length of column |
| $n$ | number of moveable blocks |
| $P$ | strength of point or line loads |
| $P_x$, $P_y$ etc. | field stresses |

| Symbol | Quantity Represented |
|---|---|
| $P_c$ | load per unit area |
| $P_h$ | horizontal load |
| $P_v$ | vertical load |
| W | width of block |
| $W_n$ | weight of block N |
| $Y_n$ | displacement of block N in Y-direction |

GREEK

| Symbol | Quantity Represented |
|---|---|
| $\gamma$ | unit weight |
| $\gamma$ | shear strain |
| $\Delta X$ | incremental rigid body translation in X-direction |
| $\Delta Y$ | incremental rigid body translation in Y-direction |
| $\Delta\theta$ | incremental rigid body rotation |
| $\epsilon$ | normal strain |
| $\lambda$ | geometric scale factor |
| $\psi$ | dynamic scale factor |
| $\rho$ | density |
| $\phi$ | angle of friction |
| $\mu$ | friction coefficient |
| $\nu$ | Poisson's Ratio |
| $\sigma$ | normal stress |
| $\sigma_c$ | uniaxial compressive strength |
| $\sigma_t$ | uniaxial tensile strength |
| $\tau$ | shear stress |
| $\pi$ | pi |
| $\sum$ | summation |

# CHAPTER 1

# *INTRODUCTION*

CHAPTER 1

INTRODUCTION:

A dominant requirement of modern rock mechanics research is the development of acceptable and efficient techniques for designing engineering structures constructed in discontinuous rock masses. This requirement has largely arisen from the need to locate and design rock structures such as open-pits, tunnels and large underground mining excavations in increasingly unfavourable environments, such as heavily fractured rock masses. The importance attached to both the economic and safety aspects of these designs has resulted in a need to produce methods of analysis which can assess, more comprehensively than previously possible, the factors controlling overall behaviour. These methods of analysis assist with engineering judgement and provide insight into the behaviour of the rock structure. Also, the advent of nuclear energy and the associated waste disposal problem, coupled with the present feasibility of extending or redeveloping existing mining operations, indicates that the demand for sophisticated design techniques will continue to increase.

The main problem addressed in this thesis is the behaviour of underground excavations located in discontinuous rock masses, with particular attention being paid to the performance of hangingwall and crown spans in mining excavations in tabular orebodies. A photograph illustrating the importance of rock discontinuities on the behaviour of a hangingwall span is shown in Figure 1.1. Apart from the reasons given above, the justification for studying this particular aspect of rock engineering is to provide insight into the factors controlling the integrity of the overall rock structure, such as the displacements induced and energy re-distributed when excavations are created in rock. For many of the problems encountered in mine design, this information is essential. Equally important from the planning engineers viewpoint is the availability of methods which enable such factors as the size and purpose of the excavation, the mining method and associated mechanisation, and the likely support requirements to be incorporated into the design process. It was with the hope of fulfilling some of these requirements



Figure 1.1: Rock discontinuities influencing hangingwall behaviour.

that the present research was undertaken.

Rock engineering has one major distinguishing feature which separates it from many of the other engineering disciplines, namely that rock engineering design is based largely on limited and inadequately defined information which can often result in extremely conservative designs. The overriding economical and safety considerations of many designs in rock are usually determined by the quality of the input information available. Also, it is equally important for the methods of analysis used in design to portray the correct response characteristics of the rock structure system, and in many instances this requires the correct modelling of the discontinuities present. Inadequacies and limitations in the modelling methods chosen will result in only restricted design information, no matter how accurate or well-defined the input data is. In mine design and, in general, for any rock structure, it is often unreasonable to design by precedent since as well as the problem of inadequate data definition, there is usually little continuity between some of the more important parameters from one location to the next. Thus, any design solution must be assessed with both the extent of problem definition and the limitations of analytical techniques used kept in mind.

Rock masses in typical mining environments often contain numerous discontinuities which have been shown to play a significant role in the engineering performance of large excavations situated within them (Fabjanczyk, 1978). Deformations measured from monitoring instrumentation installed in the immediate vicinity of such excavations indicate that displacements predicted from continuum analyses can be very inaccurate in cases where unstable geometries allow large displacements to occur. Therefore, the design of such excavations should be concerned with methods of predicting, as accurately as possible, the actual load-deformation response in jointed rock masses.

The response characteristics of a jointed rock mass to a prescribed set of physical properties and boundary conditions

is a complex problem and it is. in general, difficult to predict the final outcome with any certainty. It is important to examine all of the kinematically possible modes of deformation of jointed rock masses. An essential feature of blocky, no-tension materials is the ability for rotation of individual block units and hence non-uniformity of resulting inter-block forces (Burman, 1972). In a highly fractured rock mass, extensional, rotational and sliding deformations are all possible depending on the tensile and shear strengths of the joints and these can result in the interlocking of rock blocks, the creation of voids and the formation of point contacts between blocks. The modes of deformation possible in a discontinuous rock mass are depicted in Figure 1.2.

Such modes of failure generally give rise to large movements compared with any elastic deformation, particularly in areas where the stresses are low. The effects of block rotation result in:

a) a change in the volume of the block assemblage;
b) large force concentrations due to constraints which restrict the volume change;
c) a change in the strength characteristics.

Because of these possible variations in deformation, internal block arrangements may be formed which are consistent with the boundary conditions, but which result in large variations in internal load distribution due to the variations in contact area between blocks. These localized areas of contact produce high stress concentrations which may cause large rigid body displacements and rotations with crushing or cracking of the rock blocks ultimately possible.

The modes of deformation possible in a jointed rock mass indicate that the equilibrium state at any particular time may well be dependent on the path taken i.e. the resulting behaviour is path dependent. This means that intermediate arrangements may develop where there are several stages of partial collapse in which geometries fail and more stable ones

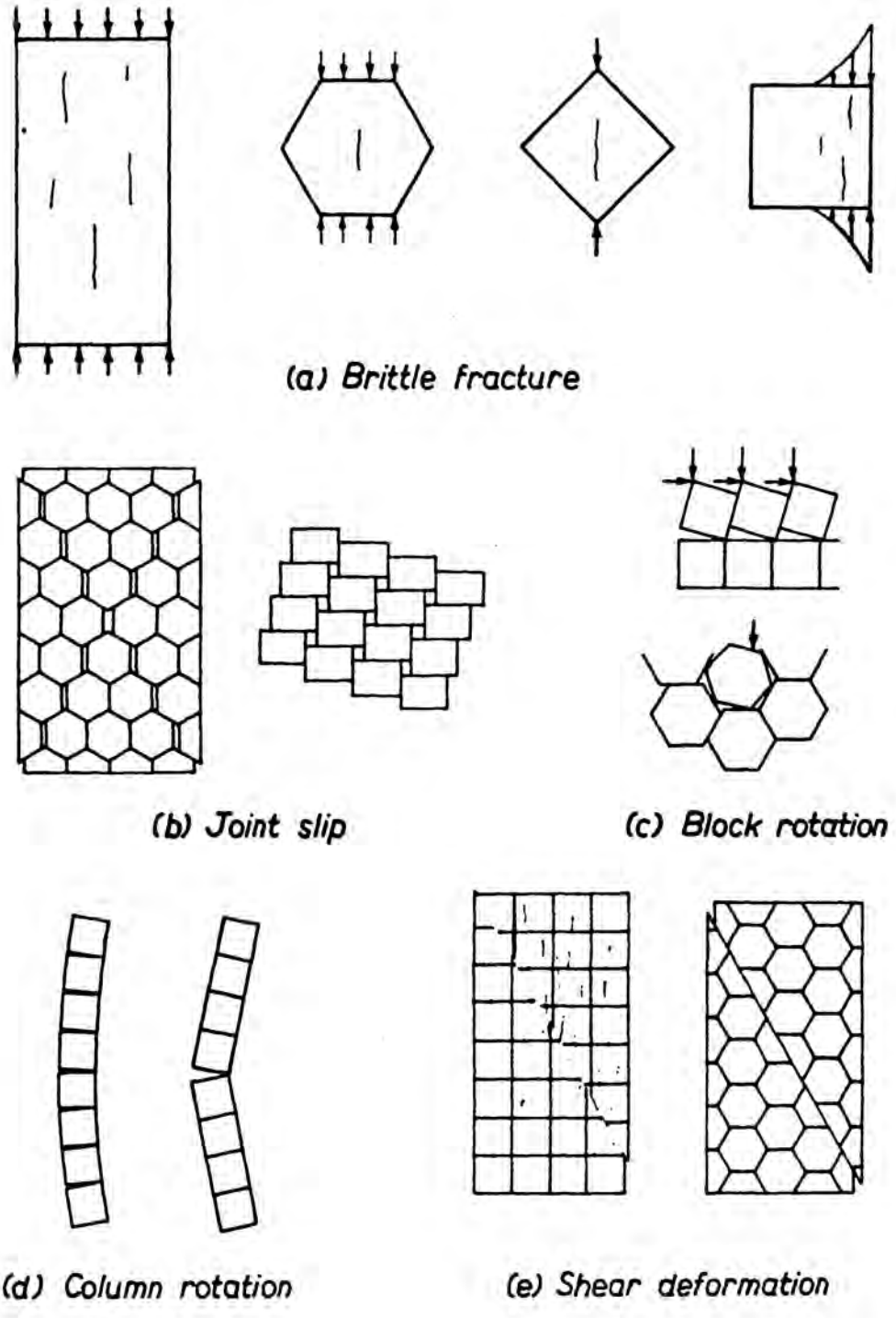



Figure 1.2: Modes of deformation possible in discontinua (after Brown, 1968).

are developed before there is a final total collapse of the rock mass.

The objectives of the research presented here are to incorporate the response characteristics of jointed rock masses into modelling techniques, specifically developed to aid in mine design. This is achieved by developing modelling techniques which allow for large scale translational and rotational movements within jointed rock masses. The work is concerned with the development of experimental and numerical methods for modelling such behaviour, with particular emphasis on the influence of the discontinuities.

A numerical method, based on an extension of the Distinct Element Method, is used to model the behaviour of rock structures constructed in jointed rock masses. In this model, the intact rock is assumed to be rigid whereas the discontinuities may be modelled according to realistic constitutive relationships. As with all numerical models, care must be exercised in interpreting the results since the solutions obtained are only as good as the quality of the input information, and a rigorous testing of the program is usually necessary to instil confidence in its use. The advantage of being able to develop and apply numerical methods to the modelling of jointed rock systems is that one is able to carefully study the major characteristics controlling the behaviour by independently varying the system parameters. Also, no prior assumption as to the failure mode is necessary, which is an advantage over analytical techniques such as limiting equilibrium.

Because of a lack of data produced from precise, properly controlled experimentation concerning inelastic behaviour, a biaxial loading apparatus was designed and constructed for an experimental investigation of underground excavations in jointed media. The medium-sized loading apparatus has been used to examine modes of deformation on plaster block models with various jointing configurations. The purpose of the laboratory tests was to accurately measure the rigid body displacements of model

elements and to compare experimental displacements with those predicted numerically. The physical modelling was selected since the experimental conditions were easily controllable while the system properties, although not able to be varied independently, could usually be sufficiently well characterised. Often, these conditions are impossible to achieve in field tests.

Chapter 2 reviews a number of analytical/numerical techniques which have been commonly used to analyze the behaviour of jointed media. A brief introduction to relaxation methods is presented and a detailed account given of a numerical relaxation procedure termed dynamic relaxation. Its applicability to mine design is assessed by way of an illustrative example. The chapter concludes with a description of an alternative relaxation algorithm, developed to overcome some of the inherent difficulties encountered with dynamic relaxation.

Chapter 3 is concerned with the validity of solutions calculated by the numerical model. Any computer program developed must be rigorously tested and compared against known solutions before employing it to solve general problems. However, comprehensive analytical or closed form solutions do not exist for general problems involving jointed rock masses. For most of the validations presented, a comparison was made with the results predicted from either alternative numerical techniques or from results based upon limiting equilibrium principles.

An extension of the numerical model to incorporate large-sized problems in general and the subsequent experimental model studies in particular, is dealt with in Chapter 4. The modifications are described, and an example of the potential and applicability of the development illustrated with reference to typical mine design problems. Comparisons between the numerical model results and those from independent techniques are also presented.

A brief review of experimental modelling techniques used for studying discontinua is given in Chapter 5. This is

followed by the design and development of a loading apparatus which allows independent control of two principal stresses on a jointed model. The results of commissioning and calibration tests are presented enabling the overall performance of the apparatus to be assessed. Details of the associated instrumentation developed for the experimental model studies, together with specifications of the modelling material, are also presented. Finally, the relationship between the model studies and the prototype is discussed.

In Chapter 6, the results of eight physical and numerical model studies are critically assessed. Comparisons between the numerical and experimental results are made and explanations offered where deviations between predicted and measured behaviour exist.

The work is summarized in Chapter 7, where the relevance of the modelling techniques developed to underground excavation design is discussed and recommendations for future research are made.

# CHAPTER 2

# *NUMERICAL METHODS FOR DISCONTINUA*

# CHAPTER 2

# NUMERICAL METHODS FOR DISCONTINUA

## 2.1. Methods Available For The Analysis of Discontinuous Rock Masses:

The methods of analysis available to the rock mechanics engineer when designing engineering structures in discontinuous rock masses are limited. The particular method(s) selected usually means that some compromise must be made between the nature of the input data/problem definition available, the assumptions inherent in the method, and the importance attached to the subsequent solutions. This is largely due to the fact that rock is usually characterized by some of the features of non-homogeneity, anisotropy, non-linearity and extensive fracturing. Hence, the chosen method(s) of analysis should be capable of taking into account these factors if a meaningful basis for design is to be established.

The discontinuous nature of many rock masses probably presents the most difficult design decision of all i.e. does the extent of fracturing throughout the rock mass warrant a continuum or a discontinuum analysis. As outlined in Chapter 1, the behaviour of a jointed rock mass is fundamentally different from the behaviour of a continuum. Before selecting particular methods of analysis, engineering judgement should be exercised where possible and it is reasonable to expect in some instances such as when the displacements are small or the jointing of minimum extent that a continuum approach would suffice. For example, Eissa (1980) reports the development of an anisotropic continuum model by which the influence of a regular joint set can be modelled. On the other hand, for more general problems an analysis based on true discontinuum behaviour is essential.

The discontinuous characterization of many rock masses has been categorized by past researchers as being intermediate between particle (heavily fractured) or

monolithic behaviour, both of which are usually amenable to continuum theory (Hammett, 1974; Muller and Hofmann, 1970). This classification has been applied by Hocking (1977) to the relative size of the rock structure (slope, underground excavation) to the material structure (discontinuity spacing, block size). Where the rock structure is either large or small compared to the material structure then a continuum analysis is justified. However, where the material structure is between the two extremes the behaviour tends to that of a discontinuum, and should be analysed as such.

The methods of analysis available to the rock mechanics engineer to examine the response characteristics of a jointed rock mass can be broadly classified into the following categories:

a) numerical studies;
b) analytical studies;
c) physical model studies.

A more comprehensive grouping has been adopted by Brown and Hudson (1972) which is discussed further in Section 5.1. Also, a review of the applicability of physical modelling techniques to the studies and analyses of jointed media is presented in Sections 5.1 and 5.4. As outlined above, many of the approaches to the analysis of discontinuum behaviour have derived from continuum theories.

The best known numerical methods based on a continuum characterization are the Finite Difference, Finite Element and Boundary Element techniques. All three methods have been applied to the analysis of discontinua but are limited by the assumptions and idealisations which are necessary and by the extent to which the response characteristics can be correctly simulated. Burman (1972) and Chappell (1972) report the development of Finite Element formulations using rigid blocks which were limited to small scale displacements

and could only model some of the discontinuum response features outlined in Chapter 1. Goodman et. al. (1968) and Hittinger and Goodman (1978) incorporated joint elements with normal and shear stiffnesses into a Finite Element formulation but again the system behaviour was restricted to essentially small scale movements. Boundary Element methods offer considerable advantages over the established Finite Difference or Finite Element techniques (Eissa, 1980) but at present they still strictly model continuum behaviour and therefore cannot be truly representative of jointed rock masses.

Limiting equilibrium methods have received favourable application in situations where the problem geometry is relatively simple and a number of realistic assumptions may be made concerning the resulting rock mass behaviour. These assumptions, usually concerning the magnitude and point of application of some forces, are necessary to ensure the problem is statically determinant. In cases of limiting equilibrium, where the failure mode is known, or can be guessed with reasonable certainty, the limiting equilibrium method can be used to determine the factor of safety and information on the distribution of forces. Goodman and Bray (1976) have employed the method to investigate the toppling failure of slopes with simple geological structures. The method has also been used extensively for problems involving the stability of wedges of rock and rock slopes excavated in jointed rock and the investigation of the stress distribution within jointed rock (Bray, 1967; Hoek, 1970).

However, in a randomly jointed rock system it may be impossible to make some of the assumptions necessary for the problem to become statically determinate. For example, the mode of failure (displacement directions) with the lowest stability may be unknown in advance or the amount of shear deformation required to mobilise the shear strength along certain discontinuities may be considerable.

The clastic model theory developed by Trollope (1968) and Trollope and Brown (1965) is another analytical approach which can be applied to the analysis of rock masses. This theory was developed to determine the force distribution within an assembly of units such as spheres and cubes. The model was used to examine arching mechanisms within block jointed models and to investigate the pressure distribution in a discontinuous foundation.

The following sections detail alternative numerical approaches to the analysis of jointed rock masses, in which the main response characteristics are correctly modelled without imposing undue limitations or assumptions. They are based on relaxation principles and attempt to overcome some of the shortcomings in the existing methods outlined above.

## 2.2. Relaxation Methods:

### 2.2.1. General:

Historically, relaxation methods were developed more than half a century ago as a means of calculating stresses and displacements in general engineering structures. Southwell (1940) describes relaxation methods developed for the calculation of stresses in highly redundant pin-jointed frameworks while an earlier development based on the same principle was reported by Hardy Cross (1932) who was concerned with problems involving moment distribution in continuous beams. These relaxation methods are characterised by the fact that the necessity of solving large numbers of simultaneous equations is eliminated. Further developments have seen the method applied to problems involving electrical and hydraulic networks, vibrating systems, and plane-potential problems.

The basis of the method as applied to frameworks or beams is to start by making the structure rigidly fixed

at every moveable joint or support and then finding the forces or fixed-end moments necessary for any loading conditions under consideration. One joint at a time is then released and the forces or fixed-end moments are modified to secure equilibrium at the released joint. This is possible by considering the appropriate unit problem whose solution enables the joint displacements (rotations) imposed to be related to the forces (moments) which must be applied in order to maintain these joint movements. For example, the simplest unit problem in a pin-jointed framework is the displacement of a joint (end-of-member) through a unit distance in some specified direction, all other joints being held fixed. This joint is then temporarily fixed again until all other joints have been released and fixed in their new positions. The procedure is repeated again and again until the desired degree of accuracy is obtained.

The above relaxation procedure can be equally applied to problems involving discontinuous rock masses, in which the rock mass is visualized as consisting of a set of discrete rigid rock blocks, each block capable of connecting in some way with adjacent blocks. Here, the block centroids correspond to the 'joints' outlined in the relaxation procedure above. For the rock blocks, both translation and rotation are considered in the unit problem and hence constraints must be applied to the centroids which prevent these movements.

The relaxation method requires the structure (in this case the discontinuous rock mass) to be initially considered in its unloaded state and to have all of its moveable members (i.e. the rock blocks) effectively fixed in position and direction by imaginary constraints (clamps). This initial clamping of the members induces no forces or moments in the structure and when any loading effect (e.g. self weight, surface loading) is applied, it is taken wholly by the constraints. This imaginary

clamping of the structure allows the various members to be initially considered separately in their structural action.

Next, suppose that the constraints on one block are relaxed and that it travels through some specified distance in some particular direction, the exact amount and nature of this movement depending on the particular unit problem employed. As the loads on each constraint are liquidated, the other blocks in the structure are kept fixed in position. Then forces will be transferred from the constraints to the inter-block contacts surrounding the released block, which usually affects the forces on neighbouring constraints as well as liquidating the forces on the constraint which has been relaxed. However, as discussed in Section 2.4.1, care is required as to when these alterations on neighbouring constraints are updated since for conditions where inelastic behaviour is possible, the final result could well be path dependent.

The amount of translation and rotation of the member during the relaxation process determines the extent to which the particular constraint is relieved of load, and the residual (out-of-balance) forces and moments can be either liquidated completely or to any desired extent. For example, if the governing unit problem permits the member to displace so as to satisfy the scalar equilibrium conditions, then the residuals should be completely liquidated when the block attains its new position.

Now, let this constraint be fixed in its new position and let some other constraint be relaxed. Then the second constraint can be relieved of load in a similar manner to that described above and the process repeated indefinitely. Numerous relaxations of each system member are usually necessary since each relaxation affects the residuals on neighbouring constraints and so loads may reappear on constraints which previous operations had

relieved.

The alterations in the constraints during progressive relaxations are usually small enough to ensure that the overall procedure eventually reduces the residual forces and moments to negligible proportions. By employing a systematic adjustment of all system members the procedure can be repeated until the desired degree of accuracy is obtained. A record of the behaviour of the structure during this systematic relaxation of constraints enables the final, unrestrained structural action to be determined by a summation of the separate contributions.

Thus, the relaxation procedure enables the complete set of simultaneous equations relating to the structure to be solved, not exactly, but with a steadily increasing accuracy.

2.2.2. Example of the Relaxation Process:

The relaxation technique is best illustrated with reference to the following trivial one degree-of-freedom example. Consider a vertical column of three rigid rock blocks which are connected by a series of springs of varying stiffnesses. The system is simply under its own weight and the motion of the blocks is assumed to be in the vertical direction. The springs resist compression as well as extension. The mass of the springs is assumed negligible to that of the blocks. Forces are positive in the upwards direction. The problem is to determine the final static equilibrium position of the spring-mass system, shown in Figure 2.1.

Consider the constraint on block N to be relaxed during iteration $t + 1$, and assume that the associated movement for this block due to out-of-balance forces in the vertical direction is $Y_N^{t+1}$. The unit problem for each block can be formulated by considering the static

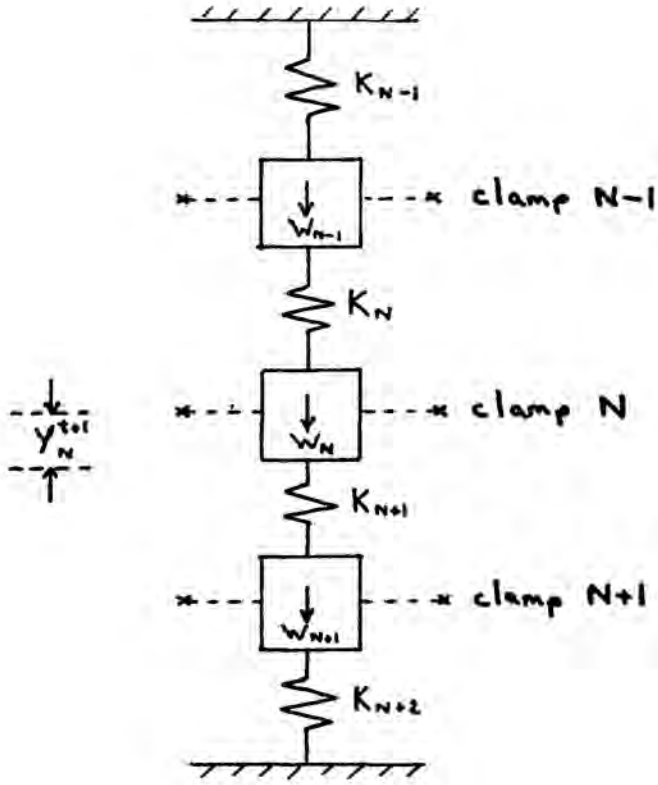



Figure 2.1: Three block relaxation example.

equilibrium requirements during each relaxation. The unit problem for block N at iteration t+1 is given by:

$$K_n\left[(Y_n^{t+1} - Y_{n-1}^{t+1}) + (Y_n^{t} - Y_{n-1}^{t}) + \ldots + (Y_n^{1} - Y_{n-1}^{1})\right]$$

$$+ K_{n+1}\left[Y_n^{t+1} + (Y_n^{t} - Y_{n+1}^{t}) + \ldots\ldots\ldots\ldots + (Y_n^{1} - Y_{n+1}^{1})\right] = W_n$$

or $F_{n,\,Wn} + F_{n+1,\,Wn} = W_n$

where

$K_n$, $K_{n+1}$ are the stiffnesses of springs N and N+1,

$Y_{n+1}^{t}$, $Y_n^{t}$, $Y_{n-1}^{t}$ are the vertical displacements (positive in downwards direction) of blocks N+1, N and N-1 at iteration t,

$F_{n,\,Wn}$, $F_{n+1,\,Wn}$ are the forces in the springs N and N+1 (positive in upwards direction) necessary to ensure static

equilibrium when block N is relaxed, and $W_n$ is the self weight of block N.

The above assumes that the clamps are relaxed in the order 1, 2, ....., N-1, N, N+1 during each iteration, although the final solution is independent of the particular relaxation sequence. The unit problem is valid for all three blocks in the system and the solution to the problem is presented in the following operations table.

Assume $W_{n-1} = W_{n+1} = 12$

$W_n = 6$ (units are of no particular significance)

$K_{n-1} = K_n = K_{n+1} = K_{n+2} = 1$

Table 2.1: Relaxation Table for Three Block Example

| relax clamp | N-1 | | N | | N+1 | |
|---|---|---|---|---|---|---|
| iteration number | $F_{n-1}$'$W_{n-1}$ | $F_n$'$W_{n-1}$ | $F_n$'$W_n$ | $F_{n+1}$'$W_n$ | $F_{n+1}$'$W_{n+1}$ | $F_{n+2}$'$W_{n+1}$ |
| 1 | 6 | 6 | 0 | 6 | 3 | 9 |
| 2 | 9 | 3 | 3 | 3 | 0 | 12 |
| 3 | 12 | 0 | 3 | 3 | -1.5 | 13.5 |
| 4 | 13.5 | -1.5 | 3 | 3 | -2.25 | 14.25 |
| 5 | 14.25 | -2.25 | 3 | 3 | -2.625 | 14.625 |
| 6 | 14.625 | -2.625 | 3 | 3 | -2.8125 | 14.8125 |
| 7 | 14.8125 | -2.8125 | 3 | 3 | -2.9063 | 14.9063 |
| 8 | 14.9063 | -2.9063 | 3 | 3 | -2.9531 | 14.9531 |
| 9 | 14.9531 | -2.9531 | 3 | 3 | -2.9766 | 14.9766 |
| 10 | 14.9766 | -2.9766 | 3 | 3 | -2.9883 | 14.9883 |

The exact solution, obtained from the static force equilibrium equations, consists of equal positive forces of magnitude 15 in springs N-1 and N+2. Thus, after 10 iterations, the relaxation procedure gives a solution which is within 0.1% of the exact solution. The exact solution cannot be obtained by the relaxation technique since the method is one of successive approximation but by repeating the process sufficiently often any desired degree of

accuracy can be obtained.

A similar treatment to that above can be applied to two-dimensional problems of rigid blocks to solve for the force and displacement distribution throughout the block system.

## 2.3. Assessment of the Dynamic Relaxation Method:

### 2.3.1. General Description of the Method:

Dynamic relaxation is, as described by Otter et. al. (1966), "a numerical technique which was developed to solve iteratively the finite difference formulations of the equations of elasticity. It is essentially a step-by-step integration of critically damped vibrations using viscous damping to obtain the steady-state solution". Dynamic relaxation was originally introduced as a method for solving dynamic elastic problems. By including a damping factor it has been shown to be capable of analysing static elastic problems. For the stress analysis of continuous structures, dynamic relaxation involves the separate consideration of the finite-difference approximations to the stress-strain and dynamic equilibrium equations (containing both inertial and viscous damping terms). By substituting sequentially the known values at each calculation stage, the necessity for solving the complete set of simultaneous equations is avoided, which is in contrast to direct finite difference or finite element methods. This results in efficient use of computer resources since, for example, memory requirements are kept to a minimum (the possibility of sparse arrays is eliminated) and the procedure is relatively simple to program. Also, non-linear and path dependent effects can be incorporated with no extra effort or complexity.

The solution procedure requires that the system equations be considered in their separated form to deal with the mixed boundary conditions. For the analysis of

elastic isotropic materials (Otter et. al., 1966) this involves the separate consideration of

a) the stress-strain relationship, and

b) the motion of an element due to internal stresses and imposed body forces. More generally, the two stages of dynamic relaxation involve the finite-difference approximations to any constitutive relationship and some governing law of motion.

It is not the intention of this section to present a detailed description of the specifics of the dynamic relaxation method but rather to review its applicability to various problems and to indicate the developments which led to it being used as a method for the analysis of discontinuous rock problems.

Otter et. al. (1966) applied dynamic relaxation to the stress analysis of continuous isotropic elastic structures in one, two and three dimensions. They determined the static stresses and displacements of various structures (e.g. elastic arch dams) subjected to loading and temperature effects. Their results showed that the method was suitable for the analysis of practical engineering problems and, in particular, that dynamic relaxation is relatively easy to program and economical in computer resources.

Parekh (1976) used dynamic relaxation to analyze steady state seepage problems of slopes and found good agreement with both independent numerical solutions and field measurements. He also recognised the inherent advantages in the method (simplicity of formulation, efficient use of memory, low execution times) when compared to finite elements or other direct methods requiring the solution of large sets of simultaneous equations.

Cundall (1971) presented a generalisation of the

dynamic relaxation calculation procedure developed by Otter et. al. (1966) which included forces and displacements, non-linearities and various laws of motion. It is, however, based on the same cyclic finite-difference solution of the separated constitutive and law of motion equations. The basic calculation cycle used by Cundall is illustrated in Figure 2.2.

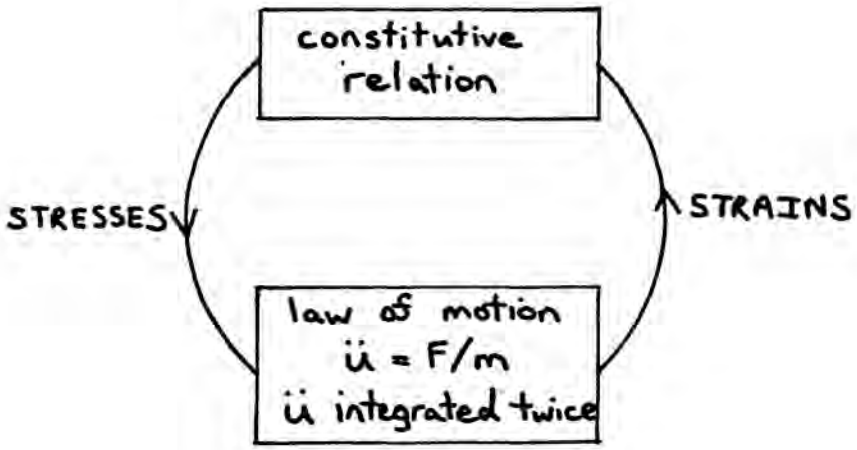



Figure 2.2: Calculation cycle for Dynamic Relaxation (after Cundall, 1976).

This calculation cycle also forms the basis for subsequent explicit finite-difference methods developed by Cundall (Cundall et. al., 1978; Cundall and Strack, 1979; Maini et. al., 1978). Cundall (1971) recognised that the general calculation procedure could be applied to many rock mechanics problems involving not only elastic, continuous, linear materials but also to the study of equilibrium conditions and progressive failure mechanisms in non-linear, inelastic, discontinua. He developed a suite of dynamic relaxation programs which were capable of analysing both the full dynamic and static solutions to continuous elastic problems. Success was also achieved in incorporating some degree of progressive failure (failing

joints) into the static dynamic relaxation formulation. However, such modelling of progressive failure in an elastic continuum would appear applicable where displacements are small and conformable and the problem geometry is not complex. Developments in this area have recently been pursued using the boundary element technique of stress analysis (Morgan, 1979; Elsworth, 1980; Townsend, 1980).

Furthermore, Cundall (1971) dispensed with the idea of modelling failure in continuous media and applied the dynamic relaxation technique to formulations which simulated both the equilibrium state and progressive, large-scale movements in a truly discontinuous medium. This approach requires the consideration of forces and displacements (rather than stresses and strains) and accommodates failure mechanisms, such as tensile and shear failure of the joints, which are characteristic of jointed rock masses. Its applicability to a system of circular discs and angular blocks was demonstrated and it was the potential of these techniques which instigated the author's interest and involvement in developing similar methods to analyse jointed rock masses.

Hocking (1977) developed a numerical formulation, based on dynamic relaxation, for the analysis of arbitrary geometries and coupled a finite element routine for the determination of stresses within blocks. His assumptions and idealisations were similar to those of Cundall (1971, 1974). The formulation included the internal stress calculation to facilitate a criterion for cracking of blocks but this was not implemented. Hocking (1977) and Ozgenoglu (1978) demonstrated the versatility of the method in a qualitative manner in studies of toppling and sliding behaviour in both jointed slopes and underground excavations.

Voegele (1978) employed a sophisticated formulation of the dynamic relaxation technique for analysing jointed

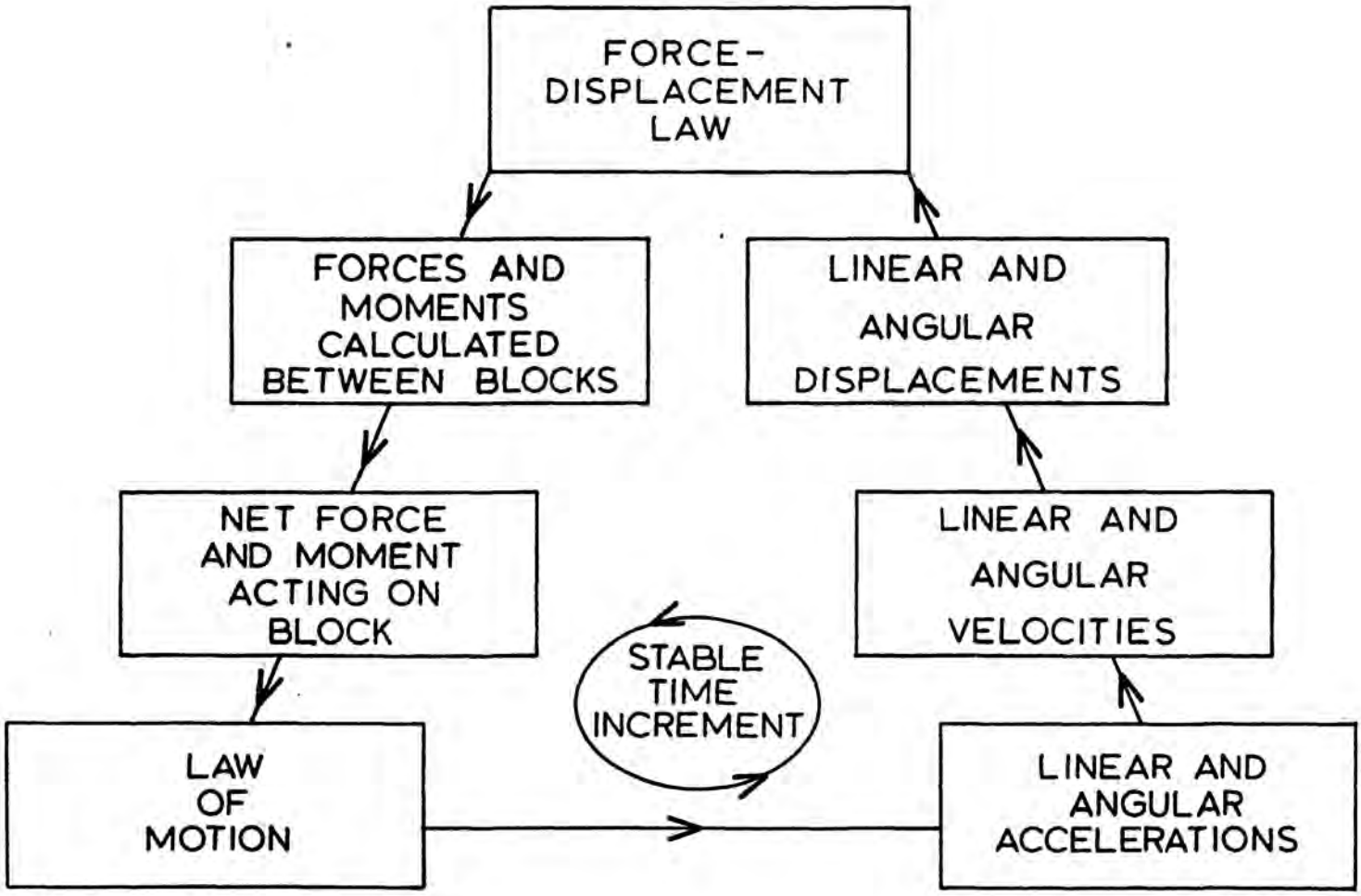
rock masses (Cundall, 1974). The main purpose of his research was to investigate, in a quantitative manner, the design of supports and the behaviour of the blocky rock mass surrounding an underground excavation. This behaviour was described in terms of ground reaction curves. Also, he carried out an extensive verification programme by comparing the numerical solutions to those based on limiting equilibrium principles.

Maini et. al (1978) and Cundall and Marti (1979) report advanced dynamic relaxation formulations which are also able to model arbitrarily shaped blocks. Additionally, programs have been developed which incorporate the cracking of blocks and allow for block deformability. Vargas (1981) is currently developing a deformable block program based on dynamic relaxation.

2.3.2. Dynamic Relaxation as Applied to Discontinuous Rock Problems:

A study was undertaken to examine, implement and assess various dynamic relaxation formulations available for the analysis of progressive, large-scale displacements in jointed media. The technique for modelling unlimited translational and rotational displacements during progressive failure in a blocky rock mass was originated by Cundall (1971a, 1971b, 1974, 1975). The program used in this study was a dynamic relaxation formulation developed by Hocking (1977) which was based on the identical calculation cycle to that instigated by Cundall (loc. cit) for determining the dynamic or quasi-static response of a discontinuum to a variety of loading conditions. The complete calculation cycle is shown in Figure 2.3.

It is relevant at this stage to discuss some of the basic features and assumptions which characterise these methods since some of these are retained in further advanced formulations (Maini et. al., 1978; Cundall and Marti, 1979) and some also relate to the alternative relaxation procedure developed and detailed in Section 2.4.




ITERATION PROCEDURE

Figure 2.3: Complete dynamic relaxation calculation cycle.

One of the fundamental assumptions made in all of the earlier formulations is that the rock structure under consideration can be represented by a network of discrete rigid blocks. This assumption implies that the rock blocks do not change their geometry as a result of applied loading or imposed constraints. At first, this may appear to place a severe restriction on the applicability of the method but it is considered to be a reasonable approximation for many rock engineering problems, particularly those located in low-stress environments. In such instances, it is common for the performance of the rock structures (slopes, tunnels, large open stopes) to be dominated by the joint properties and it seems reasonable to ignore the elastic properties of the rock material in any analysis. Care must be exercised when ignoring the rock elastic properties since in the analysis of underground excavations at depth, it is possible that the intact material response could dominate or at least control the overall behaviour to the same degree as do the discontinuities. Many crown and hangingwall failures observed and monitored around large open stopes at depths of up to 1500 m, however, indicate that discontinuous features such as faulting, bedding and jointing still control the resulting collapse mechanisms (Bridges, 1980; Fabjanczyk, 1978).

To render the system of rigid blocks statically determinate, stiffnesses are incorporated (via normal and shear springs) at discrete points along the block edges. All deformations within the rock mass are assumed to occur at the boundaries and, if necessary, the deformation properties of both the intact material and the joint can be collectively modelled.

The solution procedure also assumes that when blocks interact, the forces between blocks are located only at the block corners. Hence, forces develop where surrounding block corners penetrate block edges, and

conversely (Figure 2.4). An edge-to-edge contact is considered as two separate corner-edge contacts, while a corner-corner contact is a special case of a corner-edge contact. The prescribed force-displacement relationship for the edge component of the contact allows evaluation of the normal and shear forces at the contact points. This assumption seems reasonable since any real surface is likely to make contact at only a small number of asperities, especially if there is any tendency for rotation (Cundall, 1971).

The nature of the modes of deformation possible in a jointed rock mass (rotation, sliding, tension) indicate that the system is best described in terms of forces and displacements, rather than stresses and strains, since the former parameters remain finite regardless of the amount or nature of the resulting deformation.

The contact between two rigid blocks is modelled as a normal interaction and a shear interaction. These interactions are governed by realistic friction and stiffness laws. The normal interaction is modelled by a spring-dashpot system in parallel where contraction of the system is represented by overlapping of the blocks. In, many rock engineering structures, the normal stiffness of the joint does not control the failure process when failure is governed by joint shearing and tensile behaviour. Also, for many rock joints the normal stiffness is much greater than the shear stiffness (Barton, 1978; Goodman, 1970).

Hence, for many problems the normal forces can be simply calculated as directly proportional to the amount of overlap, i.e.

$$Fn_i = Kn \cdot \delta n_i$$

where $Fn_i$ = normal force at ith corner

$Kn$ = normal stiffness

$\delta n_i$ = normal overlap at ith corner

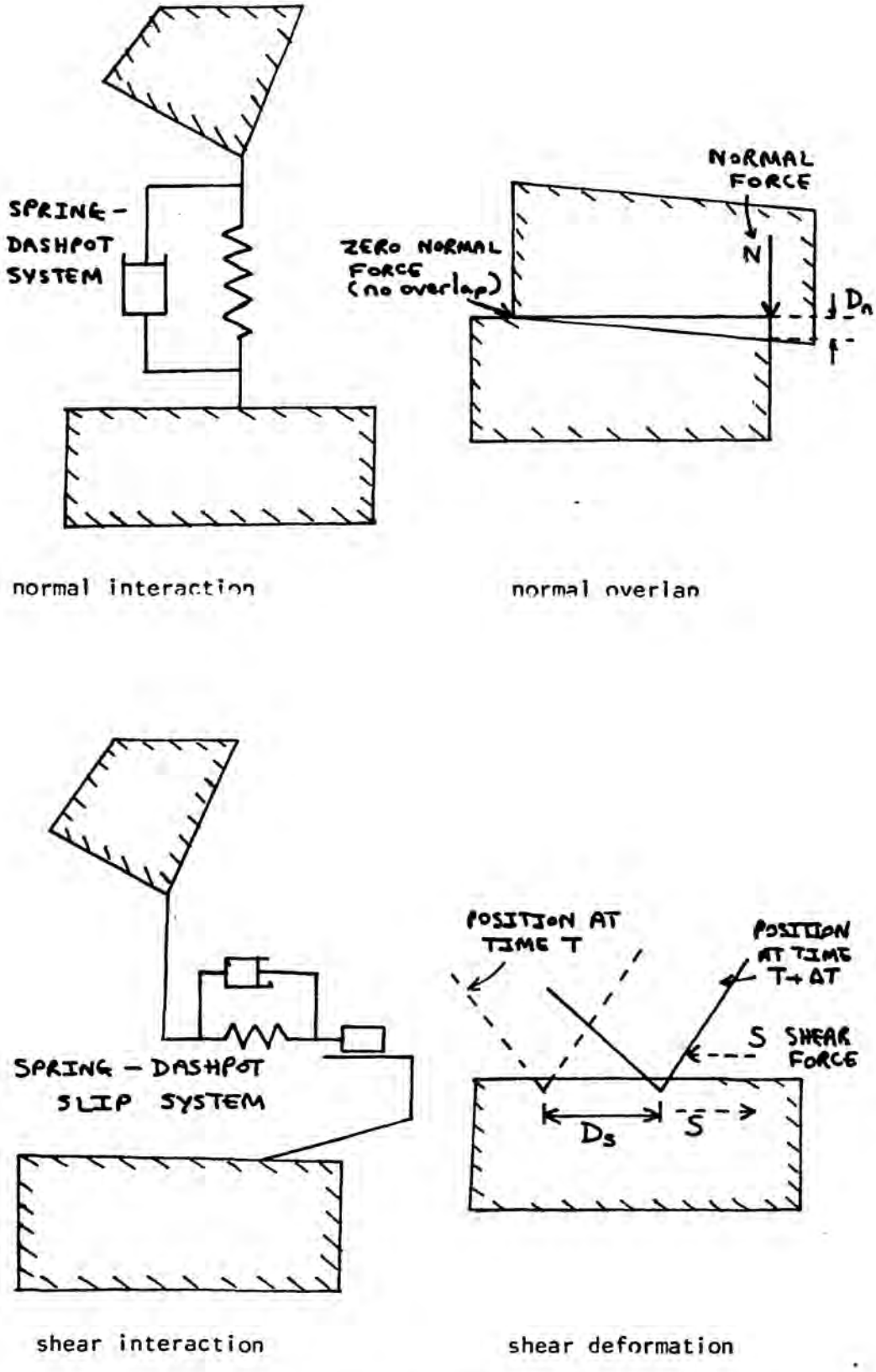



Figure 2.4: Normal and shear interactions in dynamic relaxation program (after Hocking, 1977).

This linear normal force-displacement relationship is incorporated in the numerical formulation of Hocking (1977).

Goodman (1974) indicated the highly non-linear behaviour of a typical rock joint in compression and any arbitrary normal joint characteristic may be incorporated in the solution procedure providing the behaviour is adequately defined.

The shear interaction modelled is a spring-dashpot system with a friction slider so that once slip has occurred the shear damping is removed, i.e.

$$Fs_i^{t+1} = Fs_i^{t} + Ks \cdot \delta s_i$$

where $Fs_i^{t+1}$ = new shear force at ith corner

$Fs_i^{t}$ = old shear force at ith corner

$Ks$ = shear stiffness

$\delta s_i$ = relative shear displacement of corner i along interacting block edge.

Elastic - perfectly plastic shear load-deformation behaviour for a joint is usually modelled although any general shearing characteristic can be included without extra difficulty. The shear force calculation is an incremental process since the shear force depends on the previous block movements as well as on the magnitude of the normal force. One of the advantages of the numerical model is that the joint stiffnesses may be easily modified to determine the effect on the deformation mechanism. Also, where the field response is well defined, a parametric study may possibly suggest values for the system parameters.

Two types of failure law are operative during the calculation procedure. Shearing failure is based on the Mohr-Coulomb criterion to determine if plastic shear failure can develop. Slip occurs if

$$Fs \geq \mu . Fn$$

where Fs and Fn are the total shear and normal forces acting at the contact and $\mu$ is the friction coefficient. If the shear failure law is satisfied, the shear force is set to the shear strength and slip continues until elastic conditions can be re-established.

The second type of failure occurs where joints may separate in a tensile manner. When this occurs, the magnitudes of both the normal and shear forces are set to zero until further interaction takes place.

The forces acting on each block are then resolved with respect to some convenient co-ordinate system and the components summed giving two orthogonal loads on each block equivalent to thrusts through the centre of gravity and a moment about an axis through the centre of gravity of the block.

The cyclic calculation procedure illustrated in Figure 2.3 is begun at some arbitrary time and from the geometric position of each block relative to neighbouring blocks, together with any body forces and applied surface forces, the resultant forces and moments acting on each block are determined. The blocks are able to move to new positions due to the out-of-balance forces and moments acting on them, the nature and extent of such movement being governed by the particular law of motion which the blocks obey. In the dynamic relaxation codes examined, Newton's second law of motion is used, but other laws could equally well be incorporated depending on the problem to be solved.

The linear and angular accelerations of each block are then calculated and by integrating over an incremental time step, the block velocities and displacements are calculated. Thus, the program calculates the motion of the blocks as a function of time and each new

block position generates new contact forces. After relaxing all of the blocks during any particular cycle, the procedure is repeated until a satisfactory state of equilibrium or mode of failure ensues.

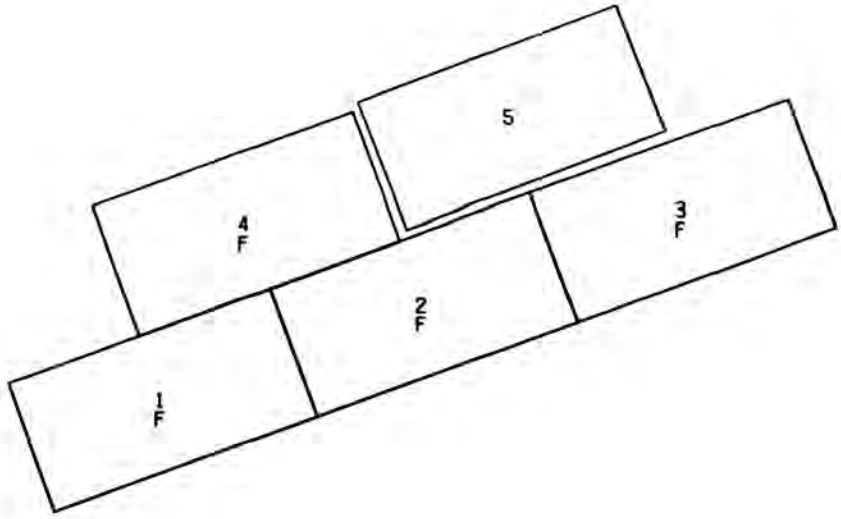
With the above law of motion, there is a restriction on the size of the permissible time step which is required to ensure a steady state solution. The stable time increment is a function of the mass and apparent stiffness (Cundall, 1971) and is usually of such a small magnitude that it leads to solution times which are, in general, excessive. The number of calculation cycles required to produce significant results, especially for 'large' problems, places severe demands on computing resources. In the dynamic relaxation formulations examined, all rigid blocks are scanned to determine a minimum value for the critical time step (based on a single degree-of-freedom system). This time step is subsequently multiplied by an arbitrary scaling factor (usually between 0.1 and 0.5) to derive a single stable time increment for the entire block system. A variable time increment, based on the mass and apparent stiffness for each block and calculated during each iteration should allow faster convergence to the final solution, thus resulting in a more efficient and economical solution procedure.

In any case, the effect of the time step may be studied by varying it and observing the results. However, if the time step exceeds its critical value then numerical instabilities will result. An example of a block 'bouncing' due to a time step larger than critical is shown in Figure 2.5. In problems where uncertainty in the final solution exists, it is advisable to re-analyse the problem with a lower time step and a correspondingly larger number of relaxation cycles.

Two types of viscous damping are incorporated in

CONSOLIDATION FOR SLIDING WHERE TIME STEP IS TOO LARGE.DT=1E-2

BLOCK PLOT NUMBER OF PROBLEM UNITS PER INCH = 0.50 CYCLE NUMBER = 20




CONSOLIDATION FOR SLIDING WHERE TIME STEP IS TOO LARGE.DT=1E-2

VELOCITY PLOT NUMBER OF PROBLEM UNITS PER INCH = 0.92 CYCLE NUMBER = 20



**Figure 2.5:** Block bouncing due to time-step greater than critical

the model by means of dash-pots connected in parallel with the normal and shear springs and by dash-pots connecting block centroids to ground. The former damping, referred to as stiffness proportional damping, damps the contact forces directly in the solution algorithm while mass proportional damping operates on the velocities. Stiffness damping prevents continuous vibration of the blocks relative to one another while mass damping can be visualised as reducing the movements of the whole block system relative to some reference frame. There are no clearly defined rules as to which type of damping should be used for particular problems, and in all of the dynamic relaxation analyses described in this work, either mass damping only or a combination of mass and stiffness proportional damping were found to give satisfactory solutions.

Thus, the development of a failure mechanism or equilibrium condition proceeds with time and the program automatically selects the mode of failure since the system fails by that mode with the lowest stability. This is in contrast to limiting equilibrium analyses which require some prior assumption as to the failure mode.

### 2.3.3. Computational Notes:

The restricted form of the dynamic relaxation procedure used here (Hocking, 1977) was not a user package and required a significant amount of user familiarity before meaningful results were obtained. There are, however, several pertinent points regarding the numerical formulation worth noting:

i) two versions of the program were available. Only the smaller version (which did not include calculation of the stress distribution within blocks) was used;

ii) the input parameters including the stable time step, the joint stiffnesses and the damping parameters were not readily optimized and a certain amount of familiarity and knowledge was required in specifying these parameters;

iii) certain routines required modification depending on the type of problem to be solved e.g. block generation and consolidation routines;

iv) a consolidation phase was performed before relevant blocks were extracted. The number of cycles for consolidation depended on the size of problem;

v) the program was run interactively, using graphics, which enabled a visual display of the results. This enabled verification of the initial block geometry and examination of subsequent block movements. Microfilm records of block geometries and displacement vectors were produced if required;

vi) a restart option was included whereby information calculated up to a particular stage may be stored and used as input to a further stage;

vii) for reasons of computer storage, the number of blocks surrounding any particular block was limited by the fact that each block corner could have a maximum of three neighbouring blocks interacting with it. Thus, for a rectangular block, the maximum number of neighbouring blocks was twelve. The neighbouring blocks were updated in user specified intervals by calling the appropriate routine;

viii) a CDC 6600 computer with 60 bit words was used. Typical central memory (C.M.) requirements for a 20 block problem were 22 K C.M. addresses, while 30 K C.M. addresses were required for a program capable of handling 160 rectangular blocks;

ix) for the excavation design problem analysed in Section 2.3.4., consisting of 150 blocks, a total of 1850 6600 seconds of CP time was needed with a typical stage of 1000 cycles requiring 450 6600 CP seconds;

x) blocks of any general shape could be modelled but it was often the case (due to continuity of jointing) that only blocks of one particular shape were required since for many mining environments rectangular shaped

blocks predominate;

xi) the program was validated against simple examples of sliding and toppling blocks and the results were in good agreement with analytical solutions. The program could adequately distinguish between stable and sliding conditions for a single block where the difference between the slope angle and the angle of friction was as low as 0.1 of a degree. More detailed and advanced validations have been conducted using this particular program by Hocking (1977) and Ozgenoglu (1978).

A listing of the rigid block program developed by Hocking (1977) is contained in Appendix VI. Also listed in Appendix VI is a generalised dynamic relaxation rigid block program (Maini et. al., 1978) which is used in subsequent chapters.

### 2.3.4. Results for an Underground Excavation Design Problem:

The applicability of an existing dynamic relaxation rigid block program (Hocking, 1977) to the analysis of a typical excavation design problem was assessed, with particular emphasis on the behaviour of the hangingwall and crown. Since the author was familiar with mining operations at Mount Isa, Australia, a typical stope in the lead-zinc section of that mine was chosen for the analysis. Briefly, the lead-zinc area is comprised of several parallel tabular orebodies of varying dimensions with shale as the dominant host rock. The shale is well bedded and jointed and can be considered to behave as a blocky material. For those orebodies whose widths are greater than about 9 m, a sub-level open stoping mining method is used. Typical dimensions for stopes mined by this method are:

| | | |
|---|---|---|
| span (vertical height) | - | 100 m |
| length(horizontal span) | - | 30-100 m |
| width (hangingwall to footwall) | - | 30 m |

Therefore, hangingwall exposures of between 30 m by 100 m and 100 m by 100 m may be formed during excavation. The main structural features in the orebodies and surrounding shale are (Brady, 1979):

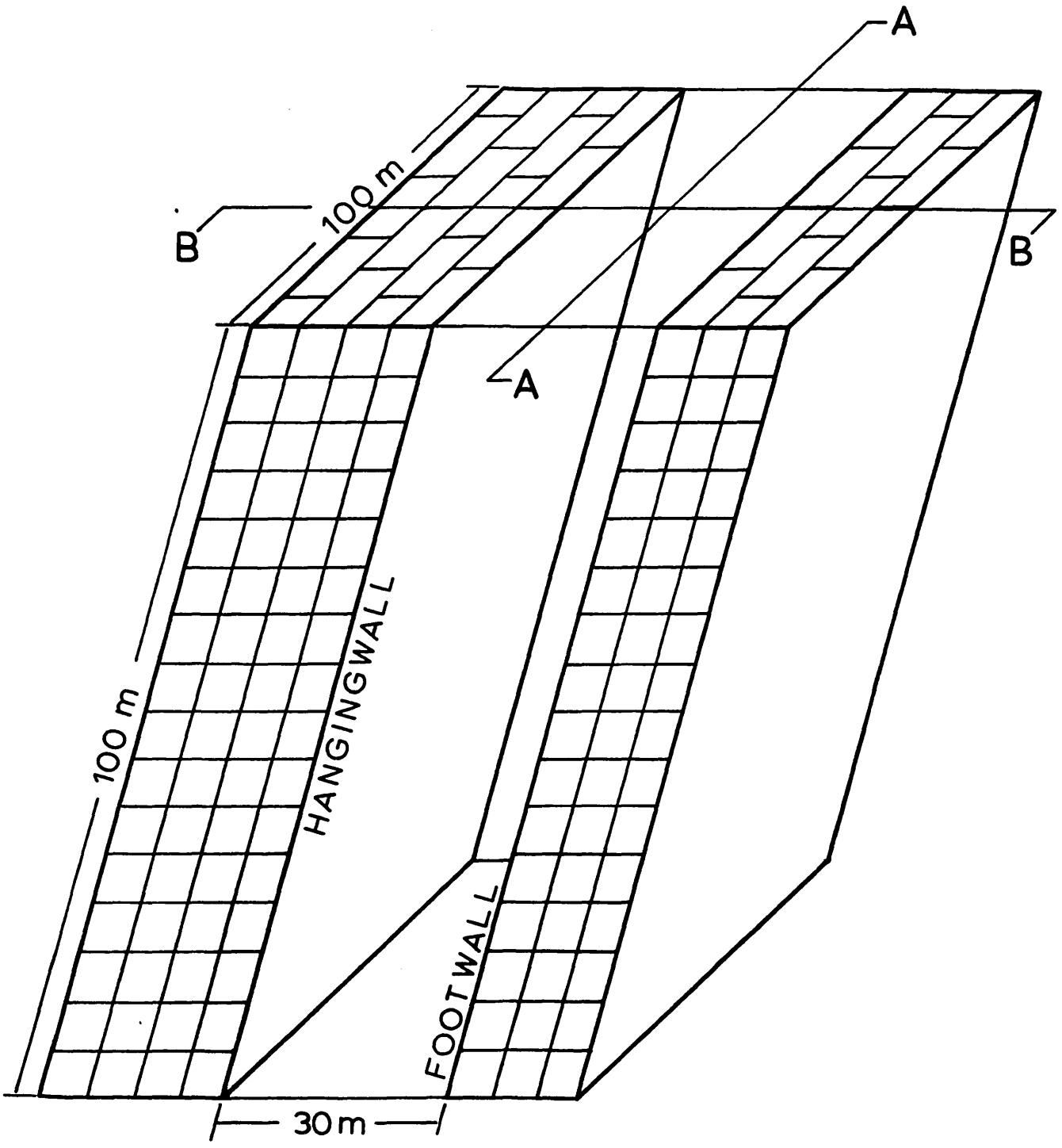
i) bedding planes dipping 60-70 degrees in a direction of approximately 270 degrees. These are the most continuous planes of weakness throughout the rock mass;

ii) a joint set dipping east at 20-25 degrees. These planes of weakness are discontinuous and rarely extend more than 1-2 m before being offset;

iii) a joint set which trends E-W and is near vertical.

Thus, the rock mass may be considered as being separated into a system of discrete blocks of intact rock by the planes of weakness. The analysis of such problems usually involves two critical sections, as shown in Figure 2.6. The vertical section (B-B in Figure 2.6) was considered to be the more important of the two as the vertical span is under gravity load.

Considering the vertical section, if the average block size is 2 m x 5 m as determined by the spacing of the joints and bedding planes, then each hangingwall column comprises 20 blocks (corresponding to a stope height of 100 m). For a representative section of hangingwall to be modelled, it is estimated that the number of columns of blocks should at least be equal to the number of joints intersecting the face of the hangingwall spanning the excavation, which for this example would mean a real distance into the hangingwall of 40 m. When using the program, arbitrary finite boundaries defining the problem domain must be chosen in a manner similar to that required by a finite element analysis. This usually involves a compromise between the accuracy of the results obtained and economic considerations. For a realistic simulation, the above problem would require between 700 and 800 blocks and based on the solution




ISOMETRIC VIEW OF UNDERGROUND
EXCAVATION DESIGN PROBLEM

Figure 2.6

times to smaller problems, it was considered uneconomical to analyse a problem containing this number of blocks.

Therefore, since only qualitative results were sought, the block size was increased, but so as to allow a representative number of joints to intersect the hangingwall and crown. The new block size was 4 m x 10 m, thereby reducing the original number of blocks by a factor of 4. With this modified block geometry, the size of the blocks with respect to the excavation size was such that the failure mechanism should be equivalent to that of the original geometry.

Once generated, the assemblage of 154 rigid blocks was consolidated under gravity using low friction conditions ($\mu = .01$) to create equilibrium throughout the block system (Figure 2.7). Consolidation was achieved by fixing a number of the boundary blocks and no external loading was applied to the system. The normal and shear stiffnesses were assigned the same value of 1.E06 computer units, this magnitude having no special significance except to keep the block overlaps as small as possible. Also, a linear normal load-deformation relationship and an elastic-plastic shear characteristic were modelled. The friction angle was then set to a value of 15 degrees, a rather low friction angle being chosen to induce large block movements. The excavation was created by the instantaneous removal of appropriate blocks.

The positions of the blocks during progressive stages of movement are shown in Figure 2.8. The geometry of the model before any visual movement occurred is shown at cycle 1200. The first indication of movement is at cycle 2000 where the columns comprising the hangingwall have moved into the excavation as a continuous unit. A distinct gap, which propagates the full extent along the back of the hangingwall, has formed between the fixed boundary and the remainder of the hangingwall. The

fixed boundary and associated gap above the stope back have prevented compressive forces from restraining the crown movement and have resulted in a very unstable crown position with increased compression of the blocks towards the footwall. Had the hangingwall boundary above the stope back been unfixed and external compressive forces been applied to the crown, then a more realistic behaviour would have ensued.

The unstable crown behaviour is seen after 3000 cycles with tilting, crushing and relative movement of the crown into the opening all observable; these features are characteristic of mine openings. Separation between blocks is initiated in a zone near the base of the hangingwall columns and simulates a plastic hinge formation. The associated velocity vector plot clearly shows the movement of basal blocks into the excavation. This hinging effect then propagates upwards through the hangingwall columns as the number of cycles is increased. After 4000 cycles the whole block assemblage is clearly unstable.

It should be noted that the excavation was created instantly and so a dynamic loading condition was imposed on the system. The alternative to this would be to gradually create the excavation by either

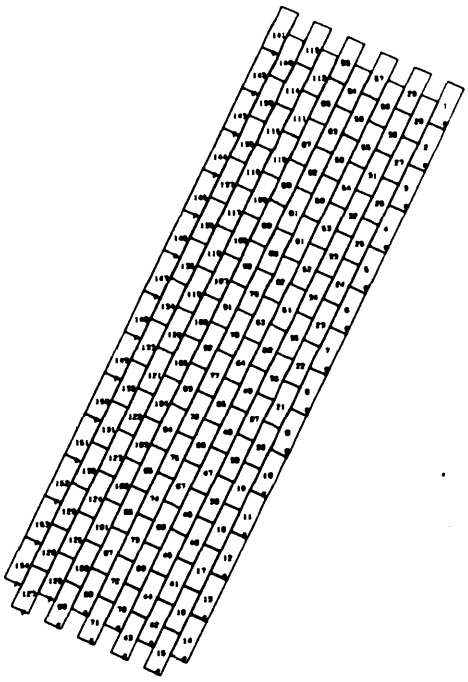
a) removing the blocks one at a time or in small groups,

or b) gradually contract the blocks in the excavation by decreasing their stiffnesses and removing when appropriate.

However, since in this example the inertial forces were relatively small, the method of extraction was not likely to greatly influence the final collapse mechanism.

CONSOLIDATION RUN FOR TYPICAL UNDERGROUND EXCAVATION DESIGN PROBLEM

BLOCK PLOT NUMBER OF PROBLEM UNITS PER INCH = 15.00 CYCLE NUMBER = 100



CONSOLIDATION RUN FOR TYPICAL UNDERGROUND EXCAVATION DESIGN PROBLEM

VELOCITY PLOT NUMBER OF PROBLEM UNITS PER INCH = 0.10 CYCLE NUMBER = 100

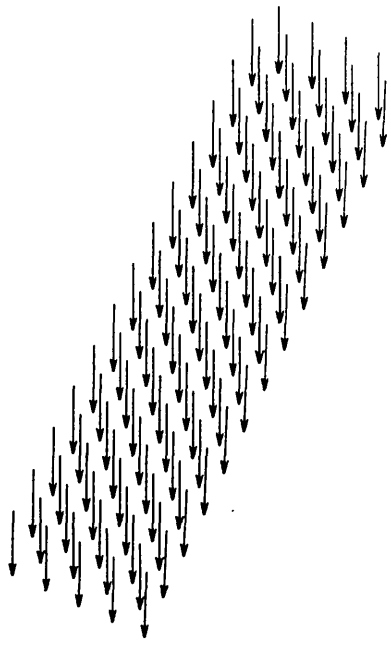


Figure 2.7

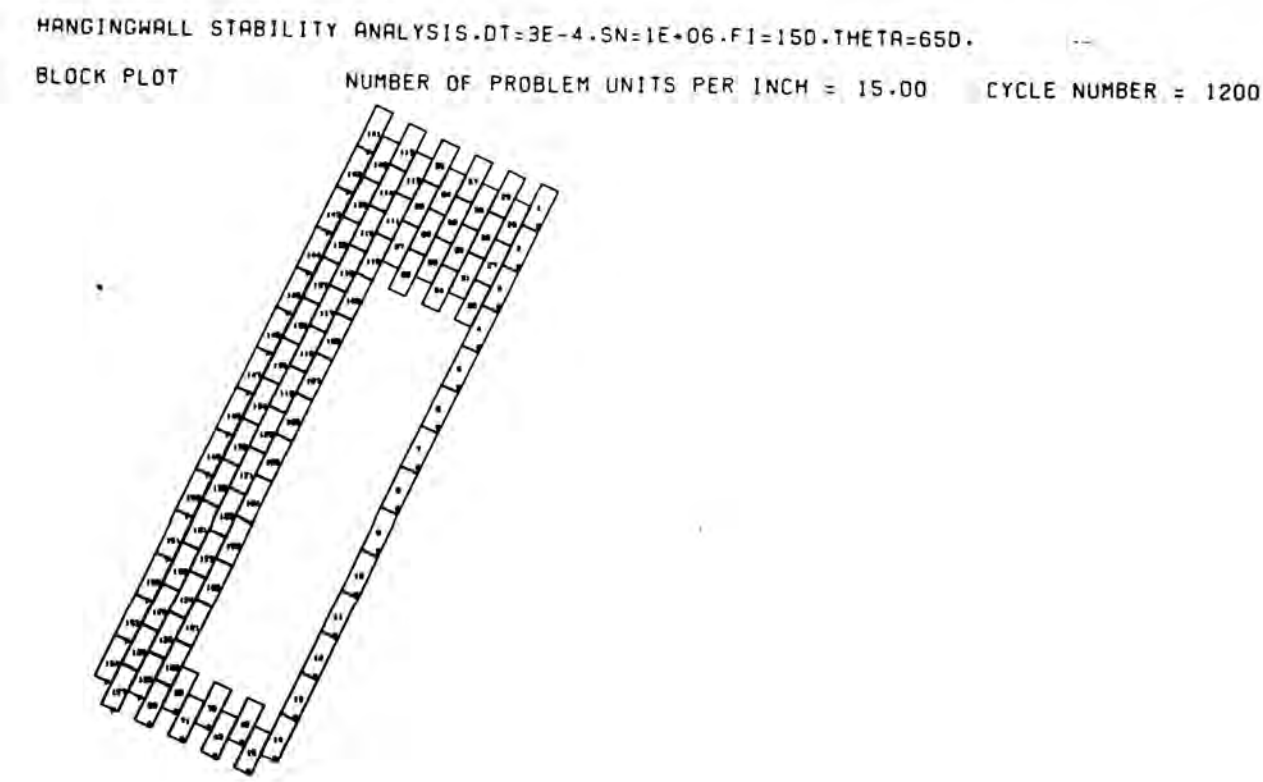
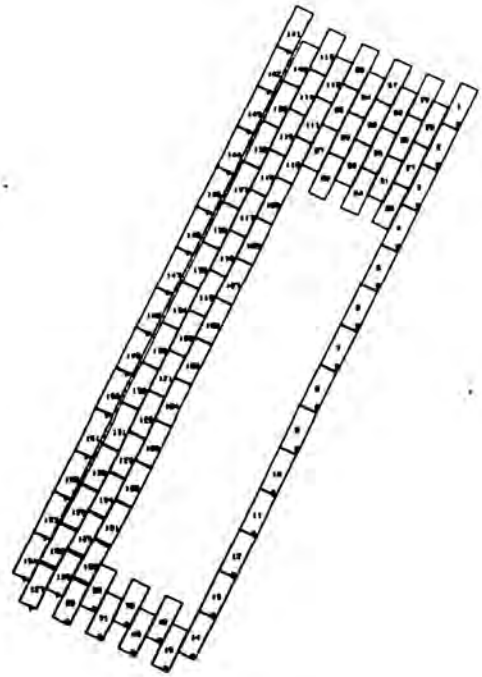

HANGINGWALL STABILITY ANALYSIS.DT=3E-4.SN=1E+06.FI=15D.THETA=65D.
BLOCK PLOT
NUMBER OF PROBLEM UNITS PER INCH = 15.00
CYCLE NUMBER = 1200
HANGINGWALL STABILITY ANALYSIS.DT=3E-4.SN=1E+06.FI=15D.THETA=65D.
VELOCITY PLOT
NUMBER OF PROBLEM UNITS PER INCH = 3.34
CYCLE NUMBER = 1200

Figure 2.8.

HANGINGWALL STABILITY ANALYSIS.DT=3E-4.SN=1E+06.FI=15D.THETA=65D.

BLOCK PLOT NUMBER OF PROBLEM UNITS PER INCH = 15.00 CYCLE NUMBER = 2000



HANGINGWALL STABILITY ANALYSIS.DT=3E-4.SN=1E+06.FI=15D.THETA=65D.

VELOCITY PLOT NUMBER OF PROBLEM UNITS PER INCH = 5.69 CYCLE NUMBER = 2000

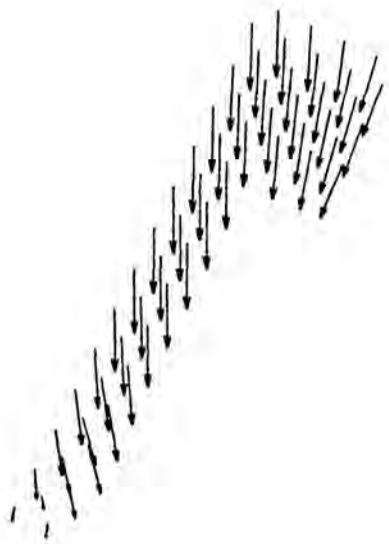
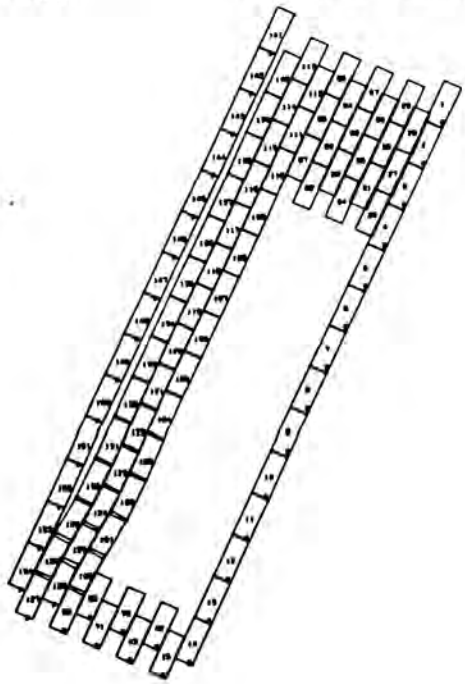


Figure 2.8 contd.

HANGINGWALL STABILITY ANALYSIS.DT=3E-4.SN=1E+06.FI=15D.THETA=65D.

BLOCK PLOT NUMBER OF PROBLEM UNITS PER INCH = 15.00 CYCLE NUMBER = 3000



HANGINGWALL STABILITY ANALYSIS.DT=3E-4.SN=1E+06.FI=15D.THETA=65D.

VELOCITY PLOT NUMBER OF PROBLEM UNITS PER INCH = 8.41 CYCLE NUMBER = 3000

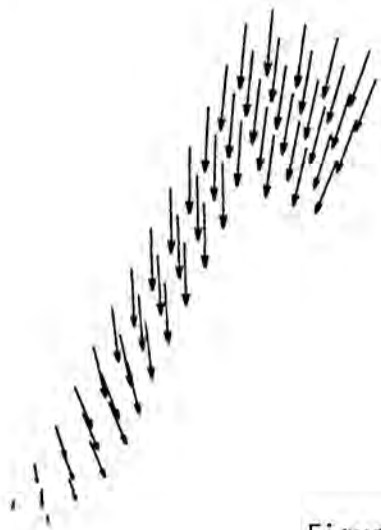
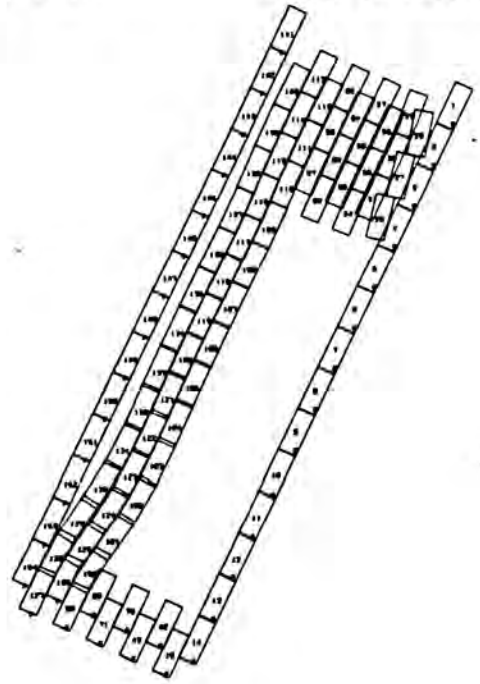


Figure 2.8 contd.

HANGINGWALL STABILITY ANALYSIS.DT=3E-4.SN=1E+06.FI=15D.THETA=65D.

BLOCK PLOT NUMBER OF PROBLEM UNITS PER INCH = 15.00 CYCLE NUMBER = 4000



HANGINGWALL STABILITY ANALYSIS.DT=3E-4.SN=1E+06.FI=15D.THETA=65D.

VELOCITY PLOT NUMBER OF PROBLEM UNITS PER INCH = 10.53 CYCLE NUMBER = 4000

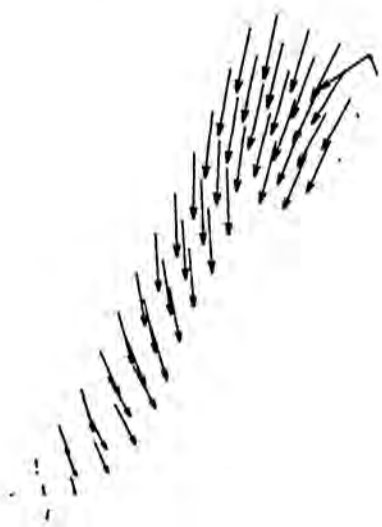


Figure 2.8 contd.

## 2.4. An Alternative Numerical Model for the Analysis of Underground Excavations in Discontinuous Rock Masses:

This section describes an alternative relaxation procedure (hereafter referred to as static relaxation) which has been developed for the two-dimensional analyses of underground excavations in discontinuous rock masses. This research was inspired by the fact that previous formulations, based on dynamic relaxation, placed rather severe demands on computing resources due to the excessive solution times encountered when 'large' problems were modelled. This is seen as a serious limitation on the program from a commercial point of view even though the results appeared in general to simulate block movements and collapse conditions compatible with those observed in practice. Since the main concern in excavation design is to determine either the equilibrium position or likely failure mode of the system, the alternative procedure was aimed at minimising demands on computer resources bearing in mind the usual limited computing facilities available on site at many mining operations.

As with the previous formulations described in Section 2.3.2, the aim of the numerical model was to allow large scale translational and rotational movements throughout the blocky rock system. This enabled the influence of the discontinuities to be examined and an appreciation of the response of the system to various loading and displacement conditions to be made. Many of the assumptions and features incorporated in the static relaxation procedure are similar to those of the dynamic relaxation techniques. The main difference between the methods lies in the nature of the unit problem, where the alternative method seeks a direct force-displacement path to equilibrium, independent of any time step and integration procedure.

2.4.1. Description of the Method:

The method of analysis used is based on the general relaxation principles developed by Southwell (1940) and Hardy Cross (1932), as discussed in Section 2.2. The method is of the same explicit nature as dynamic relaxation, each system member communicating during any iteration with only its nearest neighbours and resulting in a set of unconnected equations. This is in contrast to implicit methods which require all elements to be connected to each other (via equilibrium and compatibility) and a complete set of equations solved for each iteration. However, it is when non-linear behaviour and progressive effects in general require modelling that explicit methods are used to advantage.

The same basic calculation cycle involving the separated constitutive and law of motion equations (Figure 2.2) is used. The solution procedures of both relaxation methods differ from the classical relaxation theory in that the loads induced on each constraint due to surrounding block relaxations are updated only after all system members have been relaxed i.e. after every complete iteration. This approach is necessary to ensure that any possible path dependency is eliminated during the analysis of jointed rock mass problems where inelastic behaviour is possible. In such cases, a simultaneous relaxation technique is essential to ensure that the equilibrium condition or failure mode is independent of the path taken when relaxing constraints on system members. This results in a somewhat reduced rate of propagation of a disturbance such as loading compared to that attained with conventional successive relaxation methods such as moment distribution. Chapter 3 presents a comparison between the successive and simultaneous relaxation procedures.

The two-dimensional numerical representation of the jointed rock mass is essentially similar to that used

by previous investigators (Cundall, 1971, 1974; Hocking, 1977). In the model the rock blocks, which are of constant thickness and can be of arbitrary shape, are assumed rigid. Deformations between adjacent blocks are assumed to occur at the block interfaces only, where a joint is regarded as the boundary interface between interacting blocks. Contraction and shear movements between blocks are simulated by overlapping and sliding respectively along the interfaces in an identical manner to that used in dynamic relaxation rigid block formulations.

Contacts and associated forces between blocks are again assumed to occur at discrete points where block corners interact with neighbouring block edges and vice versa. The whole block system is statically determinate since joint stiffnesses are introduced via normal and shear springs at the contact points. The rheological models and typical force-displacement relationships for the contacts are shown in Figure 2.9. It will be noted that the normal and shear interactions shown in Figure 2.9 differ from those used in dynamic relaxation (Figure 2.4) in that no viscous dashpots are associated with the springs. Thus, energy is dissipated in the model only through friction. This means that the block assemblies will not be able to reach exact equilibrium, the deviation from equilibrium being made as small as possible by controlling the rate at which loading is applied. The philosophy here was to tolerate small continuous vibrations of blocks relative to one another providing they did not unduly affect the final equilibrium position, and be prepared, if necessary, to incorporate some form of damping at the contacts. In all subsequent comparisons with dynamic relaxation, the effect of not including viscous damping is shown to have little significance on the final results. Any solution procedure should consider the margin of uncertainty surrounding the input data where refinements in the solution procedure may not only be unnecessary, but also meaningless.

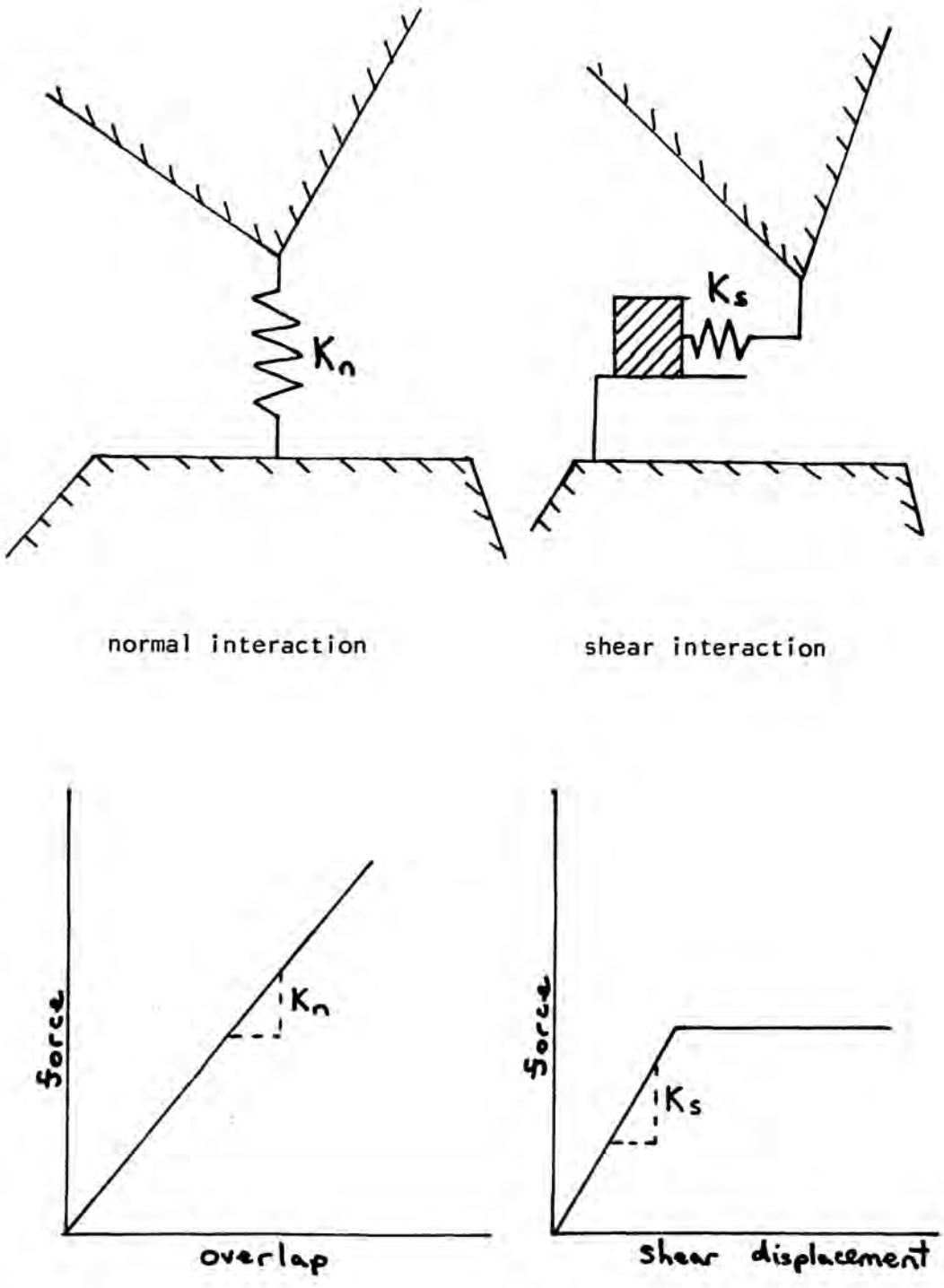
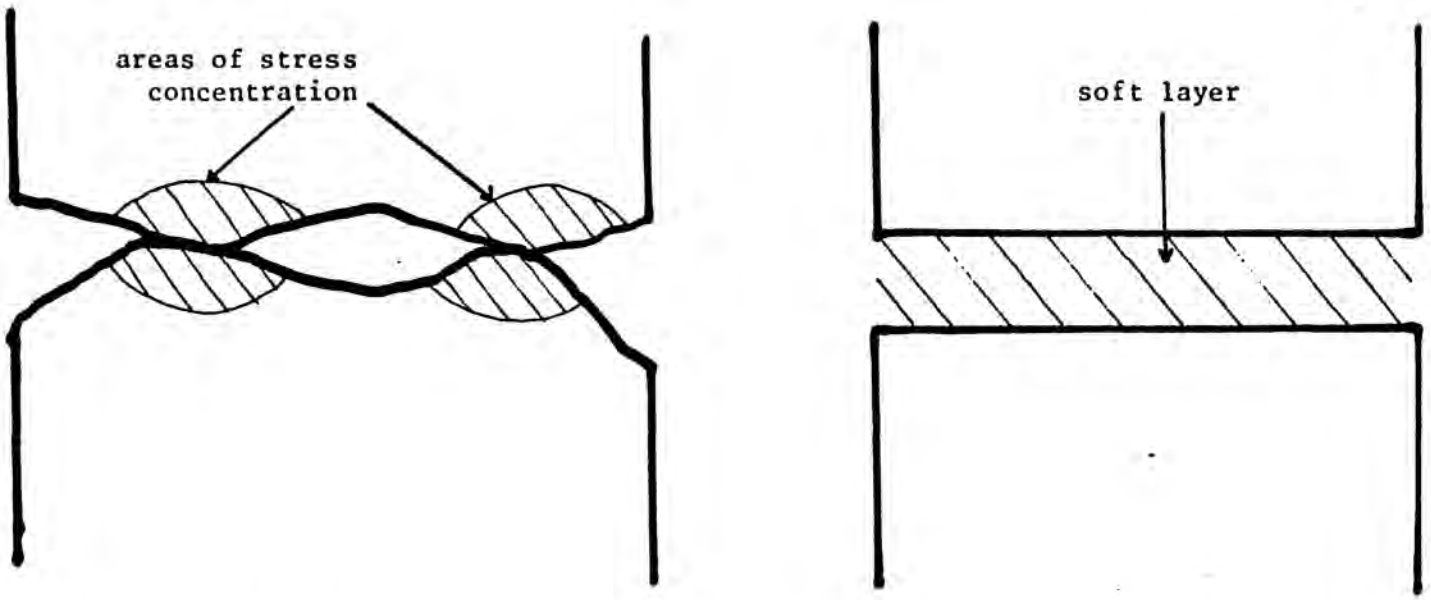



Figure 2.9: Normal and shear interactions for static relaxation model.

The stiffnesses of actual discontinuities can be visualized by considering the contact between rough hard rock surfaces with no joint infilling, as depicted in Figure 2.10. With purely elastic behaviour, the asperities are sites of stress concentration, and consequently will be associated with displacements which are large compared with those derived from the main body of the rock material. Hence, the joint can be considered as a relatively soft layer. Secondly, crushing and shearing of the asperities result in increased displacements with a consequent reduction in the effective stiffnesses. With increasing shear displacement there is increasing comminution, high spots tend to be worn away and the degree of interlocking is reduced. The consequent reduction in shear strength leads to a modified shear-displacement characteristic. Typical load-deformation characteristics for rock joints are shown in Figure 2.11.

Since the numerical algorithm is of an explicit nature whereby incremental displacements are calculated which are small compared with the corresponding cumulative displacements, it is a relatively simple procedure to model any realistic joint characteristic. This can be done by incrementing the joint stiffnesses in a piecewise linear fashion, with either the displacements or forces being used as the control, depending on the scale of the variables. Both linear and non-linear force-displacement characteristics have been successfully modelled for the normal direction while an elastic, perfectly plastic shear characteristic is common.

It should be noted that there are no special joint elements such as exist in certain finite element formulations where specific properties and behaviour are assigned to these elements (Goodman, 1976; Burman, 1972). Rather, the deformation properties of both the intact material and the joint are collectively




a) actual situation

b) schematic representation

Figure 2.10: The representation of interfaces between blocks.

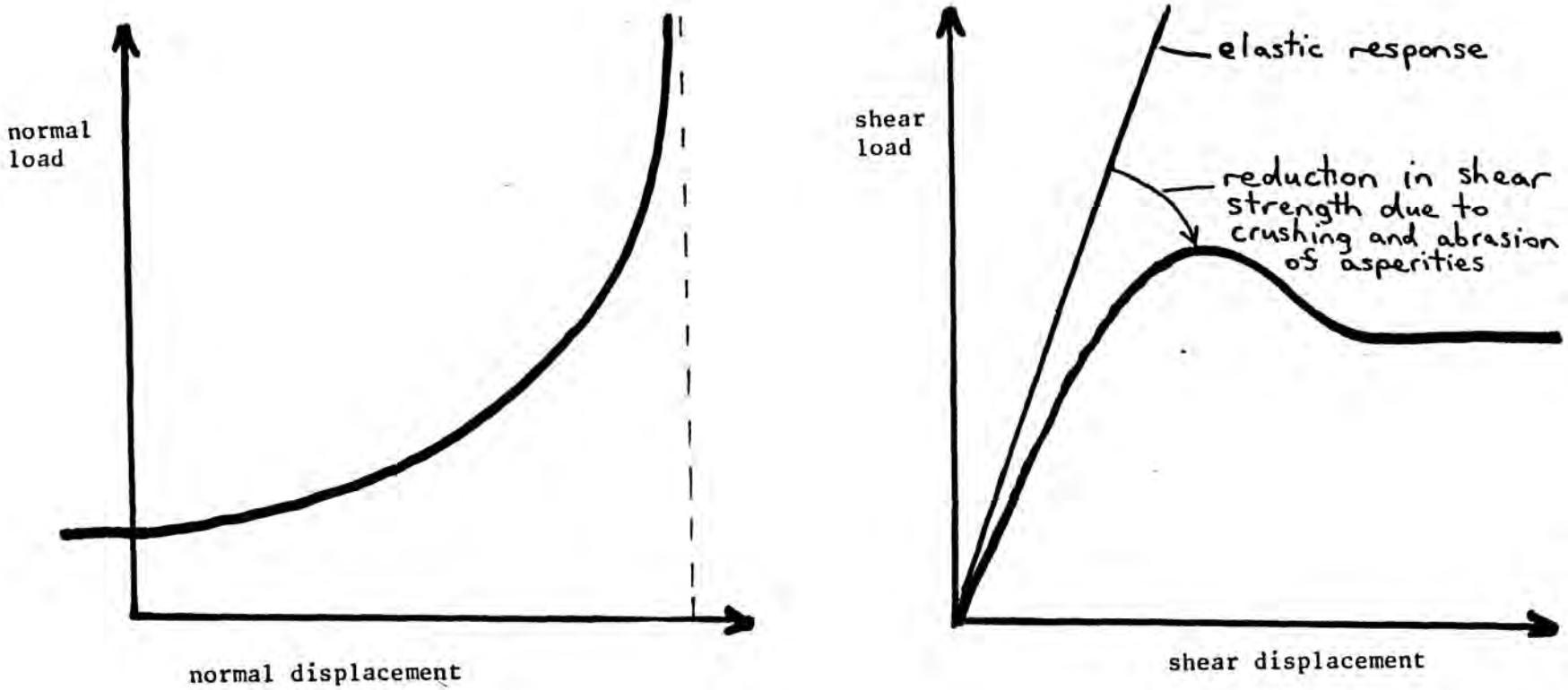



Figure 2.11: Realistic characteristics for rock joints.

considered at the block interfaces.

Thus, the rock mass model is again best suited for problems involving relatively heavily fractured rock where either hard rock, low confining pressures, large movements on discontinuities or some combination of these features is likely.

The solution is begun by applying some loading effect in turn to each of the initially unloaded rock blocks. During the first iteration, this loading effect arises from the self weight and any externally applied loading, while for subsequent iterations contact forces arising from the interaction between blocks must also be considered. Due to out-of-balance forces and moments acting on a particular member, the member will, when the appropriate constraints are relaxed, displace to a new position with three degrees of freedom; translation in the X and Y directions ($\Delta X$ and $\Delta Y$) and a rotational displacement ($\Delta\theta$). It is the method by which the members displace under the action of the out-of-balance forces and moments which, in effect, distinguishes static relaxation from alternative relaxation techniques. In the static relaxation method each member seeks a direct force-displacement path to an equilibrium position before being temporarily locked in this position until the next iteration. During each relaxation, the incremental X, Y and rotational rigid body displacements for a particular member are a function of the out-of-balance forces and moments acting on the member and the disposition of the member with respect to neighbouring members. By controlling the rate at which the loading is applied, the magnitude of the resulting displacements can be set to any desired level.

The method is illustrated with reference to the following example. Consider the rectangular rigid block

'a' in Figure 2.12 which is surrounded by four other rigid blocks giving rise to six corner-edge contacts, and hence six contact forces. These contact forces, calculated at the completion of each iteration, are incremental forces: that is, the relative incremental normal and shear displacements for a given contact point are evaluated from the centroidal displacements ($\Delta X$, $\Delta Y$, $\Delta\theta$) of the two blocks concerned. The incremental force components are then calculated and added to the forces already existing at the contact, as detailed in Section 2.3.2. Each surface of the block is then examined for the possibility of slip between it and the adjacent surface. If the conditions for slip are satisfied, the elastic response of the interface is over-ridden and the problem is analysed in terms of the forces determined from the slip criterion. Alternatively, if the incremental normal displacement indicates that the two blocks are no longer interacting, the forces for that contact are set to zero (no tensile strength).

Now, for a particular iteration N+1, say, assume that under the action of the resultant out-of-balance (residual) forces and moment existing after iteration N, the block centroid undergoes incremental translational and rotational rigid body displacements of magnitude $\Delta X^a$, $\Delta Y^a$ and $\Delta\theta^a$. This is illustrated in Figure 2.13.

Since the blocks are considered completely rigid, the incremental displacements of the block contact points can be defined in terms of the incremental displacements of the block centroid. Details of this transformation are given in Appendix I. Assuming small values for the rotation $\Delta\theta^a$, then, for each contact point i, the incremental global displacements due to incremental centroidal displacements of block 'a' ($\Delta X^a$, $\Delta Y^a$, $\Delta\theta^a$) are, to a first order approximation, given by

$$\Delta Y^a_i = \Delta Y^a + \Delta\theta^a (X_i - X_c^a)$$

and

$$\Delta X^a_i = \Delta X^a - \Delta\theta^a (Y_i - Y^a_c)$$

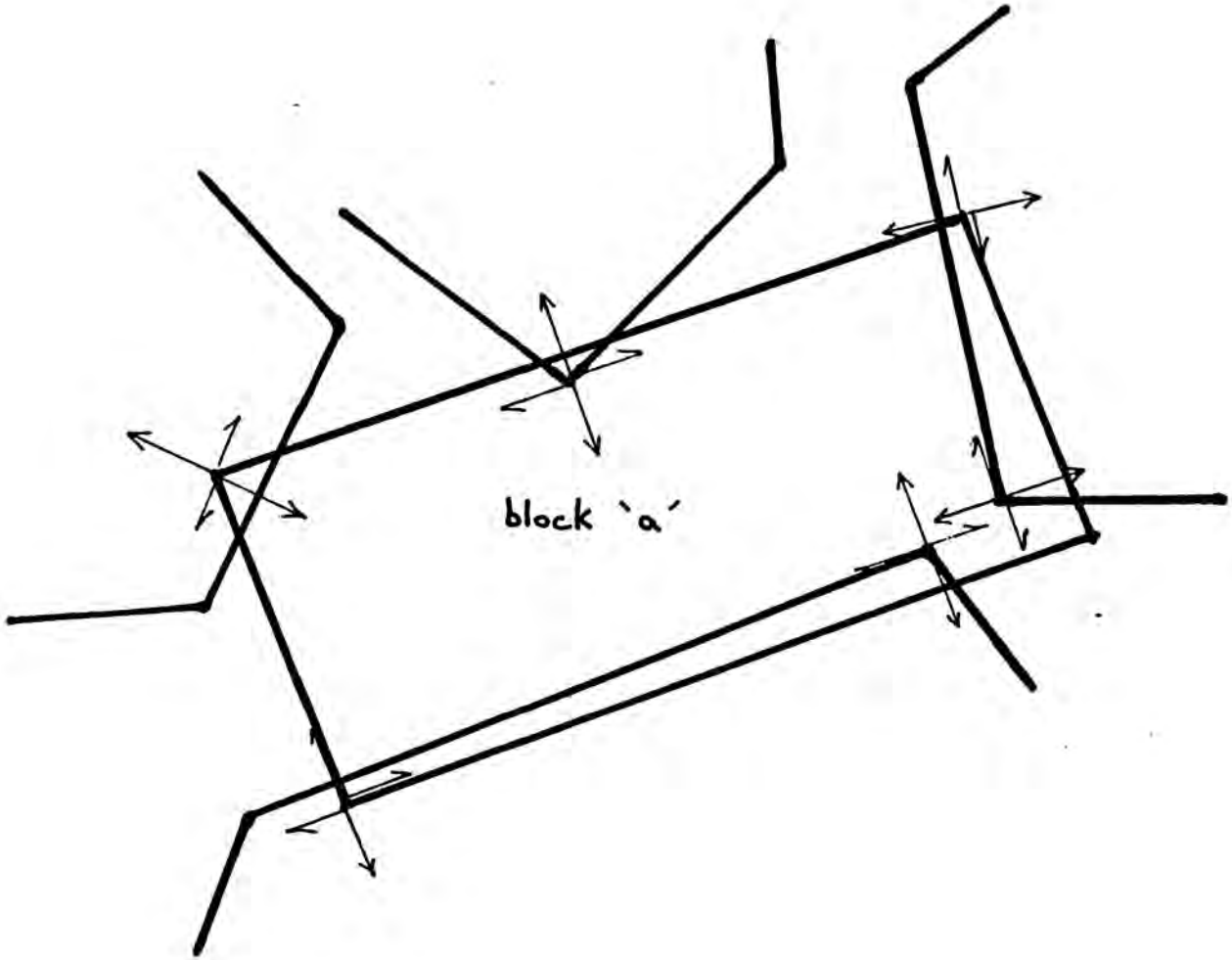



Figure 2.12: Contacts between block corners and edges

where

$X^a_c$, $Y^a_c$ are the global centroid co-ordinates of block 'a', and $X_i$, $Y_i$ are the global contact point co-ordinates.

The sign convention is as shown in Figure 2.13. Since all other surrounding blocks are temporarily fixed in position by their respective constraints, $\Delta X^a_i$ and $\Delta Y^a_i$ are the incremental displacements of block 'a' relative to the other block involved in the contact.

Incremental forces arising from these relative displacements can be evaluated by applying the force-displacement relationship for the edge component of the contact. Thus,

$$\begin{aligned}
\Delta FY^a_i &= KY_i * \Delta Y^a_i \\
&= KY_i * [\Delta Y^a + \Delta\theta^a (X_i - X^a_c)] \\
\Delta FX^a_i &= KX_i * \Delta X^a_i \\
&= KX_i * [\Delta X^a - \Delta\theta^a (Y_i - Y^a_c)]
\end{aligned}$$

where $KX_i$ and $KY_i$ are the global joint stiffnesses.

The above incremental global forces and displacements can be expressed as equivalent normal and shear components relative to the local block co-ordinates by using the relevant transformations (see Appendix II).

The solution procedure requires that for each relaxation the sum of these incremental forces ($\sum_i \Delta FX^a_i$, $\sum_i \Delta FY^a_i$) together with the residual forces acting satisfy the three equations of scalar equilibrium (force equilibrium in the X and Y directions and moment equilibrium about the centroid). Thus, for block 'a'

i) $$\sum_{i=1}^{6} FX^a_i + \sum_{i=1}^{6} \Delta FX^a_i + FX_{load} = 0$$

ii) $$\sum_{i=1}^{6} FY^a_i + \sum_{i=1}^{6} \Delta FY^a_i + W^a + FY_{load} = 0$$

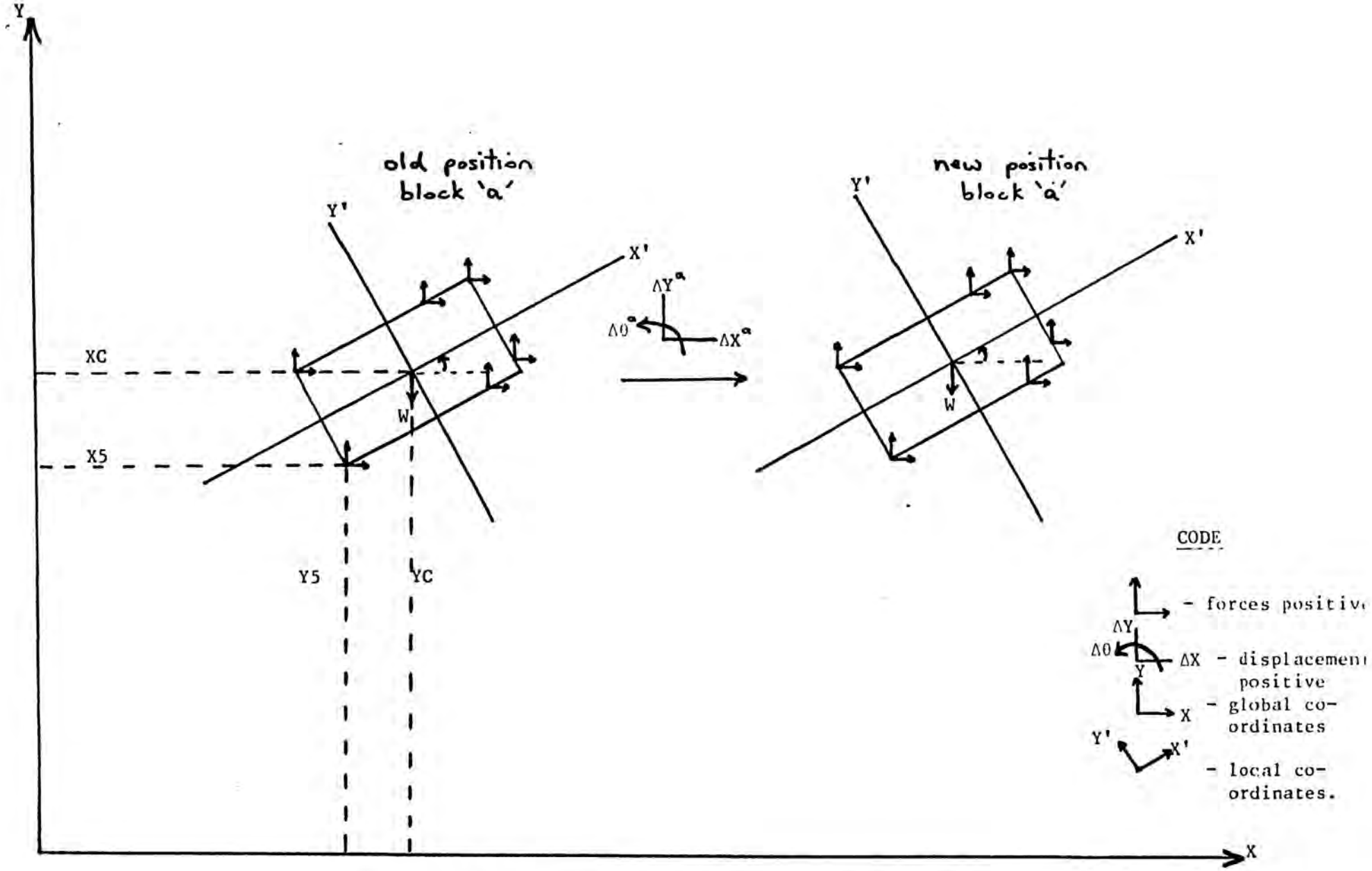



Figure 2.13: Block displacement to equilibrium position.

iii) $$\sum_{i=1}^{6} (FY^a_i + \Delta FY^a_i)(X_i - \Delta\theta^a (Y_i - Y^a_c) - X^a_c) - \sum_{i=1}^{6} (FX^a_i + \Delta FX^a_i)(Y_i + \Delta\theta^a (X_i - X^a_c) - Y^a_c) + M_{load} = 0$$

where

$\sum_i FX^a_i$, $\sum_i FY^a_i$ $FX_{load}$ $FY_{load}$, $M_{load}$, $W^a$, $X_i$, $X^a_c$, $Y_i$, $Y^a_c$ are all known; and

$FX^a_i$, $FY^a_i$ are the global contact forces for the ith contact after iteration N;

$\Delta FX^a_i$, $\Delta FY^a_i$ are the incremental global contact forces for the ith contact due to the block moving under the influence of residual forces during the $(N+1)^{th}$ iteration;

$W^a$ is the self weight of block 'a';

$FX_{load}$, $FY_{load}$, $M_{load}$ are the resultant global X, Y and moment external loads acting on the block after the Nth iteration.

These equations can be expressed in terms of the unknown displacements by the following simultaneous equations (see Appendix II):

$$a_{11}\,\Delta X^a + a_{12}\,\Delta Y^a + a_{13}\,\Delta\theta^a + XLOAD = 0$$
$$a_{21}\,\Delta X^a + a_{22}\,\Delta Y^a + a_{23}\,\Delta\theta^a + YLOAD = 0$$
$$a_{31}\,\Delta X^a + a_{32}\,\Delta Y^a + a_{33}\,\Delta\theta^a + MLOAD = 0$$

where

$$XLOAD = \sum_i FX^a_i + FX_{load}$$
$$YLOAD = \sum_i FY^a_i + W^a + FY_{load}$$
$$MLOAD = \sum_i FY^a_i\,(X_i - X^a_c) - \sum_i FX^a_i (Y_i - Y^a_c) + M_{load}$$

$\sum_i$ implies the summation over all contact points for block 'a'. Also, the matrix of coefficients is symmetric (i.e. $a_{ij} = a_{ji}$).

Hence, the solutions for $\Delta X^a$, $\Delta Y^a$ and $\Delta\theta^a$ can, in general, be obtained and the procedure repeated for all moveable blocks in the system. After all blocks

have been relaxed, the incremental forces due to the relative displacements of the blocks can be evaluated and added to the existing contact forces, and the residual forces updated in preparation for the next iteration. It is an inherent assumption in the solution procedure that incremental forces develop at all contact points during any particular iteration, regardless of whether the total force at a contact becomes tensile during that iteration. If necessary, the formation of new and deletion of obsolete contacts can be updated between iterations, together with any other relevant 'housekeeping'. Thus, a complete calculation cycle has been traced and all the necessary information to begin the next iteration (N+2) is available. The calculation procedure is shown for completeness in Figure 2.14.

The calculation is continued until the differences between incremental displacements determined from successive iterations fall below some pre-determined threshold or when the specified number of calculation cycles have been completed. Rates of convergence are discussed in the following chapters.

Thus, the method is suitable for the analysis of pseudo-static, dense assemblages of blocks. For problems in which dynamic effects are important, alternative methods, such as dynamic relaxation, should be employed.

### 2.4.2. Fortran Implementation:

It is worth discussing in brief detail some general points regarding the computer program with more detailed information, including a flow chart, user information and a listing provided in Appendix VII.

Although the 'static relaxation' solution algorithm presented in the previous section is a very simple procedure, the operations and routines necessary to allow for virtually unrestricted large scale displacements and

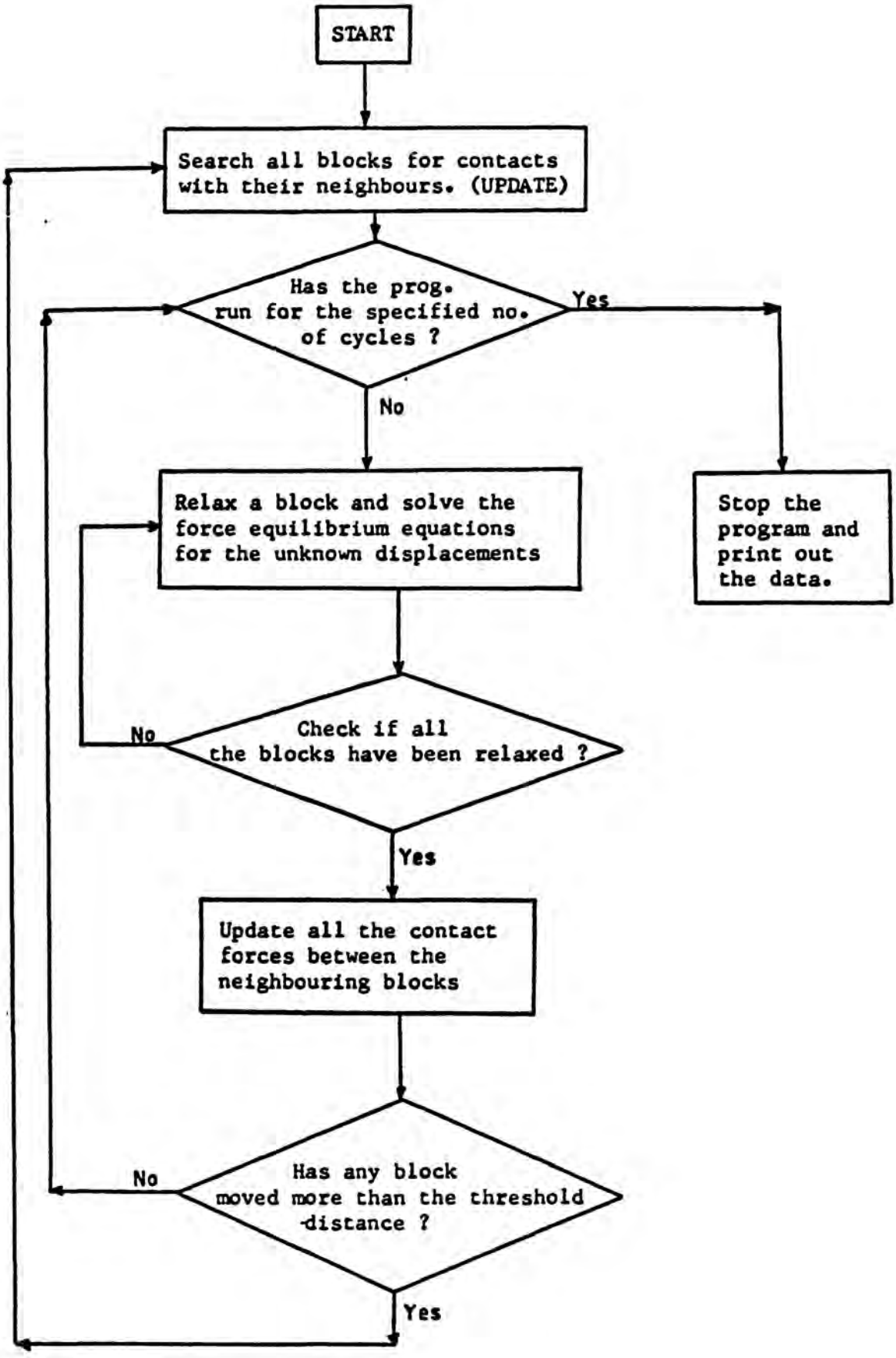



Figure 2.14: Static relaxation calculation procedure.

rotations of the system members result in a computer program of quite considerable size and complexity. The working version of the program for average sized problems required approximately 2000 Fortran statements, with an extended version developed for the analysis of large problems (discussed in Chapter 4) requiring some 200 additional statements. The terms 'average' and 'large' relate to the memory limits imposed by the particular computer and for the CDC 6600 machine used throughout this study, the maximum amount of information able to be held in core was limited to approximately 50 K words. This meant that for problems involving more than about 150 rectangular blocks it was necessary to use the extended version, although the actual memory required was largely a function of the particular geometry analysed. The program itself required approximately 20 K of core store to load. Memory requirements and allocation are fully discussed in Appendix VII..

At the time of writing the Fortran, a sophisticated Fortran version of a generalised dynamic relaxation program became available (Maini et. al., 1978). It was decided to make use of some of the novel techniques and housekeeping routines incorporated in this formulation since many of the operations entailed in both relaxation methods were more or less identical. Rather than attempt to describe the details of these features here, the reader is referred to Cundall (1974) for a full description. The efficient and economical concept of dynamic memory allocation utilizing linked lists for data storage arrays, developed by Cundall (1974), was one of the features incorporated in the static relaxation program. Other routines and ideas 'carried over' from the dynamic relaxation formulation are described in Appendix VII.

The program has been designed to make full use of the excellent graphics facilities available on the Imperial College computing system with visual output produced in

user specified intervals. This is a useful facility for enabling erroneous data to be easily detected and resulting behaviour to be comprehensively interpreted. All problems analysed produced plots of the system geometry, force distributions and block movements, this information being complemented by the relevant numerical printout. Hard copy could be made of the screen display, either via the Tektronix terminals available, or by microfilm. It should be stressed that the program has limited applicability where standard plotting facilities (e.g. Calcomp) are not available.

Input/output operations are relatively straightforward, the problem geometry being defined in card image format. A particular set of data is identified by the use of keywords on data cards. The model allows arbitrary shaped blocks to be modelled providing no block exceeds the maximum 50 allowable corners. There is no limit to the number of blocks interacting with any particular block, this being a function of the block sizes and shapes. After defining the problem geometry, the user can specify physical properties (e.g. joint stiffnesses, friction coefficient) and the appropriate boundary conditions. Different properties can be specified for different joints throughout the system, enabling anisotropy and other features such as faults to be modelled. All data are echoed on the line printer. The nature of the calculation cycle allows boundary conditions of both the force-controlled and displacement-controlled types to be modelled.

As the calculation proceeds, the user can remove blocks (to simulate excavation) and apply support loads. This is easily done by using the restart option which allows the problem to be stopped at any stage, the relevant information stored either on disk file or magnetic tape, and then later re-starting by reading the saved information back into core along with any modified

input parameters and commands. Also, the structure of the program is suitable for analysing coupled problems in which the solutions from an independent source (e.g. boundary element elastic stress analysis) can be utilized as input parameters before allowing for inelastic behaviour.

2.4.3. Problem Areas:

The solution algorithm described in Section 2.4.1. requires that each block in the system has a balanced distribution of contact points around its edges to ensure meaningful results and prevent numerical instabilities from occurring. This is tantamount to assuming some sort of mathematical good fit where the matrix containing the coefficients of the simultaneous equations does not become singular or very ill-conditioned. A singular matrix corresponds to the physical situation of one or less contacts occurring on a block or where all of the contacts are located along a single block edge.

The three simultaneous equations are solved using Gaussian elimination and in the equation solver tests for singularity or severe ill-conditioning are applied to avoid execution errors. If the equations are singular or ill-conditioned, an appropriate message is printed out in place of the solutions and execution is usually aborted. However, for analyses involving dense block assemblages (e.g. underground excavation simulations) such problems will be rarely encountered but care and familiarity with the program are necessary when relatively loosely-packed assemblages are modelled.

The above problem may be partially overcome either by allowing for a movement hysteresis between block contacts so that contacts are not suddenly broken or by introducing over-relaxation or 'fudge' factors in which the block movement is determined independently of the surrounding contact distribution. Moreover, in cir-

cumstances where the solution is intractable other factors such as compatibility with surrounding behaviour may possibly suggest values for the unknowns.

The other possible source of equation ill-conditioning concerns the relative magnitude of the contact stiffnesses on any block. In analyses where it is necessary to have widely varying joint stiffnesses (e.g. to simulate faults or very strong zones) it is possible for the equations to become very ill-conditioned since the matrix coefficients are directly proportional to the contact stiffness magnitudes (Appendix II). Again, this is highly improbable for blocks with a well-balanced distribution of contact points but could cause difficulties in unconfined situations.

Parameters governing the updating of interblock contacts are specified during data input and must be compatible with the geometry of the problem being analysed otherwise misuse of the program will result. Numerical instabilities are detected either when contact forces unrelated to the applied forces or body forces develop or when error messages are produced and unrealistic behaviour results.

# CHAPTER 3

# *VALIDATION AND EXTENSIONS OF THE STATIC RELAXATION METHOD*

# CHAPTER 3

# VALIDATION AND EXTENSIONS OF THE STATIC RELAXATION METHOD:

## 3.1. General Discussion:

Before the static relaxation method described in Section 2.4 could be applied to the analysis of general discontinuous problems, it was essential to compare the results produced from the numerical technique to existing solutions obtained from independent methods. Such comparisons instil confidence or otherwise in the subsequent use and validity of the method. These solutions for comparison with the developed numerical technique may be obtained by examining methods of analysis for jointed media from any of the following groups:

a) analytical methods
b) limiting equilibrium methods
c) numerical methods
d) physical modelling techniques
e) actual field measurements

The comparisons detailed in this chapter are concerned with results derived from methods associated with the first three groups. Subsequent chapters deal with comparisons between the numerical technique and solutions from the other groups. The solutions to jointed rock mass problems from either analytical methods (e.g. anisotropic elastic analyses) or approximate techniques of analysis such as limiting equilibrium usually involve approximations and simplifying assumptions as to the overall material representation and behaviour. However, it is important that the methods selected be capable of modelling the significant parameters incorporated in the static relaxation model.

As outlined by Voegele (1978) "the problem of verifying the accuracy of solutions calculated by numerical techniques designed for the analysis of discontinua is compounded by the lack of analytical solutions that describe the behaviour of a jointed rock mass". This usually means

that approximate methods must be chosen for comparison to determine whether acceptable results are being generated by the numerical technique. The static relaxation method is itself an approximate technique for calculating the response behaviour of a jointed rock mass. Hence, meaningful comparisons between it and other methods will only be forthcoming where the assumptions concerning the geometrical and physical properties and material behaviour for the methods involved are similar. Also, the results generated by the static relaxation method can only be considered as representative of actual rock mass behaviour if a mimimum of realistic assumptions regarding material behaviour have been made.

The following sections document some of the comparisons and validation runs that have been conducted with the static relaxation method to verify that the program performs satisfactorily. The following examples formed part of a sequence of rigorous tests of the program logic. During the course of these tests certain problem areas and program malfunctions were identified and the relevant modifications were included where necessary. Comparisons were made using not only analytical and limiting equilibrium methods but also using results from numerical techniques specifically developed for the analysis of jointed rock masses. The idealised geometries and simple properties relating to many of the following examples should not be considered as limitations imposed by the static relaxation method. Rather, such configurations were convenient for the generation of results from the approximate techniques providing the comparisons.

## 3.2. Validation Tests:

### 3.2.1. Sixteen Rectangular Block Test:

The object of this test was to show the path independency of the static relaxation program. Sixteen rectangular blocks of aspect ratio 2 : 1 were consolidated

under self weight and external loading with a friction coefficient of 0.36 ($\phi$ = 20 degrees). Figure 3.1 shows the corner forces developed from a 'forwards' relaxation path, each iteration beginning with the bottom, left-hand corner block. Figure 3.2 shows the force distribution and magnitudes developed for the identical problem but with the relaxation path having been reversed starting from the top, right-hand corner block. Examination of the force and displacement plots together with the numerical printout after 50 calculation cycles reveals that the solutions for both cases are identical, even though slip has taken place.

3.2.2. Continuum Validation:

One part of the validation of the rigid block model is to test its elastic response. The most convenient way of doing this is to design the model so that it represents an elastic continuum, since solutions exist for a wide range of elastic continuum problems. In the limit of very high joint stiffnesses, an assemblage of blocks should be a representation of a continuum. Appendix III indicates the way in which the model stiffnesses should be chosen so that this simulation is achieved. The block geometry shown in Figure 3.3 was selected to represent an elastic continuum by incorporating the appropriate normal and shear stiffnesses. The blocks were assumed to be of unit thickness. The model was tested under self weight and the edges of boundary blocks were subjected to confining compressive forces.

The closed form solution was obtained by application of the standard Kirsch equations to determine the stresses and displacements at 25 specific points in an infinite plate containing a circular hole of unit radius and subjected to a hydrostatic stress field of unit magnitude. Plane strain conditions were assumed and the elastic modulus of the plate was 1000 units with a Poisson's ratio of zero. The grid points at which the stresses and displacements were evaluated formed the corners of the 16 rectangular blocks.

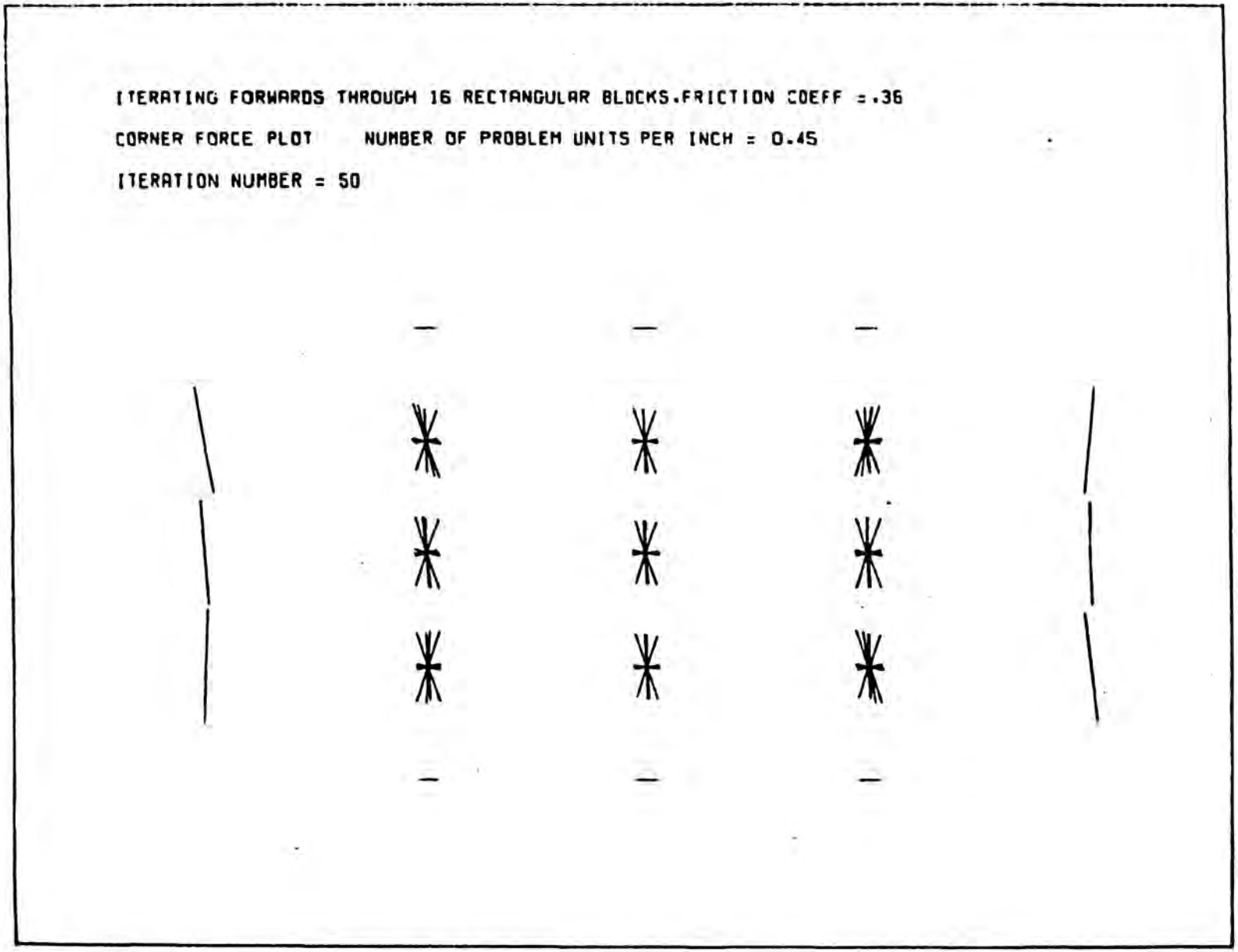



Figure 3.1: A 'forwards' relaxation path

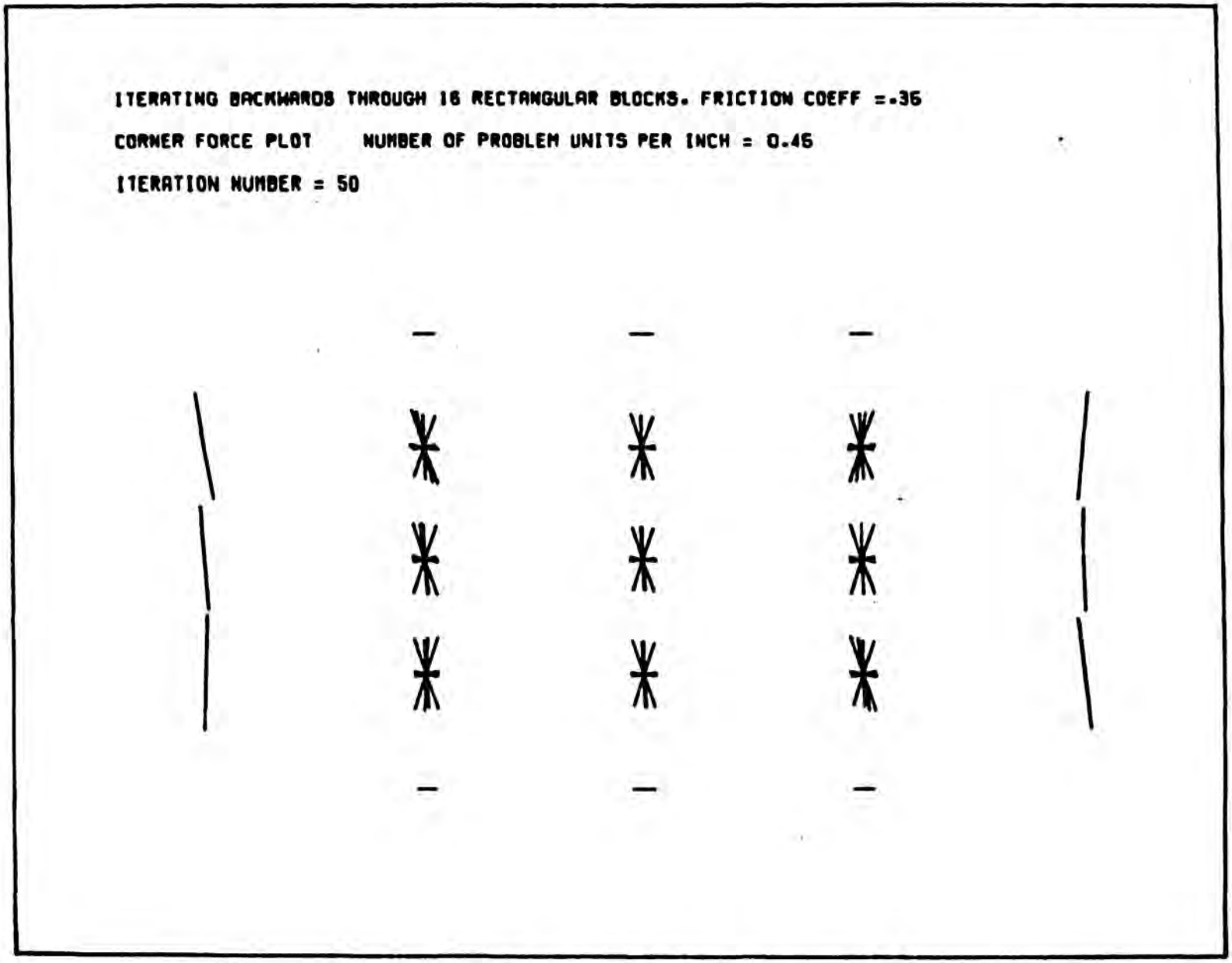



Figure 3.2: A 'backwards' relaxation path.

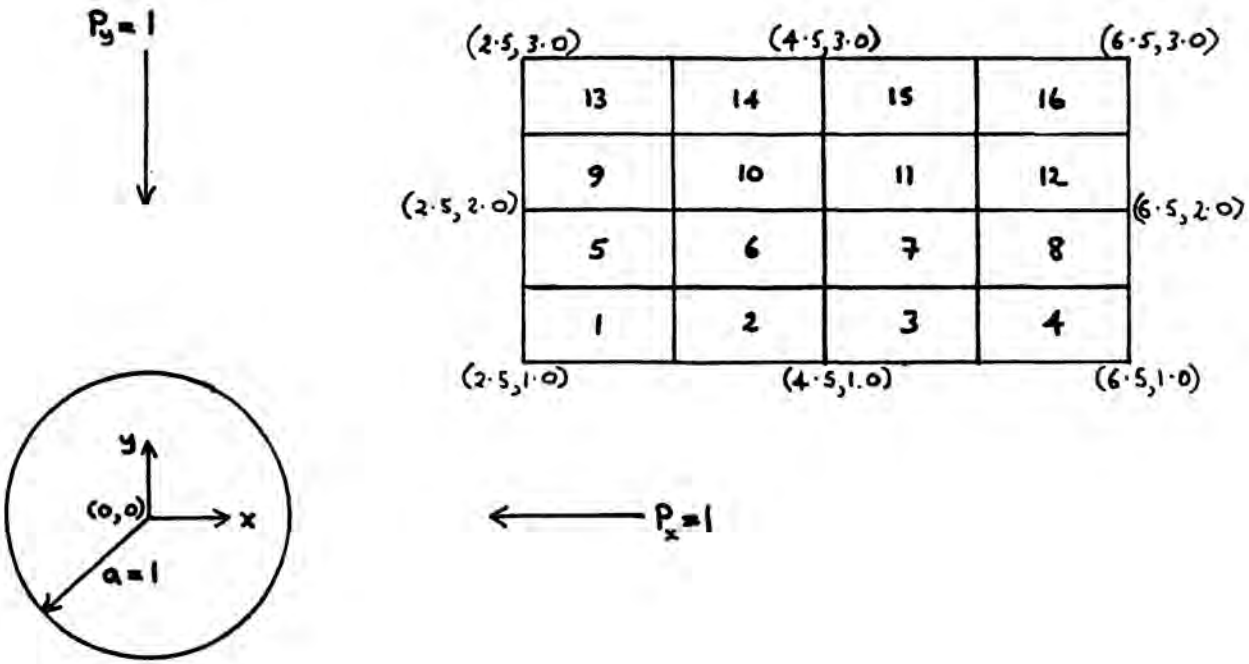



Figure 3.3: Block geometry for elastic continuum validation

The stresses at the grid boundary points were integrated to give statically equivalent forces acting at the points and these forces were used as input to the numerical model. The grid point nearest to the circular hole was a distance of 2.7 radii from the hole centre, which gave a maximum variation in the boundary forces of about 11%.

The forces generated by the static relaxation method for interior grid points are compared with those derived from the Kirsch equations in Table 3.1. The maximum deviation between the analytical and numerically predicted normal forces is less than 1%, which indicates that the agreement between the two sets of results is satisfactory.

Larger errors (up to 15%) are encountered when the shear forces are compared. However, these errors have little meaning and should be calculated on the basis of the magnitude of the largest forces acting since a normal force acting at a point affects the shear force on a plane removed from the point.

Table 3.2 compares the results of closed form and static relaxation solutions for displacements of grid points relative to the grid point nearest the hole. Again, there is satisfactory agreement between the two sets of results.

A similar problem to that above was analysed but with all 25 stress determination points much closer to the hole, as shown in Figure 3.4. The grid point nearest to the hole was now a distance of 1.12 radii from the hole centre, which generated a maximum variation in the boundary forces of approximately 60%. Table 3.3 compares the results of closed form and static relaxation solutions for normal and shear forces at interior grid points for this case. The maximum deviation between the closed form and static relaxation normal forces is about 28%. This occurs at grid point (2.0, 0.5) which is adjacent to the grid point nearest the boundary of the hole. For all other grid points

Table 3.1: Comparison of forces calculated using static relaxation method and closed form solution, around circular hole in an infinite plate.

| | NORMAL FORCES | | SHEAR FORCES | |
|---|---|---|---|---|
| block number | C.F.S.[1] | S.R.[2] | C.F.S. | S.R. |
| 1 | .2353 | .2324 | .0108 | .0107 |
| | .2367 | .2348 | .0116 | .0119 |
| | .5252 | .5261 | .0340 | .0370 |
| | .5263 | .5296 | .0430 | .0502 |
| 6 | .2394 | .2392 | .0128 | .0130 |
| | .5220 | .5218 | .0212 | .0193 |
| | .5200 | .5209 | .0173 | .0193 |
| | .2417 | .2415 | .0071 | .0072 |
| | .2423 | .2416 | .0074 | .0072 |
| | .5145 | .5160 | .0192 | .0210 |
| | .5150 | .5158 | .0228 | .0210 |
| | .2408 | .2398 | .0130 | .0130 |
| 11 | .2437 | .2437 | .0078 | .0078 |
| | .5130 | .5139 | .0135 | .0125 |
| | .5120 | .5138 | .0115 | .0125 |
| | .2448 | .2448 | .0049 | .0046 |
| | .2452 | .2446 | .0051 | .0046 |
| | .5093 | .5116 | .0123 | .0133 |
| | .5097 | .5114 | .0142 | .0133 |
| | .2443 | .2438 | .0079 | .0078 |
| 16 | .2458 | .2459 | .0053 | .0049 |
| | .5085 | .5105 | .0093 | .0083 |
| | .5080 | .5099 | .0082 | .0075 |
| | .2462 | .2461 | .0053 | .0049 |

1. Closed Form Solution
2. Static Relaxation Method

Table 3.2: Comparison of displacements calculated using static relaxation method and closed form solution, around circular hole in an infinite plate. Displacements are in x-direction, relative to point x = 2.5, y = 1.0. (E = 1000, $\nu$ = 0)

| point | | C.F.S. | S.R. |
|---|---|---|---|
| x | y | | |
| 3.5 | 1.0 | -9.1900 E-04 | -9.1765 E-04 |
| 4.5 | 1.0 | -1.8668 E-03 | -1.8579 E-03 |
| 5.5 | 1.0 | -2.8310 E-03 | -2.8196 E-03 |
| 6.5 | 1.0 | -3.8050 E-03 | -3.7939 E-03 |
| 2.5 | 2.0 | 1.0100 E-04 | 1.4711 E-04 |
| 3.5 | 2.0 | -8.7000 E-04 | -8.2460 E-04 |
| 4.5 | 2.0 | -1.8410 E-03 | -1.7931 E-03 |
| 5.5 | 2.0 | -2.8150 E-03 | -2.7667 E-03 |
| 6.5 | 2.0 | -3.7950 E-03 | -3.7462 E-03 |
| 2.5 | 3.0 | 1.8100 E-04 | 2.6825 E-04 |
| 3.5 | 3.0 | -8.2000 E-04 | -7.3328 E-04 |
| 4.5 | 3.0 | -1.8050 E-03 | -1.7236 E-03 |
| 5.5 | 3.0 | -2.7950 E-03 | -2.7097 E-03 |
| 6.5 | 3.0 | -3.7820 E-03 | -3.6954 E-03 |

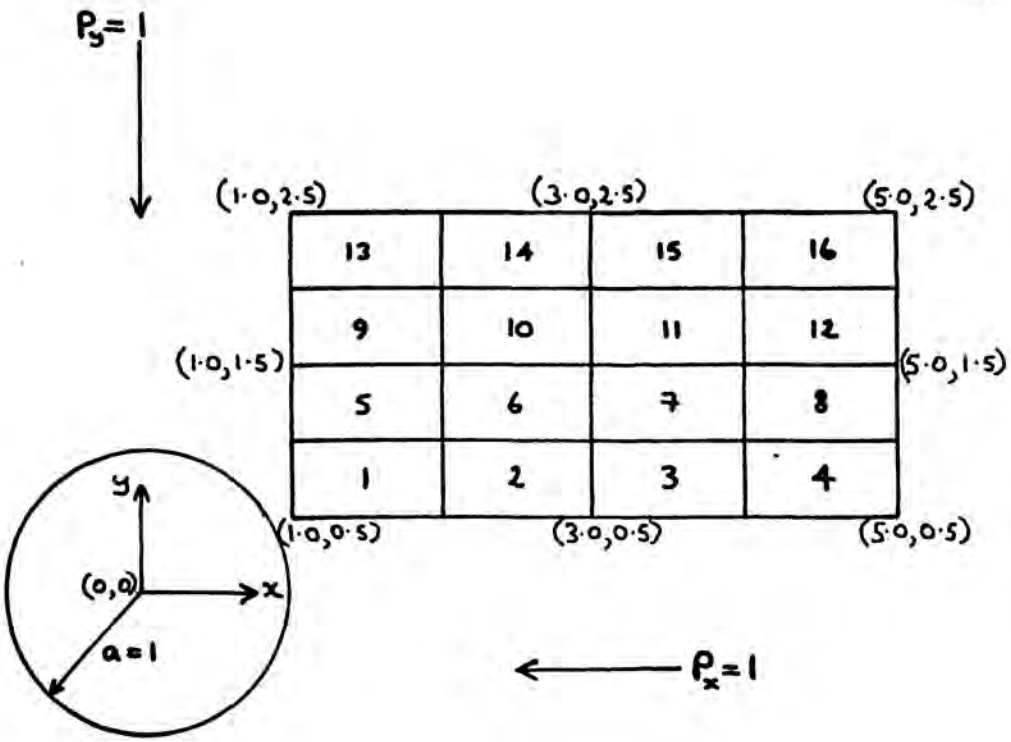



Figure 3.4: Modified block geometry for elastic continuum validation.

Table 3.3: Comparison of forces calculated using static relaxation method and closed form solution, around circular hole in infinite plate. Severe variation in boundary conditions.

| | NORMAL FORCES | | SHEAR FORCES | |
|---|---|---|---|---|
| block number | C.F.S.[1] | S.R.[2] | C.F.S. | S.R. |
| 1 | .2053 | .1486 | .0318 | .0353 |
| | .2126 | .1823 | .0359 | .0432 |
| | .5400 | .5482 | .1367 | .1610 |
| | .5200 | .5241 | .1933 | .2607 |
| 6 | .2263 | .2074 | .0395 | .0428 |
| | .5533 | .5498 | .0633 | .0608 |
| | .5467 | .5484 | .0467 | .0608 |
| | .2323 | .2169 | .0159 | .0211 |
| | .2345 | .2259 | .0168 | .0211 |
| | .5252 | .5256 | .0493 | .0604 |
| | .5238 | .5242 | .0632 | .0604 |
| | .2325 | .2243 | .0390 | .0428 |
| 11 | .2387 | .2324 | .0178 | .0213 |
| | .5245 | .5248 | .0297 | .0341 |
| | .5225 | .5249 | .0238 | .0341 |
| | .2407 | .2383 | .0093 | .0119 |
| | .2416 | .2402 | .0097 | .0119 |
| | .5150 | .5168 | .0252 | .0327 |
| | .5150 | .5174 | .0303 | .0327 |
| | .2406 | .2416 | .0178 | .0213 |
| 16 | .2433 | .2440 | .0100 | .0116 |
| | .5142 | .5181 | .0173 | .0174 |
| | .5133 | .5159 | .0147 | .0154 |
| | .2442 | .2468 | .0100 | .0114 |

1. Closed Form Solution

2. Static Relaxation Method

the deviations are less than half the maximum with a 3.8% error in the normal forces for the centre grid point.

The displacements for the case of a severe variation in the boundary conditions are compared in Table 3.4. The maximum deviations occur for relative displacements in the x-direction for points closest to the hole.

The effect of the block size on the magnitude of the forces was examined by analysing the initial case of fairly uniform boundary conditions with 32 square blocks. The maximum variations in the normal force magnitudes at the 25 original grid points were found to be less than 2%, which indicated the results were not significantly affected by the particular discretisation.

Table 3.4: Comparison of displacements calculated using static relaxation method and closed form solution, around circular hole in an infinite plate. Severe variation in boundary conditions. Displacements are in x-direction. ($E = 1$, $\nu = 0$)

| point | | relative to point | | C.F.S. | S.R. |
|---|---|---|---|---|---|
| x | y | x | y | | |
| 2.0 | 0.5 | 1.0 | 0.5 | 0.671 | 0.593 |
| 3.0 | 0.5 | " | " | 1.524 | 1.279 |
| 4.0 | 0.5 | " | " | 2.446 | 2.125 |
| 5.0 | 0.5 | " | " | 3.398 | 3.059 |
| 2.0 | 1.5 | 1.0 | 1.5 | 1.012 | 1.009 |
| 3.0 | 1.5 | " | " | 1.959 | 1.928 |
| 4.0 | 1.5 | " | " | 2.911 | 2.858 |
| 5.0 | 1.5 | " | " | 3.875 | 3.815 |
| 2.0 | 2.5 | 1.0 | 2.5 | 1.057 | 1.090 |
| 3.0 | 2.5 | " | " | 2.059 | 2.144 |
| 4.0 | 2.5 | " | " | 3.042 | 3.153 |
| 5.0 | 2.5 | " | " | 4.022 | 4.137 |

The numerical model was also checked for the problem of an infinite vertical line load on the surface of a semi-infinite medium. A configuration of nine square blocks was chosen, as shown in Figure 3.5. The closed form stresses were obtained from the integrated Boussinesq solution (Poulos and Davis, 1974). The stresses were integrated as before to obtain equivalent forces at the grid points. The geometry selected gave a maximum variation in the boundary forces in excess of 200%, the radial distance to the nearest point being 5.83 units. The magnitude of the infinite vertical line load was 100 units. All blocks were of unit thickness. Table 3.5 compares the results of closed form and static relaxation solutions for normal and shear forces at interior grid points. In contrast to the previous case, the maximum deviations occur between the theoretical and numerically predicted normal forces. The largest errors occur adjacent to the boundary having the maximum variation in boundary conditions, with average deviations being in the order of 5 to 7%.

Finally, continuum tests were performed for the cases of uniaxial (unconfined) compression and direct shear. For both cases, the continuum was modelled with nine square blocks and the generated displacements were in perfect agreement with the independent analytical solutions.

It should be noted that in all the above continuum simulations the contacts, once created, were locked in position. This avoided the necessity of continually varying the contact stiffness magnitude depending on the number and nature of the contacts. This seems a reasonable assumption since movements within the continuum system are likely to be at least a magnitude smaller than those encountered in its discontinuous counterpart. However, slip was still possible in the shear direction, providing the conditions for slip were satisfied.

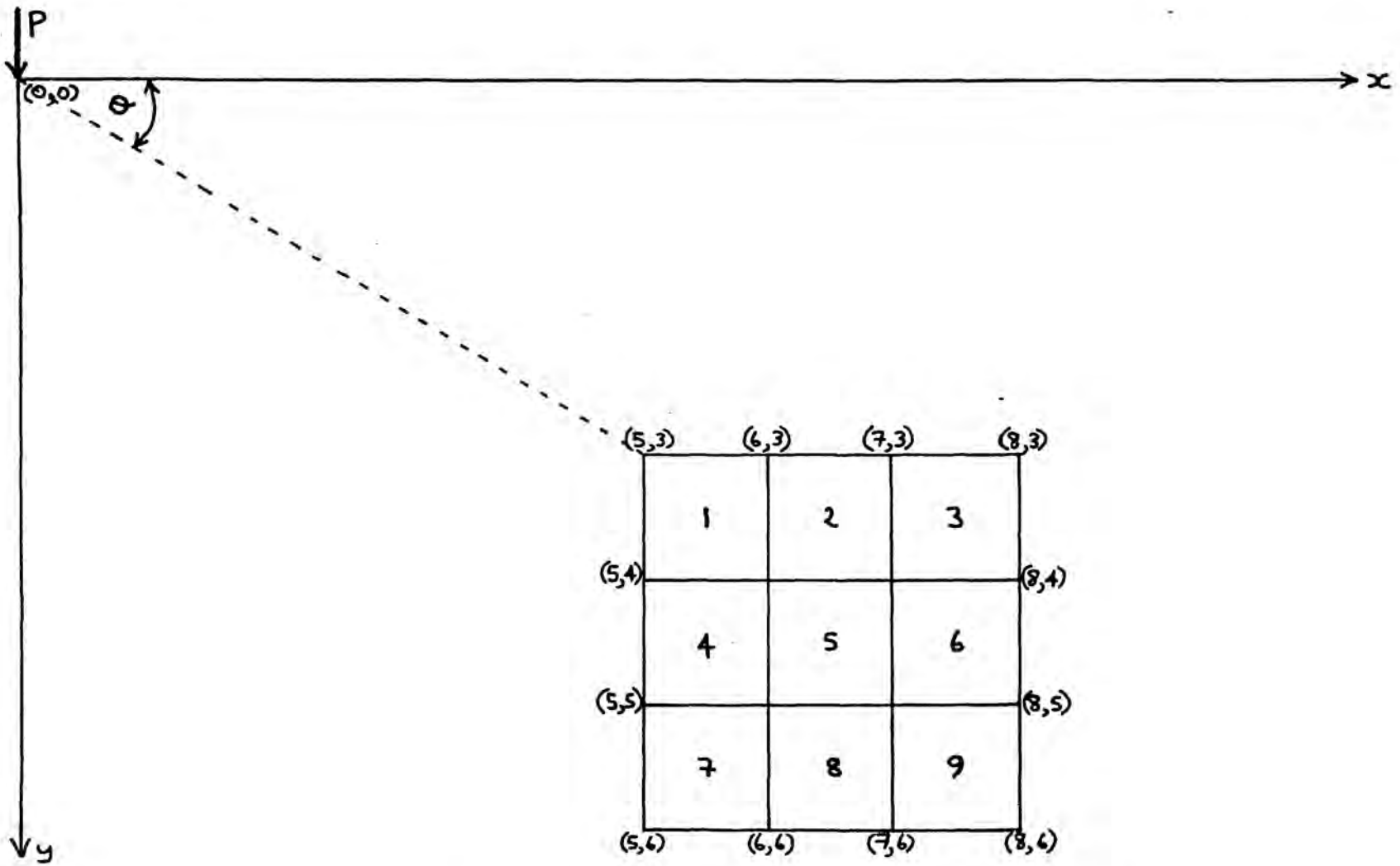



Figure 3.5: Normal line load on a semi-infinite medium.

Table 3.5: Comparison of forces calculated using static relaxation method and closed form solution, for infinite vertical line load in a semi-infinite mass.

| | NORMAL FORCES | | SHEAR FORCES | |
|---|---|---|---|---|
| block number | C.F.S.[1] | S.R.[2] | C.F.S. | S.R. |
| 1 | 1.3975 | 1.3540 | 1.3119 | 1.0790 |
| | 1.4686 | 1.3790 | 1.2975 | 1.2280 |
| | 1.2434 | 1.0470 | 1.3860 | 1.3920 |
| | 1.4175 | 1.4220 | 1.4888 | 1.4940 |
| 5 | 1.5916 | 1.6370 | 1.2321 | 1.1990 |
| | .9551 | 1.0760 | 1.1945 | 1.1340 |
| | .8408 | .7394 | 1.1059 | 1.1340 |
| | 1.4417 | 1.5040 | .9594 | .9308 |
| | 1.4592 | 1.3790 | .9016 | .9308 |
| | .5711 | .4754 | .9392 | .9919 |
| | .6630 | .8048 | 1.0347 | .9919 |
| | 1.6434 | 1.5480 | 1.1811 | 1.1990 |
| 9 | 1.4481 | 1.5840 | .7612 | .7995 |
| | .4276 | .6066 | .7747 | .7870 |
| | .3729 | .4146 | .7057 | .8102 |
| | 1.4195 | 1.4540 | .6787 | .8434 |

1. Closed Form Solution
2. Static Relaxation Method

### 3.2.3. Comparison with Dynamic Relaxation:

Several comparisons with the static relaxation method have been made in subsequent chapters using the dynamic relaxation rigid block program listed in Appendix VI (Maini et. al., 1978). Two comparisons are presented in this section. In the first, the block geometry shown in Figure 3.6 was modelled, the aims being to compare the final force magnitudes and to examine rates of convergence towards the final solution. The block system in Figure 3.6 was modelled under self weight until equilibrium was attained. The properties for the runs were as follows:

| | |
|---|---|
| contact stiffnesses | : $K_n$ = 1.0 E+08 |
| | $K_s$ = 0.0 |
| friction coefficient | : 0.01 |
| density | : $\rho$ = 2500.0 |
| applied gravity | : $g_y$ = -9.81 |
| moveable block height | : 2.5 |
| moveable block width | : 5.0 |
| damping (mass- and stiffness-proportional) | : 0.1 at frequency 300. |
| fraction of critical time-step | : 0.1 |
| number of moveable blocks | : 5 |

The results for this first example are presented in Table 3.6. The results show the rapid rate of convergence achieved with the static relaxation method, whereby all forces are within 0.2% of their final equilibrium values after 30 iterations. This is in contrast to dynamic relaxation (D.R.) where after 30 iterations the forces deviate by up to 23% from corresponding equilibrium values. Only after 100 iterations are the D.R. calculated forces within 0.2% of the final solution. A comparison of the equilibrium contact forces indicates that the maximum variation is approximately 1.5%.

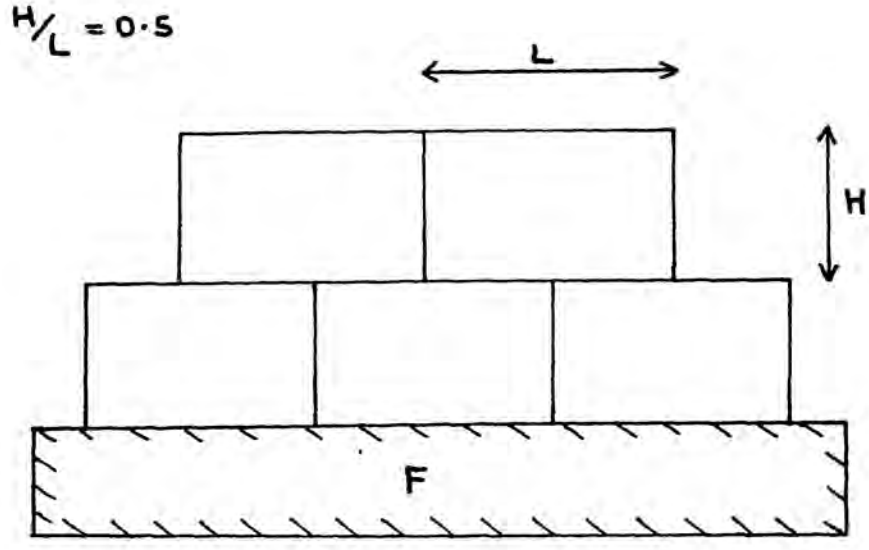



Figure 3.6: Block geometry for comparison with dynamic relaxation - first test.

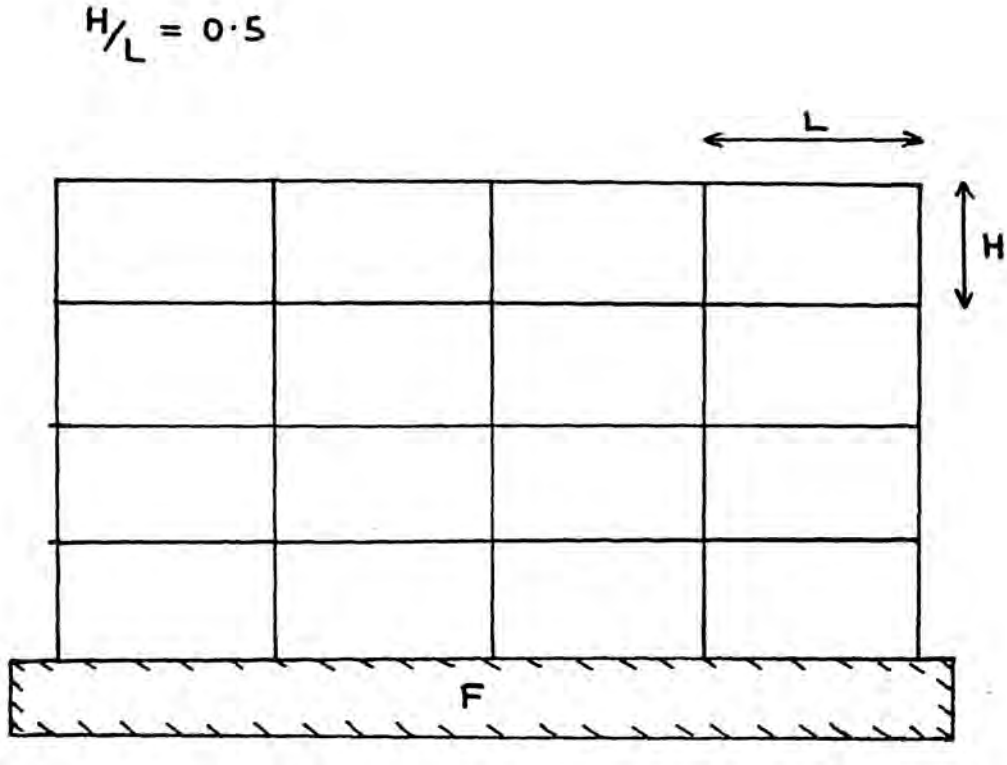



Figure 3.7: Block geometry for comparison with dynamic relaxation - second test

Table 3.6: Comparison of normal forces calculated using static relaxation and dynamic relaxation rigid block methods, for 5 rectangular blocks (2 : 1) sitting on fixed block.

| iteration number | S.R.[1] | | | D.R.[2] | | |
|---|---|---|---|---|---|---|
| | FORCE | | | FORCE | | |
| | A | B | C | A | B | C |
| 10 | 1.918 | 2.547 | .806 | | | |
| 20 | 1.968 | 2.914 | .871 | | | |
| 30 | 1.971 | 2.952 | .876 | 1.791 | 2.468 | .739 |
| 40 | 1.971 | 2.955 | .877 | | | |
| 50 | 1.971 | 2.956 | .877 | | | |
| 60 | | | | 1.949 | 2.882 | .849 |
| 90 | | | | 1.964 | 2.946 | .862 |
| 100 | 1.971 | 2.956 | .877 | 1.965 | 2.958 | .863 |

N.B. all forces * E + 05

1. Static Relaxation Method
2. Dynamic Relaxation Method

In the second test, the 16 rectangular block geometry shown in Figure 3.7 was examined with both relaxation techniques. External loading was applied to block edges located along the two vertical sides and along the top horizontal boundary. The applied loads were approximately 100 times the individual block weight. Table 3.7 presents a comparison between representative normal and tangential contact forces throughout the block system. The agreement between the two sets of results is reasonable considering the differences between the two relaxation methods. With the dynamic relaxation method, the applied forces were input at the block centroids whereas the loading was located at the corners of the boundary edges in the static relaxation model. Hence, block rotations and associated tangential forces could be expected to be generally higher in the S.R. model, as is shown in Table 3.7.

Table 3.7: Comparison of normal and tangential forces calculated using static and dynamic relaxation rigid block methods, for 16 rectangular blocks (2 : 1).

| block number | S.R.[1] FORCES | | D.R.[2] FORCES | |
|---|---|---|---|---|
| | normal | tangential | normal | tangential |
| 5 | 1.836 | 0.643 | 1.841 | 0.645 |
| 5 | 2.771 | 0.489 | 2.753 | 0.429 |
| 6 | 3.026 | 0.320 | 3.038 | 0.390 |
| 6 | 3.237 | 0.340 | 3.339 | 0.440 |
| 6 | 2.774 | 0.264 | 2.796 | 0.258 |
| 6 | 2.533 | 0.234 | 2.577 | 0.258 |
| 11 | 2.974 | 1.041 | 2.864 | 1.004 |
| 11 | 2.055 | 0.719 | 1.974 | 0.688 |
| 11 | 2.376 | 0.832 | 2.354 | 0.824 |
| 11 | 2.668 | 0.793 | 2.670 | 0.786 |
| 16 | 3.820 | 0.732 | 3.837 | 0.687 |
| 16 | 2.898 | 0.207 | 2.804 | 0.189 |

N.B. all forces * E + 04

1. Static Relaxation Method
2. Dynamic Relaxation Method

Further extensive comparisons between the static and dynamic relaxation methods have been made by Warner (1979), who compared results after block removal for problems involving approximately 100 blocks. In general, satisfactory agreement between the two techniques was obtained and a comparison of the efficiency between the two methods for one particular case is illustrated in Figure 3.8.

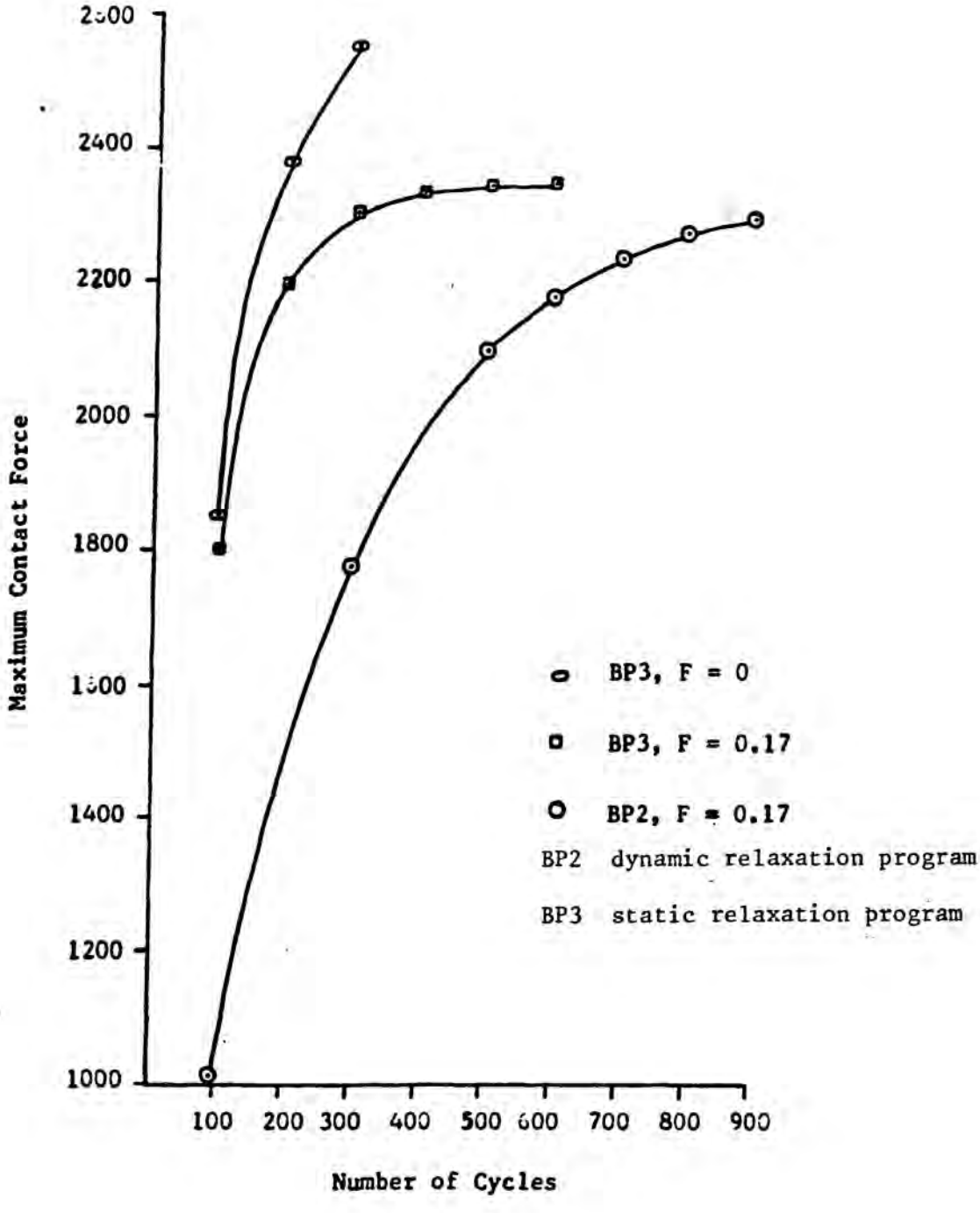



Figure 3.8: Comparison of rates of consolidation for 83 block model using different programs and angles of friction

### 3.2.4. Comparison with Deformable Block Program:

The block configuration shown in Figure 3.9 consisting of five square blocks sitting on top of a larger fixed block was used in this example. The problem was analysed using static relaxation and dynamic relaxation rigid block methods and a dynamic relaxation program which allowed for block deformability (Vargas, 1981). The following properties were modelled:

| | | |
|---|---|---|
| contact stiffnesses | : | $K_n$ = 1.0 E + 10 |
| | | $K_s$ = 1.0 E + 10 |
| friction coefficient | : | F = 2.0 |
| elastic modulus | : | E = 1.0 E + 10 |
| density | : | $\rho$ = 2500.0 |
| applied gravity | : | $g_y$ = -9.81 |
| moveable block height | : | H = 10 |
| moveable block width | : | W = 10 |
| damping (mass- and stiffness-proportional) | : | 0.1 at frequency 300. |
| fraction of critical time-step | : | 0.1 |
| number of moveable blocks | : | n = 5 |

Initially, a comparison was made between the static relaxation and deformable block methods by allowing the system to attain equilibrium under self weight only. The results for the normal forces obtained from these two methods are presented in Table 3.8. The maximum error between corresponding forces is less than 10% and the relative agreement between force magnitudes is satisfactory.

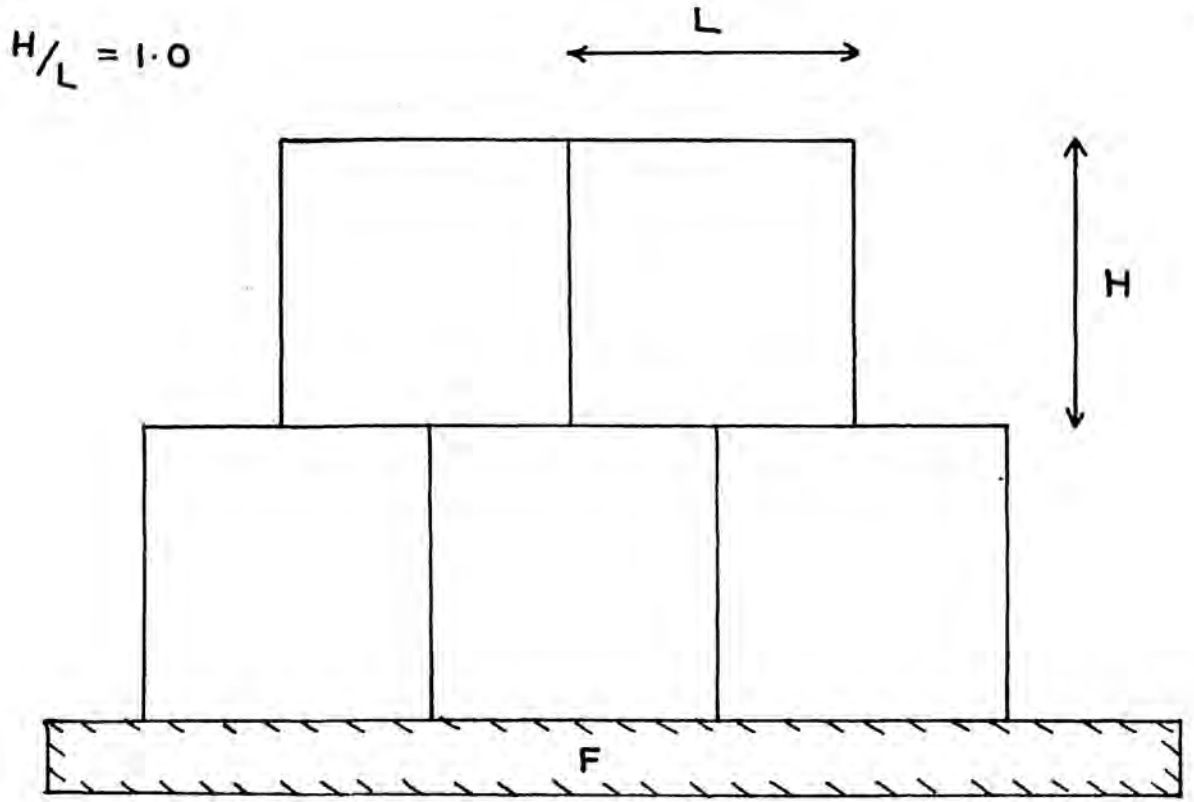



Figure 3.9: Block geometry for comparison with deformable block program.

Table 3.8: Comparison of normal forces calculated using static relaxation and deformable block methods, for 5 square blocks sitting on fixed block. Self weight only.

| STATIC RELAXATION FORCES (* E + 06) | DEFORMABLE BLOCK FORCES (*E + 06) | PERCENTAGE DEVIATION |
|---|---|---|
| 1.941 | 1.801 | 7.5 |
| 2.092 | 1.946 | 7.0 |
| 2.099 | 1.950 | 7.1 |
| 0.876 | 0.801 | 8.5 |
| 0.598 | 0.564 | 5.7 |
| 0.591 | 0.561 | 5.0 |
| 0.388 | 0.356 | 8.3 |

To examine the effect of increased loading on the force distribution, loads of magnitude 50 and 500 times the block weight were applied to the top two blocks. The results of increased loading for both the normal and tangential forces calculated by the various methods are presented in Tables 3.9 and 3.10. As expected, the ex-

Table 3.9: Comparison of normal and tangential forces calculated using static relaxation, dynamic relaxation and deformable block methods, for 5 square blocks sitting on fixed block. Loads of 50 times block weight applied to top blocks.

| STATIC RELAXATION FORCES (* E + 07) | | DYNAMIC RELAXATION FORCES (* E + 07) | | DEFORMABLE BLOCK FORCES (* E + 07) | |
|---|---|---|---|---|---|
| normal | tangential | normal | tangential | normal | tangential |
| 3.324 | 0.636 | 3.199 | 0.655 | 3.300 | 0.495 |
| 4.376 | 0.636 | 4.363 | 0.668 | 4.191 | 0.522 |
| 4.780 | 0.000 | 4.918 | 0.000 | 4.988 | 0.017 |
| 4.104 | 0.428 | 3.754 | 0.413 | 4.567 | 0.420 |
| 3.191 | 0.428 | 3.252 | 0.413 | 2.504 | 0.310 |

Table 3.10: Comparison of normal and tangential forces calculated using static relaxation and deformable block methods, for 5 square blocks sitting on fixed block. Loads of 500 times block weight applied to top blocks.

| STATIC RELAXATION FORCES (* E + 08) | | DEFORMABLE BLOCK FORCES (*E + 08) | |
|---|---|---|---|
| normal | tangential | normal | tangential |
| 3.325 | 0.636 | 3.293 | 0.499 |
| 4.376 | 0.636 | 4.199 | 0.525 |
| 4.779 | 0.000 | 4.988 | 0.014 |
| 4.107 | 0.428 | 4.581 | 0.391 |
| 3.190 | 0.428 | 2.493 | 0.307 |

ternally applied loading has caused larger deviations between the contact force magnitudes of the rigid block and deformable block methods. The maximum error encountered for the highest load case (Table 3.10) was approximately 22%, with errors of between 5% and 10% existing between the largest forces.

A comparison of the corner displacements obtained using the three methods for the case of external loads of 50 times the individual block weight is presented in Table 3.11. The agreement between the vertical displacements for both rigid block methods is to within 4% but, as expected, there is a large discrepancy between these displacements ($N_r$) and those calculated from the deformable block program ($N_d$). The ratio $N_r/N_d$ in some instances exceeds 4.0.

Table 3.11: Comparison of x and y displacements calculated using static relaxation, dynamic relaxation and deformable block methods, for 5 square blocks sitting on fixed block. Loads of 50 times block weight applied to top blocks.

| | block number | DISPLACEMENTS FROM | | |
|---|---|---|---|---|
| | | S.R.[1] | D.R.[2] | D.B.[3] |
| x - direction | 1 | - .4150 E-03 | - .4960 E-03 | - .8081 E-03 |
| | | .6360 E-03 | .6680 E-03 | .1378 E-02 |
| | | .6360 E-03 | .6680 E-03 | .6222 E-03 |
| | | - .4150 E-03 | - .4960 E-03 | - .6261 E-03 |
| | 2 | 0.0 | .500 E-09 | - .8706 E-04 |
| | | 0.0 | .120 E-07 | .3351 E-03 |
| | | 0.0 | .120 E-07 | - .3351 E-03 |
| | | 0.0 | .500 E-09 | .8706 E-04 |
| y - direction | 1 | - .3324 E-02 | - .3199 E-02 | - .8293 E-02 |
| | | - .3324 E-02 | - .3199 E-02 | - .1292 E-01 |
| | | - .4376 E-02 | - .4364 E-02 | - .1954 E-01 |
| | | - .4376 E-02 | - .4364 E-02 | - .9184 E-02 |
| | 2 | - .4780 E-02 | - .4919 E-02 | - .9981 E-02 |
| | | - .4780 E-02 | - .4919 E-02 | - .1996 E-01 |
| | | - .4780 E-02 | - .4919 E-02 | - .1996 E-01 |
| | | - .4780 E-02 | - .4919 E-02 | - .9981 E-02 |

1. Static Relaxation Method
2. Dynamic Relaxation Method
3. Deformable Block Method

3.2.5. Loading of a Jointed Foundation:

The network of equilateral triangular rigid blocks shown in Figure 3.10 formed the model for this test. In the model, all blocks were assumed to be of unit thickness. The objectives were to examine the mechanism of failure generated by the static relaxation method and to compare the magnitude of the collapse load to that obtained from limit theory.

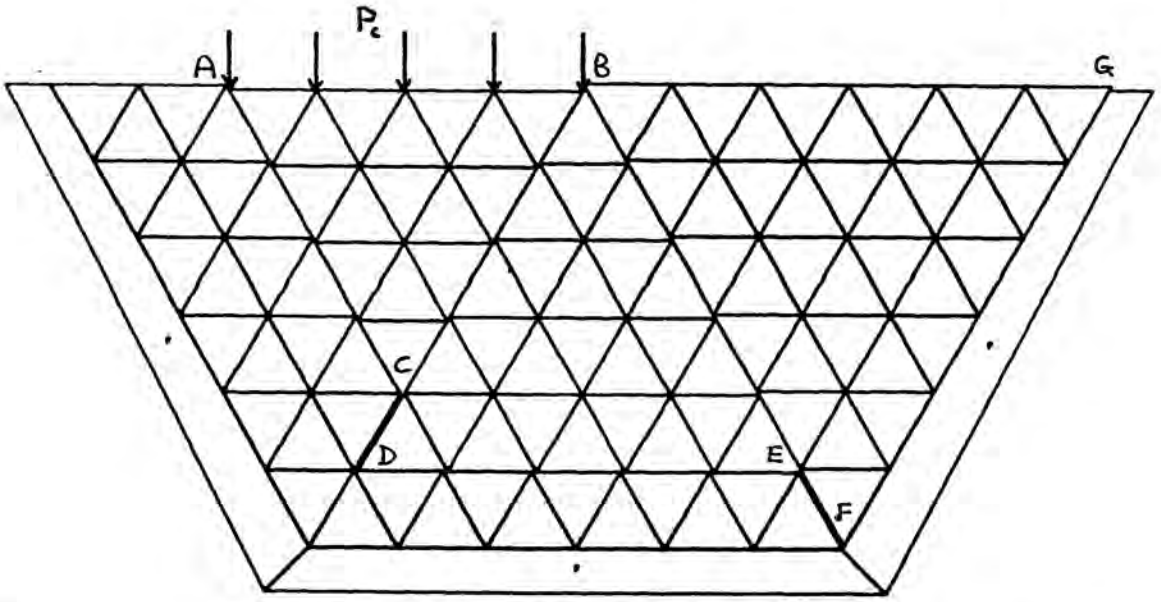
A strip loading of magnitude $P_c$ per unit area was applied to the faces of the four blocks indicated in Figure 3.10. Bray (1981) has determined the collapse load $P_c$ for the particular block configuration shown in Figure 3.10 using upper bound limit theory which produces a solution equivalent to a limiting equilibrium analysis. The limit theory analysis assumes the mode of failure for the three large triangular blocks to be that indicated in Figure 3.10 and an infinitesimal spacing of the blocks is also assumed. For the particular case of a friction coefficient of 0.364 ($\phi$ = 20 degrees), Bray found the collapse load to be 220.5 units, assuming values for the system parameters b, c and $\delta$ specified in Figure 3.10. The limit theory solution also assumes the shear strength of the discontinuities is $C + \sigma \tan \phi$, where C is the cohesion and $\phi$ the angle of friction.

The block geometry illustrated in Figure 3.10 was modelled using the static relaxation method for strip loads approximately ten percent greater and less than the theoretical collapse load, namely $P_c$ = 200.0 and $P_c$ = 250.0. The results for the case $P_c$ = 250.0 are shown in Figure 3.11, and the results show that the block system is unstable for this magnitude of loading since the shear strength along all of the boundaries has been exceeded. Similar block displacements were generated for the case $P_c$ = 200.0. However, the frictional resistance along the boundaries was not fully mobilised indicating the block

STRIP LOAD OF INTENSITY FY=-1ON APPLIED TO BLOCKS 90.92.94.96

BLOCK PLOT NUMBER OF PROBLEM UNITS PER INCH = 7.00

CYCLE NUMBER = 300 SCALE . 1 INCH = ____




Δr masses expected to slip : ACB
BDE
BFG

mode of failure assumed in limit theory solution

Contact stiffnesses :

Kn = 1.0 E+04

Ks = 1.0 E+04

γ = 9·81 E-03

c = 0·01

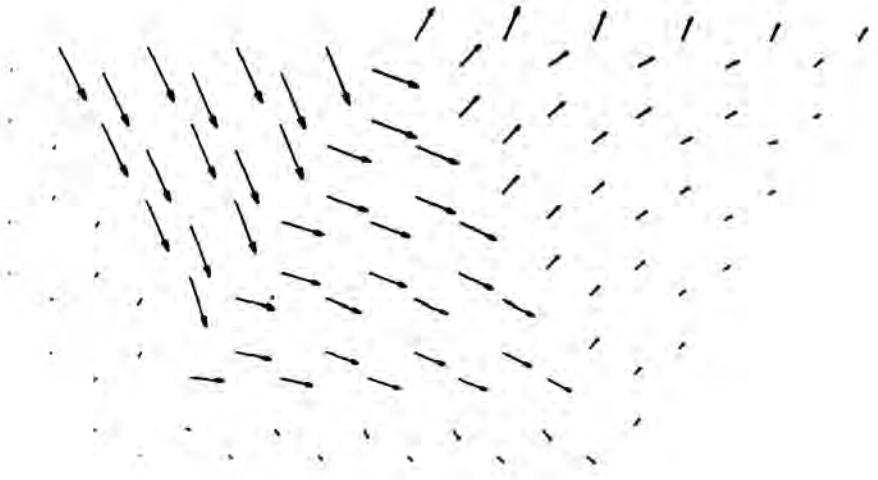
b = 40·0 for 1st block
= 50·0 for 2nd block
= 60·0 for 3rd block

Figure 3.10: Foundation of triangular blocks

STRIP LOAD OF INTENSITY -62.5 APPLIED TO BLOCKS 90,92,94,96

INCREM.DISPL.PLOT NUMBER OF PROBLEM UNITS PER INCH = 0.00001079

CYCLE NUMBER = 300 SCALE . 1 INCH = ____



STRIP LOAD OF INTENSITY -62.5 APPLIED TO BLOCKS 90,92,94,96

TOTAL DISPL.PLOT NUMBER OF PROBLEM UNITS PER INCH = 0.01303793

CYCLE NUMBER = 300 SCALE . 1 INCH = ____

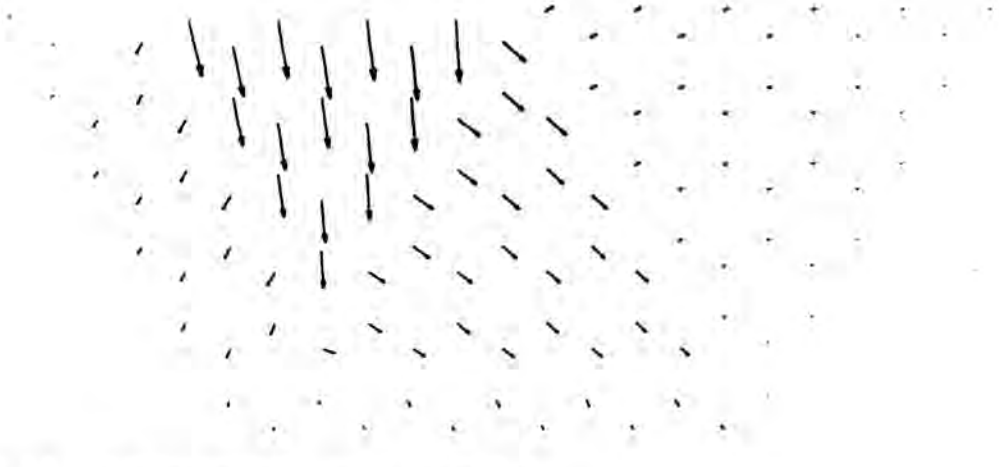


Figure 3.11: Strip loading of $P_c$ = 250.0

system was capable of sustaining further load.

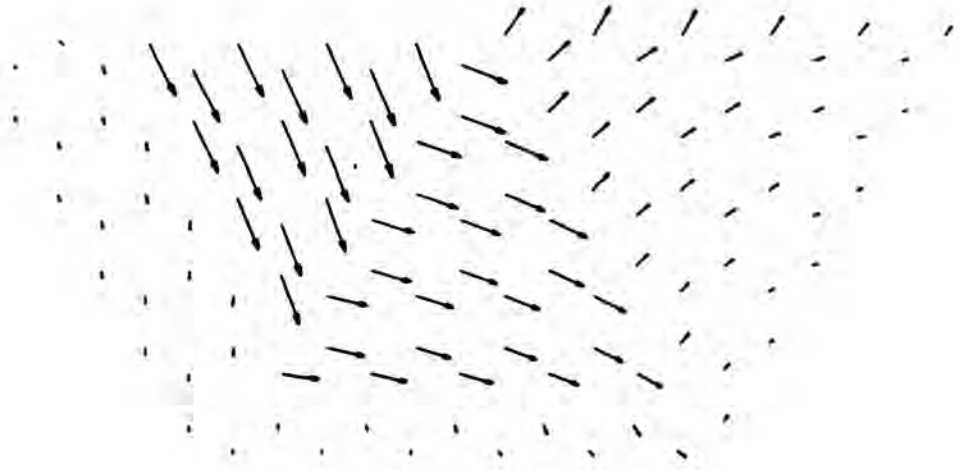
A similar procedure to that above was performed for a lower friction angle, namely tan $\phi$ = 0.05. The limit theory collapse load for this case is 17.6 units (Bray, 1981). Using the static relaxation method, strip loads of magnitude 20.0 and 15.0 were modelled. Again, the block system was found to be stable for the lower load and unstable for the high load. The results for $P_c$ = 20.0 are shown in Figure 3.12.

The slightly modified block geometry in which all joint sets are continuous (Figure 3.13) was also modelled. For a friction coefficient of 0.364 ($\phi$ = 20 degrees), the collapse load for similar loading and system properties to those before is 102.8 units (Bray, 1981). However, a failure mechanism similar to that shown in Figure 3.11 could not be generated for loads greater than the theoretical collapse load. The results for a loading approximately four times greater than the collapse load ($P_c$ = 400.0) are shown in Figure 3.13. It was concluded that in this case the system remained stable due to interlocking between rock blocks.

STRIP LOAD OF INTENSITY FY=- 5N APPLIED TO BLOCKS 90.92.94.96

INCREM.DISPL.PLOT NUMBER OF PROBLEM UNITS PER INCH = 0.00000325

CYCLE NUMBER = 300 SCALE . 1 INCH = _____



STRIP LOAD OF INTENSITY FY=- 5N APPLIED TO BLOCKS 90.92.94.96

TOTAL DISPL.PLOT NUMBER OF PROBLEM UNITS PER INCH = 0.00302500

CYCLE NUMBER = 300 SCALE . 1 INCH = _____

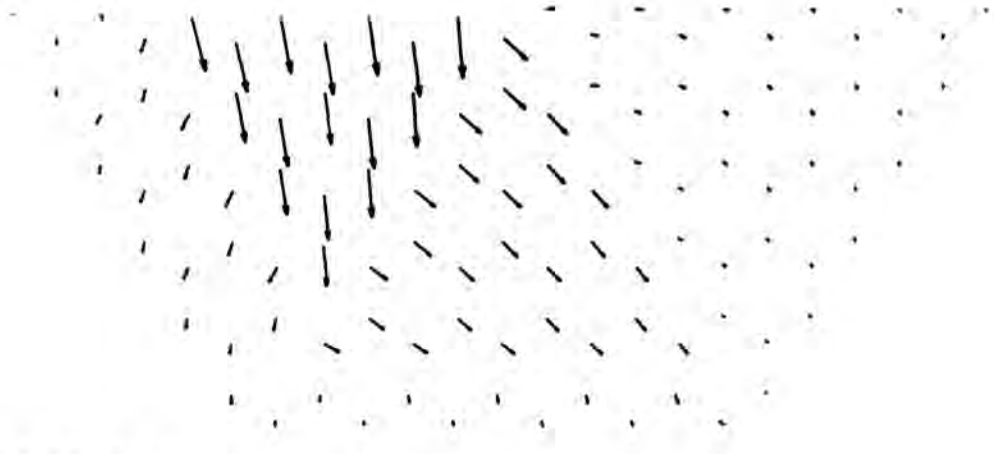
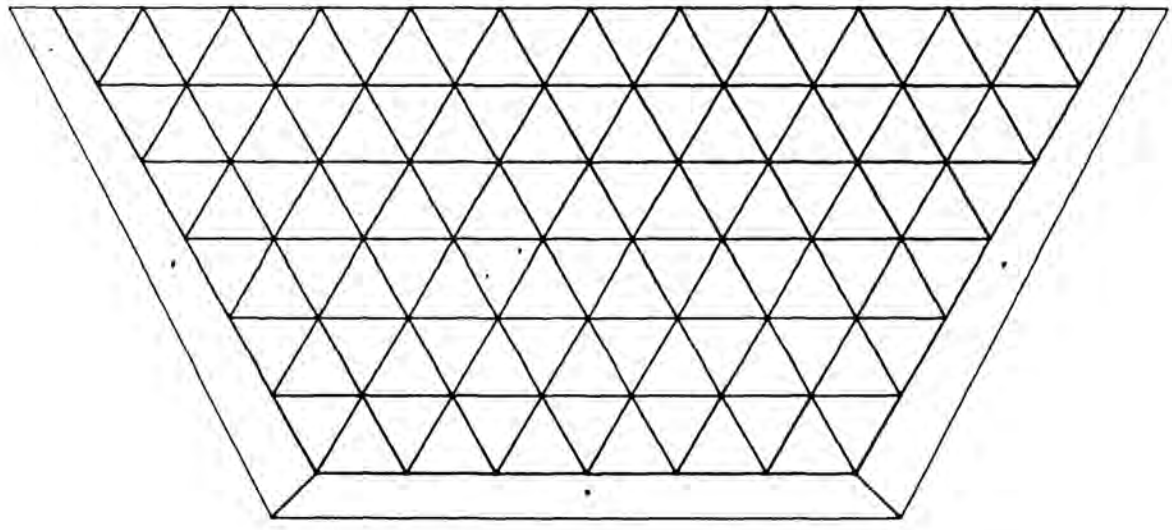


Figure 3.12: Strip loading of $P_c$ = 20.0

STRIP LOAD OF INTENSITY FY=-100N APPLIED TO BLOCKS 90,92,94,96

BLOCK PLOT NUMBER OF PROBLEM UNITS PER INCH = 7.00

CYCLE NUMBER = 1000 SCALE . 1 INCH = ____



STRIP LOAD OF INTENSITY FY=-100N APPLIED TO BLOCKS 90,92,94,96

CORNER FORCE PLOT NUMBER OF PROBLEM UNITS PER INCH = 28.21299622

CYCLE NUMBER = 1000 SCALE . 1 INCH = ____

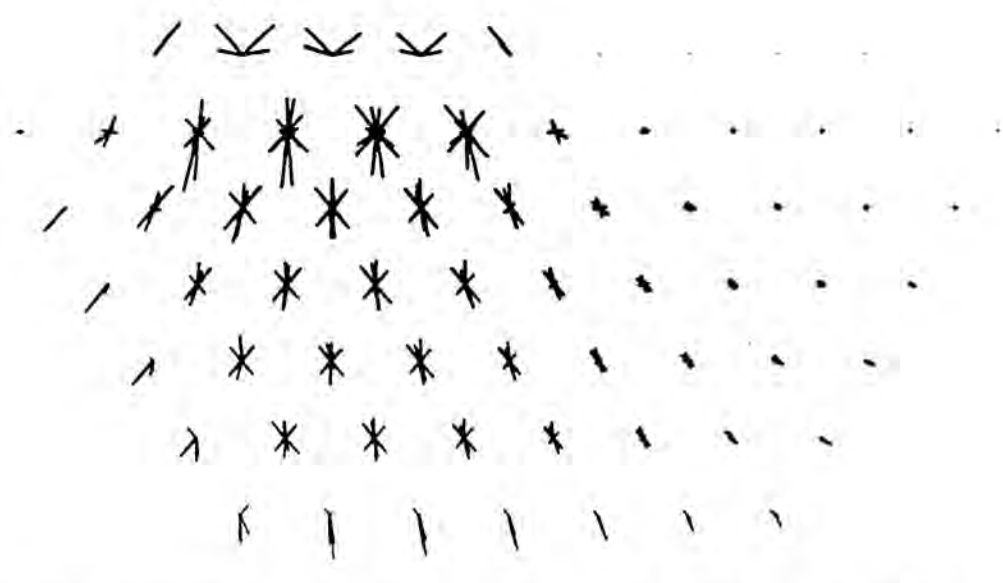
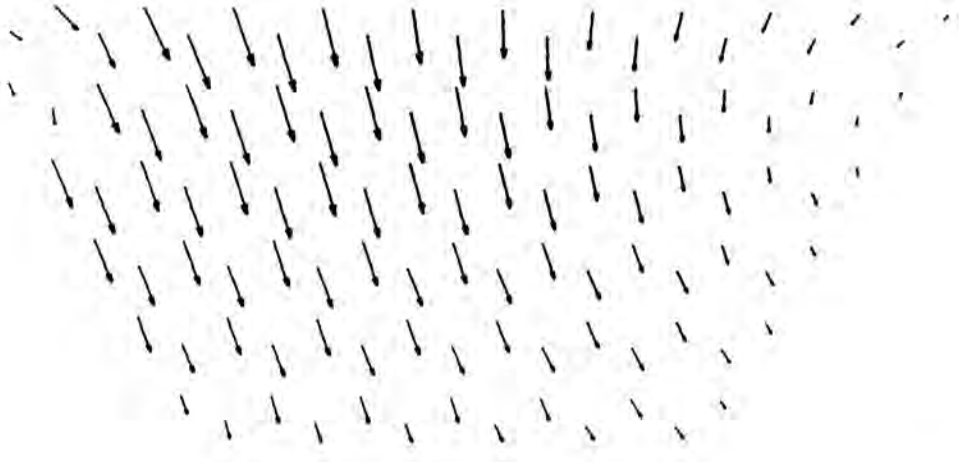


Figure 3.13: Modified block geometry for foundation problem - $P_c$ = 400.0

STRIP LOAD OF INTENSITY FY=-100N APPLIED TO BLOCKS 90.92.94.96

INCREM.DISPL.PLOT NUMBER OF PROBLEM UNITS PER INCH = 0.00000007

CYCLE NUMBER = 1000 SCALE . 1 INCH = _____



STRIP LOAD OF INTENSITY FY=-100N APPLIED TO BLOCKS 90.92.94.96

TOTAL DISPL.PLOT NUMBER OF PROBLEM UNITS PER INCH = 0.00876715

CYCLE NUMBER = 1000 SCALE . 1 INCH = _____

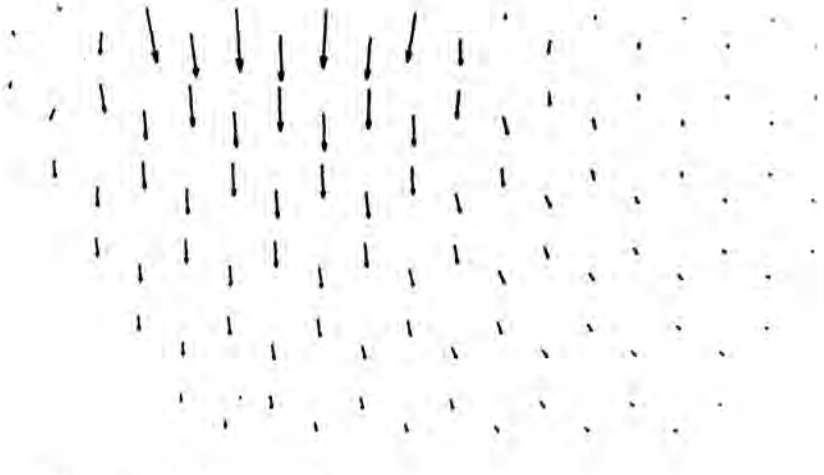


Figure 3.13 contd.

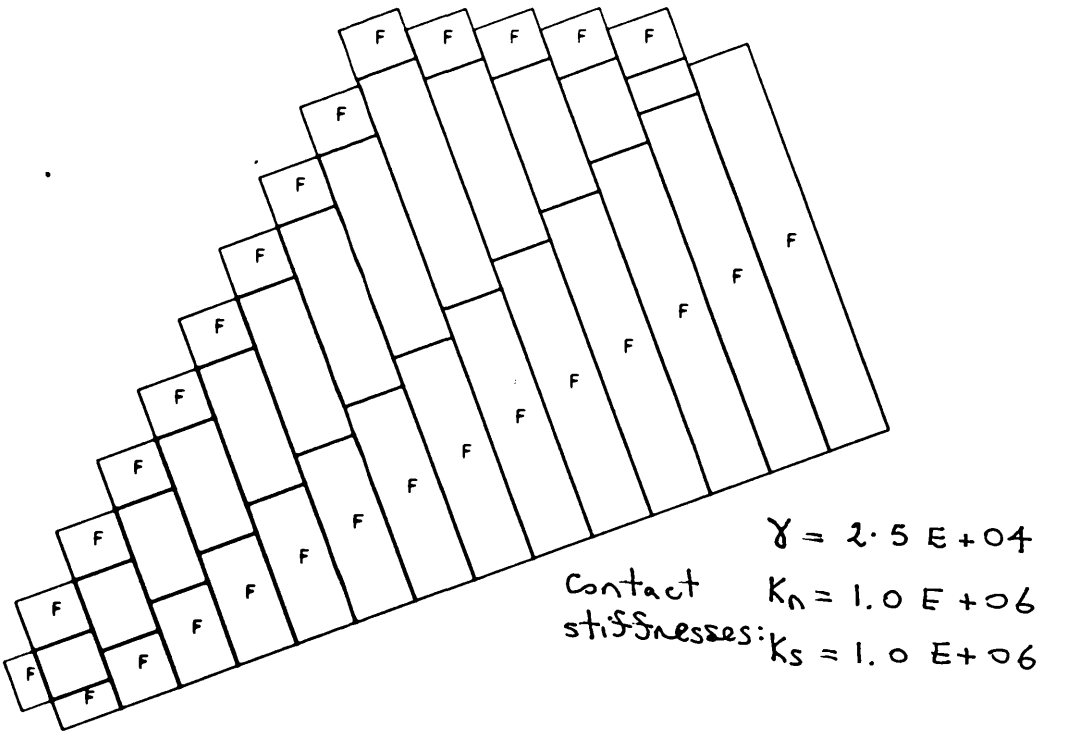
3.2.6. Block Toppling Model:

Several investigators, notably Hocking (1977); Ozgenoglu (1978), Voegele (1978), and Maini et. al. (1978) have compared limiting equilibrium solutions for systems of toppling blocks (Goodman and Bray, 1976) with dynamic relaxation rigid block methods. It was considered worthwhile to perform a similar comparison using the static relaxation method.

The thirteen block geometry used in the computer simulation is shown in Figure 3.14 and the geometry was the same as that analysed by Goodman and Bray (1976). For a particular value of the friction coefficient (in this case $\mu = .393$), Goodman and Bray's analysis gives the magnitude and distribution of all interblock forces when the system is just on the point of failure. Also, the mechanism of collapse is predicted and for $\mu = .393$, the three upper blocks remain stable, the lower block slides on the base while remaining blocks undergo rotation about their lower corners. There are two major assumptions in the limiting equilibrium solution, these being that full frictional resistance develops at each contact point and contact points have specific locations.

The dimensions and block properties used in the model were identical to those used by Goodman and Bray. This enabled a direct comparison between the inter-block forces calculated by both methods. The coefficient of friction used in the computer run was set to .393 for all sides of all blocks to ensure compatibility with the limiting equilibrium solution. The aim of this test was two-fold: firstly, to compare the mode of failure and secondary to compare contact force magnitudes in regions where the mode of failure was similar.

Figure 3.14 shows the block configuration used in the consolidation phase with restraining blocks indicated by an 'F'. The blocks were consolidated under



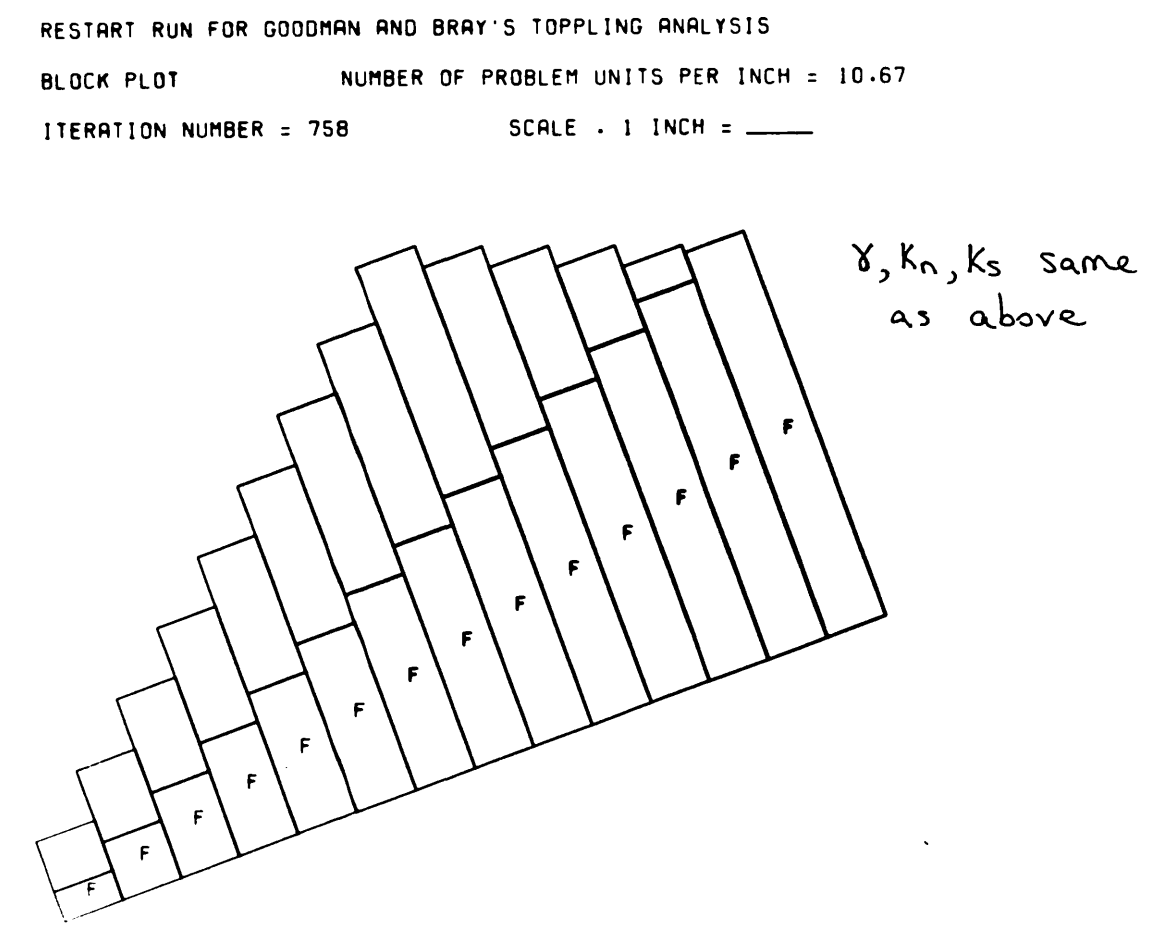
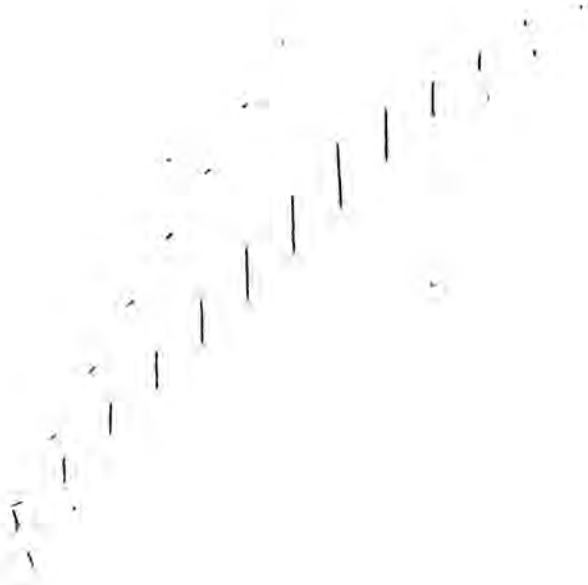




Figure 3.14: Thirteen block toppling model.

RESTART RUN FOR GOODMAN AND BRAY'S TOPPLING ANALYSIS

CORNER FORCE PLOT  NUMBER OF PROBLEM UNITS PER INCH = 9.48

ITERATION NUMBER = 758  SCALE . 1 INCH = _____



RESTART RUN FOR GOODMAN AND BRAY'S TOPPLING ANALYSIS

DISPLACEMENT PLOT  NUMBER OF PROBLEM UNITS PER INCH = 0.00000003

ITERATION NUMBER = 758  SCALE . 1 INCH = _____



Figure 3.1 contd.

self weight before the restraining blocks were removed to perform the stability test. As with other problems, a restart file was saved at the end of consolidation. The stability test indicated a slightly different mode of failure to that calculated from limiting equilibrium in the toe region of the slope. The lower four blocks were sliding rather than toppling whereas only the lower block was sliding with limiting equilibrium. The reason for this discrepancy is probably due to the different contact point locations in both methods. This problem is discussed fully by Maini et. al. (1978).

Table 3.12 and Figure 3.15 compare the magnitude of inter-block forces developed and a satisfactory correlation exists between the computer and analytical results for those blocks having the same mode of failure.

Table 3.12: Comparison of inter-block contact force magnitudes using limiting equilibrium and static relaxation method, for 13 toppling block model.

| | S.R.[1] | | | L.E.[2] | | |
|---|---|---|---|---|---|---|
| block number n | $R_n$ | $S_n$ | $S_n/R_n$ | $R_n$ | $S_n$ | $S_n/R_n$ |
| 13 | 1409.6 | 513.0 | .3639 | 1404.8 | 511.3 | .3640 |
| 12 | 3359.5 | 1222.7 | .3640 | 3354.7 | 1221.0 | .3640 |
| 11 | 5309.0 | 1932.0 | .3639 | 5304.6 | 1930.7 | .3640 |
| 10 | 7360.0 | 2506.0 | .3405 | 7197.2 | 2494.8 | .3466 |
| 9 | 9146.0 | 2731.0 | .2986 | 8942.7 | 2684.3 | .3000 |
| 8 | 8091.0 | 2527.0 | .3123 | 7894.4 | 2414.5 | .3058 |
| 7 | 7245.0 | 2341.0 | .3231 | 7046.9 | 2168.9 | .3078 |
| 6 | 6387.0 | 2170.0 | .3398 | 6192.9 | 1906.4 | .3078 |
| 5 | 5562.0 | 2025.0 | .3641 | 5325.2 | 1609.4 | .3022 |
| 4 | 4729.0 | 1858.0 | .3929 | 4424.9 | 1229.3 | .2778 |
| 3 | 3836.9 | 1508.4 | .3930 | 3423.5 | 591.8 | .1729 |
| 2 | 2940.5 | 1155.5 | .3930 | 1020.7 | 1700.8 | -1.6667 |
| 1 | 2030.4 | 797.9 | .3930 | 6075.0 | 2387.5 | .3930 |

1. Static Relaxation Method
2. Limiting Equilibrium Method

$R_n$, $S_n$ are the normal and shear forces on the base of block n.

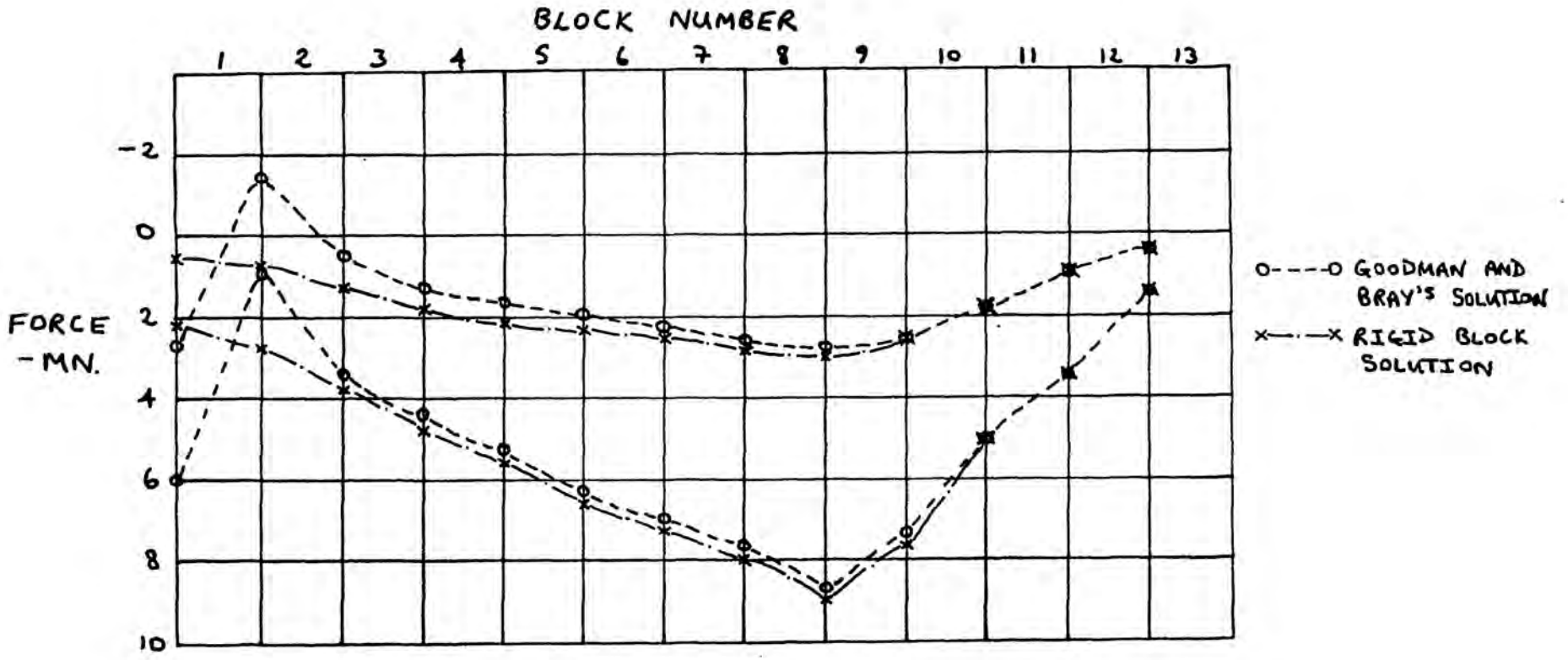
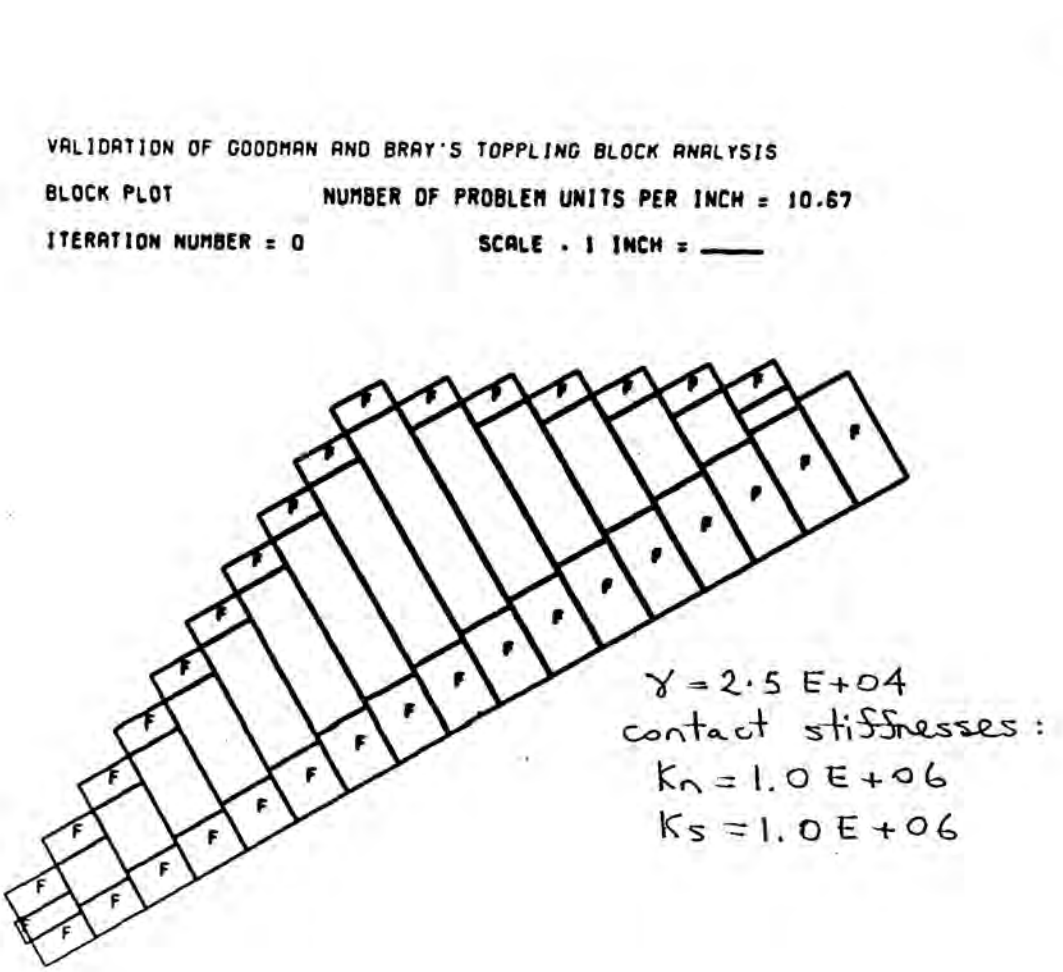



Figure 3.15: Comparison of forces for 13 block toppling model.

A limiting equilibrium solution was also available for the sixteen block geometry shown in Figure 3.16 (Goodman and Bray, 1976). The same problem was analysed with static relaxation and the results for this analysis are presented in Table 3.13. The modes of failure for this case are very similar, the only difference being that block number 3 topples with static relaxation whereas limiting equilibrium predicts sliding behaviour. There is excellent agreement between inter-block force magnitudes listed in Table 3.13, the deviations again being most likely due to the differences in contact force locations.



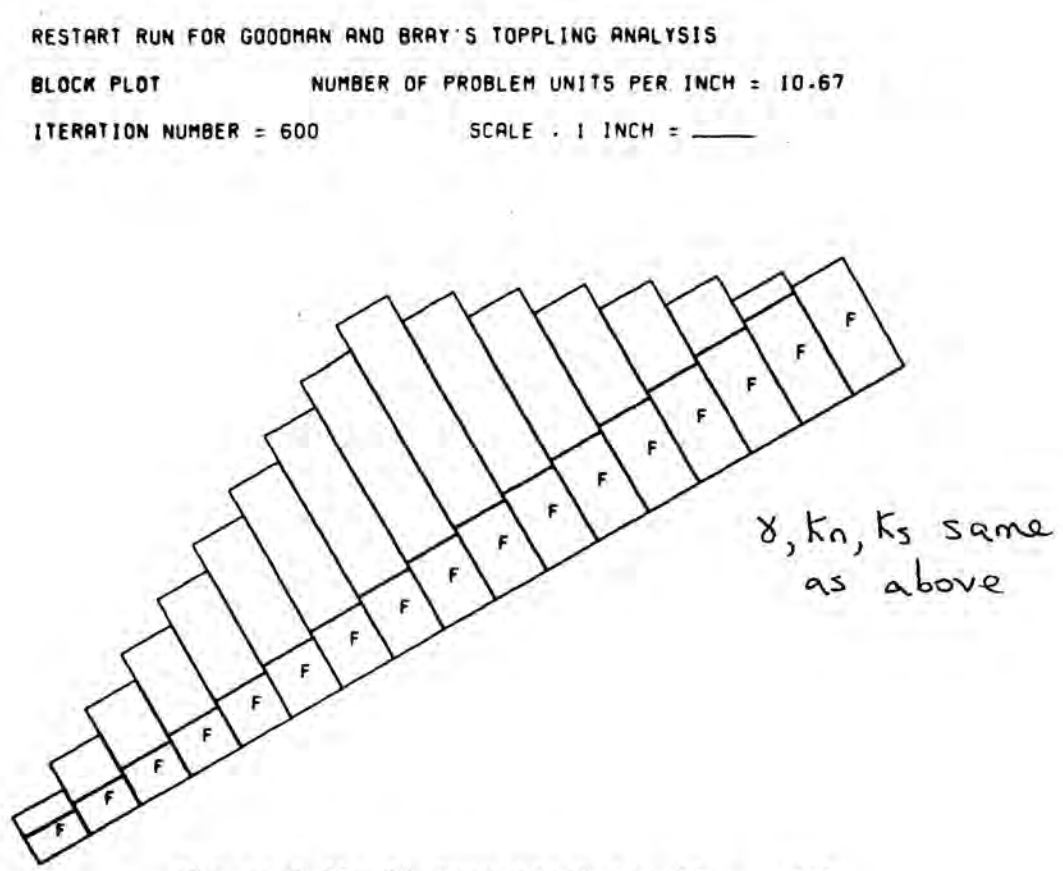
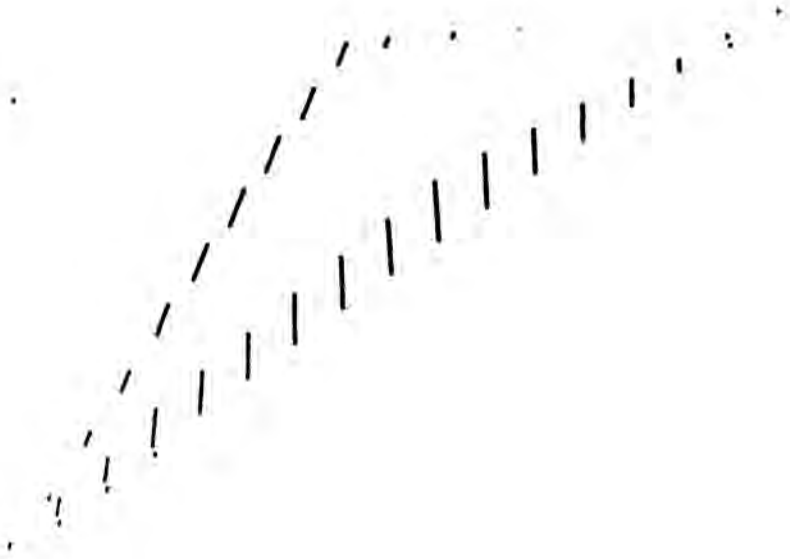




Figure 3.16: Sixteen block toppling model

RESTART RUN FOR GOODMAN AND BRAY'S TOPPLING ANALYSIS

CORNER FORCE PLOT  NUMBER OF PROBLEM UNITS PER INCH = 8.57

ITERATION NUMBER = 600  SCALE . 1 INCH = ____



RESTART RUN FOR GOODMAN AND BRAY'S TOPPLING ANALYSIS

DISPLACEMENT PLOT  NUMBER OF PROBLEM UNITS PER INCH = 0.00000002

ITERATION NUMBER = 600  SCALE . 1 INCH = ____



Figure 3.16 contd.

Table 3.13: Comparison of interblock forces using limiting equilibrium and static relaxation method, for 16 toppling block model.

| | S.R.[1] | | | | L.E.[2] | | | |
|---|---|---|---|---|---|---|---|---|
| block number n | $R_n$ | $S_n$ | $S_n/R_n$ | $P_n$ | $R_n$ | $S_n$ | $S_n/R_n$ | $P_n$ |
| 16 | 866.0 | 500.0 | .577 | 0 | 866.0 | 500.0 | .577 | 0 |
| 15 | 2165.5 | 1250.0 | .577 | 0 | 2165.0 | 1250.0 | .577 | 0 |
| 14 | 3464.0 | 1999.7 | .577 | 0 | 3464.0 | 2000.0 | .577 | 0 |
| 13 | 4578.0 | 2465.0 | .538 | 0 | 4533.4 | 2457.5 | .542 | 0 |
| 12 | 5678.0 | 2956.0 | .521 | 263.6 | 5643.4 | 2966.8 | .526 | 292.5 |
| 11 | 6828.0 | 3507.0 | .514 | 778.3 | 6787.6 | 3520.0 | .519 | 825.7 |
| 10 | 7707.0 | 3721.0 | .483 | 1490.0 | 7662.1 | 3729.3 | .487 | 1556.0 |
| 9 | 7168.0 | 3408.0 | .475 | 2735.0 | 6933.8 | 3404.6 | .491 | 2826.7 |
| 8 | 6202.0 | 3254.0 | .525 | 3796.0 | 6399.8 | 3327.3 | .520 | 3922.1 |
| 7 | 5913.0 | 3259.0 | .551 | 4513.0 | 5872.0 | 3257.8 | .555 | 4594.8 |
| 6 | 5386.0 | 3197.0 | .594 | 4732.0 | 5352.9 | 3199.5 | .598 | 4837.0 |
| 5 | 4873.0 | 3152.0 | .647 | 4517.0 | 4848.1 | 3159.4 | .652 | 4637.5 |
| 4 | 4441.0 | 3137.0 | .706 | 3852.0 | 4369.4 | 3152.5 | .722 | 3978.1 |
| 3 | 3486.7 | 2695.0 | .773 | 2706.0 | 3707.3 | 2912.1 | .785 | 2825.6 |
| 2 | 2510.2 | 1971.2 | .785 | 1398.0 | 2471.4 | 1941.3 | .785 | 1413.5 |
| 1 | 1266.5 | 994.7 | .785 | 415.4 | 1237.1 | 971.8 | .785 | 472.2 |

1. Static Relaxation Method
2. Limiting Equilibrium Method

$R_n$, $S_n$ are the normal and shear forces on the base of block n.

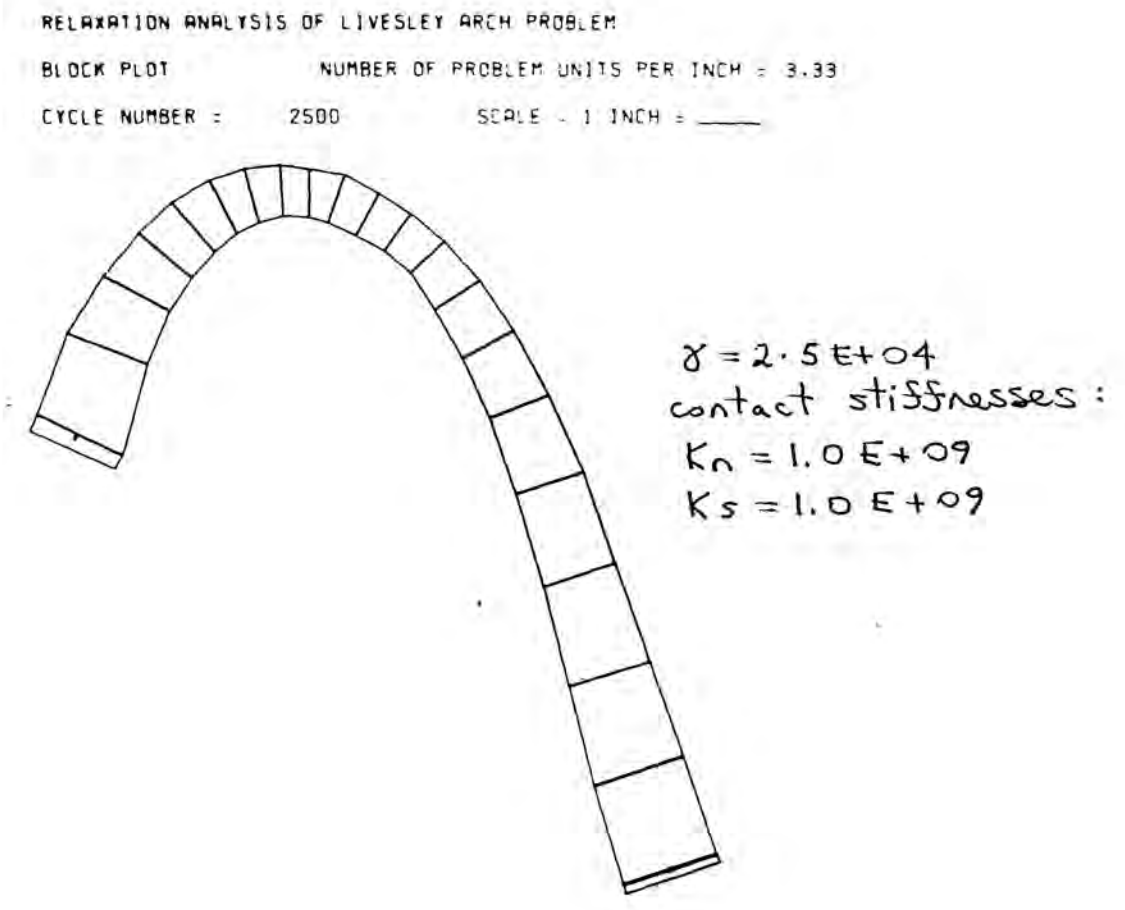
$P_n$ is the normal force acting on the upper side of block n.

### 3.2.7. Collapse Analysis of Mason ry Arches:

As discussed later in Chapter 6, the concept of arching is of fundamental importance to the load distribution within jointed media. To examine the mechanisms associated with the development of arches in jointed media, a particular mason ry arch was analysed using the static relaxation method and the behaviour was compared to an independent solution. Voegele (1978) also analysed a particular type of mason ry structure (Voussoir arch) using a dynamic relaxation rigid block method and found good agreement with theoretically predicted behaviour.

The particular mason ry structure examined in this example was the jointed arch analysed by Livesley (1978), as shown in Figure 3.17. Livesley (1978) presents an analysis whereby the collapse load of a mason ry arch or dome of arbitrary shape can be formulated as a problem in limit analysis. In this procedure, in which the structure is formed from rigid blocks, the load factor is maximised subject to the equilibrium equations of the structure and linear constraints imposed by criteria of failure at the block interfaces. The rigid blocks shown in Figure 3.17 were each assumed to be of constant thickness with the faces of the blocks perpendicular to the plane of the arch.

Livesley (1978) formulated two limit-analysis problems for the mason ry arch, the first being concerned with whether the arch could support its own weight. If this solution existed, then the second problem concerned the magnitude of applied loading necessary to cause collapse of the structure. Unfortunately, numerical values for the system properties were not specified by Livesley (1978). However, the problem was analysed with the static relaxation method using realistic parameters, the aim being to compare the collapse mechanisms generated by both methods.



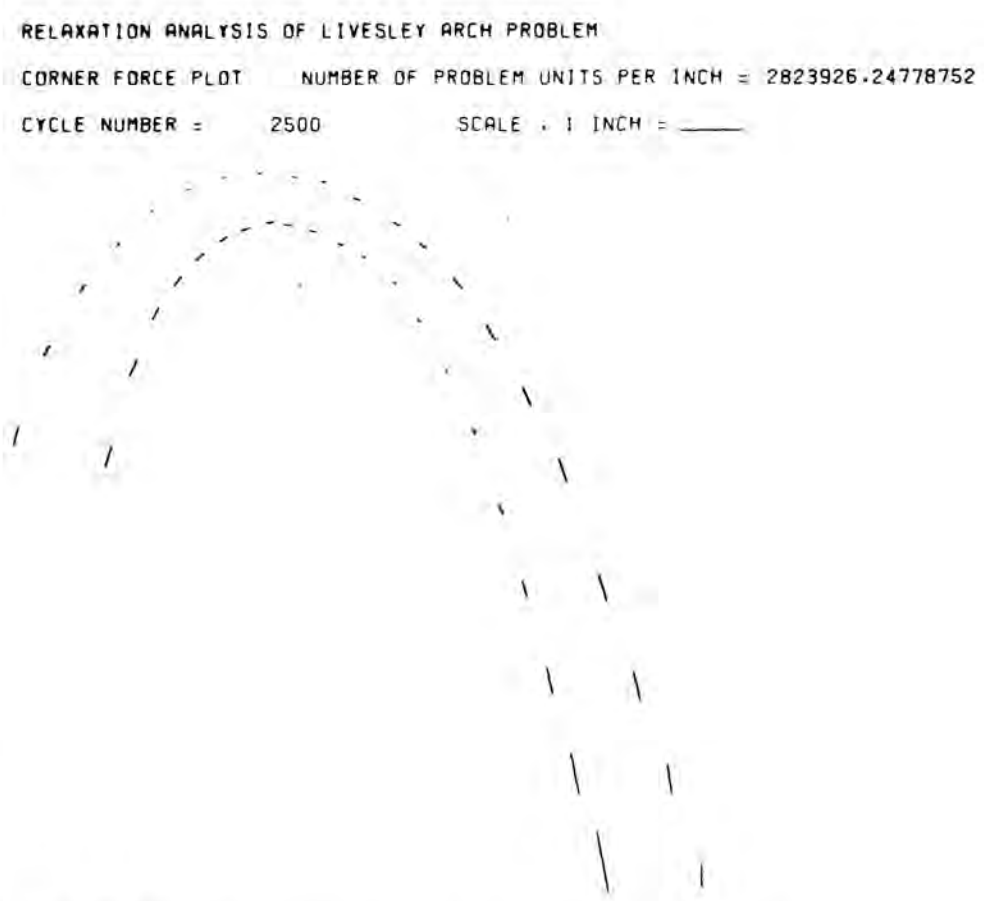
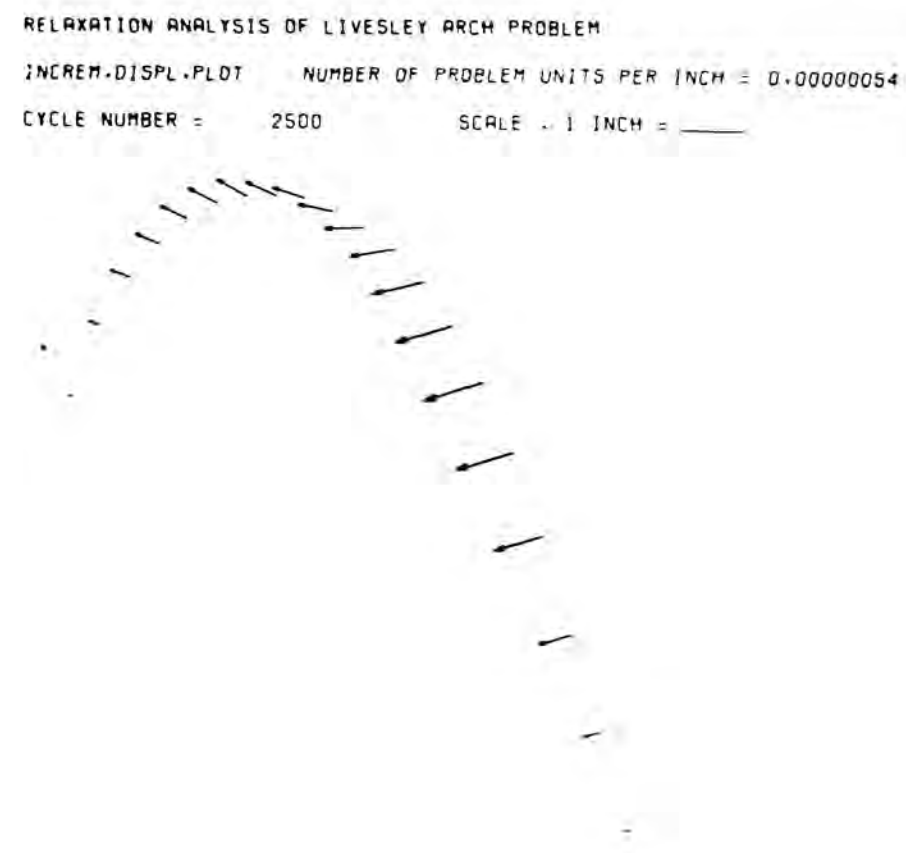




Figure 3.17: Masonry arch problem under self weight



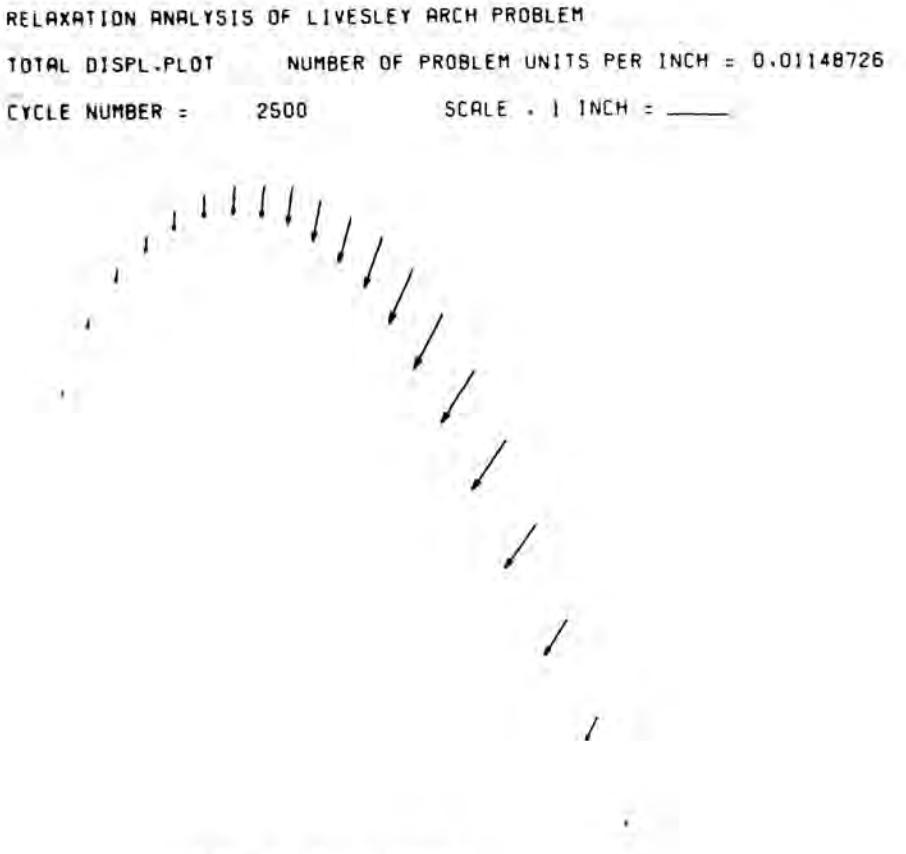
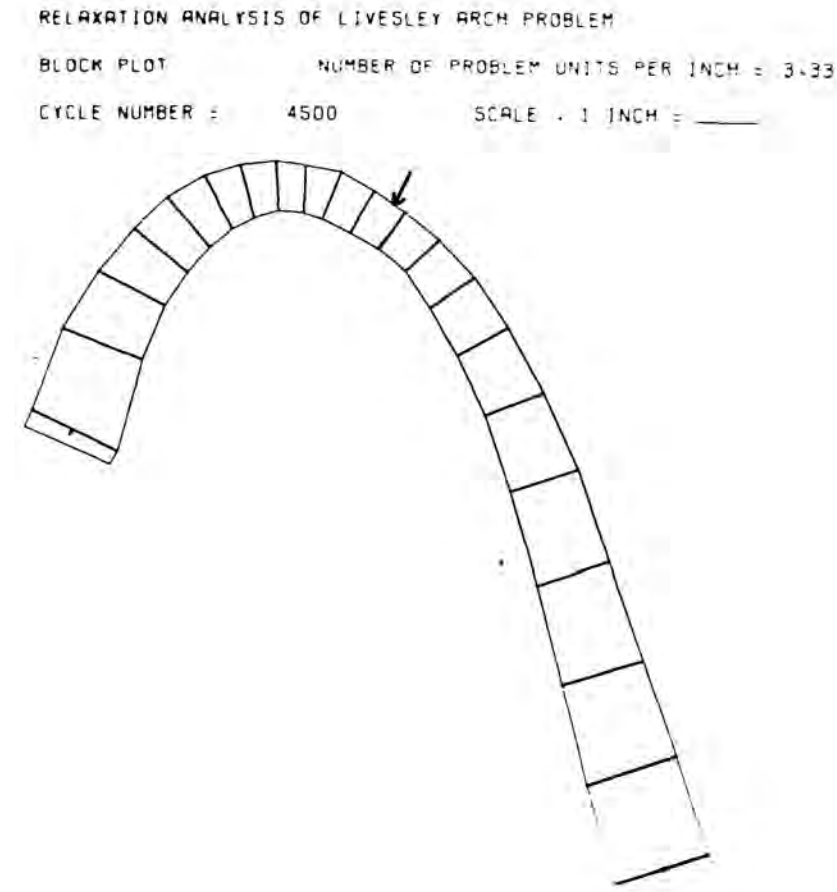




Figure 3.17 contd.

Initially, the system was analysed under self weight with the static relaxation method and it was found that the arch could support its own weight. The contact forces between and displacements of members after 2500 iterations of self weight loading are shown in Figure 3.17. At this stage, the incremental block displacements were less than 1% of the maximum incremental displacements while the shear forces along all block interfaces did not exceed the corresponding shear strengths. The analysis of Livesley (1978) also showed that the system could support its own weight.

To investigate the collapse mechanism, a point load of magnitude 50 times the block weight was applied to a mid-span block, as indicated in Figure 3.18. The problem was analysed for a further 2000 iterations, re-starting from the file saved at the end of self weight loading (Figure 3.17), and the results after a cumulative 4500 iterations are shown in Figure 3.18. The contact force plot agrees favourably with the approximate line of thrust obtained from limit analysis (Figure 3.19). The mid-span hinges are detected on the force plot by the absence of contact forces. The collapse mechanism generated with static relaxation predicted three hinges as with the limit analysis but the position of the middle hinge located on the extrados between the abutment hinge and the loaded block was slightly different. The position of the middle hinge from static relaxation was located one block interface nearer to the loaded block. This discrepancy in hinge location could be due to the assumption in the limit analysis of Livesley (1978) that the limiting shear force associated with sliding at a block interface is independent of the normal component of force across the interface.



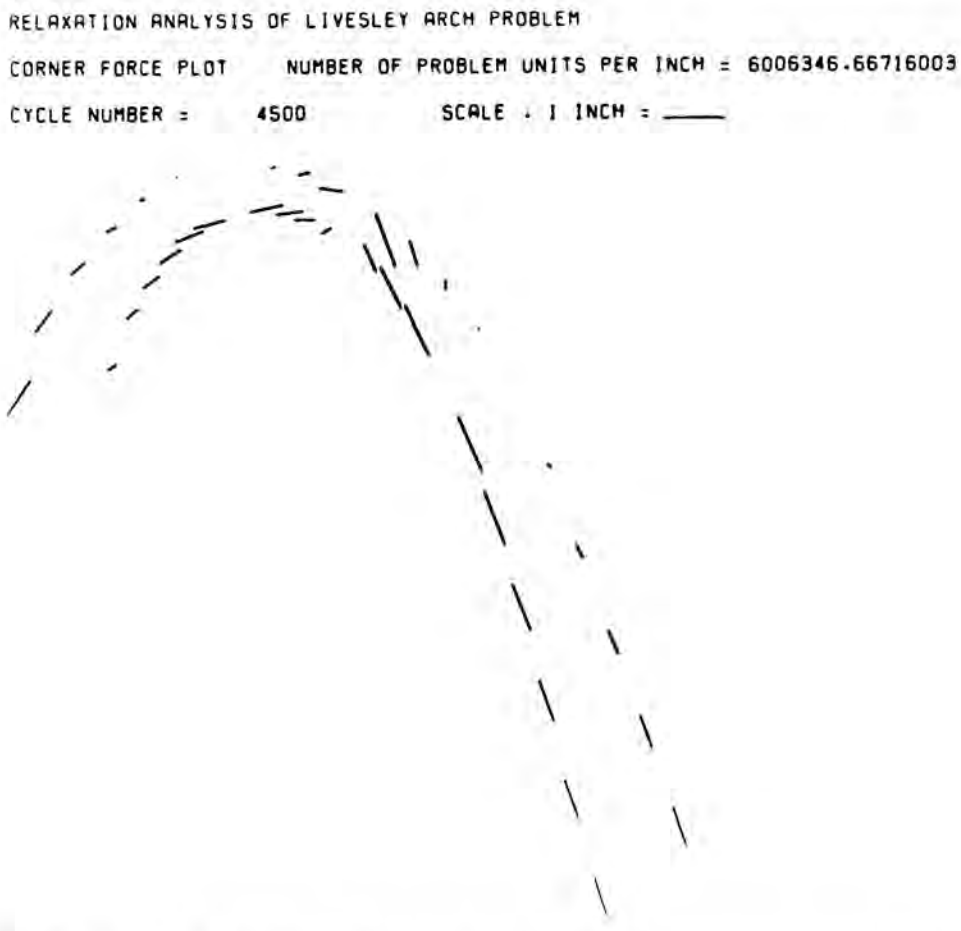




Figure 3.18: Masonary arch analysis under external loading

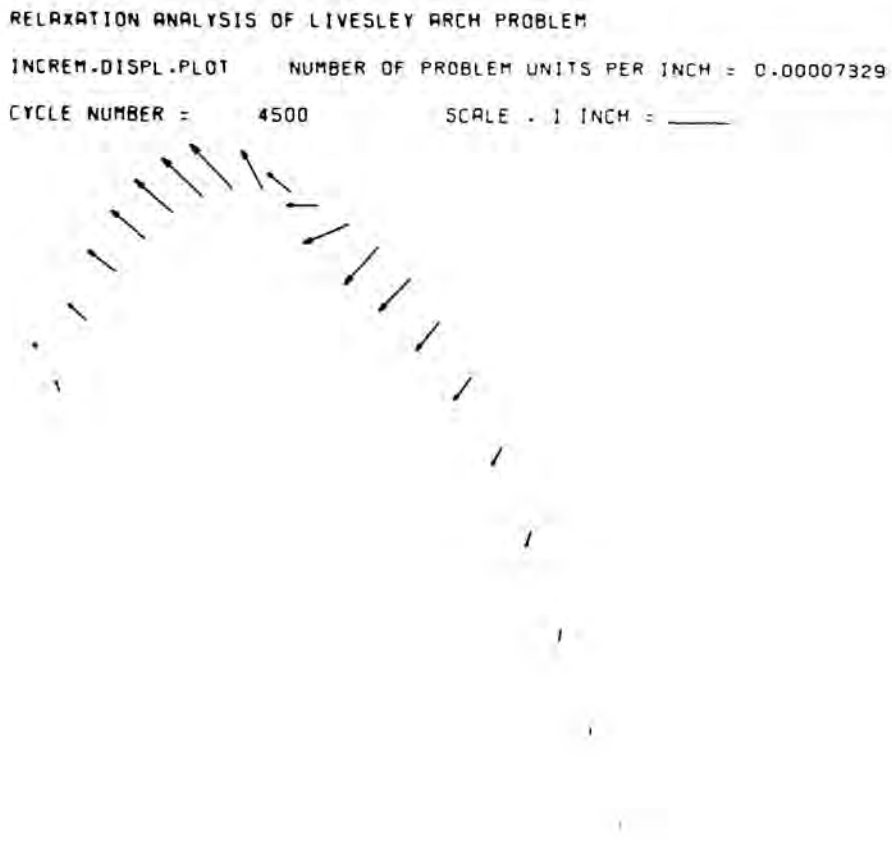






Figure 3.13 contd.

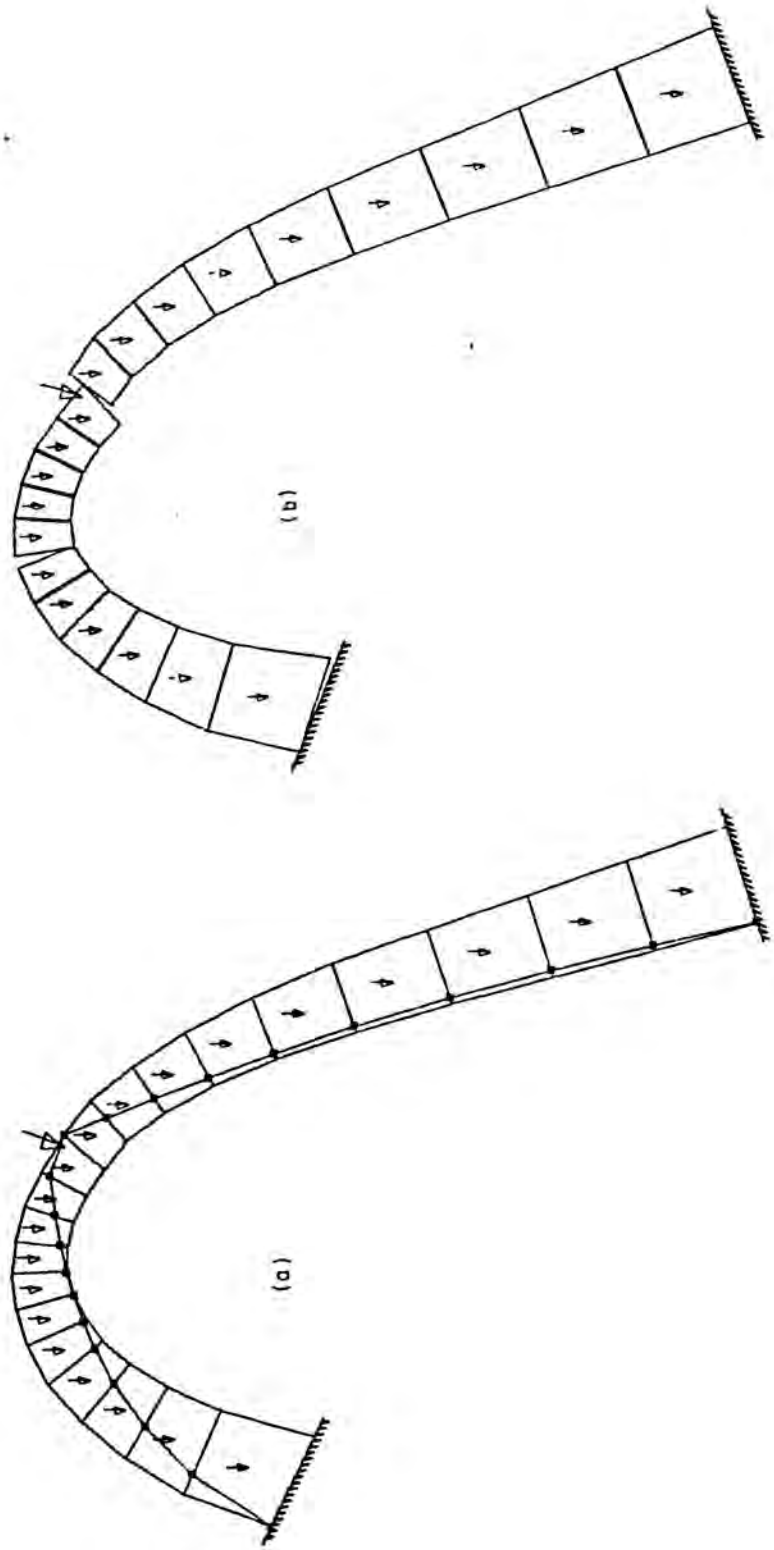



Figure 3.19: Plots of (a) line of thrust and (b) collapse mechanisms, for a typical arch (after Livesley, 1978).

3.2.8. Simultaneous Versus Successive Relaxation:

The difference between simultaneous and successive relaxation was outlined in Section 2.4.1. In order to determine if there was any difference in the solution reached by these two methods after consolidation, the block geometry shown in Figure 3.20 was analysed using both procedures. The rock mass has two mutually perpendicular joint sets orientated at 75 and 15 degrees to the horizontal. The joints were assigned normal and shear stiffnesses of 1000 and 100 units respectively, and the friction angle was set at 1 degree for consolidation. The simultaneous relaxation procedure is independent of the numbering sequence of the blocks, as demonstrated in Section 3.2.1. However, the successive relaxation procedure may not be and so a consistent order was adopted. Blocks were created, and therefore numbered, starting in the top right corner of the model and progressing down each column from right to left.

Figure 3.21 is the total displacement plot for the successive relaxation after 224 iterations. This and the corner force plot are exactly the same as the results obtained with 300 iterations of simultaneous relaxation. The first obvious difference is that the successive relaxation procedure converges faster than simultaneous relaxation, and hence in terms of computer time successive relaxation is more efficient. A comparison is presented below:

| | Successive Relaxation | Simultaneous Relaxation |
|---|---|---|
| No. of cycles : | 224 | 300 |
| No. of computer: units (CDC 6600) | 3.74 | 4.58 |
| Relative cost : | 81.6% | 100% |

This shows a saving in computer costs for successive relaxation of approximately 20%. It is interesting to note that dynamic relaxation required in the region of 1000

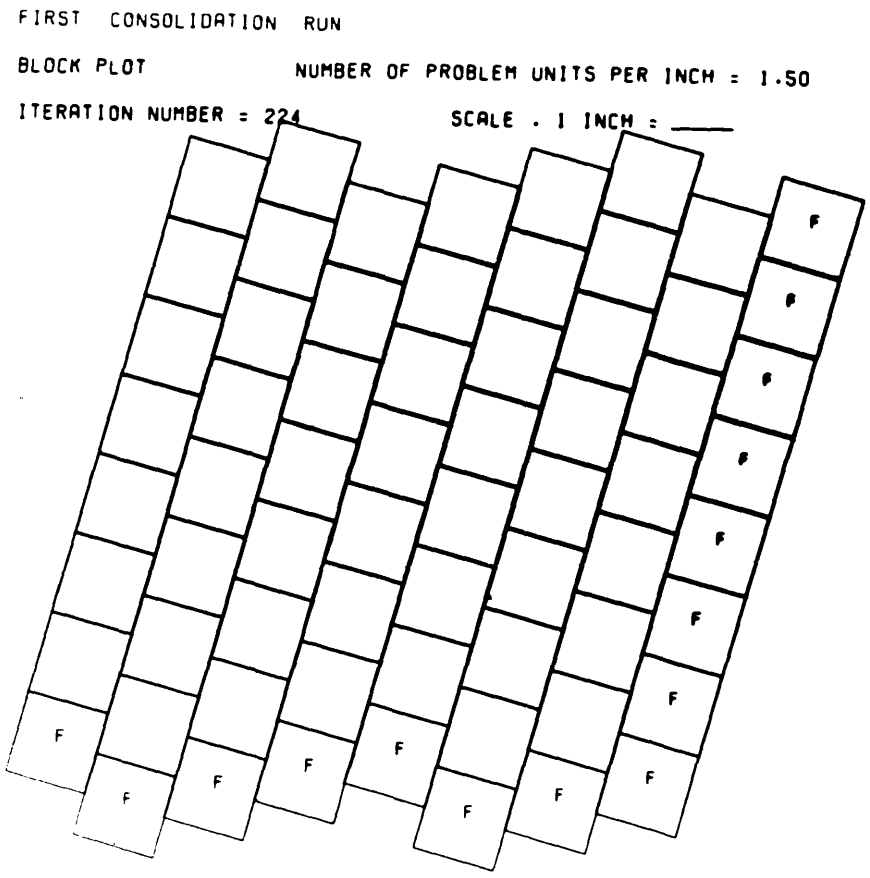



Figure 3.20: Block geometry used for simultaneous and successive relaxation.

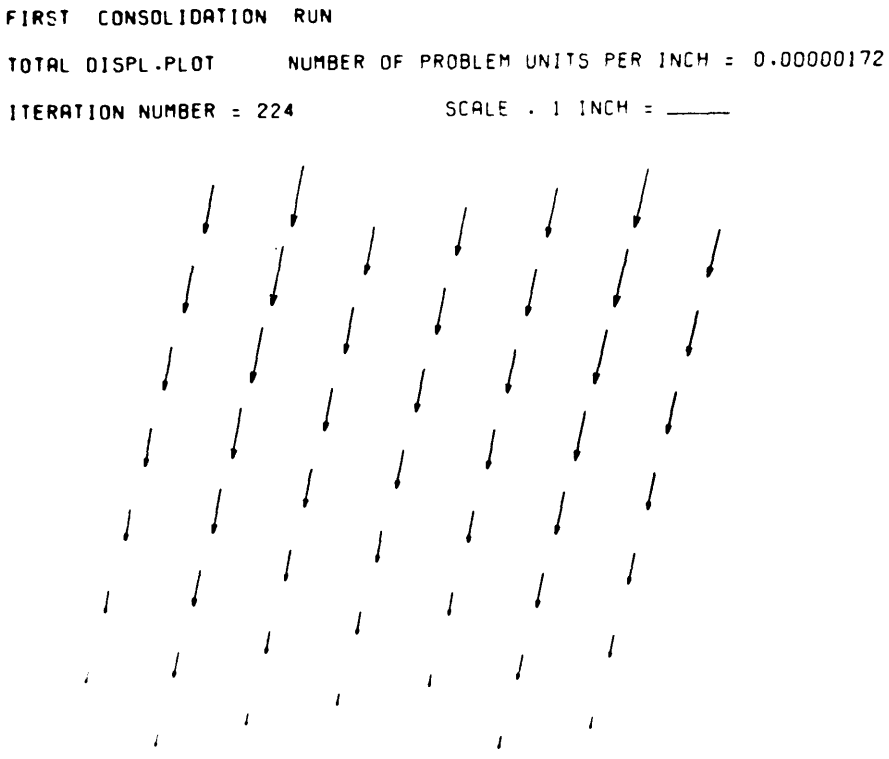



Figure 3.21: Total displacement plot for successive relaxation

iterations to achieve an equivalent consolidated state, using mass proportional damping and a critical time-step fraction of 0.1.

In Figure 3.22 plots of the maximum resultant out-of-balance forces in the vertical direction against the number of cycles for both relaxation procedures are presented. The out-of-balance forces have been normalised against the individual block weight. The graphs show that, as expected, convergence is initially faster with successive relaxation.

Although the comparison presented here indicated that economies could be achieved by using a successive relaxation procedure, a great amount of care and judgement are usually necessary to ensure that the successive relaxation solution is, in fact, path independent. For many problems, this will depend upon the nature of the geometry and the resulting displacements.

# Simultaneous & Successive Relaxation

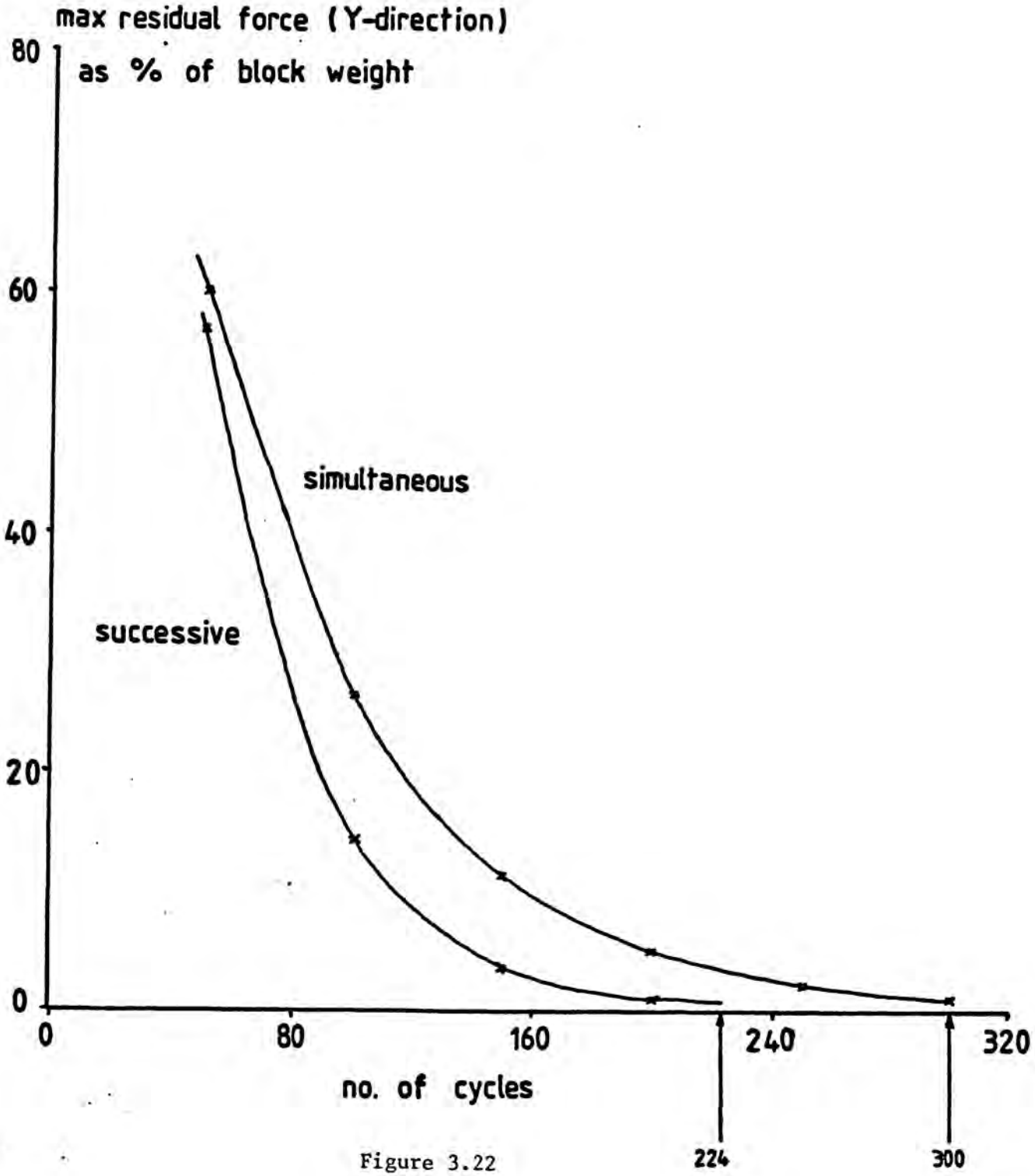



Figure 3.22

## 3.3. Summary:

The validation tests presented in this chapter indicate that the static relaxation method is capable of analysing jointed rock mass behaviour in which large scale translational and rotational movements can occur. The method was compared to elastic and inelastic solutions which involved the mechanisms of sliding, toppling and arching. In light of the assumptions governing the static relaxation method and the solutions used for comparison, agreement was generally very good between both the mechanisms of failure predicted and the magnitudes of the block forces and displacements. The agreement was best where the assumptions inherent in both methods were similar. The versatility of the static relaxation method was demonstrated by comparing the predicted solutions with results obtained from either analytical, limiting equilibrium or numerical modelling.

The validations performed highlight the major advantages of the method in that no mode of failure or combination of failure mechanisms need be assumed. However, as illustrated by the example in Section 3.2.5, intuitive failure modes may not always develop. The other major advantage of the method is that it may be applied to realistic, practical problems involving complex geometries for which some of the other methods may break down.

Comparisons between the static relaxation method and other independent techniques are not confined to this chapter alone. In the remaining chapters both quanlitative and quantitative correlations are made with field behaviour and with the results of physical and numerical modelling of jointed media.

Therefore, it can be concluded from the validations presented here together with the results of additional tests and comparisons performed but not discussed in this chapter that the static relaxation program works as intended.

# CHAPTER 4

# *APPLICATIONS TO MINE DESIGN*

# CHAPTER 4

# APPLICATIONS TO MINE DESIGN:

## 4.1. General:

The relaxation program described in Section 2.4 and Appendix VII was restricted in general use since only problems consisting of less than a certain number of bricks could be analysed. The capacity of the original program was largely determined by the type of computer available. For the CDC 6600 machine used in this study, the user was limited to a maximum of 50 K of core store. This meant that approximately 100 rectangular bricks could be analysed with the original program, the exact number of bricks depending on the shape of the bricks and the nature of the jointing. For a particular brick, the memory space required increased as the number of corners increased while offset jointing patterns required less memory than sets of through-going joints. These memory requirements are similar to those demanded by generalised dynamic relaxation formulations (Maini et. al., 1978).

Obviously, for the subsequent experimental model studies involving in excess of 400 square bricks, modifications to the relaxation programs were necessary if comparisons between the laboratory and numerical experiments were to be made. Also, for typical mine design problems, the facility for handling large sized problems is essential. The basic structure of the original program was designed to enable flexibility with subsequent modifications. In this respect, the original program has been modified to allow for an unlimited number of rock bricks constituting a jointed rock assemblage, by storage of the problem data during job execution on mass storage files.

## 4.2. Changes to Data Structures:

It was necessary to make several changes to the data structures in order that the program could analyse general problems. The major change made involved the use of

sequential scratch files for the storage of contact information during execution. The sequentially linked contact data arrays (Figure A.8, Appendix VII) constituted the major portion of the data storage requirements for any analysis. For example, 70% of the memory required for data storage was used by the contact information in a problem comprising fifty rectangular, staggered bricks. For many problems, the quantity of information was too large to be simultaneously held in core and this necessitated the use of files to store the relevant data and later read it back into core. Since large amounts of contact data were usually involved, the files were designed to handle this data.

Care is necessary when using files since the input/output operations needed to shuffle data in and out of core are relatively expensive and can markedly affect the execution costs. The efficient use of both core and files is essential and in the specification of files, only those file structures that are permissible in all large computer systems should be used. This is to ensure that the program is as machine independent as possible.

The data structures illustrated in Appendix VII were modified in the following way. The large singly-dimensioned array Q (existing permanently in core) stored data relating to the problem, as before, but was modified to exclude the contact data arrays. The contact data arrays for each brick were stored sequentially, but unlinked, on scratch files LUM and LUN. Variable length segments of the contact data were read into core from these files when necessary, and this information was stored in the array AO. The efficient use of core required that real and integer arrays be equivalenced. The occupation of core is shown in Figure 4.1. The layout of the memory contained in arrays Q and AO is shown schematically in Figures A.10 and A.11 in Appendix VII. The size of each contact data array was reduced to 14 words, since no storage space was required to link one array to another.

The information contained in each array was also slightly modified, as shown in Figure A.9, Appendix VII.

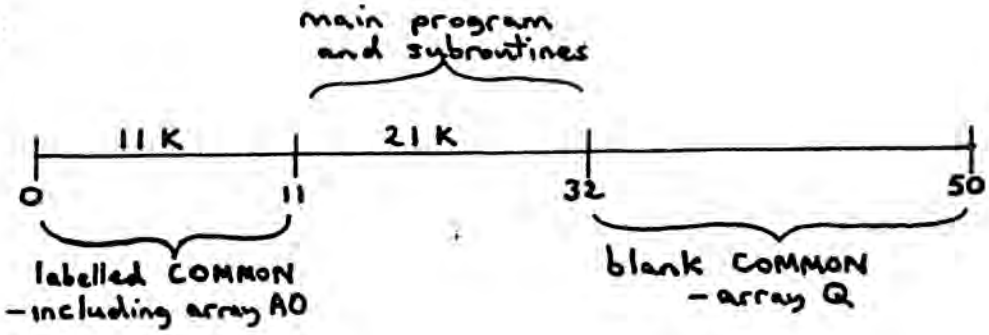



Figure 4.1 - Occupation of CDC 6600 core by the program.

The unformatted sequential access file LUN containing the contact data information is initially created and subsequently updated in subroutine UPDATE (for listing, see Appendix VII). File LUN consists of JC00 records, each scratch file record being LREC words in length. Each record consists of NBL blocks (blocking factor) and each block contains the LBL words of contact data array information.

Thus

$$LREC = NBL * LBL$$

and

$$JC00 = \frac{NCONT * LBL}{LREC} + 1$$

where NCONT is the total number of contacts for all bricks.

In the program, LBL was set to 14 and 100 blocks were stored in each record. Therefore, the scratch file record length was 1400 words. The contact data begins at the beginning of the first record and as many records of 1400 words as necessary are written for all contacts. The program always writes the contact data consecutively to the

file LUN i.e. the contact data for bricks 1, 2, 3,- - - X is contained on record 1, that remaining for brick X and for bricks X + 1, X + 2, - - - - on record 2, etc. The structure of file LUN is shown in Figure 4.2. Files LUN and LUM have equivalent structuring, the convention being always to read from LUM and write to LUN.

Since the files are too large to be held simultaneously in core, NPREC consecutive records are held in core (in array AO) at any one time. However, the nature of the calculations performed requires that as well as efficient file access, a certain amount of contact information be stored in array AO. This is because of the explicit nature of the solution procedure which requires not only access to the contact information for the particular member being relaxed, but also access to the contact data for neighbouring members. For any geometry this means that the brick numbering sequence (bricks are automatically numbered by the program at input) should be such that the difference between neighbouring brick numbers is as small as possible. This problem is analogous to that encountered in the finite element method where it is essential to keep the difference between adjacent element numbers to a minimum for formulations using a frontal solver for symmetric banded systems of equations.

The number of records held in core (NPREC) is usually in the order of five to seven, the exact value of NPREC (specified during input) depending on the problem geometry being analysed. As stated above, brick arrangements having a staggered brickwork pattern require less memory than those formed from through-going joint sets since fewer contacts exist in the former case. As an example, consider the two brick arrangements shown in Figure 4.3 which are part of a larger model consisting of some 400 25 mm square bricks and having overall dimensions of 500 mm square (representing the subsequent model studies described in Chapter 6).

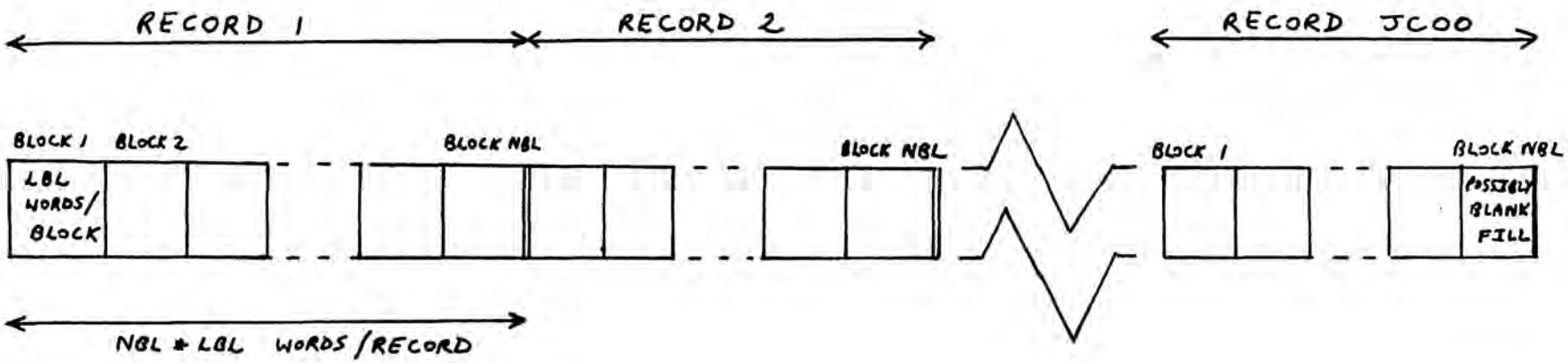
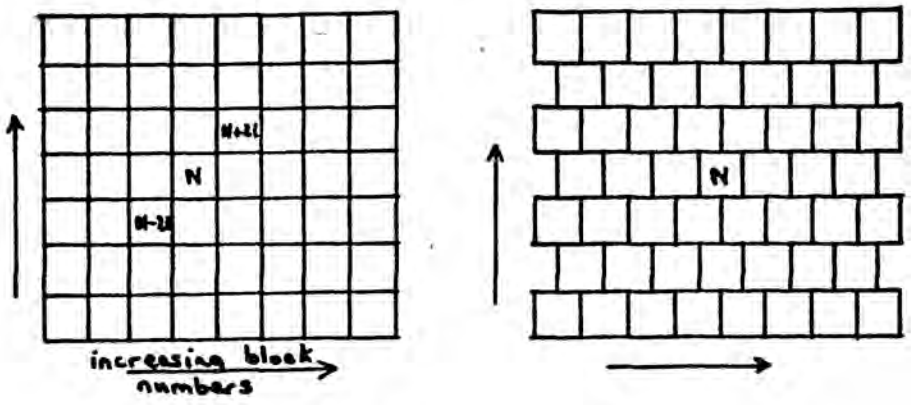



Figure 4.2: Structure of file LUN (record length = 1400 words)




a) continuous pattern b) staggered pattern

Figure 4.3 - Two Different Brick Arrangements

Then, for brick N in the continuous joint pattern, there are a possible maximum of 16 contacts, from surrounding members (4 for each edge). If all possible contacts exist for all bricks, the contact data arrays for only 6.25 bricks can be written onto each record of 1400 words. Since the maximum difference between neighbouring brick numbers is 42, at least nine records of contact information must be held in core. These records are shown schematically in Figure 4.4.

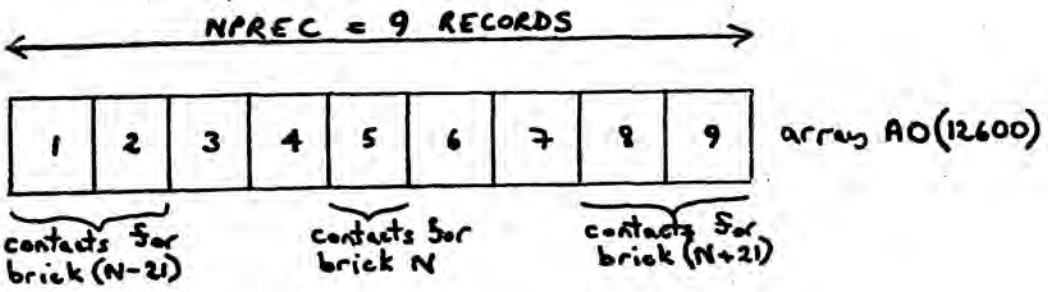



Figure 4.4 - Schematic of Records in Array AO.

For the staggered pattern, however, the average number of contacts from surrounding bricks is 8. Thus, in general, the contact data for twice as many bricks can be stored on each record than with the continuous jointing pattern. This results in only five records of contact information being required in array AO. Thus, some familiarity of the relationship between data structures and problem geometry is required if efficient use of core is to be made.

At the end of the calculation procedure, all information necessary for a restart including the brick and box data in array Q and the contact data on the scratch file LUN is written to an unformatted sequential binary file which is saved on magnetic tape. The information is then read from magnetic tape back into central memory or onto scratch file to facilitate a subsequent restart.

A listing of the modified program, together with relevant user information, is contained in Appendix VII.

## 4.3. Application of Modified Program to Mine Design:

The main purpose of the program restructuring detailed above was to specifically enable the experimental model studies described in Chapter 6 to be modelled numerically, and hence allow for comparisons between the physical and numerical modelling techniques. However, the modified program can also assist in mine design by allowing large, realistic problem geometries to be examined. The potential of the numerical technique for application to mine design is illustrated in the following examples.

### 4.3.1. Example Runs:

The rock block geometry shown in Figure 4.5 was selected as being representative of many mining environments in which the rock mass is characterised by a primary continuous joint set (e.g. bedding planes) and a secondary off-

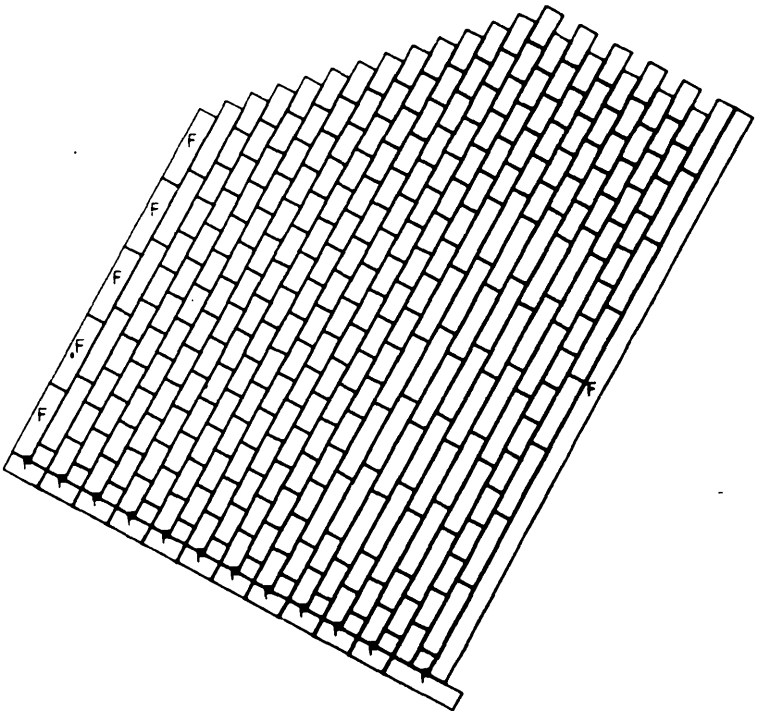
set joint set. The tabular lead-zinc orebodies at Mount Isa, Australia are an example of excavations located in such rock masses (Brady, 1977; Baczynski, 1977). The rock geometry shown in Figure 4.5 consisted of 24 columns of rectangular blocks of varying aspect ratios, the primary joint set being inclined at 60 degrees counter-clockwise to the horizontal. A total of 314 blocks were included in the model. It should be noted that an idealized geometry was chosen for these examples in which the block shapes and system parameters were not necessarily representative of particular prototypes. Hence, the results are primarily qualitative but are useful in highlighting the influence of various parameters.

The model was initially consolidated under self weight only by fixing a number of the boundary blocks (those indicated by an 'F' in Figure 4.5). During consolidation, the normal and shear stiffnesses were set equal to 1.0 E + 04 computer units*, a low friction coefficient of 0.01 was assumed and the block weights were in the order of 0.5 to 1.0 computer units. These numerical values for the stiffness and friction parameters applied to all blocks. Consolidation was continued for 700 iterations, during which a stage of 100 iterations required approximately 180 CP secs (6600) of execution time. After consolidation, the maximum incremental rigid block displacements were less than 5% of their initial values, while there was a 2.7% increase in the maximum contact force magnitude from iteration 600 to iteration 700. The force and displacement conditions at the end of consolidation are shown in Figure 4.5. The consolidation file was saved on magnetic tape for later restarting.

The friction coefficient was subsequently set to 0.577 ($\phi$ = 30 degrees) and the 32 larger rectangular blocks representing the orebody were removed in various sequences to simulate different mining methods. Only the behaviour of unsupported openings is examined in the following

* values for Kn and Ks same throughout all examples for both pre- and post-consolidation

PARAMETRIC STUDY OF MINING EXCAVATIONS IN A BLOCKY MEDIUM-CONSOL 500-700 CYCLES
BLOCK PLOT NUMBER OF PROBLEM UNITS PER INCH = 16.67
ITERATION NUMBER = 700 SCALE . 1 INCH = ———




PARAMETRIC STUDY OF MINING EXCAVATIONS IN A BLOCKY MEDIUM-CONSOL 500-700 CYCLES
CORNER FORCE PLOT NUMBER OF PROBLEM UNITS PER INCH = 14.56692621
ITERATION NUMBER = 700 SCALE . 1 INCH = ———

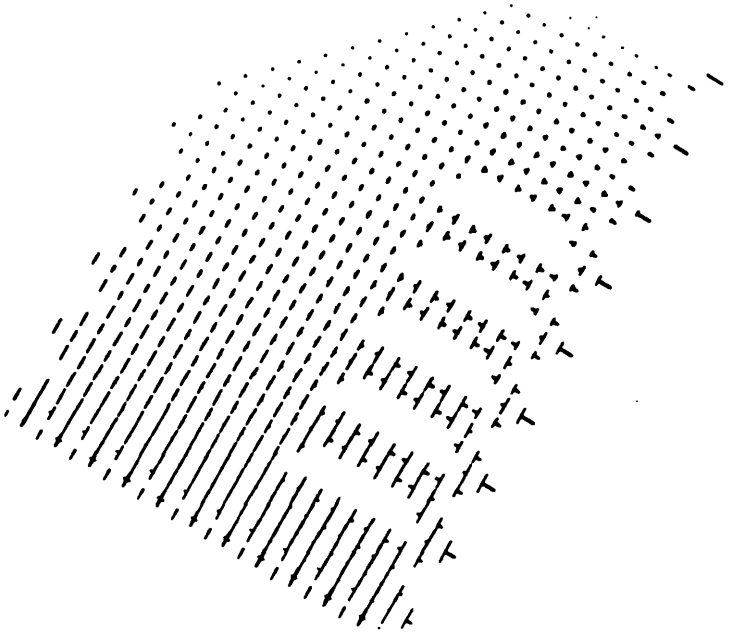
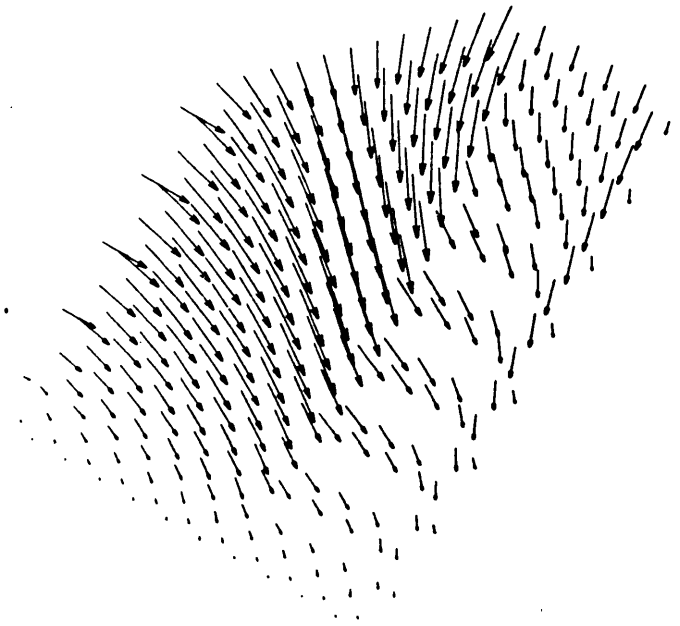


Figure 4.5.

PARAMETRIC STUDY OF MINING EXCAVATIONS IN A BLOCKY MEDIUM-CONSOL 500-700 CYCLES
INCREM.DISPL PLOT NUMBER OF PROBLEM UNITS PER INCH = 0.00000171
ITERATION NUMBER = 700 SCALE . 1 INCH = _____



PARAMETRIC STUDY OF MINING EXCAVATIONS IN A BLOCKY MEDIUM-CONSOL 500-700 CYCLES
TOTAL DISPL PLOT NUMBER OF PROBLEM UNITS PER INCH = 0.00209883
ITERATION NUMBER = 700 SCALE . 1 INCH = _____

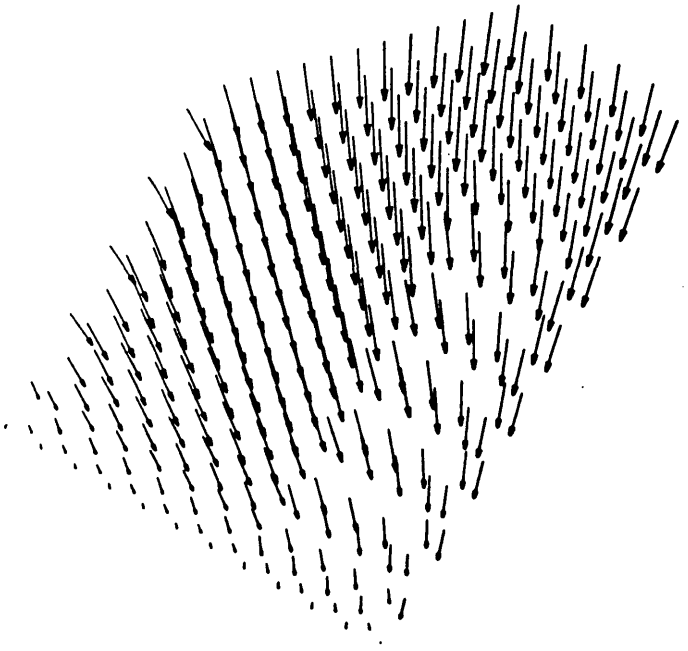


Figure 4.5 contd.

examples but the facility exists in the program to apply support forces or specified displacements to relevant blocks.

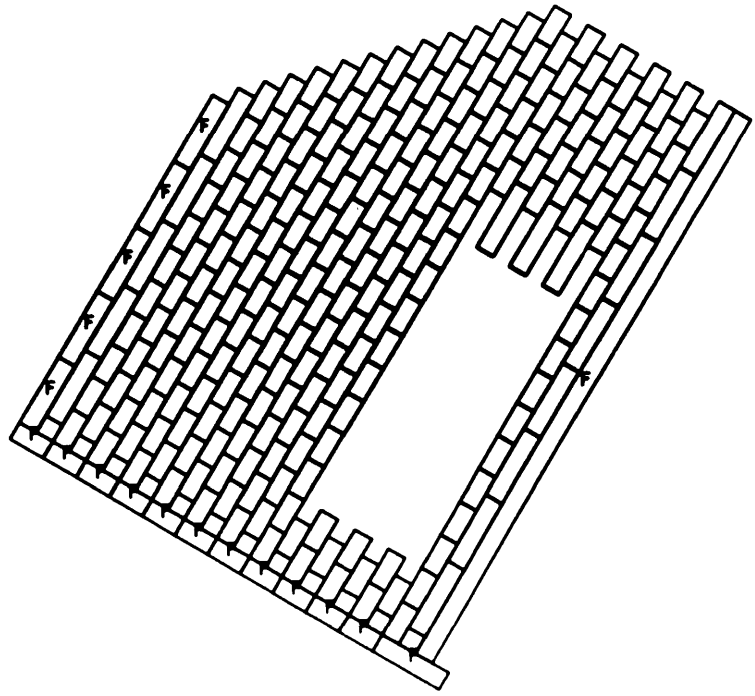
Firstly, the 32 blocks were simultaneously removed upon restarting to simulate mass blasting of the excavation, and the behaviour of the material surrounding the opening for 250 iterations after block removal is illustrated in Table 4.1 and Figure 4.6. The nature of the block displacements meant that a very large number of iterative cycles would have been necessary to model large deformation behaviour or allow for the attainment of equilibrium. Thus, for both practical and economical reasons, execution was somewhat arbitrarily terminated in all of the following examples. The maximum cumulative displacements listed in Table 4.1 imply that the hangingwall is unstable after 950 iterations. This is confirmed by the numerical print-out

Table 4.1: MASS BLASTING RESULTS

| iteration number | $max^m$. contact force magnitude | $max^m$. cumulative resultant translation |
|---|---|---|
| 700 | 3.64 | 0.00 |
| 750 | 3.58 | 4.70 E-04 |
| 800 | 3.70 | 6.19 E-04 |
| 850 | 3.93 | 9.06 E-04 |
| 900 | 4.12 | 1.19 E-03 |
| 950 | 4.28 | 1.46 E-03 |

which shows the maximum block translation and rotation for each iteration oscillating about a mean value and not steadily decreasing to an equilibrium condition. The displacement plots of Figure 4.6 clearly show the unstable hangingwall zone extending from the opening face into the overlying material for the first five columns. The shear strength of the upper and lower cross-joints for the three immediate hangingwall columns has been exceeded after 950 iterations. The largest displacements are located at mid-span of the exposed hangingwall. The contact force print-out reveals that the mid-span joints have opened

REMOVING ALL EXCAVATION BLOCKS TO SIMULATE MASS BLASTING.0-250 CYCLES RESTART
BLOCK PLOT NUMBER OF PROBLEM UNITS PER INCH = 16.67
ITERATION NUMBER = 950 SCALE . 1 INCH = _____



REMOVING ALL EXCAVATION BLOCKS TO SIMULATE MASS BLASTING.0-250 CYCLES RESTART
CORNER FORCE PLOT NUMBER OF PROBLEM UNITS PER INCH = 17.09837469
ITERATION NUMBER = 950 SCALE . 1 INCH = _____

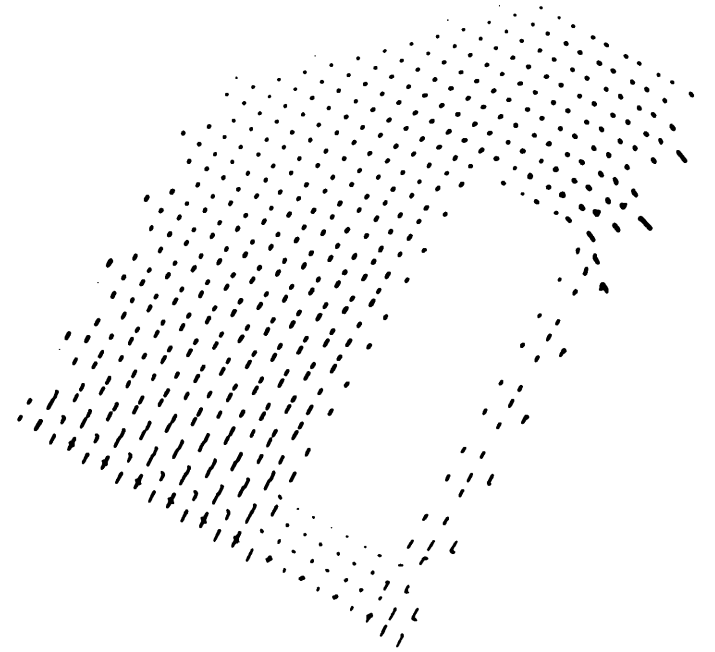
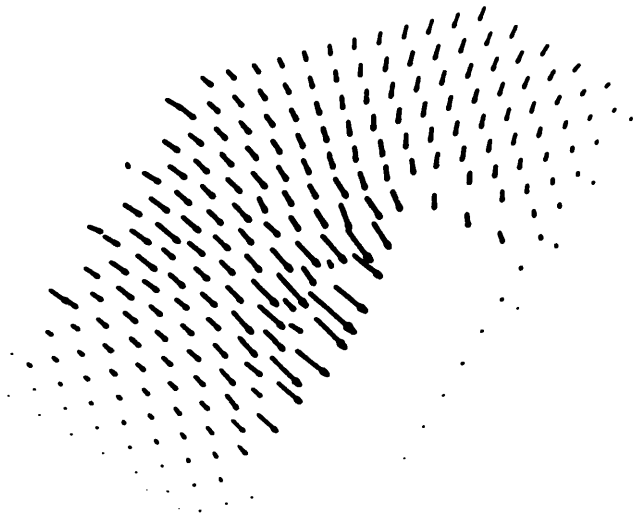


Figure 4.6

REMOVING ALL EXCAVATION BLOCKS TO SIMULATE MASS BLASTING.0-250 CYCLES RESTART
INCREM.DISPL PLOT NUMBER OF PROBLEM UNITS PER INCH = 0.00000708
ITERATION NUMBER = 950 SCALE . 1 INCH = _____



REMOVING ALL EXCAVATION BLOCKS TO SIMULATE MASS BLASTING.0-250 CYCLES RESTART
TOTAL DISPL PLOT NUMBER OF PROBLEM UNITS PER INCH = 0.00146479
ITERATION NUMBER = 950 SCALE . 1 INCH = _____



Figure 4.6 contd.

adjacent to the excavation indicating a beaming action of the immediate column with both ends effectively pinned. Also, the force distribution indicates that lateral forces in the hangingwall have been eliminated. The hangingwall action suggests that a support system will have most effect if the central span displacements of the country rock can be adequately controlled. The crown displacements, although of lesser magnitude than those in the immediate hangingwall rows, indicate a compression of the material towards the footwall which could eventually result in crushing and collapse of the crown. The inward displacements of material in both the footwall and floor are probably due to reactions from the fixed boundaries.

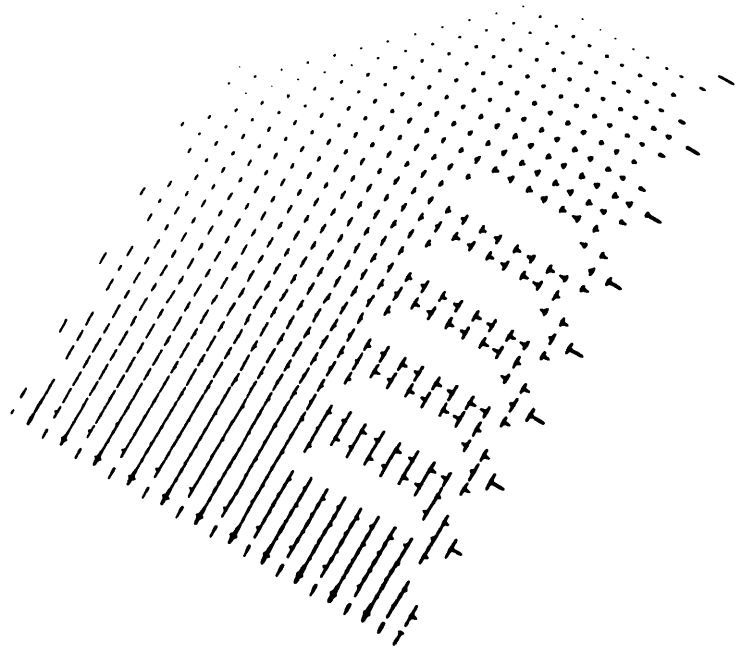
An interesting comparison was obtained between the mass blasting results of Table 4.1 and Figure 4.6 and those for the same example analysed with dyanmic relaxation. The generalised dynamic relaxation program listed in Appendix VI was modified to incorporate the features described in Section 4.2. Consolidation was achieved by using mass proportional damping and a critical time-step fraction (based on single degree-of-freedom) which varied between 0.1 and 0.25. The same stiffness and friction parameters were used and consolidation was again carried out for 700 calculation cycles. At this stage equivalent magnitudes of contact force and block displacement to those before had been generated, this being achieved through optimisation of the time-step. The dynamic relaxation program was also slightly more economical to run, with approximately 150 CP secs of execution time (c.f. 180 CP secs for static relaxation) required for 100 iterations. Figure 4.7 shows the dynamic relaxation results and the consolidated states of both relaxation techniques are seen to be almost identical.

The force and displacement conditions existing after an equivalent period of block removal are presented in Table 4.2 and Figure 4.8. Again, there is a marked

CONSOLIDATION OF MINE DESIGN PROBLEM USING DYNAMIC RELAXATION

CORNER FORCE PLOT  NUMBER OF PROBLEM UNITS PER INCH = 15.564041619

CYCLE NUMBER = 700  SCALE . 1 INCH = _____



CONSOLIDATION OF MINE DESIGN PROBLEM USING DYNAMIC RELAXATION

INCREM.DISPL.PLOT  NUMBER OF PROBLEM UNITS PER INCH = 0.000002496

CYCLE NUMBER = 700  SCALE . 1 INCH = _____

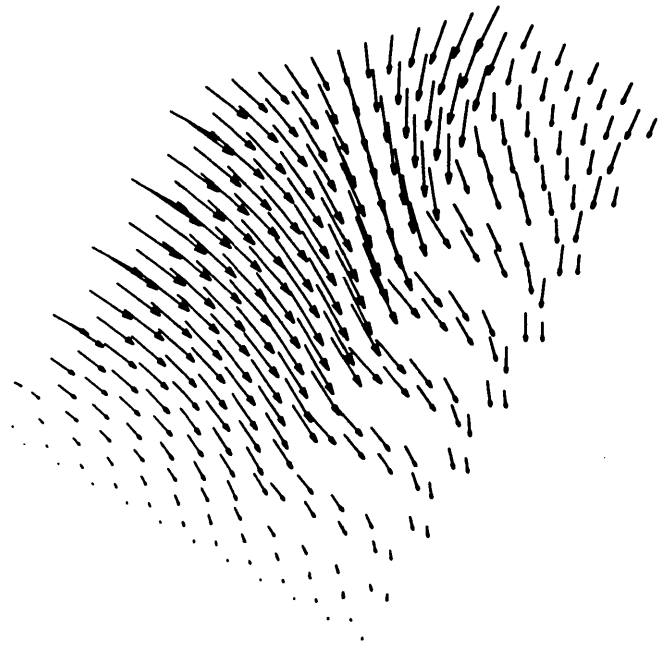


Figure 4.7

CONSOLIDATION OF MINE DESIGN PROBLEM USING DYNAMIC RELAXATION

TOTAL DISPL.PLOT NUMBER OF PROBLEM UNITS PER INCH = 0.002564064

CYCLE NUMBER = 700 SCALE . 1 INCH = _____

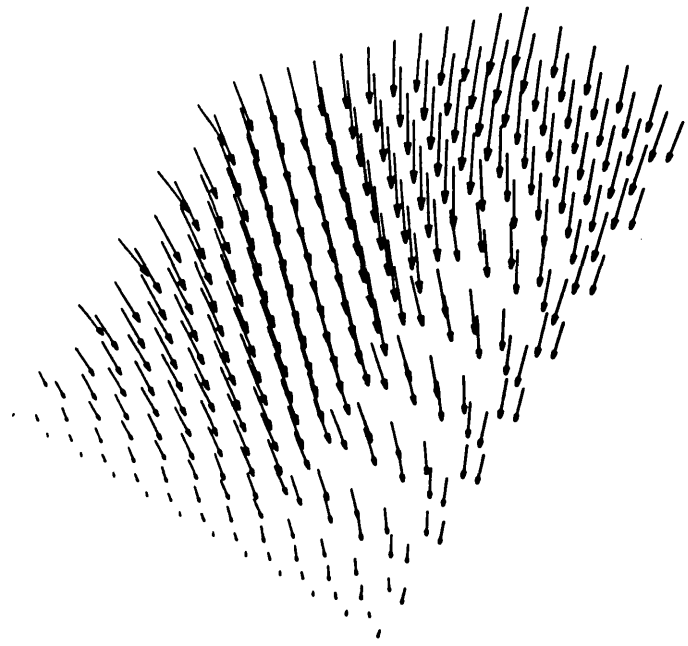


Figure 4.7 contd.

MASS BLASTING SIMULATION WITH DYNAMIC RELAXATION. 0-250 CYCLES RESTART

CORNER FORCE PLOT NUMBER OF PROBLEM UNITS PER INCH = 18.015200720

CYCLE NUMBER = 950 SCALE . 1 INCH = _____

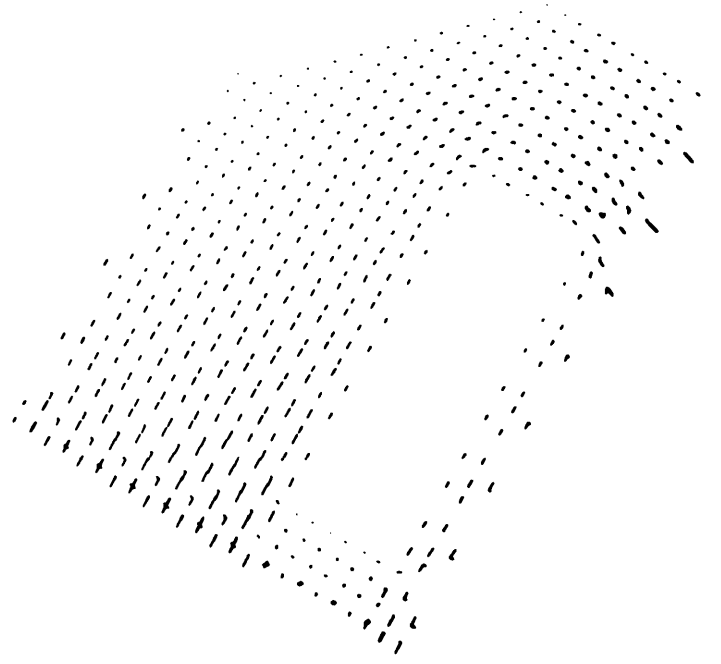
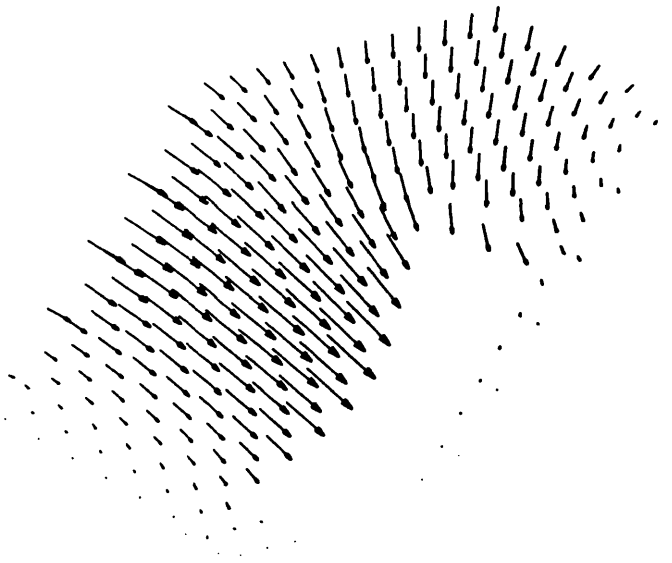


Figure 4.8

MASS BLASTING SIMULATION WITH DYNAMIC RELAXATION. 0-250 CYCLES RESTART

INCREM.DISPL.PLOT NUMBER OF PROBLEM UNITS PER INCH = 0.000002822

CYCLE NUMBER = 950 SCALE . 1 INCH = _____



MASS BLASTING SIMULATION WITH DYNAMIC RELAXATION. 0-250 CYCLES RESTART

TOTAL DISPL.PLOT NUMBER OF PROBLEM UNITS PER INCH = 0.000882676

CYCLE NUMBER = 950 SCALE . 1 INCH = _____

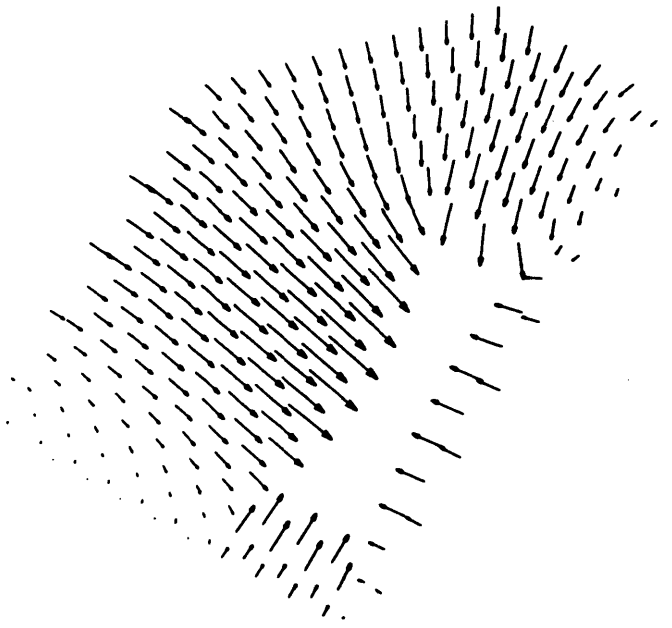


Figure 4.8 contd.

similarity between the force and displacement distributions produced by both relaxation techniques.

Table 4.2: MASS BLASTING RESULTS WITH DYNAMIC RELAXATION

| iteration number | $max^m$. contact force magnitude | $max^m$. cumulative resultant translation |
|---|---|---|
| 700 | 3.89 | 0.00 |
| 750 | 3.86 | 4.72 E-04 |
| 800 | 4.03 | 6.66 E-04 |
| 850 | 4.20 | 9.88 E-04 |
| 900 | 4.36 | 1.28 E-03 |
| 950 | 4.50 | 1.57 E-03 |

The displacements listed in Table 4.2 indicate that the hangingwall is unstable, the force and displacement magnitudes after 950 iterations being between 6% and 7% higher than those in Table 4.1. This is due to the larger forces existing at the end of consolidation with dynamic relaxation. The same potential hangingwall failure zone is delineated in the displacement plot of Figure 4.8.

The author was fortunate to be associated with base friction studies of underground openings in jointed media conducted by May (1979). Although these studies involved much larger deformations than those generated by the numerical models, some interesting correlations concerning the initial behaviour could be made. A jointed configuration containing an opening similar to that shown in Figure 4.6 was examined using the base friction method. The failure mechanism of the hangingwall, shown in Figure 4.9, involved buckling and collapse into the excavation of the first five columns. The displacements of these same columns define the potentially unstable hangingwall zone in Figures 4.6 and 4.8. The initial base friction response of the hangingwall was a progressive inwards deflection of the immediate columns accompanied by opening along both joint sets, these features also being identified in the numerical simulations.

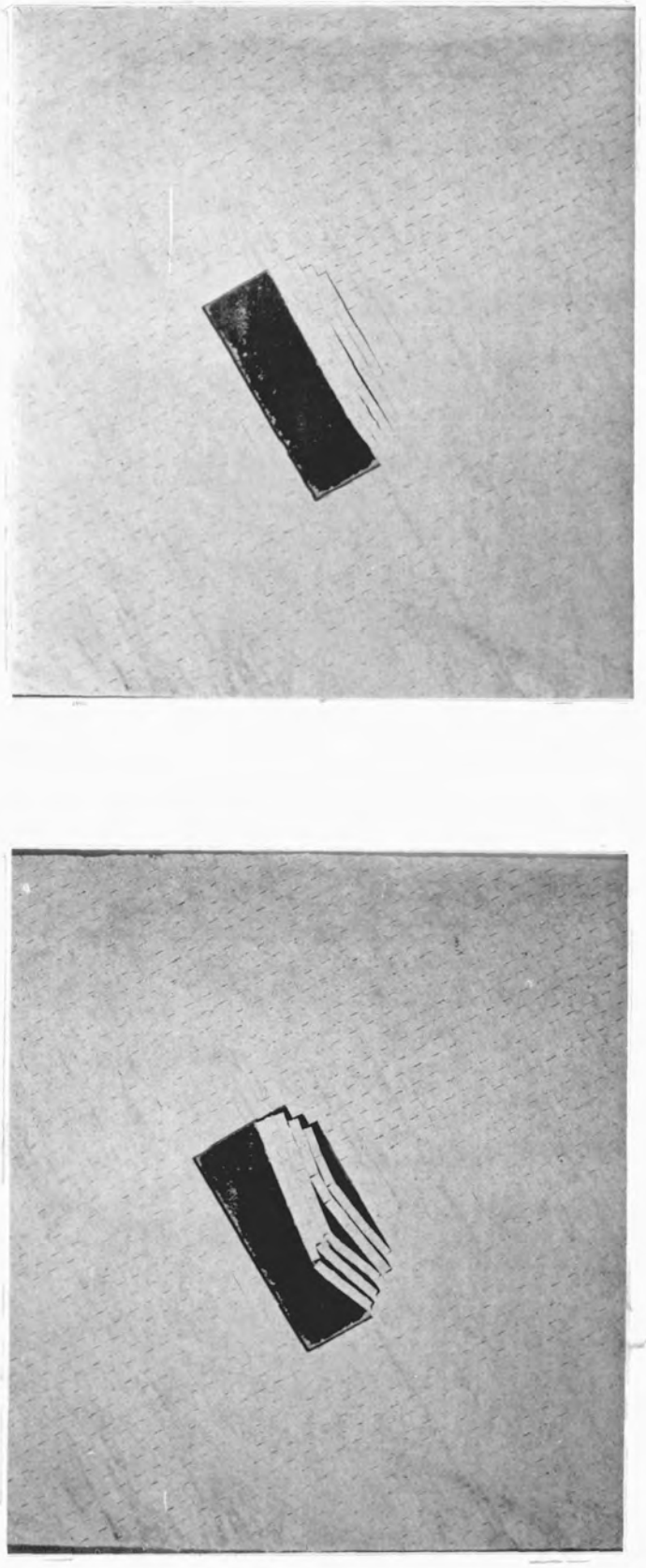


Figure 4.9: Base friction model study.

To simulate the open-stoping method of mining using the numerical model, the opening was created in three stages. The friction coefficient was set to 0.577 upon restarting and the central column of four blocks was extracted first to generate a cut-off slot. After 50 iterations the slot was widened by removing the two adjacent columns and after a further 100 iterations the opening was extended to its full size and the problem run until a total of 950 iterations had been achieved. The three stages of block removal are illustrated in Figure 4.10 and the results during this particular extraction sequence are tabulated in Table 4.3. A comparison between Tables 4.1 and 4.3 reveals that the results from mass blasting and open stoping after equivalent periods of execution time are very similar, suggesting that

Table 4.3: OPEN STOPING RESULTS

| iteration number | $max^m$. contact force magnitude | $max^m$. cumulative resultant translation |
|---|---|---|
| 700 * | 3.64 | 0.00 |
| 750 ** | 3.66 | 6.21 E-04 |
| 800 | 3.73 | 9.76 E-04 |
| 850 *** | 3.83 | 1.44 E-03 |
| 900 | 3.99 | 9.54 E-04 |
| 950 | 4.25 | 1.23 E-03 |

* cut-off slot created

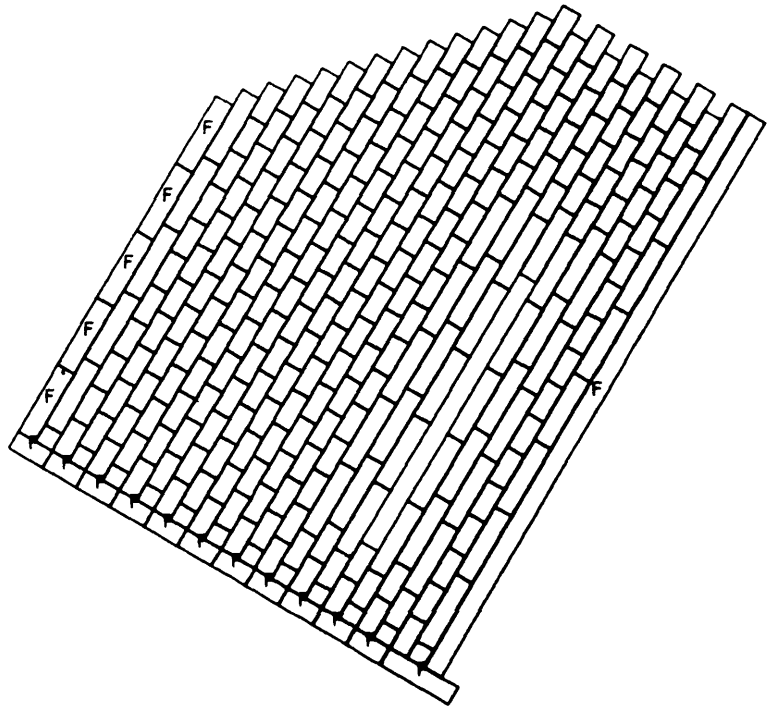
** opening three columns wide

*** opening full size

the ultimate response of the country rock for this particular problem is not greatly influenced by the mining method. Also, the force and displacement plots from open stoping are in close agreement with those from mass blasting.

Another mining method commonly encountered in tabular orebodies is cut-and-fill mining. To examine the behaviour of the country rock due to this mining method, the block extraction sequence shown in Figure 4.11 was modelled. Groups of blocks were progressively extracted up-dip in a

REMOVING BLOCKS GRADUALLY TO SIMULATE OPEN STOPING.0-250 CYCLES RESTART
BLOCK PLOT NUMBER OF PROBLEM UNITS PER INCH = 16.67
ITERATION NUMBER = 750 SCALE . 1 INCH = ———




REMOVING BLOCKS GRADUALLY TO SIMULATE OPEN STOPING.0-250 CYCLES RESTART
BLOCK PLOT NUMBER OF PROBLEM UNITS PER INCH = 16.67
ITERATION NUMBER = 800 SCALE . 1 INCH = ———

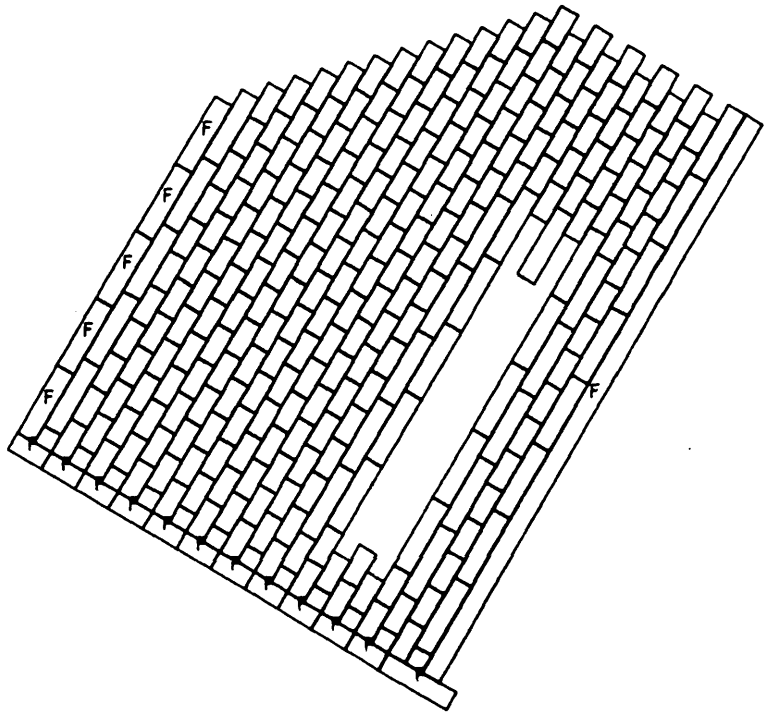
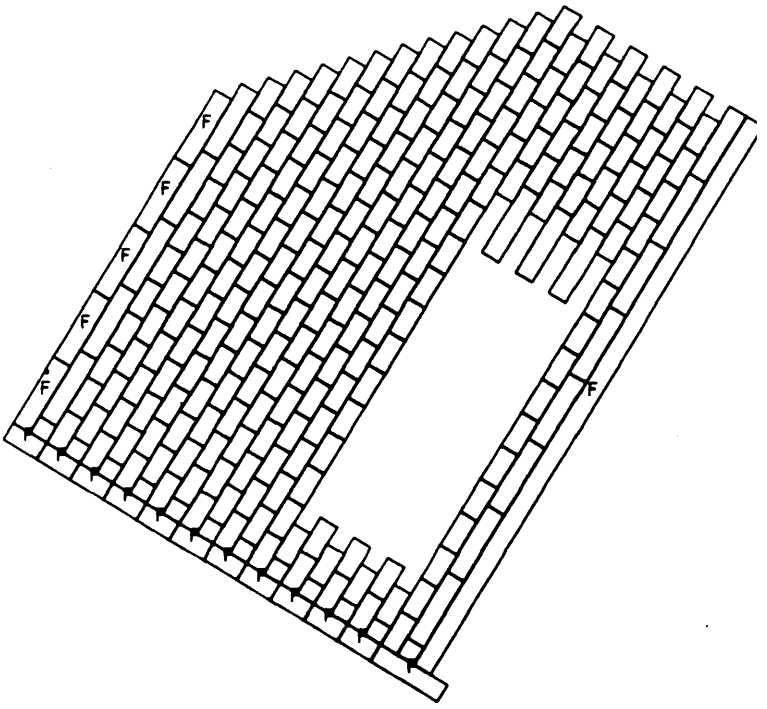



Figure 4.10

REMOVING BLOCKS GRADUALLY TO SIMULATE OPEN STOPING.0-250 CYCLES RESTART
BLOCK PLOT NUMBER OF PROBLEM UNITS PER INCH = 16.67
ITERATION NUMBER = 950 SCALE . 1 INCH = _____




REMOVING BLOCKS GRADUALLY TO SIMULATE OPEN STOPING.0-250 CYCLES RESTART
CORNER FORCE PLOT NUMBER OF PROBLEM UNITS PER INCH = 17.01077423
ITERATION NUMBER = 950 SCALE . 1 INCH = _____

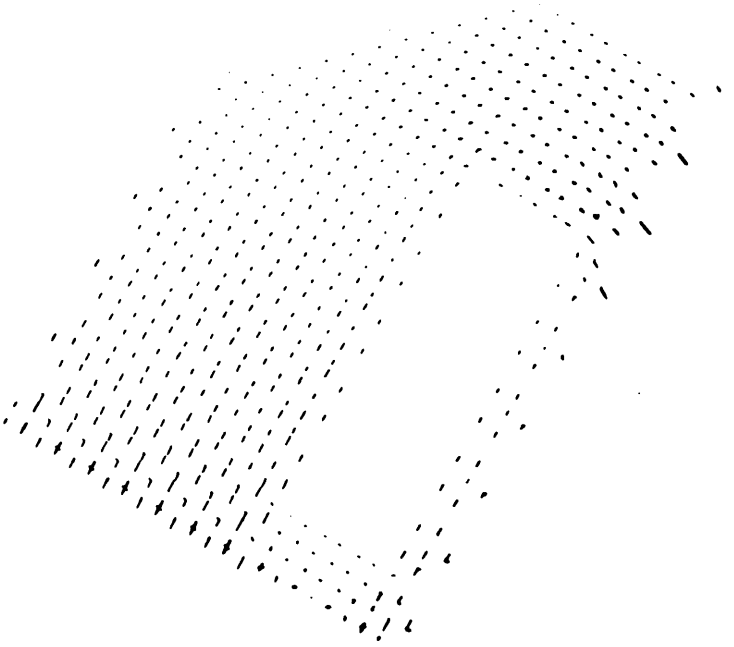
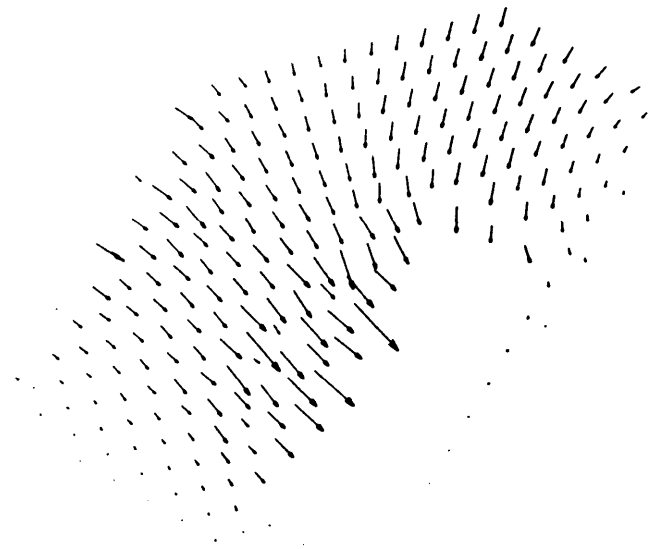


Figure 4.10 contd.

REMOVING BLOCKS GRADUALLY TO SIMULATE OPEN STOPING.0-250 CYCLES RESTART
INCREM.DISPL PLOT NUMBER OF PROBLEM UNITS PER INCH = 0.00000709
ITERATION NUMBER = 950 SCALE . 1 INCH = _____



REMOVING BLOCKS GRADUALLY TO SIMULATE OPEN STOPING.0-250 CYCLES RESTART
TOTAL DISPL PLOT NUMBER OF PROBLEM UNITS PER INCH = 0.00123208
ITERATION NUMBER = 950 SCALE . 1 INCH = _____

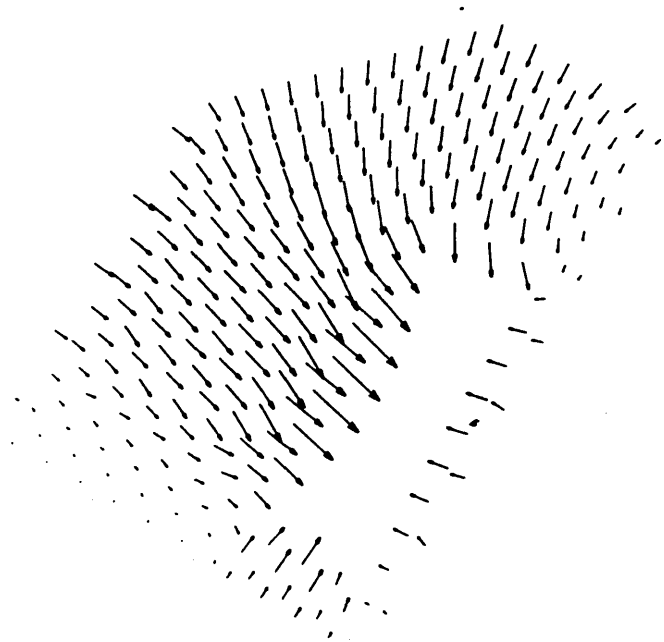


Figure 4.10 contd.

series of five stages, with an interval of 50 iterations between each stage. The same consolidation file as for mass blasting and open stoping was used, the friction coefficient being set to 0.577 at the restart.

The resulting behaviour for 250 calculation cylces after restarting is presented in Table 4.4 and Figure 4.11. Again, there are no significant deviations in the resulting behaviour to suggest that cut-and-fill mining is preferable to either mass blasting or open stoping.

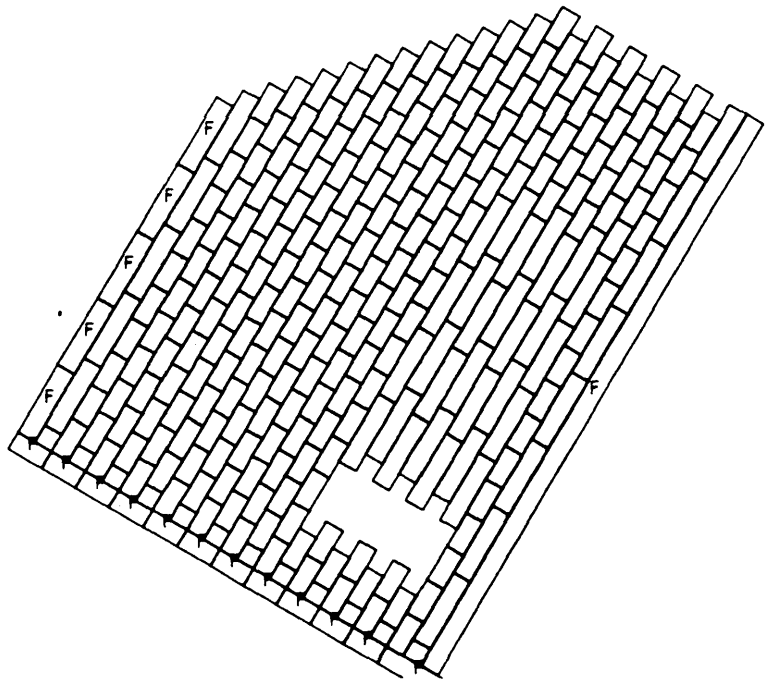
Table 4.4: UP-DIP CUT-AND-FILL RESULTS

| iteration number | $max^{m}$. contact force magnitude | $max^{m}$. cumulative resultant translation |
|---|---|---|
| 700 | 3.64 | 0.00 |
| 750 | 3.70 | 5.76 E-04 |
| 800 | 3.78 | 5.79 E-04 |
| 850 | 4.01 | 5.97 E-04 |
| 900 | 4.22 | 8.03 E-04 |
| 950 | 4.43 | 1.05 E-03 |

However, the total displacement plot at iteration 950 indicates that the block displacements have been influenced by the particular mining sequence since the displacements in the immediate hangingwall have a significant down-dip component. This is not surprising since the lower section of the opening controls the behaviour of the hangingwall over a longer portion of the test and where slip along the joints occurs, it would be unreasonable to expect a displacement distribution similar to that from the alternative mining methods. The consequence of having the opening at its full size for only 50 iterations is a 28% decrease in the maximum resultant translation compared with mass blasting and a 3.5% increase in the maximum contact force.

An interesting comparison with the cut-and-fill method described above was to reverse the block extraction sequence to simulate the highly improbable case of a down-dip cut-

REMOVING BLOCKS GRADUALLY TO SIMULATE CUT-AND-FILL MINING.0-200 CYCLES RESTART
BLOCK PLOT NUMBER OF PROBLEM UNITS PER INCH = 16.67
ITERATION NUMBER = 750 SCALE . 1 INCH = _____




REMOVING BLOCKS GRADUALLY TO SIMULATE CUT-AND-FILL MINING.0-200 CYCLES RESTART
BLOCK PLOT NUMBER OF PROBLEM UNITS PER INCH = 16.67
ITERATION NUMBER = 800 SCALE . 1 INCH = _____

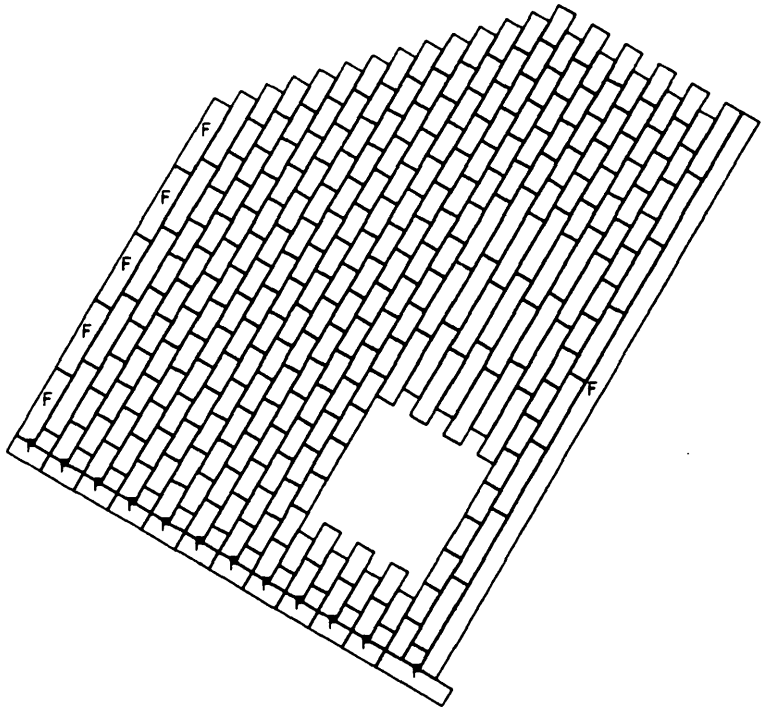
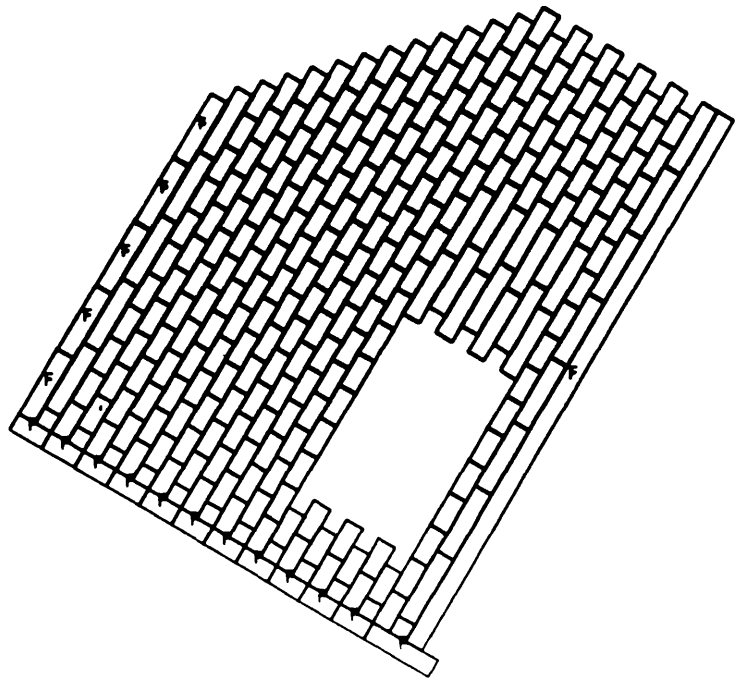



Figure 4.11

REMOVING BLOCKS GRADUALLY TO SIMULATE CUT-AND-FILL MINING.0-200 CYCLES RESTART
BLOCK PLOT NUMBER OF PROBLEM UNITS PER INCH = 16.67
ITERATION NUMBER = 850 SCALE . 1 INCH = _____



REMOVING BLOCKS GRADUALLY TO SIMULATE CUT-AND-FILL MINING.0-200 CYCLES RESTART
TOTAL DISPL PLOT NUMBER OF PROBLEM UNITS PER INCH = 0.00059721
ITERATION NUMBER = 850 SCALE . 1 INCH = _____

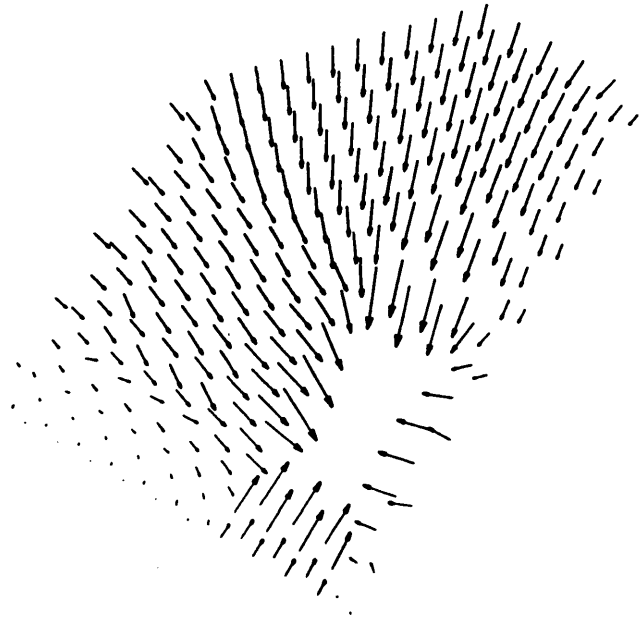
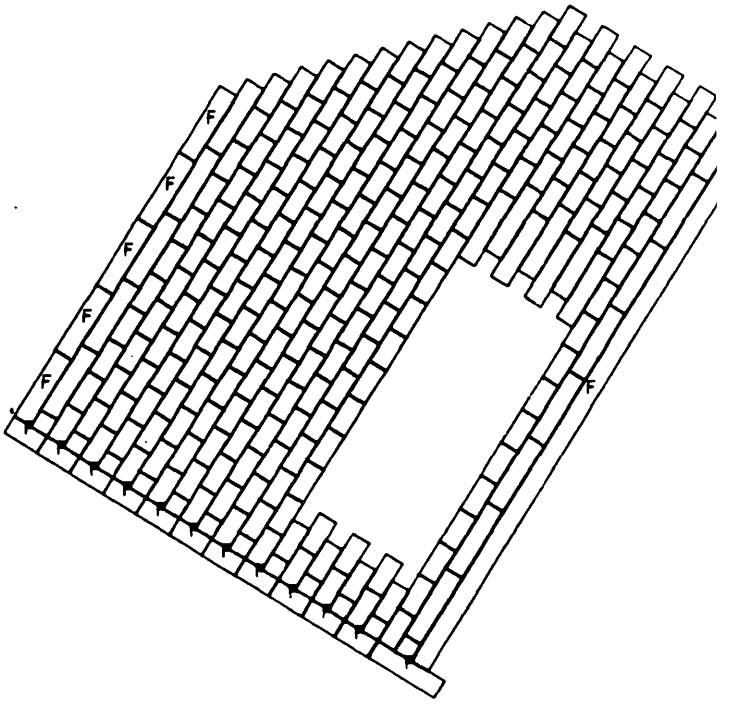


Figure 4.11 contd.

REMOVING BLOCKS GRADUALLY TO SIMULATE CUT-AND-FILL MINING.0-200 CYCLES RESTART
BLOCK PLOT NUMBER OF PROBLEM UNITS PER INCH = 16.67
ITERATION NUMBER = 900 SCALE . 1 INCH = _____




REMOVING BLOCKS GRADUALLY TO SIMULATE CUT-AND-FILL MINING.200-250 CYCLES RESTART
BLOCK PLOT NUMBER OF PROBLEM UNITS PER INCH = 16.67
ITERATION NUMBER = 950 SCALE . 1 INCH = _____

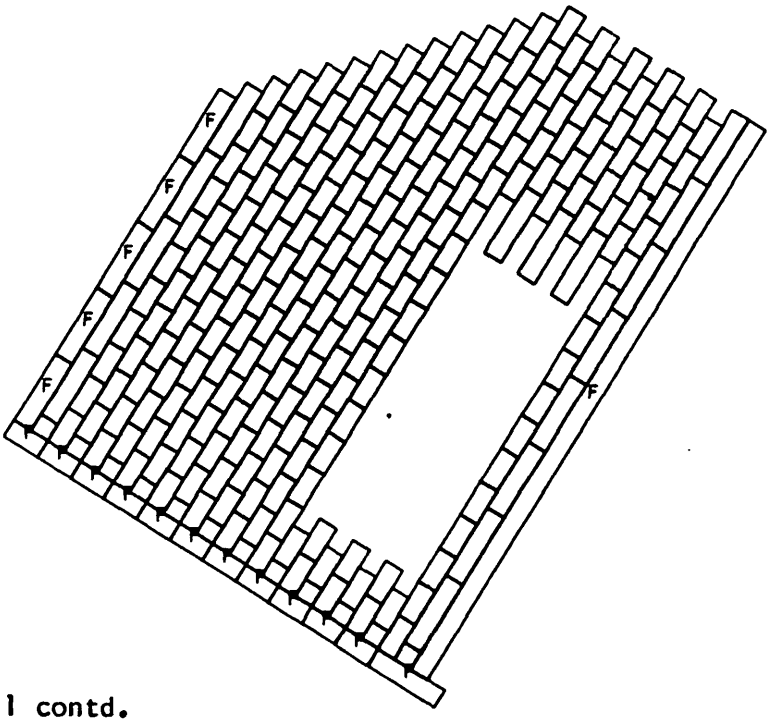
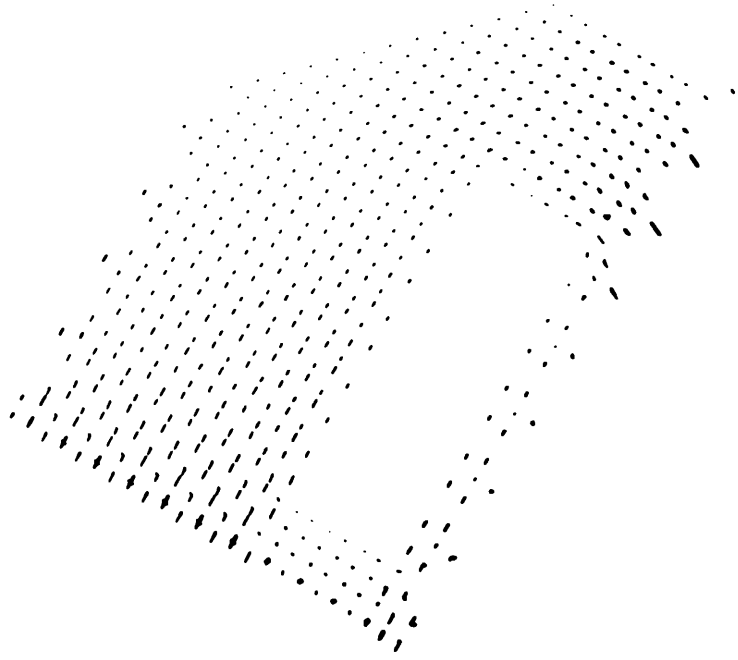



Figure 4.11 contd.

REMOVING BLOCKS GRADUALLY TO SIMULATE CUT-AND-FILL MINING.200-250 CYCLES RESTART
CORNER FORCE PLOT NUMBER OF PROBLEM UNITS PER INCH = 17.71668374
ITERATION NUMBER = 950 SCALE . 1 INCH = _____



REMOVING BLOCKS GRADUALLY TO SIMULATE CUT-AND-FILL MINING.200-250 CYCLES RESTART
TOTAL DISPL PLOT NUMBER OF PROBLEM UNITS PER INCH = 0.00104837
ITERATION NUMBER = 950 SCALE . 1 INCH = _____

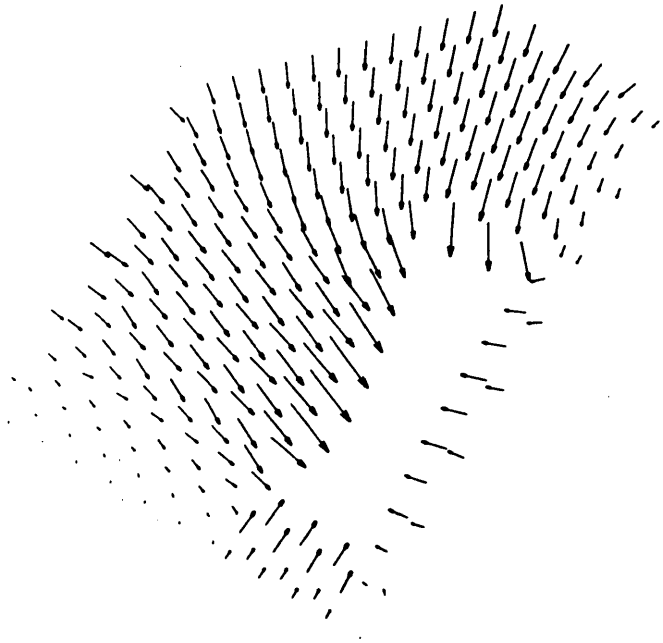


Figure 4.11 contd.

and-fill mining operation. Each stage of block removal was again performed in intervals of 50 iterations, and the results at the end of the 250 iterations subsequent to consolidation are presented in Table 4.5 and Figure 4.12. The contact force and cumulative displacement magnitudes after 250 iterations are almost identical for both cut-and-fill extraction sequences but the slight variations in the

Table 4.5: DOWN-DIP CUT-AND-FILL RESULTS

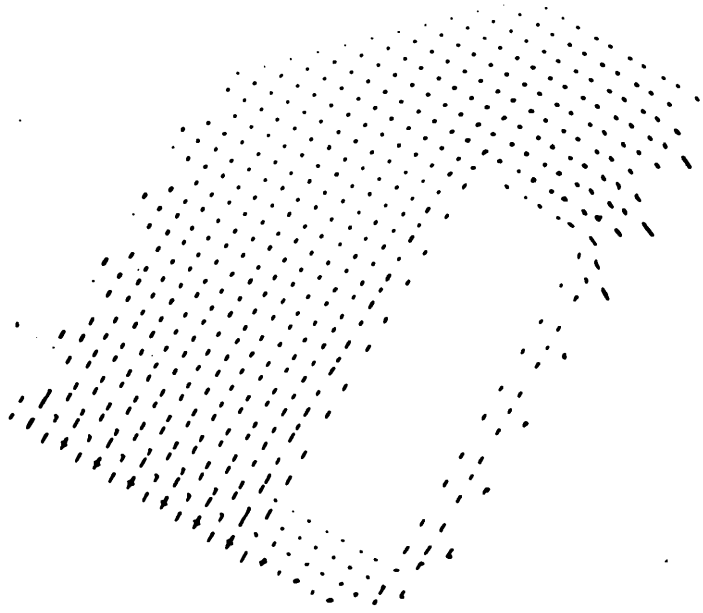
| iteration number | $max^m$. contact force magnitude | $max^m$. cumulative resultant translation |
|---|---|---|
| 700 | 3.64 | 0.00 |
| 750 | 3.69 | 1.37 E-04 |
| 800 | 3.60 | 4.47 E-04 |
| 850 | 3.93 | 6.30 E-04 |
| 900 | 4.18 | 7.77 E-04 |
| 950 | 4.42 | 1.03 E-03 |

force and displacement magnitudes indicate that the final behaviour is path dependent. In contrast to the up-dip extraction sequence, the largest opening closures are now located in the upper hangingwall.

To examine the effect of an increase in depth on the resulting behaviour, forces were applied to the edges of external blocks. The five blocks along the left-hand boundary were freed and external forces of magnitude ten times the block weight were applied to these blocks and to the blocks located at the top of each column. Equal loads were applied at both corners of the block edges. This resulted in a horizontal to vertical pressure ratio of 0.5. The system of blocks was consolidated under the external loading and self weight for 300 iterations, restarting from the original consolidation file, and an updated consolidation file was saved for later restarting. The physical properties were the same as in the previous examples.

For the tests under external loading, the presence

REMOVING BLOCKS GRADUALLY DOWN-DIP TO SIMULATE CUT-AND-FILL MINING
CORNER FORCE PLOT NUMBER OF PROBLEM UNITS PER INCH = 17.69282122
ITERATION NUMBER = 950 SCALE . 1 INCH = _____



REMOVING BLOCKS GRADUALLY DOWN-DIP TO SIMULATE CUT-AND-FILL MINING
TOTAL DISPL PLOT NUMBER OF PROBLEM UNITS PER INCH = 0.00103457
ITERATION NUMBER = 950 SCALE . 1 INCH = _____

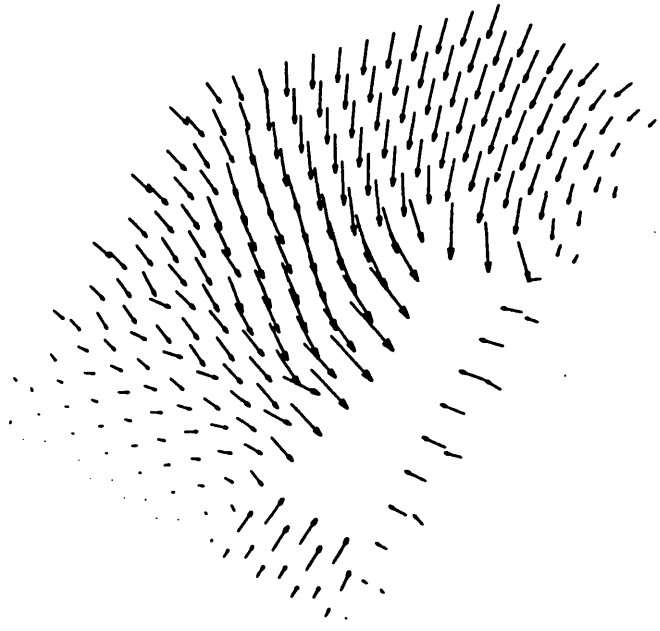


Figure 4.12

of the problem boundaries close to the openings is likely to influence the results and hence this limitation should be recognised when assessing the results. The influence of the external forces was examined by initially mass blasting for 200 iterations. The results for this are reproduced in Table 4.6 and Figure 4.13 (a). In contrast to the self weight case, movements of approximately equal magnitude now occur in both hangingwall and crown regions. Also, the displacements show no clearly defined zone of potential hangingwall instability. The external loading has caused

Table 4.6: MASS BLASTING UNDER EXTERNAL LOADING

| iteration number | $max^m$. contact force magnitude | $max^m$. cumulative resultant translation |
|---|---|---|
| 1000 | 8.49 | 0.00 |
| 1050 | 9.24 | 7.49 E-04 |
| 1100 | 9.87 | 1.17 E-03 |
| 1150 | 10.58 | 1.56 E-03 |
| 1200 | 11.53 | 1.88 E-03 |

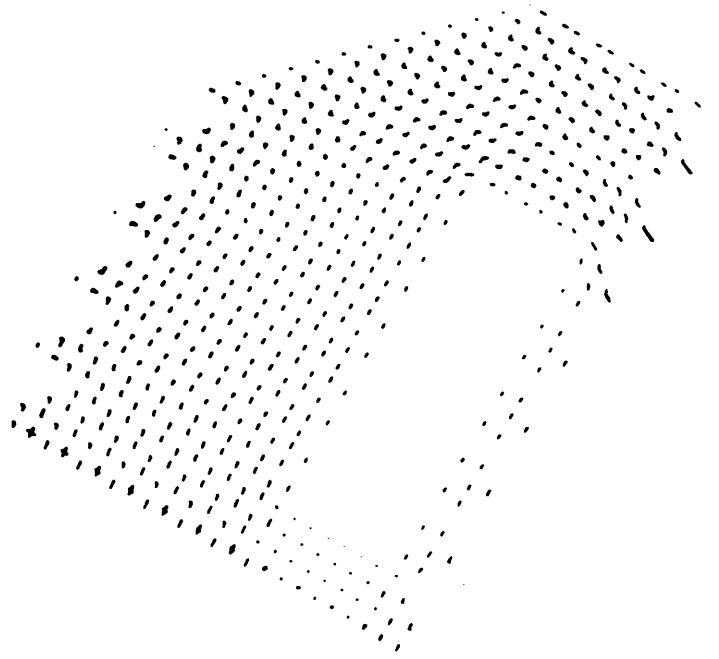
considerable down-dip displacement components as well as sub-vertical displacements for all crown blocks. A comparison with the self weight case reveals that the contact forces have increased approximately threefold while there has been less than a 100% increase in the displacement magnitudes. More importantly, however, is the steady convergence in the displacement magnitudes towards an equilibrium condition indicating increased stability over the self weight case. This stability is highlighted by the lateral thrusts observable in the force distribution of Figure 4.13(a).

The case where surrounding openings shield the crown from lateral confining pressures was simulated by reconsolidating without lateral loading being applied to the blocks located along the upper stepped boundary. As shown in Figure 4.13(b), the largest displacements for this case occur in the crown, the crown moving monolithically towards the opening by sliding along the steeply

MASS BLASTING OF SINGLE OPENING WITH EXTERNAL LOADING

CORNER FORCE PLOT  NUMBER OF PROBLEM UNITS PER INCH = 46.129186872

CYCLE NUMBER = 1200  SCALE . 1 INCH = _____



MASS BLASTING OF SINGLE OPENING WITH EXTERNAL LOADING

TOTAL DISPL.PLOT  NUMBER OF PROBLEM UNITS PER INCH = 0.001876710

CYCLE NUMBER = 1200  SCALE . 1 INCH = _____

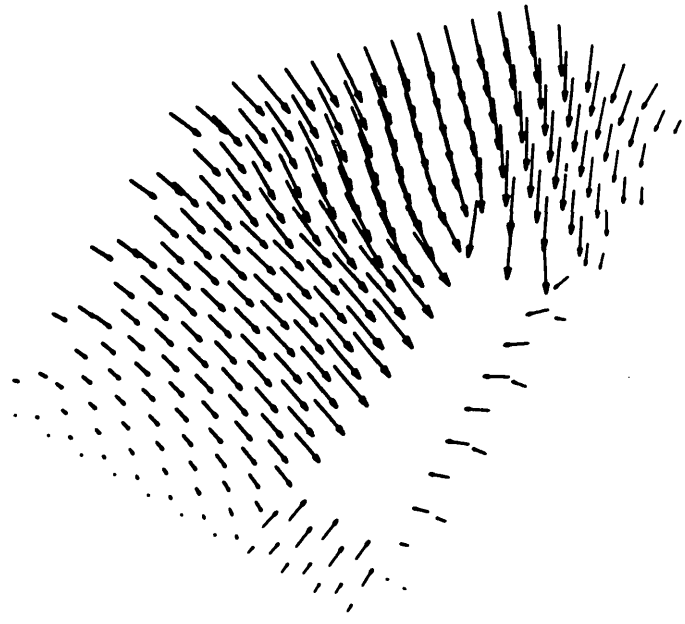
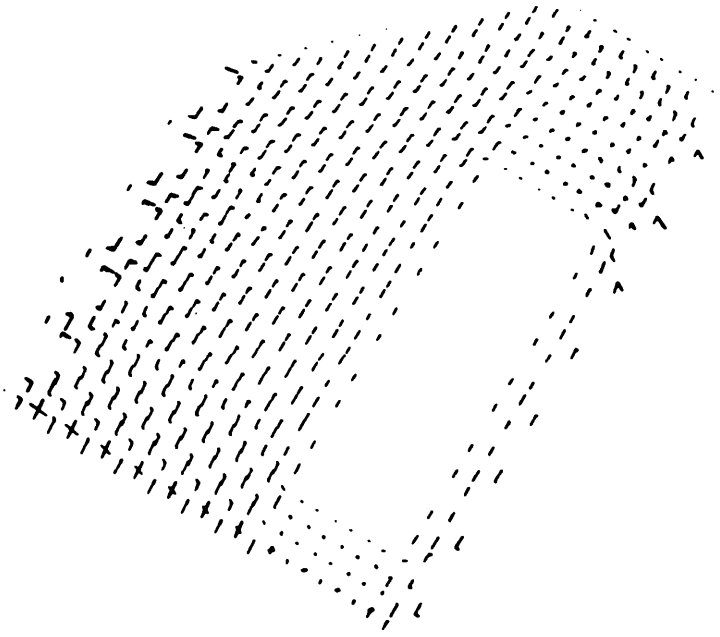


Figure 4.13a

MASS BLASTING SIMULATION UNDER EXTERNAL LOADING. 250 CYCLES RESTART
CORNER FORCE PLOT NUMBER OF PROBLEM UNITS PER INCH = 23.64851371
ITERATION NUMBER = 1200 SCALE . 1 INCH = _____



MASS BLASTING SIMULATION UNDER EXTERNAL LOADING. 250 CYCLES RESTART
TOTAL DISPL PLOT NUMBER OF PROBLEM UNITS PER INCH = 0.00253845
ITERATION NUMBER = 1200 SCALE . 1 INCH = _____

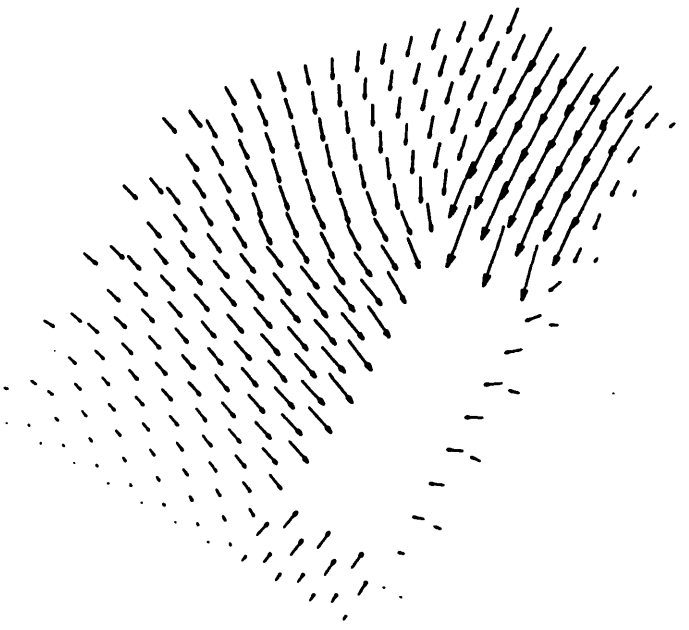


Figure 4.13b

inclined bedding planes. These large displacements arise since the crown region is in an effectively unconfined state.

The simultaneous mass blasting under full external loading of the two adjacent openings shown in Figure 4.14 was modelled for 400 iterations. The purpose of this simulation was to examine the behaviour of the rib pillar so formed. The results for this case are presented in Table 4.7 and Figure 4.14. The displacement plots illustrate the extent to which the rib pillar has been

Table 4.7: SIMULTANEOUS MASS BLASTING UNDER EXTERNAL LOADING

| iteration number | $max^m$. contact force magnitude | $max^m$. cumulative resultant translation |
|---|---|---|
| 1000 | 8.49 | 0.00 |
| 1100 | 9.81 | 1.82 E-03 |
| 1200 | 11.44 | 3.09 E-03 |
| 1300 | 13.03 | 4.26 E-03 |
| 1400 | 14.31 | 5.35 E-03 |

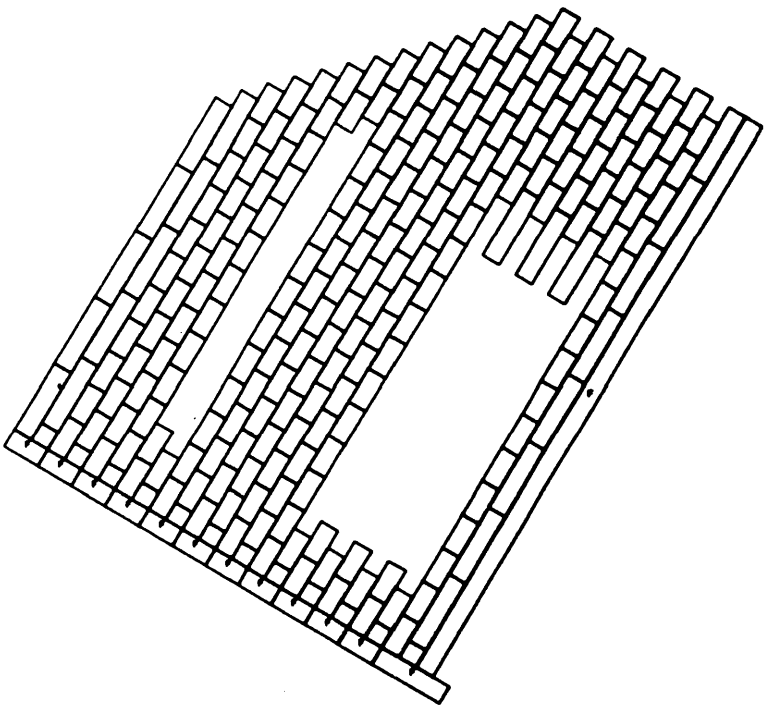
shielded from the lateral loading. The hangingwall displacements of the primary opening now have considerable down-dip components, steadily decrease in magnitude from the crown to the floor of the opening, and have magnitudes less than half those for the hangingwall of the secondary opening. Also, the contact force distribution indicates that the rib pillar is in an unconfined state with each of the seven columns acting independently of adjacent columns. In the crown above the rib pillar lateral stabilising forces are predominant and larger displacements occur in the crown of the primary stope than in its hangingwall.

As an alternative to the simultaneous mass blasting of two adjacent openings detailed above, the secondary opening was created subsequent to the initial opening. This was achieved by restarting from the file saved at the end of mass blasting of the primary opening under external

SIMULTANEOUS MASS BLASTING OF TWO ADJACENT OPENINGS WITH EXTERNAL LOADING

BLOCK PLOT NUMBER OF PROBLEM UNITS PER INCH = 16.67

CYCLE NUMBER = 1400 SCALE . 1 INCH = _____



SIMULTANEOUS MASS BLASTING OF TWO ADJACENT OPENINGS WITH EXTERNAL LOADING

CORNER FORCE PLOT NUMBER OF PROBLEM UNITS PER INCH = 57.234038481

CYCLE NUMBER = 1400 SCALE . 1 INCH = _____

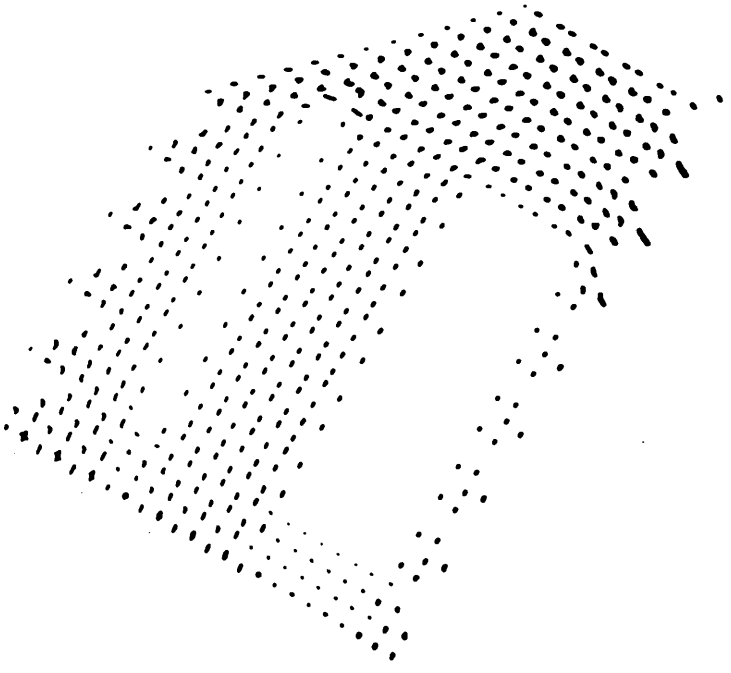
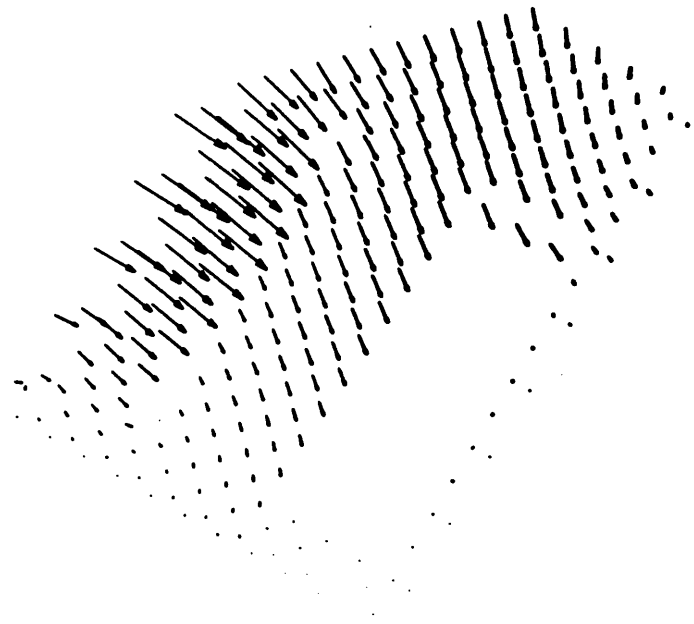


Figure 4.14

SIMULTANEOUS MASS BLASTING OF TWO ADJACENT OPENINGS WITH EXTERNAL LOADING

INCREM.DISPL.PLOT NUMBER OF PROBLEM UNITS PER INCH = 0.000010697

CYCLE NUMBER = 1400 SCALE . 1 INCH = _____



SIMULTANEOUS MASS BLASTING OF TWO ADJACENT OPENINGS WITH EXTERNAL LOADING

TOTAL DISPL.PLOT NUMBER OF PROBLEM UNITS PER INCH = 0.005352411

CYCLE NUMBER = 1400 SCALE . 1 INCH = _____

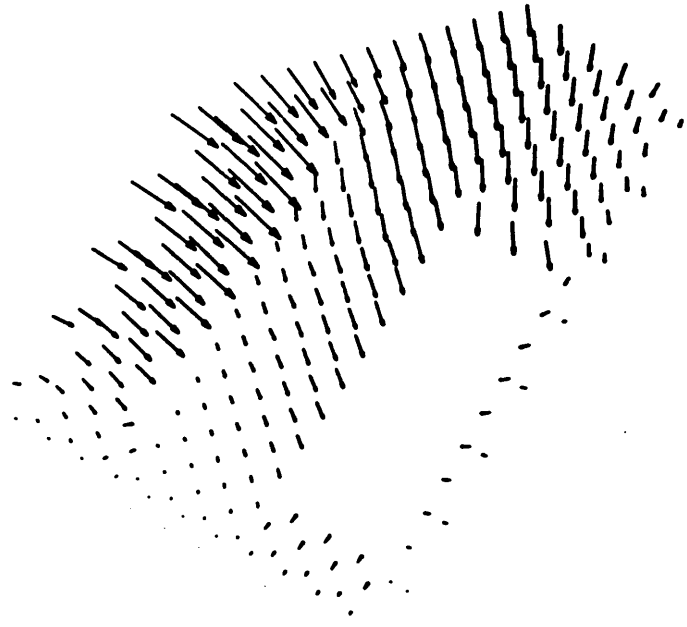


Figure 4.14 contd.

loading (Figure 4.13a). The behaviour of this model was investigated for a further 200 iterations and the results are presented in Table 4.8 and Figure 4.15. There is very close agreement between the force and incremental displacement distributions of this model and those for the simultaneous mass blasting test. The contact force magnitudes for both models deviate by less than 3%. Although the cumulative displacements subsequent to consolidation are approximately 15% smaller for this case, the cumulative displacements for the 200 iterations since the creation of the second opening are exactly half those obtained after 400 iterations of the simultaneous extraction model. There are, as expected, slight variations between the total displacement distributions for both cases.

Table 4.8: MASS BLASTING OF SECONDARY OPENING SUBSEQUENT TO PRIMARY OPENING.

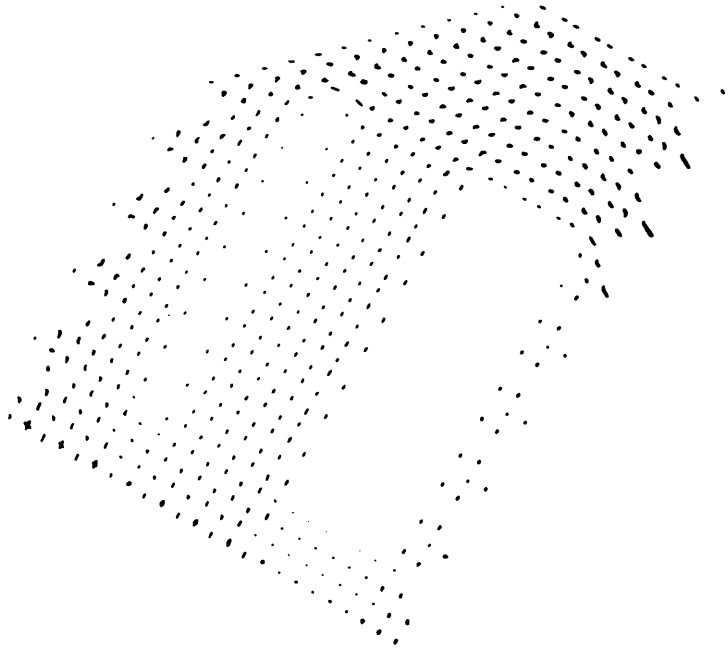
| iteration number | $max^m$. contact force magnitude | $max^m$. cumulative resultant translation |
|---|---|---|
| 1200 | 11.53 | 1.88 E-03 |
| 1250 | 12.58 | 2.50 E-03 |
| 1300 | 13.41 | 3.23 E-03 |
| 1350 | 14.11 | 3.92 E-03 |
| 1400 | 14.71 | 4.54 E-03 |

To investigate the response of a crown pillar to external loading seven overlying blocks were extracted, as shown in Figure 4.16. These blocks were removed after the 200 iterations of mass blasting of the primary opening (Figure 4.13a). The force plot of Figure 4.16 indicates that the crown pillar is capable of transmitting the lateral forces but is shielded from the effects of the forces representing the overburden load. This has increased the stability of the crown pillar although there is no evidence of arching in the immediate roof of the primary opening due to the high aspect ratio of the blocks. The crown displacements are now considerably smaller than those in the

MASS BLASTING OF ADJACENT OPENING SUBSEQUENT TO CREATION OF FIRST OPENING

CORNER FORCE PLOT  NUMBER OF PROBLEM UNITS PER INCH = 58.858587720

CYCLE NUMBER = 1400  SCALE . 1 INCH = _____



MASS BLASTING OF ADJACENT OPENING SUBSEQUENT TO CREATION OF FIRST OPENING

INCREM.DISPL.PLOT  NUMBER OF PROBLEM UNITS PER INCH = 0.000013036

CYCLE NUMBER = 1400  SCALE . 1 INCH = _____

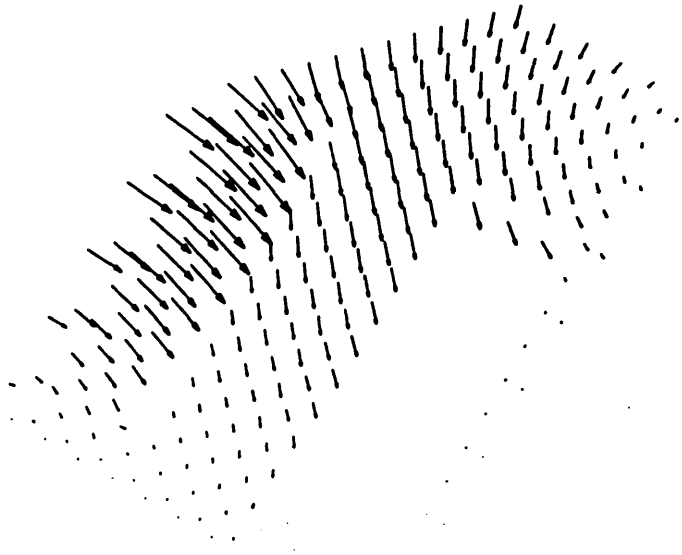


Figure 4.15

MASS BLASTING OF ADJACENT OPENING SUBSEQUENT TO CREATION OF FIRST OPENING

TOTAL DISPL.PLOT NUMBER OF PROBLEM UNITS PER INCH = 0.004543377

CYCLE NUMBER = 1400 SCALE . 1 INCH = _____

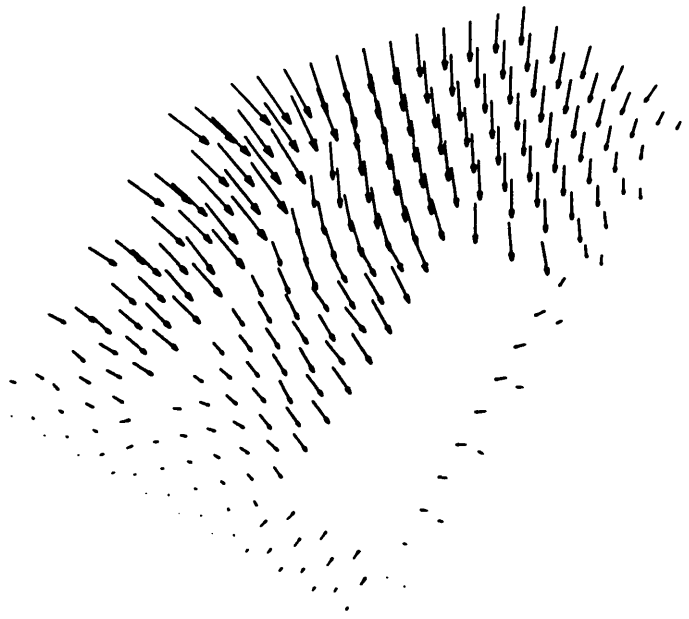


Figure 4.15 contd.

MASS BLASTING OF OVERLYING OPENING CREATING CROWN PILLAR

BLOCK PLOT NUMBER OF PROBLEM UNITS PER INCH = 16.67

CYCLE NUMBER = 1400 SCALE . 1 INCH = _____

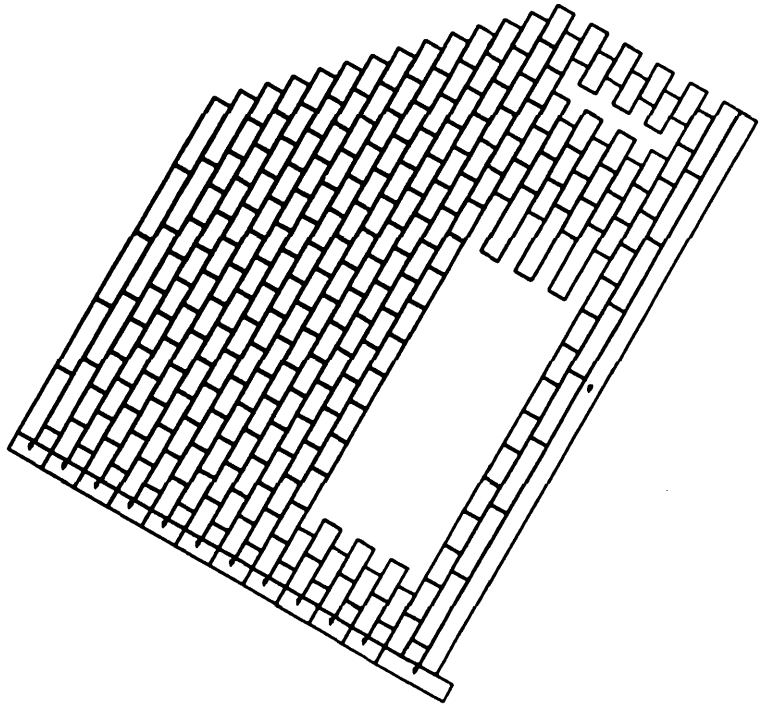
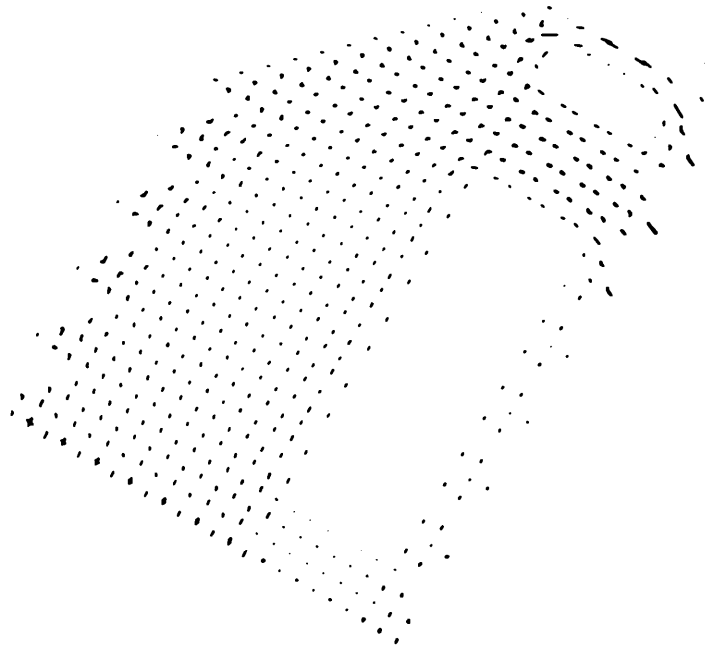


Figure 4.16

MASS BLASTING OF OVERLYING OPENING CREATING CROWN PILLAR

CORNER FORCE PLOT NUMBER OF PROBLEM UNITS PER INCH = 57.792733984

CYCLE NUMBER = 1400 SCALE . 1 INCH = _____



MASS BLASTING OF OVERLYING OPENING CREATING CROWN PILLAR

TOTAL DISPL.PLOT NUMBER OF PROBLEM UNITS PER INCH = 0.009884437

CYCLE NUMBER = 1400 SCALE . 1 INCH = _____

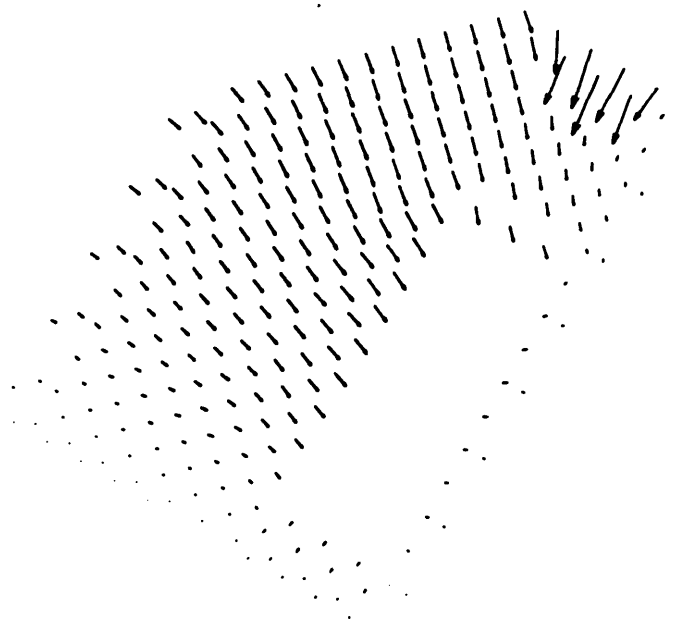


Figure 4.16 contd.

hangingwall and have been further displaced towards the footwall.

Finally, the results are presented in Figure 4.17 of tests carried out with stiffnesses differing from those used for the above tests. The behaviour of laminar structures was investigated by assigning different stiffnesses to each joint set. For the case shown in Figure 4.17(a) the ratio of the normal and shear stiffnesses for the cross-joints to those of the continuous joints was 10,000 to 1.* These conditions therefore simulated the case where only one set of jointing was predominant, namely the bedding of the steeply dipping strata. The force distribution at the completion of 200 iterations subsequent to the creation of the primary opening clearly illustrates the effect of the varying stiffnesses. All hangingwall columns are now able to accommodate considerable lateral forces while the inward displacements of blocks in the hangingwall have been reduced to approximately half those of the original mass blasting test (Figure 4.13a). Also, the inward displacements of the crown blocks are between four and five times greater than the hangingwall displacements since the stabilising forces generated by shearing along the cross-joints have been greatly reduced.

Figure 4.17(b) shows the effect of a competent zone of material in the hangingwall. Field information from Mount Isa (Lang, 1979) indicates that stronger silica dolomite intrusions in the hangingwall country rock often become exposed when the weaker jointed material between the excavation and the competent zone collapses into the opening. The competent zone was modelled by increasing the normal and shear stiffnesses by a factor of 100 for all blocks comprising the fifth hangingwall column in from the opening face. Figure 4.17(b) shows the discontinuity in displacement magnitudes either side of the competent zone with the immediate hangingwall displacement magnitudes approximately five times greater.

* $K_n = 1.0\ E+04$, $K_s = 1.0$

MASS BLASTING OF SINGLE OPENING WITH SINGULAR JOINT SET

CORNER FORCE PLOT NUMBER OF PROBLEM UNITS PER INCH = 33.974355155

CYCLE NUMBER = 1200 SCALE . 1 INCH = _____

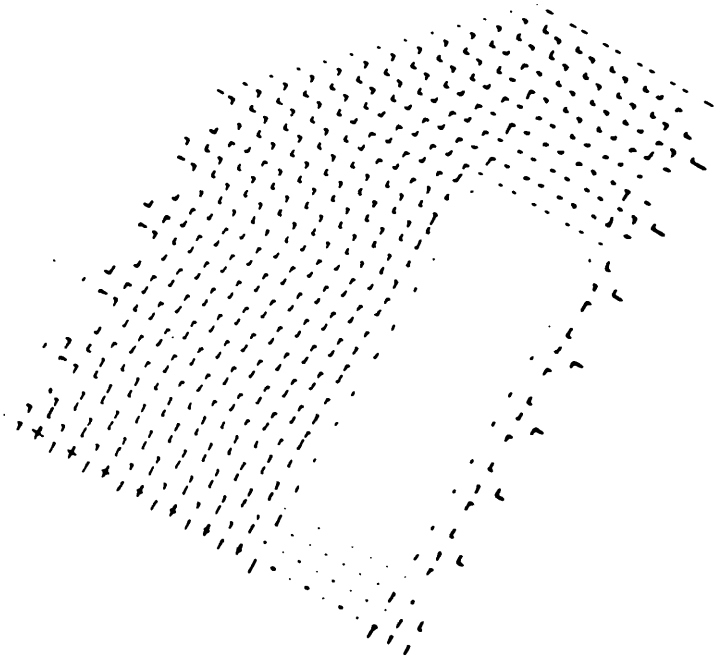


Figure 4.17a

MASS BLASTING OF SINGLE OPENING WITH FAULT ZONE IN HANGINGWALL

TOTAL DISPL.PLOT NUMBER OF PROBLEM UNITS PER INCH = 0.005119256

CYCLE NUMBER = 1200 SCALE . 1 INCH = _____

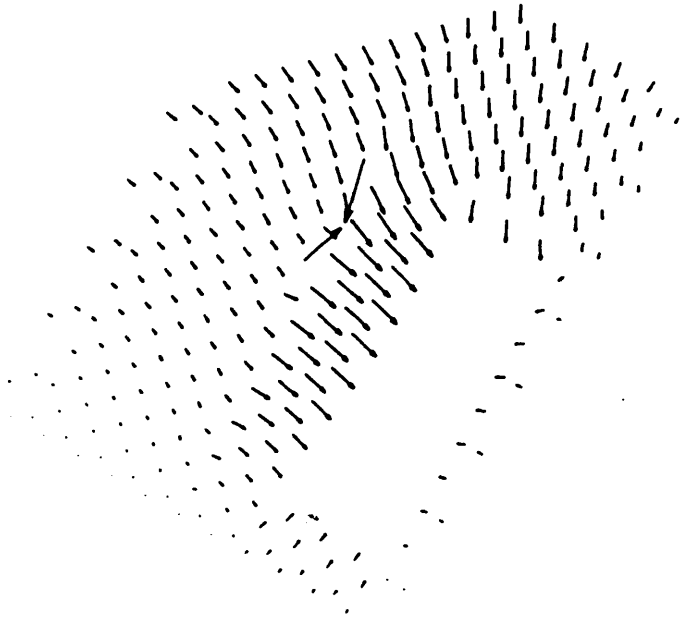


Figure 4.17b

4.3.2. Summary:

The above examples demonstrate the potential and applicability of the numerical technique to mine design. Although the examples chosen were primarily qualitative, they are of great assistance in defining possible mechanisms by which the rock mass deforms. Comparisons made with the results from dynamic relaxation and base friction studies indicate that the static relaxation method is a valid tool for aiding in mine design.

# CHAPTER 5

# *DEVELOPMENT OF A PHYSICAL MODELLING TECHNIQUE*

CHAPTER 5

# DEVELOPMENT OF A PHYSICAL MODELLING TECHNIQUE

## 5.1. Introduction:

The use of modelling techniques in certain engineering disciplines to study the response of a proposed structure to imposed conditions is by no means new. The literature is replete with examples of advanced and sophisticated models (both analytical/numerical and physical) in such fields as aerodynamics, fluid mechanics and mechanical design. Modelling techniques in these fields have developed due to factors such as the ease and accuracy of obtaining information and the economies and simplicity of model construction compared to that of any full scale field equivalent.

The development of sophisticated physical modelling techniques related to the mining industry appears to have originated during the early sixties (Barron and Larocque, 1962; Everling, 1964; Hobbs, 1966). This has been mainly due to the need for a fundamental understanding of the factors and mechanisms involved in mining rock mechanics as mining technology advances. Consequently, numerous and varied modelling techniques have been developed worldwide to assist in this understanding. The noticeable benefits in production and safety accruing from the scientific methods and principles upon which mining model studies have been based has demanded that model work in certain areas attain very advanced levels.

In the design and loading of models to study mechanisms of deformation in underground structures it is necessary to consider the type of model to use and the information required to perform the analysis. In selecting the type of model for study the choice is made between models which can be classified into the following groups (Brown and Hudson, 1972):

i) analytical models

ii) numerical models
iii) 'rigid' block mechanistic models
iv) photo-elastic models
v) material or fracture models

The above models will offer either qualitative or quantitative information which can then be used to determine the behavioural mechanisms of prototype mining structures. The amount of relevant information deriving from any model study primarily depends on

a) the degree to which properties and conditions in the prototype can be characterized by the model and
b) the sophistication of the instrumentation employed to monitor stress and deformation conditions throughout the model.

Photo-elastic models have been extensively used to determine the stress distribution in both continua and discontinua (Ergun, 1970; Chappell, 1972). With this technique, openings of any shape can be analysed and the method has been successfully applied to excavations in jointed media, highlighting some of the fundamental characteristics of jointed rock, such as slip and block rotation. However, a major disadvantage of the photo-elastic method is that no knowledge of displacements or strain in the surrounding material can be obtained.

Geomechanical model studies have assumed widespread appeal in many situations in which the determination of the behaviour of underground openings in geometrically complex situations has been sought (Heuer and Hendron, 1971; Krsmanovic and Milic, 1964; Barton, 1978). A geomechanical model is defined as one in which a scale model of the proposed underground structure is constructed in a material which accurately models the properties of the in-situ rock mass and is then loaded in such a manner as to reproduce the stress state which exists in the prototype. Such modelling requires dynamic

similitude to be closely approached if scale models are to faithfully reproduce deformation and failure of the actual geological structure. The failure to attain or adequately control some of the stringent similitude requirements has resulted in certain geomechanical model studies becoming invalid and others yielding only limited information in light of their original objectives. This highlights the fact that some modelling techniques are of limited applicability to the prediction of the behaviour of underground excavations in rock and for a rational design solution, a sound knowledge of the limitations of the particular technique employed is essential.

In this respect, the usefulness of structural and kinematic models should not be underestimated (Erguvanli and Goodman, 1972). Structural models, in which the proposed engineering structure alone is modelled without due regard to the surrounding environment, can provide valuable research and design information for such structures as arch dams. Kinematic models offer the advantage of quickly and easily identifying possible degrees of freedom and weak points of underground structures in jointed and layered rock masses, although not indicating the exact nature or magnitude of expected deformations.

Apart from physical model studies of the sort briefly outlined above, other methods currently available for analysing discontinuous, non-linear behaviour for rock excavations fall into the analytical/numerical category. No detailed description of these methods is warranted at this point, suffice to say that they play an important role if only in the fact that they appear to offer a choice in the method of analysis. However, as one becomes familiar and subsequently versatile with the various modelling techniques available, it is realised that they do in fact offer complementary approaches to the same problem, one method usually displaying the limitations or advantages of the other. It is often the

case that a complete solution to any mining design problem will only be forthcoming if some contribution from each group of techniques has been made.

Ideally, the research and design phase of any proposed engineering structure should include as many varied and suitable modelling appreciations as possible. The number and nature of modelling techniques ultimately employed depends on such factors as the importance placed on the final results and the facilities and equipment available. It is this complementary characteristic inherent in many of the available modelling techniques which becomes of great assistance in the development and subsequent validation of any new design method. It is on this basis that the physical modelling technique described in this Chapter has been developed and utilized. In order to gain further insight into both the limitations and validity of the numerical static relaxation model developed for the analysis of discontinuous rock masses, a biaxial loading apparatus was designed, constructed, calibrated and commissioned. It is the purpose of this chapter to convey the reasoning behind and the details of the development of a suitable physical modelling technique and it is intended to present the failures as well as the successes of the exercise.

## 5.2. Scope of the experimental programme:

The overall experimental programme incorporated two specific and distinct phases:

1) the development of a geomechanical model loading apparatus together with suitable modelling and experimental techniques;

2) the testing of a number of jointed models to study their behaviour and to compare such behaviour with the predictions of other independent techniques.

The first phase included the development of

(a) a suitable modelling material
(b) the design, construction and calibration of a loading apparatus, and
(c) instrumentation for quantitatively measuring the performance of the jointed models.

It should be emphasised that certain of the experimental techniques and design procedures adopted throughout the course of this first phase of the study had already been standardized and successfully proven by the work of past investigators (Hoek, 1965; John, 1969; Rosenblad, 1969; Ergun, 1970; Heuer and Hendron, 1971; Gonano, 1974) and that on no account should all of the design characteristics be considered original. Moreover, by incorporating established techniques into the overall design it was hoped to produce a practical and efficient system to assist not only the present research but also that of future investigators contemplating similar studies.

In the second phase, the behaviour of spans of openings located in discontinua was to be quantitatively examined with particular emphasis on

i) the nature and orientation of the jointing;
ii) the size, shape and number of openings;
iii) the ratio and magnitude of the applied boundary loading.

It was required that these variables should all be capable of adequate definition and control throughout the geomechanical model to enable valid comparisons to be made between the results so obtained and those of similar experiments analysed with alternative techniques, such as numerical modelling. The discrete element displacements surrounding the excavation(s) would provide the basis for comparison, these displacements being accurately determined under controlled loading conditions using a single photograph photogrammetric technique. It was believed that such comparisons would complement the validation of the

static relaxation numerical model described in Chapter 2, this being the main objective of the experimental programme. Due to the lack of data available from precise, properly controlled experimentation concerning inelastic behaviour, it was felt that the proposed experimental work would provide deeper insight and understanding into the mechanics of jointed media while at the same time yield further confidence (or otherwise) concerning the use of numerical techniques for analysing discontinua.

## 5.3. Design Requirements:

With regard to the model studies for which the loading apparatus was required, the basic requirements of the design were as follows:

i) the ability to apply uniformly distributed loads to diametrically opposing edges of dimensions 500 mm x 50 mm;

ii) to allow for sufficiently large deformations at the loaded edges with the load distribution remaining undisturbed as the loading and boundary deformations increase;

iii) that any induced shear stresses at the loaded model boundaries be kept as small as possible compared with the normal stresses;

iv) to permit failure of most model materials and some weak rocks, the rig must be capable of applying loads in the order of 450,000 N;

v) the vertical and horizontal loads should be independent and maintain a constant ratio to each other for the duration of loading;

(vi) similitude considerations were of no importance and hence no provision was required for a loading or restraint to be applied to the model faces, unless to prevent buckling;

(vii) since the model element displacements are to be measured, the model must not be obscured, nor the

instrumentation hindered, by the loading frame.

A review of the literature was then carried out, bearing in mind the above considerations, to assess the successes and limitations of loading techniques developed and employed by past researchers.

## 5.4. Review of previous work:

Geomechanical model studies have in the past had widespread appeal in many situations in which the determination of the behaviour of underground openings in geometrically complex situations has been sought. However, such studies have often been fraught with numerous problems and hence a considerable portion of the reported research has either been invalidated or must be analysed with such limitations kept in mind.

If the requirements of similitude are rigorously satisfied then the behaviour of the model simulates the prototype in all respects. However, most researchers have had to be content with a compromise between some of the more critical similitude aspects such as joint spacing (Barton, 1978; Heuer, 1971). The failure to satisfy such critical aspects of similitude as the boundary loading conditions and model material properties has generally handicapped the degree of understanding of the major factors influencing the behaviour of underground openings in rock. Model studies and experimental techniques employed in past research have, however, provided a wealth of valuable information to aid in the understanding of the performance characteristics and factors to be considered when analysing both continua and discontinua.

Techniques employed in the past to effect a uniform and frictionless transfer of load from the load source to the model boundaries can be broadly classified into three groups:

i) the solid platen method;
ii) the mechanical, load distributing method;

iii) the flexible membrane method.

Each method has met with varying degrees of success in producing a uniform and frictionless loading and, in general, the more sophisticated the loading mechanism becomes the more accurate and predictable the resulting load distribution.

The problems pertaining to the "rigid" platen loading technique are all too well known. When carefully prepared rock or model specimens are loaded either uniaxially or triaxially with the specimen ends in direct contact with steel platens, a very non-uniform stress distribution is usually induced in the vicinity of the edges due to lateral restraint. Severe interface friction losses in the order of 50% of the applied loading have been reported by Hobbs (1966), Ergun (1970), and Muller and Pacher (1965). The other main disadvantage of this system is that any relative displacement between the loading device and the model elements is unacceptable. Where some differential displacement is initiated at a model boundary, stress concentrations will be induced in the model and hence a non-uniform load distribution will result. Attempts to overcome the frictional restraint problem by lubricating the sample ends with graphite, molybdenum disulphide and other solid lubricants have been made. Ductile, low friction inserts sandwiched between the specimen edges and steel load transfer plates to allow for lateral expansion have also been introduced (Hoek, 1965; Rosenblad, 1969; Muller and Pacher, 1965). However, such techniques are limited since the possible intrusion of the lubricants into pores and cracks on the specimen surface coupled with the extrusion (plastic flow) of the low modulus insert gives rise to radial tensile stresses which induce longitudinal splitting of the specimen (Rosenblad, 1969; Gonano, 1974). With such mechanisms it is virtually impossible to effect a complete load transfer with no friction loss and most researchers have been forced to accept friction losses in the order of 5% to 10% of the applied normal load (Heuer and Hendron, 1971; Ergun, 1970).

A more promising approach to the end effects problem has been the development and use of brush platens (Brown and Gonano, 1974; Ergun, 1970). By utilizing numerous slender steel loading pads placed between the model and the loading source, the end restraint problem is completely suppressed since any lateral deformation of the specimen is accompanied by bending of the loading pads. In this respect, it is surprising that the brush platen technique has experienced only limited use in studies requiring uniform load application, one possible reason being the expense and effort entailed in producing suitable platens. The inability to adequately control the load distribution in the 'rigid' platen technique has plagued many promising geomechanical model studies, and has consequently resulted in the development of more suitable loading mechanisms.

A widely accepted and proven technique to overcome the major difficulties encountered using solid platens involves a mechanical, load distributing mechanism. With this method, (in principle similar to brush platens), load is transferred from the source (e.g. hydraulic jacks) to the continuous or discontinuous model by means of a pyramid of increasingly larger stacks of loading elements (Heuer and Hendron, 1971; Rosenblad, 1969; Hoek, 1965; Gonano, 1974). At the boundaries of discontinuous models, each loading element ideally bears against only one constituent model element. Hence, the problem of interface friction is largely overcome since each model element and loading platen pair are free to rotate, translate and/or displace in an axial direction independently. Experience has shown that for two-dimensional model loadings involving large boundary deformations, the mechanical load distributing mechanism will maintain an acceptable uniform load distribution in the vicinity of the model boundaries. However, the manufacturing of and restraints required for these loading elements generally result in an expensive and somewhat complicated loading apparatus with associated complexities in design and difficulties in locating component malfunctions.

An alternative mechanical loading system in which each model element located along the model boundaries is loaded directly from the load source, rather than from a network of progressively smaller loading elements, offers considerable advantages (Jagger, 1967; Barron and Larocque, 1962; Everling, 1964). This method of load transfer formed the basis of the loading system adopted in this study.

There have been several reported attempts at utilizing the third technique of load transfer, namely the transmission of load to the model edges via flexible membranes (Moore, 1966; John, 1969; Ergun, 1970). While appearing to offer an attractive alternative to the relatively complicated mechanical loading mechanisms described above, they too can experience serious difficulties and shortcomings. A loading apparatus incorporating flexible membranes is often limited by the small pressures that it can apply and by the restricted nature of the boundary deformations it can withstand before the membranes rupture. John (1969) reports on flexible loading pads made from a rubberised fabric capable of a maximum working pressure of about 0.3432 MPa and although the pads were covered on both sides by double layers of a low friction insert (Teflon), it was not possible to eliminate friction between the pressure pads and the experimental system. Ergun (1970) developed a much more versatile and rugged loading system incorporating flexible membranes which demonstrated excellent loading characteristics even for high pressure work (up to 55 MPa). His design employed the novel technique of utilizing slender steel loading pads (similar to brush platens) to transmit pressure from the rubber membrane to the model. The considerable, and as yet non-standardized, effort entailed in the manufacture of such seals, together with the suspect nature of some of the quoted differential movements attainable by such an apparatus, provided sufficient justification for selecting a mechanical loading mechanism for loading the discontinuous

models in this particular study.

## 5.5. Design philosophy for the loading apparatus:

For the particular design of loading apparatus needed to fulfil the objectives of this study, there existed a certain degree of inflexibility since several of the design considerations were already inherently prescribed if compatibility was to be maintained between the physical model and its numerical counterpart. The numerical model had been developed for two-dimensional, plane stress situations and hence these same conditions must be duplicated by the loading apparatus if meaningful comparisons and results were to be extracted. It is pertinent at this stage to note that the two-dimensional model for jointed media is equivalent to the unfavourable situation in which an excavation is created with its long axis parallel to the strike of the predominant joint set and that in model tests designed to simulate prototype conditions, a plane strain condition is almost mandatory. However, for the model tests designed here to duplicate conditions in and verify particular numerical experiments, a plane stress condition was preferable since this was the situation which existed in the numerical model. It is important to realise that this was the premise upon which the loading apparatus was designed, i.e. to duplicate conditions compatible with the numerical model and not necessarily to simulate the behaviour of the field prototype. However, the philosophy was to keep the design as flexible as possible to facilitate adaptation if required at a later stage or by future researchers.

Designing the loading apparatus in this manner actually overcomes some of the more difficult aspects in traditional geomechanical design since, for example, similitude no longer becomes of real concern providing that the model material properties have been sufficiently well characterized. Nonetheless, it is still considered beneficial to be able to relate the physical model tests,

however crudely, to field prototype conditions, if only to determine the extent of deviation of the physical model from its full scale equivalent.

One of the first, and perhaps most difficult of all the design decisions to be made, concerned the optimum model size. Certain factors, such as ease of measurement and instrumentation, suggested that 'large' scale models would be preferable (Ergun, 1970; Heuer and Hendron, 1971), whilst other factors such as construction time, efficiency of production of model material and more importantly economic considerations generally tended to favour 'smaller' model sizes (Hoek, 1965; Gonano, 1974). After much deliberation and some preliminary calculations concerning buckling stability, the type of loading, the reaction frame necessary to resist the loads and economic implications, the loading apparatus was designed so as to accommodate discontinuous models having in-plane dimensions of 500 mm square and allowing a maximum out-of-plane thickness of 50 mm. Previous research (Ergun, 1970; Gonano, 1974) has shown that such slab or plate-shaped models, in which the out-of-plane dimension is an order of magnitude less than in-plane dimensions, greatly assist in the attainment of uniform load conditions on the model edges or faces.

Another decision of prime importance concerned the nature of the boundary loading. A uniform normal load distribution together with the absence of large shearing forces along the model boundaries is an essential prerequisite in order to ensure a known stress state throughout the model. This was, in fact, considered to be the factor of paramount importance in the design and as such deserved due recognition if maximum benefit was to derive from subsequent work. A mechanical load distributing system whereby each individual loading element connected directly to a separate hydraulic cylinder was the loading mechanism adopted for this study.

Economic considerations, together with the equipment facilities already available, will largely determine the ultimate design of any loading apparatus. It was thought that the loading system adopted for this study would be capable of meeting the necessary design specifications of applying a uniform load to all four lateral sides of the model and yet allow freedom of movement at the boundaries.

The inherent necessity for a plane stress condition in the loaded model indicated that a biaxial loading system would suffice. It was decided that the load should be actively applied to all four lateral sides rather than loading the model on two adjacent sides and pushing it against a passive reaction on the opposing sides, as has frequently been employed in the past (Muller and Pacher, 1965; Gonano, 1974). Such a directly loaded system ensures that loading symmetry is maintained, and that any friction present between the model and the loading platens is equally disposed about subsequent excavations. It should be borne in mind that previous designs incorporating similar biaxial loading systems have often met with limited success, displaying such undesirable secondary effects as out-of-plane slabbing and shearing failures due to induced loads. In situations where it is required that failure be governed by the stress concentrations existing around model excavations, it has often been necessary in the past to modify certain designs and incorporate a restraint normal to the plane of the model i.e. to apply a plane strain condition (Hoek, 1965; Ergun, 1970; Gonano, 1974). The necessity for a plane strain condition usually applies to model studies of excavations in continuous media and presents added complexity to the design as well as hindrance to subsequent instrumentation and measurements. For the proposed series of opening tests to be conducted in discontinuous media, it was considered that such secondary effects would be suppressed and that a biaxial, plane stress loading system should adequately fulfil the

design requirements.

The other major design consideration for the loading system was that it be sufficiently flexible i.e. be able to maintain a constant load distribution under quite severe boundary deformations. Although large, irregular boundary deformations were not anticipated, some degree of flexibility in the loading system was required due to the likely possibility of the zone of influence of any reasonably sized opening in a discontinuous model extending to at least some of the loaded boundaries. A design to inhibit boundary deformations would result in either model dimensions of an intolerably large magnitude or place a severe restriction on the size of permissible model openings, both of which would limit the proposed program of experiments. Hence, some compromise was necessary and a flexible loading system was required.

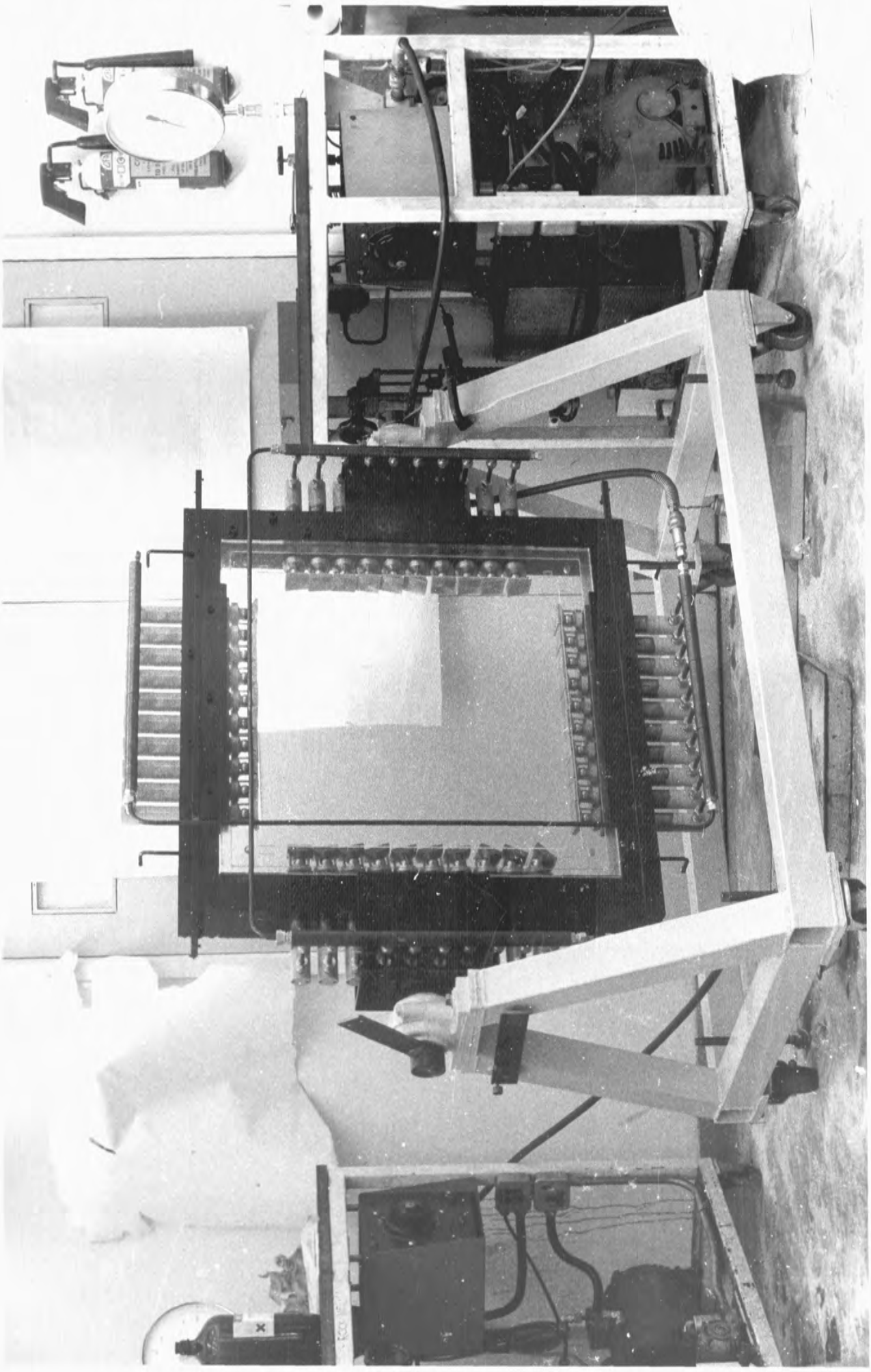
## 5.6. Model Loading Apparatus:

An overall view of the loading apparatus is shown in Figure 5.1.

### 5.6.1. Loading Mechanism:

The loading mechanism chosen to meet the design specifications is a completely mechanical one whose basic features are similar to those systems adopted by previous investigators (Hoek, 1965; Rosenblad, 1969; Gonano, 1974; Hobbs, 1966; Heuer and Hendron, 1971). The system consists of a network of forty hydraulic loading cylinders (jacks) of which ten are housed in series along each of the four component members of the outer reaction frame, as illustrated in Figure 5.2. All cylinders are identical Enerpac 5 tonne jacks (Model RC-55) capable of operating at pressures up to 70 MPa. Each 'push-type' jack is of a single-acting, solid plunger design with a 133 mm stroke. Each jack has an effective pressure area of 640 sq.mm., a collapsed height

Figure 5.1: Overall view of loading apparatus



of 216 mm, and a cylinder outside diameter of 38 mm. The jacks are self-retracting. Each jack plunger connects directly to a loading element, the platen device threading into the internal $\frac{3}{4}$-16 UNF plunger thread for a thread depth of 16 mm.

The loading apparatus was designed to accommodate discontinuous models 500 mm square by 50 mm thick. The ten hydraulic jacks located along each member of the outer reaction frame are capable of applying a total maximum force of 0.445 MN to any one particular model edge. For a model element thickness of 50 mm, this represents a maximum principal in-plane field stress of approximately 18 MPa. Obviously, a reduction in the maximum model thickness will accordingly increase the transmitted pressure applied to each model edge. This maximum available pressure of 18 MPa for 50 mm thick models was considered more than adequate for the experimental model studies. The unconfined compressive strength of the model material was approximately 25 MPa and applied pressures well below the maximum available were envisaged if elastic deformations of the model constituents were to be kept to a minimum. This was an essential prerequisite for the validation of the numerical model. However, to maintain the versatility of the loading apparatus, jacks of sufficient order were incorporated to ensure failure of most model materials and some weak rocks, but the apparatus would be severely restricted in its ability to test strong competent rock or its equivalent, and this would most likely entail a complete redesign.

### 5.6.2. Loading Platens:

The loading platen units, each of which connects directly to a hydraulic jack, are shown schematically in Figure 5.3. The spatial distribution of the loading platens is seen in Figure 5.2. Each platen has rectangular base dimensions of 50 mm by 48.3 mm, enabling

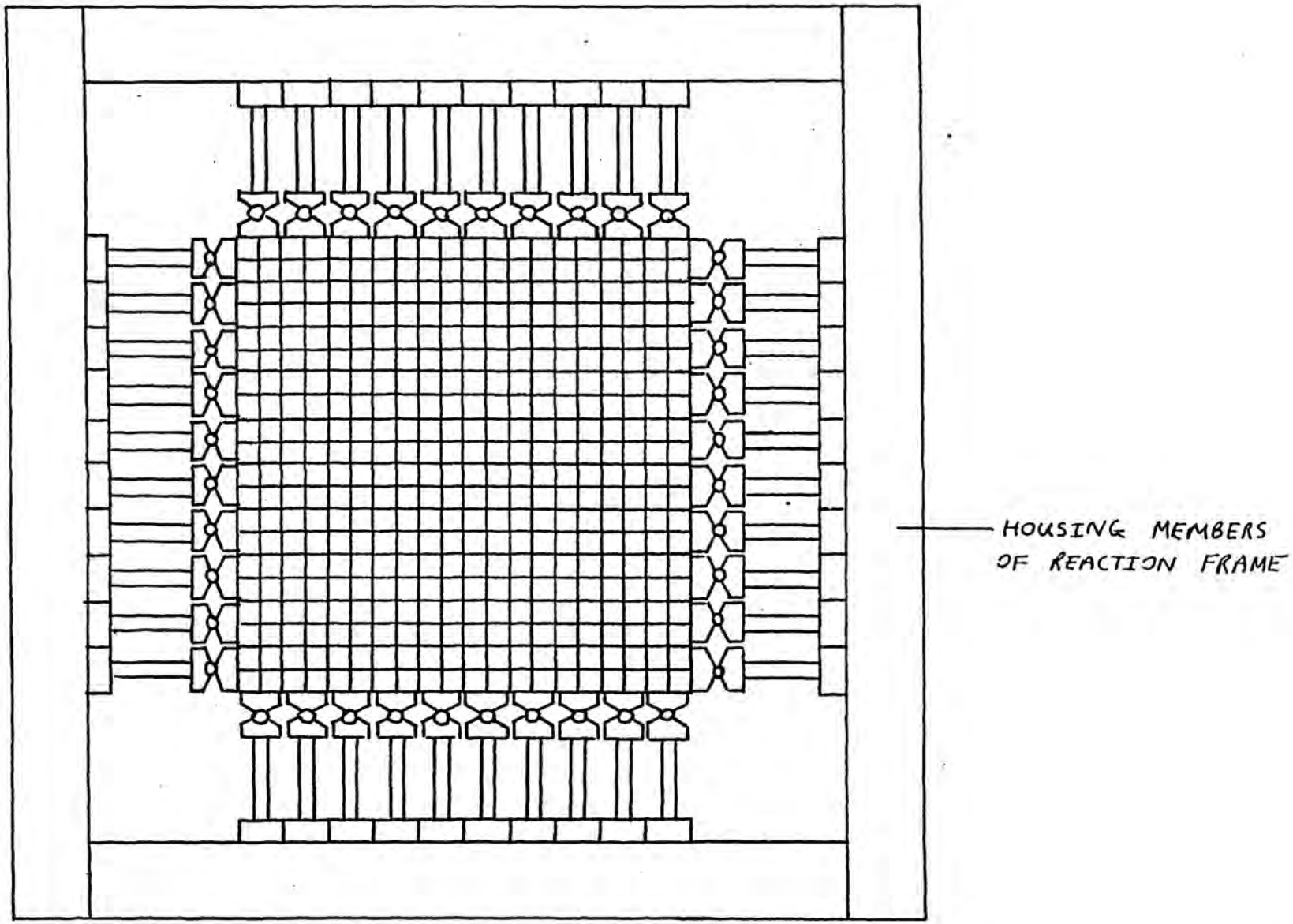



Figure 5.2: Biaxial Loading Apparatus Showing Platen-Model Loading Arrangement.

the platens to be positioned along each model edge in a manner similar to that shown in Figure 5.2. Interference between opposing platens at the corners of the model is not a problem since these platens have a 3 mm steel shim attached to their base. The components have been designed to allow a 2 mm gap between adjacent platens along any one edge, thus affording complete freedom of movement (in-plane) to each platen. With such an arrangement, each platen assembly is in direct contact with two complete 25 mm by 50 mm boundary model elements (Figure 5.2) or three offset elements. Although not an ideal load distributing mechanism in situations where large differential boundary movements between adjacent elements are likely, the compromise mechanism proved successful for the series of model experiments undertaken.

The problem of induced shear stresses along each model edge due to lateral movement between the loading platens and the boundary model blocks has been largely overcome by the incorporation of a pin-jointed mechanism (via a 25 mm dia. ball-bearing) between the jack plunger and platen-model interface, Figure 5.3. Each platen and set of model blocks which it bears against are thus free to move as a unit with the pin-joint eliminating any turning moments since the line of action of the axial load always passes through the same point. Shear stresses will still arise due to the angle of obliquity of the line of action, but for the amount of lateral movement anticipated in the experimental tests, the magnitude of such stresses could be tolerated without significantly affecting the load distribution.

The loading platens shown in Figure 5.3 were manufactured from EN31 high strength, case-hardening steel with accurate machining to the required dimensions. The 25 mm dia. ball-bearings, also manufactured from EN31 steel, were chosen to provide a large enough bearing area at the contacts to prevent local yielding of the steel

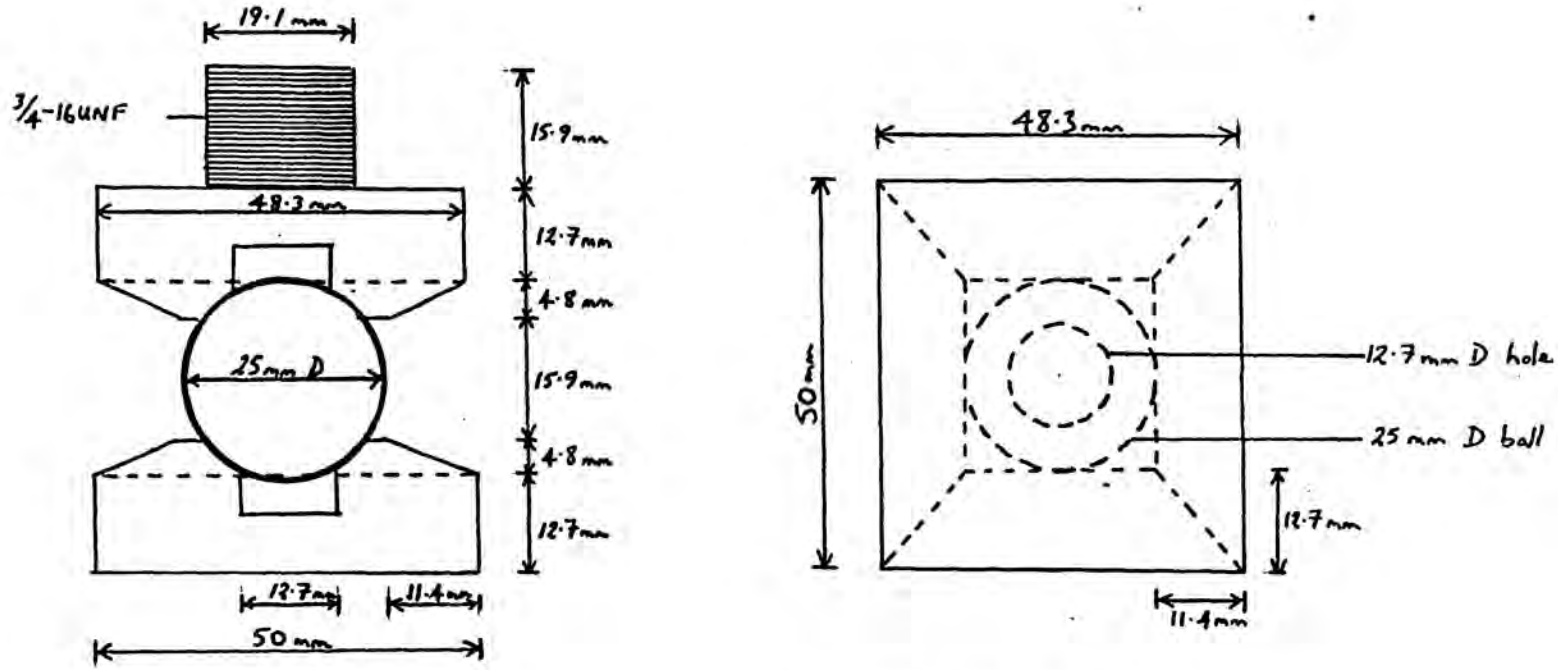



Figure 5.3: Loading Platen Assembly

under high contact stresses. Although relatively high contact stresses can arise in these areas, the machined components were maintained in their "soft" condition. It was not considered worthwhile to carry out surface hardening of the platens for the range of testing pressures anticipated. However, prior to testing strong rock material, the platens should undergo a heat treatment process.

Some support was desirable between each jack plunger-contact platen pair to prevent component damage in the unlikely event of a complete collapse of the experimental model. This support, provided by means of three flexible steel springs (38 mm long, 5 mm O.D.) evenly spaced around the platen circumference, ensured free component movement as well as greatly simplifying the loading procedure. A layer of polytetrafluroethylene self-adhesive low friction tape (known commercially under the trade names "Teflon" or "PTFE") was applied to the base of the contact platens. The tape (50 mm wide, 0.1 mm thick, and with a friction coefficient of about .05) was found to be necessary to ensure adequate load transfer from the load source to the model. This is detailed further in Section 5.7.2.

5.6.3. Reaction Frame:

The planar, outer reaction frame housing the necessary number of jacks was constructed from four 75 mm x 75 mm square section EN3B mild steel bars. The four central housing sections are braced at the corners via 75 mm x 20 mm rectangular section EN3B mild steel outer plates. Each housing section contains ten 38 mm diameter circular holes drilled 75 mm deep, the jack housing holes being spaced at 50 mm intervals along the axis of each bar. Mounting brackets constructed from EN8 mild steel plate are bolted to the inner side of each bar, the diameter of the threaded hole in each bracket flush with the housing hole. The specifications and

arrangement of the mounting brackets are shown in Figures 5.2 and 5.4. The collars of the hydraulic jacks thread into the $1\frac{1}{2}$-16 UN-2B thread on the mounting brackets, ensuring that under general loading conditions the reaction frame is mostly in tension.

A prototype mounting bracket was initially tested by loading a housed hydraulic cylinder as near to its specified maximum capacity as possible before any component failure was detected. The mounting bracket withstood the maximum load capacity of the hydraulic jack without any visual distortion to either the bracket, housing section, bolts or jack thread. On the basis of this test, the complement of mounting brackets were then manufactured. The mounting brackets also enabled the removal and replacement of individual jacks without completely dismantling a particular housing section. Each hydraulic jack station and attachments were individually numbered to facilitate ready reassembly.

High tensile strength bolts (Unbrako type, 12 mm BSW x 112 mm long) connected the central housing sections with the outer steel plates at the four corners of the reaction frame. The bolts had to be capable of withstanding the combined effects of tensile and shear behaviour, the exact nature of the bolt action depending on the magnitude and type of loading applied to the model. Some problems were encountered in the preliminary testing of the assembled apparatus with, in one particular case, the high tensile bolts failing completely at one corner (see Section 5.7.4).

To minimise bending stresses in the reaction members and, in some instances, to provide adequate representation for the field prototype or to control any expected failure, previous loading systems have been constructed to be as stiff as is reasonably possible. For the loading apparatus developed in this study, the reaction frame could

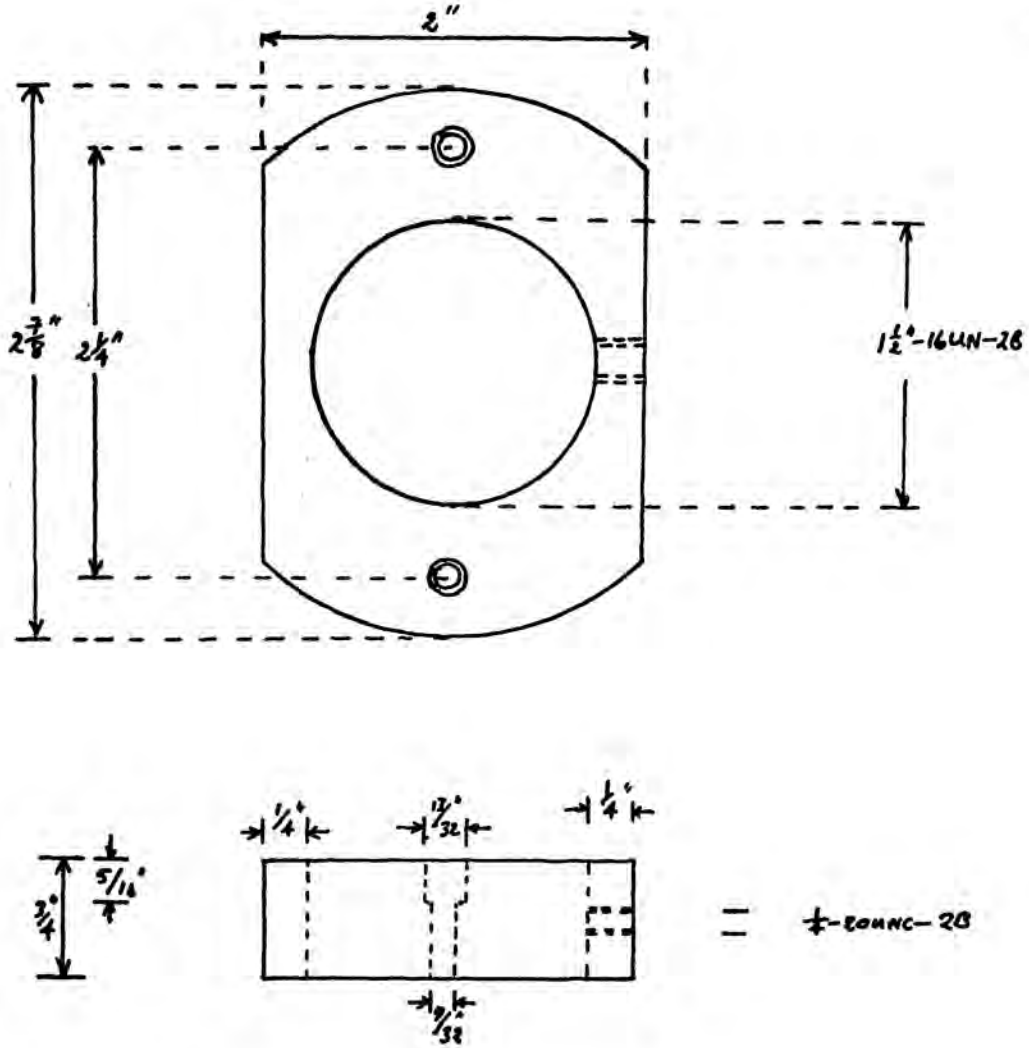



Figure 5.4: Mounting bracket specifications

have been made considerably stiffer if a rigid brace or tie-bar was used to connect the mid-points of opposing members. However, when construction and instrumentation requirements for the proposed model tests are considered, the feasibility of pursuing some of these more readily apparent modifications is limited. For the magnitude and range of operating pressures contemplated in the model studies, it was calculated that bending stresses induced in the reaction frame members would not exceed their design limits. However, it is suggested that for studies involving 'large' loading pressures, e.g. biaxial tests on competent rock, serious consideration be given to an integral rather than assembled reaction frame.

One pair of perspex windows 0.75 m square were made from a 25 mm thick clear perspex plate. The purpose of the windows was to offer protection in case of a sudden collapse of the loaded model and one plate also assisted model construction when the rig was locked horizontally. The size of the perspex windows was slightly smaller than the inner perimeter of the reaction frame, the windows fitting into this opening and held in place via brackets attached to the reaction frame.

5.6.4. Hydraulic Circuit:

The loading system was designed to operate up to a maximum hydraulic pressure of 70 MPa. At this pressure the jacks will each exert a maximum thrust of 4.5 tonnes. However, this magnitude of loading has not been realized in the model studies completed to date. The layout of the hydraulic circuit used in the biaxial loading apparatus is shown in Figure 5.5.

The hydraulic pressure was generated by two variable speed pump units, the pump in each console being driven at 1400 revolutions per minute by a 1.5 horsepower motor. The multi-piston pump was immersed in an oil reservoir and supplied the outlet line. The outlet pressure was

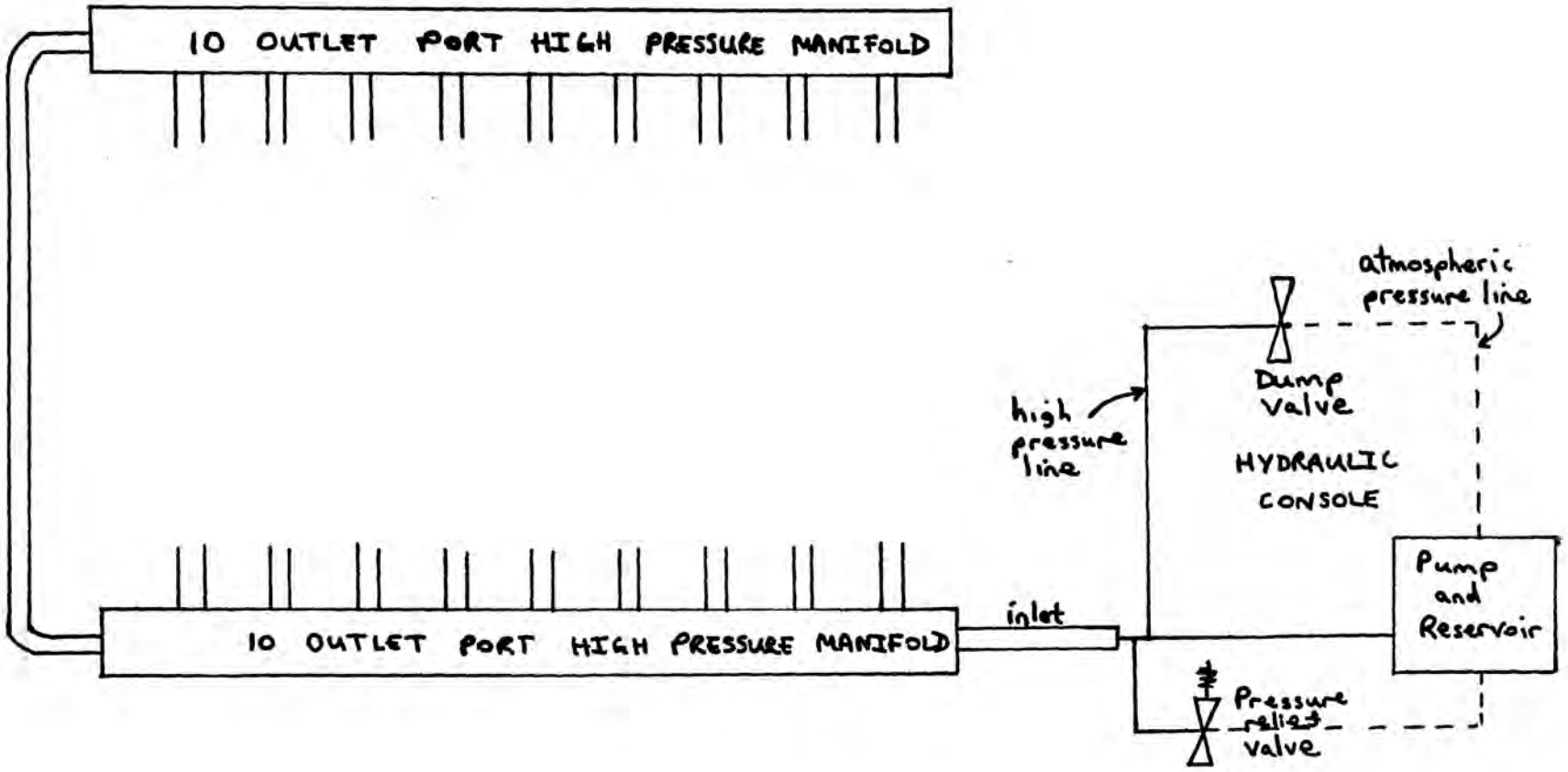



Figure 5.5: Hydraulic circuit layout

controlled by a spring-loaded release valve which sent excess oil back to the reservoir. In this manner, the speed of rotation of the pump influenced only the volume of oil which was delivered and to a first approximation did not affect the pressure. The two sets of diametrically opposing jacks were activated from the same hydraulic feed network, the consoles being capable of maintaining constant pressure to an accuracy of $\pm$ 0.014 MPa. In order to provide sudden relief of the load for emergency use e.g. when the model failed, an additional dump valve was available on each console.

Pressures were measured by using two accurate and calibrated pressure gauges attached to the hydraulic consoles. A suite of gauges was available depending on the magnitude of pressure required. While not entirely satisfactory because it was a rather remote measurement, the pressure recording system adopted here was considered the most practical. A detailed calibration of the loading system is described in Sections 5.7.1, 5.7.2 and 5.7.3.

All of the jacks housed in a given circuit were connected to each other in series via high pressure hydraulic tubing (9 mm O.D.) and appropriate couplings (high pressure Ermeto type). The distributing manifold to which each of the feeds to the jacks connected, was constructed from sections of 25 mm O.D. mild steel pipe having an internal bore of 6 mm diameter. These lengths of pipe threaded into one another to create a manifold 500 mm in length with a bleeding valve attached to the manifold at the end of each hydraulic circuit.

Thus, the hydraulic loading system was such that the vertical and horizontal loading applied to the model could be independently controlled, thereby enabling simulation of many of the typically encountered loading environments in mining operations. Independent control of the hydraulic jacks in each bank was not necessary for the present studies but it would involve a relatively minor

modification that would contribute significantly to the versatility of the loading apparatus.

5.6.5. Housing Frame:

The housing frame, supporting the biaxial apparatus, was designed to be and is a functional component of the complete loading system. The frame consists of a rectangular base 1.4 m x 0.9 m manufactured from 100 mm square tube with 'A' frames mounted at each end. Plummer blocks with internal braces were bolted to the top of each 'A' frame to enable rotation of the loading rig. This was achieved by welding stub axles 50 mm in diameter to a channel section on each side of the rig, each channel section being bolted to the reaction frame at mid-height. Each channel section straddled the hydraulic jacks with the manifold pipes locating through holes in the channel section.

A locating device was clamped to the protruding end of each stub axle enabling the rig to be locked in suitable preparatory or testing positions. The rotation axis for the rig was fixed at a height of 0.75 m above the ground floor, this proving to be a suitable working height when the rig was locked in the horizontal position. Castors 100 mm in diameter and facilitating easy transportation were clamped to the base of the housing frame at each corner, one pair of castors being fixed while the other pair were free to swivel. Attached to the castors were stabilizing screw jacks which also acted as levellers when there were irregularities in the floor.

## 5.7. Calibration and Preliminary Testing of the Biaxial Loading Apparatus:

Before it could be put to reliable use for the proposed experimental model tests, the biaxial loading apparatus had to be thoroughly and rigorously commissioned to ensure that the design requirements were being adequately met. To achieve this, a series of tests was performed,

each test having been so devised as to enable the behaviour of at least one of the pertinent design specifications to be carefully examined. Subsequent modifications and improvements to the apparatus were implemented on the basis of the results obtained from this testing programme.

The following calibration tests were performed and are presented in the order in which the testing proceeded.

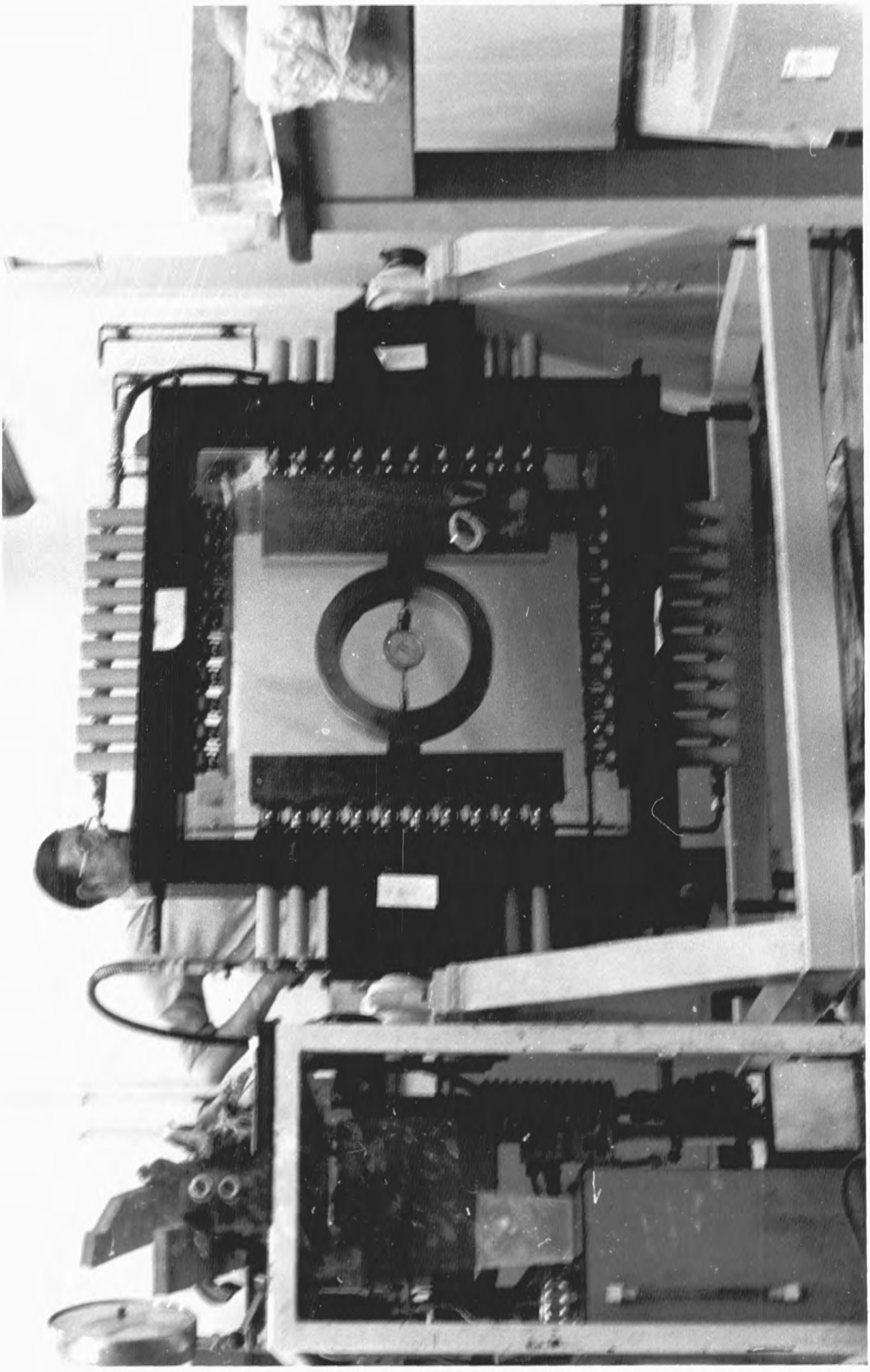
5.7.1. Proving Ring Test:

A 56 tonnes calibration ring and steel bridge arrangement was inserted into the loading apparatus as shown in Figure 5.6. The purpose of the test was to calibrate the 20 rams connected to each hydraulic circuit. For several different loading levels, the transmitted load as indicated on the proving ring dial gauge and the combined sum of the product of the circuit pressure and ram effective area for each of the 20 jacks, were in satisfactory agreement, variations between loads being within 5% of each other.

5.7.2. Loading of a Strain-Gauged Continuous Plate:

A solid 500 mm square x 50 mm thick aluminium plate (HP 30 type), upon which an arrangement of 10 mm electrical strain gauge rosettes were glued to either face, constituted the experimental test specimen. The exact positioning of the strain gauges is shown in Figure 5.7. The purpose of the test was to investigate, for a variety of uniaxial and biaxial loading conditions, the uniformity of strain (and hence stress) distribution along the edges of the solid plate model and throughout its interior in both the normal and lateral loading directions. The load transmitting ability of the platens could then be assessed and any loading variations inherent in the apparatus itself would be highlighted by testing uniaxially in both directions and also biaxially under different loading paths.

Figure 5.6: Proving ring test



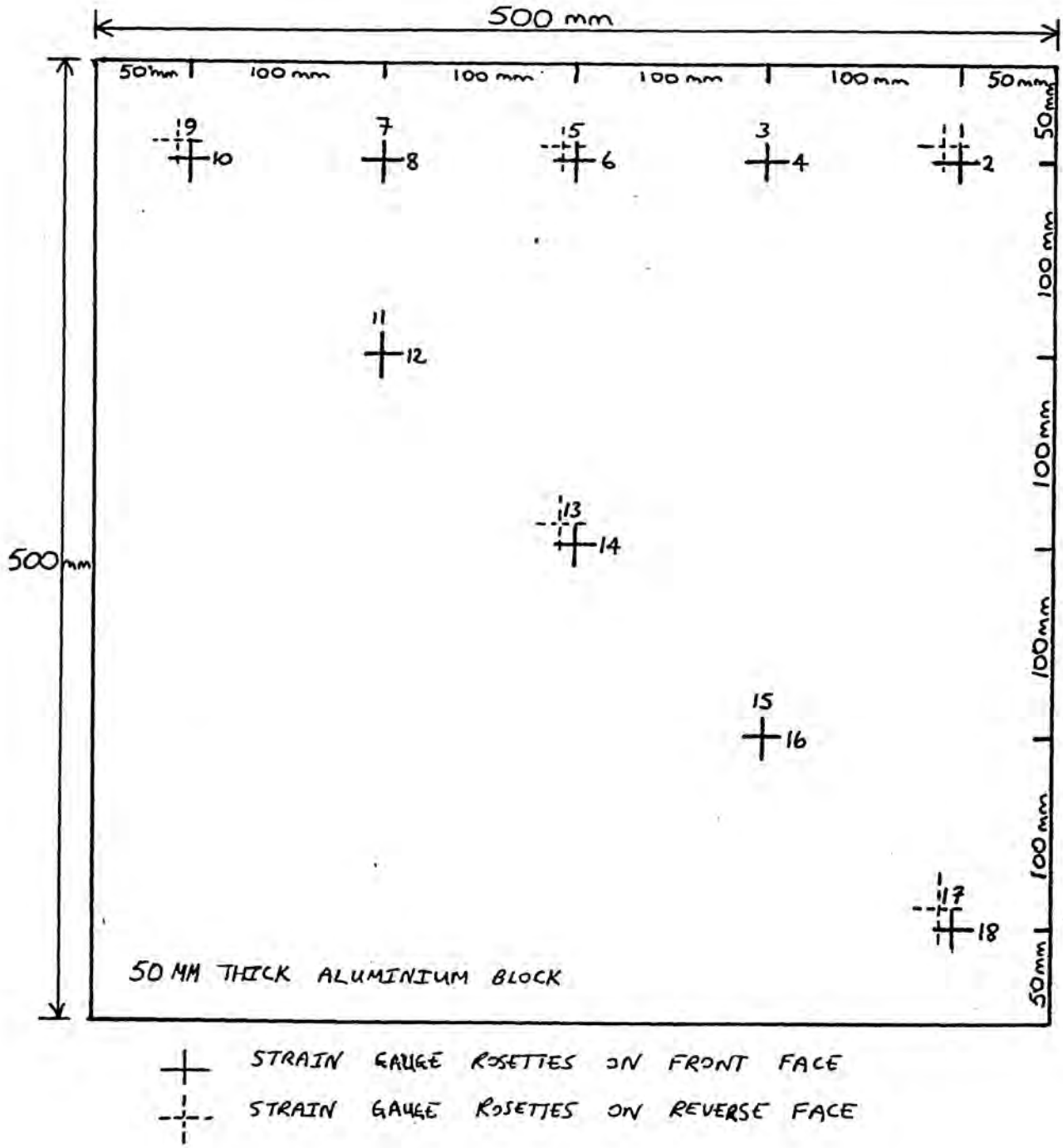



Figure 5.7: Arrangement of Strain Gauges for Measurement of Strain Distribution in Solid Plate Model.

The plate was tested under the apparatus design condition of plane stress and the strains were recorded by the conventional technique using standard Huggenberger multi-channel strain recording equipment. Some typical strain readings are shown in Table 5.1 for the uniaxial tests in which each of the four loading edges of the biaxial apparatus in turn pressurized the strain-gauged edge of the aluminium block. In these initial tests the block was subjected to pressures of up to 14 MPa with no low friction insert placed between the machined block edges and the steel platens. It is obvious from these initial results that the strain distribution obtained is far from satisfactory and that the local influence (or edge effects) of the platens appears to extend considerably further than 50 mm in from each edge. The disturbance is particularly marked in the vicinity of the plate corners.

To help overcome such undesirable edge effects, it was necessary to attach a strip of 'PTFE' low friction tape (with pressure sensitive side facing the model) to the base of each steel platen. The same uniaxial tests as above were then repeated and the results are presented in Table 5.2. They indicate that the strain distribution produced by the modified platens was adequate to satisfy the design requirement of applying a uniform normal load distribution while confining induced shear stresses to the scale of individual contacts. The normal strain deviation throughout the aluminium block was well within 5% of the mean normal strain while the results show lower values of lateral strain in the mid-section of the loaded edge indicating a slight frictional effect. Such results are not surprising since the five strain gauge rosettes parallel to the edge were located at a depth into the model equal to the width of the platens and slight deviations in strain at this depth were to be expected. The strains measured at a greater depth into the model confirm that undesirable edge effects have, in fact, been eliminated.

| Gauge No. | Edge A | | Edge B | | Edge C | | Edge D | |
|---|---|---|---|---|---|---|---|---|
| | Norm | Rev | Norm | Rev | Norm | Rev | Norm | Rev |
| 1 | 155· | 147· | 154· | 171·5 | 154· | 155·5 | 151·5 | 160·5 |
| 2 | -53·5 | -38·5 | -41· | -44.5 | -45·5 | -39· | -42.5 | -42.5 |
| 5 | 166· | 164·5 | 182· | 167·5 | 186· | 159· | 180·5 | 169 |
| 6 | 3· | -8 | 7· | 2.5 | -15·5 | 12·5 | -2· | -1·5 |
| 9 | 156· | 131·5 | 162·5 | 141·5 | 153· | 147·5 | 159· | 145· |
| 10 | -43· | -45·5 | -28·5 | -30·5 | -29· | -44.5 | -30·5 | -38 |
| 13 | 200·5 | 189·5 | 208· | 200· | 201·5 | 193·5 | 200· | 200· |
| 14 | -81·5 | -78·5 | -70·5 | -74·5 | -78·5 | -70 | -73· | -78· |
| 17 | 134· | 133·5 | 157·5 | 144· | 151· | 143· | 154·5 | 144·5 |
| 18 | -49· | -46·5 | -43·5 | -36·5 | -51·5 | -41· | -49· | -42·5 |

Table 5.1 : Actual Strains for Four Uniaxial Tests: Values in Microstrain, Applied load = 356,100N - ve sign indicates tension. A,B,C,D refer to loading edge of frame in contact with strain-gauged edge of block. Gauge numbers as in Figure 4. Norm and Rev refer to either face or block, Norm facing the normal viewing direction.

| Gauge No. | Edge A | | Edge B | |
|---|---|---|---|---|
| | Norm | Rev | Norm | Rev |
| 1 | 184· | 171· | 170·5 | 183·5 |
| 2 | -64·5 | -54·5 | -53·5 | -56·5 |
| 5 | 175· | 171· | 179· | 171·5 |
| 6 | -48·5 | -47· | -47· | -43· |
| 9 | 173· | 176· | 185·5 | 171·5 |
| 10 | -53· | -59· | -54·5 | -50· |
| 13 | 185·5 | 175· | 182·5 | 181·5 |
| 14 | -62·5 | -62· | -58·5 | -58· |
| 17 | 180·5 | 170·5 | 176·5 | 179· |
| 18 | -62·5 | -56· | -54· | -56· |

Table 5.2: Actual Strains for Two Uniaxial Tests with PTFE Tape on Platens: Values in microstrain, Applied load = 356,100N, - ve sign indicates tension.

In order to provide a comparison with the experimental strain distribution as well as ensuring the correct load magnitude was being transmitted to the model, a series of numerical experiments using the boundary element method of stress analysis were performed. A formulation which predicts the strain distribution in a homogeneous, isotropic and linear elastic material was selected. Two differing arrangements of boundary elements along the loaded model face were constructed with the mid-points of appropriate elements corresponding as near as possible to the actual positions of the strain gauge rosettes on the aluminium block.

One arrangement of elements along the loaded model edges consisted of fifteen equally spaced and uniformly loaded elements while the other arrangement attempted to simulate the exact nature of the physical model with uniformly loaded elements representing the platens interspersed with smaller unloaded elements representing the small gaps between the platens. Representative properties for the aluminium plate were selected (E between 6.55E04 and 6.89E04 MPa, $\nu$ = .32) since the exact value of the plate properties were unknown. The results for the numerical uniaxial tests using the same magnitude of load as for the experimental results of Tables 5.1 and 5.2, are presented in Table 5.3 and Figure 5.8. Although the magnitude of normal and lateral strain was generally 5-10% higher in the numerical experiments (due to representative material properties), the strain distribution was remarkably similar to that obtained experimentally.

Under biaxial loading conditions, strain distributions were obtained which yielded results essentially compatible with those for the uniaxial loading of the plate. Two sets of biaxial tests were performed with K (vertical to horizontal load ratio) having values of 1 and 0.5. Path dependency of frictional effects was checked during

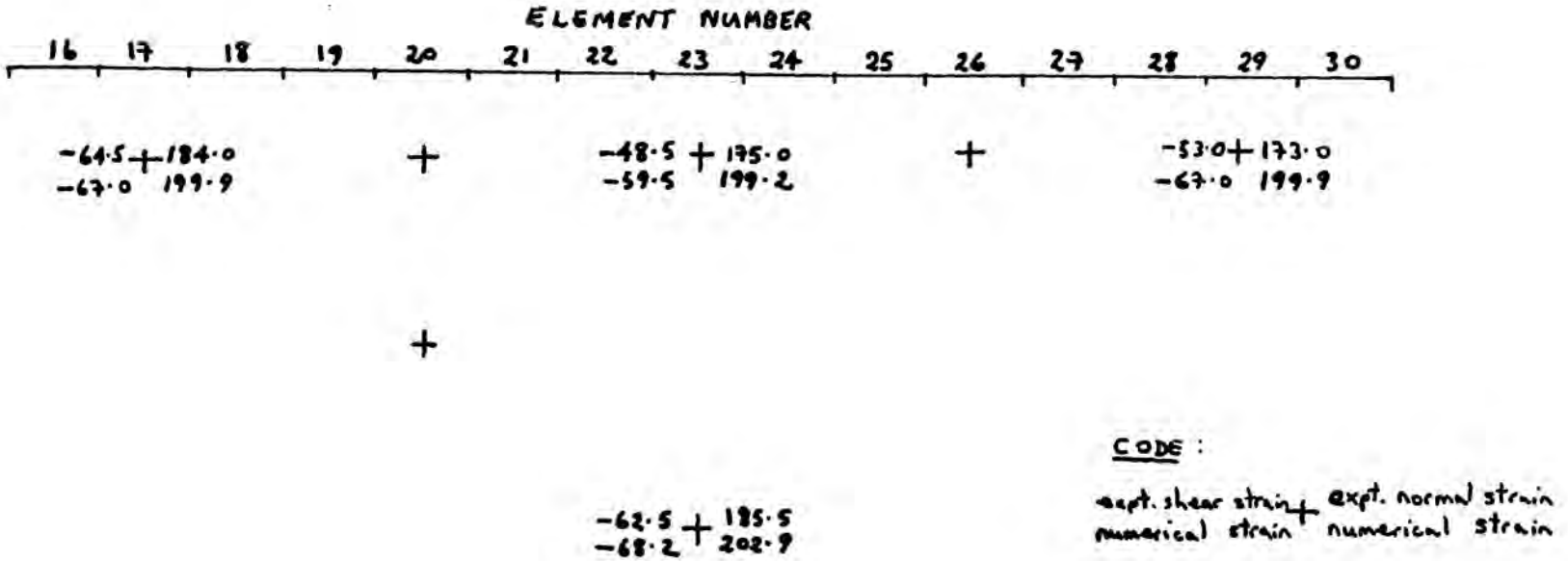



Figure 5.8: Comparison of experimental and numerical strains.

Table 5.3: Comparison of experimental and numerical strains, for uniaxial loading of continuous plate. P = 13.8 MPa. E = 6.55 E+04 MPa, $\nu$ = .32.

| Experimental strain | | Numerical strain | |
|---|---|---|---|
| normal | lateral | normal | lateral |
| 184.0 | - 64.5 | 189.9 | - 64.0 |
| 175.0 | - 48.5 | 189.1 | - 56.3 |
| 173.0 | - 53.0 | 189.9 | - 64.0 |
| 185.5 | - 62.5 | 193.0 | - 65.0 |

Table 5.4: Comparison of experimental and numerical strains, for biaxial loading (hydrostatic) of continuous plate. P = 6.86 MPa, E = 6.55 E+04, $\nu$ = .32.

| Experimental strain | | Numerical strain | |
|---|---|---|---|
| normal | lateral | normal | lateral |
| 67. | 67. | 65.6 | 67.8 |
| 63. | 68.5 | 68.0 | 65.9 |
| 65.5 | 67. | 68.1 | 66.7 |
| 62.5 | 69. | 66.7 | 67.7 |

Table 5.5: Comparison of strains before and after removal of central plug for discontinuous plate. P = 4 MPa.

| Before plug removed | | After plug removed | |
|---|---|---|---|
| normal | lateral | normal | lateral |
| 54. | - 15. | 53. | - 17. |
| 53. | - 14. | 55. | - 17. |
| 57. | - 15. | 56. | - 17. |
| 49. | - 13. | 46. | - 13. |

the biaxial tests by initially applying the vertical load before the horizontal load and then subsequently reversing the stressing procedure. The similarity between the results of such loadings, as well as between the uniaxial and biaxial results, indicated that the frictional edge effects had been reduced to within acceptable limits and that a satisfactory load transfer system had been accomplished. A comparison between the experimental and numerical results for a hydrostatic biaxial test with a pressure of 6.86 MPa applied to each plate edge is presented in Table 5.4.

### 5.7.3. Differential Boundary Displacement Test:

The logical progression in the calibration programme was to next examine the strain distribution obtained when a differential movement occurred at the model-platen loading interface. To achieve this, two experimental procedures were devised and implemented.

Firstly, an aluminium block similar to that described in Section 5.7.2 was cut and arranged as shown in Figure 5.9. This discontinuous plate model was used in order to obtain a differential boundary displacement by withdrawing an appropriate sized central rectangular section whilst under load. The plate components were each strain gauged, as seen in Figure 5.9, and strains were recorded both before and after any differential boundary movement occurred. Separate tests were performed with each of the four loading edges of the apparatus in contact with the differential strain-gauged boundary to determine if symmetrical loading conditions had been preserved following boundary displacements. The results of such loading tests, carried out at stress levels of 2 MPa and 4 MPa respectively, indicated that the strain distributions within the plate were uniform to within 5% with strain variations about the mean value being slightly less, as expected, for the higher stress level. Table 5.5 indicates the strain distribution throughout

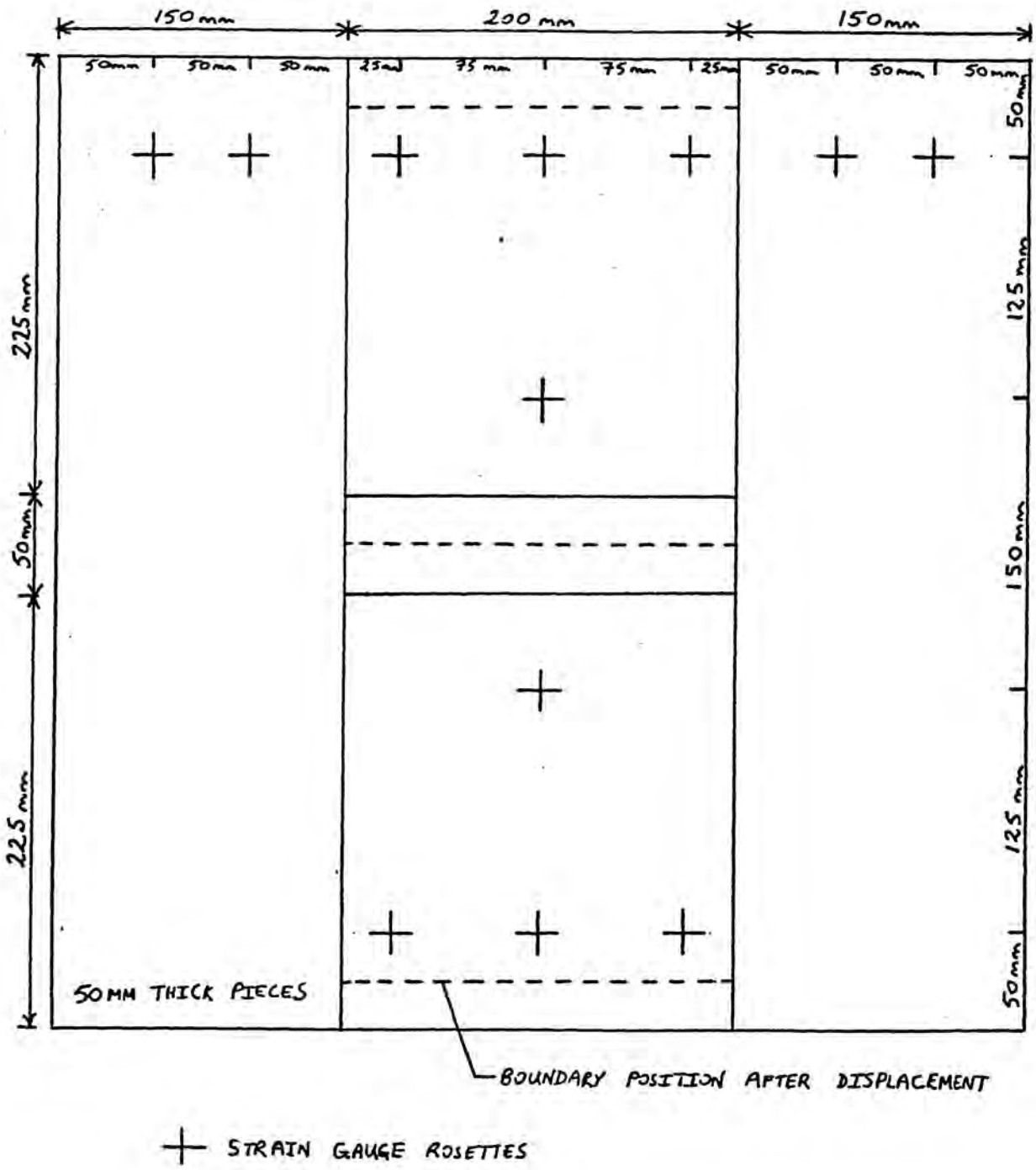



Figure 5.9: Arrangement of Strain Gauges for Measurement of Strain Distribution in Discontinuous Plate Model.

the discontinuous plate for an applied pressure of 4 MPa. The maximum in-plane boundary displacement examined during these tests was 25 mm. However, there was no reason to suspect that larger boundary displacements could not be sustained and at the same time apply uniform loading. The theoretical amount of differential boundary movement possible would be governed by the 130 mm stroke of each jack plunger, provided platen-element contacts were compatible.

In the second simulated discontinuous model experiment, a differential column test similar to that described by Gonano (1974) was performed. Again, the objective of this test was to obtain a measure of the uniformity of load distribution under non-uniform boundary displacements. The test arrangement consisted of three columns loaded in parallel with a weaker 200 mm x 50 mm x 500 mm column to undergo subsequent failure located between the two stronger outer columns, as shown in Figure 5.10. The two outer 150 mm x 50 mm x 500 mm columns of stronger section provided the remaining platens with a reaction. The failure specimens were manufactured from a montmorillonite gypsum plaster and water mixture in a ratio of 1 : 2 : 2 by weight. The resulting uniaxial compressive strength for the cured mixture was approximately 5 MPa, this low strength arising from the fact that the porosity of the resultant plaster mix had been substantially increased.

Initially, the two identical reaction columns were made from a plaster-water mixture having a stiffness only slightly greater than that of the failure specimen. In the second series of tests, the reaction columns from the discontinuous aluminium plate model were used resulting in an outer column contraction considerably less than that for the failure specimen at maximum load. A total of eight failure specimens were cast and cured, with four specimens being loaded to failure for each type of outer

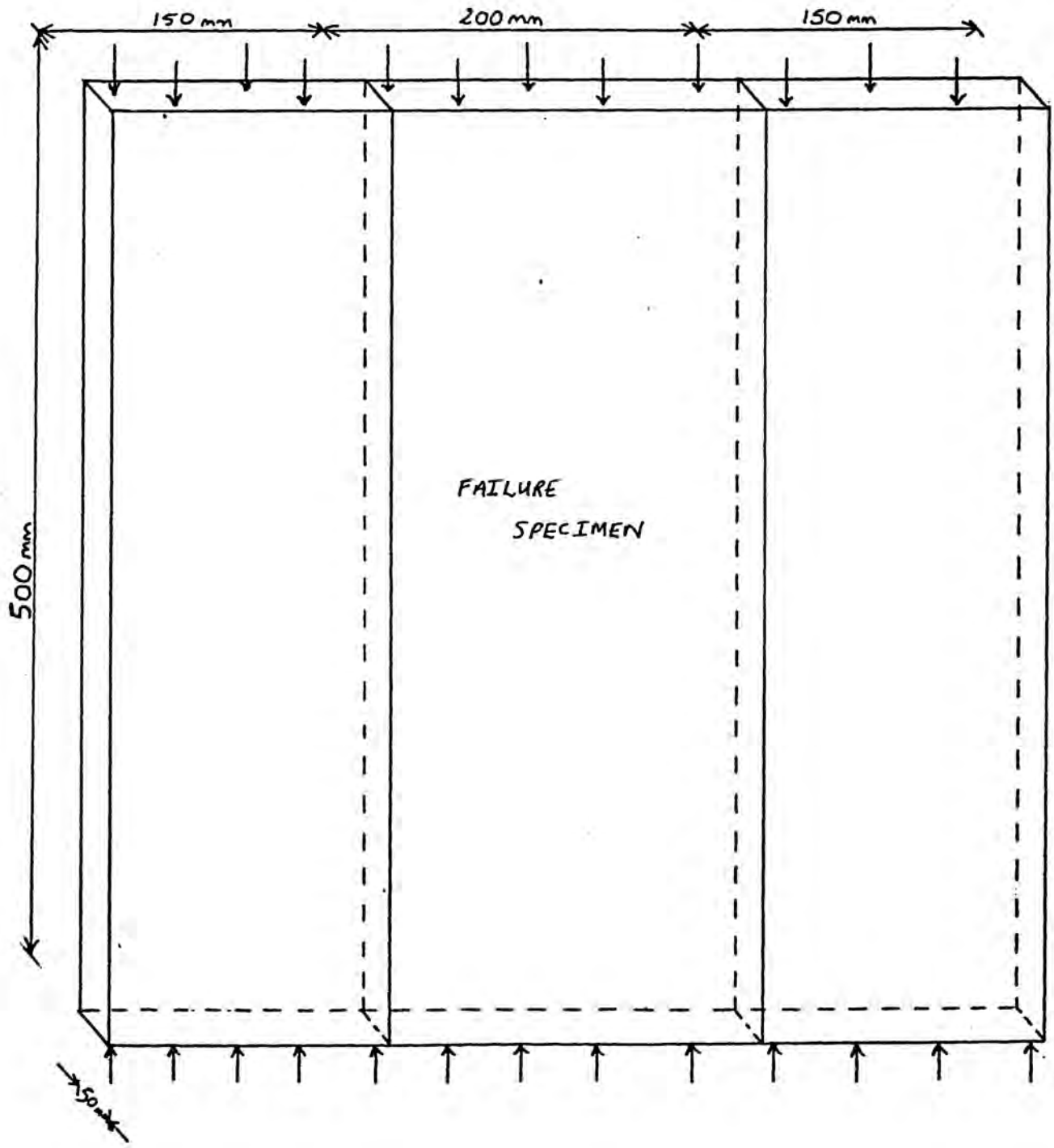



Figure 5.10: Arrangement for Differential Boundary Displacement Test.

column. The inability of the loading apparatus to accommodate differential boundary displacements would be indicated by a greater failure load required for the second series of tests i.e. those tests incorporating very stiff outer reaction columns.

The results for each test series confirmed that there was no significant variation in the average total failure load for each central column, the failure load averaging 0.047 MN with a 5% variation about the mean value. Also, from the brittle nature and consistency of failure modes one could infer that the design requirements were being adequately achieved. A typical failure specimen is shown in Figure 5.11.

5.7.4. Stiffness Test:

As discussed in Section 5.6.3, it was calculated as highly unlikely that bending stresses and resulting deformations of the steel members comprising the reaction frame would cause significant problems for the level of operating loads contemplated for the model tests. Some knowledge of the stiffness of the loading apparatus was, however, desirable and this was obtained through the accurate measurement (via strategically positioned dial gauges) of the resulting frame deformations as a model was loaded.

The solid aluminium plate used in the calibration test of Section 5.7.2 constituted the test model and was subjected to uniaxial loading. The magnitude and nature of the reaction frame deformations for two uniaxial tests, each applying a reaction force of 0.177 MN to diametrically opposing steel members, are presented in Figure 5.12. The resulting deformations obtained may be regarded as the maximum possible under equivalent loading since uniaxial loading situations are the most unfavourable to the overall stiffness of the apparatus.



Figure 5.11. Montmorillonite failure specimen

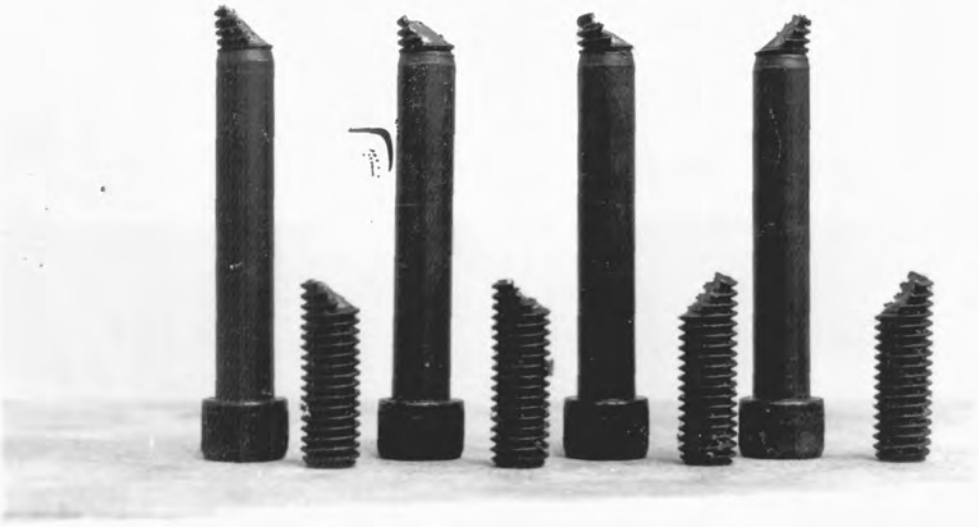


Figure 5.13. Failed high tensile bolts

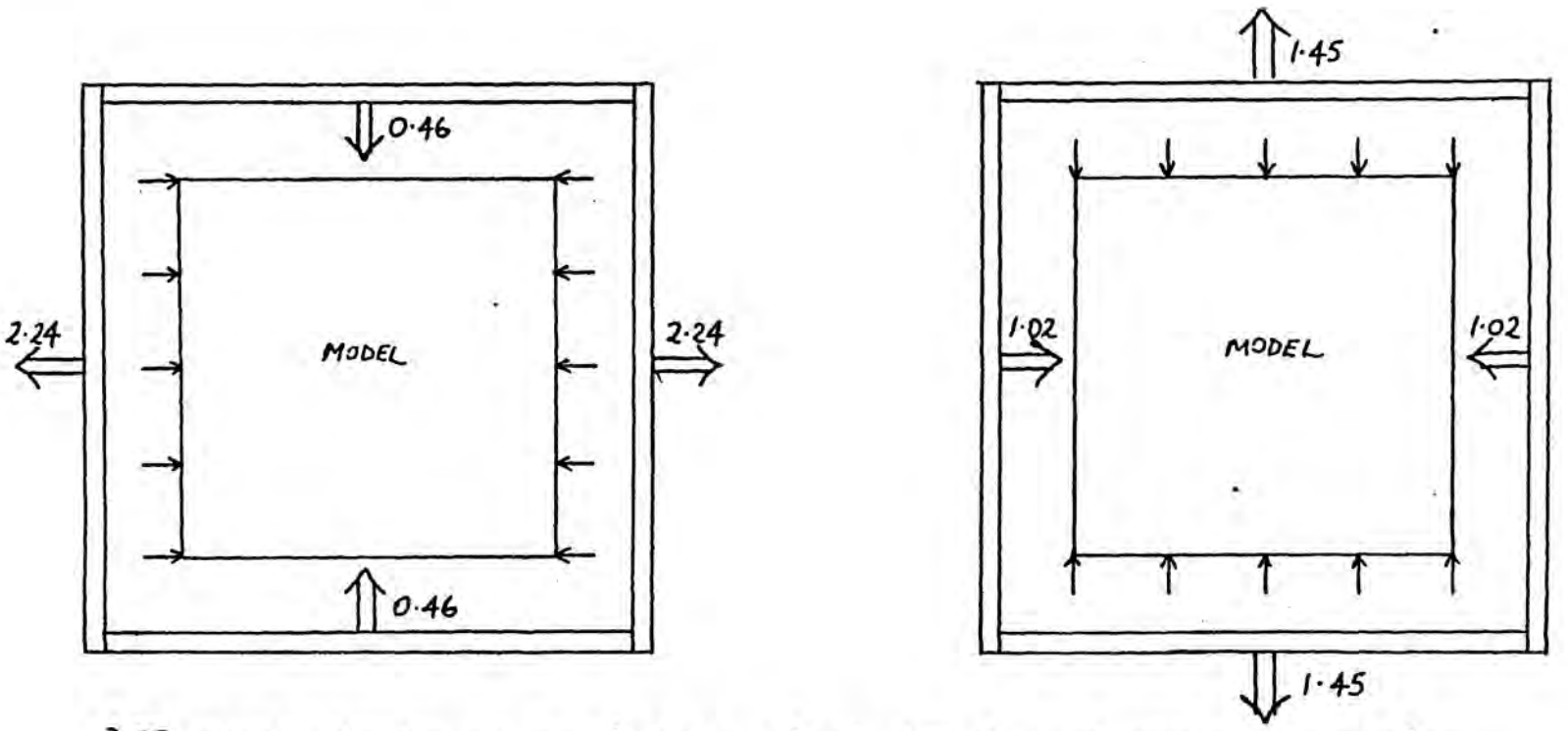



Figure 5.12: Results for Stiffness Test of Reaction Frame when Model Uniaxially Loaded to 176,600N.

The high tensile strength bolts connecting the various sections of the housing frame are under a combined action of shear and tensile behaviour during any particular loading. The maximum possible reaction load capable of being withstood by the apparatus prior to total failure of the connecting bolts was determined and found to be within 10% of the ultimate loading capacity available. Examination of the failed bolts (Figure 5.13) confirmed that a combined shear-tensile behaviour was indeed being induced in the bolts.

One important and unforeseen aspect of the loading apparatus behaviour resulting from this test was a lateral, rigid body translation of the reaction frame along the pivot stub axles. The extent of this movement was directly proportional to the magnitude of the loads applied to the model. Such movement was due to the fact that the reaction frame was asymmetrically braced to the housing frame (via the locating device) when the rig was in the vertical testing position. Obviously, this movement was undesirable in light of the subsequent photogrammetrical techniques to be employed. The incorporation of two reaction frame stabilisers, welded to the base of the housing frame at either end, inhibited this rigid body movement. Further testing showed that such lateral movement could be adequately controlled by these stabilisers for the range of operating pressures anticipated.

5.7.5. Static Friction Test:

A double shear test was performed to measure the effective coefficient of static friction at the model-platen interface for various normal loads and shearing displacements. A solid plaster slab was positioned and loaded between the vertical platens to the required normal load, after which load was applied to one of the two remaining edges since one bank of jacks had been previously disconnected from the second hydraulic circuit. The experimental set-up is shown in Figure 5.14. Shearing

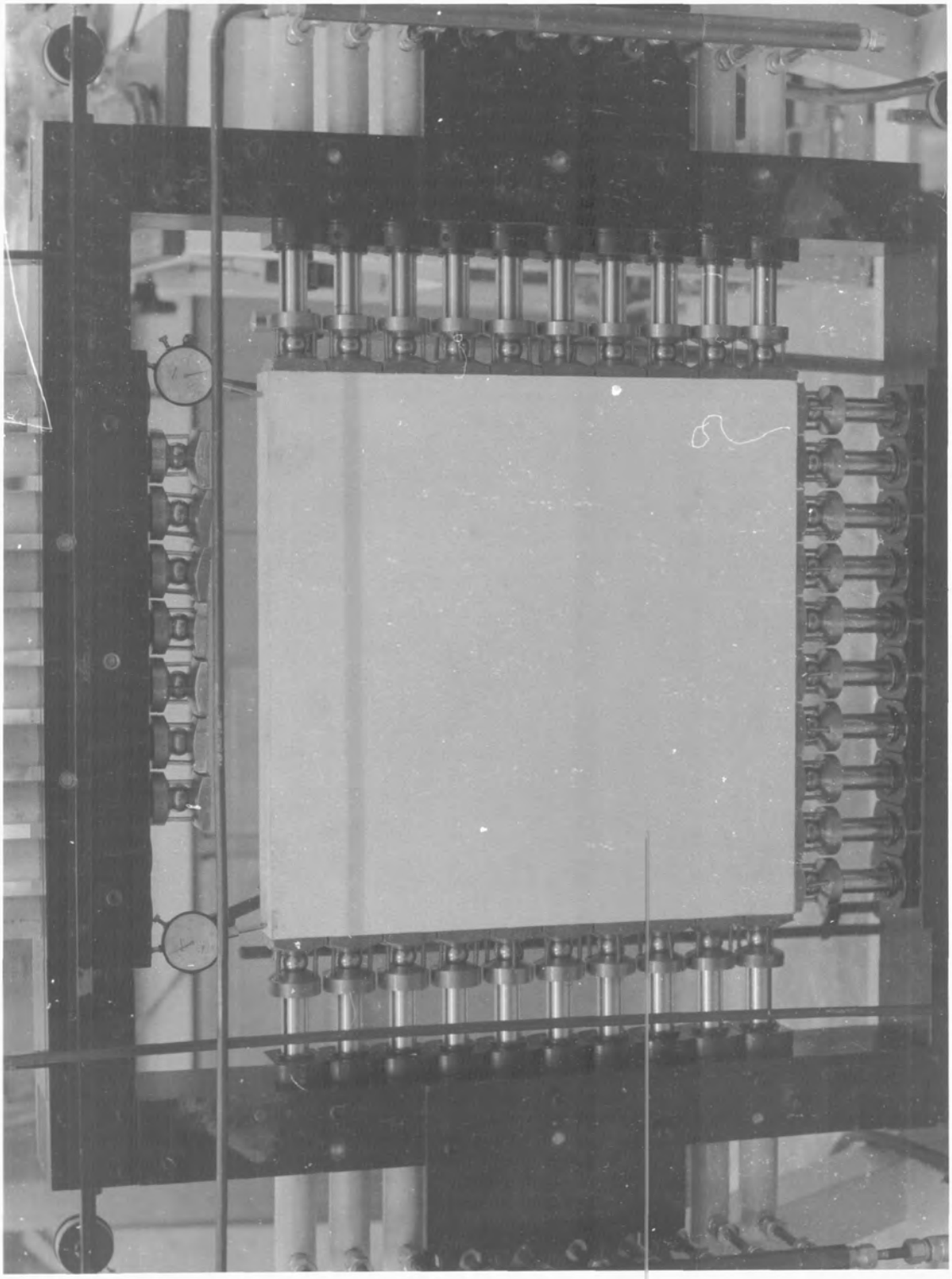


Figure 5.14: Double shear test

loads were recorded for displacements of up to 5 mm, since this was considered to be the maximum shear displacement likely in the experimental tests. Results suggested that a friction coefficient in the vicinity of .05 could be reasonably assumed, this value being difficult to precisely define since shear load was found to increase less than proportionally with normal load. This means that on average approximately five percent of the applied normal loading was taken up in friction along the model edges.

5.7.6. Preliminary Tests:

In addition to the basic calibration tests described above, further additional experimentation was performed before proceeding to the main experimental programme of model tests. The objectives of this were:

i) to further confirm and establish the reliability and performance of the loading apparatus, correcting for faults or otherwise as the need arose;

ii) to standardise the sequence of events necessary for a complete testing cycle, thereby minimising the variability in operational procedure between successive experiments;

iii) to aid in the characterisation of the model material and to confirm the casting and model preparation technique;

iv) to emphasise the advantages and disadvantages associated with particular discontinuous geometries;

v) to compare, where possible, any results with those obtained from independent techniques.

In some of the preliminary tests conducted, solid plaster slabs containing circular and rectangular openings were cast and loaded to determine if satisfactory failure modes were induced around the opening under a plane stress condition. Figure 5.15 shows the failure mode of a 100 mm

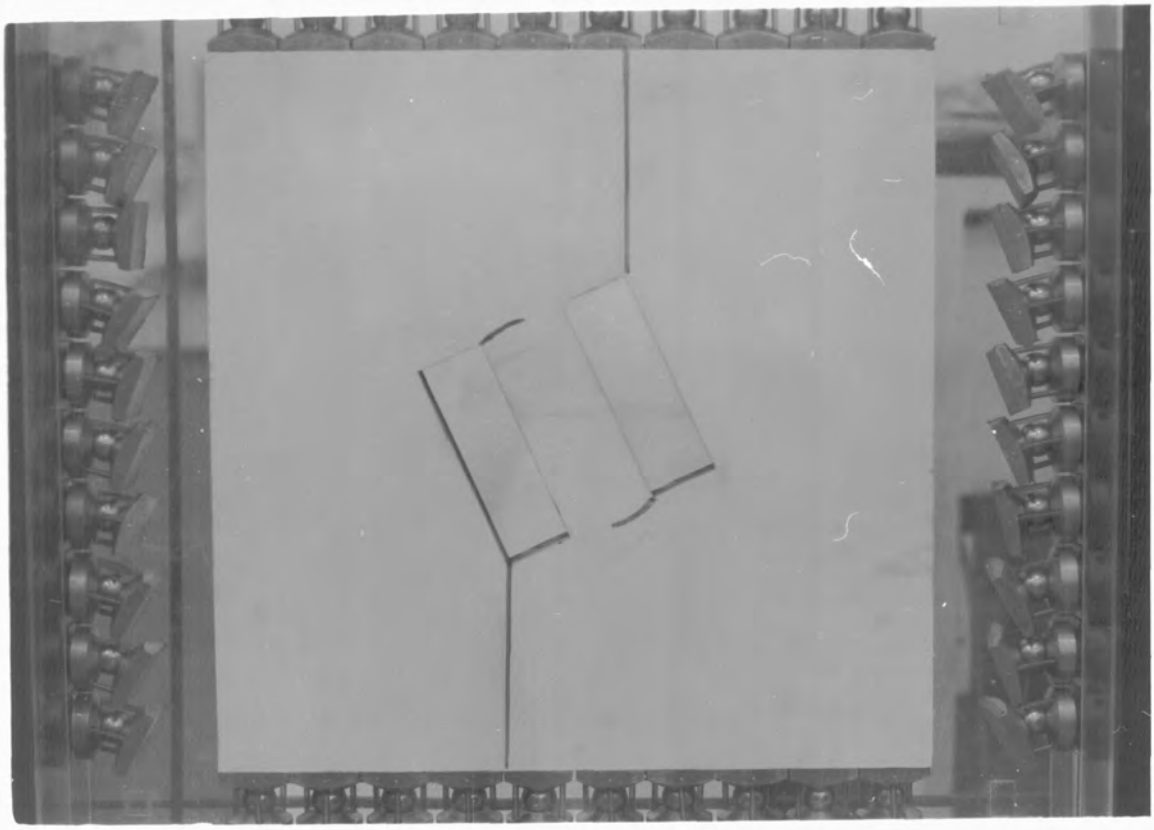


Figure 5.16: Failure mode for 2 rectangular openings

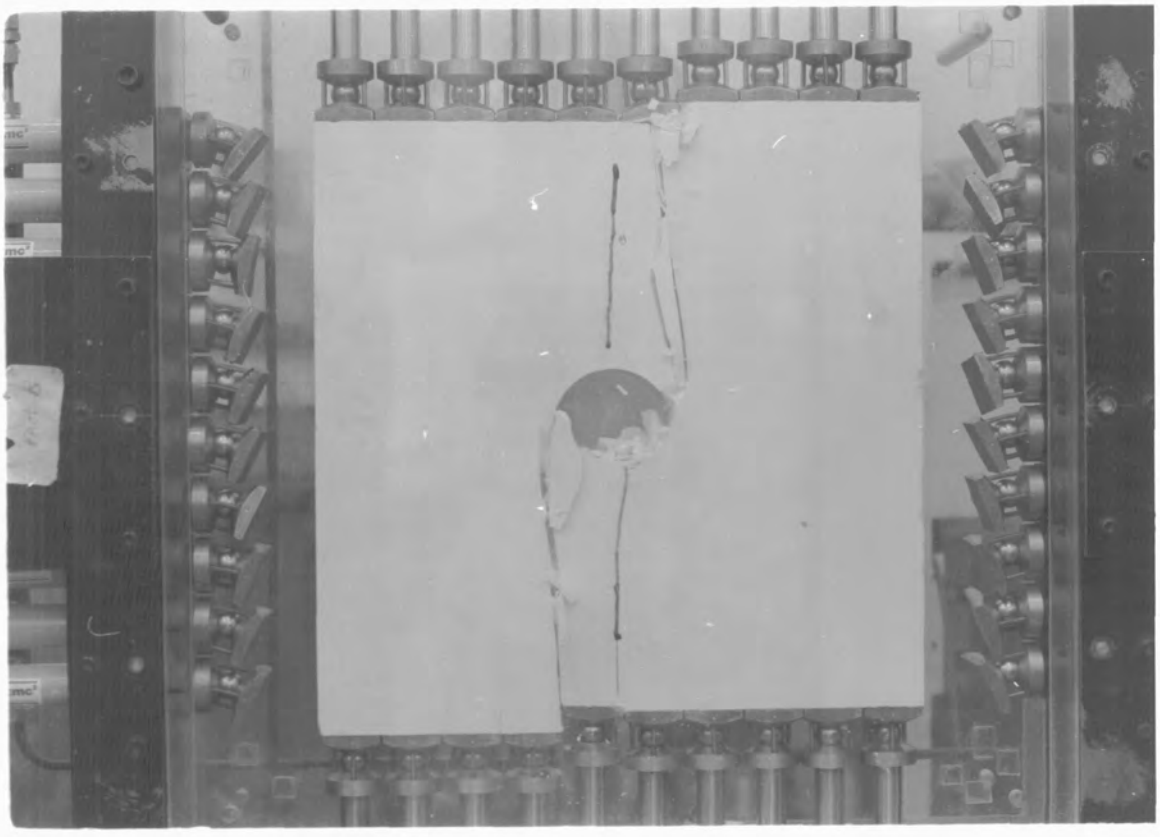


Figure 5.15: Failure mode for 100 mm dia. circular tunnel.

diameter circular tunnel subjected to a vertical uniaxial field stress. Tensile cracking in the crown and invert of the tunnel commenced at a hydraulic circuit pressure of 10.3 MPa, which represents a uniaxial tensile strength for the plaster mixture of approximately 2.55 MPa. As the pressure increased, the tensile cracks became wider and radiated towards the specimen edges. Crushing at the spring line was also evident due to the theoretical stress concentration factor of 3.0 existing at the central section of the walls.

Two rectangular openings with an aspect ratio of 3 : 1 were also subjected to a uniaxial vertical loading and the resulting failure mode is shown in Figure 5.16. Again, a combination of tensile and compressive failures was evident.

It was encouraging to note that in the preliminary tests involving continuous plaster slabs, failure was in accordance with theoretical stress concentrations surrounding the openings and was not governed by failures unaffected by the presence of the opening, such as slabbing or shearing.

Preliminary testing of openings in discontinuous plaster models was also performed. This provided valuable insight for the controlled experiments described in Chapter 6 and enabled the effect of variables such as the size of opening, and ratio and magnitude of the applied loading, to be examined.

From the results of the calibration and preliminary testing it was concluded that the loading apparatus was capable of fulfilling the design requirements of applying a uniform distribution of loading to the lateral sides of the model whilst being capable of deforming non-uniformly. Deviations from intended behaviour were noted and remedied where possible and modifications carried out

with the aim of keeping the complexity of design and operational procedure to a minimum.

## 5.8. Buckling Stability Calculations:

It was essential that the size of the model selected for the experimental tests be such that failure of the loaded model due to out-of-plane buckling would not occur, so that all ensuing block movements were restricted to the plane of the model. This is not to be confused with any in-plane buckling mechanisms present around the walls and roofs of underground openings which can contribute significantly to the overall behaviour of the mine structure. Preliminary calculations to determine a suitable model size were performed and are briefly outlined in this section. The results of these calculations, together with the experiences and conclusions of other researchers (Ergun, 1970), were carefully assessed before appropriate model dimensions were decided upon.

The problem of eliminating out-of-plane buckling once model dimensions have been fixed may be overcome by either increasing the model thickness or restraining the model faces sufficiently by loading or confining them between rigid plates, both methods not always being feasible or convenient. The literature reports several instances (Heuer and Hendron, 1971; Gonano, 1974) in which loading apparatus designs have had to undergo such modifications to meet their design requirements and this would tend to suggest, in some cases, a lack of insight in their initial planning phase.

Ergun's work (loc.cit) on testing experimentally both brick and solid columns showed that the critical buckling load of a brick column was substantially less (in some cases by more than 50%) than that of a similar solid column under identical loading conditions.

Euler's critical buckling formula enables the

critical buckling load for a solid column with both ends pinned and subjected to uniform applied stresses to be determined. The formula is:

$$F_{cr} = \frac{\pi^2 EI}{L^2}$$

where

Fcr = critical buckling load (MN)
E = Youngs modulus of column (MPa)
I = moment of inertia of cross-section ($m^4$)
L = length of the column (m)
A = cross-sectional area ($m^2$)
$\sigma_c$ = uniaxial compressive strength (MPa)

The length of column ($L_t$) at which the transition between compression and buckling type failures will occur is defined as follows:

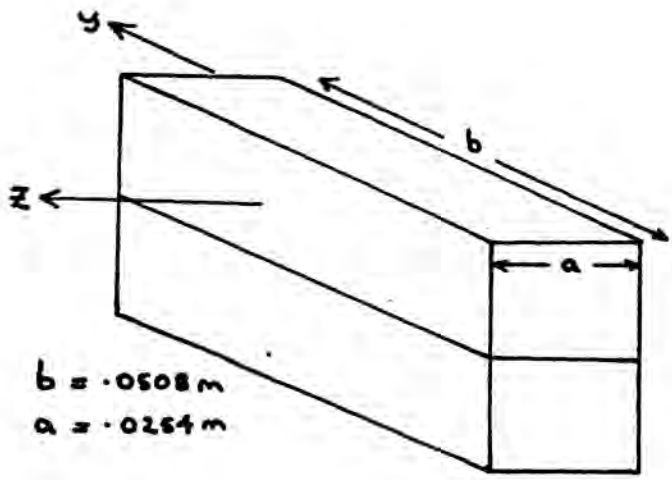
$$\sigma_c = \frac{F_{cr}}{A} = \frac{\pi^2 EI}{L_t^2 A}$$

or, on rearranging, the minimum length for buckling to occur is:

$$L_t = \left(\frac{\pi^2 EI}{A\sigma_c}\right)^{\frac{1}{2}}$$

For discontinuous columns constructed from the plaster blocks to be used in the model studies:-

E = 8630.0 MPa
$\sigma_c$ = 20.7 MPa
A = 0.00129 $m^2$
Iy = $6.94 \times 10^{-8}$ $m^4$; Iz = $2.775 \times 10^{-7}$ $m^4$




then

1) the minimum length of column for buckling to occur about the horizontal y-axis is:

$$L_{ty} = \left( \frac{\pi^2 \times 8630 \times 6.94 \times 10^{-8}}{1.29 \times 10^{-3} \times 20.7} \right)^{\frac{1}{2}} \text{ m}$$

$$= 0.471 \text{ m}$$

and about the horizontal z-axis is:

$$L_{tz} = \left( \frac{\pi^2 \times 8630 \times 2.775 \times 10^{-7}}{1.29 \times 10^{-3} \times 20.7} \right)^{\frac{1}{2}} \text{ m}$$

$$= 0.941 \text{ m}$$

2) the critical buckling load about the z-axis for a 0.5 m long column is:

$$F_{cr} = \left( \frac{\pi^2 \times 8630 \times 2.775 \times 10^{-7}}{.5 \times .5} \right) \text{ MN}$$

$$= 0.0945 \text{ MN}$$

In the experimental model studies, $L_{ty}$ will be of no concern during biaxial loading since a restraint against buckling failure in this direction is provided by the

platens applying the lateral pressure. Therefore, only conditions for out-of-plane buckling i.e. about the z-z axis, need be examined.

Ergun's work also showed that when the length of the brick column is close to the minimum column length for buckling to occur ($L_t$), then the actual critical failure load for the discontinuous column has a variation of between 30 to 40 percent less than the Fcr predicted by Euler's theory. Therefore, for a 0.5 m long brick column with cross-sectional area 0.00129 $m^2$, it is reasonable to assume an actual critical failure load somewhere in the vicinity of 0.050 MN. For the proposed experimental model studies, it was considered unlikely that loads on individual brick columns would exceed at most 0.010 MN and hence it was concluded that buckling should not be a problem.

Preliminary tests on a biaxially loaded brick model 500 mm square x 50 mm thick containing 20 bricks along each model edge indicated no evidence of buckling instability for the range of operating pressures anticipated. Any departure from the uniform load distribution assumed throughout the brick column in the above calculations will lead to a reduction in the amount of load capable of being sustained before failure occurs. Hence, care should be taken in the model material preparation to ensure that tolerances between plaster bricks are kept as small as possible.

## 5.9. Instrumentation of the Model:

The purpose of the instrumentation system was to provide comprehensive and permanent quantitative data from which, to a suitable level of accuracy, the rigid body displacements of particular model elements could be calculated. A photogrammetric technique was adopted to provide this information.

The measurement of displacement or strain is basic to understanding the response of engineering models and prototypes to applied loading. Techniques previously employed to measure displacements have encompassed instrumentation in the mechanical, electrical and optical fields. Before selecting a particular measurement technique, it is important to clearly define the exact nature of the information required since there are two fundamentally very different techniques available. Displacements and strains may be monitored at discrete points on or within the model (e.g. by strain gauging and potentiometers) or alternatively whole field deformation methods such as photogrid coatings, photogrammetry and Moire methods may be utilized.

The model studies to be conducted highlighted the need for a relatively simple experimental method for determining the planar displacement fields. There were several requirements stipulated for the instrumentation system including the following:

i) the information is recorded simultaneously and contained as a permanent record that can be interpreted at any convenient time;

ii) the information record is such as to enable whole field displacements to be determined, if required;

iii) experiments need not be repeated if more detailed information of a particular zone is subsequently required;

iv) the instrumention in no way interferes with the behaviour of the model;

v) the accuracy of the calculated displacements should be in the order of $\pm$ .1 mm to .2 mm at true scale;

vi) use be made, where possible, of existing equipment and efficient techniques.

A literature survey was carried out bearing in mind the above considerations and it was decided to use a recent development in close-range non-topographical

photogrammetry as the displacement measuring method. Recent successes with this method are reported by Chiat et al. (1979) and Robinson and Minton (1979). Serious consideration was also given to Moire methods (Theocaris, 1962; Moore, 1965) and stereogrammetric techniques (Butterfield et. al., 1970; Wickens and Barton, 1971; Atkinson, 1972) but these were eventually discarded either because the method was not sufficiently well standardized for the application in question or because of the expensive and involved nature of the subsequent data reduction. Also, because all block movements were essentially in the same plane and only differential movements were required, then consideration could be given to a method based on the analysis of single photographs rather than from the stereoscopic viewing of multiple photographs.

The photogrammetric method adopted for the data reduction enabled the rigid body displacements of the discontinuous model elements to be determined. This was achieved by taking two exposures: one before the model was loaded and the second exposure when the jointed model had undergone deformation. The planimetric positions of model elements on each exposure were then derived and a comparison of the spatial co-ordinates enabled calculation of the translational and rotational components of displacement.

5.9.1. <u>The Equipment:</u>

The main requirement of the photography was that the whole plan area of the 500 mm square model, together with the surrounding reference tapes providing photogrammetric control, be contained on the one negative. Preliminary tests showed that this was feasible without diminishing the resolution of points on the negative in any way. To achieve this complete coverage, a single non-metric Sinar monorail camera was used to photograph the model from an object distance of approximately 1.1 m.

A non-metric camera was selected simply because a metric camera i.e. one designed specifically for photogrammetric purposes, was not available.

Karara (1975) states the following advantages and disadvantages of a non-metric camera compared to a metric camera.

Advantages:

i) general availability;

ii) flexibility in focusing range;

iii) can be hand-held and therefore orientated in any direction;

iv) the price is considerably less than for metric cameras;

Disadvantages:

i) the lenses are designed for high resolution at the expense of high distortion;

ii) instability of interior orientation;

iii) lack of fiducial marks;

iv) the absence of level bubbles and orientation provisions precludes the determination of exterior orientation before exposure.

The Sinar camera had a focal length of 150 mm, a format of 95 mm x 120 mm, aperture values from 5.6 to 45 and a wide choice of exposure times including B setting which was used for the model experiments. An area of approximately 80 mm square on each negative corresponded to the discontinuous model. This gave a scale of the photography of approximately 1 : 6.25 and since displacements in the order of .1 mm full scale were sought, it required an analytical instrument capable of measuring the negative image co-ordinates to an accuracy in the region of .02 mm, or to a corresponding degree of accuracy if negative enlargements were to be analysed. The Sinar

camera is shown in Figure 5.17. All photographs were taken with Kodak gravure positive film having an estar thick base of 0.18 mm. The negative format was 102 mm x 127 mm.

Two analytical instruments were considered for the measurement of the image co-ordinates. Firstly, a Pye two-dimensional measuring microscope with a specified accuracy of $\pm$ 0.01 mm in each orthogonal direction and capable of accommodating the negative within its 200 mm x 100 mm operating area, was available. A photograph of the instrument is shown in Figure 5.18. The measuring microscope was illuminated from underneath by a convenient light source. The second choice of analytical instrument, used only in the preliminary stage, was a SAC sonic digitizing table which had a specified resolution of 0.1 mm. The philosophy governing this latter method was to print enlargements of the original negatives to approximately three quarters of the full scale size (350 mm x 350 mm). The information was then digitized from the enlarged print since the operating area of the table was 650 mm x 650 mm.

The use of a digitizer had obvious advantages in that it was comfortable to operate and had facilities for the automatic recording of all relevant information and thus formed a fast and efficient system while also minimising sources of human error. However, the inability of the digitizer to adequately resolve small-scale displacements coupled with its inconsistency regarding the reproducibility of results meant that the more cumbersome measuring microscope became the choice of analytical instrument used in this study. Reliable but limited quantitative information was preferable to numerous results defying or misleading interpretation.

Individual markers or targets located on specific model elements were not required since the image resolution

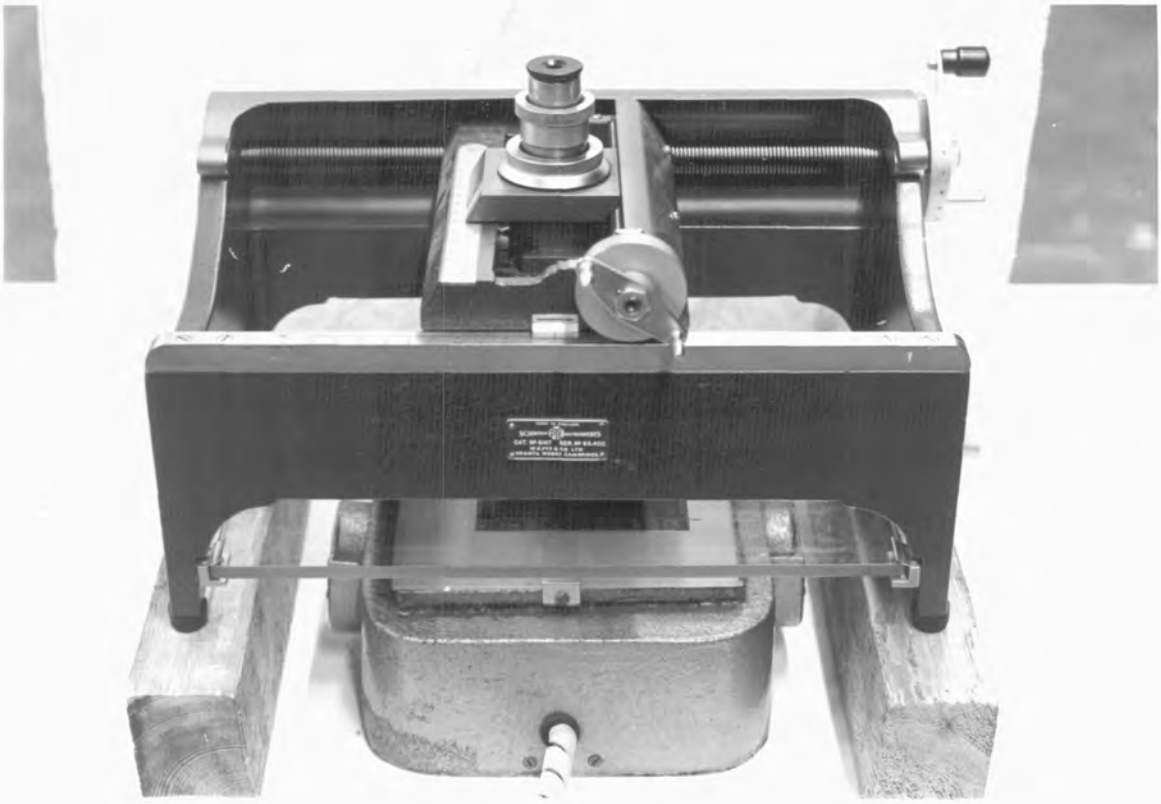


Figure 5.18: Eye measuring miscroscope

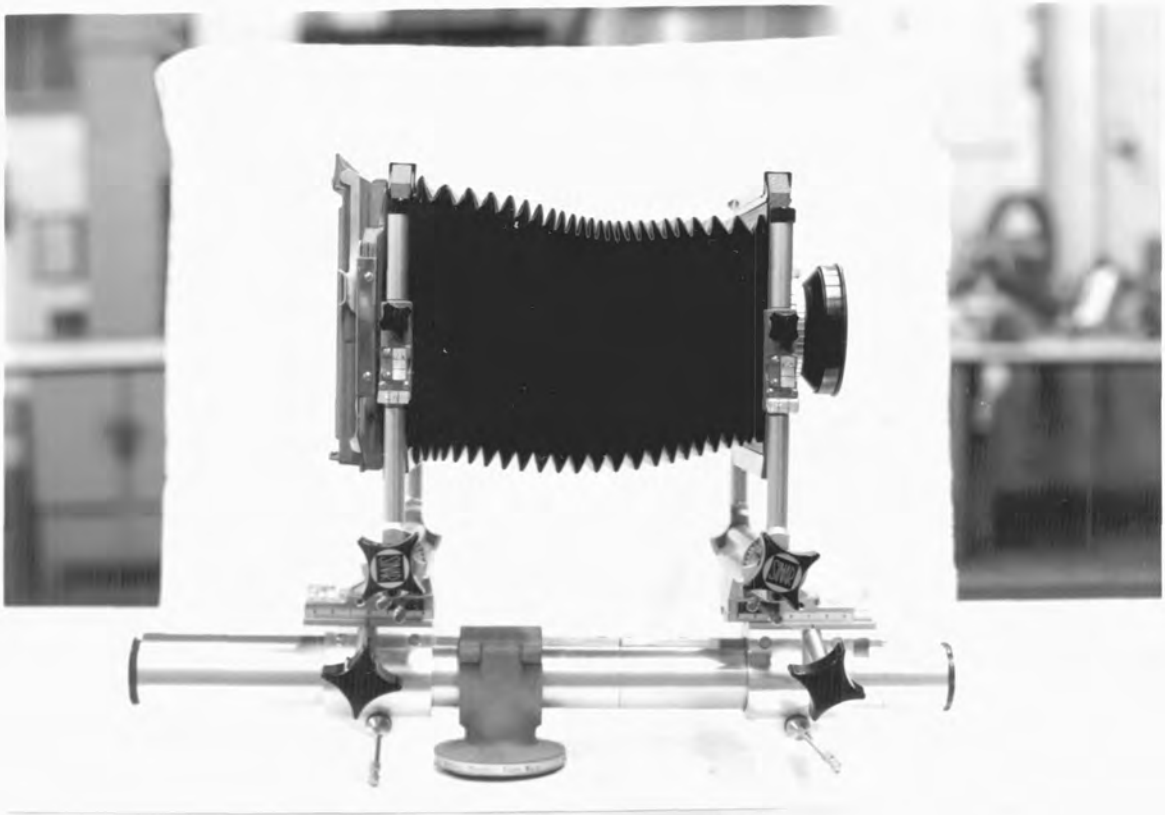


Figure 5.17. Sinar monorail camera

of the model geometry at the required scale was sufficient for the measuring microscope photograph analyser. Any dependence on the use of targets would severely limit the photogrammetry since the system would become inflexible and produce information only at pre-determined discrete locations, unless of course sufficient targets were employed. The photo co-ordinates of the model element corners were measured and recorded directly, these co-ordinates being subsequently transformed into global co-ordinates to allow the global displacement components of particular element corners to be determined. The resultant negative format of dark grey model elements separated by white lines representing the jointing between them provided adequate definition for the element corners. Alternating tones of grey elements assisted the resolution since the model had been carefully constructed, inverting adjacent elements to form a chequered pattern.

Since accurate and small-scale measurements were to be determined it was essential to establish a satisfactory photogrammetric control over the complete model area. Photogrammetric control consists of any points whose positions are known in an object-space reference co-ordinate system and whose images can be positively identified in the photographs. Such control was necessary since it enabled all the parameters of both the 'interior orientation' and'exterior orientation' of the exposure camera to be calculated with high accuracy. This subsequently enables the calculation of the space co-ordinates for all of the negative measurements previously collated.

Photogrammetric control for the model experiments was provided by points on a rectangular reference frame which surrounded the perimeter of the model. Sections of surveying tape were attached to the reference frame and a control point was defined as the intersection of a selected graduation line with an edge of the tape. The

photogrammetric reference frame was attached to the housing frame of the loading apparatus, and stood in a vertical plane approximately 75 mm in front of the plane of the model. After each model test, the reference frame had to be disconnected to enable the loading apparatus to pivot from the vertical to the horizontal position. Hence, space co-ordinates for all control points had to be re-calculated for each separate test.

Small sections of the same surveying tape provided control points located in the plane of the model near the corners and at the corners of the reaction frame. The control points on the reaction frame were used to determine if it was maintaining a stationary position under the applied loading. The photogrammetric control set-up is illustrated in Figure 5.19. A minimum of thirteen control points were surveyed and the space co-ordinates of these points were determined using triangulation. The space (ground) co-ordinates of control points determined by geodetic operations were assumed to be errorless.

Two Vickers V22 six-second theodolites were used with the theodolite stations located approximately 2.4 m from the model and 1.9 m apart. The tripod legs for mounting the theodolites were set into holes in the concrete floor. With the theodolites arranged as above, the accuracy was such that 2.5 minutes of arc on each theodolite corresponded to a distance of approximately 0.1 mm on the model. A photograph of the theodolite arrangement is shown in Figure 5.20. The distance between the theodolite stations was measured by tape but this distance was not critical since accurate distances between points on the model were available for the reduction of data to space co-ordinates. An arbitrary origin was chosen for the 3-dimensional space co-ordinate system to ensure that values for the space and photo planes increase in the same general direction along both X and Y axes and that Z values increase from the

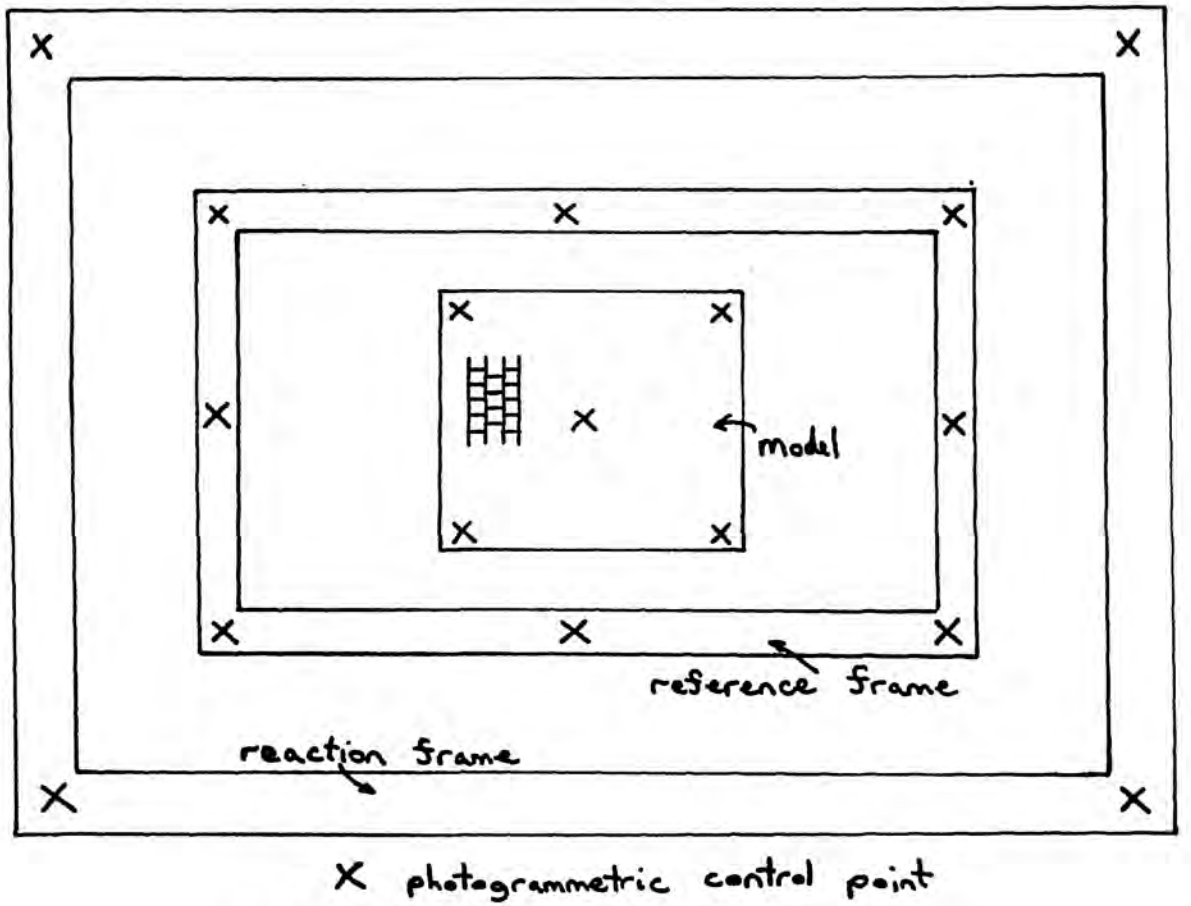



Figure 5.19: Photogrammetric control arrangement

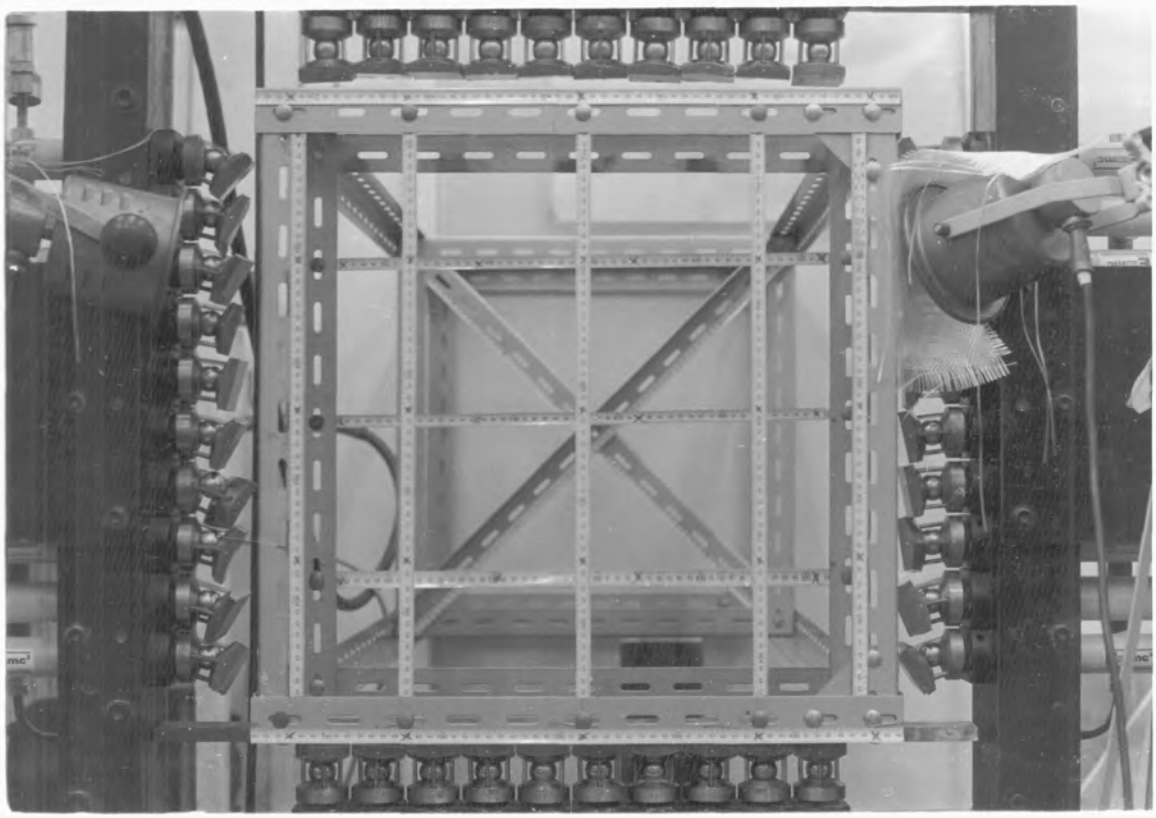


Figure 5.21: Camera calibration set-up

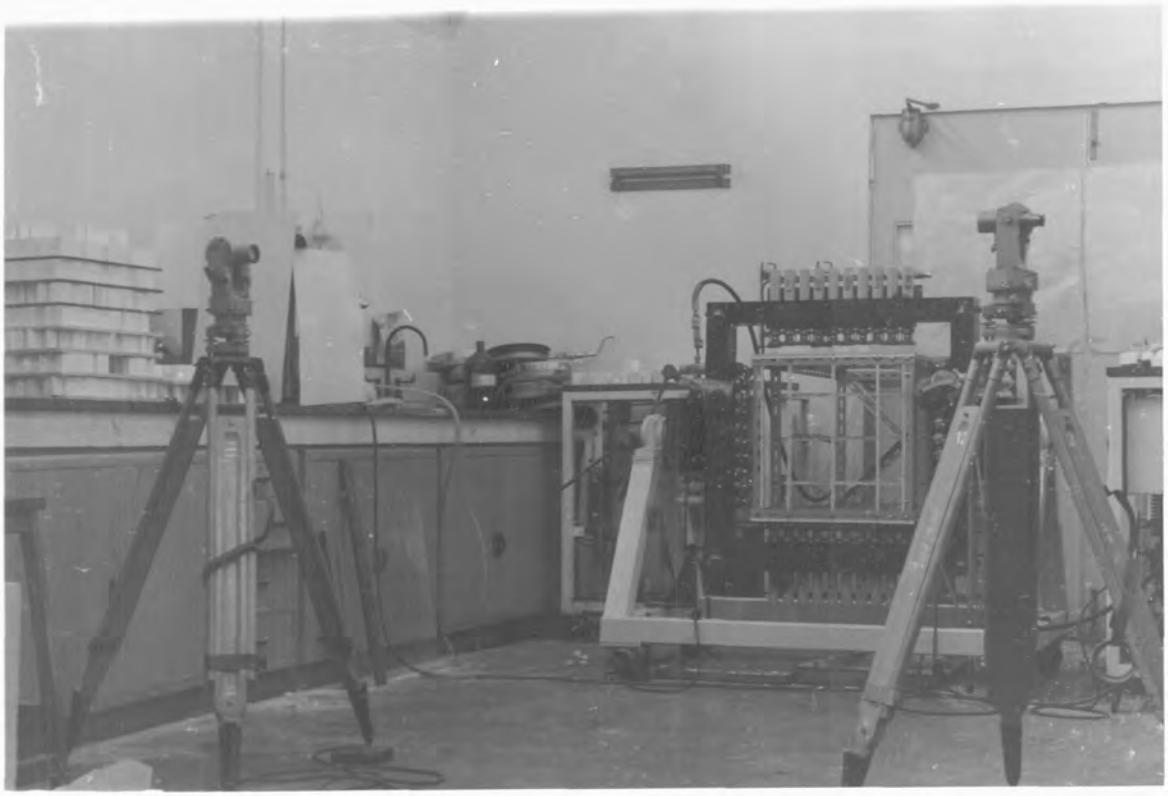


Figure 5.20: Theodolite arrangement

object towards the camera. Otherwise, the space co-ordinates were of no particular significance.

5.9.2. Experimental Procedure and Interpretation:

Once a satisfactory photogrammetric control had been constructed and validated, the model tests could then proceed with the subsequent determination of all relevant space co-ordinates and ultimately model element differential displacements. Some familiarisation tests were initially conducted to standardise the complete process and ensure that all photographic and experimental equipment and computer programs were functioning correctly.

The plane of the camera film was arranged to be as nearly parallel to the plane of the model as possible. Also, the X and Y axes of the space system were approximately parallel to the X and Y axes, respectively, on the photograph. The camera was mounted on a tripod with the legs of the tripod locating into holes in the concrete floor for extra stability. Photographs were taken without the perspex safety sheet covering the model and the white opaque nature of the model bricks meant that only a minimal amount of flood lighting in addition to the fluorescent room lighting was required.

In each model the first photograph taken before any loading had been applied was used as a static reference datum to establish the initial ('zero') space co-ordinates. The negative was analysed using a Pye travelling microscope to measure the photo co-ordinates of element corners. To calculate the three unknown centroidal rigid body displacements of a particular element the planimetric positions of at least three corners were needed, and since the blocks were of square section, it was decided to record the co-ordinates of all four corners. Representative blocks throughout the model were selected for co-ordinate determination with the advantage of analysing only those blocks most clearly

defined on the negative since no pre-selection process was necessary. Besides recording the co-ordinates of particular blocks in each model, which usually numbered between 30 and 40, the photo co-ordinates of at least five of the control points were recorded. Also, the photo co-ordinates for two points on each of the four edges of the negative, as near to the corners of the frame as possible, were recorded. These edge points were used to derive photo co-ordinates for the centre of the negative, as required by the computer program.

The above measurement procedure was then used to analyse subsequent photographs and derive the space co-ordinates for the displaced block positions. These were then compared with the initial space co-ordinates to calculate the differential global displacements of the block corners. Finally, the three centroidal displacements of each block (two translational and one rotational) could be deduced from a knowledge of the block geometry and the corner differential displacements. This is outlined in Appendix I.

A computer program was available to convert the photo co-ordinates into planimetric rectangular co-ordinates. The program is based on transformation formulae quoted by Hirvonen (1971) to establish the absolute orientation of each photograph. The program will either calibrate a camera or calculate the X and Y space co-ordinates of points with known Z co-ordinates from single photographs taken with a camera of known interior orientation. For calibration, the elements of both 'interior orientation' and 'exterior orientation' of the exposure camera are determined accurately, if the space co-ordinates of at least five suitable ground control points are supplied. For co-ordinate determination only, the six parameters of 'exterior orientation' are calculated and only three suitably placed ground control points are necessary. The program was used

in either mode and in each case produced X and Y space co-ordinates for any number of additional points provided their Z co-ordinates were known. A listing of the program is contained in Appendix IV.

5.9.3. Camera Calibration:

Since a non-metric camera was used to supply the photographs for the photogrammetric measuring technique, it was necessary to establish to a reasonable level of accuracy the parameters of 'interior orientation'. Faig (1975) describes a non-metric camera as one which has an interior orientation that is completely or partially unknown and frequently unstable. He also states that a non-metric camera does not have fiducial marks and lists a number of parameters which define the 'interior orientation' including focal length or principal distance, position of the principal point on the photograph, and lens distortion. It should be emphasized here that the computer program described in the last section could be used either to determine the 'interior orientation' parameters in the same adjustment as the other unknowns (i.e. in calibration mode) or it could assume the 'interior orientation' parameters to be known whereby only the elements of 'exterior orientation' would be calculated. The advantage of using the program in calibration mode is that the effect of instability of the non-metric camera is eliminated since the measurements of unknown points are determined from the same photograph that is used for the determination of the 'interior orientation'.

The philosophy governing the camera calibration performed in this study was to provide a sufficiently large number of well-distributed and geodetically determined ground control points so that a measure of the lens distortion could be obtained. A rectangular, box-shaped open frame was constructed from sections of handy-angle, similar to the wooden frame used by Robinson (1979). Attached to the frame members, located at various sections

along its length, were strips of surveying tape which established the ground control points. A number of points on each tape were then surveyed from the two theodolite stations providing an adequate distribution of points throughout the field of view. The frame was positioned in the biaxial loading apparatus with the same camera setting as that used for the subsequent model studies and several photographs of the calibration frame were taken using the Sinar camera. The camera setting was such as to ensure a sufficient depth of field so that all control points could be easily resolved on the analyser. The calibration set-up is shown in Figure 5.21.

The results for two of the camera calibration experiments analysed with the travelling microscope are presented in Table 5.6. A plot of the residuals for one test is shown in Figure 5.22 and it can be seen that the pattern of lens distortion is rather even with no concentration of large errors in the corners of the frame. This is confirmed by the fact that there is very little change in the 'interior orientation' parameters when the control points located at the extremeties of the frame are discarded in the analysis. The pattern of lens distortion obtained for the Sinar camera differs quite markedly from that of other researchers using non-metric cameras e.g. Robinson (1979). This is due to the fact that the co-ordinates of the principal point are accurately calculated simultaneously with the reduction of the other data and do not assume a pre-determined location such as the centre of the photograph. A residual is defined as follows:

$$\text{Residual} = \left[\begin{pmatrix}\text{calc.photo co-ords.}\\ \text{relative to p.p. as origin}\end{pmatrix} + \begin{pmatrix}\text{co-ords. of p.p.}\\ \text{relative to photo}\\ \text{centre as origin}\end{pmatrix}\right] - \left[\begin{pmatrix}\text{photo co-ords. as read}\\ \text{from analyser}\end{pmatrix} - \begin{pmatrix}\text{co-ords. of photo}\\ \text{centre}\end{pmatrix}\right]$$

It is obvious that if the principal point and the photograph centre are assumed to coincide, then large residuals

Table 5.6: Results of camera calibration tests

| Number of ground control points | S.E. of photo co-ordinate reading (mm) | Principal distance (mm) | Co-ordinates of principal point relative to centre of photograph as origin (mm) | |
|---|---|---|---|---|
| | | | x | y |
| 37 | .020 | 175.85 | -1.084 | .356 |
| .33 * | .020 | 175.80 | -1.163 | .390 |
| 37 | .019 | 174.92 | 1.488 | -.423 |
| 33 * | .017 | 174.85 | 1.526 | -.530 |

* Four corner points omitted.

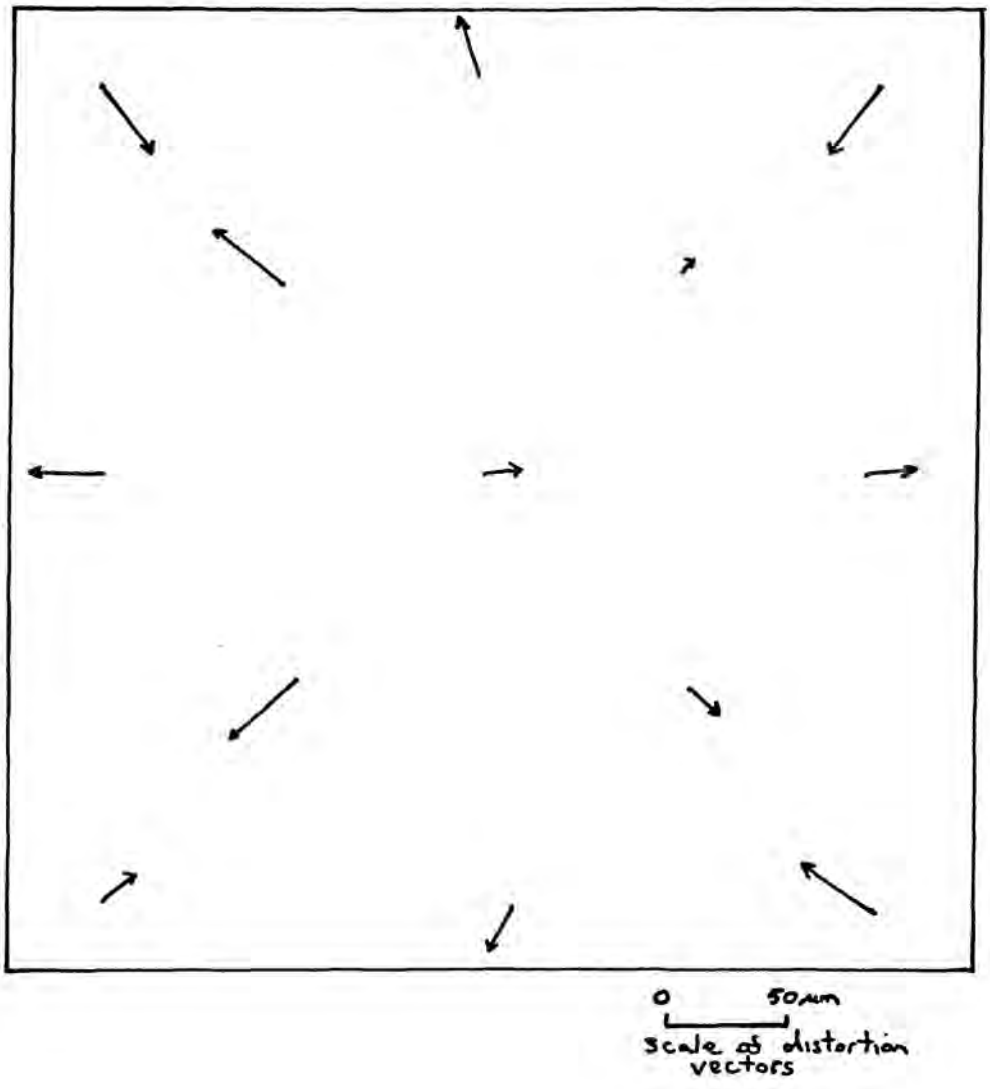



Figure 5.22: Plot of lens distortion vectors

will result.

5.9.4. Error Analysis:

A random selection of 22 independent analyses showed that the standard error for a photo co-ordinate reading varied between .008 mm and .035 mm with an average standard error of .023 mm. Robinson (1979) obtained an average standard error of .026 mm for 17 arbitrarily selected photographs analysed with the same travelling microscope. Robinson devised an experimental procedure which enabled an approximate estimate of the accidental observation error, which forms a component of the overall standard error, to be assessed. His analysis produced a standard error of observation of .003 mm. This value could be compared with that obtained from an analysis of the deviations of control point residuals from their mean values for identical control points in several of the model photographs. This produced a standard error of observation of .004 mm.

An estimate of the standard error of a space (ground) co-ordinate could be assessed from an analysis of the ground co-ordinates of identical control points determined for the various photographs analysed during a model test. An average value for this standard error of .05 mm was calculated which meant that the standard error for a block corner displacement would be approximately .07 mm ($\sqrt{2} * .05$) due to the subtraction of the corresponding corner ground co-ordinates.

Several alternative sources of error were possible with the instrumentation technique adopted. Since a non-metric camera was used with film rather than stable plates, it was likely that lack of flatness of the film could cause errors. Any major errors arising from the film flatness would be detected during the analysis stage since the separations between several points in the field of view were known to a high accuracy. The camera was set

up as for the model studies and several photographs were taken of points whose separation was accurately known. The difference between the known and photographically determined separation was minimal, the difference being of the same order as the standard error for the displacements as calculated above.

Another source of possible error was in assuming that the Z ground co-ordinates of all unknown points were accurately known. Actually, as discussed in Section 5.9.2, a constant Z ground co-ordinate was assumed for all these points both before and after testing. However, it was possible either as a result of poor model construction or any out-of-plane movement during testing that this assumption may not always have been justified. Robinson (loc. cit.) quotes a formula to determine the error in a ground co-ordinate due to any discrepancy in the Z co-ordinate as:

Error in ground co-ordinate =

$$\frac{\text{Error in height}}{\text{Camera height}} \times \text{Radial distance of the point}$$

where the camera height is the height of the camera perspective centre above the reference field and the radial distance of the point is the distance from the centre of the model to the point at which the error in the ground co-ordinate is required. Considering the worst possible case in which a block has a Z co-ordinate variation before and after testing of 2.5 mm and is located at one of the model corners, the error in the ground co-ordinates would have a magnitude of approximately 0.4 mm. For small variations in height the error decreases accordingly and during all of the model tests conducted both visual and measured results suggested no significant out-of-plane movements. Hence, the justification for assuming a constant height for all unknown points during the analysis was verified.

It was considered unnecessary to correct the image co-ordinates of the block corners or control points for lens distortion. Absolute values for the co-ordinates were of little consequence since only the magnitude of the difference between a set of co-ordinates was sought. It was considered very unlikely that any correction for lens distortion would significantly alter the differential displacement since the correction would be applied to block corners whose positions on the negatives were almost identical. This has also been postulated by past researchers using similar single photograph techniques (Chiat et. al., 1979).

The use of a single photograph photogrammetric technique incorporating an ordinary camera, not specifically calibrated for photogrammetric work, may have led to various sources of small errors in determining the absolute block positions. However, since only relative displacements were required, errors tended to be compensated for and did, in general, maintain tolerable levels. Moreover, in positions where errors are present, then other factors such as compatibility with surrounding behaviour will highlight erroneous results and possibly suggest values for the unknowns. Thus, the method is considered suitable for the application in question. A summary of the complete photogrammetry technique is presented in Appendix IV.

5.9.5. Other Instrumentation:

Apart from the main photogrammetric process outlined above, some secondary instrumentation was incorporated during certain tests. Accurate dial gauges were used to indicate the initial stages of movement and to subsequently maintain a constant rate of movement during shear tests. However, they were found to interfere with the failure mechanism in some block-jointed models and had to be used with great caution.

The applied stresses were measured by monitoring the hydraulic pressures supplied to each hydraulic circuit. Accurate pressure gauges were located on each hydraulic console and were calibrated to give directly the average stress applied to each model edge.

## 5.10. Modelling Material:

The literature contains numerous well-documented reports on the development of suitable modelling materials for particular applications, such as Rosenblad (1968), Barton (1970), Heuer and Hendron (1971), Barron and Larocque (1962) and Brown and Trollope (1967). In the past, the majority of modelling materials developed have been concerned with simulating the properties of the prototype material in as many of its behavioural properties as possible and at least correctly simulating those of greatest importance. Modelling is not, however, only concerned with achieving similarity conditions and some compromise is usually necessary, taking into account factors such as model scale, material costs, preparation time and testing procedure. Modelling materials have developed over the years since no satisfactory technique has been discovered whereby the actual prototype material may be used to advantage in model tests. This is because of the excessive size and loading capacity which would be required to test the model and of the problems associated with obtaining a representative prototype sample. Hence, 'artificial' rock materials have had to be developed and manufactured and this has necessitated the use of efficient preparation techniques since typical discontinuous model studies require mass production of component elements.

The purpose of the modelling material manufactured and used in this study was not to represent the scaled mechanical properties of a particular prototype but to provide a material whose basic features could be sufficiently well characterised and were suitable for the proposed series of experimental and numerical model studies.

However, it was still considered appropriate to be able to relate the experimental model studies, albeit however crudely, to their full scale equivalent if only to examine the extent of the deviation of the model studies from reality. This is discussed in Section 5.10.3.

5.10.1. Requirements of Modelling Material:

Before a suitable model material could be selected and preliminary testing conducted, several requirements had to be considered. These were that the ensuing model material must:

i) be easily obtainable in economical quantities and not require expensive equipment;

ii) have material properties which are uniform throughout each specimen and reproducible between specimens from different batches;

iii) have minimum variation in the cast dimensions to ensure that subsequent behaviour is not governed by irregularities in shape;

iv) have strength parameters of sufficient magnitude so that the elastic deformation of the material under the proposed experimental loading is as small as possible;

v) be easily fabricated into the desired shapes with a minimum time delay between casting and testing;

vi) when cured, exhibit strengths and failure modes similar to typical rock materials;

vii) have a casting and setting procedure which minimizes undesirable features such as excessive bleeding, shrinkage or distortion and entrapped air bubbles.

With the above requirements in mind, an extensive literature search was conducted to examine the modelling materials developed by previous investigators. It would be true to say that the majority of model materials used previously have been based on a non-granular gypsum plaster or cement media either with or without aggregate

granular materials such as sand which are commonly used to increase the internal friction angle of the material. The use of fillers or retarders has also been usefully employed with such mixtures to either aid the manufacturing process or to influence the mechanical properties. There are several reasons for preference being given to a plaster based mix to simulate geological materials in structural models and these include the brittle nature of the resulting material under load, the ability to give similitude with prototype rocks, the large range of strengths obtainable by varying the mix proportions, the relative ease of casting and moulding, and the uniform and reproducible properties achieved between specimens. However, the manufacture of plaster modelling materials is not without problems (Stimpson, 1970; Heuer and Hendron, 1971) and care must be taken to ensure that excessive bleeding and shrinkage during setting and hydration does not affect the desired properties or that the presence of air bubbles does not create a low density, easily compacted material.

It was decided to select a non-granular plaster-water mixture as the model material for the experimental, block-jointed studies. Such a model material falls into the 'non-plastics-non-metallic-brittle' group of non-granular media as proposed by Stimpson (1970). A high strength industrial plaster (trade name Crystacal LX; supplied by British Gypsum Limited) was mixed with water in the specific ratio of 2.25 : 1 by weight respectively. Setting and hardening of the mixture was a very rapid process and only volumes of manageable proportions were mixed. Specific details of the exact mixing technique are contained in Appendix V. Eissa (1974) conducted tests on specimens manufactured from the same plaster and the dependence of uniaxial compressive strength on both the plaster-water ratio and curing time are shown in Figures 5.23 and 5.24. As can be seen from these graphs, along with those produced by other investigators (Russel

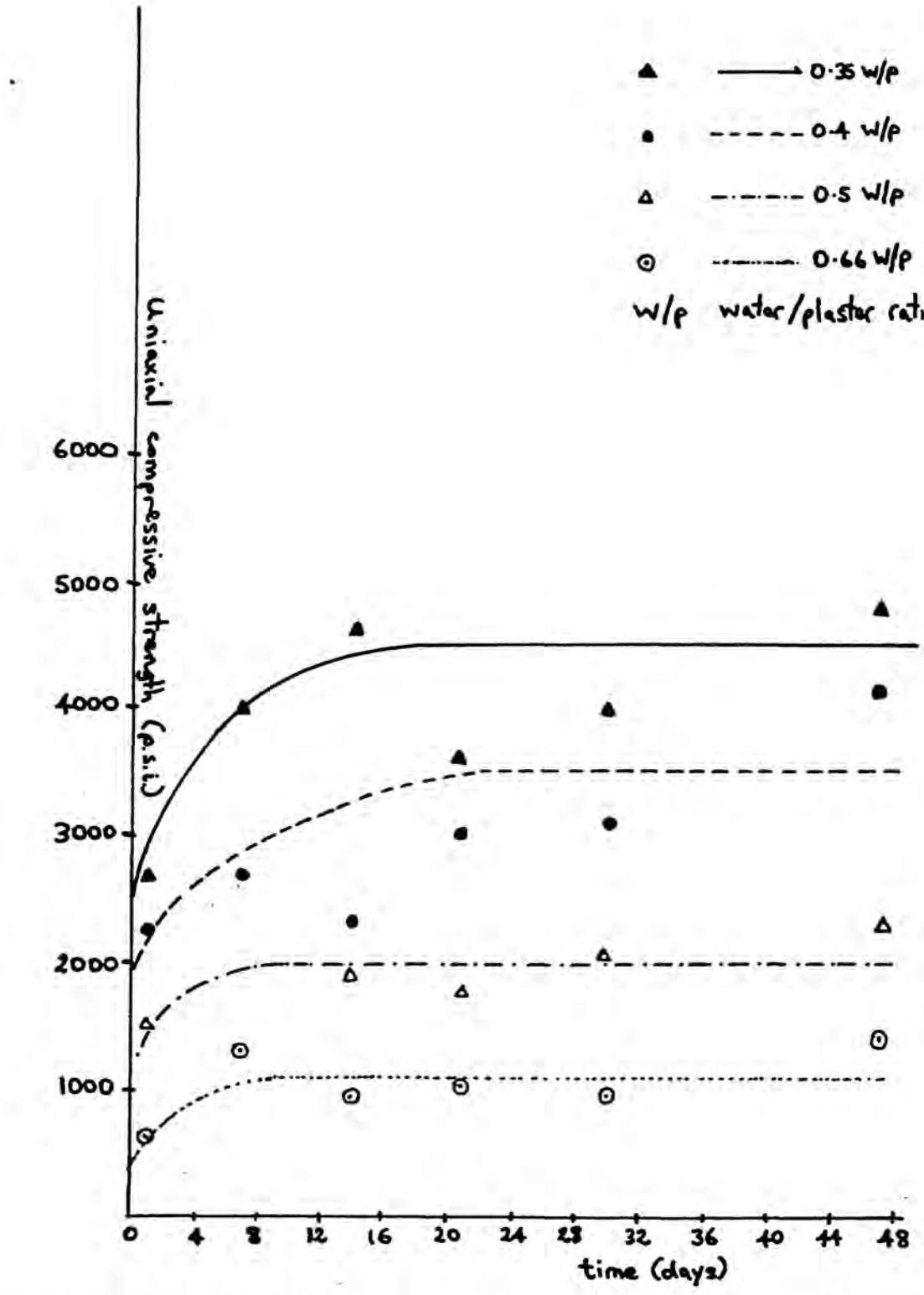



Figure 5.23: Uniaxial compressive strength versus curing time for plaster (after Eissa, 1974).

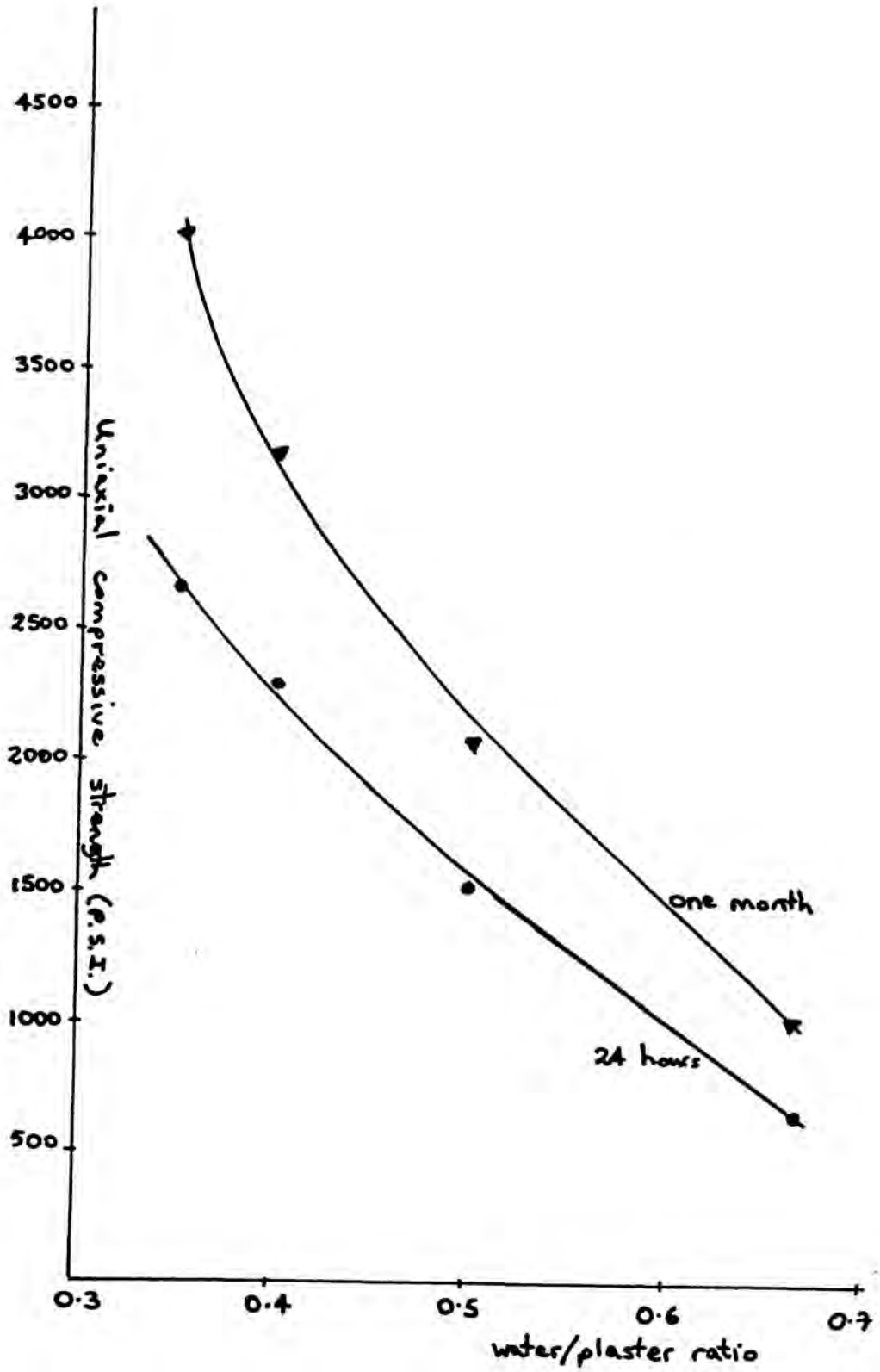



Figure 5.24: Uniaxial compressive strength versus water/plaster ratios and drying time (after Eissa, 1974).

and Blakey, 1956), the mechanical properties, particularly uniaxial compressive strength and Young's modulus, can be varied over a wide range by varying the plaster/water ratio of the mix. In general, the higher the plaster/water ratio the stronger is the resultant dry plaster specimen. However, there are upper and lower limits to the practical amount of water which can be used in the casting phase.

The reversible chemical process in which the 'as-received' plaster (calcium sulphate hemihydrate) is hydrated to form a gypsum plaster (calcium sulphate dihydrate) involves the absorption of water and the generation of heat.

$$CaSO_4.\tfrac{1}{2}H_2O + 3/2\ H_2O \rightleftharpoons CaSO_4.2H_2O + \text{heat}$$

Only 18.6 percent of water by weight is theoretically required during the hydration process to become chemically bound with the gypsum plaster to form, according to Heuer and Hendron (1971), "an inter-knitted network of monoclinic gypsum crystals giving the mass its strength". However, a considerably greater amount of water is necessary to ensure a mix is produced which has a sufficient viscosity to enable thorough mixing and pouring and yet not allow segregation to occur. This additional 'free' water present during the casting and curing stages has a very important influence on the resulting properties and means that a proper curing process in which the optimum water content is attained is the most critical part of the material preparation.

The criterion adopted for the curing process was to allow the plaster blocks to attain constant weight by allowing the excess water to be lost through diffusion and evaporation in air at room temperature. It has been common to speed up the drying process by placing the specimens in an oven at an elevated temperature (Barron and Larocque, 1962, suggest 35°C as a safe drying

temperature) but care must be taken not to reverse the chemical process by driving off the chemically bound water and so form the hemihydrate or even possibly the anhydrite. Raphael (1960) showed that this breakdown of gypsum plaster occurs at a temperature of about 55°C, although there is much confusion in the literature as to a 'safe' drying temperature.

The curing time required to achieve constant weight was a period of approximately three weeks, depending on sample size and shape. After losing the excess water, the gypsum plaster should theoretically achieve a constant maximum strength although Brown and Trollope (1967), who cured for 28 days at constant humidity and temperature, found a slight increase in strength after this time. After the zero free moisture condition had been reached and the specimen was subjected to normal room temperature and humidity conditions, it did not pick up moisture from the atmosphere. This aided the experimental procedure since there was no limitation placed upon the length of exposure of the specimens to normal testing conditions.

From the above discussion it is clear that the method of preparation has a marked influence on the nature of the model material. The method of mixing and decisions regarding time of mixing, use of accessory constituents, moulding technique, and curing procedure must be strictly adhered to, once adopted.

Ergun (1970) has investigated the effect of block tolerances on the stress distribution and strength of a discontinuous medium. He demonstrated experimentally that the stress distribution in a jointed mass was greatly affected by the presence of voids along joints due to the non-parallelness and non-squareness of the block faces. Point contacts were created which produced areas of high stress concentration even under relatively low applied stresses. It was necessary, therefore, to adopt a

satisfactory casting procedure to produce large quantities of plaster blocks with acceptable tolerances. Initially, perspex moulds were used to cast the plaster blocks and these are shown in Figure 5.25. However, serious difficulties were experienced with these moulds since the mould dimensions became unstable after dismantling and reassembly of the component pieces several times. Also, perspex itself has a major disadvantage in that its thickness varies considerably over a length but this was partially accounted for in the initial mould design. The time consuming, unstable, and tedious nature of casting the model material using these moulds soon led to the search for a more efficient process.

Moulds manufactured from urethane rubber (Adiprene L-100) were chosen largely because of the successes obtained with it by Ergun (1970). Six rubber moulds were cast from a 'male' steel master mould. The resulting rubber mould was dimensionally stable and each mould could produce 36 square plaster blocks (25 mm x 25 mm x 50 mm), as shown in Figure 5.26. A volume of mix sufficient to fill three of these moulds was adopted as the standard mix quantity. Actual block dimensions differed slightly between moulds (this being a function of the mould manufacturing process) but by careful grading and assorting of blocks, tolerances to within .025 mm could be achieved. This variation in length and thickness between faces was randomly surveyed for a number of specimens throughout the experimental programme to ensure adequate quality control. Such tolerances were similar to those quoted by Ergun (1970) and therefore it could be reasonably expected that problems associated with inaccurate block dimensions would be minimised. There was no need to use a release agent as the plaster stripped easily from the rubber mould and it was found that the extraction of the set blocks from the mould was greatly assisted by heating the mould in an oven for about 15 minutes (to about $40^{\circ}C$). Due to the differential rates of expansion, the bricks

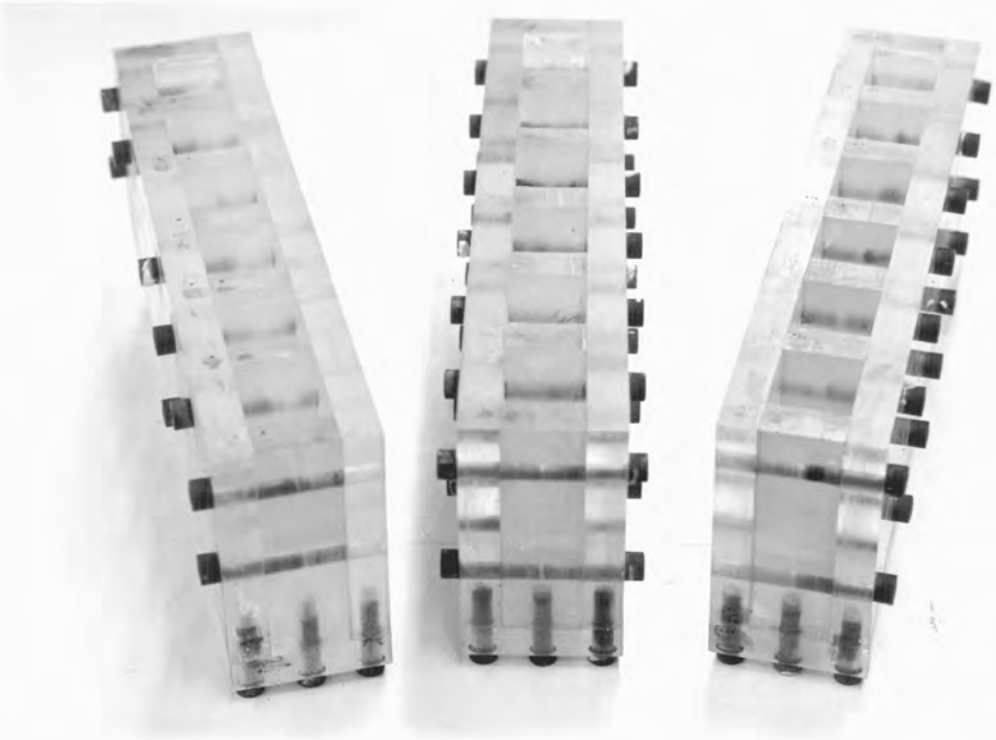


Figure 5.25: Perspex moulds

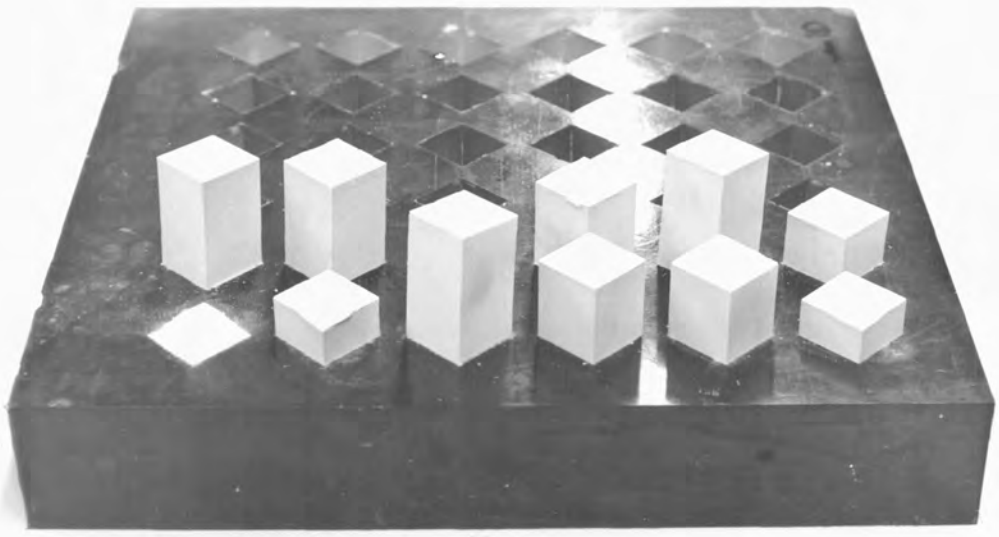


Figure 5.26: Urethane rubber moulds

were then easily removed under light pressure and placed on glass trays to cure at room conditions. Special techniques were developed for making the odd shaped edge pieces required for a discontinuous model with inclined jointing. These were manufactured at a similar time to the bricks and a stockpile was kept of all component pieces so that they could be used in model construction as and when required.

5.10.2. Properties of Modelling Material:

The main mechanical properties determined for the dry plaster blocks were uniaxial compressive strength, Young's modulus, uniaxial tensile strength, Poisson's ratio and the interface sliding friction angle. Initially, specimens with various plaster/water ratios ranging from 1.5 : 1 to 2.5 : 1 were tested as curing proceeded and the results agreed favourably with the general trends of results obtained by previous investigators i.e. uniaxial compressive strength and Young's modulus increased with increasing plaster/water ratio while Poisson's ratio remained nearly constant.

Uniaxial compression tests were performed throughout the experimental programme on random specimens selected from assorted batches. The uniaxial compression test was used as the standard control test throughout and specimens were also tested the same day as the experiments were performed. The specimens had a length to diameter ratio of 2 : 1 and the tests were carried out in a soft loading machine using solid spherical platens with cross-sections similar to those of the specimens. The tests indicated a uniaxial compressive strength ($\sigma_c$) of 27.85 MPa with a maximum variation of between 5 and 10%. Uniaxial compression tests provided control whenever a new bag of Crystacal LX plaster was used. The plaster specimens were characterised by a brittle failure mode with typical failures shown in Figure 5.27. The cones formed at the ends of some specimens indicated an 'end effects' problem

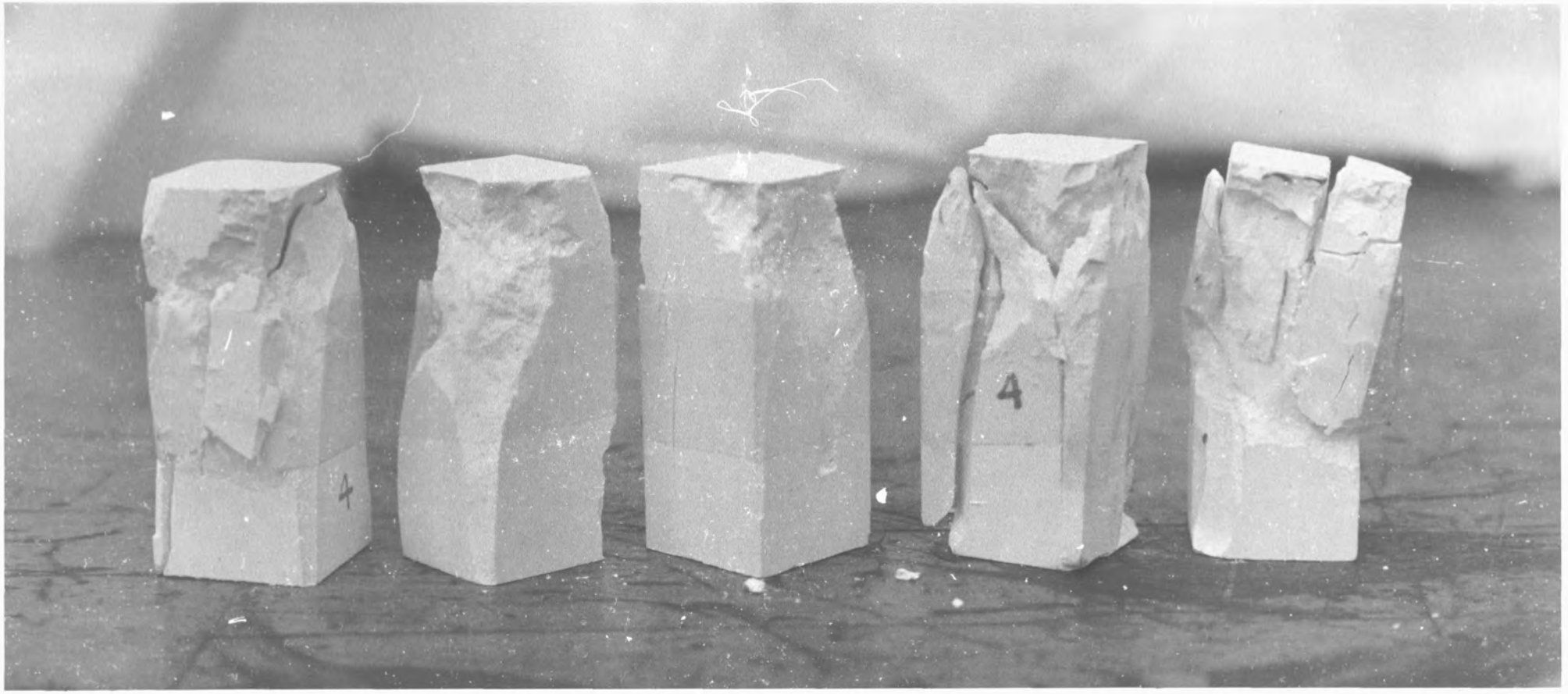



Figure 5.27: Typical plaster failures

and would probably account for the considerable standard error in the uniaxial compressive strength.

Young's modulus (E) and Poisson's ratio ($\nu$) were measured by strain gauging the plaster blocks at mid-height. Loading was initially cycled up to approximately 50% of the uniaxial compressive strength before finally loading to failure. A typical stress-strain curve is shown in Figure 5.28 and it can be seen that the material behaves in a linear fashion except for initial 'bedding-in' effects. This high initial strain is not surprising in view of the highly porous nature of the material with some investigators reporting complete collapse of similar plaster materials under confining pressure alone during triaxial tests. An average value for Young's modulus was $1.088 \times 10^4$ MPa with a 4% variation while Poisson's ratio remained constant at 0.2. This value for Poisson's ratio varied slightly from the quoted average value of 0.24 in the literature and the discrepancies could well be due to the testing procedure.

The technique used for determining the tensile strength has been reported in Section 5.7.6 where the uniaxial tensile strength ($\sigma_t$) was determined as 2.55 MPa. The above results give values for the modulus ratio ($E/\sigma_c$) and compressive/tensile ratio ($\sigma_c/\sigma_t$) of approximately 390 and 11 respectively, which are not uncharacteristic of many common rock types.

Simple sliding tests gave the interface friction angle of the plaster bricks as 35 degrees, although this value increased slightly to 37 or 38 degrees under higher normal loads. The density of the cured plaster was $1.45 \times 10^3$ Kg/m$^3$. No triaxial tests were necessary.

The properties for the selected model material outlined above adequately met the considerations specified earlier and no major difficulties in using the material

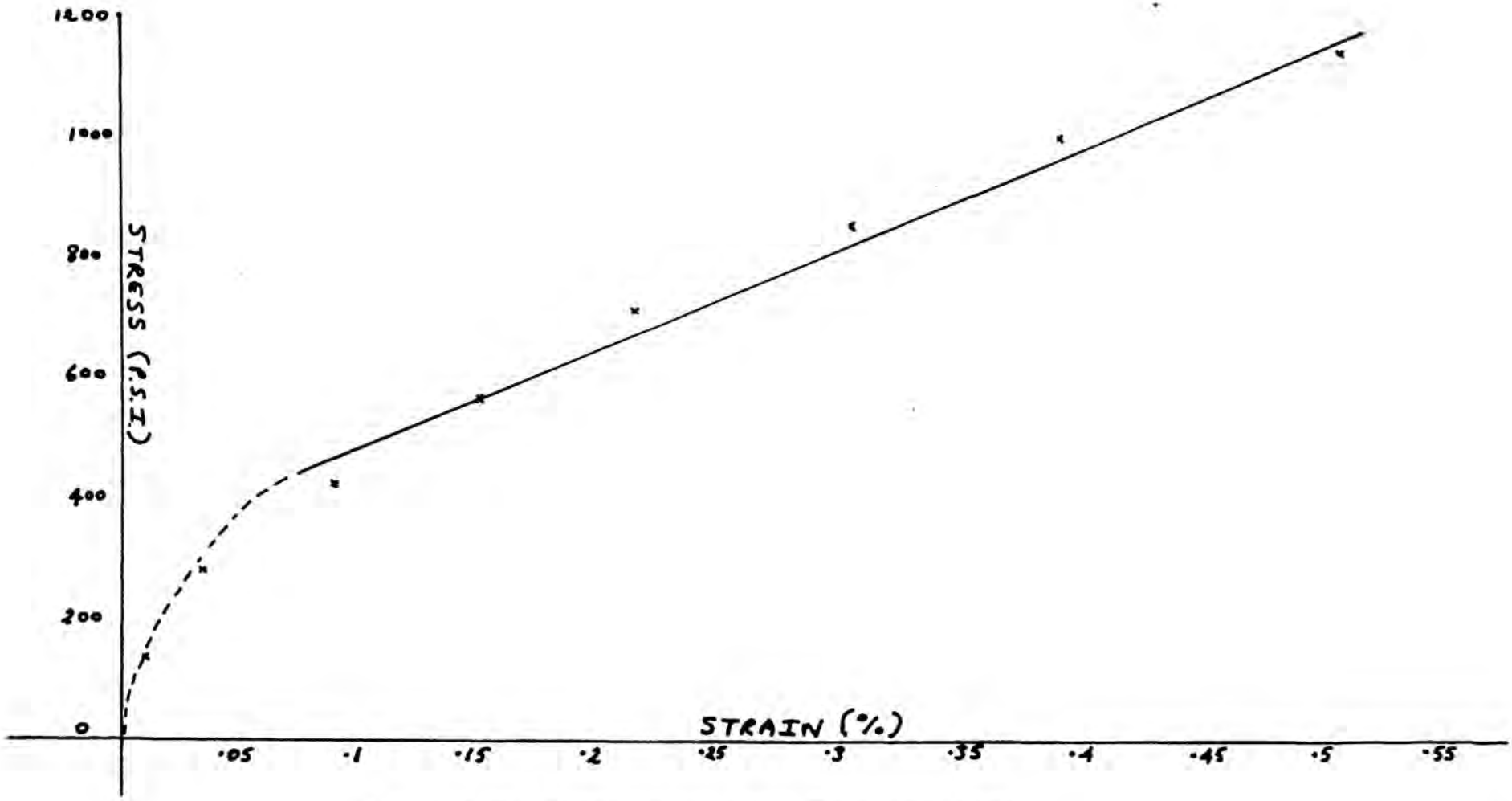



Figure 5.28: Stress-strain graph for plaster used.

could be foreseen.

5.10.3. Relationship to Prototype:

As previously discussed, it was considered useful to relate the model material and jointed model studies to a real physical situation. The prototype may be regarded as a segment of a long straight horizontal underground excavation at a depth which is several times greater than the excavation height.

The requirements for similitude between model and prototype are specified by the techniques of dimensional analysis. Basically, this consists of constructing a number of independent dimensionless parameters. These are factors formed by the combination of pertinent variables considered to influence the system behaviour and a set of fundamental dimensions such as those of force and length for a static system. The dimensionless parameters allow scale factors and model laws to be developed. The similitude condition is then achieved if each dimensionless factor is the same for both model and prototype and by measuring selected variables in the model, the corresponding values of variables in the prototype can be predicted. If gravity loading is incorporated, then three dimensionless parameters determine the similitude requirements for the system. These are the geometric scale factor, the dynamic (or strength) scale factor and the density factor. If similitude exists, then the following relationship is true:

$$\left(\frac{\rho g L}{E}\right)_m = \left(\frac{\rho g L}{E}\right)_p$$

where subscripts m and p refer to model and prototype respectively and $\rho$ , $g$ , L and E represent the density, gravitational acceleration, length and elastic modulus for each system. It will be noted that the above expression involves the equivalence of two dimensionless parameters, providing the gravitational acceleration is assumed the same for both model and prototype. The above

relationship can then be expressed as

$$\left(\frac{\rho_m}{\rho_p}\right)\left(\frac{Ep}{Em}\right) = \left(\frac{Lp}{Lm}\right)$$

$$\text{or } \psi \cdot \left(\frac{\rho_m}{\rho_p}\right) = \lambda$$

where $\psi$ = dynamic scale factor

and $\lambda$ = geometric scale factor

For this relationship to be satisfied it is obvious that a model material with a high density and low strength must be sought. The geometric scale factor implies that the distance between any two points in the model must bear a constant ratio to the corresponding points in the prototype. Geometric scales reported in the literature vary widely from 10 : 1 used by Everling (1964) to 300 : 1 used by Barton (1978), this factor being largely determined by economic considerations.

For the purposes of this exercise, let the geometric scale factor be 30 : 1, and assume an average density for rock of $2.5 \times 10^3$ Kg/m$^3$. Then

$$\frac{\rho_m}{\rho_p} = \frac{1.45}{2.5} = 0.58$$

and $$\psi = 30/.58 = 51.72$$

That is, the ratio of model and prototype densities (0.58) gives a stress scale ($\psi$) of 51.72 : 1 when the geometric scale ($\lambda$) is 30 : 1. Now, consider a typical model study, as shown in Figure 6.3, in which the 175 mm x 25 mm model opening represents an underground excavation with dimensions 5.25 m x 0.75 m in a segment of the prototype simulating horizontal and vertical dimensions each of 15 m. The average stresses applied to the model boundaries to initiate failure during testing were approximately 0.86 MPa vertically and 0.18 MPa horizontally. These represent

vertical and horizontal field stresses in the prototype of 44.84 MPa and 9.31 MPa respectively which would typically indicate an underground excavation buried some 1500 m to 2000 m below the surface, with a K factor of 0.20. It is interesting to note that the scaled model material properties imply a uniaxial compressive strength and Young's modulus for the prototype rock of approximately 1440 MPa and $5.63 \times 10^5$ MPa respectively. These are excessively large values for most rock types and failure of the intact rock blocks would be considered highly unlikely under the applied loads, a fact borne out from the model studies.

The joint spacing is, however, realistic with both continuous and discontinuous sets having a spacing of 0.75 m in a plane perpendicular to the excavation axis. Such values for joint spacing and rock block size have been measured in the field (Brady, 1977; Baczynski, 1977). Also, an interface friction angle for the model material of approximately 35 degrees is not uncharacteristic of the residual friction angle occurring in many rock joints.

Hence, the model studies examined here can be considered as 'overstiff' representations of actual mining environments and if prototype properties are to be realistically simulated, then a model material with reduced strength properties must be employed. Also, serious consideration would have to be given to developing sufficient frictional strength within the model material (between 25 degrees and 50 degrees) to agree with that of the prototype material.

As an alternative to the above analysis, if the model material and prototype densities are considered as variables whose influence on the behaviour of underground excavations is insignificant, then body forces may be neglected. In this case the field stresses are the most significant forces influencing the excavation behaviour.

When this condition is assumed, the geometric and strength scale factors are independent and may be selected arbitrarily. This is probably a more valid approach when examining the degree of similarity between the prototype and the experimental model studies discussed in Chapter 6. Again, let the geometric scale factor be 30 : 1 and assume an average prototype modulus of elasticity of $5.4 \times 10^4$ MPa. Then the strength scale factor ( $\psi$ ) will be given approximately as:

$$\psi = {}^{Ep}/_{Em} = 5.4/1.1 = 5 : 1$$

which is greatly reduced from that obtained when the strength scale factor was dependent on the geometric scale.

## 5.11. Conclusions:

A suitable physical modelling technique has been developed for studying excavations in two-dimensional, plane stress, discontinuous models. The requirement for the precise measurement of the displacements of the jointed model constituents during the proposed experimental studies highlighted the need for an accurate and predictable biaxial loading system. The design requirements for the loading system have been attained. A model material was developed with sufficient strength parameters to minimise elastic deformations under the applied experimental loadings.

Preliminary testing has indicated that confidence in the use of, and validity in the results produced from experiments conducted with the loading apparatus has been achieved. Excavation geometries and jointing patterns which enable the simulation of most field prototype situations are readily modelled with the apparatus, although similitude was of no real concern for the present programme of experiments.

# CHAPTER 6

# *RESULTS OF PHYSICAL AND NUMERICAL MODEL STUDIES*

# CHAPTER 6

# RESULTS OF PHYSICAL AND NUMERICAL MODEL STUDIES

## 6.1. Objectives and General Discussion:

The objectives of the two dimensional model studies of underground excavations in discontinuous media reported in this section were twofold:

i) to examine the inelastic deformations throughout discontinuous media containing openings with particular attention being paid to the load-deformation response of certain critical areas, and the particular factors influencing the mass behaviour;

ii) to compare the results of similar model studies carried out using both physical and numerical methods.

The importance of utilising independent techniques for studying relatively complex problems such as the load distribution throughout a discontinuum has been highlighted by the studies of past researchers. Chappell (1972) conducted numerical experiments on excavations in block jointed media in which he extracted relevant blocks either before or subsequent to the applied loading. From the results of his numerical modelling he concluded that the load distribution was independent of the load path since the resultant magnitude and patterns of force were the same for both methods of block extraction. The results of his physical model experiments, however, showed that the final load distribution was, in fact, very much influenced by the loading history. Upon closer examination he was able to explain the discrepancy between the results of the two methods of analysis as a function of numerical processes involved in his numerical technique.

Barton (1978) performed large scale two-dimensional physical model tests to study the deformation and stability of large openings excavated in jointed near-surface rock masses. Complementary to his physical modelling, sophisticated jointed finite element studies were under-

taken to enable a comparison with the experimental results and at the same time provide a check on the performance of the numerical model.

There are many factors which influence the load distribution in a jointed rock mass. In general, these factors are more difficult to control in a scaled physical model of a rock structure than in its numerical counterpart, especially where conditions of similitude must be satisfied. Also, it is desirable that the load distribution and deformation behaviour surrounding underground excavations in jointed media should be determined by the presence of the excavations alone with secondary effects such as block non-alignment and joint misfit being kept to an absolute minimum. It is solely on this basis that valid comparisons or otherwise between physical and numerical modelling may be drawn.

Ergun (1970) and Chappell (1972) showed that the following factors influence the load distribution in a jointed rock mass:

i) joint roughness and planarity i.e. the presence of voids along joints;

ii) squareness or orthogonality of the jointing systems;

iii) equality in size between contiguous blocks;

iv) block geometry;

v) the ratio of the applied loads;

vi) the inclination of the joints to the direction of the applied principal stresses;

vii) loading sequence and loading history.

Chappell (1972) considers the above factors to mainly influence the initial load conditions. When this initial state is disturbed by creating an underground excavation, mechanisms of deformation such as slip, separation and rotation may be initiated which result in a redistribution of load.

## 6.2. Testing Procedure:

Several discontinuous models containing excavations were constructed and loaded with the model behaviour at particular loading stages recorded on photographs for later analysis. The models were constructed from 25 mm square x 50 mm thick plaster of paris bricks, the details of which have been described in Chapter 5 and Appendix V. Care was taken during model construction to ensure that bricks of as near equal size and shape as possible were selected from the cured, graded batches. This was necessary to minimise the effects of block non-alignment and joint misfitting, factors which if not adequately controlled have been shown to dominate the subsequent load distribution and deformation behaviour within the discontinuous mass (Ergun, 1970).

It is recognised that block defects will exist but providing they are not relatively large or can be sufficiently controlled, they should not significantly affect the load distribution nor control the failure mechanisms resulting from the placement of openings in such media. However, as discussed later, the influence of such defects is very much dependent on the level of loading applied.

The particular geometrical configurations modelled are illustrated in Figure 6.1. The continuous joint set was either horizontal, vertical or inclined at 30, 45 or 60 degrees to the horizontal. In the original experimental programme, it was proposed to model situations in which both joint sets were continuous. Several preliminary physical modelling experiments were performed with both joint sets through-going and orientated horizontally and vertically or at $\pm 45$ degrees. For these geometries, anticipated failure mechanisms were not always generated and crushing and slabbing of block corners was predominant. It was concluded that ~~true~~ expected behaviour was being prevented by interlocking between adjacent block units due to the combined effects of slight variations in

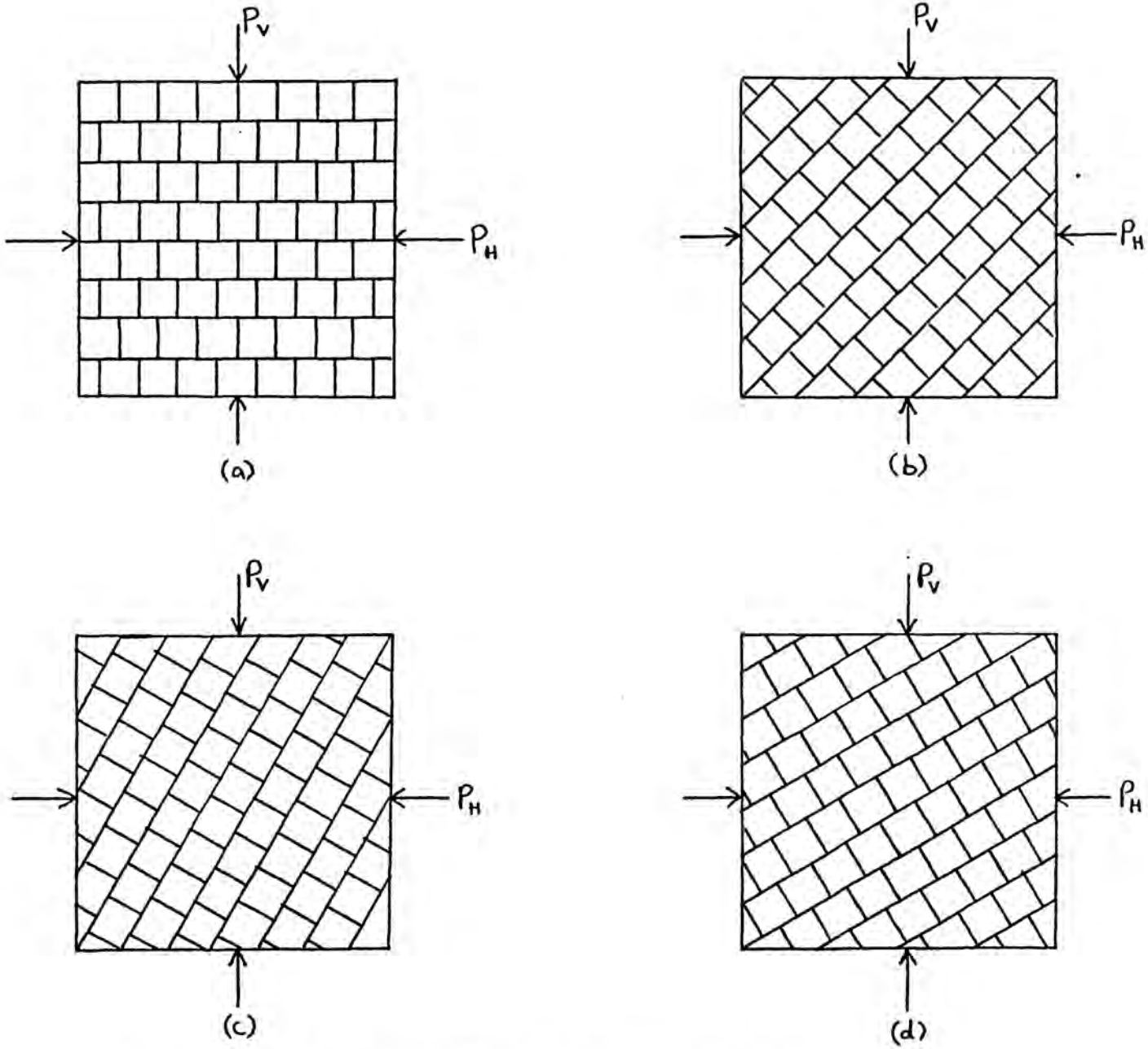



Figure 6.1: Joint Patterns Used in Model Experiments

block tolerances and a certain amount of joint 'shuffling' during loading and unloading.

Additional problems also arose when the joints were inclined at ± 45 degrees since blocks were able to slide along adjacent edges simultaneously. This resulted in concentrated corner to corner loading which induced an effective tensile stress condition throughout the block and in some instances resulted in blocks splitting. This effect has also been noted by Brown (1968, 1970) in triaxial compression experiments on plaster block-jointed models.

In view of the problems associated with continuous jointing, it was decided to abandon the proposed programme and to concentrate on configurations which overcame these inherent difficulties. The revised modelling program shown in Figure 6.1 would cause no loss of generality as far as the objectives of this study were concerned and could be regarded as being more representative of prototype situations. As seen in Figure 6.1, each experiment in the revised program consisted of two sets of orthogonal joints, one set being continuous with a secondary, staggered system forming a stacked brickwork pattern.

The dimensions of the discontinuous physical models were 500 mm square by 50 mm thick and all models were tested under plane stress conditions. Rectangular openings with typical dimensions of 150 mm by 25 mm were created prior to load application. This post-loading sequence was adopted after careful consideration had been given to other methods available. Initially, pre-loading tests were performed in which relevant blocks were extracted whilst under load. These proved to be rather unsatisfactory since the methods chosen to remove the blocks were all deemed to have interfered with the failure mechanism. In some cases, the vibrations associated with block removal resulted in separation along the joints while the model was under small stabilising boundary loads. In this respect, the methods of block extraction

adopted by Ergun (1970) and Chappell (1972) must be regarded with caution.

To the author's knowledge, no satisfactory method of block extraction for a preloaded, jointed physical model has, as yet, been achieved. It is appropriate to reiterate here that the overriding objective of the physical model studies was to provide a basis for comparison with the results of numerical experiments, and as such it was irrelevant whether the models were postloaded or blocks were removed subsequent to applied loading. For the proposed experiments, it would seem logical to choose the extraction/loading sequence which caused least complications.

Thus, the post-loading modelling procedure adopted implies that the loading sequence and history for a prototype situation have not been correctly simulated and any attempt to correlate the model results with prototype behaviour must recognise this fact, especially where load path dependent phenomena such as slip and rotation are present. It is also important to note that the magnitude of the applied loading was primarily chosen to induce failure mechanisms (e.g. slip and rotation) in the jointed models and not necessarily to simulate prototype conditions.

A comparison of the behaviour of postloaded and preloaded models containing identical geometries and subjected to the same load magnitudes was made by Chappell (1972). He concluded that the joints for the postloaded model were stiffer than those for the preloaded case since blocks in the preloaded model tended to rotate more. He also noted that stress concentrations on blocks surrounding any opening were larger for the preloaded model.

The typical size of the opening(s) selected for each model as specified above was such as to allow a representative number of joints to intersect the opening, thus permitting the salient features of load and deformation behaviour of a jointed medium to be examined. The opening

size is relatively large compared with the overall model dimensions and problems in satisfying boundary conditions were expected for some model geometries.

The zone of influence for an opening in an elastic medium is approximately 5 : 1, but becomes significantly larger for openings in discontinuous media (Bray, 1978). Studies on the influence of openings in jointed media were carried out by Ergun (1970) using 1000 mm square by 25 mm thick models containing 170 mm square openings excavated under load. He demonstrated that the failure zone extended to the loaded boundaries depending on the orientation of the jointing and the ratio of applied loading. For the joint configurations shown in Figure 6.1, it was anticipated that the zone of influence would extend to the loaded boundaries for some models. This required, as discussed in Chapter 5, the loading system to be as flexible as practically possible to accommodate the likely boundary deformations.

It is recognized that where considerable deformations of the loaded boundaries occur, the resulting load distributions along these boundaries will be markedly non-uniform and impossible to quantify. Consequently, any comparison between the physical and associated numerical model results would be of limited relevance. Therefore, conditions of minimum boundary deformations in the physical models were a prerequisite when comparisons with the numerical results were made. Such conditions were determined both visually and by monitoring the hydraulic pressure gauges to ensure satisfactory boundary conditions existed when photogrammetry was utilized.

Models with multiple openings were also examined to determine the response due to the interaction of openings. All of the models were loaded using the biaxial loading rig described in Chapter 5.

For the construction and testing of discontinuous

plaster brick models containing excavations, the following experimental procedure was adopted.

i) the loading frame was locked into the horizontal position with one of the 25 mm thick perspex safety windows secured on the underside beneath the loading platens;

ii) the discontinuous model was carefully constructed from the appropriately sized bricks, the brick ends being supported by the perspex sheet. Each brick was individually examined to ensure that all its edges were perfectly smooth and planar, and free of any dust or other asperities, before it was included in the model. Each model consumed approximately 400 whole bricks and no bricks were reused after any one test. In any one row or column of the model, alternate bricks were inverted (from their cast position) to minimise joint misfitting. This produced a chequered pattern on the resulting model photographs which greatly assisted the subsequent photogrammetric analysis;

iii) with all the blocks in place and weights placed over the upper face to prevent buckling (Figure 6.2) the model was consolidated by applying small horizontal and vertical loads to each model edge. The model was then rotated from a horizontal to a vertical position. Both the horizontal and vertical pressures were then increased by equal increments to give transmitted pressures of approximately 0.3 MPa, the loads being cycled several times;

iv) after consolidation, the model was returned to the horizontal position and the loading removed. The bricks forming the excavation were then easily extracted and small horizontal and vertical pressures were reapplied to the model edges via the loading platens. To maintain joint alignment, the horizontal and vertical pressures were never permitted to fall below these initial magnitudes until the testing was completed. The model plane was returned to the vertical position and secured in place via the locating device;

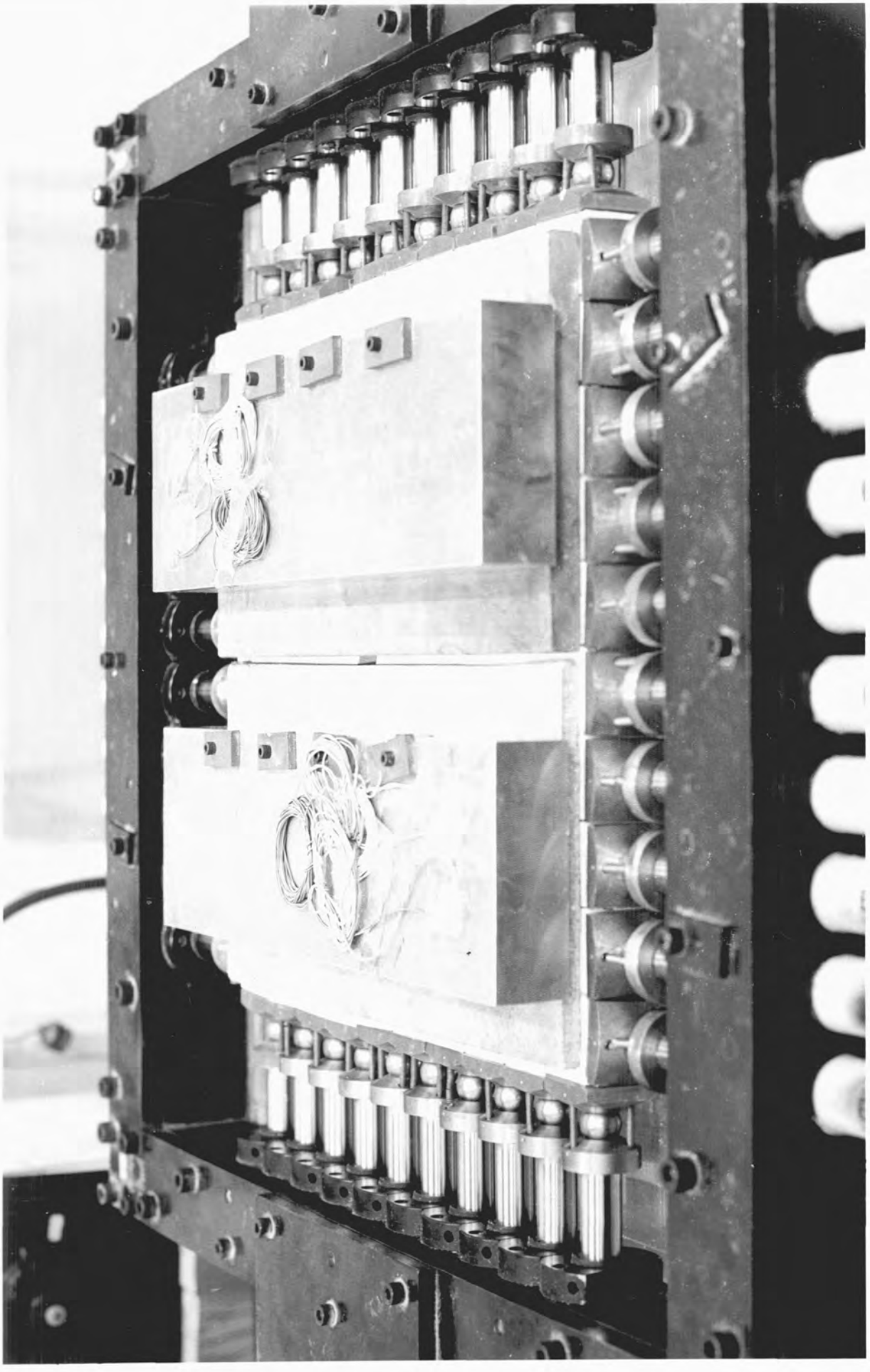


Figure 3.2: Preliminary model loading.

v) the rectangular frame providing the points for photogrammetric control was bracketted to the housing section;

vi) the horizontal and vertical pressures were then increased in equal increments to a desired level after which a photograph was taken to establish the 'zero' positions for the model elements;

vii) either the horizontal or vertical gauge pressure was then increased (usually in increments of · 345 MPa) while the other pressure was held constant until visible or detected signs of failure took place in the model. Photographs were taken after each load increment during the loading stages. An average of 12 photographs were taken for each model test;

viii) careful visual observation of the model behaviour after each load increment was carried out together with a detailed inspection of the bricks surrounding the excavation(s) after unloading.

A summary of the model testing programme is presented in Table 6.1. For each discontinuous model experiment discussed below several preliminary trial runs were necessary to ascertain the load and deformation characteristics for the particular model. These trial experiments also enabled the testing procedure to be rigorously evaluated and modified where necessary. The consistency between the load-deformation response for each series of preliminary model tests ensured that the correct model behaviour was being quantitatively assessed in the final experiments. These trials also proved that the design requirements of the loading apparatus were being satisfactorily achieved. Each model experiment required approximately 8 hours for assembly and complete testing.

The following section details the results of several two-dimensional physical model studies of rectangular underground openings in discontinuous media. Only a limited number of representative photographs for each model

Table 6.1: Summary of model testing program

| Model | Orientation to horizontal(degrees) | | Pv> Ph | No. of openings |
|---|---|---|---|---|
| | Cont. Joints | Discont. Joints | | |
| 6.3.1 | horizontal | vertical | yes | 1 |
| 6.3.2 | vertical | horizontal | yes | 1 |
| 6.3.3 | ± 45 | ± 45 | yes | 1 |
| 6.3.4 | ± 45 | ± 45 | no | 1 |
| 6.3.5 | 60 | 30 | yes | 1 |
| 6.3.6 | 30 | 60 | yes | 1 |
| 6.3.7 | 60 | 30 | yes | 2 |
| 6.3.8 | 60 | 30 | yes | 2 |

are presented in the following discussion. The numbers assigned to each test indicate the chronological order in which the experimentation was undertaken. In all cases, the results of the physical modelling precede the presentation of the numerical results.

## 6.3. Results of Physical and Numerical Model Studies:

### 6.3.1. Model I: Continuous Horizontal Joints and Discontinuous Vertical Joints. Rectangular Opening 175 mm by 25 mm with Long Axis Horizontal (Pv > Ph).

Physical Model Study:

Model I was assembled with the horizontal joint set continuous and a staggered vertical joint system. After initial consolidation and prior to final loading a planar rectangular opening 175 mm long and 25 mm high was created, the long axis of the opening being parallel to the horizontal continuous joint set. Seven discontinuous joints intersected the roof and floor of the opening. The hangingwall consisted of 10 rows of blocks leaving 4 rows between the keystone block of the kinematically feasible triangular wedge (termed the suspended zone) and the upper loaded boundary.

A photograph of the model geometry under a small initial loading (Pv = .138 MPa, Ph = .155 MPa) establishing the 'zero' block positions is shown in Figure 6.3. Careful examination of the initial set-up was required to ensure that all blocks in the immediate hangingwall were mating each other and to detect any joint separations or interlocks that had developed under the relatively small stabilising thrust.

When this condition was satisfied, the vertical boundary pressure was increased in increments of .086 MPa while the horizontal boundary pressure was held constant throughout at .155 MPa. The vertical pressure was increased until observable movements occurred, such as those shown in Figures 6.4 and 6.5, where the ratio

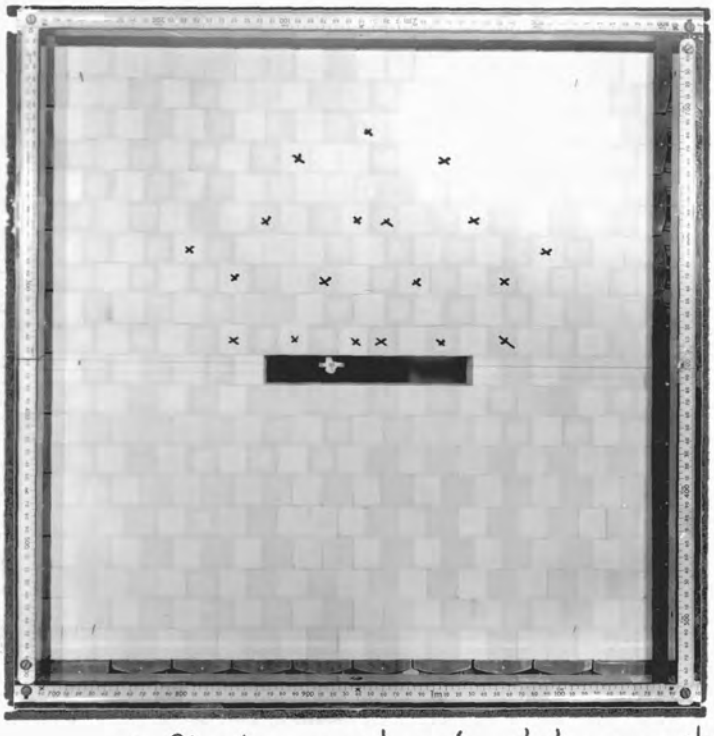



Figure 6.3: Model I under initial loading.

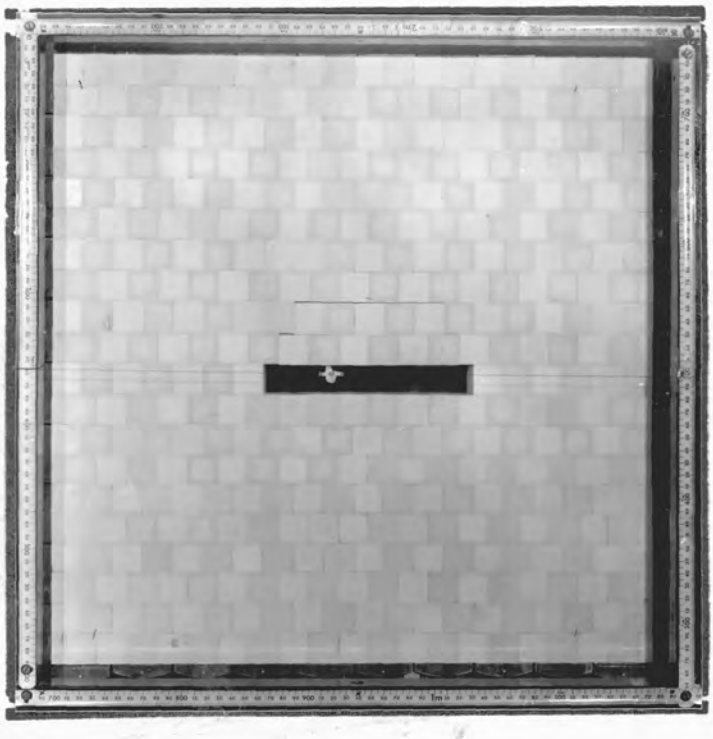


Figure 6.4: Model I - Pv/Ph = 4.5.

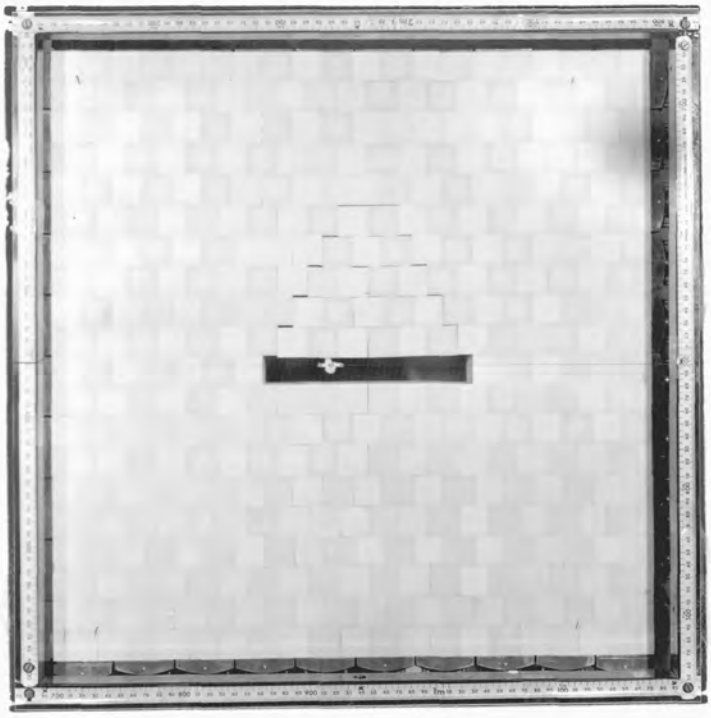


Figure 6.5: Model I - Pv/Ph = 9.0

$\gamma = 0.466$
contact stiffnesses: } for Fig.'s 6.3, 6.4, 6.5
$K_n = 1.088\ E+10$
$K_s = 1.088\ E+10$

Pv/Ph of the forces applied in the vertical (Pv or Fv) and horizontal (Ph or Fh) directions is 4.5 and 9.0 respectively.

Figures 6.4 and 6.5 are representative of the progressive nature of the hangingwall failure mechanism observed as the vertical load is increased. Under relatively small vertical loads the rows of blocks immediately spanning the opening would undergo slip and rotation mechanisms, with, in general, higher loads needed to generate these deformation mechanisms in overlying rows. The asymmetry of the deformation between hangingwall and footwall for the particular configuration considered here (horizontally bedded) suggests that body forces are of significance for Model I. The magnitude of body forces and mechanistically developed contact forces are evaluated in the numerical section.

The block movements shown in Figures 6.4 and 6.5 were analysed photogrammetrically producing the translational and rotational block displacements plotted in Figures 6.6 and 6.7. The maximum translational movement for a Fv/Fh ratio of 9.0 is approximately twice that for a ratio of 4.5.

In these plots, the magnitude of the block rotation (in radians) has been printed alongside each resultant displacement vector, the particular blocks analysed being indicated in Figure 6.3. The similarity between both sets of displacement vectors confirms that the photogrammetric method is indeed able to adequately resolve both the magnitude and direction of block movements encountered in such experimentation.

Upon completion of loading, this and future experimental models were carefully dismantled to detect if and where plaster blocks had failed. Shearing and tensile type plaster failures were readily distinguished from the nature of the resulting fracture surface. Tensile failures produced a rough, clean surface throughout the plaster

RESULTS FOR EXPERIMENTAL MODEL STUDY NUMBER 1

CONT.JOINTS HORIZ. DISCONT.JOINTS VERT. OPENING 175MM=25MM. PV.GT.PH.

PLOT OF TRANSLATIONAL AND ROTATIONAL BLOCK DISPLACEMENTS-ROT.PRINTED IN RADIANS

NUMBER OF PROBLEM UNITS PER INCH = 0.00109 METRES. SCALE IS 1 INCH = _____

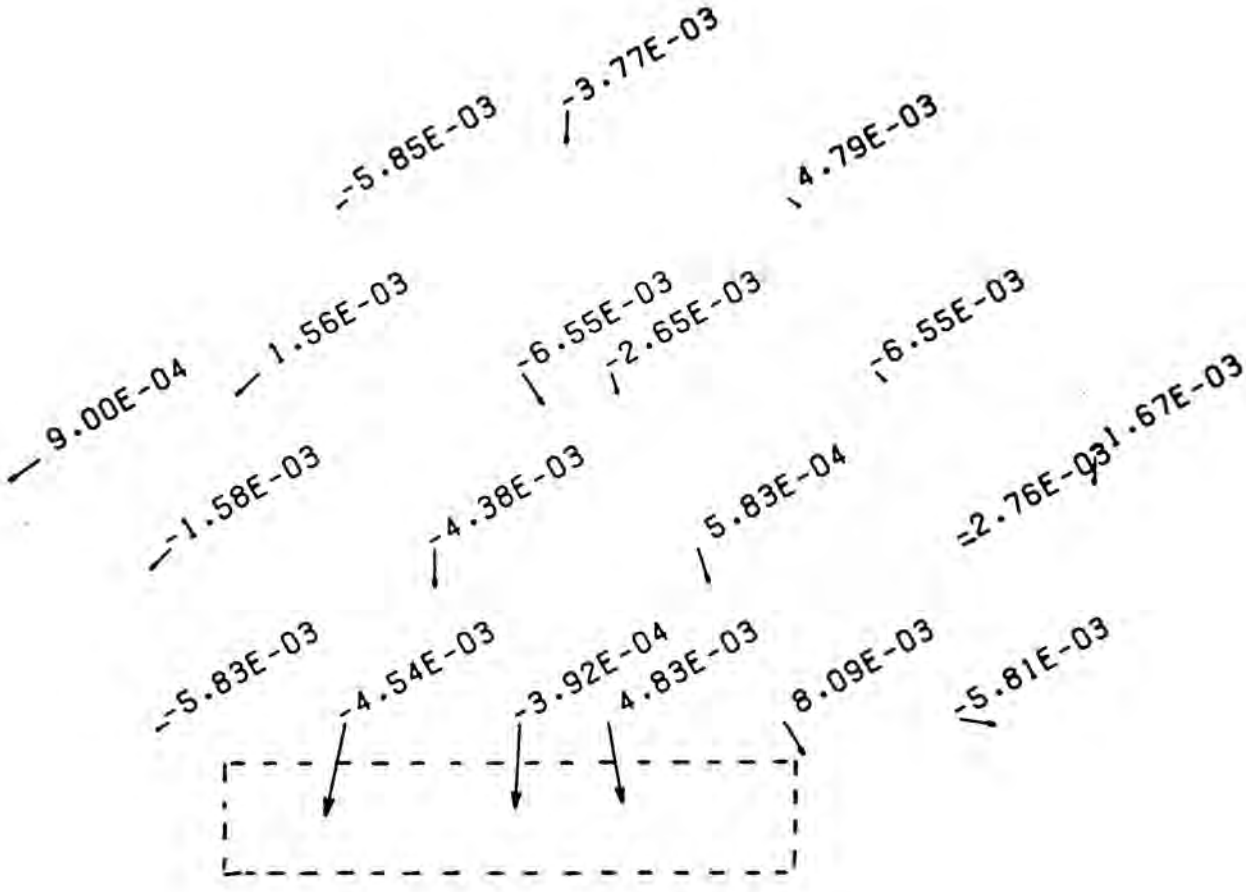



Figure 5.8

RESULTS FOR EXPERIMENTAL MODEL STUDY NUMBER 1

CONT.JOINTS HORIZ. DISCONT.JOINTS VERT. OPENING 175MM=25MM. PV.GT.PH.

PLOT OF TRANSLATIONAL AND ROTATIONAL BLOCK DISPLACEMENTS-ROT.PRINTED IN RADIANS

NUMBER OF PROBLEM UNITS PER INCH = 0.00197 METRES.- SCALE IS 1 INCH = _____

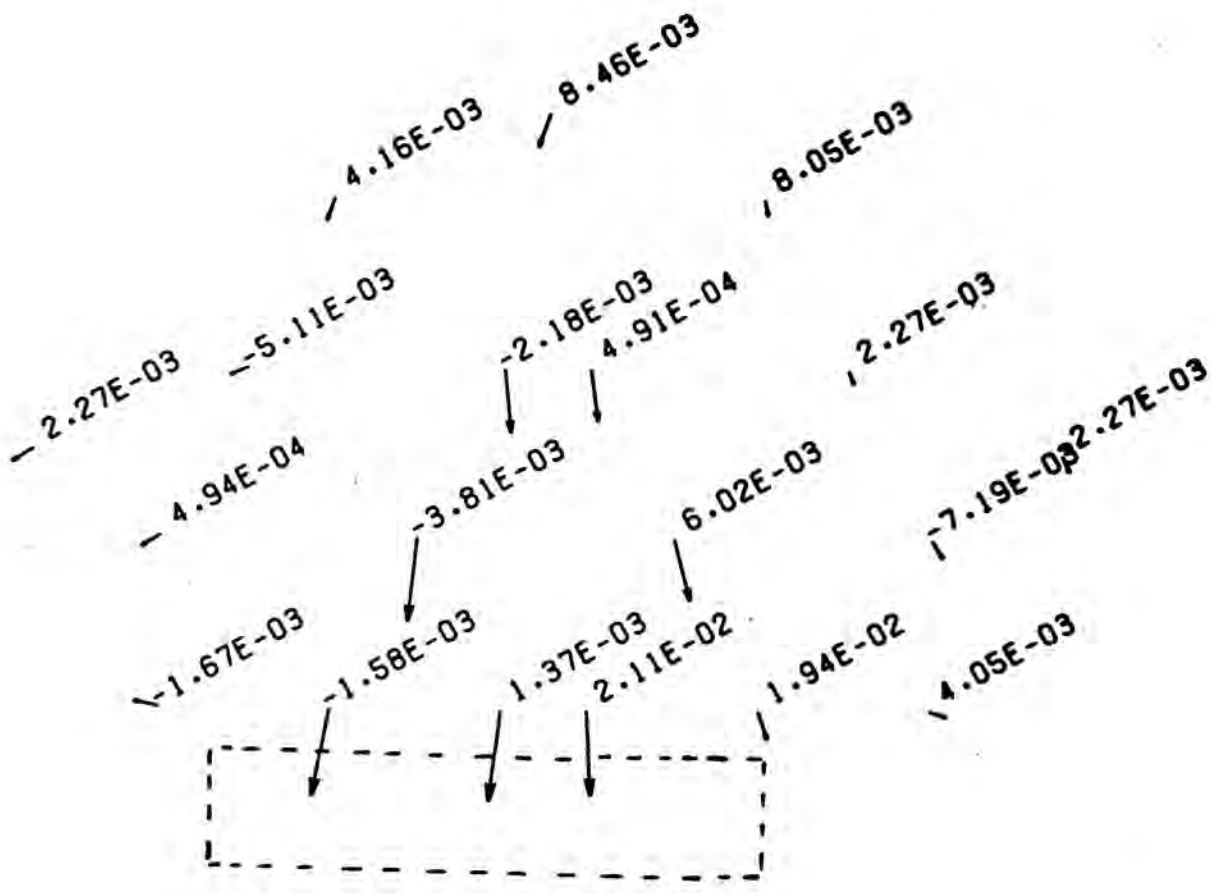



Figure 6.7

matrix while a smooth, powdery surface indicated shearing failure. For Model I, two types of tensile failure were observed. Block splitting due to effective tensile stresses ('Brazilian type loading') was detected at mid-height of the hangingwall and immediately adjacent to the suspended zone. This failure occurred when the Fv/Fh ratio was between 4.5 and 9.0, and indicated that the extent of the suspended zone is not necessarily defined solely by the geometry of the model opening.

The second type of tensile failure was located along the vertical edges of blocks contiguous with the suspended zone. Hinge formation and shear sliding of adjacent blocks created an effective tensile strain condition which caused slabbing to occur at the lower corners of these edges. Slabbing is predominant in some subsequent model studies but the extent of such failure for Model I is negligible. Slabbing failure was observed for the footwall row immediately adjacent to the opening.

There are several important aspects of the load and deformation behaviour of a jointed medium which are highlighted by the experimental results obtained from Model I. It is obvious from the magnitude of the resulting block displacements and associated joint separation that mechanisms of inelastic deformation incorporating some combination of slip and rotation have occurred. Such movement is far in excess of the displacements obtained when a similar opening is excavated in an equivalent elastic continuum, as detailed in the following numerical section.

The mechanism of failure in the immediate hanging-wall is of a progressive nature with movement extending upwards roughly 70% of the span distance from the row of blocks adjacent to the opening to the keystone block as the vertical pressure is increased. It is interesting to note that detectable movement of the keystone block was not observed for the range of boundary pressures applied.

The rows of blocks within the suspended zone display behaviour characteristic of beaming action in order to achieve stability of the suspended zone. As outlined by Trollope (1966), failure involves both the mechanisms of slip and rotation. Rows of blocks were observed to slide into the opening in shear along the vertical joints with attendant beaming ('bending') of each row necessary to maintain stability by developing lateral thrusts. The ultimate collapse state, although not observed in these studies, would be due to compressive failure of the hinges. Such actions mean that each row is eventually relieved of any superincumbent load and behaves independently of adjacent rows in supporting itself. This beaming action comprising vertical joint separation and associated hinge formation is most evident for the row of blocks immediately adjacent to the opening (Figure 6.5).

The ability of the suspended zone to contribute towards overall load transmission throughout the blocky mass is therefore seriously diminished as inelastic movements occur and the load originally shed by this zone must be transferred to surrounding areas (Terzaghi, 1946; Trollope, 1966). The redistribution of load is achieved by the formation of load arches around the triangular shaped suspended zone. This has been previously demonstrated photoelastically by Chappell (1972) and numerically, using dynamic relaxation, by Voegele (1978).

Arching causes concentrations of load to develop with the possible failure of the model constituents either through excessive compressive or tensile loading. As seen earlier, the nature of block movements throughout a discontinuous medium is conducive to the creation of effective tensile stress or strain conditions. These conditions may well govern the ultimate stability of the jointed mass.

Voegele (1978) discusses the fundamental difference in behaviour of the destressed zone surrounding an ex-

cavation in either an elastic continuum or a jointed medium. For both models, a similar load distributing arch forms in the stable material surrounding the destressed (suspended) zone but whereas, for the elastic case, the weight of material in the destressed zone is supported through the development of tensional forces, in the jointed model a second arching mechanism is initiated to support the suspended zone. The block movements necessary to induce this secondary roof arching are clearly evident in Figure 6.5.

This concept has important implications for the design of support requirements for excavations in jointed media. A design based on supporting the total dead weight of the suspended material may be unnecessarily conservative and financially intolerable. Also, incorrect placement and alignment of the support may inhibit secondary arching mechanisms within the suspended mass. This was witnessed when a small upward artificial support was applied to the mid-point of the bottom row of blocks spanning the excavation. This caused the mid-span vertical tension joint to partially close and resulted in complete collapse of the triangular opening, the rows sliding out in shear along the vertical joints.

An important factor influencing the extent to which secondary arching occurs is the nature and magnitude of the horizontal thrust originally present. A horizontal thrust of sufficient magnitude may completely inhibit slip and rotation surrounding the excavation causing the resulting load distribution to approach that of a continuum. This has been demonstrated experimentally by Ergun (1970) who subjected openings in continuously jointed media to hydrostatic type loads.

The effect of the magnitude of horizontal thrust was examined in several trial experiments by increasing the horizontal pressure to a maximum of three times the adopted experimental value of .155 MPa. Correspondingly higher

vertical pressures were required to achieve similar stages of progressive failure when compared with the experimental model. As the horizontal thrust increased in magnitude, rotation of blocks became less pronounced. At the maximum lateral thrust examined (.465 MPa) the failure mechanism was predominantly shear sliding of the suspended rows along the vertical joints with minimal 'bending' of the rows.

Numerical Analysis of Model I:

Numerical simulations of all model studies were analysed using the static relaxation procedure described in Chapter 2. The main purpose of the numerical analyses undertaken was to enable comparisons between both the mechanisms and actual magnitudes of deformation to be made with the physical model results, thereby providing a check on the performance of the numerical model.

Because of the repetitive and idealised nature of each model geometry, routines were written for automatically generating the system of blocks, given the relevant parameters such as joint spacings and directions. The idealized block geometry shown in Figure 6.8 which consisted of 218 square and rectangular (aspect ratio 2 : 1) blocks formed the basic model used for the numerical analyses of Model I. This model was a compromise of the larger 400 plus block physical situation (Figure 6.3) and was considered justified due to quasi-symmetry between hangingwall and footwall and economic computing considerations.

Model I required 46 K. words of central memory for execution on the CDC 6600 machine. Also, the execution time required for 400 iterations was approximately 480 CP secs (6600). If the complete model geometry was represented it could be reasonably expected that the execution time would be roughly doubled for the same number of iterations.

As with all subsequent numerical analyses, the continuous and discontinuous joints were modelled as smooth, planar features. Also, all input data and numerical calculations were expressed in S.I. units.

Nominal dimensions for the length of each square block edge were chosen as 1 computer unit, the density of the block material being 0.0475 computer units. This produced a numerical block weight of 0.4660 computer units, equivalent to the measured mean weight of 0.0475 Kgf.

In the initial analyses for Model I, joint stiffnesses proportional to the plaster elastic modulus and block geometry were calculated (Appendix III ) and it was assumed that these normal and shear stiffnesses were equal and remained constant throughout, their magnitudes being 1.088E + 10 computer units for square blocks. It was anticipated that the maximum boundary pressures would not exceed 1 MPa for any model and hence a friction coefficient of 0.754, based on experimental tests, was used. The cohesion was set to zero.

The above parameters were typical of the geometrical and physical properties required for each model study. The facility existed in the program for assigning different values of the above properties to any individual block or group of blocks, and this was utilized when necessary.

The boundary conditions were of both the force-controlled and displacement-controlled type. Usually, each model consisted of one or more boundaries of fixed blocks with the remaining boundaries subjected to applied forces. Occasionally, prescribed displacements were imposed on boundary blocks. Loading, represented by forces (in compatible computer units) at block corners along relevant boundary block edges was calculated as equivalent to the uniform experimental transmitted pressures. Additionally, these loads were independent of lateral and vertical displacements and remained constant

at their selected levels until either increased or decreased for a further period of constant loading.

As noted previously, the output from the numerical model was substantially enhanced by the facility to produce graphical plots at user specified intervals. Plots of the problem geometry, interblock contact forces, and both incremental and total block displacements were produced during each execution stage.

Presentation of the relevant plots will be included in the following discussion, where appropriate. Numerical dumps of selected contact force data and block data complemented the graphical output. Other printout during problem execution enabled one to determine whether convergence to a stable equilibrium condition, or otherwise, was occurring.

The model geometry shown in Figure 6.8 was subjected to 500 iterations of initial loading equivalent to horizontal and vertical uniform boundary pressures of .155 MPa and .138 MPa respectively. The criterion used in all analyses to establish when a satisfactory state of equilibrium had been achieved was to examine the resultant out-of-balance X, Y and rotational force sums. Incremental translational and rotational block movements, expressed as percentages of initial movements, also indicated whether or not the system of blocks was converging to a static equilibrium position.

For Model I the maximum out-of-balance forces were to within 3% of typical applied boundary loads, indicating an acceptable initial load distribution after 500 iterations. The maximum unbalanced forces were in the downward vertical direction and were located within the suspended zone or immediately above it.

Plots of the load distribution and cumulative block displacements at the conclusion of initial loading are

STATIC RELAXATION RUN FOR MODEL EXPERIMENT NUMBER 1
BLOCK PLOT NUMBER OF PROBLEM UNITS PER INCH = 1.33
ITERATION NUMBER = 500 SCALE . 1 INCH = _____

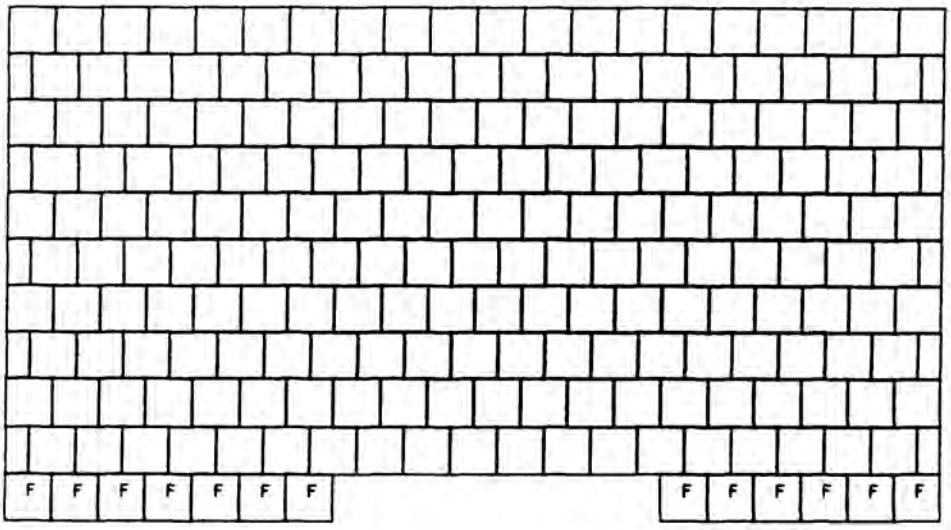



Figure 6.8

STATIC RELAXATION RUN FOR MODEL EXPERIMENT NUMBER 1
CORNER FORCE PLOT NUMBER OF PROBLEM UNITS PER INCH = 750.954765969
ITERATION NUMBER = 500 SCALE . 1 INCH = _____

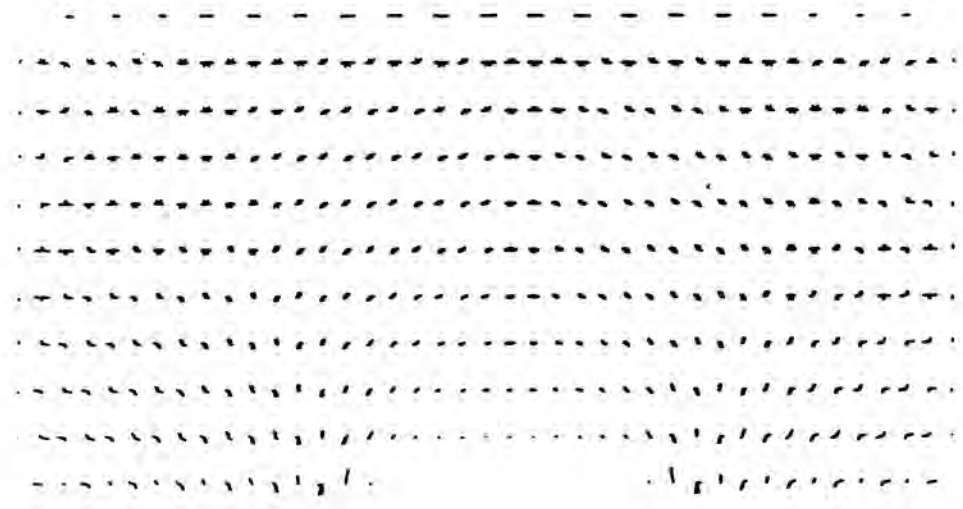
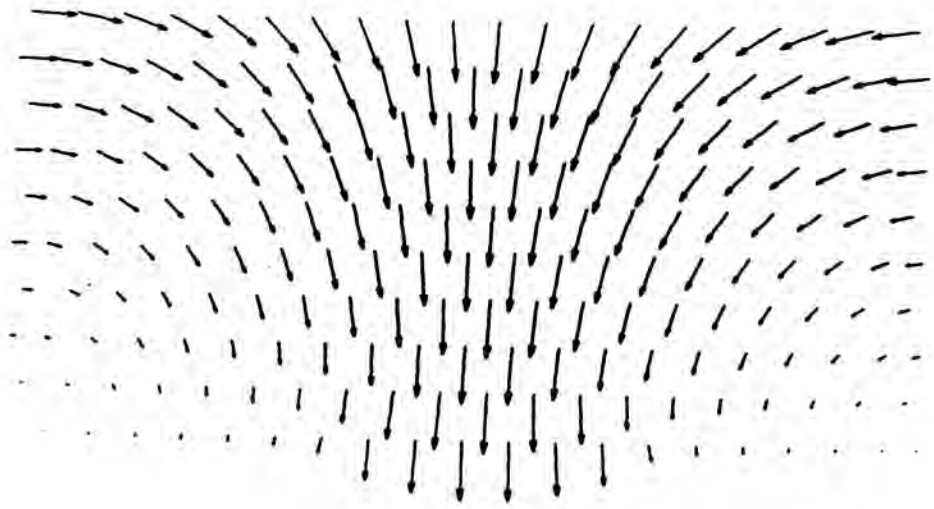


Figure 6.9

STATIC RELAXATION RUN FOR MODEL EXPERIMENT NUMBER 1
INCREM.DISPL PLOT NUMBER OF PROBLEM UNITS PER INCH = 0.000000000
ITERATION NUMBER = 500 SCALE . 1 INCH = ____



STATIC RELAXATION RUN FOR MODEL EXPERIMENT NUMBER 1
TOTAL DISPL PLOT NUMBER OF PROBLEM UNITS PER INCH = 0.000000080
ITERATION NUMBER = 500 SCALE . 1 INCH = ____

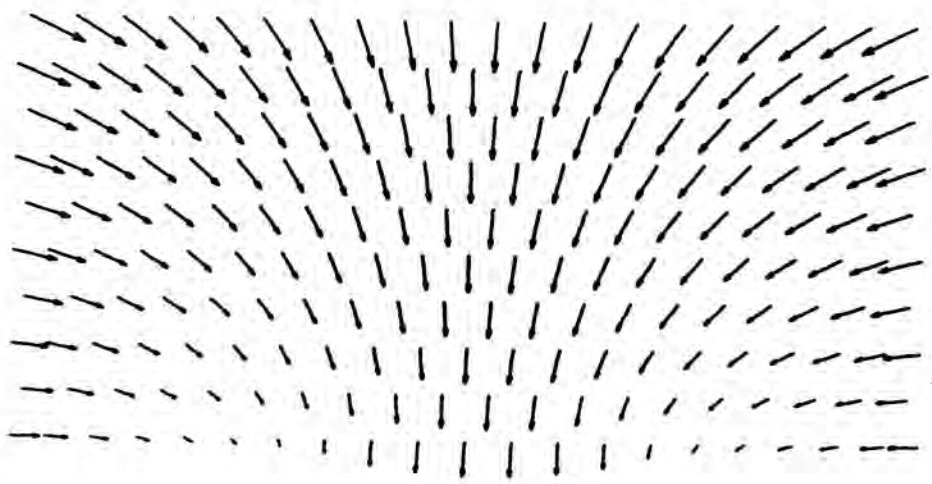


Figure 6.9 contd.

shown in Figure 6.9. The force plot shows that arching of the load above the excavation has already commenced with beaming action in the immediate overlying row. The contact force printout indicates tension at the base of the three mid-span vertical joints.

Due to the very small movements in relation to the block sizes a dump of the contact data was required to detect separations along joints and zones of slippage. This information enabled a magnified illustration of the geometry and associated force distribution throughout the suspended zone to be depicted, as shown in Figure 6.10. The magnitudes of normal forces only are shown.

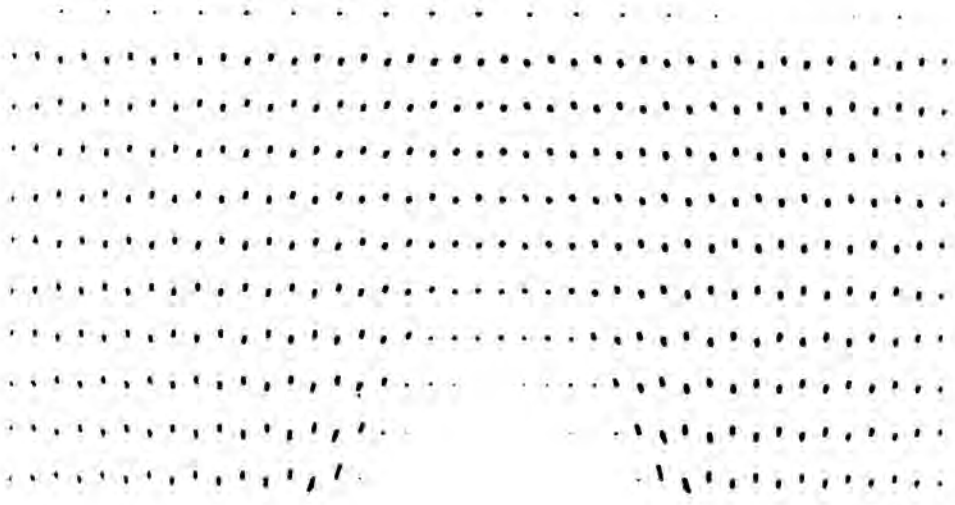
Sliding in shear along the vertical abutment joints combined with beaming action have isolated the first row from overlying rows. Data for all other rows indicated no slip or joint separations had occurred. There is a force concentration of approximately 1.5 times the vertical load on abutment blocks, with the normal forces throughout the suspended zone at no point exceeding the level of the applied loads.

Similar situations of independent behaviour for the immediate row spanning the opening were encountered in preliminary physical modelling of Model I.

The restart facility in the numerical model was then used to increase the vertical load while leaving the horizontal pressure constant at .155 MPa. After initial loading, the total displacements for each block were zeroed to enable a comparison to be made with the displacements analysed photogrammetrically. 400 iterations of vertical loading (Pv : Ph ratio of 4.5) produced the results shown in Figure 6.11.

The increase in vertical pressure has resulted in a substantial arching of the load throughout the inherently stable zone surrounding the triangular wedge. Tension in

RESTART RUN FOR MODEL EXPERIMENT 1 WITH INCREASING VERTICAL LOAD.PV=-2.828MPA.
CORNER FORCE PLOT NUMBER OF PROBLEM UNITS PER INCH = 2890.947266750
ITERATION NUMBER = 900 SCALE . 1 INCH = _____



RESTART RUN FOR MODEL EXPERIMENT 1 WITH INCREASING VERTICAL LOAD.PV=-2.828MPA.
TOTAL DISPL PLOT NUMBER OF PROBLEM UNITS PER INCH = 0.000000226
ITERATION NUMBER = 900 SCALE . 1 INCH = _____

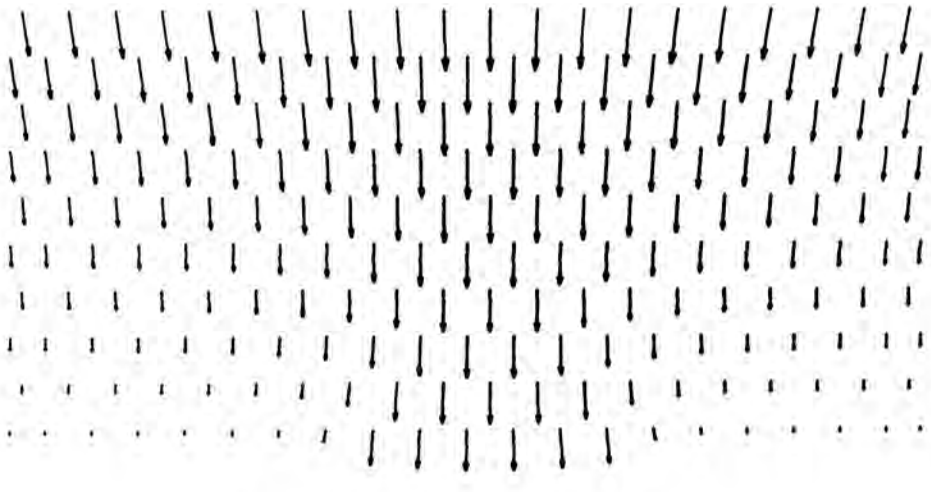


Figure 6.11

the vertical joints for the first 3 overlying rows indicates good mechanistic agreement with the physical model (Figure 6.4) in which the same rows produced beaming through the actions of slip and rotation.

The magnified deformations after this intermediate loading stage are shown in Figure 6.12, together with relevant force magnitudes. The translational and rotational block movements at corresponding execution stages were approximately ten times larger than those for the initial loading phase.

After a cumulative 900 iterations, full frictional resistance had been mobilised along the sides of the stable opening for the first four rows. However, block movements had been reduced to some 2% of the translational and rotational movements obtained at the commencement of this loading.

The actual magnitudes of the translational and rotational displacements for blocks in the hangingwall predicted by the numerical model showed little agreement with photogrammetric results and were in general between one and two orders of magnitude too low, as shown in Table 6.2.

To simulate the final loading state the external loads along the top row of blocks were increased to equivalent values and the problem was restarted using the dump file saved at the completion of the previous loading stage. The final loading (Pv : Ph ratio of 9.0) was applied for a further 400 iterations at which stage the maximum unbalanced force on any block was within 2.5% of the maximum applied external load. Also, final incremental translational and rotational displacements were less than 0.1% of their cumulative totals.

The largest out-of-balance forces were again those acting vertically on blocks within the suspended zone,

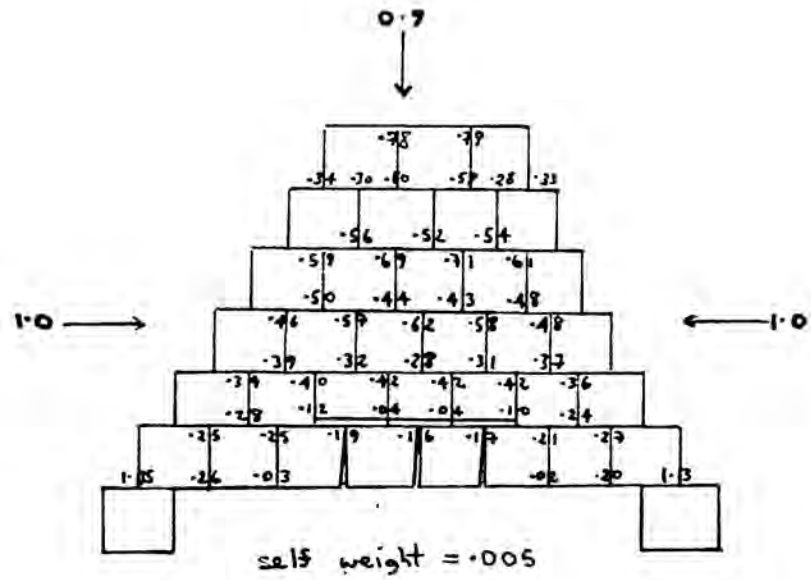



Figure 6.10: Model I under initial loading showing normal force magnitudes.

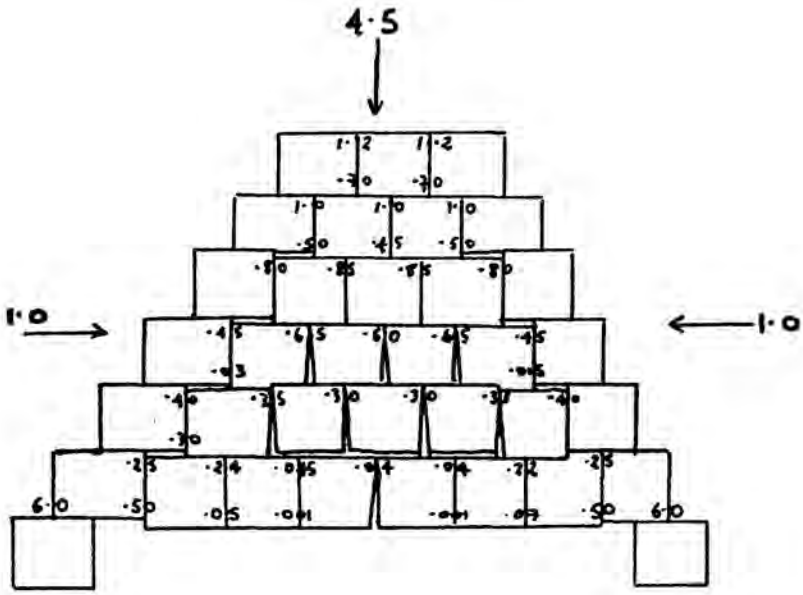



Figure 6.12: Model I - $P_V/P_H$ = 4.5 showing normal force magnitudes.

Table 6.2: Numerical and Photogrammetric Displacements for Model I

| Load Ratio Pv/Ph | Block Number | Static Relaxation Displacements (mm) | | | Boundary Element Displacements(mm) E=1.088E+04 ·MPa $\nu$ = .2 | Photo-grammetric Displace-ments (mm) |
|---|---|---|---|---|---|---|
| | | Kn=Ks=1.088 E + 10 | Kn=Ks=1.088 E + 09 | Measured Stiffnesses | | |
| 9.0 | 20 | .0024 | .0244 | .1220 | .0075 | .59 |
| | 22 | .0132 | .1205 | 1.0577 | .0158 | 1.90 |
| | 24 | .0148 | .1403 | .9821 | .0238 | 1.97 |
| | 61 | .0064 | .0663 | .3315 | .0130 | .43 |
| | 64 | .0144 | .1364 | .8736 | .0233 | 1.77 |
| | 103 | .0113 | .1147 | .4817 | .0225 | .39 |
| | 106 | .0155 | .1511 | .8435 | .0275 | 1.38 |
| | 145 | .0155 | .1558 | .7011 | .0290 | .51 |
| | 168 | .0181 | .1821 | .8195 | .0335 | .75 |
| 4.5 | 20 | .0010 | | | | |
| | 22 | .0050 | | | | |
| | 24 | .0059 | | | | |
| | 61 | .0028 | | | | |
| | 68 | .0057 | | | | |
| | 103 | .0048 | | | | |
| | 106 | .0063 | | | | |
| | 145 | .0065 | | | | |
| | 168 | .0076 | | | | |

the maximum values occurring for the four blocks in the third overlying row. This indicates incomplete vertical force transmittal to the first two rows of roof blocks and that these rows are capable of supporting themselves independently by interaction with the opening abutments.

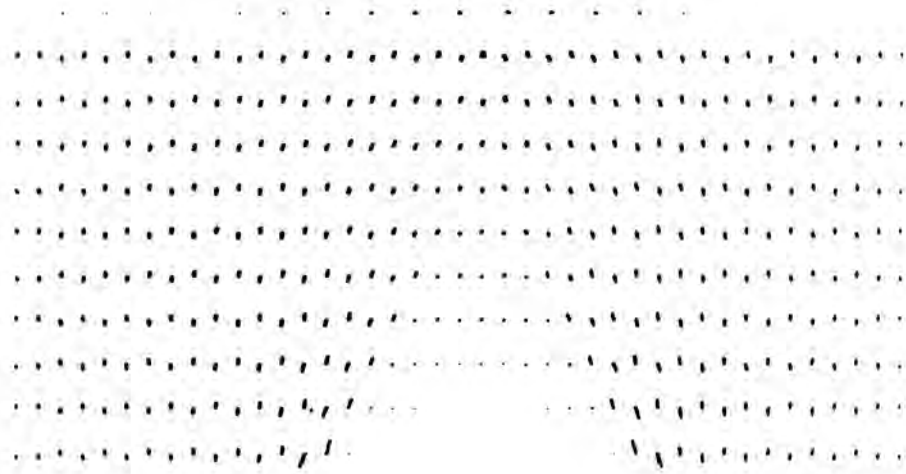
Figure 6.13 is an obvious extension of the intermediate stage where the arching has become steeply inclined and has penetrated high into the roof material overlying the keystone block. The large arching forces produced in the sides of the opening correlate well with the observed tensile failure in the physical model.

The 'punching-in' effect of over- and underlying blocks creates loading conditions on the blocks surrounding the suspended zone similar to the Brazilian test. The magnitude of these interaction forces predicted by the numerical model after final loading is such that the uniform tensile stress calculated from theory approaches the tensile strength of the plaster. A doubling of the vertical load has resulted in a two-fold increase in the abutment loads, as indicated in Figure 6.14.

The small magnitude of contact forces in the suspended zone (Figure 6.13) indicates that body forces could be an important factor in determining ultimate behaviour. The ratio of typical applied boundary forces to block weight is in the order of 1000 : 1 for all models while the magnitude of contact forces throughout the suspended zone is approximately 100 times the body forces. However, for the first two rows, the contact forces between mid-span blocks are of the same order of magnitude as the body forces.

Beaming has extended to the fourth row in order to support the superincumbent load. The mechanistic response of the suspended zone is again in good agreement with the physical model. The numerical results indicate slip and rotation for the first five rows with a stable

RESTART RUN FOR MODEL EXPERIMENT 1 WITH INCREASING VERTICAL LOAD. PV=-5.483 MPA
CORNER FORCE PLOT NUMBER OF PROBLEM UNITS PER INCH = 5777.403548372
ITERATION NUMBER = 1300 SCALE . 1 INCH = ____



RESTART RUN FOR MODEL EXPERIMENT 1 WITH INCREASING VERTICAL LOAD. PV=-5.483 MPA
TOTAL DISPL PLOT NUMBER OF PROBLEM UNITS PER INCH = 0.000001527
ITERATION NUMBER = 1300 SCALE . 1 INCH = ____

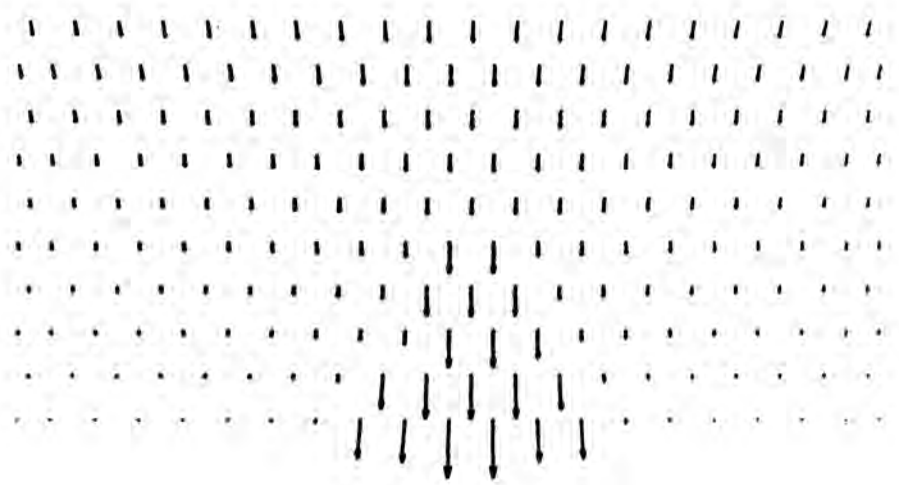


Figure 6.13

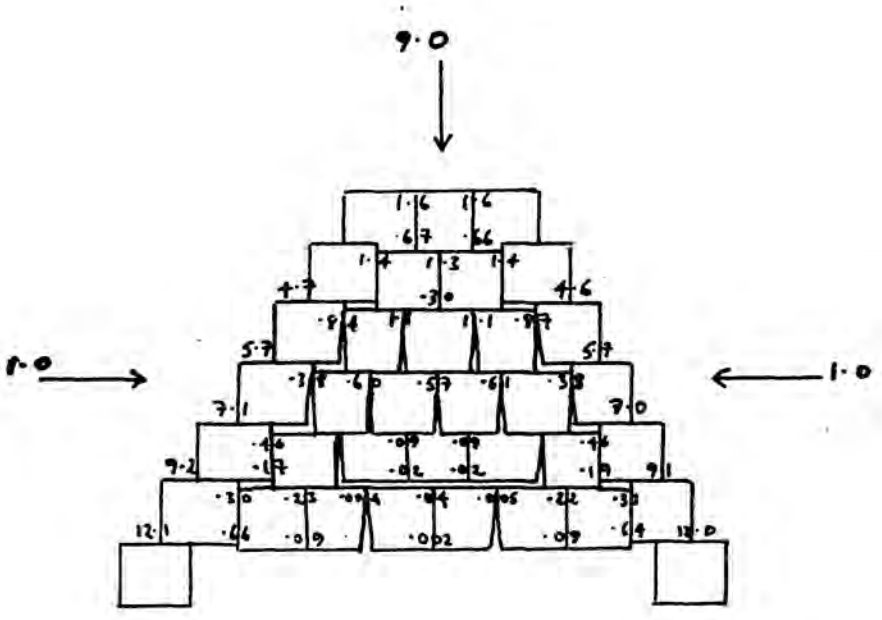



Figure 6.14: Model 1 - $P_V/P_H$ = 9.0 showing normal force magnitudes.

keystone block.

The magnitudes of the numerically predicted displacements, shown in Table 6.2, are still very much less than those measured photogrammetrically. The displacements for corresponding block positions in an isotropic elastic continuum containing a similar opening with equivalent physical properties were determined using the boundary element method of analysis. These results, analysed under similar loading conditions to the discontinuous numerical model, are tabulated in Table 6.2.

Both continuum and discontinuum analyses predict displacements of the same order of magnitude. Although the failure mechanisms generated from both physical and numerical modelling reported above show close correlation, there is a major discrepancy in the actual magnitudes of the rigid block displacements predicted by both models. In general, the numerical model displacements were between 1% and 10% of those measured experimentally. This discrepancy is thought to be mainly due to the following factors:

i) the geometry modelled numerically is an overstiff representation of the actual physical situation; and

ii) failure processes in the physical model such as tensile splitting and slabbing of the blocks.

In the above simulations, values for the normal and shear joint stiffnesses were derived by considering the discrete block model to represent an elastic continuum. This assumption is however, highly suspect in that it would require the joints (interfaces between contiguous block units) in the physical model to be perfectly mating with closed, smooth planar surfaces. Also, for the low magnitudes of experimental pressures used it is probable that the joints will display marked non-linear stiffnesses. Block defects such as misfits, non-planar surfaces and tolerances do exist and will play a significant role in

the resulting mass behaviour. Therefore, it was considered important to investigate in more detail the physical properties of block jointed media.

Size effects problems have continually plagued studies of discontinuous media (Gonano, 1974; Chappell, 1972). Chappell (1972) determined mass moduli for stackings of square photoelastic blocks of varying sizes but similar to the geometrical configuration of Model I. He recognised that "unavoidable defects were introduced while manufacturing" and conducted deformability studies on jointed models without openings to measure the influence of such defects. His work showed that for geometries similar to Model I and comprising photoelastic blocks 25 mm square or less, the effective mass moduli were approximately 10% of the values for the intact material.

It was possible to determine if movements corresponding to these reduced moduli were being produced in the physical model studies by considering the differential displacements of the four corner points measured photogrammetrically. Although virtually at the limits of the photogrammetric resolution, these results indicated mass movements at least an order of magnitude larger than those calculated using intact material properties. Therefore, it was essential to modify the normal and shear stiffnesses if meaningful comparisons were to be made with the photogrammetric displacements.

Initially, both normal and shear stiffness were reduced arbitrarily by a factor of ten and the effect on the block displacements was noted. After an equivalent period of loading to that before the displacement magnitudes had, in general, increased in magnitude by the same amount that the stiffnesses had been reduced. This brought the numerical displacements considerably closer in agreement with corresponding photogrammetric values, as seen in Table 6.2.

An extension of the above model was to further decrease the stiffnesses of blocks within and immediately adjacent to the suspended zone. The purpose here was to crudely simulate possible mechanisms such as slabbing along the sides of the opening. Several computational runs were performed and for the particular case where the ratio of stiffnesses for blocks contiguous to the opening to those removed from the opening was .05, the displacements for the suspended zone were approximately double those of the initial reduced stiffness model. The force distribution for this model (Figure 6.15) was similar to that in the original analyses, but with definition of the suspended zone and attendant arching more pronounced due to increasing block movements.

Although the arbitrarily reduced stiffness models provided a reasonable approximation for the jointed mass deformability, it was decided to ascertain as accurately as possible the variation and actual magnitude of both normal and shear stiffnesses for the range of loading anticipated in this and future model studies.

The normal stiffness was measured on a plaster block jointed model which was geometrically similar to Model I. The model contained no openings and the deformations were measured between suitable points by a mechanical extensometer (accurate to .0025 mm). The gauge length to block size ratio was 8 for all measurements. Initially, a hydrostatic loading was applied after which the vertical load was increased incrementally to the desired level. The results are shown in Figure 6.16 and the non-linear behaviour is tabulated in Table 6.3.

Table 6.3: Measured Normal Stiffnesses*

| Actual Displ. Da(mm) | Elastic Displ. De(mm) | Normal Pressure (MPa) | Ratio Da/De | Normal Stiffness (Kn elastic=1.088E+10) |
|---|---|---|---|---|
| .0750 | .001575 | >.138,<.224 | 47.6 | 2.286 E + 08 |
| .1000 | .003150 | >.224,<.397 | 31.7 | 3.432 E + 08 |
| .0850 | .003150 | >.397,<.569 | 27.0 | 4.030 E + 08 |

* above stiffnesses used in subsequent examples

MODEL EXPT.1.WITH PV=-5.483 MPA.AND VARIABLE STIFFNESSES THROUGHTOUT MODEL
CORNER FORCE PLOT  NUMBER OF PROBLEM UNITS PER INCH = 5300.704503242
ITERATION NUMBER = 1600  SCALE . 1 INCH = _____

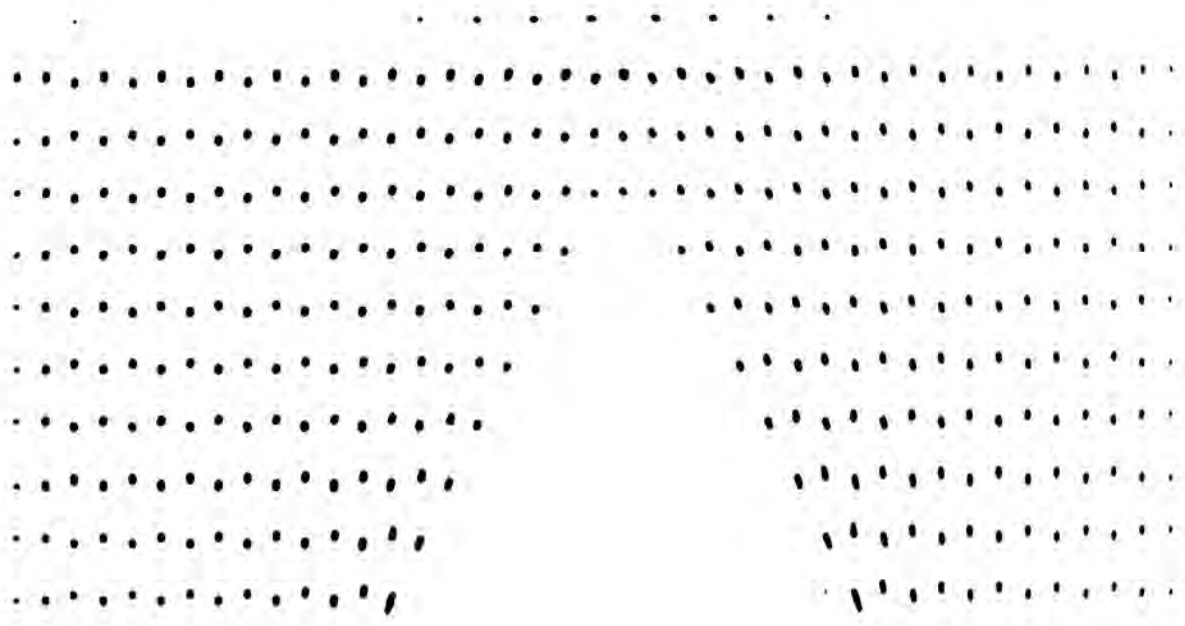


Figure 6.15

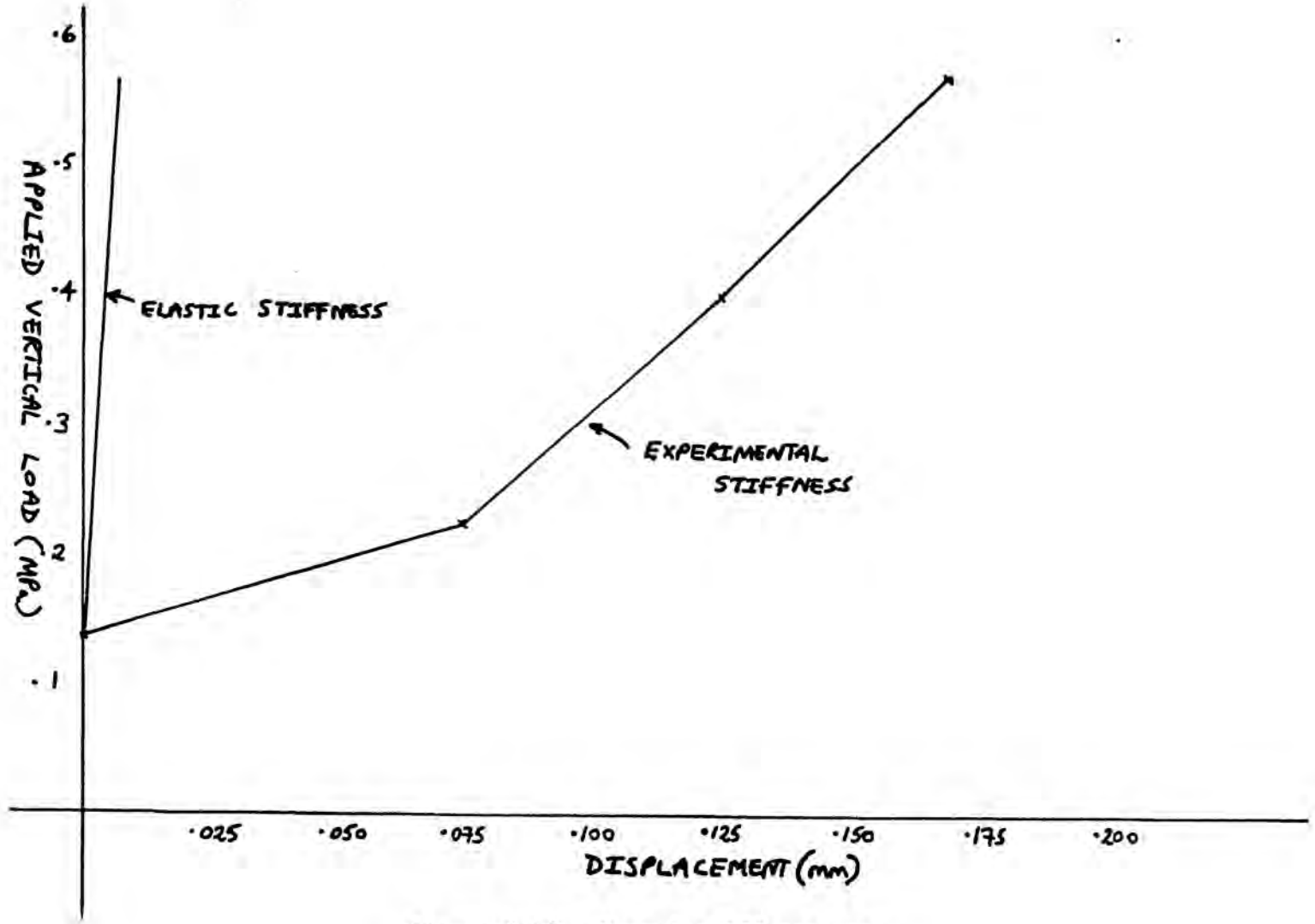



Figure 6.16: Normal stiffness test

The normal stiffnesses listed in Table 6.3 were selected as parameters for the model tests. These values were assumed valid where the applied loading was outside the range of experimental pressures used in the stiffness test.

The numerical modelling procedure involved applying the load in increments equivalent to the stiffness test pressures, selecting the corresponding normal stiffness, and allowing sufficient iterations for the load to propagate throughout the system before altering the stiffness and load parameters for subsequent stages.

The shear stiffness was determined from double shearing tests on models containing openings where there was a continuity of jointing in the vertical direction, as seen in Figure 6.17. For selected values of the normal force, the shear load was increased so as to produce a constant shearing rate of 0.25 mm per minute as the mass failed monolithically towards the opening. The displacements were measured via dial gauges (.0025 mm resolution) and the results of such tests are presented in Table 6.4.

TABLE 6.4: MEASURED SHEAR STIFFNESSES

| Actual Displ. Da(mm) | Elastic Displ. De(mm) | Normal Load (N) | Ratio Da/De | Shear Stiffness (Ks elastic=1.088E+10 |
|---|---|---|---|---|
| 1.5 | .025 | 8,007 | 60 | 1.813 E + 08 |
| .25 | .005 | 8,007 | 50 | 2.176 E + 08 |
| .25 | .0064 | 2,002 | 39 | 2.790 E + 08 |
| .50 | .0106 | 4,003 | 47 | 2.315 E + 08 |

The results listed in Table 6.4 were obtained until continuous displacement under constant shear load was achieved. The shear-force shear-displacement curves showed some non-linearity but average values were calculated for each test.

In the numerical modelling, a constant shear stiffness of 2.176 E + 08 computer units was assumed.* The

* this value for Ks assumed for subsequent examples

normal and shear stiffnesses derived above were assumed valid for all of the jointed model configurations examined (Figure 6.1). Also, it was thought that the reduced loading rate would assist in the attainment of a satisfactory equilibrium condition.

Model I was re-analysed incorporating the measured stiffnesses and the results in Table 6.2 show that the numerically predicted displacements are now in satisfactory agreement with the photogrammetric displacements. The failure mechanism generated was still similar to that established from the elastic stiffness model, which indicates that joint stiffnesses, if of sufficient relative magnitude, do not significantly affect the mode of failure. The influence of the physical properties (normal and shear stiffness, interblock friction coefficient) is examined further in Model VI.

Therefore, the numerical results obtained for Model I show that the numerical model is capable of predicting the mode of failure for the particular configuration (horizontally bedded) considered. It has been shown that by selecting realistic input parameters, a satisfactory correlation between the displacement magnitudes for both physical and numerical experiments is achieved. These results provided much insight into, and justification for, continuing with the additional studies.

6.3.2. Model II: Continuous Vertical Joints and Discontinuous Horizontal Joints. Rectangular Opening 150 mm by 25 mm with Long Axis Horizontal (Pv > Ph).

Physical Model Study:

Model II was assembled with the vertical joint set continuous and a discontinuous horizontal joint set, as shown in Figure 6.17. The opening was created such that a zone six blocks wide and extending to either vertically loaded boundary was free to slide into the opening along the continuous jointing system. Four columns of abutment

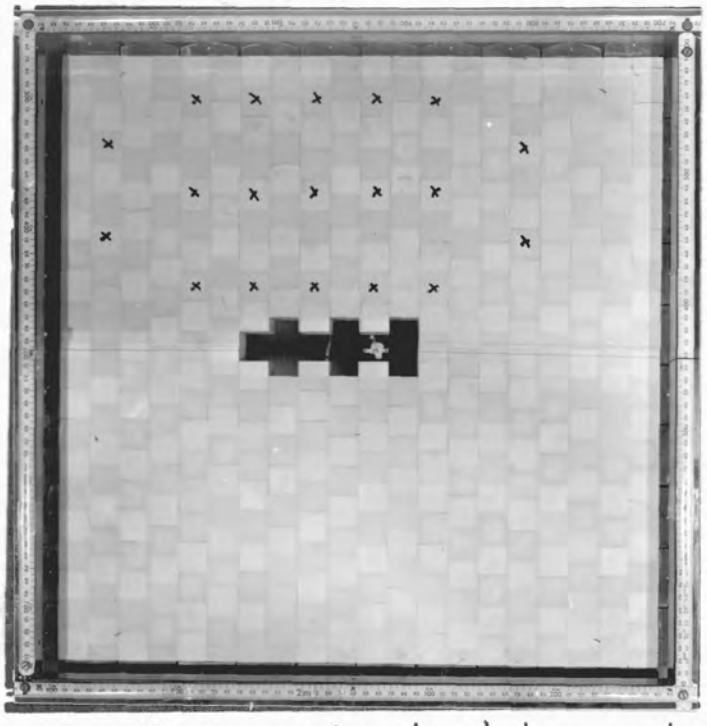



Figure 6.17: Model II under initial loading.

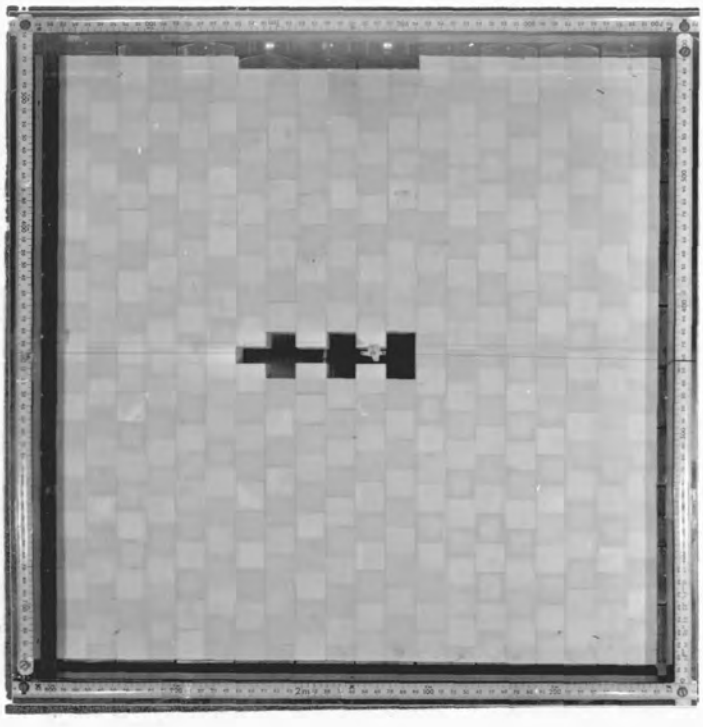


Figure 6.18: Model II - sliding along vertical joints.

bricks on either side of the opening provided the reaction. The two potential sliding zones were not symmetrical about the opening, the zone above the opening having one additional row of blocks between the opening face and the loaded edge.

The objective was to examine the effect of the continuity of vertical jointing. It was expected that such a configuration would inhibit the formation of arching and thereby allow the mass to fail monolithically. Model II was in fact the double shearing test used to determine the coefficient of sliding friction and shear stiffness properties discussed previously. Several trial experiments were performed to determine these properties.

The model geometry in Figure 6.17 shows the 'zero' block positions under initial pressures of Pv = .138 MPa and Ph = .155 MPa. After initial loading the vertical pressure was increased while the horizontal pressure was maintained constant throughout at the initial level of 0.155 MPa. The vertical loading was applied so as to produce a constant displacement rate of .5 mm per minute for the shorter of the two sliding zones (i.e. the zone beneath the opening in Figure 6.17). Displacements for this zone were measured by dial gauges (accurate to .0025 mm) until sliding under a constant vertical loading was achieved (in this case Pv = .388 MPa).

Thereafter, displacements were analysed photogrammetrically, and Figure 6.18 shows the model geometry after sliding along the vertical joints of about half a block length.

The photogrammetric results for the translational and rotational displacements corresponding to Figure 6.18 are presented in Figure 6.19, the particular blocks analysed being indicated in Figure 6.17.

In general, once sliding had commenced under a

RESULTS FOR EXPERIMENTAL MODEL STUDY NUMBER 2

VERT.CONT.JOINTS. HORIZ.DISCONT.JOINTS. OPENING 150MM HORIZ. PV.GT.PH.

PLOT OF TRANSLATIONAL AND ROTATIONAL BLOCK DISPLACEMENTS-ROT.PRINTED IN RADIANS

NUMBER OF PROBLEM UNITS PER INCH = 0.01106 METRES. SCALE IS 1 INCH = _____

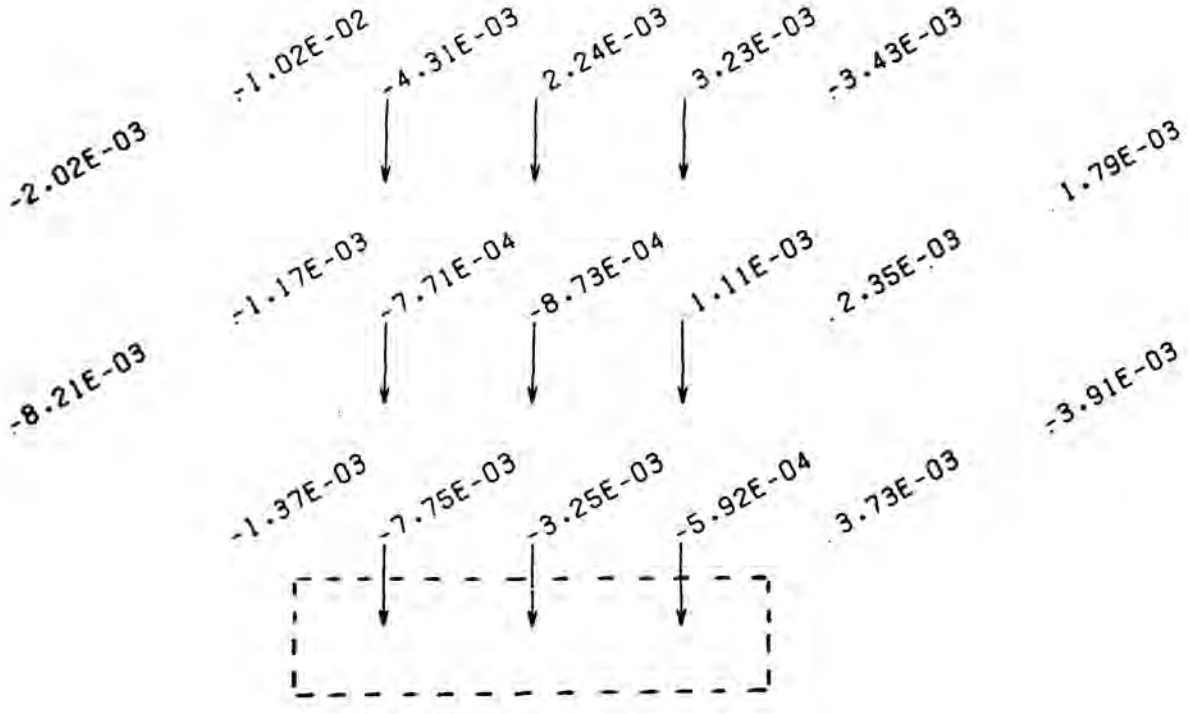



Figure 6.19

constant vertical pressure, it was not necessary to decrease the vertical pressure in order to stop sliding. After sliding movements of approximately 2 to 3 mm, the sliding stopped due to interlocking between blocks along the joints. The situation shown in Figure 6.18 was photographed during such an interlocking stage.

To initiate further sliding, the vertical pressure was increased approximately 5% over the level required to maintain the previous sliding, with the vertical pressure ultimately decreasing to the same level as before once sliding started.

The coefficient of sliding friction along the vertical continuous joints was determined from shearing tests under constant horizontal pressures ranging from .155 MPa to .620 MPa. The average value for the friction coefficient was found to be .84 with a variation of $\pm$ 10% depending on the magnitude of the normal load. Under low normal loads (Ph = .155 MPa), the value of the friction coefficient averaged .75 with the value steadily increasing to around .9 for the maximum experimental load of .620 MPa. The coefficient of friction calculated for the lowest normal pressure compares favourably with that determined for simple unconfined sliding tests, as discussed in Chapter 5.

The results obtained from this model study provide further evidence as to the satisfactory performance of the loading rig. Due to asymmetry of the sliding zones about the opening, the hangingwall zone would require a proportionately higher vertical pressure to induce sliding along the vertical boundaries because of the larger horizontal confining load.

The alternative geometry, in which both potential sliding zones were symmetrical about the opening, was subjected to the same normal boundary pressure as before and as expected a proportionally higher shear load (4.5%) was required to maintain a constant shearing rate. How-

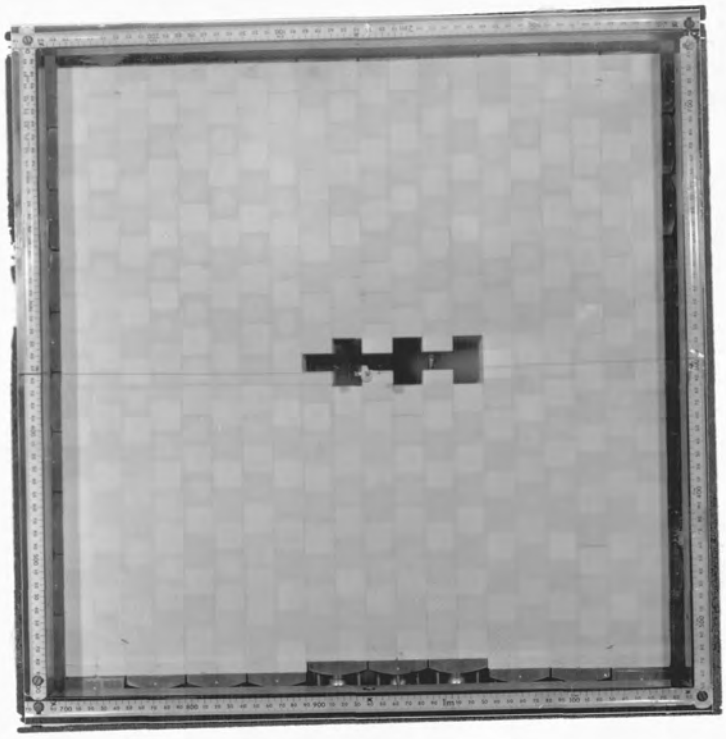


Figure 6.20: Model IIA - sliding along vertical joints.

ever, as shown in Figure 6.20, only the zone nearest to the hydraulic feed inlet failed monolithically.

Numerical Analysis of Model II:

The block arrangement used for the computer simulation of Model II is shown in Figure 6.21. The modelled geometry consisted of 140 square and rectangular blocks (aspect ratio 2 : 1) and was representative of the actual sliding zone examined in the laboratory model. This configuration was again chosen on the basis of economic computing considerations.

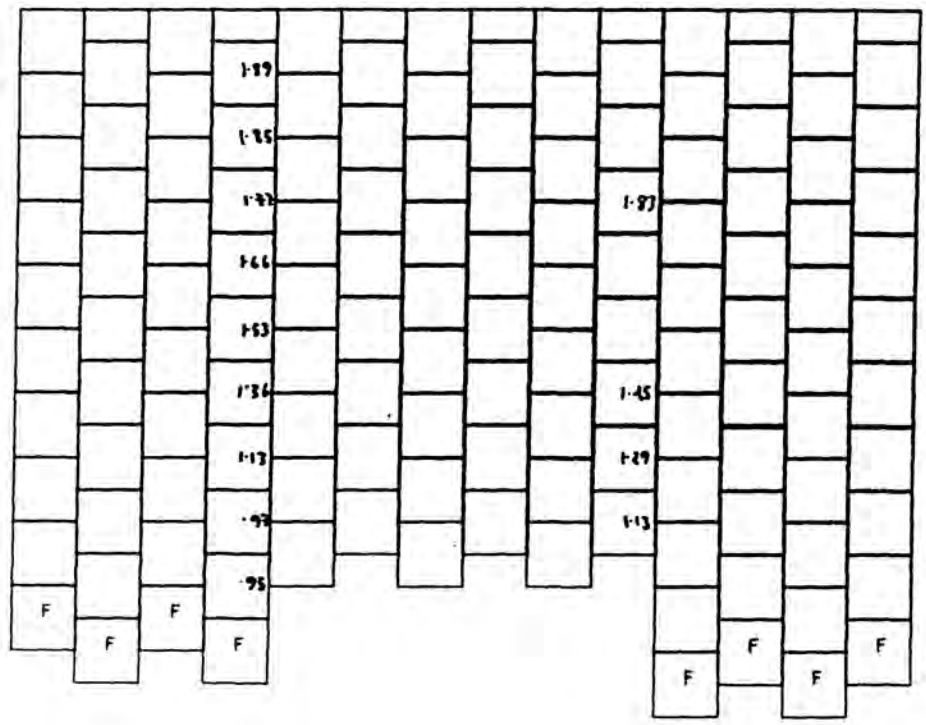
The main objective of the numerical experiments was not to compare actual displacement magnitudes but primarily to examine the failure mechanism and associated load distribution for a Pv/Ph ratio similar to that used in the physical model.

The physical properties input into the numerical model were the experimentally determined normal and shear stiffnesses (see Section 6.3.1) and a friction coefficient of .75 corresponding to the normal pressure. All boundary blocks (except those fixed) had three degrees of freedom.

The idealised computer model was subjected to 700 iterations of initial loading equivalent to vertical and horizontal uniform boundary pressures of .138 MPa and .155 MPa respectively. The load distribution and block displacements at the conclusion of initial loading are shown in Figure 6.21.

It is seen that due to the presence of the opening, a small amount of arching has occurred, resulting in a non-uniform normal load distribution along the vertical joint planes intersecting the opening. The magnitudes of these forces are depicted in Figure 6.21. Total normal forces greater in magnitude than the applied edge loads exist along the vertical joint planes for blocks located roughly

STATIC RELAXATION RUN FOR MODEL EXPERIMENT 2 - INITIAL LOADING
BLOCK PLOT NUMBER OF PROBLEM UNITS PER INCH = 1.00
ITERATION NUMBER = 700 SCALE . 1 INCH = _____




STATIC RELAXATION RUN FOR MODEL EXPERIMENT 2 - INITIAL LOADING
CORNER FORCE PLOT NUMBER OF PROBLEM UNITS PER INCH = 1041648.69318547
ITERATION NUMBER = 700 SCALE . 1 INCH = _____

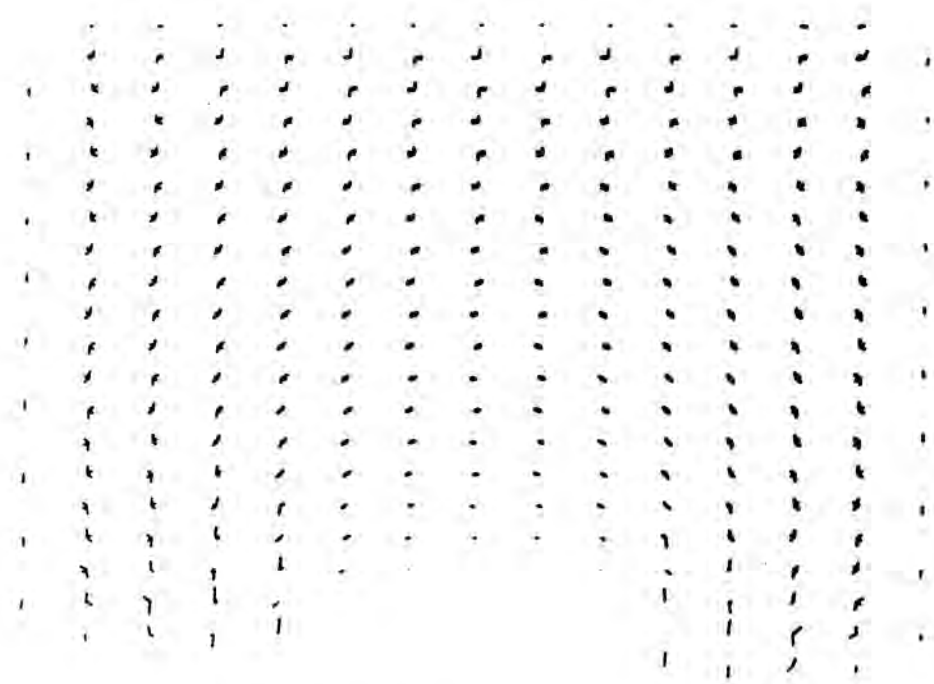
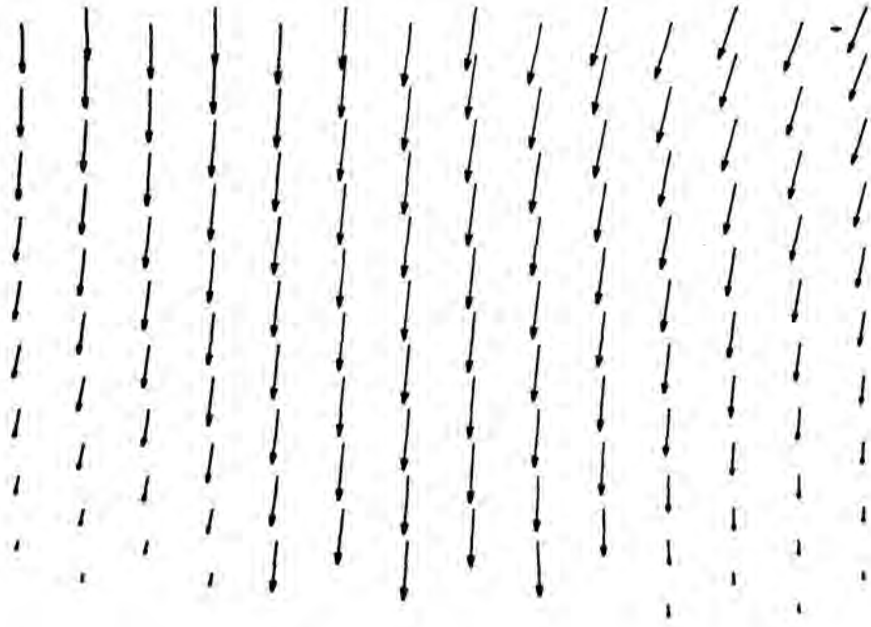


Figure 6.21

STATIC RELAXATION RUN FOR MODEL EXPERIMENT 2 - INITIAL LOADING
INCREM.DISPL PLOT NUMBER OF PROBLEM UNITS PER INCH = 0.00000006
ITERATION NUMBER = 700 SCALE . 1 INCH = ——



STATIC RELAXATION RUN FOR MODEL EXPERIMENT 2 - INITIAL LOADING
TOTAL DISPL PLOT NUMBER OF PROBLEM UNITS PER INCH = 0.00012506
ITERATION NUMBER = 700 SCALE . 1 INCH = ——

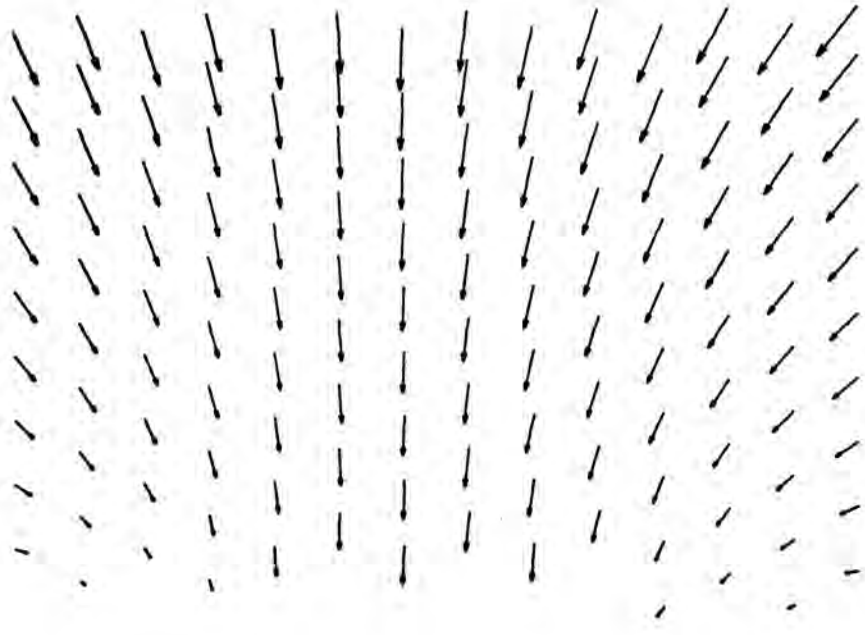


Figure 6.21 contd.

between the mid-height of the potential sliding zone and the vertically loaded boundary. This confirms that arching of the load has developed.

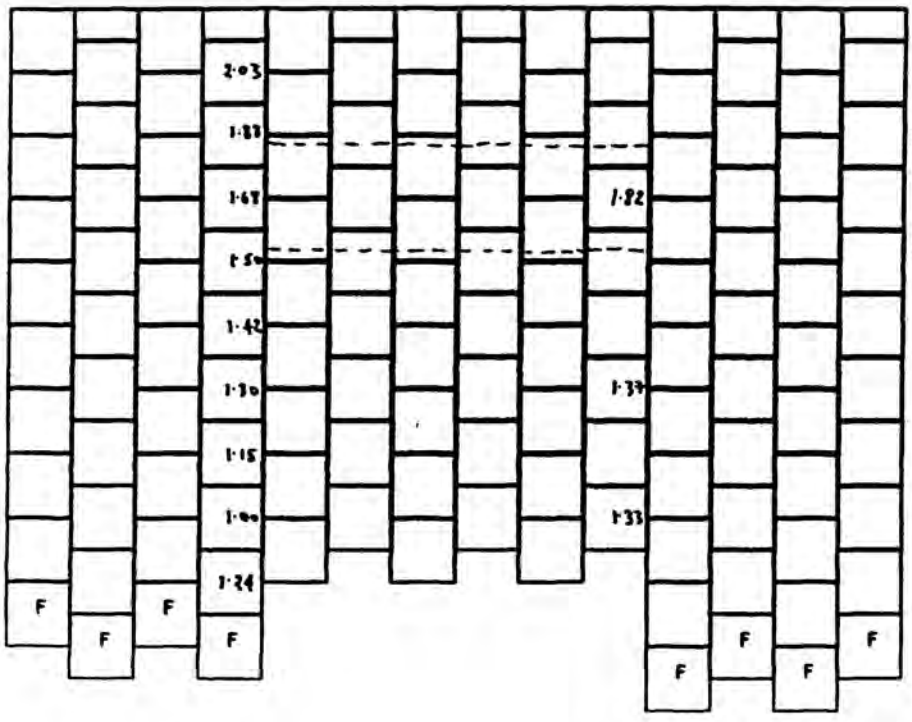
The simulation was then restarted from the initial loading phase and was subjected to 400 iterations of increased vertical loading equivalent to the constant loading required to maintain sliding in the physical model (i.e. Pv/Ph = 2.5). The results at the end of these 400 iterations are shown in Figure 6.22.

Sliding along the vertical joints has been restricted to blocks within the relaxed zone delineated in the block plot. The actual magnitude of normal forces across the vertical planes has not been significantly altered during the increase in vertical loading, with a maximum variation of 10% for blocks within the stable region. A more uniform force distribution has also resulted across the vertical planes of the sliding zone.

The effect of an increase in the vertical load was examined by setting the load ratio Pv/Ph to 3.34 and allowing the loading to distribute for 400 iterations, again restarting after the initial stage. The sliding zone had propagated somewhat nearer to the loaded boundary, as shown in the block plot of Figure 6.22, but still does not correlate with the monolithic sliding mechanism observed in the physical model.

It is assumed that this discrepancy between failure mechanisms of the physical and numerical models is due to the different boundary conditions occurring in both models. In the physical model, the blocks in contact with the loading platens are largely restricted to movements in the direction of the applied loading with only a limited rotation possible about the horizontal, out-of-plane block axes. Thus, block rotations and corresponding large normal forces across the vertical slide planes are inhibited in the physical model and a monolithic sliding zone

RESTART RUN FOR MODEL EXPERIMENT 2 WITH INCREASING VERTICAL LOAD. PV=1.552MPA.
BLOCK PLOT NUMBER OF PROBLEM UNITS PER INCH = 1.00
ITERATION NUMBER = 1100 SCALE . 1 INCH = ____




RESTART RUN FOR MODEL EXPERIMENT 2 WITH INCREASING VERTICAL LOAD. PV=1.552MPA.
CORNER FORCE PLOT NUMBER OF PROBLEM UNITS PER INCH = 2173259.11186909
ITERATION NUMBER = 1100 SCALE . 1 INCH = ____

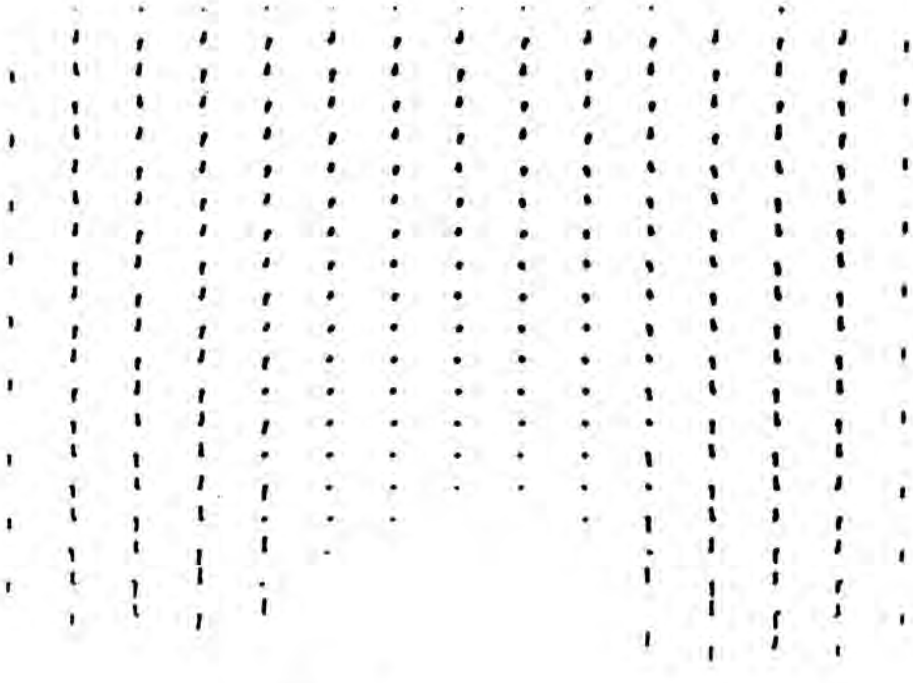
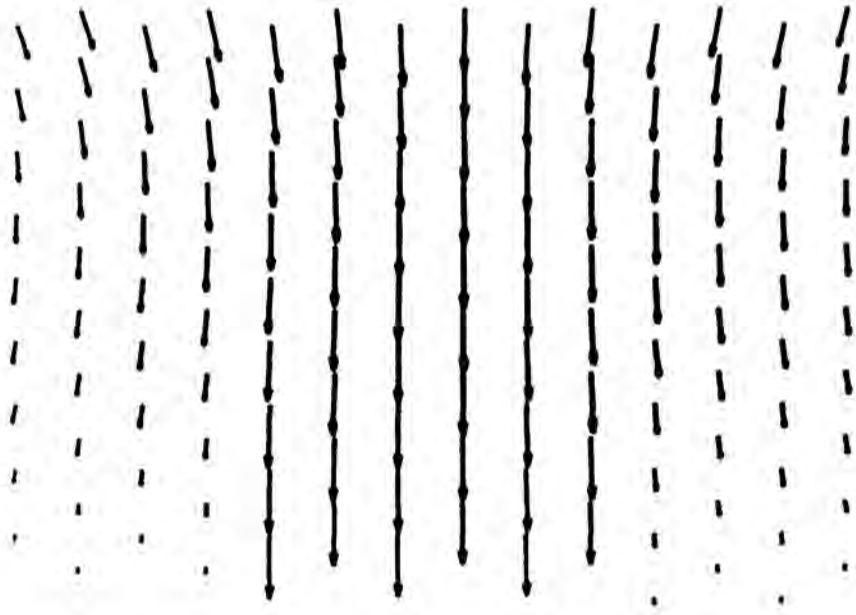


Figure 6.22

RESTART RUN FOR MODEL EXPERIMENT 2 WITH INCREASING VERTICAL LOAD. PV=1.552MPA.
INCREM.DISPL PLOT NUMBER OF PROBLEM UNITS PER INCH = 0.00000035
ITERATION NUMBER = 1100 SCALE . 1 INCH = ——



RESTART RUN FOR MODEL EXPERIMENT 2 WITH INCREASING VERTICAL LOAD. PV=1.552MPA.
TOTAL DISPL PLOT NUMBER OF PROBLEM UNITS PER INCH = 0.00022658
ITERATION NUMBER = 1100 SCALE . 1 INCH = ——

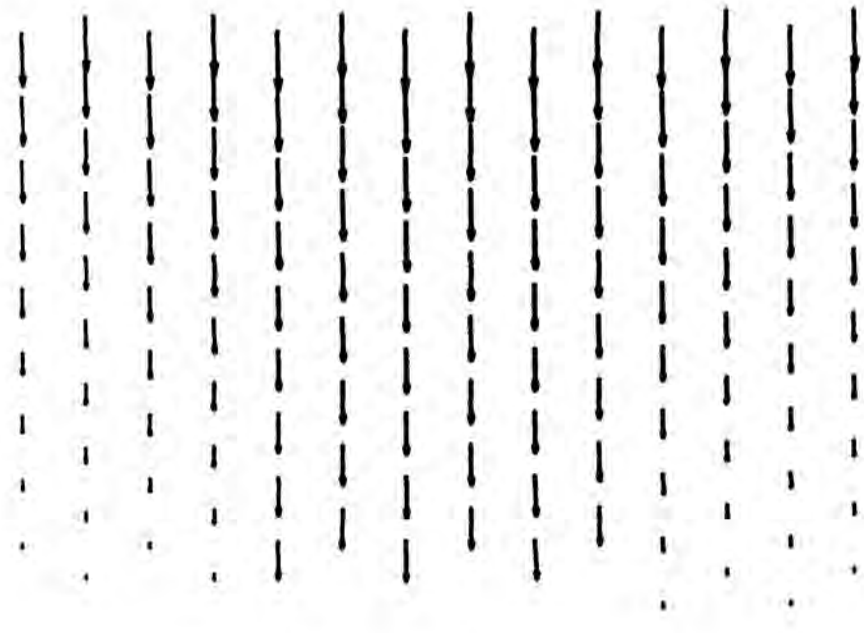


Figure 6.22 contd.

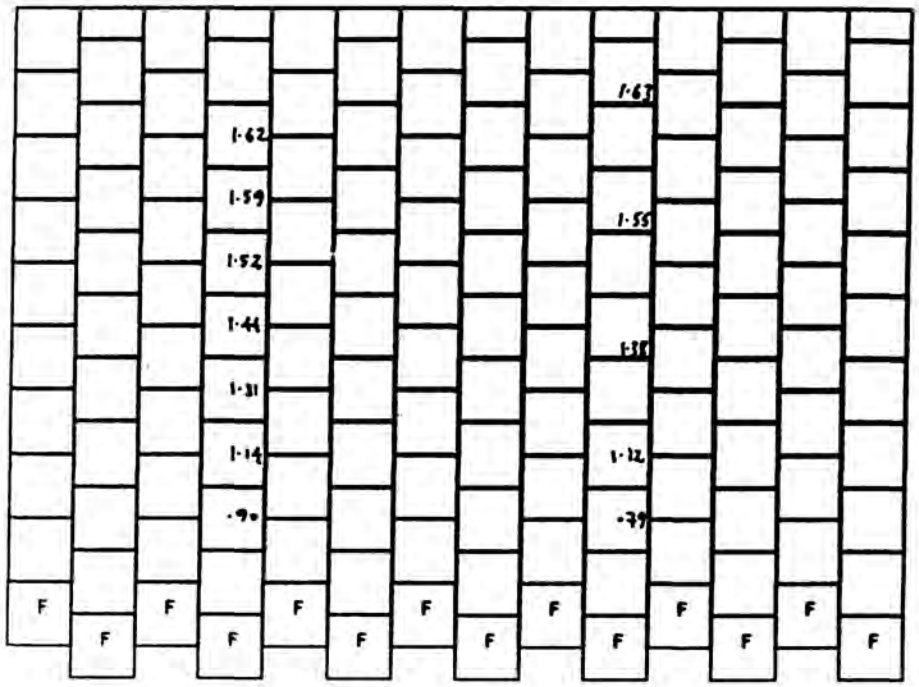
results.

The numerically calculated rotations of vertically loaded boundary blocks were approximately an order of magnitude greater than rotations for blocks located at mid-height of the sliding zone. To confirm that rotations of blocks near the loaded boundary were induced in the numerical model and were not a function of the particular geometry, an alternative block geometry shown in Figure 6.23 was modelled. With this arrangement, the model was initially loaded before creating the excavation and this resulted in a relatively uniform force distribution along each vertical plane, as shown in Figure 6.23.

After initial loading, the six base blocks were removed and the vertical pressure increased to give a Pv/Ph ratio of 2.5. The force distribution and displacement plots after 400 iterations of this increased loading are shown in Figure 6.24 and a marked similarity with the results of the post-loaded case (Figure 6.22) is apparent. Also, the magnitudes of the normal forces across the vertical sliding planes were in close agreement with those of the initial model, the maximum deviation being within 6%.

Therefore, Model II has shown that in situations where the jointing was intuitively selected to suppress arching mechanisms, the mode of failure predicted numerically did not correlate with the monolithic failure obtained in the physical model. This was due to the development of extensive near boundary arching in the numerical model and the deviation in failure modes between models illustrates the influence of boundary conditions on the resulting failure. However, for regions removed from the boundaries, there was close agreement between the failure modes and the philosophy for the following model studies was to concentrate on modes of failure immediately surrounding the openings.

INITIAL LOADING FOR MODEL EXPERIMENT 2 WITH ALL BASE BLOCKS FIXED. 0-400 CYCLES
BLOCK PLOT NUMBER OF PROBLEM UNITS PER INCH = 1.00
ITERATION NUMBER = 400 SCALE . 1 INCH = ____




INITIAL LOADING FOR MODEL EXPERIMENT 2 WITH ALL BASE BLOCKS FIXED. 0-400 CYCLES
CORNER FORCE PLOT NUMBER OF PROBLEM UNITS PER INCH = 709123.25567486
ITERATION NUMBER = 400 SCALE . 1 INCH = ____

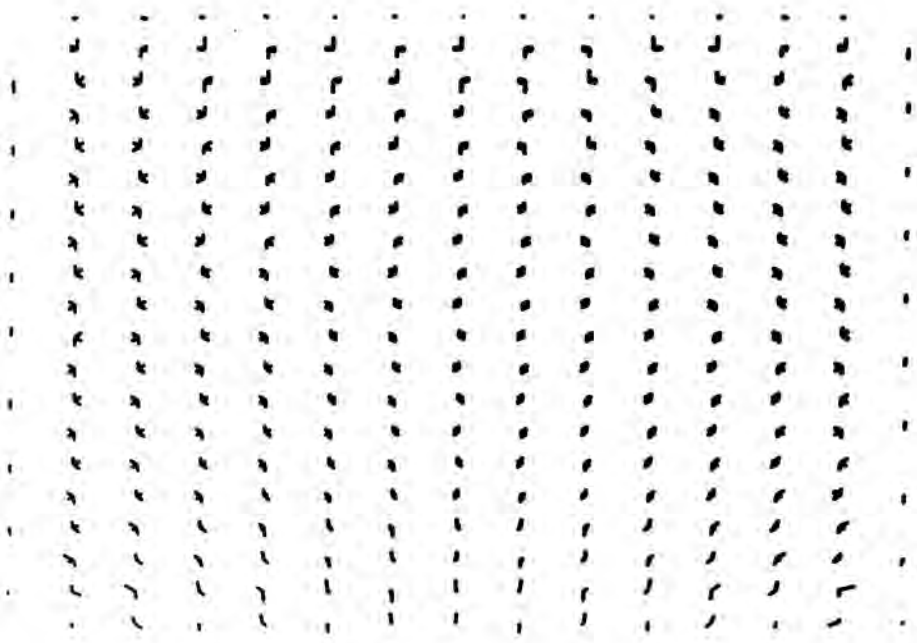
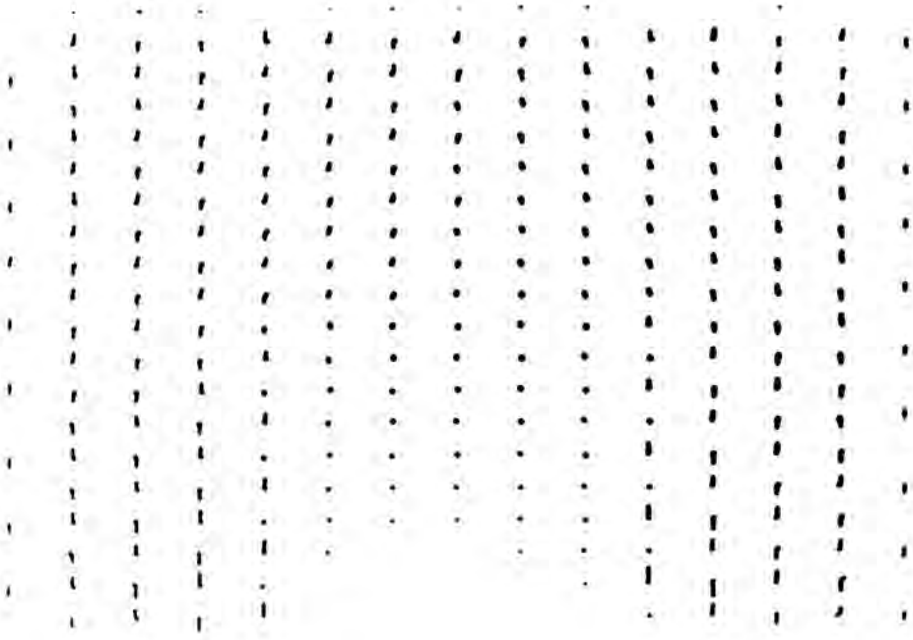


Figure 6.23

REMOVING 6 BASE BLOCKS FOR EXPERIMENT 2 UNDER VERTICAL LOADING. PV=1.552MPA.
CORNER FORCE PLOT NUMBER OF PROBLEM UNITS PER INCH = 2344834.12883324
ITERATION NUMBER = 800 SCALE . 1 INCH = ____



REMOVING 6 BASE BLOCKS FOR EXPERIMENT 2 UNDER VERTICAL LOADING. PV=1.552MPA.
TOTAL DISPL PLOT NUMBER OF PROBLEM UNITS PER INCH = 0.00025506
ITERATION NUMBER = 800 SCALE . 1 INCH = ____

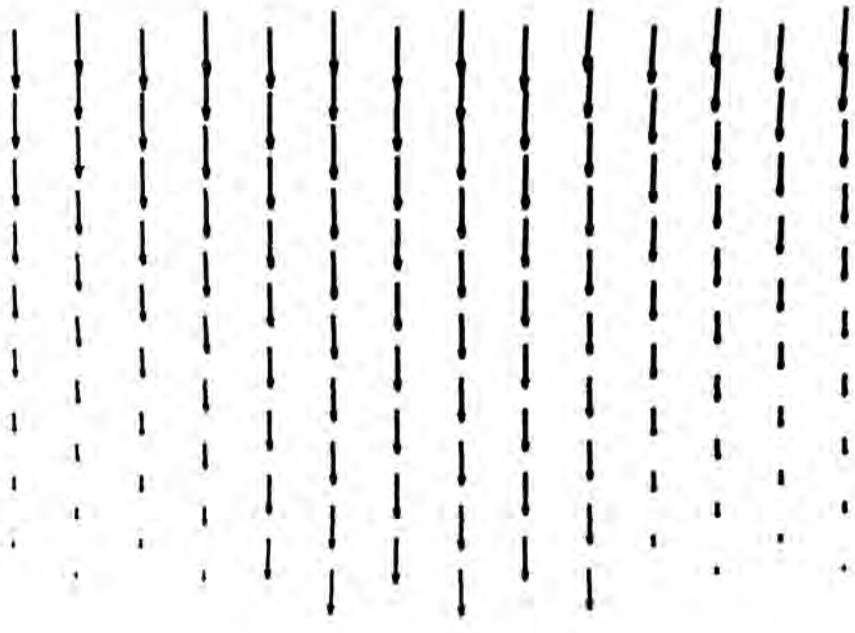


Figure 6.24

6.3.3. Model III: Continuous Joints at 45 degrees to Horizontal, Discontinuous Orthogonal Joints. Opening 150 mm by 25 mm Parallel to Continuous Jointing (Pv > Ph).

Physical Model Study:

Model III was constructed with the continuous joint set orientated at 45 degrees counter-clockwise to the horizontal and the staggered discontinuous joints orthogonal to the continuous jointing, as shown in Figure 6.25. Triangular shaped plaster blocks were accurately manufactured and these were used in conjunction with rectangular blocks (aspect ratio 2 : 1) to provide planar boundaries for loading. Each model edge comprised 14 triangular blocks, each hypotenuse being in direct contact with the loading platens. The opening was created in the centre of the model and was such that six of the discontinuous joints intersected the hangingwall and footwall faces. The hangingwall consisted of 13 rows of blocks while the footwall consisted of 12 rows.

The objective of this model study was to examine the effect of the inclination of the joint sets on the overall stability of the opening, and to provide a basis for comparison with the failure modes and displacement magnitudes predicted for similar situations analysed numerically.

Figure 6.25 shows the model geometry in the vertical test position subsequent to the application of the initial boundary pressures (Pv = .147 MPa, Ph = .112 MPa). The loading procedure was similar to that for Model I whereby the vertical pressure was increased incrementally (in steps of .086 MPa) while the horizontal pressure remained constant throughout at .112 MPa. Photographs of the model were taken systematically during the vertical load application and movement in the model was detected either visually or by a sudden reduction in the applied pressure.

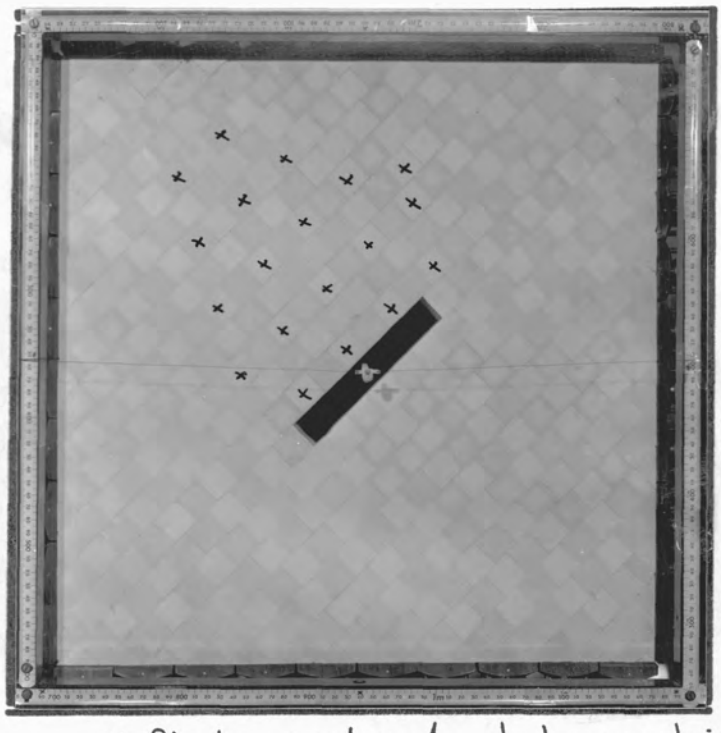



Figure 6.25: Model III under initial loading.

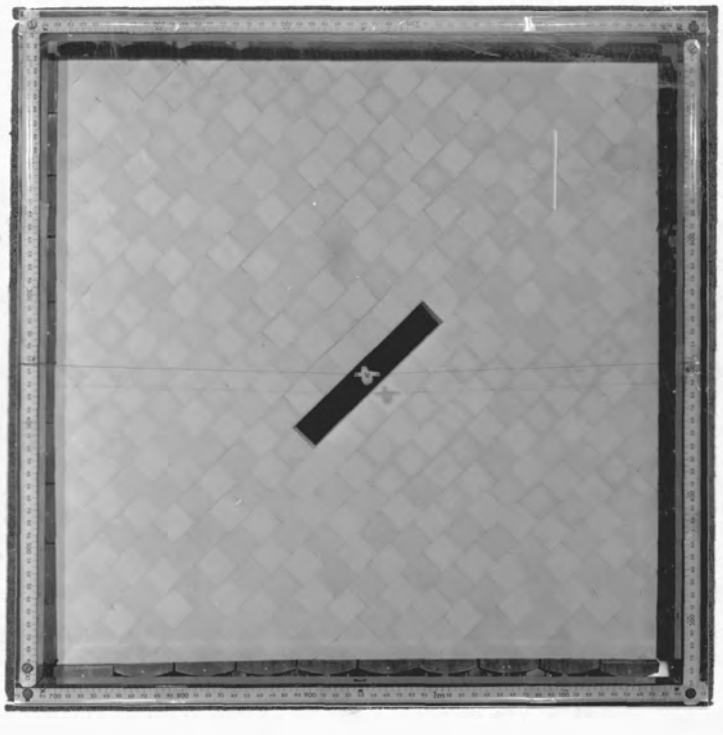


Figure 6.26: Model III - Pv/Ph = 4.8.

In Figure 6.26, the failure state at a vertical pressure of .534 MPa is shown. Separation along both sets of joints surrounding the opening is clearly evident together with the development of beaming action in the immediate overlying hangingwall rows. Slip along and separation of the joints has extended beyond the boundaries of the kinematically feasible triangular zone identified in Model I.

Figure 6.27 shows the extension of the failure mode at an advanced stage of collapse (Pv =.71 MPa) in which the influence of the opening has propagated to the vertically loaded boundary. A symmetrical failure pattern is induced in both footwall and hangingwall. For the hangingwall, the unstable zone is defined by stepped up-dip and down-dip boundaries. The down-dip boundary propagates from the lowermost discontinuous joint intersecting the opening and arises from block rotations and shear sliding towards the opening. The up-dip boundary does not intersect the opening and is characterised by the same slip and rotation mechanisms. Bending of the rows contained between these two boundaries is well defined with large separations formed along the uppermost joints intersecting the opening.

As seen in Figure 6.27, this beaming is asymmetric for the first 3 rows, is located at the mid-span for the fourth and fifth rows and then forms a two-block wide zone which extends to the vertically loaded boundary. This narrow upper rotation zone has been termed a 'kink band' by past researchers (Hammett, 1974; May, 1979).

It is noted that a substantial amount of edge slabbing has occurred along the lower stepped hangingwall hinge zone. It is essential that such undesirable effects are absent or have minimal extent when photogrammetry is employed. Hence, the displacements for particular blocks (identified in Figure 6.25) were determined photogrammetrically for the Pv/Ph ratio of 4.8 (Figure 6.26).

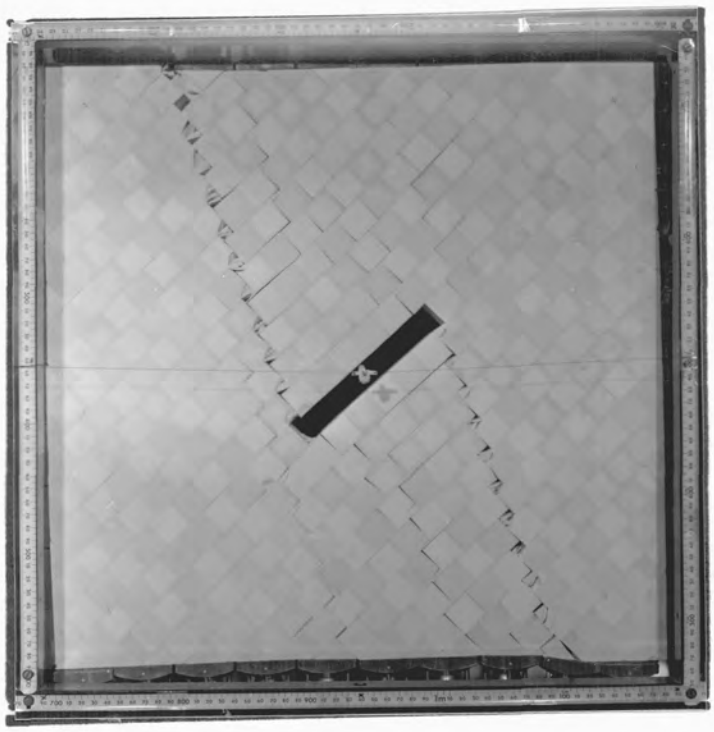


Figure 6.27: Model III - Pv/Ph = 6.3.

These displacements are shown in Figure 6.28 in which the influence of the opening is seen to have most effect on the first 5 hangingwall rows adjacent to the opening. Rows outside this zone have the major component of movement sub-parallel to the continuous jointing, this movement being most pronounced at the down-dip end. The absence of movement towards the opening at the down-dip end confirms that slabbing of the edges, if present, is not influencing behaviour at this stage.

Failure of certain plaster blocks was observed for the load ratio Pv/Ph of 4.8. Cracking in the up-dip crown (abutment) block was observed together with slabbing of block edges along the stepped boundary delineated in Figure 6.27. This slabbing had not developed along the discontinuous joints for rows immediately spanning the opening but was located along four block edges in overlying rows.

Due to the joint inclination, Model III is considerably stiffer than the horizontally and vertically jointed models examined previously since each increment in vertical load represents a corresponding increase in the stabilising thrust. This results in a progressive failure mechanism with large independent movements of overlying rows into the opening (Figure 6.27).

Numerical Analysis of Model III

Figure 6.29 illustrates the basic geometry used for the numerical modelling experiments of Model III. 239 square, rectangular and triangular shaped blocks were selected as representative of the hangingwall of the physical model, this arrangement being considered justified on the grounds of quasi-symmetry between hangingwall and footwall, and preferable in terms of computing economics.

Model III required 51 K words of central memory for execution on the CDC 6600 machine. Execution time for 400

RESULTS FOR EXPERIMENTAL MODEL STUDY NUMBER 3

INCLINED JOINTING + AND - 45 DEGS. OPENING 150MM=25MM. VERT.PRESS.GT.HORIZ.PRESS

PLOT OF TRANSLATIONAL AND ROTATIONAL BLOCK DISPLACEMENTS-ROT.PRINTED IN RADIANS

NUMBER OF PROBLEM UNITS PER INCH = 0.00262 METRES. SCALE IS 1 INCH = _____

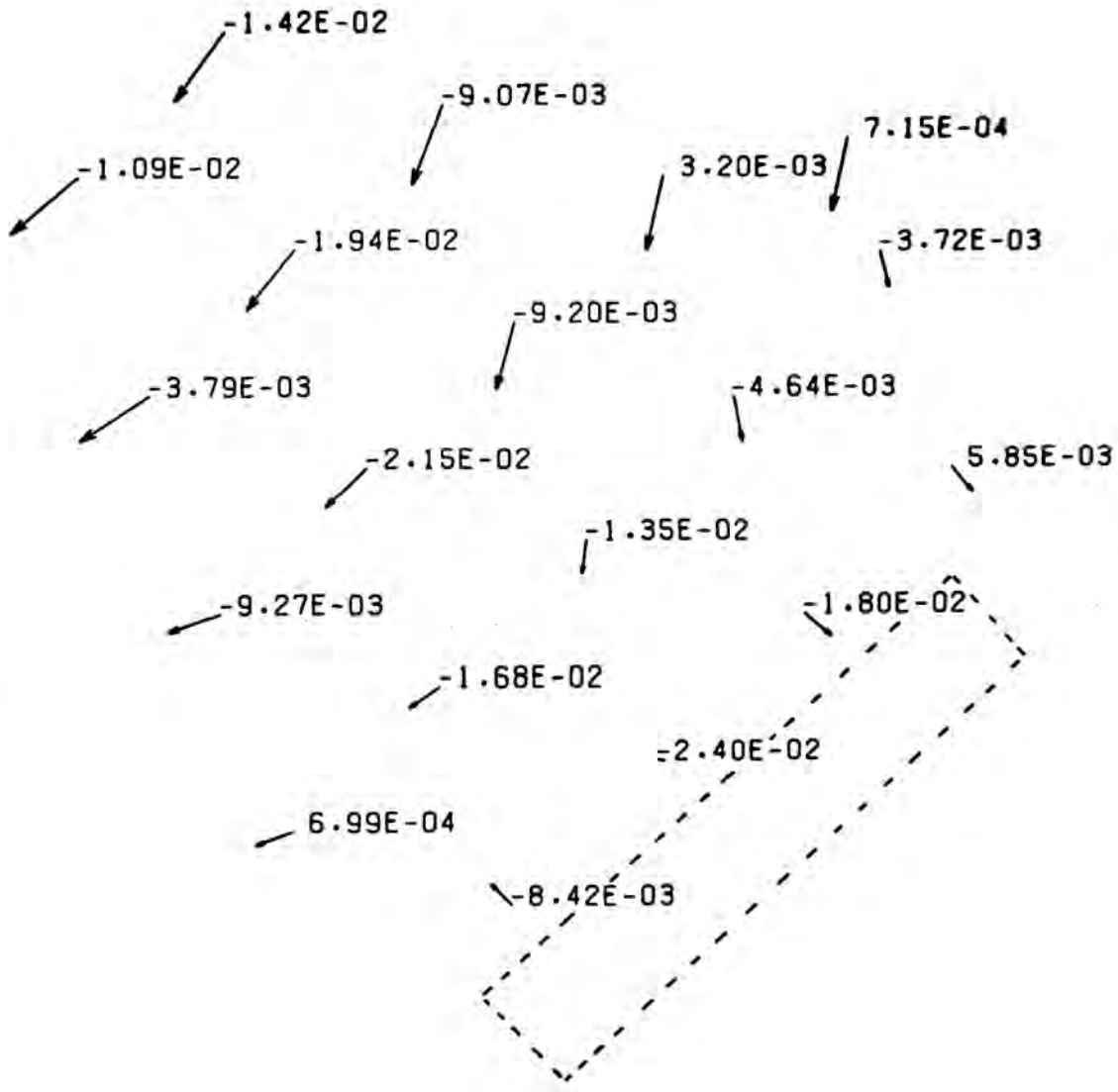
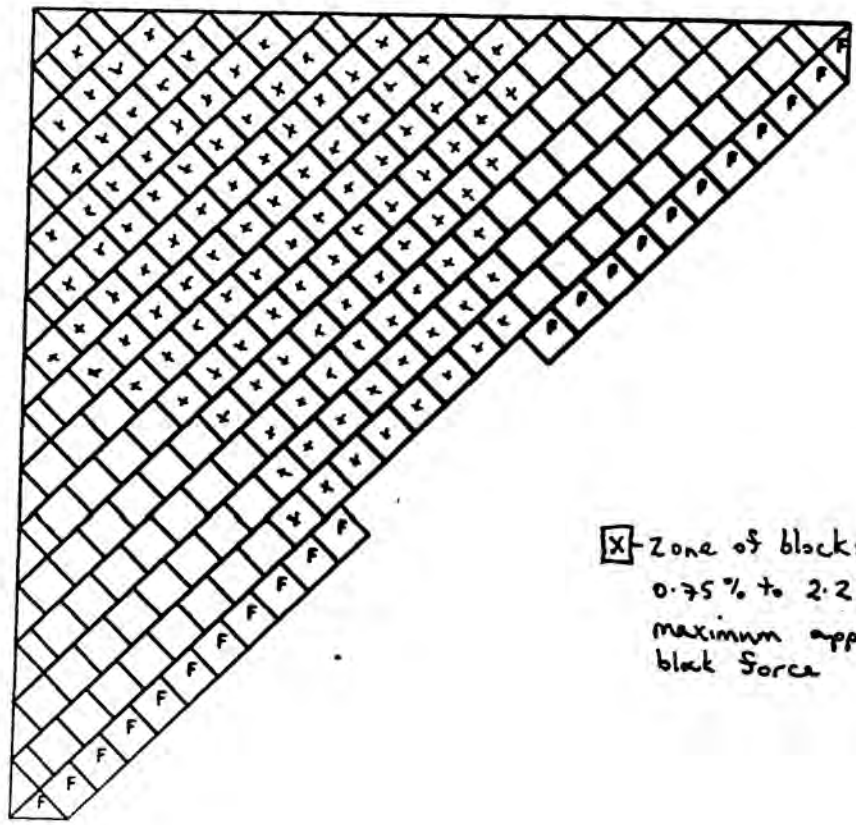



Figure 6.23

INITIAL LOADING FOR MODEL EXPERIMENTS 4 & 3. 0-400 CYCLES
BLOCK PLOT NUMBER OF PROBLEM UNITS PER INCH = 1.56
ITERATION NUMBER = 400 SCALE . 1 INCH = ____




INITIAL LOADING FOR MODEL EXPERIMENTS 4 & 3. 0-400 CYCLES
CORNER FORCE PLOT NUMBER OF PROBLEM UNITS PER INCH = 552.428178237
ITERATION NUMBER = 400 SCALE . 1 INCH = ____

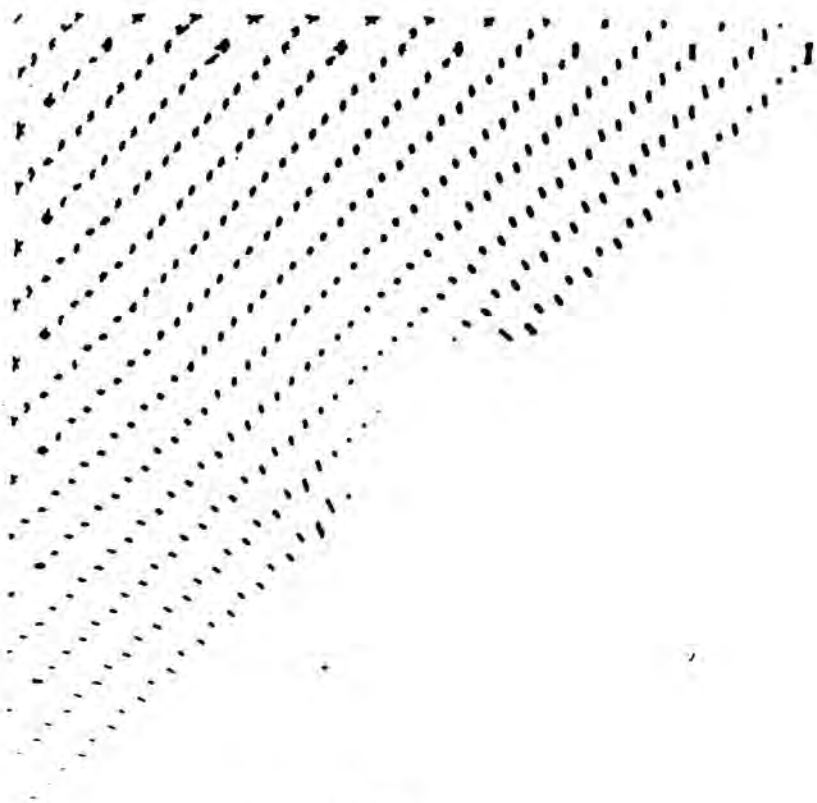
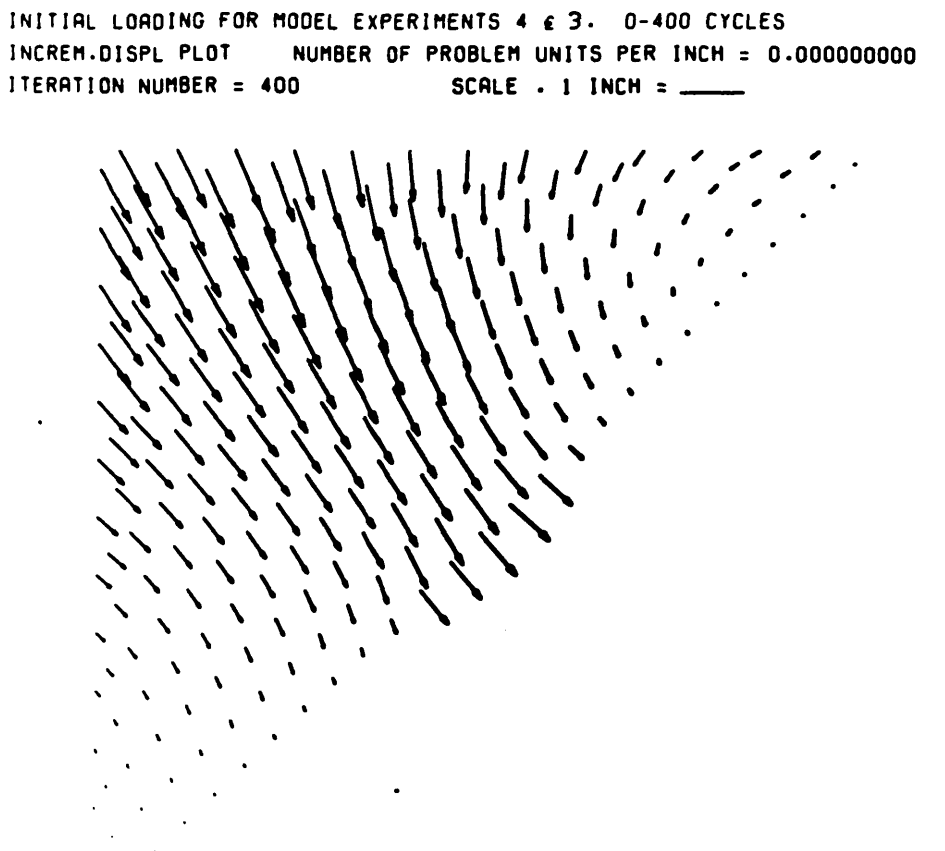


Figure 6.29



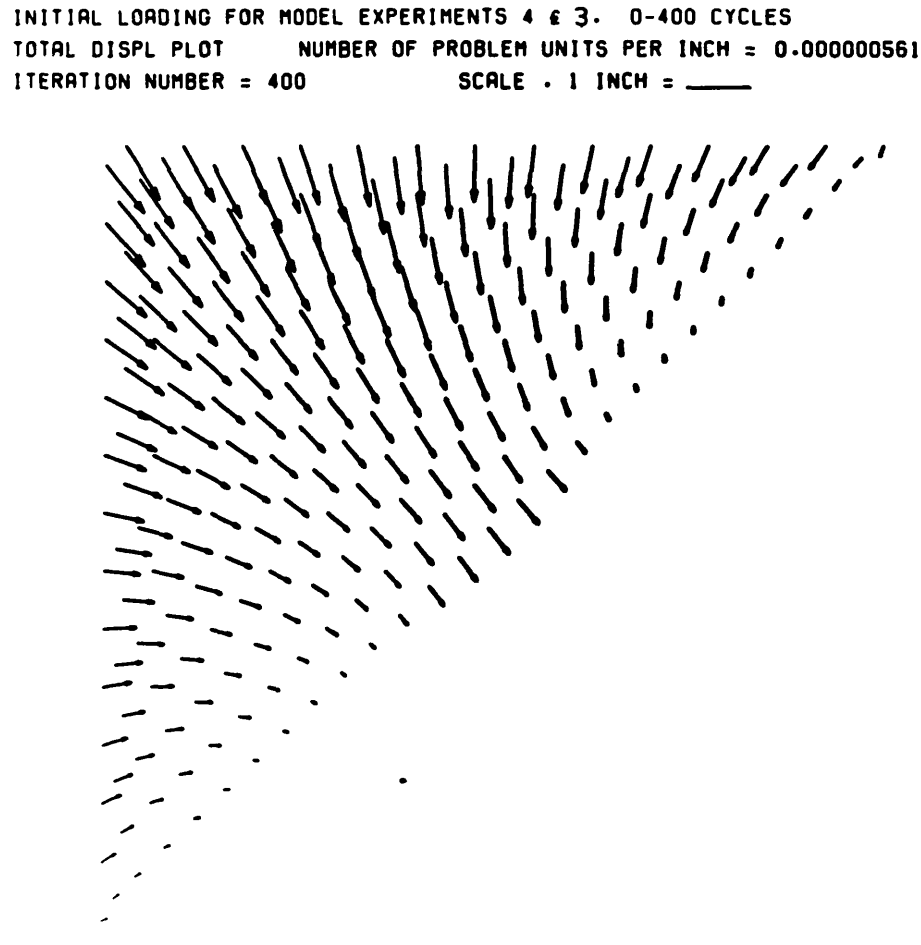




Figure 6.29 contd.

iterations was approximately 525 CP secs. (6600).

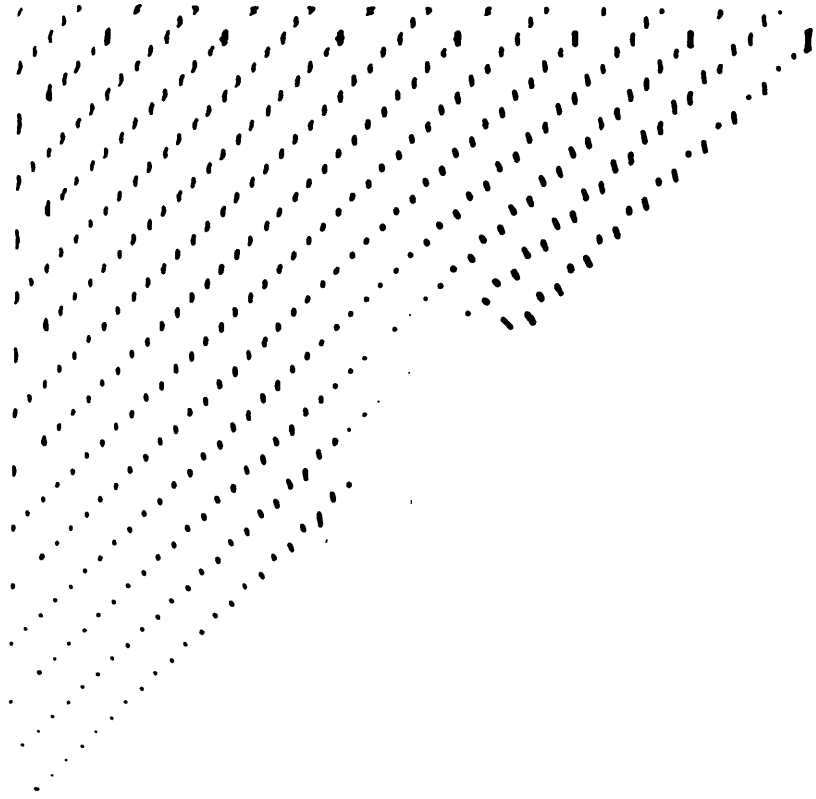
The triangular blocks were designated as externally loaded blocks, the corner forces input via these blocks being calculated as equivalent in magnitude to the uniformly distributed pressures applied to the physical model. The non-linear joint stiffnesses enabled a direct comparison between displacement magnitudes to be made.

Initial loading (equivalent to Pv = .147 MPa, Ph = .112 MPa) was applied to the numerical model for 400 iterations, after which the incremental block movements were to within 1% of those at the beginning of loading while the maximum out-of-balance force-sum was in the vertical direction with a magnitude of 2.2% of the maximum applied block load. Figure 6.29 shows the zone of blocks having out-of-balance vertical forces between 0.75% and 2.2% of the maximum applied loading.

The load distribution and resulting block displacements due to the initial loading are also shown in Figure 6.29. It is seen in the force plot that the two hangingwall rows adjacent to the opening have been shielded from the effects of the boundary loading due to arching action. The contact force printout indicates full frictional resistance has been mobilised along the uppermost and lower-most joints intersecting the opening for these two rows. Separation has also taken place along the continuous joint between these two rows.

Increased vertical loading equivalent to the experimental pressure of .534 MPa was then applied for 400 iterations using the restart facility, and the results at the end of this are seen in Figure 6.30. The force distribution at the end of initial loading (Figure 6.29) shows a similar pattern to that observed after increased loading (Figure 6.30), the maximum force concentrations being located on abutment blocks surrounding the up-dip end of the opening. Tensile failure was in fact observed for

INCREASED VERTICAL LOADING FOR EXPERIMENT 3. PV=2.138MPA. 400-800 CYCLES RESTART
CORNER FORCE PLOT NUMBER OF PROBLEM UNITS PER INCH = 1867.365397672
ITERATION NUMBER = 800 SCALE . 1 INCH = _____



INCREASED VERTICAL LOADING FOR EXPERIMENT 3. PV=2.138MPA. 400-800 CYCLES RESTART
TOTAL DISPL PLOT NUMBER OF PROBLEM UNITS PER INCH = 0.000001764
ITERATION NUMBER = 800 SCALE . 1 INCH = _____

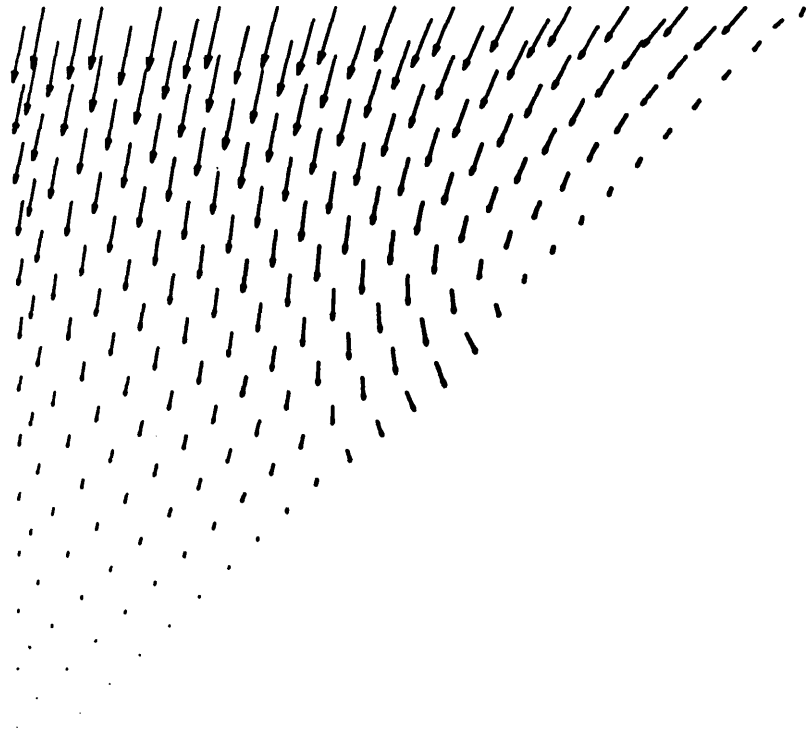


Figure 6.30

the up-dip crown block in the physical model.

The interblock normal force distribution for the first four hangingwall rows spanning the opening is quantitatively presented in Figure 6.31, together with a magnified representation of the joint separations. The body forces are insignificant when compared with the normal forces of Figure 6.31, their magnitude being approximately 1% of typical contact forces.

As in the physical model, specific boundaries have been induced in the hangingwall defining the unstable zone. Interblock slip, rotation and associated hinge formation are located along the same down-dip stepped boundary with the nature of joint separations identical for both models. However, slip has been confined to the discontinuous joints of the first four rows only. The location of the up-dip hinge zone predicted numerically differs slightly to that observed in Figure 6.27, by extending along a similar parallel stepped path but displaced one block width nearer to the opening. This is probably due to the influence in the physical model of the footwall hinge zone inducing substantial rotation of the up-dip crown block.

The contact force printout indicated that slip was occurring along the first five rows of this upper boundary and joint separations for the first two rows corresponded with up-dip physical model separations. Also, the location of the third compressive hinge located between the upper and lower hinge zones was in close agreement with the beaming observed experimentally in Figures 6.26 and 6.27. This beaming was pronounced for the first three rows. Separation along the continuous jointing between the four immediate hangingwall rows was predicted numerically, which confirms the independent action of each of these rows spanning the opening.

The numerically determined displacements of Figure 6.30 indicate that the influence of the opening has

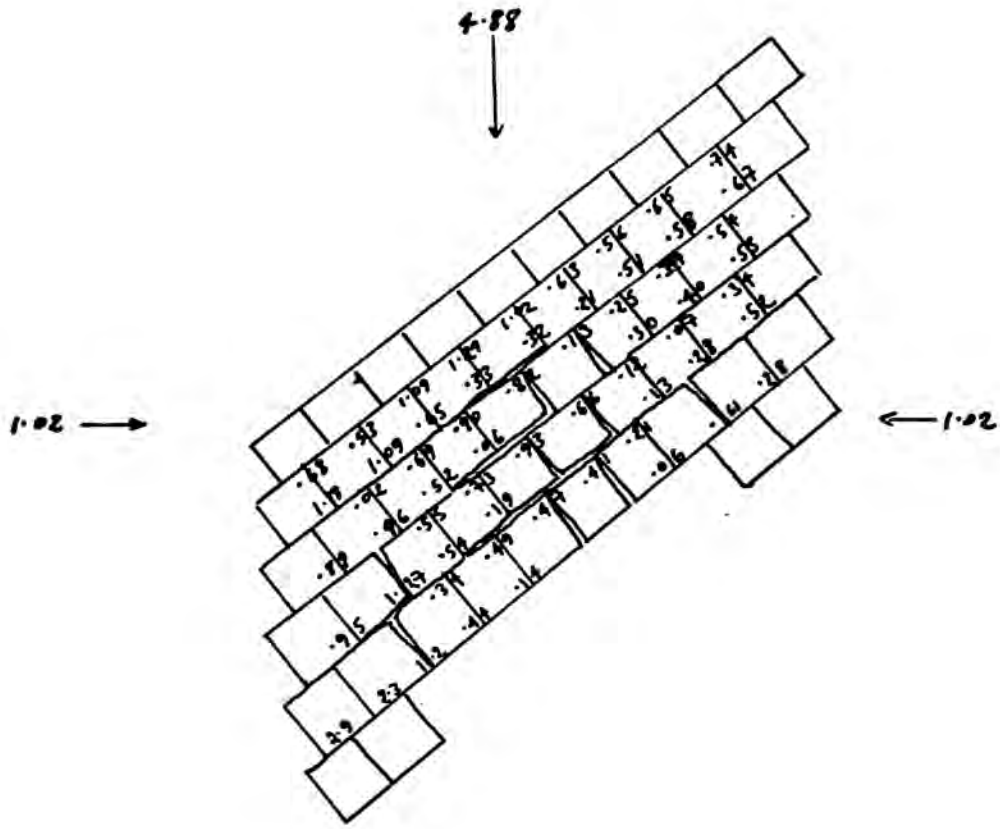



Figure 6.31: Model III - $P_V/P_H$ = 4.8 showing normal force magnitudes.

significantly affected the first five hangingwall rows. This agrees favourably with the photogrammetric displacement pattern in Figure 6.28.

However, a discrepancy exists between the total block displacement magnitudes predicted numerically and corresponding photogrammetric displacements. This difference is highlighted in Table 6.5 where numerical values are, in general, an order of magnitude less than corresponding measured values. It is considered that this dis-

| Block Number | Numerical Displ. Dn(mm) | Photogrammetric Displ. Dp(mm) | Ratio Dp/Dn) |
|---|---|---|---|
| 35 | .065 | .84 | 12.9 |
| 37 | .110 | .21 | 1.9 |
| 39 | .120 | 1.05 | 8.8 |
| 41 | .040 | .94 | 23.5 |
| 87 | .085 | 1.26 | 14.7 |
| 89 | .120 | 1.15 | 9.6 |
| 91 | .150 | 1.05 | 7.0 |
| 93 | .145 | 1.36 | 9.4 |
| 95 | .135 | 1.15 | 8.5 |
| 133 | .130 | 1.68 | 12.9 |
| 135 | .170 | 1.78 | 10.5 |
| 137 | .195 | 2.10 | 10.8 |
| 139 | .200 | 2.31 | 11.6 |
| 171 | .200 | 2.52 | 12.6 |
| 173 | .215 | 2.36 | 11.0 |
| 175 | .245 | 2.62 | 10.7 |
| 201 | .230 | 2.62 | 11.4 |
| 203 | .270 | 2.62 | 9.7 |

Table 6.5: Numerical and Photogrammetric Displacements for Model III.

crepancy in displacement magnitudes is due to

a) the presence of block fracturing and slabbing in the physical model and

b) the fact that the numerical simulation was arbitrarily

stopped while inelastic movements such as slip were still occurring.

Of course, in situations where execution is terminated before a satisfactory equilibrium state is achieved, no valid comparisons between numerical and other independent displacement magnitudes is possible. It was considered impractical in terms of computing economics to continue the numerical simulation in the hope of achieving equilibrium at some later stage.

Photogrammetric displacements had been determined where there was minimal block fracturing and so it is likely that the incompatibility between displacement magnitudes is due mainly to the second factor. However, the fact that relative block displacements were in close agreement coupled with the similarity between modes of failure predicted by both modelling techniques provided sufficient evidence to confirm that the numerical model is capable of analysing discontinua containing openings with inclined jointing.

6.3.4. Model IV: Continuous Joints at 45 degrees to Horizontal; Discontinuous Orthogonal Joints. Opening 150 mm by 25 mm Parallel to Continuous Jointing (Ph > Pv).

Physical Model Study:

Model IV was constructed using the same joint geometry as Model III (Figure 6.25), and contained an opening of identical location and size to that of Model III. The purpose of this experiment was to examine failure mechanisms and block displacements induced as the horizontal pressure was increased under a small constant vertical pressure.

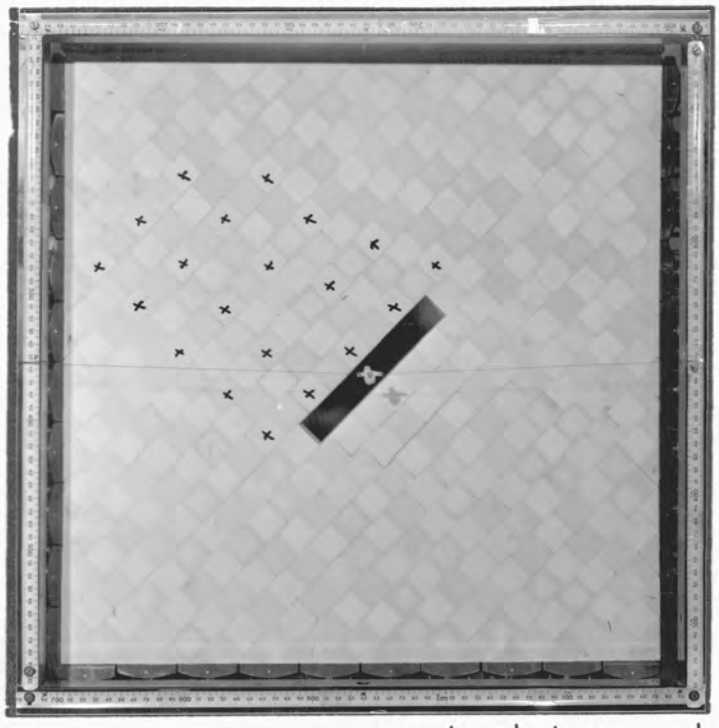
Since both sets of joints were oriented at $\pm$ 45 degrees, Models III and IV were identical except that for Model IV the body forces were now orthogonal to the major

load. This provided the opportunity to confirm that the failure mechanisms examined throughout the series of model studies were, in fact, due to the nature of the loading, joint geometry, and influence of the opening, rather than to some positional malfunction inherent in the loading apparatus.

The model geometry (Figure 6.25) was subjected to the same initial loading as Model III (Pv = .147 MPa, Ph = .112 MPa) necessary to establish the reference block positions for photogrammetry. The horizontal pressure was then increased in increments of .086 MPa until significant movements of blocks surrounding the opening had been detected. Figure 6.32 shows the mechanisms of failure in both footwall and hangingwall for a horizontal pressure of .431 MPa. It is apparent that at this horizontal pressure, considerable separation of the two immediate footwall rows has developed while separation along the discontinuous joints is also well defined for both footwall and hangingwall. The significant movement of the two immediate footwall rows into the opening coincides with the presence of corner slabbing along the down-dip joints intersecting the opening.

The next increment of horizontal pressure (Ph = .517 MPa) resulted in a considerable displacement of the immediate hangingwall row into the opening with associated slabbing and an extension of the failure mechanism is shown in Figure 6.33, for a Pv/Ph ratio of 0.21.

Again, upper and lower stepped boundaries delineating the stable and unstable zones were characteristic of the failure mechanism. As seen in Figure 6.33, these boundaries propagated along sub-horizontal paths to intersect the horizontally loaded edges. For the hangingwall, a stepped upper boundary initiated from the uppermost joint intersecting the opening and is indicative of differential block rotations and shear sliding between adjacent blocks whose edges lie along this path. In Figure 6.32, tensile



x Blocks analysed photogrammetrically

Figure 6.32: Model IV - Pv/Ph = 0.34.

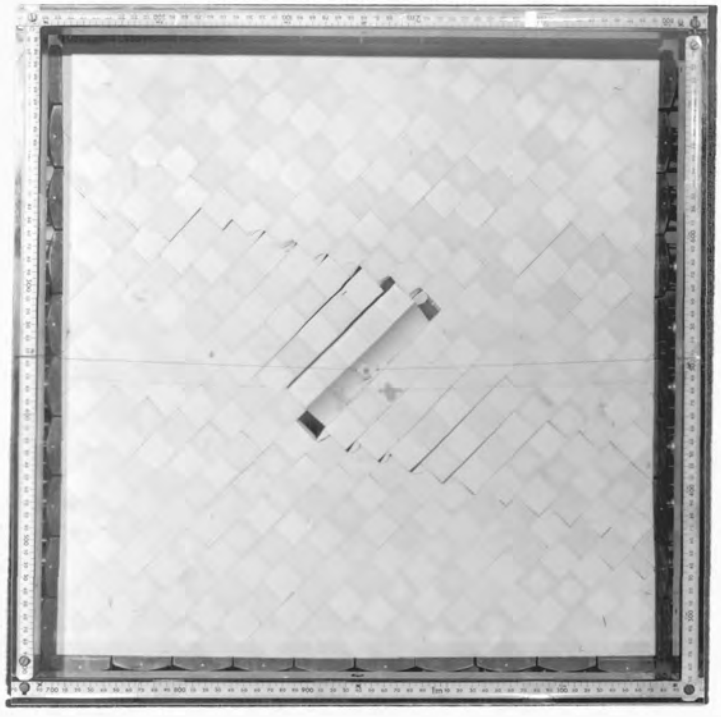


Figure 6.33: Model IV - Pv/Ph = 0.21.

separation and associated hinge formation is visible for the first five rows along this upper boundary. Also, the initiation of slabbing was detected in the second row.

The lower boundary is not as clearly defined in Figure 6.32 but careful observation reveals joint separations for the first three hangingwall rows which results in an unstable zone seven blocks wide spanning the opening between these two parallel boundaries. Bending of the immediate hangingwall rows is well defined for, and in the vicinity of, the lower-most joint intersecting the opening. Joint separations corresponding to this beaming are present in the first five rows and are asymmetrically located towards the lower hinge zone for rows immediately spanning the opening.

Displacements for hangingwall blocks were determined photogrammetrically for the load ratio Pv/Ph of .34 (Figure 6.32) since minimum fracturing of blocks occurred at this load level. Qualitatively, the extent of fracturing visible in the hangingwall of Figure 6.32 was considerably less than that present in the photogrammetrically analysed stage of Model III. The photogrammetric displacements for Model IV are presented in Figure 6.34 and they indicate that the influence of the opening has extended to the fifth hangingwall row, at least. The direction of the up-dip displacement vectors implies that slabbing is having no effect on the model behaviour.

The maximum translational block displacement measured was 55% of that in Model III, which supports the observation of a reduced level of fracturing for Model IV.

The similarity between failure modes for Models III and IV confirms that the loading apparatus is satisfying design considerations and enables further confidence to be placed in the results of subsequent studies.

RESULTS FOR EXPERIMENTAL MODEL STUDY NUMBER 4

INCLINED JOINTING + AND - 45 DEGS. OPENING 150MM=25MM. HORIZ.PRESS.GT.VERT.PRESS

PLOT OF TRANSLATIONAL AND ROTATIONAL BLOCK DISPLACEMENTS-ROT.PRINTED IN RADIANS

NUMBER OF PROBLEM UNITS PER INCH = 0.00142 METRES. SCALE IS 1 INCH = ____

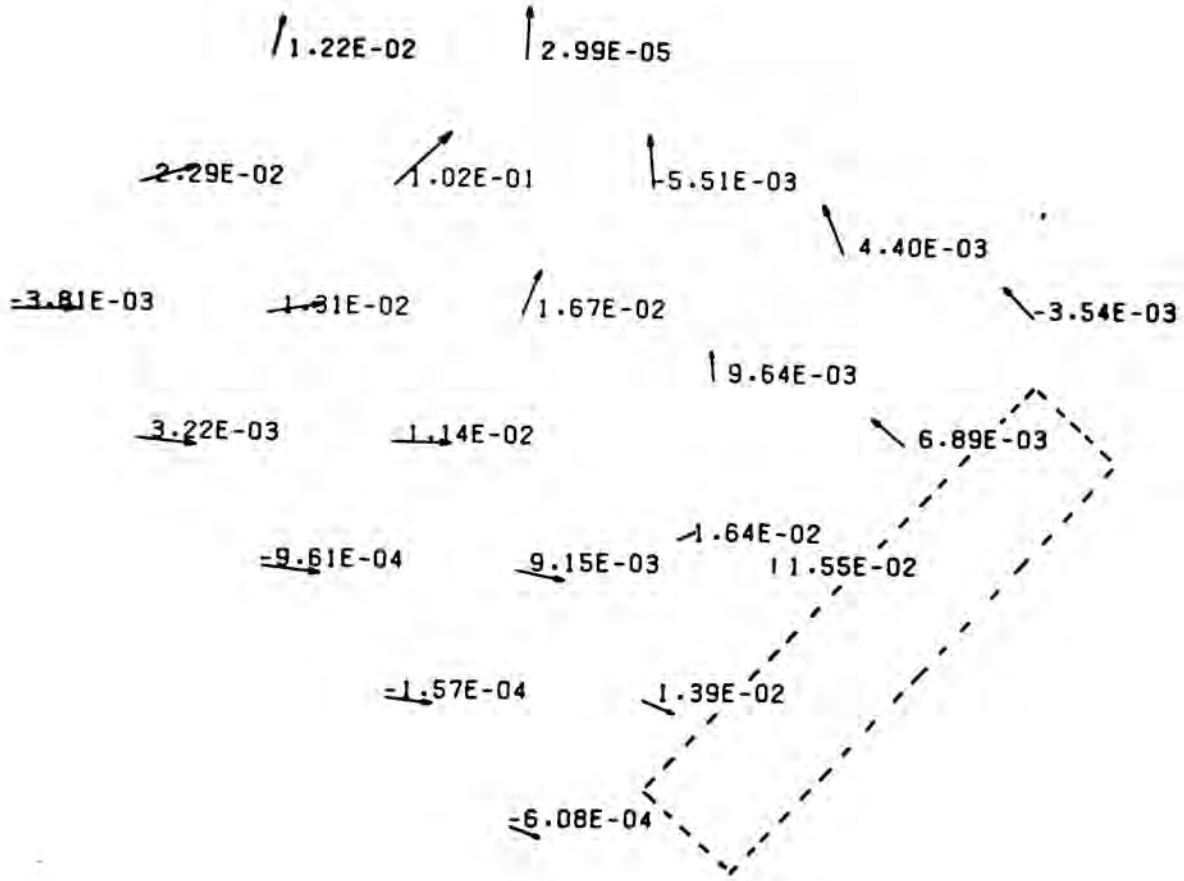



Figure 6.34

Numerical Analysis of Model IV:

The identical geometrical representation (Figure 6.29) and input parameters to those of Model III were used in the numerical experiments for Model IV. Since initial loading was the same for both studies, a preliminary loading phase was not necessary, the same restart file being applicable for both Models III and IV.

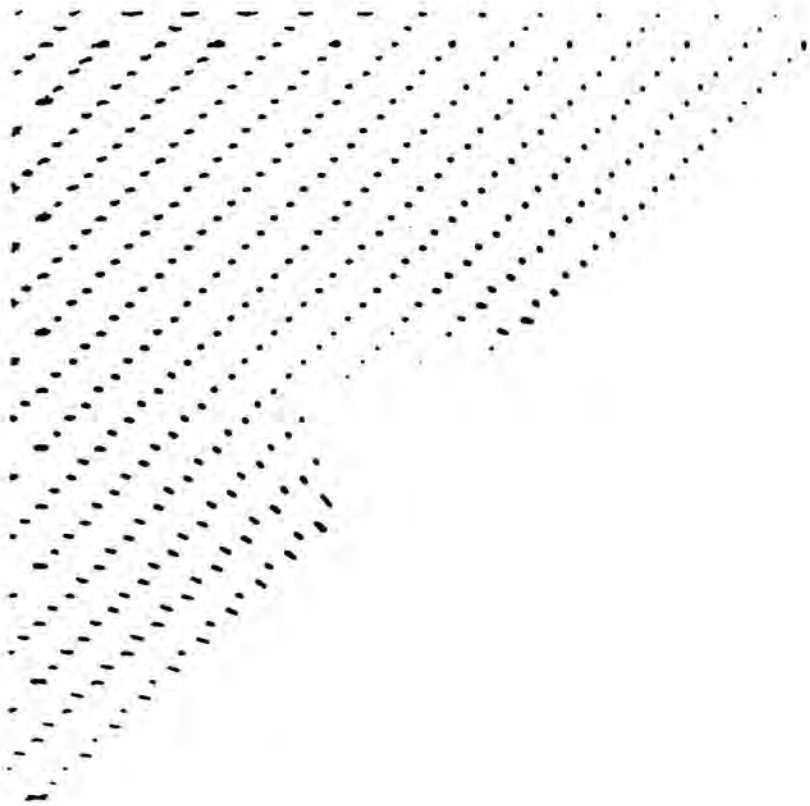
Increased horizontal loading equivalent in magnitude to the uniformly distributed experimental pressure of .431 MPa was applied to the numerical model via the restart facility. This loading was applied for a further 400 iterations and the final results are shown in Figure 6.35. Incremental movements after final loading were approximately 10% of initial movements.

Arching of the load in the surrounding material is predominant with large horizontal force components in the vicinity of the abutments. The maximum forces are located in the stable zone surrounding the down-dip end. Figure 6.35 shows a similar force distribution within the unstable hangingwall zone to that of Model III (Figure 6.30), with the first four rows adjacent to the opening being shielded from the influence of the increased horizontal pressure.

The normal contact force distribution throughout the potentially unstable hangingwall zone for the five rows spanning the opening is presented in Figure 6.36. Typical interblock forces are, on average, two orders of magnitude greater than body forces.

The numerically predicted but grossly magnified joint separations of Figure 6.36 illustrate that slip and separation have initiated along an identical 'saw-tooth' shaped upper boundary as that determined in the physical model. Separation occurs along this sub-horizontal path for the immediate row only but the nature of the force distribution for overlying rows suggests that extension of

INCREASED HORIZONTAL LOADING FOR EXPERIMENT 4. PH=1.655MPA. 400-800 CYCS RESTART
CORNER FORCE PLOT NUMBER OF PROBLEM UNITS PER INCH = 1577.157708371
ITERATION NUMBER = 800 SCALE . 1 INCH = _____



INCREASED HORIZONTAL LOADING FOR EXPERIMENT 4. PH=1.655MPA. 400-800 CYCS RESTART
TOTAL DISPL PLOT NUMBER OF PROBLEM UNITS PER INCH = 0.000001479
ITERATION NUMBER = 800 SCALE . 1 INCH = _____

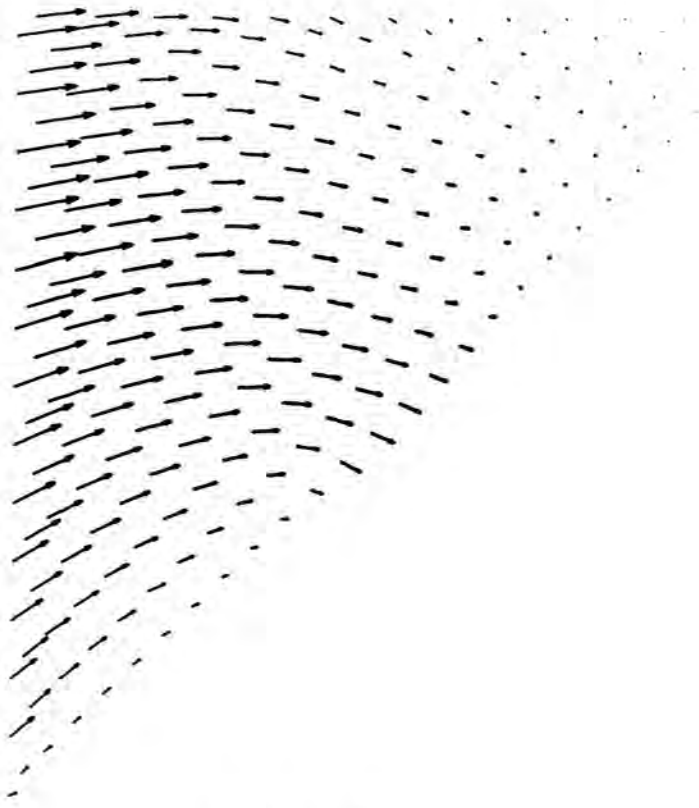


Figure C.35

this hinge zone is imminent (Figure 6.36). Full mobilisation of frictional resistance has occurred along the upper boundary for the first three rows.

The lower boundary predicted by the numerical model is characterised by similar block movements to those present in the physical model. However, as was the case with Model III, its actual location differs slightly by being displaced one block length towards the opening. This results in an unstable six block row spanning the opening. The discrepancy in the lower boundary position was again considered to be due to the diagonal row of fixed blocks preventing the footwall hinge zones from influencing hangingwall behaviour. Tensile separation, due to clockwise rotation of blocks towards the opening, occurs along the down-dip discontinuous joints for the first two rows while the ratio of shear to normal forces after final loading indicates that the shear strength of the first four rows of the lower boundary is exceeded.

The nature and location of the complementary mid-span hinge formation is similar for both models. As shown in Figure 6.36, this separation is most pronounced for the three adjacent overlying rows. Separation between the continuous joints for the first four rows indicates that these rows are primarily concerned with achieving stability through interaction with the sides of the stable opening and do so by undergoing the particular slip, rotation, separation and hinging mechanisms discussed above.

The numerically determined displacement field (Figure 6.35) is similar in pattern to the photogrammetric flow field (Figure 6.34) except in the vicinity of the crown abutment region. It is likely that the reduced reactions induced along the fixed barrier of blocks (evident in Figure 6.35) cause this discrepancy. A more realistic simulation of the crown region would be obtained by accurately modelling the force distribution along the

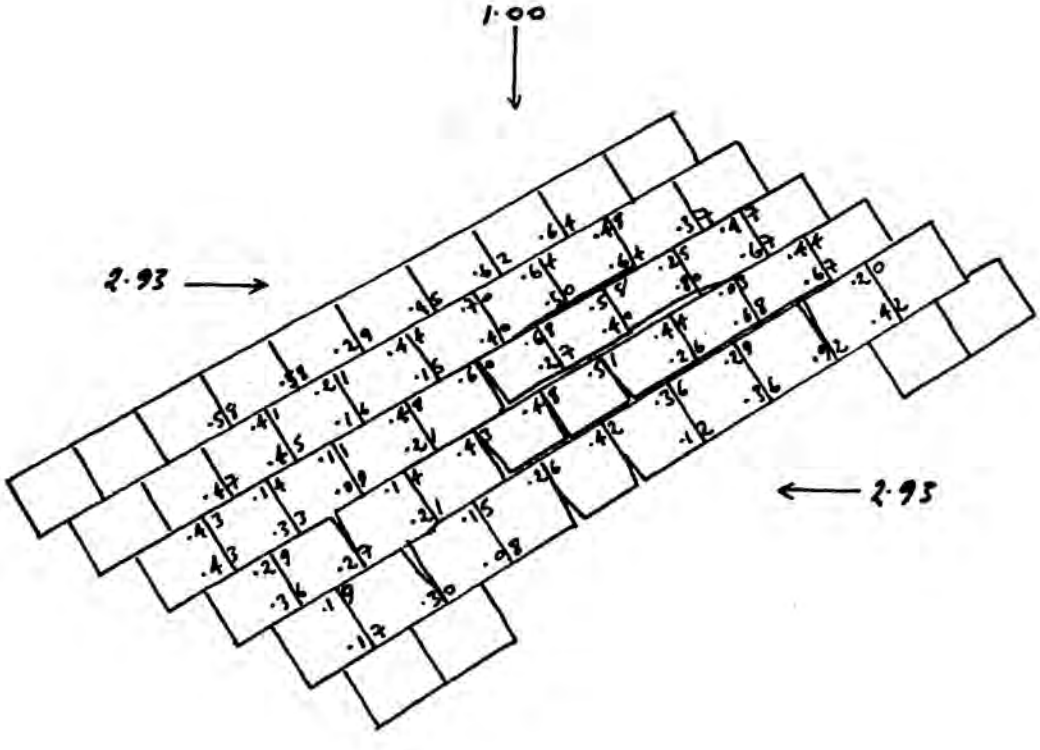



Figure 6.36: Model IV - $P_V/P_H$ = ·34 showing normal force magnitudes.

upper diagonal boundary. A comparison between the pattern of displacements, however, indicates excellent relative correlation between displacement vectors for all other zones.

With slip still occurring in the three immediate hangingwall rows of the numerical model after the duration of increased loading, any comparison which involves the predicted displacement magnitudes at this stage is of limited relevance. However, Table 6.6 presents the resultant total displacements for down-dip blocks along with the corresponding measured values. It is noted that the deviation between physical and numerical displacements for Model IV is approximately half that in Model III (Table 6.5). This suggests that the discrepancy between measured

| Block Number | Numerical Displ. Dn(mm) | Photogrammetric Displ. Dp(mm) | Ratio Dp/Dn |
|---|---|---|---|
| 33 | .035 | .568 | 16.2 |
| 35 | .100 | .682 | 6.8 |
| 64 | .120 | .341 | 2.8 |
| 86 | .110 | .852 | 7.7 |
| 88 | .130 | .909 | 7.0 |
| 131 | .165 | 1.079 | 6.5 |
| 133 | .160 | 1.070 | 6.7 |
| 168 | .210 | 1.136 | 5.4 |
| 170 | .195 | 1.022 | 5.2 |
| 197 | .245 | 1.193 | 4.9 |
| 199 | .230 | 1.079 | 4.7 |

Table 6.6: Numerical and Photogrammetric Displacements for Model IV.

and computed displacements is a direct function of the amount of slabbing present.

Therefore, the main conclusions to be drawn from the physical and numerical modelling of Models III and IV are that both techniques produce analogous failure mechanisms in the material surrounding the opening. The

extent of movements predicted in the numerical models were however, limited, largely by the inability to simulate physical processes.

6.3.5. Model V: Continuous Joints at 60 Degrees to Horizontal; Discontinuous Orthogonal Joints. Opening 150 mm by 25 mm Parallel to Continuous Jointing ($Pv > Ph$).

Physical Model Study:

Model V was constructed with the continuous joint set orientated at 60 degrees counter-clockwise to the horizontal and the discontinuous joint set perpendicular to the through-going joints, as shown in Figure 6.37. Specially shaped boundary blocks were manufactured by casting 500 mm plaster lengths against replicas of the outer 'saw-tooth' shaped model edges, these being cut into ten 47.5 mm lengths, and the planar faces of the irregularly shaped units being in direct contact with individual loading platens. These components were prepared from the same plaster mixture used to cast the square blocks.

Apart from these edge pieces, the model was constructed from square blocks, all blocks coming from the same graded batch. The opening was created in the centre of the model with the long axis parallel to the continuous jointing such that six discontinuous joints intersected both the hangingwall and footwall opening faces. Both the footwall and hangingwall were anti-symmetric about the long axis of the opening, each consisting of 12 rows of blocks.

The objective of this experiment was to determine the influence of the steeply inclined jointing on the behaviour of material surrounding the opening, and was considered especially significant since many prototype excavations are located in similar geometries.

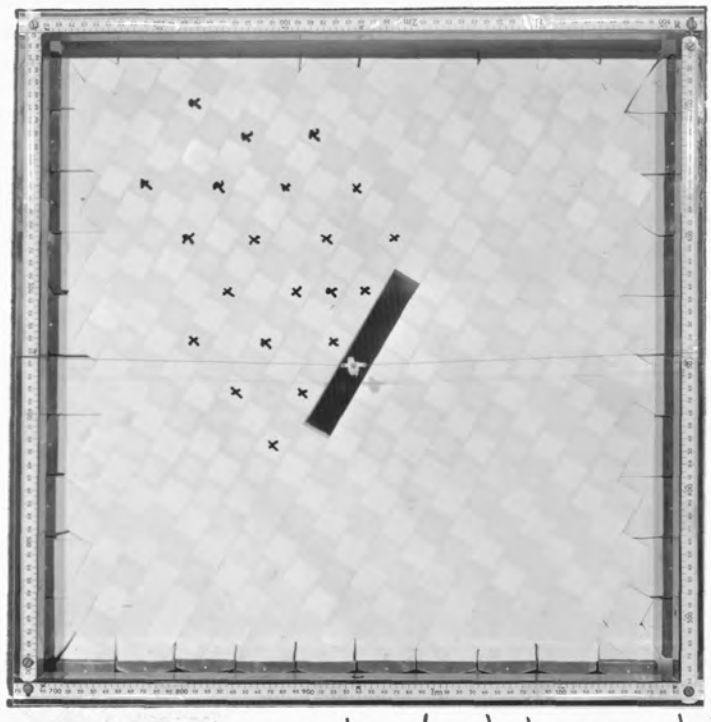



Figure 6.37: Model V under initial loading.

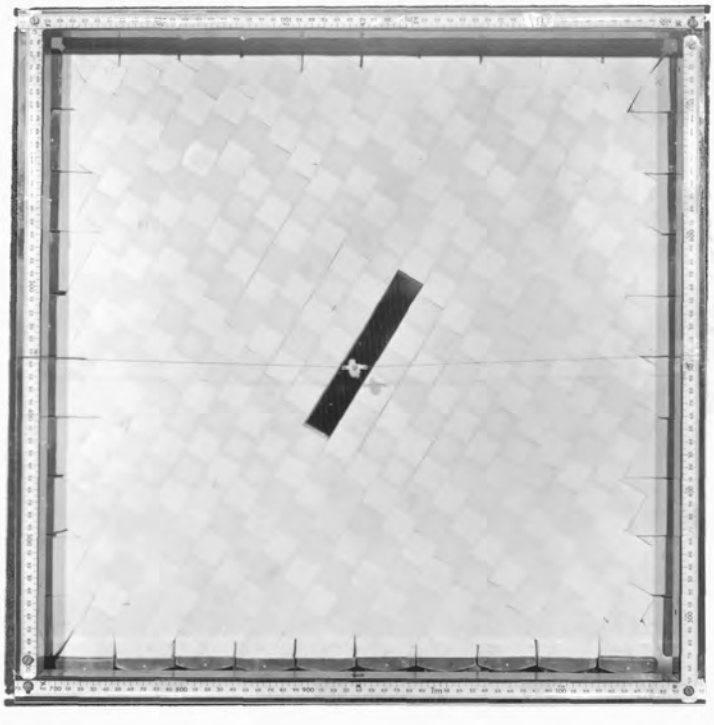


Figure 6.38: Model V - Pv/Ph = 5.2.

Figure 6.37 shows the physical model after application of the initial boundary pressures (Pv = .156 MPa, Ph = .112 MPa) and prior to subsequent loading. Loading the model to failure was accomplished by increasing the vertical pressure in increments of 0.086 MPa while maintaining the horizontal pressure constant at the initial value of .112 MPa. In Figure 6.38, the deformed model geometry under a loading ratio of Pv : Ph = 5.2 is shown.

Separation along both continuous and discontinuous joint sets surrounding the opening has occurred in an anti-symmetric manner about the long opening axis and for the hangingwall, the first four overlying rows have clearly separated from the overlying rows. For the geometry illustrated in Figure 6.38, slip and separation along the discontinuous joints propagate to either vertically loaded boundary, with interference due to edge loading effects giving rise to local variations near the boundary extremities.

The unstable hangingwall zone for Model V is characterised by two clearly defined boundaries. The lower hangingwall boundary initiates from the lower-most discontinuous joint intersecting the opening and is formed from a combination of slip and rotation with associated separation and hinge formation. The behaviour of blocks so producing this boundary is similar to that described for Models III and IV, but because of the particular joint orientations modelled, the inclination to the horizontal of the lower stepped path is considerably reduced from that of earlier models. The actual angle of inclination is between 40 and 45 degrees, and this results in the lower boundary being unable to reach the vertically loaded edge (c.f. Figure 6.27).

The mode of failure in the up-dip region of the hangingwall is quite different to that discussed for Models III and IV. For Model V, one upper hangingwall

boundary delineating the potentially unstable zone is prominent. This again is formed from a combination of block slippage and rotation mechanisms and initiates from the upper-most discontinuous joint intersecting the opening. The upper boundary, being parallel to its lower counterpart, intersects the vertically loaded model edge and results in an unstable zone five blocks wide spanning the opening.

Hinge formation at opposite ends of the discontinuous joints forming the stable sides of the opening indicates that each hangingwall row is displaying characteristics similar to a two-hinged structural beam. The failure mode for Model V thus differs from those of Models III and IV in that the development of a third hinge zone due to beaming action between the upper and lower stepped hinge zones has been suppressed.

Due to the particular jointing configuration examined here, an increase in the vertical pressure represents a corresponding larger increase in the stabilising thrusts generated orthogonal to the discontinuous joint set. The magnitudes of the lateral thrusts developed in this case were sufficient to inhibit bending of rows and attendant mid-span joint separation. The continuous joint separation for overlying rows along the full five block span demonstrates the independent behaviour of each hangingwall row.

The magnitude of the translational and rotational rigid block displacements for particular hangingwall blocks (Figure 6.37) were determined photogrammetrically from the deformed model geometry shown in Figure 6.38. These results are plotted to scale in Figure 6.39. The influence of the opening on the overlying hangingwall rows is clearly evident for up-dip blocks whilst blocks surrounding the down-dip opening extremity have their major component of translational movement sub-parallel to

[illegible] FOR EXPERIMENTAL MODEL STUDY NUMBER 5

[illegible] JOINTS AT 60 DEGS.TO HORIZ. OPENING 150MM=25MM. PV.GT.PH.

[illegible] OF TRANSLATIONAL AND ROTATIONAL BLOCK DISPLACEMENTS-ROT.PRINTED IN RADIANS

[illegible] PROBLEM UNITS PER INCH = 0.00396 METRES. SCALE IS 1 INCH = _____

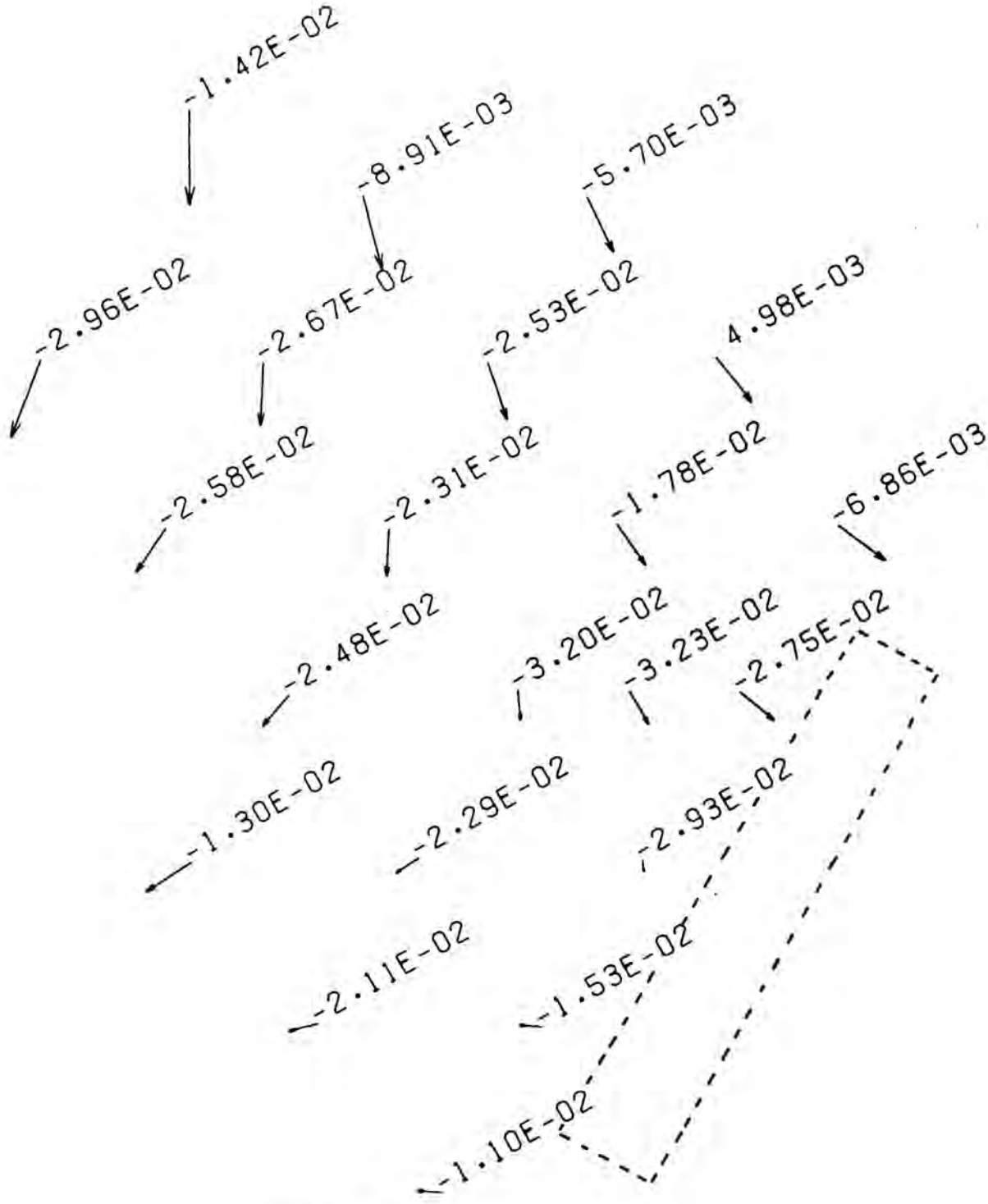



Figure 6.39

the continuous jointing.

For the loading ratio of Pv : Ph = 5.2, the extent of tensile slabbing along both upper and lower hinge zones was quite extensive. This fracturing occurred suddenly for vertical boundary pressures between .534 MPa and .577 MPa. The magnitude of the largest resultant displacement of approximately 4 mm (Figure 6.39) gives some indication of the amount of fracturing developed.

The final collapse state for Model V is shown in Figure 6.40 and is a continuation of the mode of failure described above. A secondary rotation band at approximately mid-span has created a prominent 3-block-wide kink band which extends to the loaded boundaries on both the footwall and hangingwall sides. The stepped paths defining the unstable zones have still not penetrated beyond the opening extremities. A measure of the versatility of the loading platens was demonstrated for ensuing deformations of the model edges.

Numerical Analysis of Model V:

The geometry selected to represent the hangingwall in the numerical modelling experiments is shown in Figure 6.41. Again, this configuration was chosen on the grounds of system symmetry and computing considerations. The model consisted of a total of 187 square and triangular shaped blocks, the six fixed triangular blocks located along the vertical edge being necessary to prevent excessive movement of edge blocks.

Initially, only the square blocks were modelled but this was unacceptable since shear sliding of the edge blocks dominated overall behaviour. This highlights the difficulty in numerically simulating the physical model boundary conditions. For the physical model, the platen-model material interface is such that the externally loaded blocks are effectively fixed in the direction

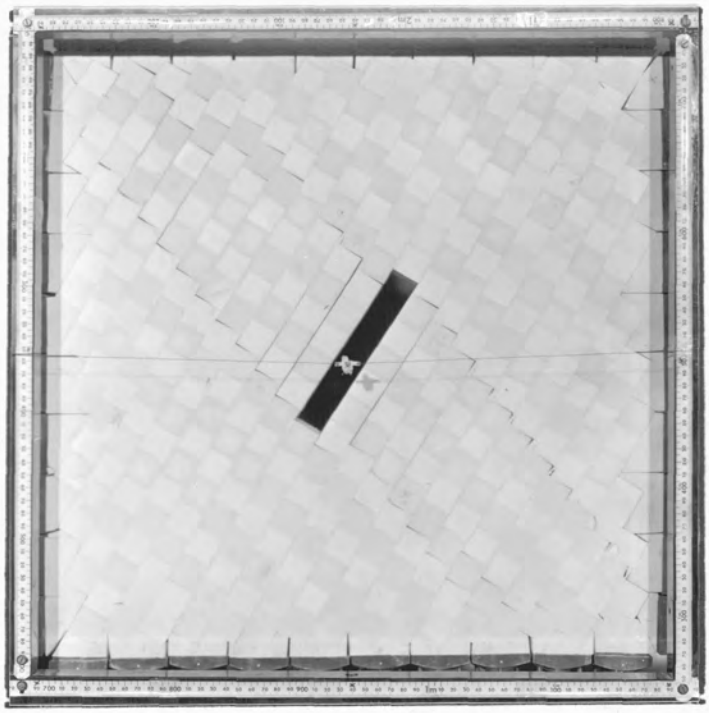
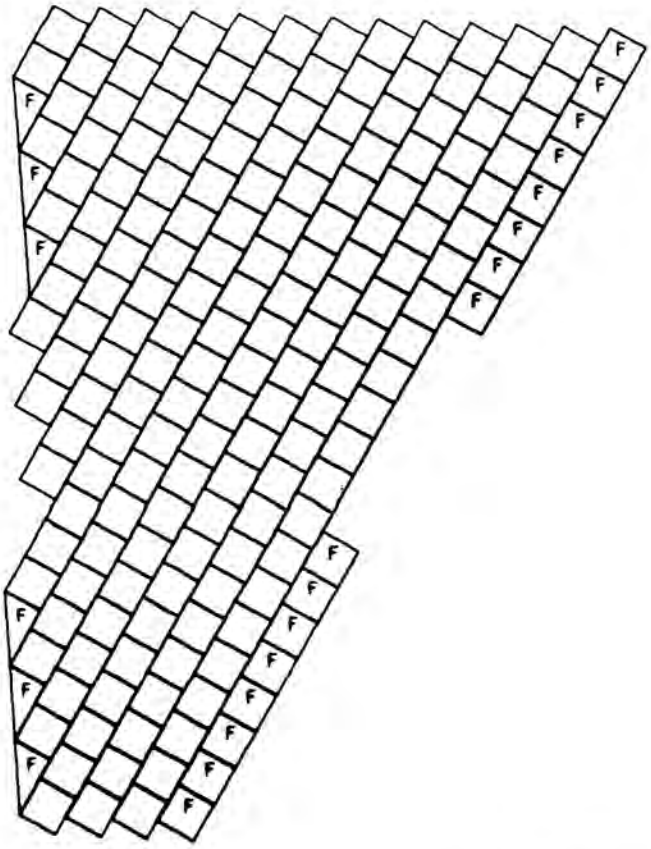


Figure 6.40: Model V - Pv/Ph = 6.5.

STATIC RELAXATION RUN FOR MODEL EXPERIMENT NUMBER 5 - INITIAL LOADING
BLOCK PLOT NUMBER OF PROBLEM UNITS PER INCH = 1.56
ITERATION NUMBER = 400 SCALE . 1 INCH = ____



STATIC RELAXATION RUN FOR MODEL EXPERIMENT NUMBER 5 - INITIAL LOADING
CORNER FORCE PLOT NUMBER OF PROBLEM UNITS PER INCH = 660.812219119
ITERATION NUMBER = 400 SCALE . 1 INCH = ____

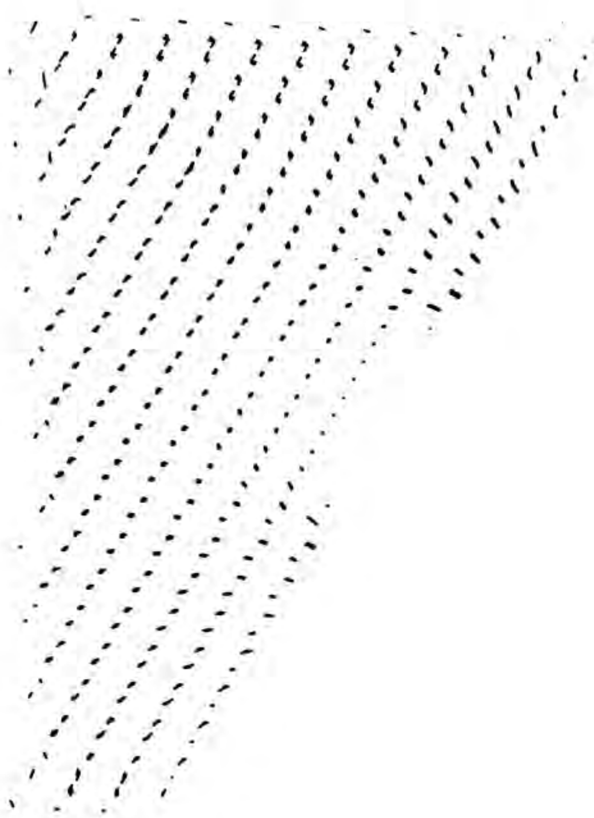
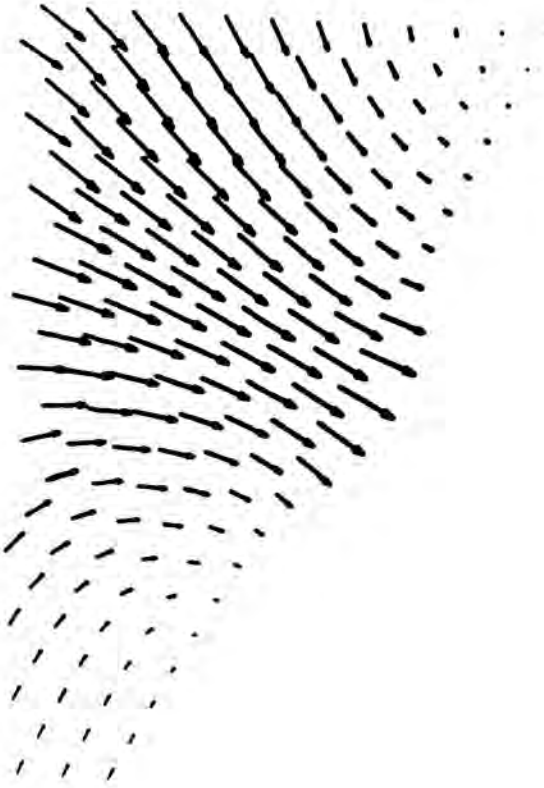


Figure 6.41

STATIC RELAXATION RUN FOR MODEL EXPERIMENT NUMBER 5 - INITIAL LOADING
INCREM.DISPL PLOT NUMBER OF PROBLEM UNITS PER INCH = 0.000000000
ITERATION NUMBER = 400 SCALE . 1 INCH = ____



STATIC RELAXATION RUN FOR MODEL EXPERIMENT NUMBER 5 - INITIAL LOADING
TOTAL DISPL PLOT NUMBER OF PROBLEM UNITS PER INCH = 0.000000577
ITERATION NUMBER = 400 SCALE . 1 INCH = ____

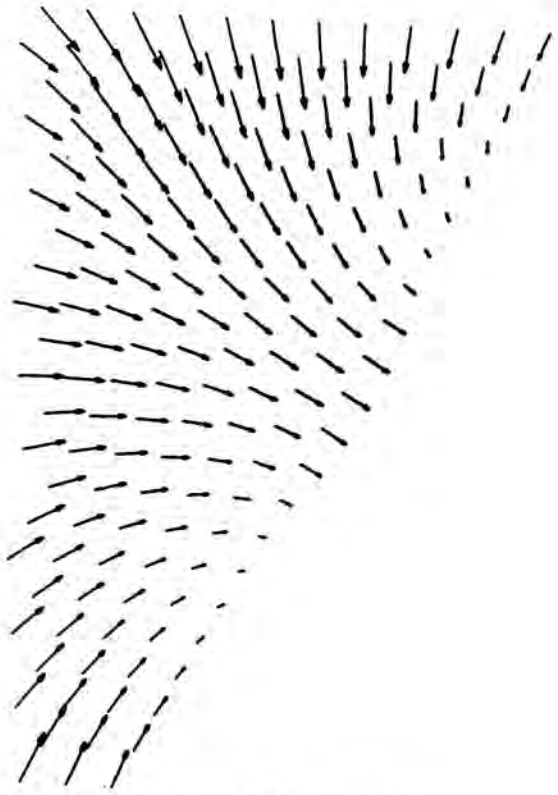


Figure 6.41 contd.

opposing the applied loading, but free to displace in other directions. Unfortunately, such a facility was not available in the numerical model.

It was considered unnecessary to incorporate the specially shaped load distributing units used in the physical model so all square blocks whose edges comprised part of an external boundary, or were in contact with the fixed triangular blocks, were designated as externally loaded blocks. The joint properties (stiffnesses and friction coefficient) were assigned the same values as used in previous experiments, both normal and shear stiffnesses representing the mass deformability.

The initial loading phase consisted of applying forces along relevant external block edges equivalent to the experimental pressures of Pv = .156 MPa and Ph = .112 MPa. The model was subjected to this loading for 400 iterations, which was considered sufficient in view of the satisfactory load distribution achieved in Models III and IV for a similar duration of loading. The results after initial loading are shown in Figure 6.41. At this stage, maximum incremental block displacements were to within 2.5% of initial values while the maximum out-of-balance force sum was less than 2% of typical applied loads.

The force distribution (Figure 6.41) indicates arching of the load has commenced with the first two rows spanning the opening being shielded from the boundary loading. This is confirmed by the interblock contact force printout which reveals separation along the continuous and discontinuous joints for the immediate hanging-wall row together with full mobilisation of frictional resistance along the joints intersecting the opening extremities.

Upon restarting, the model was subjected to a further 400 iterations of increased vertical loading, the

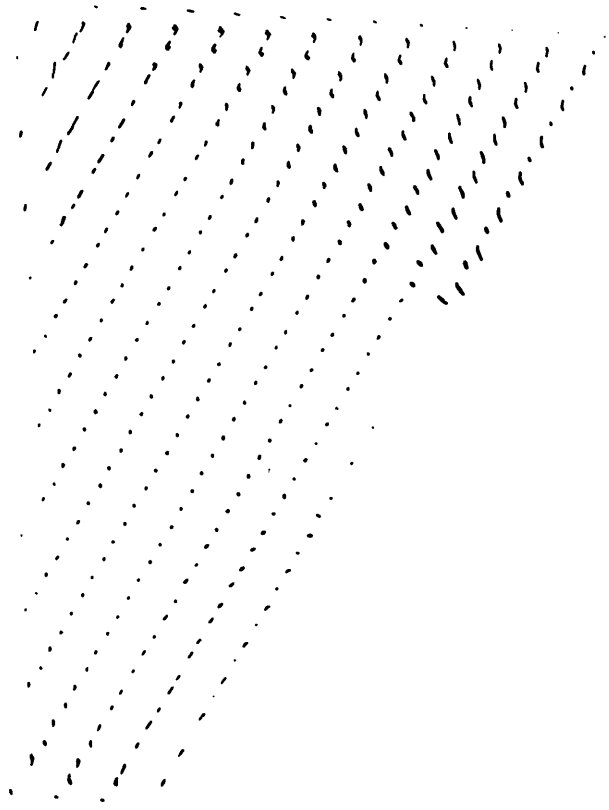
applied corner forces being calculated as those equivalent to the experimental pressure at which the model displacements were measured photogrammetrically (i.e. .577 MPa). Again, the increased loading was incrementally applied with corresponding stiffness values. The results obtained at the end of this process are shown in Figure 6.42. The force distribution shows a marked contrast to that of earlier examples with virtually all the overlying rows between the opening and the loaded boundaries displaying similar load distributions.

The complete load arch is not observable in the force plot of Figure 6.42 although the large abutment forces, especially surrounding the up-dip end, indicate that significant load transfer has taken place. The ratio of the maximum up-dip abutment forces to those down-dip is approximately 2.8 while there has been an approximate threefold increase in the up-dip abutment forces due to an increase in the Pv/Ph ratio from 1.4 to 5.2.

The normal contact forces for blocks within and adjacent to the unstable zone spanning the opening are quantitatively presented in Figure 6.43 where the model geometry has once again been magnified to illustrate the location and nature of resulting joint separations. The locations of upper and lower hinge zones coincide with those observed in the physical model (Figure 6.38) but differ in extent with separations along joints being confined to the first two rows for the numerical model computations. The force distribution for overlying rows suggests that block movements necessary for the continuation of upper and lower hinge zone formation are occurring. An encouraging aspect of the numerical results is the lack of any mid-span joint separation, except the sole hinge formed up-dip in the immediate row.

The ratio of shear to normal loads existing along

INCREASED VERTICAL LOADING FOR EXPERIMENT 5. 400-800 CYCLES RESTART
CORNER FORCE PLOT NUMBER OF PROBLEM UNITS PER INCH = 2650.533023453
ITERATION NUMBER = 800 SCALE . 1 INCH = _____



INCREASED VERTICAL LOADING FOR EXPERIMENT 5. 400-800 CYCLES RESTART
TOTAL DISPL PLOT NUMBER OF PROBLEM UNITS PER INCH = 0.000001977
ITERATION NUMBER = 800 SCALE . 1 INCH = _____

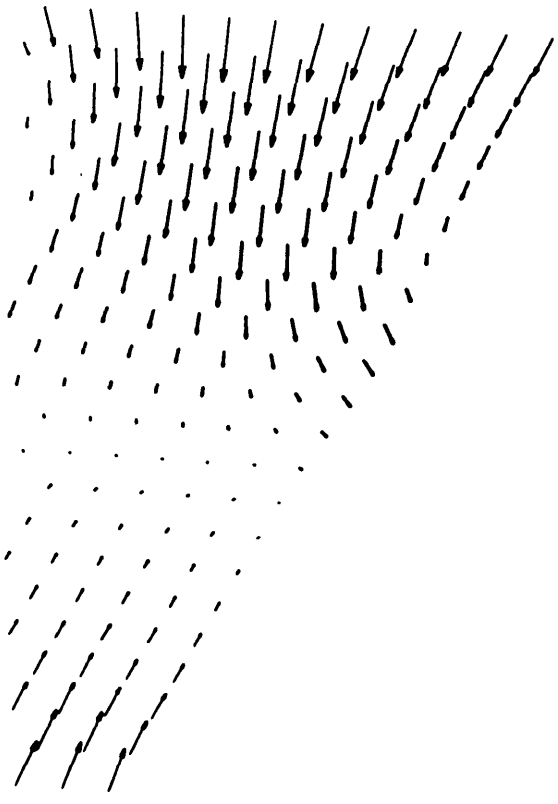


Figure 6.42.

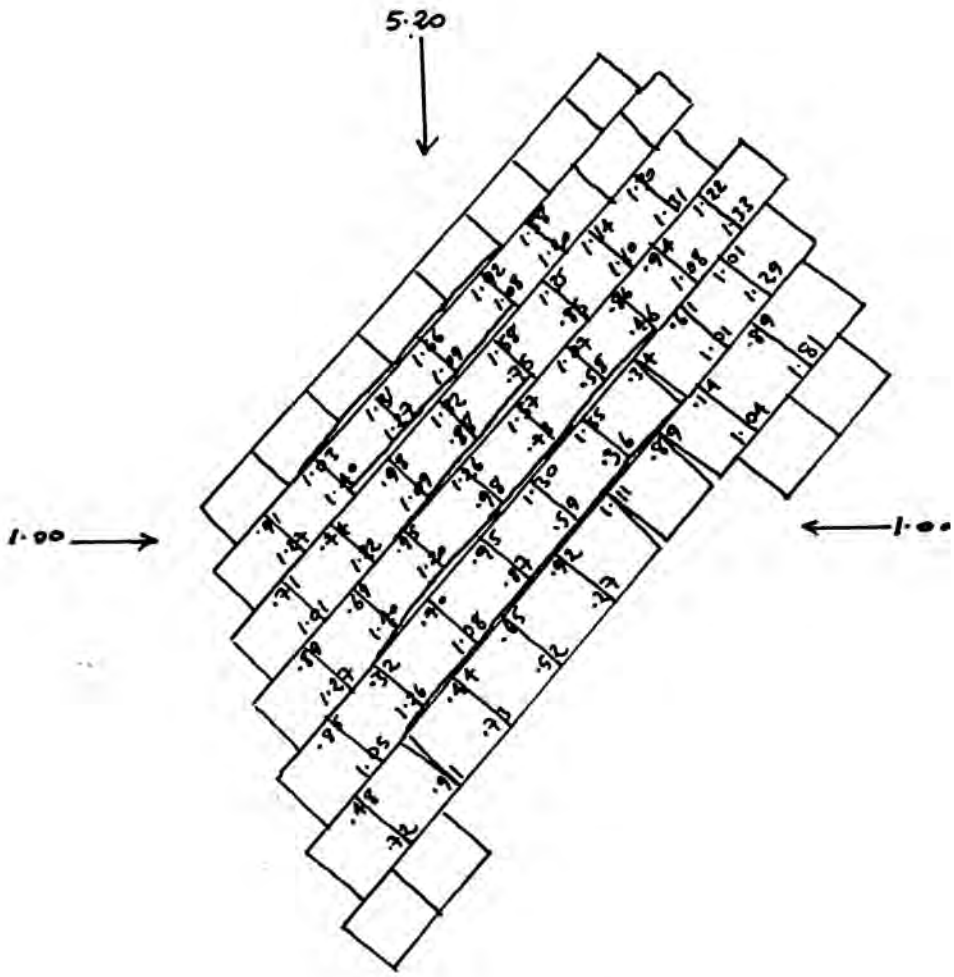



Figure 6.43: Model V - $P_V/P_H$ = 5.20 showing normal force magnitudes.

the discontinuous joints indicated that the joint shear strength was not exceeded in any of the overlying rows. Separations between blocks must therefore be largely due to block rotations and fracturing. The increase in rotation magnitude for Model V can be judged by comparing Figure 6.39 with Figures 6.28 and 6.34. Separation between the continuous joints prevails for all overlying rows within the potentially unstable zone. This separation extends along the entire five block span for the first two rows while for upward rows separation between only down-dip blocks occurs and propagates to the loaded edges.

Thus, as with the physical model, the situation after increased loading is one in which each hangingwall row is displaying behaviour independent of neighbouring rows, with load transmittal from overlying rows being minimal or non-existant.

The trends of the displacement fields illustrated in Figure 6.42 show a strong resemblance to the photogrammetric vectors of Figure 6.39. Again, the correspondence is best in areas removed from the influence of the fixed barrier. The incremental translational and rotational displacements after final loading were some 4% of initial values even though full frictional resistance had not been mobilised along any of the joints throughout the medium.

A comparison between numerical and physical model resultant displacement magnitudes is presented in Table 6.7 and it is noted that the difference between both sets of displacements is of the same order as that determined for Model III (Table 6.5). It is interesting to note that the degree of slabbing observable along hinge zones for both Models III and V is of a similar degree, which again suggests that this fracturing phenomenon is largely responsible for the displacement discrepancy, rather than

the fact that execution was terminated prematurely.

| Block Number | Numerical Displ.Dn(mm) | Photogrammetric Displ. Dp(mm) | Ratio Dp/Dn |
|---|---|---|---|
| 30 | .128 | 1.90 | 14.9 |
| 52 | .131 | 1.58 | 12.1 |
| 74 | .132 | 1.27 | 9.6 |
| 76 | .188 | 2.06 | 11.0 |
| 78 | .197 | 2.38 | 12.1 |
| 114 | .129 | 1.58 | 12.2 |
| 116 | .223 | 1.90 | 8.5 |
| 118 | .254 | 2.53 | 10.0 |
| 120 | .282 | 2.69 | 9.5 |
| 146 | .176 | 2.22 | 12.6 |
| 148 | .276 | 2.69 | 9.7 |
| 150 | .321 | 3.17 | 9.9 |
| 168 | .189 | 3.49 | 18.5 |
| 171 | .335 | 3.96 | 11.8 |

Table 6.7: Numerical and Photogrammetric Displacements for Model V.

6.3.6. Model VI: Continuous Jointing 30 Degrees to Horizontal; Discontinuous Orthogonal Joints. Opening 150 mm by 25 mm Parallel to Continuous Jointing (Pv > Ph).

Physical Model Study:

Model VI was constructed with the continuous jointing orientated at an angle of 30 degrees clockwise from the horizontal and an orthogonal staggered joint system. The complete model geometry is illustrated in Figure 6.44 and was equivalent to that of Model V rotated clockwise through 90 degrees. Similar edge pieces to those used in Model V were manufactured to ensure satisfactory load transfer to the blocky model. The opening, created prior to load application, was located in the centre of the model which resulted in both footwall and hangingwall being anti-symmetric about the major

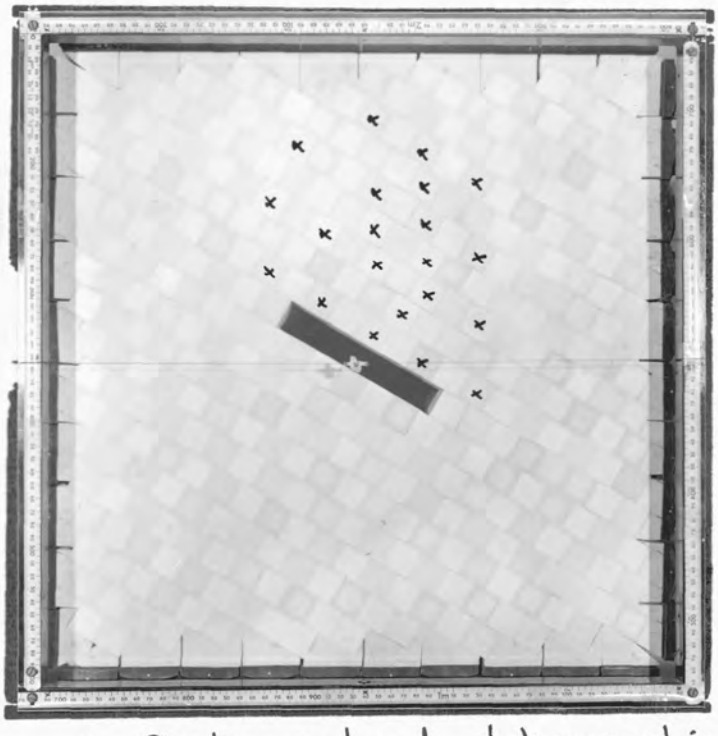



Figure 6.44: Model VI under initial loading.

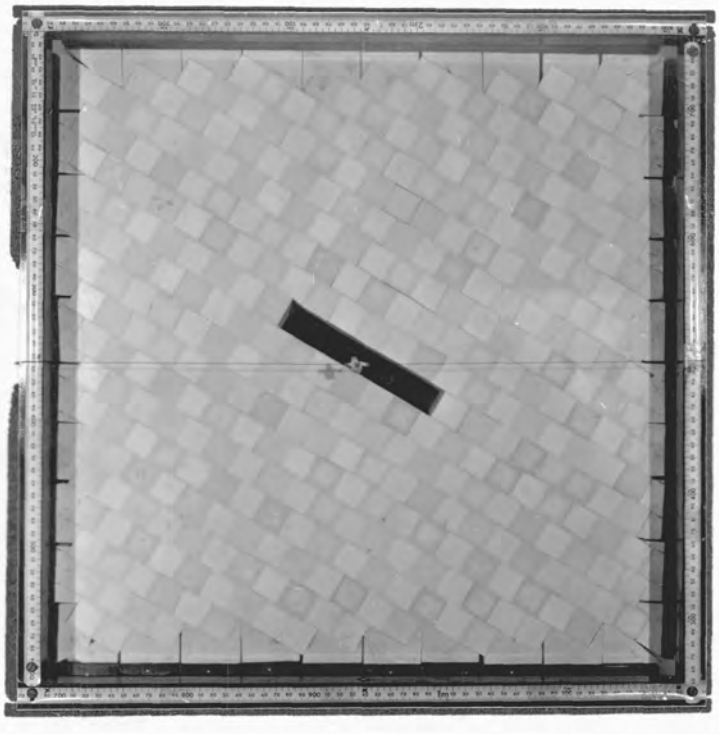


Figure 6.45: Model VI - Pv/Ph = 6.2.

opening axis. Six discontinuous joints intersected the major opening faces.

Other things being equal, it was thought that the reduced inclination of the continuous jointing would, under an increasing vertical load, induce greater shear forces along the discontinuous joint set with a consequent greater mobilisation of the slip mechanism. The purpose of this model study was to establish the exact nature and extent of such movement by examining the results from both physical and numerical experimentation.

After relevant blocks had been removed to create the opening, the initial boundary pressures were applied (Pv = .190 MPa, Ph = .155 MPa) and the housing frame rotated so that all testing was conducted in the sub-vertical plane. The experimental procedure for Model VI involved incrementing the vertical pressure gradually while maintaining the horizontal pressure constant at the initial value of .155 MPa. Block displacements were analyzed photogrammetrically when the vertical pressure had attained .965 MPa i.e. for a vertical to horizontal load ratio of 6.2.

After the large discrepancies encountered between measured and predicted displacement magnitudes for the previous three experiments, a Pv/Ph ratio was sought in which the extent of block fracturing was kept to an absolute minimum. The geometry shown in Figure 6.45 (Pv/Ph = 6.2) was chosen on this basis. The failure mode surrounding the opening for Model VI displayed similar characteristics to failure modes of previous models. A lower stepped hinge zone was evident in the hangingwall about which differential rotation of blocks into the opening occurred. This resulted in separation along the upward ends of the discontinuous joints, visible for the first four rows. The lower boundary initiated from the lower-most joint intersecting the opening and

extended along a sub-vertical path towards the vertically loaded model edge.

Failure in the region of the up-dip opening extremity consisted of two distinct zones of joint separation with associated hinge formation. The beginning of a complementary upper hinge zone, parallel to the lower but separated from it by a span of six blocks, was evident for the two immediate rows. This upper boundary originated from the joint bisecting the crown block edge and involved separations identical to those in the down-dip hinge zone. The second up-dip hinge zone represents the 'bending' action necessary for stability. This results in compressive hinge formation along the backs of hangingwall rows and is the most pronounced of the three hinging zones present.

Unfortunately, the hinge zones are not readily identified in Figure 6.45 but become apparent with increased magnification. Separation between hangingwall rows was also prominent especially in the vicinity of the down-dip hinge zone.

The photogrammetric displacement vectors determined for the twenty-one hangingwall blocks identified in Figure 6.44 are presented in Figure 6.46. The value of the maximum resultant translational displacement of approximately 1 mm is indicative of much reduced block movements compared to those of previous model experiments with inclined joints. The influence of the opening is seen to affect all overlying rows with sub-vertical block movements towards the opening at the up-dip end. The vertical component of movement away from the opening at the down-dip end (reverse sliding due to block rotation) indicates that slabbing along the lower boundary is not influencing behaviour.

Considerable movement of hangingwall rows into the

RESULTS FOR EXPERIMENTAL MODEL STUDY NUMBER 6

CONTINUOUS JOINTS AT 30 DEGS.TO HORIZ. OPENING 150MM=25MM. PV.GT.PH.

PLOT OF TRANSLATIONAL AND ROTATIONAL BLOCK DISPLACEMENTS-ROT.PRINTED IN RADIANS

NUMBER OF PROBLEM UNITS PER INCH = 0.00109 METRES. SCALE IS 1 INCH = _____

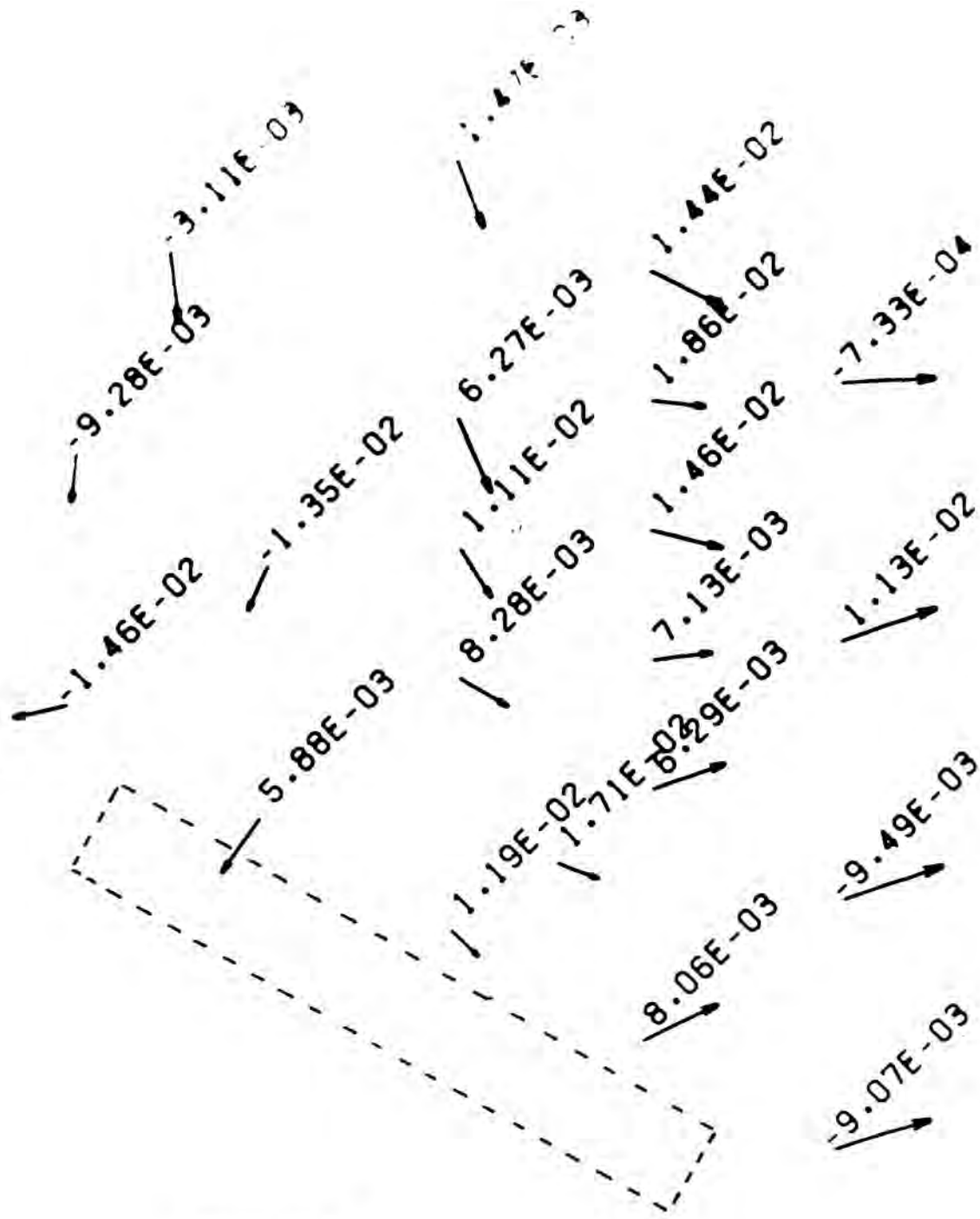



Figure 6.46

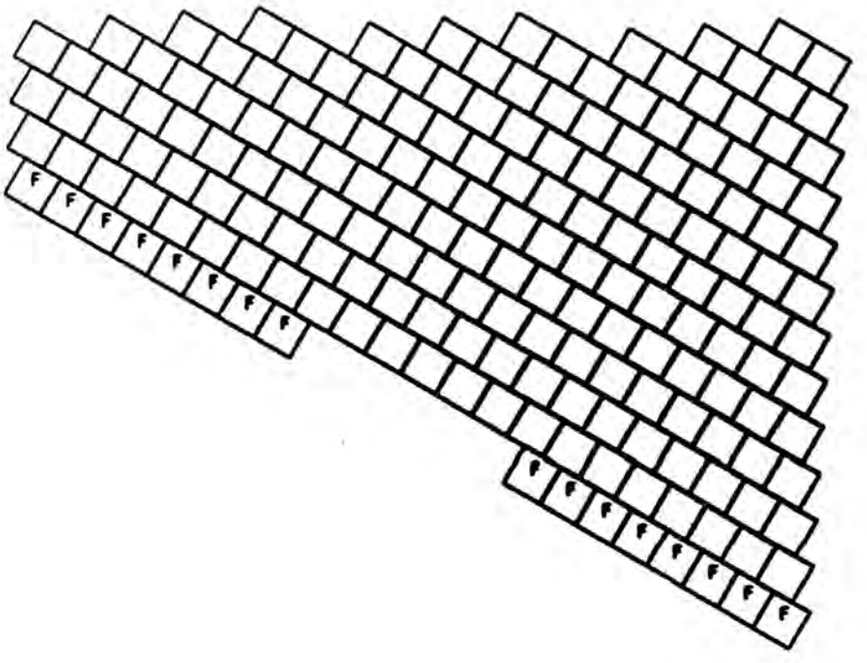
opening along the lower hinge zone occurred when the Pv/Ph ratio reached 7.2. This movement was accompanied by extensive slabbing of block edges which formed the stable sides of the opening.

Numerical Analysis of Model VI:

The local co-ordinates of square blocks used for the numerical simulations of Model VI were identical to those of Model V, the global geometry being obtained by a co-ordinate transformation through an angle of 330 degrees compared with 60 degrees used to generate the global geometry of Model V. The hangingwall of Model VI was represented by 181 square blocks as shown in Figure 6.47, the triangular fixed blocks used in the previous experiment not being required due to the reduced angle of inclination of the continuous jointing. The same external blocks as Model V were used for transmitting boundary loads while joint stiffness and friction parameters were also identical.

Initial loading was conducted for 400 iterations and consisted of applying corner forces to appropriate block edges, these being equivalent to the uniformly distributed experimental pressures of Pv = .190 MPa, Ph = .155 MPa. Figure 6.47 illustrates both the force distribution and displacement fields generated during this preliminary stage. At the end of initial loading, incremental translational and rotational rigid body displacements had been reduced to 1% and .5% respectively of their maximum initial values. Also, the largest out-of-balance force-sum on any block was within 2% of the maximum applied boundary load which indicated that sufficient calculation cycles had been allowed for convergence to equilibrium. The force distribution (Figure 6.47) shows that considerable load transfer has occurred between the material overlying and surrounding the first two rows. This is confirmed by the contact

INITIAL LOADING FOR MODEL EXPERIMENT 6 . 0-400 CYCLES
BLOCK PLOT NUMBER OF PROBLEM UNITS PER INCH = 1.50
ITERATION NUMBER = 400 SCALE . 1 INCH = _____

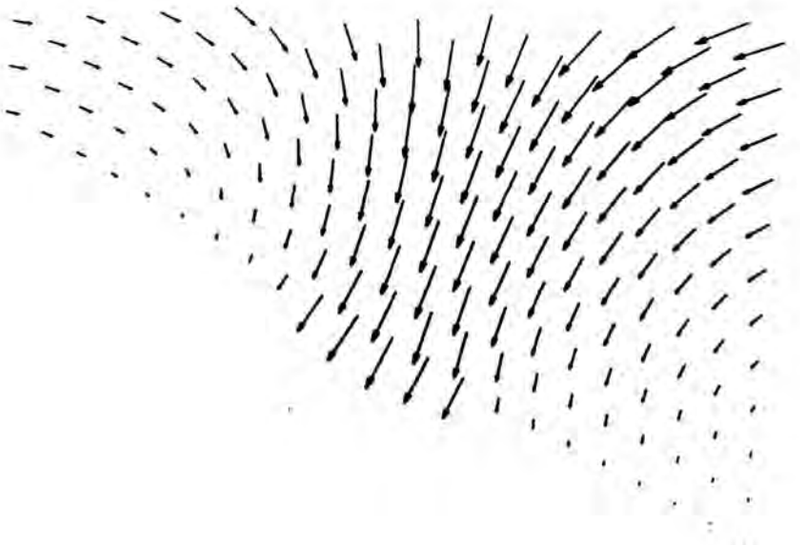


INITIAL LOADING FOR MODEL EXPERIMENT 6 . 0-400 CYCLES
CORNER FORCE PLOT NUMBER OF PROBLEM UNITS PER INCH = 923.831292236
ITERATION NUMBER = 400 SCALE . 1 INCH = _____



Figure 6.47

INITIAL LOADING FOR MODEL EXPERIMENT 6 . 0-400 CYCLES
INCREM.DISPL PLOT NUMBER OF PROBLEM UNITS PER INCH = 0.000000001
ITERATION NUMBER = 400 SCALE . 1 INCH = _____



INITIAL LOADING FOR MODEL EXPERIMENT 6. 0-400 CYCLES
TOTAL DISPL PLOT NUMBER OF PROBLEM UNITS PER INCH = 0.000000825
ITERATION NUMBER = 400 SCALE . 1 INCH = _____

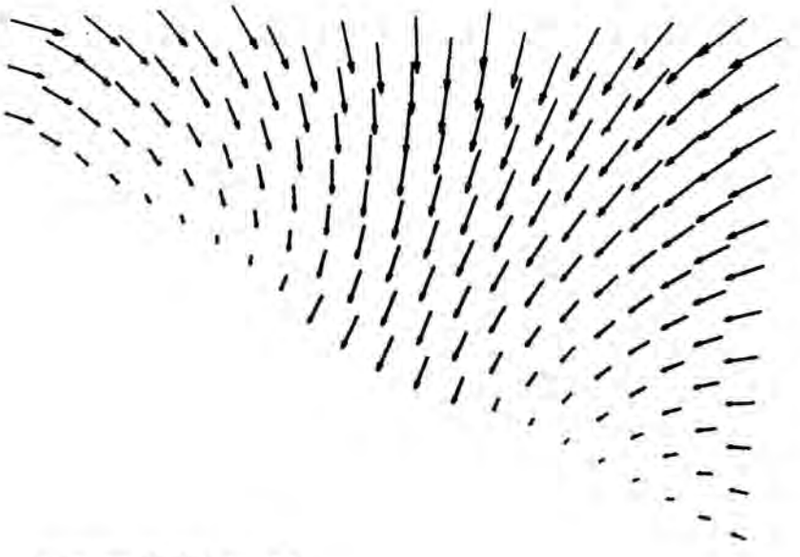


Figure 6.47 contd.

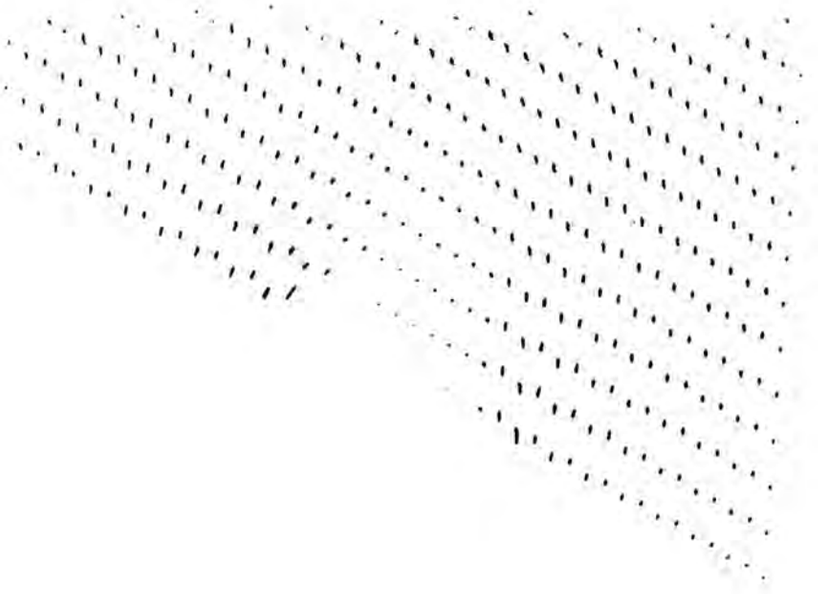
force printout which indicates slip along the upper and lower discontinuous joints for these two rows accompanied by initial separation along both joint sets.

The problem was restarted by increasing the corner forces acting in the vertical direction in order to represent the physical model test conditions at which photogrammetry was employed (i.e. Pv = .965 MPa). The results at the conclusion of 400 iterations of increased loading are presented in Figure 6.48. Adequate external force propagation is reflected by maximum out-of-balance forces less than 2.5% of applied vertical block loads after increased loading. Examination of the force distribution reveals that the major effect of an increase in vertical loading has been to extend the unstable zone of hangingwall material towards the loaded boundary. This has resulted from further load transfer to the surrounding material and the complete arching pattern illustrating the demarcation between stable and unstable zones is clearly evident from Figure 6.48. The independent behaviour of each overlying row is apparent, particularly at the down-dip end of the opening.

Large abutment compressive forces have subsequently developed, these attaining maximum values at the up-dip end of the opening. Figure 6.49 details the normal contact force magnitudes between contiguous blocks for the six hangingwall rows adjacent to the opening. The failure mechanism predicted numerically and depicted in Figure 6.49 bears a strong correlation to that achieved with the physical model. Hinge formation and associated joint separation have occurred in identical positions for both physical and numerical models but again the extent of movement is less for the numerical results.

The predicted displacement fields (Figure 6.48) show that the effect of the opening has propagated to the vertically loaded boundary forming a sink-like flow field

INCREASED VERTICAL LOADING FOR EXPERIMENT 6 .400-800 CYCLES RESTART
CORNER FORCE PLOT NUMBER OF PROBLEM UNITS PER INCH = 4298.980013163
ITERATION NUMBER = 800 SCALE . 1 INCH = _____



INCREASED VERTICAL LOADING FOR EXPERIMENT 6 .400-800 CYCLES RESTART
TOTAL DISPL PLOT NUMBER OF PROBLEM UNITS PER INCH = 0.000003462
ITERATION NUMBER = 800 SCALE . 1 INCH = _____

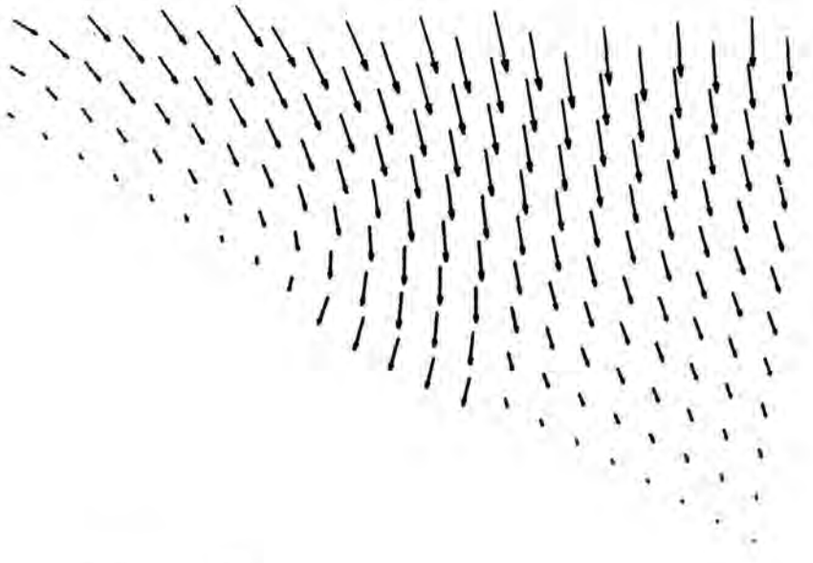


Figure 6.48

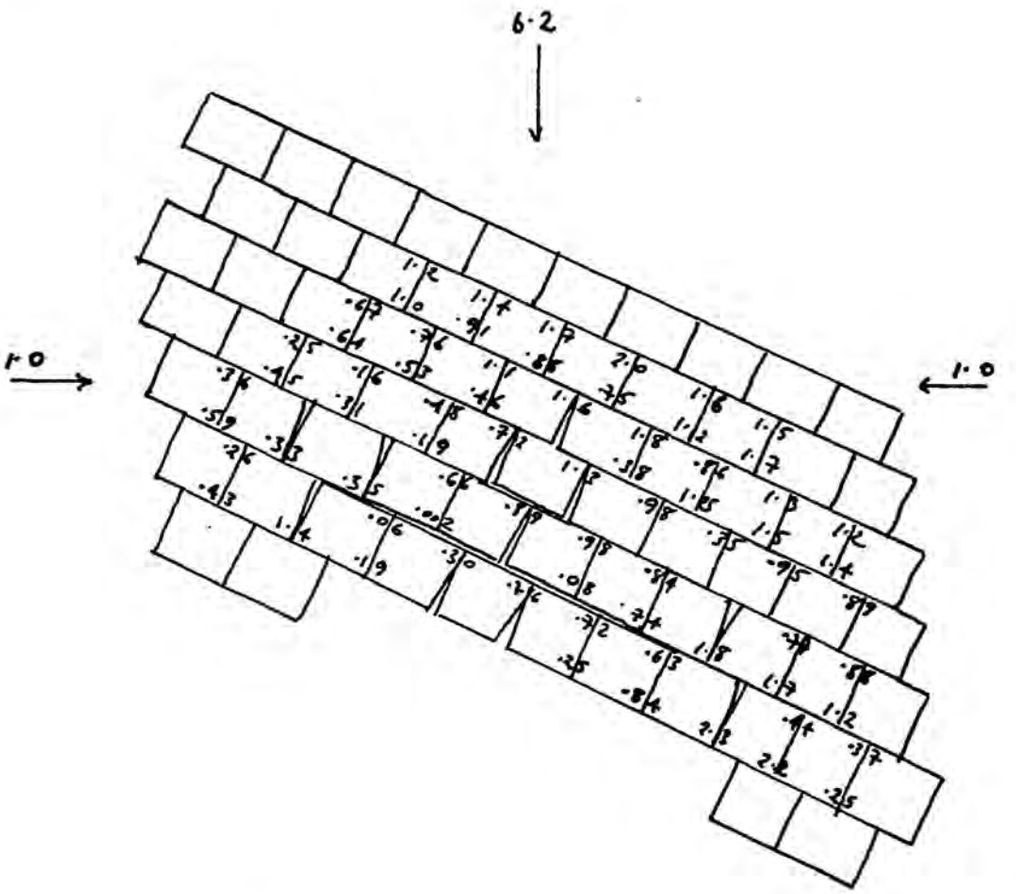



Figure 6.49: Model VI - $P_V/P_H$ = 6.2 showing normal force magnitudes.

towards the opening for overlying rows. A discrepancy in the direction between measured (Figure 6.46) and predicted (Figure 6.48) displacement vectors at the down-dip opening end is probably due to the influence of the free and fixed boundaries used in the respective models. However, remaining displacement vectors of both models show good agreement in both direction and relative magnitude.

The absolute displacement magnitudes obtained from both models are tabulated in Table 6.8 and the agreement between the two sets is considerably better than for Models III, IV and V. For the loading state of Figure 6.48,

| Block Number | Numerical Displ.Dn(mm) | Photogrammetric Displ. Dp(mm) | Ratio Dp/Dn |
|---|---|---|---|
| 26 | .184 | .70 | 3.8 |
| 28 | .215 | .39 | 1.8 |
| 51 | .223 | .44 | 2.0 |
| 68 | .158 | .52 | 3.3 |
| 70 | .194 | .52 | 2.7 |
| 72 | .247 | .59 | 2.4 |
| 92 | .263 | .61 | 2.3 |
| 107 | .254 | .76 | 3.0 |
| 110 | .284 | .87 | 3.1 |
| 112 | .281 | .78 | 2.8 |
| 128 | .306 | .57 | 1.9 |
| 139 | .343 | .78 | 2.3 |
| 141 | .332 | .85 | 2.6 |
| 143 | .298 | 1.00 | 3.4 |

Table 6.8: Numerical and Photogrammetric Displacements for Model VI.

slip is still occurring towards the opening for the first four rows within the unstable hangingwall zone. This means that additional iterations would be necessary to determine if an equilibrium state develops or collapse ensues. Economic computing considerations, however, prevented further execution. Execution time for Model VI

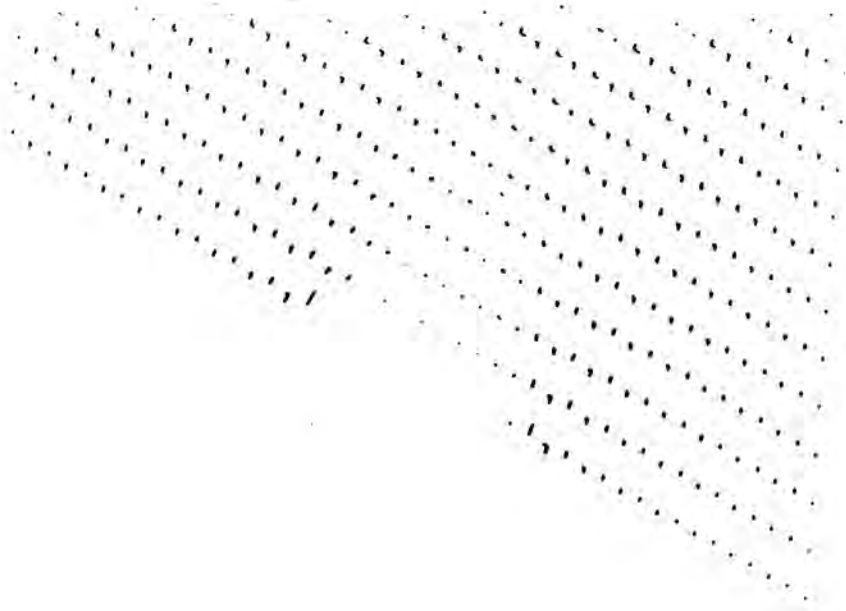
was approximately 370 CP secs. (6600) for 400 iterations.

A study of the influence of joint stiffness and friction parameters was performed numerically with Model VI. The results for a ratio of normal to shear stiffness (Kn/Ks) of ten obtained using the same magnitude and duration of increased vertical loading as above are shown in Figure 6.50. The normal stiffness remained unaltered during these parametric studies, the value of the shear stiffness being reduced to obtain the desired Kn/Ks ratio.

As seen in Figure 6.50, the total block displacements are dramatically affected by a change in stiffness ratio; in this particular case there has been an increase in displacement magnitudes of approximately 100%. Also, the increased block movements have created a modified force distribution with contact forces within the unstable zone deviating markedly, but typically at least double those shown in Figure 6.48. The mode of failure has also been altered by the variation of Kn/Ks. For the Kn/Ks value of ten, the beaming action of overlying rows was more pronounced, extending to the fifth row and propagating nearer to the lower hinge zone. This in turn tended to displace the lower hinge zone further downdip thus increasing the span of the unstable zone. A direct result of these increased block movements was an extension of separation along the continuous jointing for the first four rows.

The consequence of a further increase in the Kn/Ks ratio to 100 was investigated. This resulted in a mechanism of failure bearing little resemblance to that of the physical model. Separation was present along most of the discontinuous joints overlying the opening for the first three rows and resulted in hinge locations completely different to those shown in Figure 6.48.

INCREASED VERTICAL LOADING FOR EXPERIMENT 6 .400-800 CYCLES RESTART
CORNER FORCE PLOT NUMBER OF PROBLEM UNITS PER INCH = 5775.582496995
ITERATION NUMBER = 800 SCALE . 1 INCH = _____



INCREASED VERTICAL LOADING FOR EXPERIMENT 6 .400-800 CYCLES RESTART
TOTAL DISPL PLOT NUMBER OF PROBLEM UNITS PER INCH = 0.000009459
ITERATION NUMBER = 800 SCALE . 1 INCH = _____

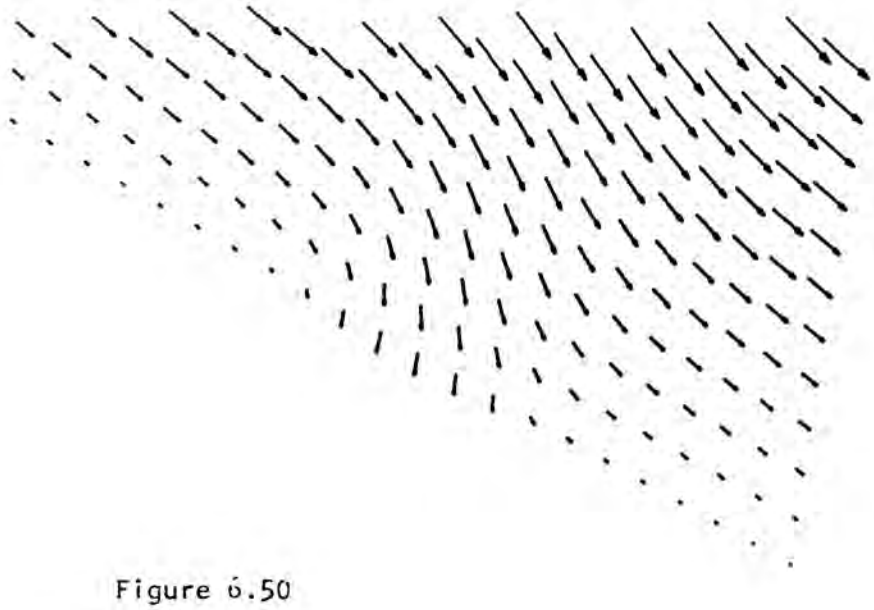
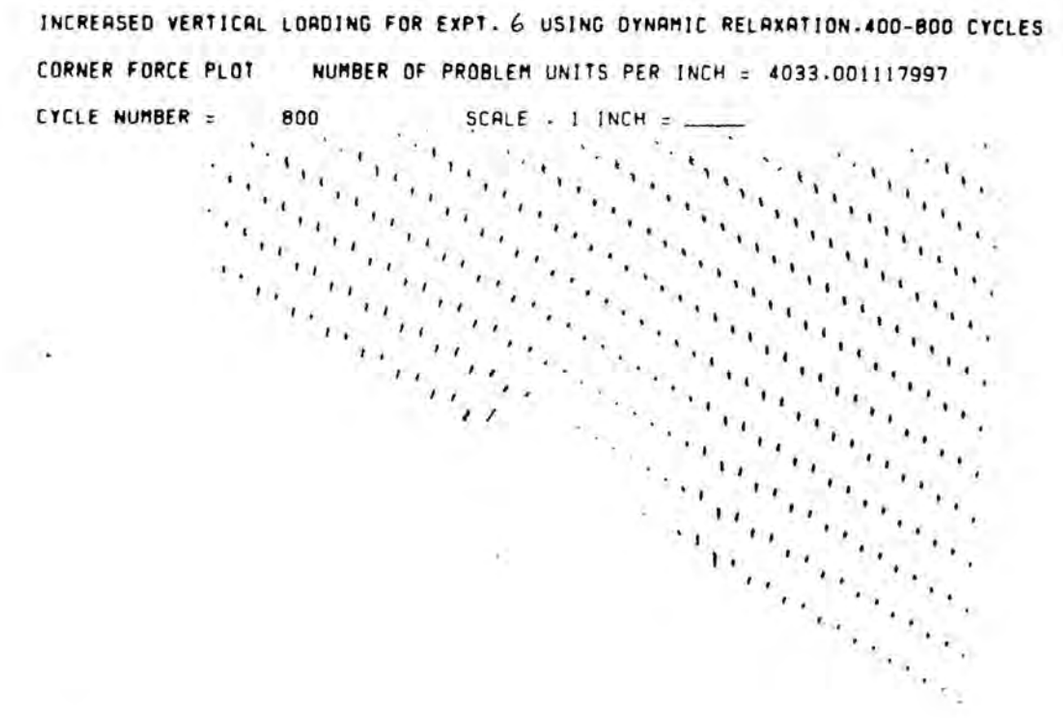


Figure 6.50

Thus, it is seen that the ratio of Kn/Ks has a major influence on the resulting model behaviour. The dependence of failure mechanisms upon the Kn/Ks ratio indicates that the normal and shear stiffness magnitudes determined experimentally and used in the numerical simulations are an adequate representation of the deformability properties in the model studies. A more refined study using Kn/Ks ratios in the range of 1.25 to 1.50, say, may account for some of the earlier discrepancies encountered between physical and numerical results. Unfortunately, the limitation of time prevented this from being carried out. However, the importance of modelling accurate normal and shear stiffnesses in situations where the mode of failure and associated displacements are of concern has been highlighted.

A study of the influence of the friction coefficient was performed by reducing its value from .75 to .70, while maintaining the stiffness values at their original level. Such a change in the friction coefficient had no effect on the mechanism of failure and resulted in only slight variations (1% to 2%) in the resultant displacements. There was however, an occasional significant deviation between corresponding normal forces with those in the reduced friction model being up to 20% smaller.

Cundall and Strack (1979) have also examined the effects of significant changes in the friction angle and stiffness ratio on the force distribution throughout an assembly of discs. They showed that where the friction coefficient was of sufficient magnitude, the resulting behaviour was very much dependent on the shear stiffness since slip commences at a far later stage. The same conclusion can be extrapolated to the present study where the high friction coefficient of the plaster-plaster interfaces infers that slip cannot initiate early in the numerical tests and that the shear force is therefore determined for a considerable period as a function of the shear stiffness and not of


INCREASED VERTICAL LOADING FOR EXPT. 6 USING DYNAMIC RELAXATION.400-800 CYCLES
CORNER FORCE PLOT NUMBER OF PROBLEM UNITS PER INCH = 4033.001117997
CYCLE NUMBER = 800 SCALE . 1 INCH = _____

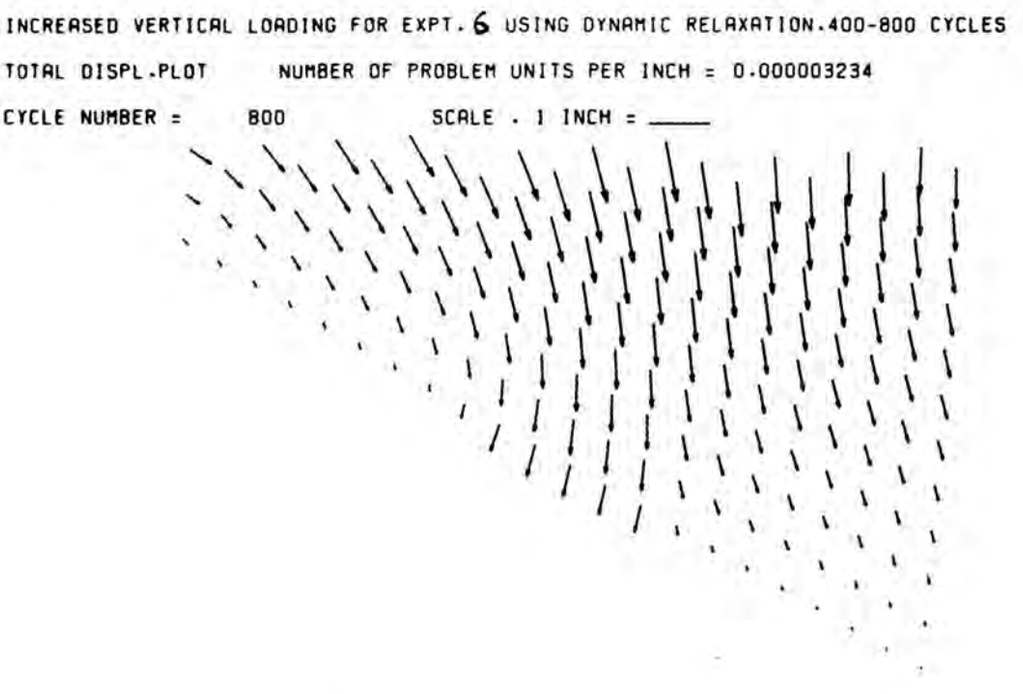

INCREASED VERTICAL LOADING FOR EXPT. 6 USING DYNAMIC RELAXATION.400-800 CYCLES
TOTAL DISPL.PLOT NUMBER OF PROBLEM UNITS PER INCH = 0.000003234
CYCLE NUMBER = 800 SCALE . 1 INCH = _____

Figure 6.51.

the normal force, as is the case when slip is occurring.

An interesting comparison was achieved by analysing the identical model geometry and input parameters of Model VI using dynamic relaxation. The results after an equivalent period of increased vertical loading are presented in Figure 6.51 and the similarity with those of Figure 6.48 is striking. The force distributions obtained from both relaxation techniques are in excellent agreement with corresponding forces from dynamic relaxation in general 6% to 7% less, this being a reflection on the reduced block movements (approximately 6.5%) achieved from the dynamic relaxation algorithm after the same number of iterations. Some other interesting facts to emerge from the comparison of the two relaxation techniques were that, for dynamic relaxation, incremental displacements had reduced to 5.5% of initial displacements (c.f. 1.5%) while the maximum out-of-balance force sum for dynamic relaxation was 2.75% of typical boundary loads (c.f. 2.5%). However, despite the minor discrepancies in force and displacement magnitudes an identical failure mechanism was predicted by each relaxation technique indicating that both numerical models are capable of generating realistic results.

6.3.7. Model VII: Continuous Joints at 60 Degrees to Horizontal; Discontinuous Orthogonal Joints. Two Openings 150 mm by 25 mm and 75 mm Apart, Parallel to Continuous Jointing (Pv > Ph).

Physical Model Study:

Tests on jointed models containing multiple openings were performed using the same model and opening sizes as for the previous single opening studies. The sequence of model construction, opening creation and subsequent loading followed the same procedure as before, and photogrammetry was employed to determine the plaster block locations at the completion of both initial and final loading stages.

The objective of the tests was to examine both qualitatively and quantitatively the influence of multiple openings on the jointed system with particular emphasis on the behaviour of the contained pillar material.

Model VII was constructed similar to Model V with the continuous jointing orientated at 60 degrees counter-clockwise from the horizontal and with an orthogonal discontinuous joint set. The same arrangement of specially manufactured edge pieces was used to ensure uniformity in the transmitted loads along each of the four loaded boundaries. For Model VII, the two openings were located on either side of the model centre leaving a rib pillar 75 mm wide between both openings. The long axes of the openings were parallel to the continuous jointing with six joints of the staggered system intersecting both the footwall and hangingwall faces of each excavation.

A photograph of the model geometry in the test position after initial loading has been applied is shown in Figure 6.52. The initial loading yielded a Fv/Fh ratio of 1.3, the vertical and horizontal pressures having magnitudes of .147 MPa and .112 MPa respectively. The transition from the initial stage to the stage at which photogrammetry was applied was achieved by increasing the vertical pressure by 335% (i.e. to Pv = .491 MPa) while the horizontal pressure was held constant. This produced a ratio Fv/Fh of 4.4 for the photogrammetric determinations. As in previous studies, the pressure was incrementally increased until some indication of movement in the vicinity of the opening was detected. The block locations for the load ratio Fv/Fh of 4.4 are shown in Figure 6.53.

The mode of failure seen in both the hangingwall and footwall of Figure 6.53 bears a strong resemblance to failure mechanisms examined previously for single openings constructed in similar jointing (Figure 6.38, Model V). For Model VII, separation is prominent along both joint

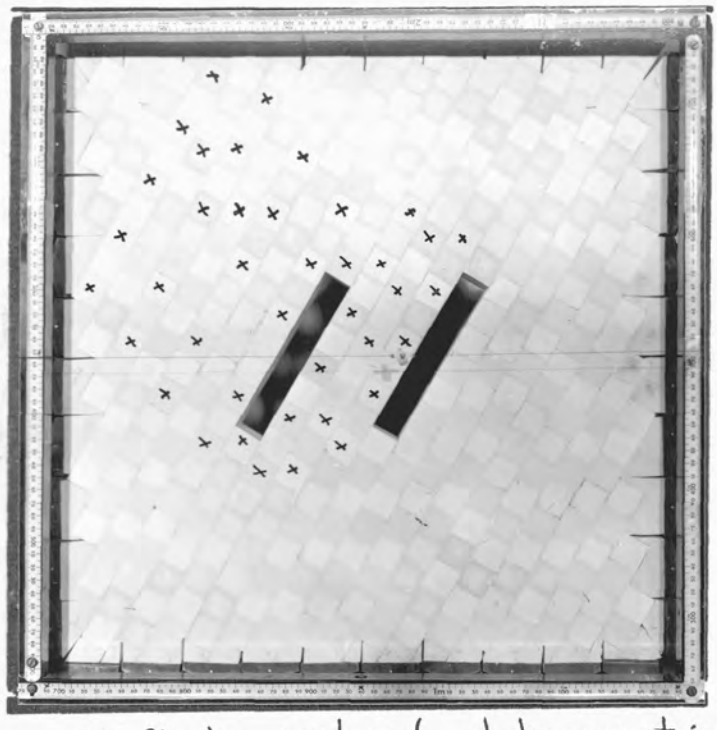



Figure 6.52: Model VII under initial loading.

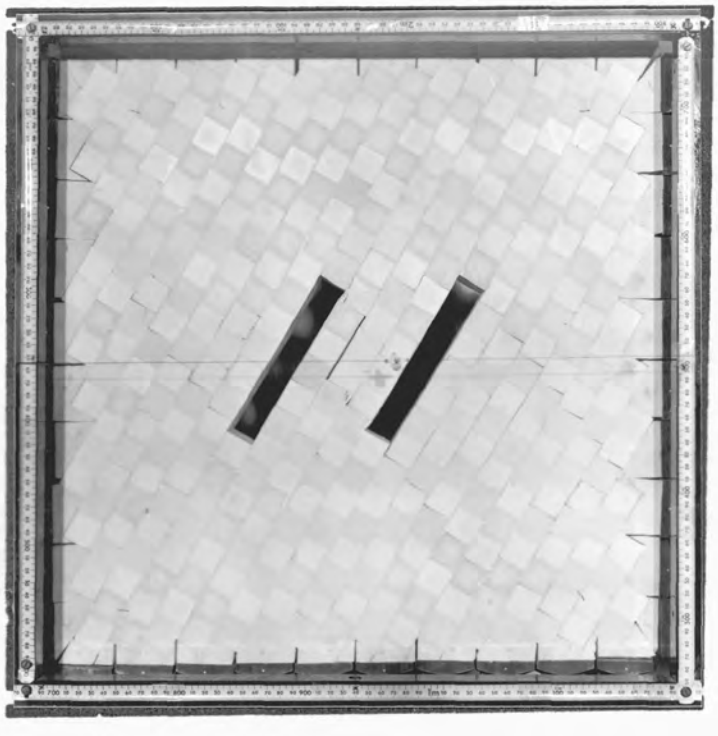


Figure 6.53: Model VII - Pv/Ph = 4.4.

sets indicating that slip and rotation mechanisms have been initiated. The unstable zone is defined by two stepped hinge zones which propagate from the opening extremities to the loaded boundaries. The reduction in transverse confinement along the continuous jointing due to block removal has also caused overlying rows to behave independently.

The behaviour of the pillar material is interesting to note. The load distribution throughout the pillar is non-uniform with a uniaxial condition in the central portion and biaxial states at either end due to incomplete release of lateral confining pressures. Therefore, it is anticipated that increases in the vertical loading will induce significant movements within the pillar. In Figure 6.53, substantial amounts of slip and rotation have occurred throughout the pillar associated with which is tensile failure along the joints intersecting the opening. Bending of the rows creating joint separations and compressive hinges has occurred at each pillar end adjacent to the opening face where the lateral confinement has been released. Separation along both joint sets is observed indicating strut-like action of the blocky rows forming the pillar.

The photogrammetric displacement vectors for the particular blocks indicated in Figure 6.52 are presented in Figure 6.54. It is seen that the displacements in the central pillar region are greatly reduced from those displacements occurring throughout the opening abutments. A similar zone of inflexion is also located in the central region of the hangingwall. The flow field of Figure 6.54 illustrates that opposing block movements at either end are subjecting the pillar to a couple stress effect which produces the large joint separations in the central pillar region.

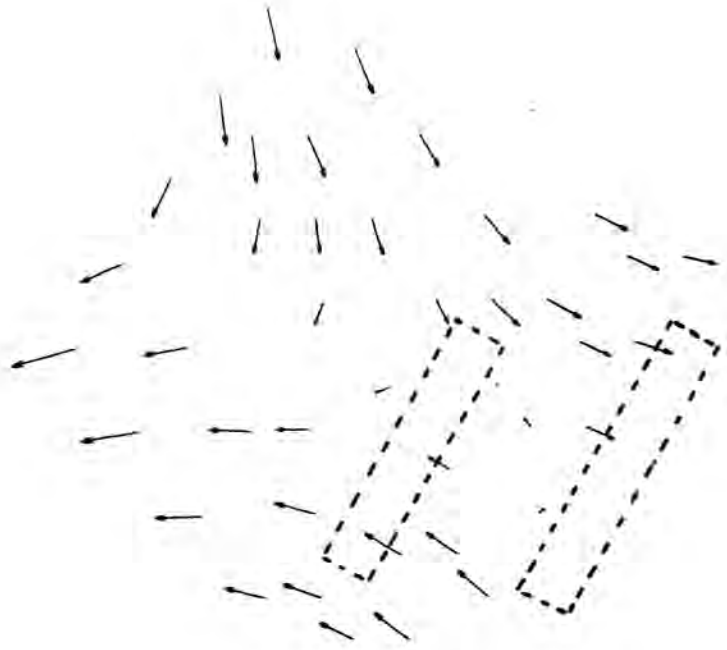
The results of the above physical model study have

RESULTS FOR EXPERIMENTAL MODEL STUDY NUMBER 7

CONT.JOINTS AT 60 DEGS.TO HORIZ. TWO OPENINGS WITH PILLAR 75MM WIDE. PV.GT.PH.

PLOT OF TRANSLATIONAL BLOCK DISPLACEMENTS

NUMBER OF PROBLEM UNITS PER INCH = 0.00338 METRES. SCALE IS 1 INCH = _____



RESULTS FOR EXPERIMENTAL MODEL STUDY NUMBER 7

CONT.JOINTS AT 60 DEGS.TO HORIZ. TWO OPENINGS WITH PILLAR 75MM WIDE. PV.GT.PH.

PLOT OF TRANSLATIONAL AND ROTATIONAL BLOCK DISPLACEMENTS-ROT.PRINTED IN RADIANS

NUMBER OF PROBLEM UNITS PER INCH = 0.00338 METRES. SCALE IS 1 INCH = _____

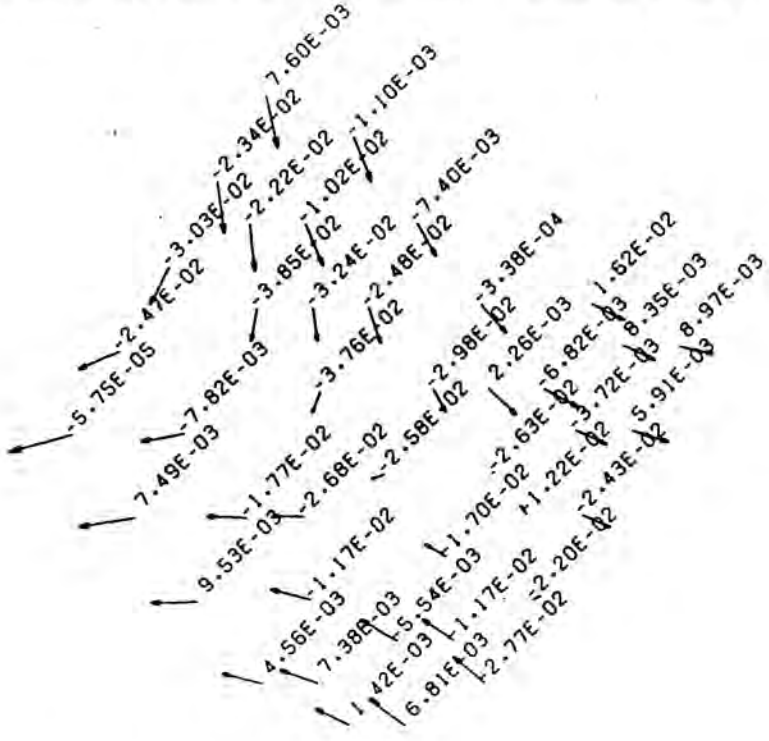



Figure 6.54.

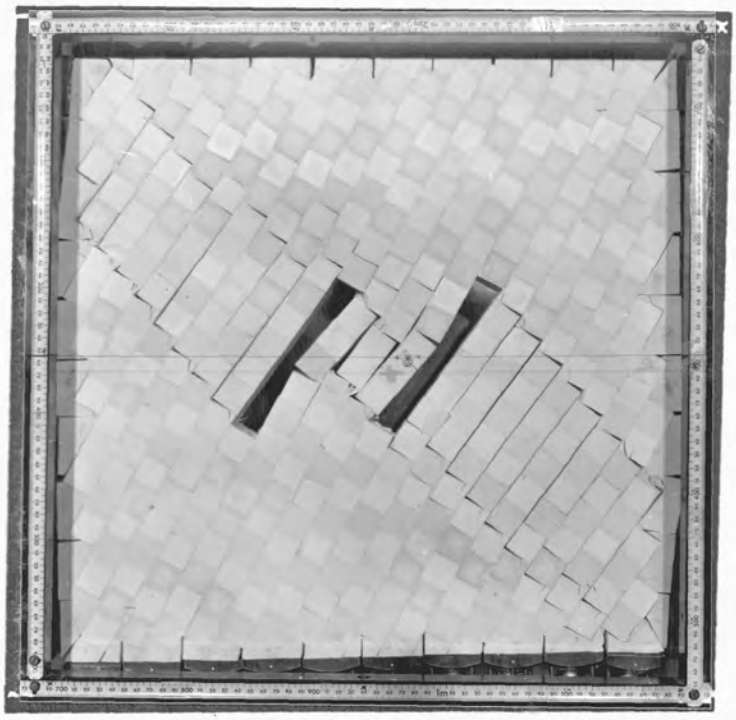


Figure 6.55: Model VII - Pv/Ph = 5.2.

highlighted several possibilities available for remedial action in the overall design, if necessary. If Model VII was a dynamically scaled representation of some prototype geometry in which pillar stability was a critical factor, then serious consideration could be given to either

a) a redesign involving the relative positions of the openings; or

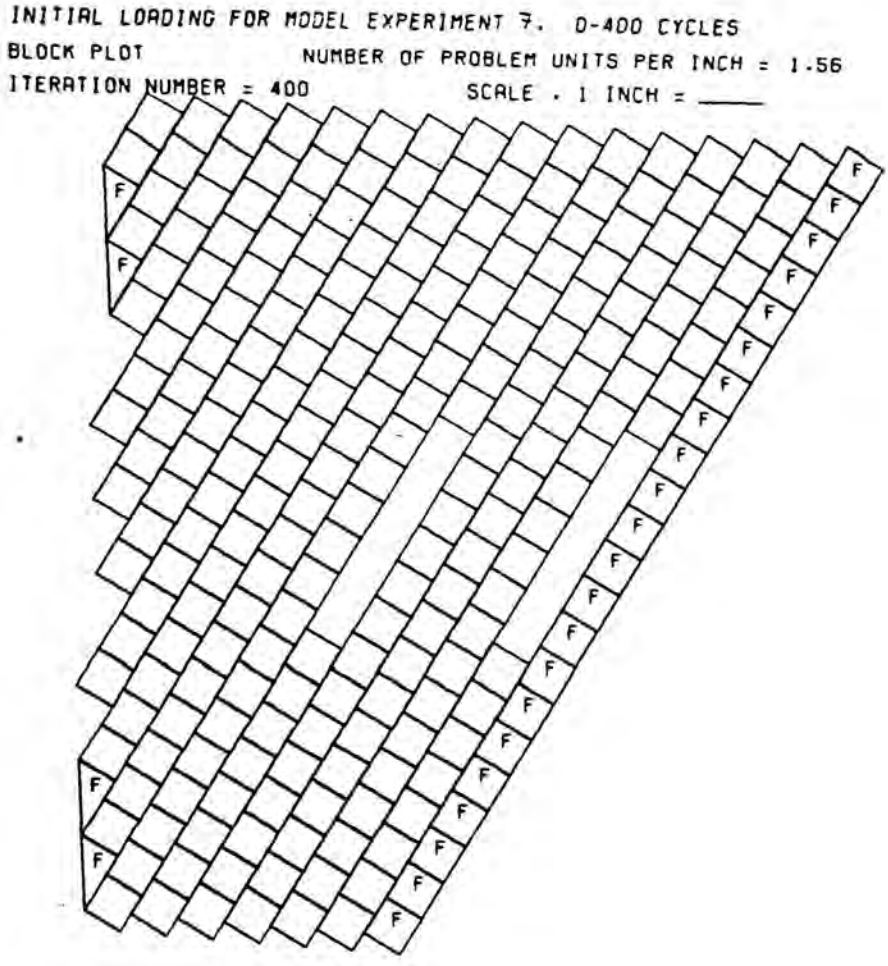
b) the placement of adequate support at the pillar ends to counter movement of material into the opening; as a means of ensuring the overall integrity of the mine structure.

For the geometry shown in Figure 6.52, an increase in the horizontal load under a smaller constant vertical load would result in little deformation throughout the pillar material due to the effective load shielding by both openings.

The model geometry at an advanced loading stage (Pv = .586 MPa) is shown in Figure 6.55. The collapse state is a continuation of the failure mechanisms described above with gross instability of the pillar evident.

Numerical Analysis of Model VII:

The numerical representation of the hangingwall geometry of Model VII is shown in Figure 6.56. Computing considerations again rendered it impractical to consider the complete model geometry and a compromise was reached in which 245 square and triangular blocks were used. The demands placed on computer resources by Model VII were similar to those required by Models III and IV. As for Model V, fixed triangular edge blocks were necessary to prevent sliding along the continuous jointing from dominating the overall behaviour. The input parameters representing the block physical properties were the same as those for previous tests with inclined jointing.


INITIAL LOADING FOR MODEL EXPERIMENT 7. 0-400 CYCLES
BLOCK PLOT NUMBER OF PROBLEM UNITS PER INCH = 1.56
ITERATION NUMBER = 400 SCALE . 1 INCH = _____

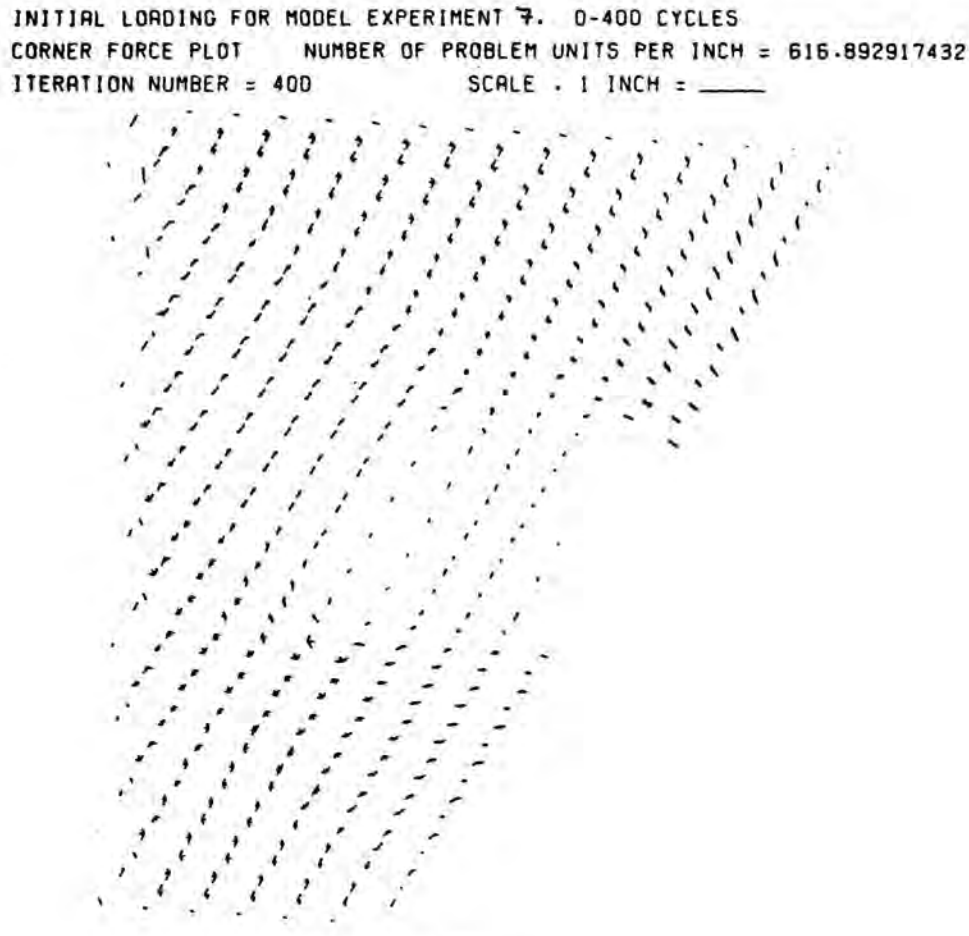
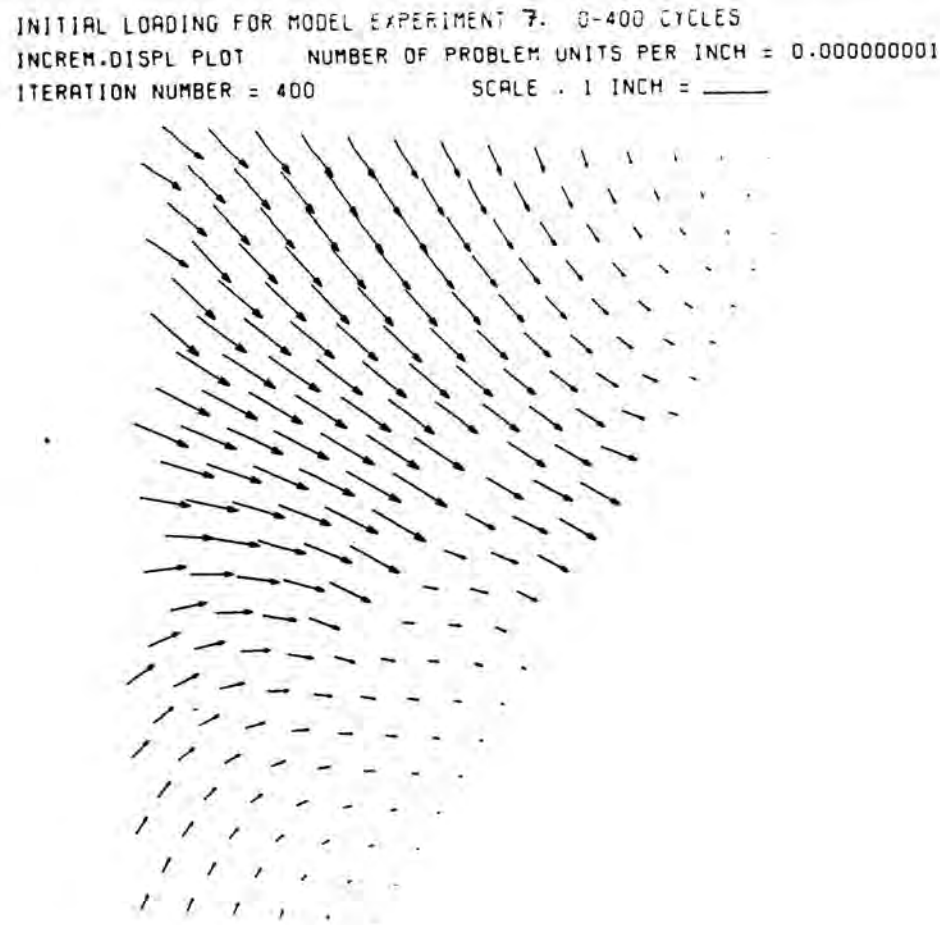

INITIAL LOADING FOR MODEL EXPERIMENT 7. 0-400 CYCLES
CORNER FORCE PLOT NUMBER OF PROBLEM UNITS PER INCH = 616.892917432
ITERATION NUMBER = 400 SCALE . 1 INCH = _____

Figure 6.56



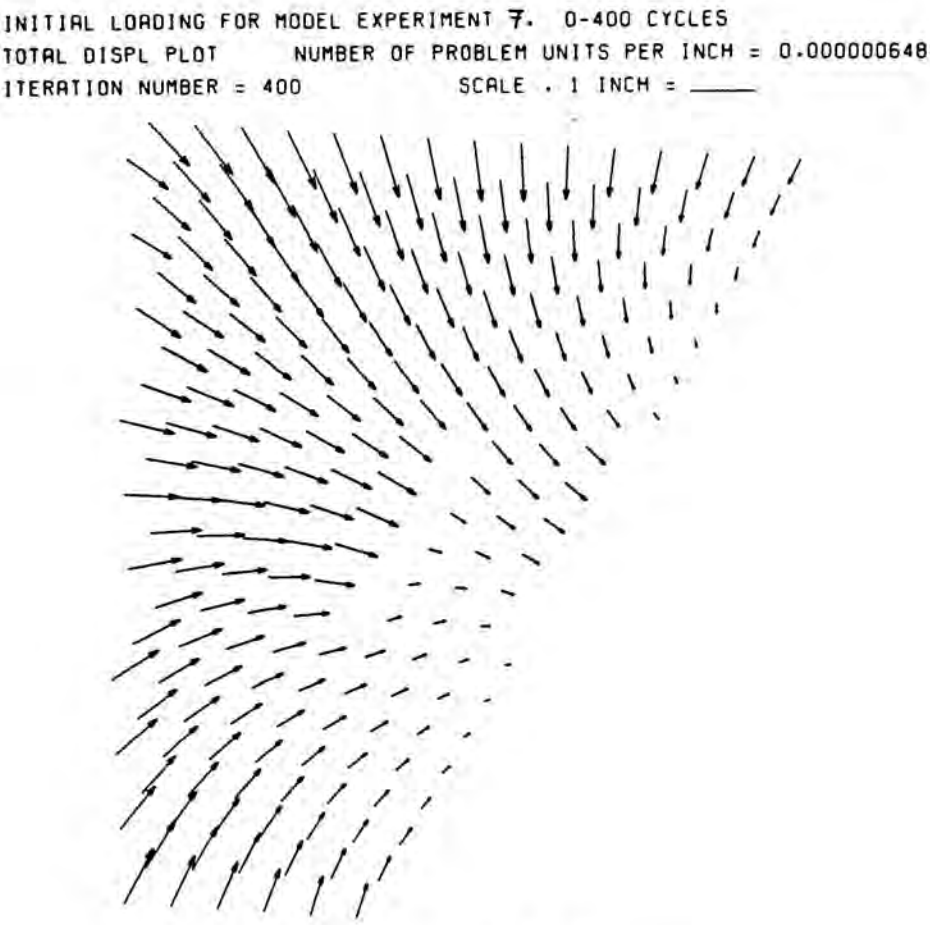
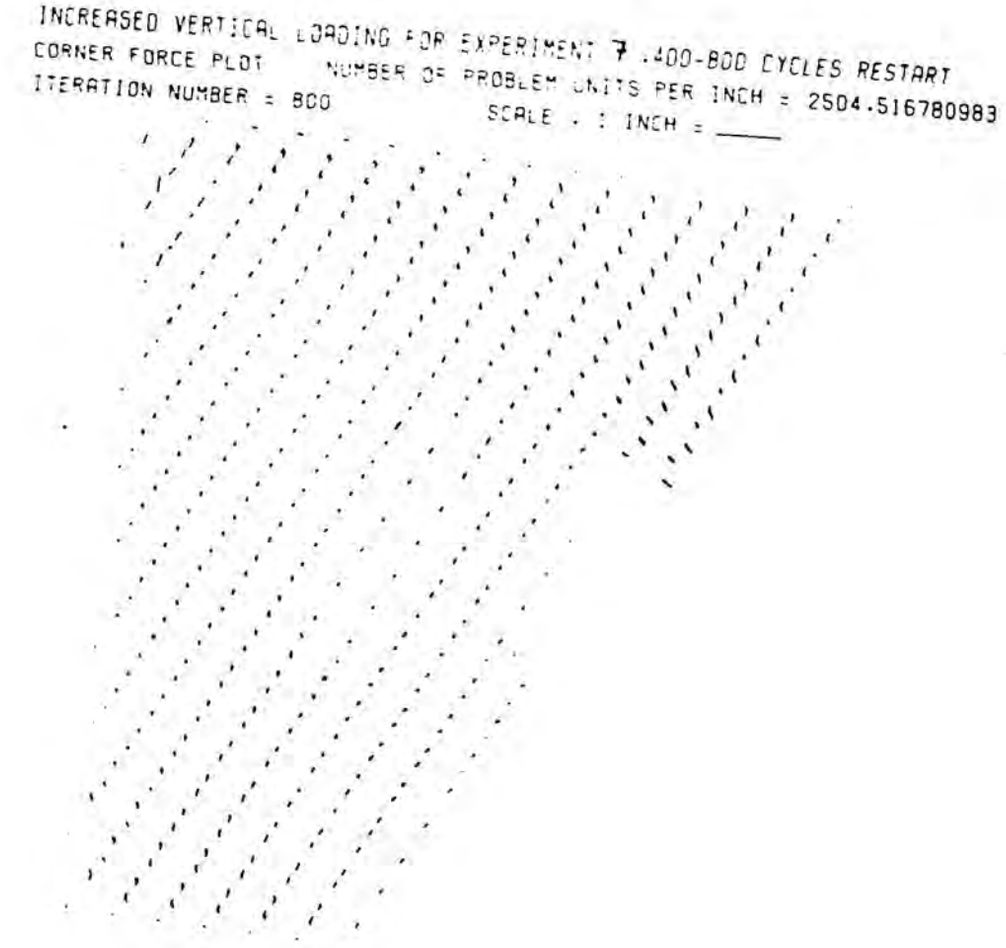




Figure 6.56 contd.

Initially, the model was subjected to 400 iterations of numerical loading equivalent to the preliminary loading in the physical model (Pv = .147 MPa, Ph = .112 MPa). In view of the satisfactory convergence to equilibrium for Models III and IV (239 blocks) after 400 iterations, the same number of calculation cycles was considered sufficient for this test. To confirm this, the largest incremental block displacement after the 400 iterations was 1.3% of the maximum initial value while the maximum out-of-balance force sum was approximately 3.5% of typical external loads. The vector force and displacement plots after initial loading are shown in Figure 6.56. The force distribution at this stage demonstrates the independent behaviour of the rows of blocks comprising the pillar and unstable hangingwall zone. The effect of the release in lateral confining pressures is particularly noticeable throughout the pillar and for those hangingwall rows immediately surrounding the openings, with some transfer of load evident between rows removed from the openings. Separation along the continuous jointing throughout the pillar and for the immediate hangingwall row is confirmed by the contact force printout. At the end of initial loading, no slip was occurring along either joint set.

The corner force and block displacement plots after a further 400 iterations of increased vertical loading are shown in Figure 6.57. The final loading was such that the Fv/Fh ratio was 4.4, which was identical to that at which photogrammetry was employed in the physical model. The distribution of contact forces illustrated in Figure 6.57 is an extension of the force pattern obtained after initial loading with all hangingwall rows now behaving independently and minimal interactions between contiguous rows.

The contact data reveals that separation between hangingwall rows has extended to the vertical boundary which correlates well with the joint separations observed in the physical model, Figure 6.53. The maximum forces


INCREASED VERTICAL LOADING FOR EXPERIMENT 7 .400-800 CYCLES RESTART
CORNER FORCE PLOT NUMBER OF PROBLEM UNITS PER INCH = 2504.516780983
ITERATION NUMBER = 800 SCALE . 1 INCH = ____

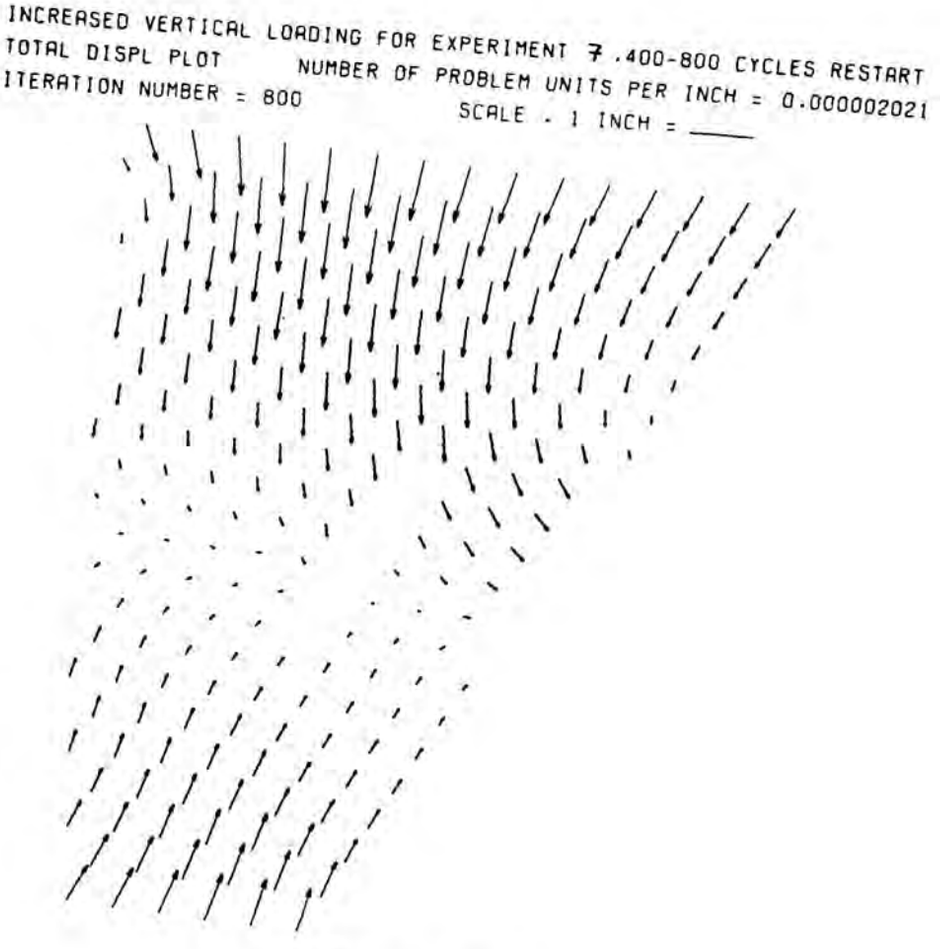

INCREASED VERTICAL LOADING FOR EXPERIMENT 7 .400-800 CYCLES RESTART
TOTAL DISPL PLOT NUMBER OF PROBLEM UNITS PER INCH = 0.000002021
ITERATION NUMBER = 800 SCALE . 1 INCH = ____

Figure 6.57

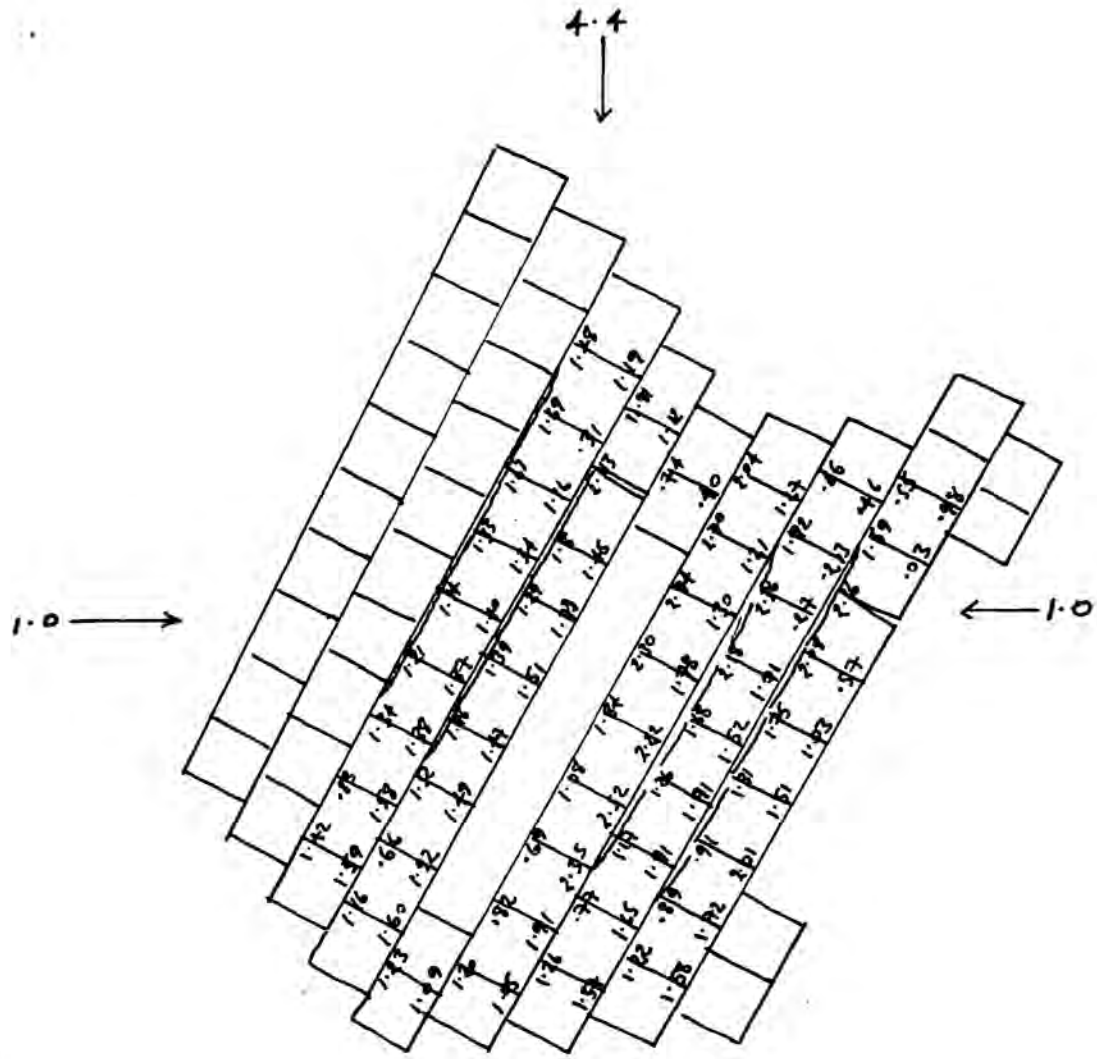



Figure 6.58: Model VII - $P_V/P_H$ = showing normal force magnitudes.

are seen to develop throughout the crown abutment area and acquire magnitudes three to four times those of typical forces occurring in the pillar and hangingwall regions. The contact force magnitudes and magnified joint separations for the pillar and hangingwall are specified in Figure 6.58. The failure mechanism calculated by the numerical model shows similar characteristics to the experimental failure mode especially in the up-dip region where effects due to the fixed barrier have less influence. Although block movements are less extensive, the location of the hinging zones and nature of joint separations predicted numerically compare favourably with experimental results and the contact forces indicate compatible block movements where separations have not yet occurred.

There is good relative agreement between the trend of up-dip displacement vectors for both models. A comparison between numerical and photogrammetric displacement magnitudes is presented in Table 6.9.

Again, a discrepancy between the two sets of values exists with numerical displacements being approximately an order of magnitude less than the corresponding photogrammetric results. This deviation is thought to be primarily due to the substantial slabbing present along each hinge zone and throughout the pillar.

6.3.8. Model VIII: Continuous Joints at 60 Degrees to Horizontal; Discontinuous Orthogonal Joints. Two Openings 150 mm by 25 mm and 50 mm Apart, Parallel to Continuous Jointing (Pv > Ph).

Physical Model Study:

Model VIII was constructed similar to Model VII with the objective being to examine the effect of decreasing the pillar thickness. To achieve this, the two central openings were separated by a pillar consisting of two rows of blocks. Otherwise, the two models were equivalent in

| Block Number | Numerical Displ.Dn(mm) | Photogrammetric Displ.Dp(mm) | Ratio Dp/Dn |
|---|---|---|---|
| 50 | .113 | 1.62 | 14.4 |
| 52 | .137 | 2.03 | 14.9 |
| 54 | .102 | 1.83 | 18.0 |
| 72 | .101 | .54 | 5.4 |
| 74 | .152 | 1.89 | 12.5 |
| 76 | .149 | 1.83 | 12.3 |
| 95 | .126 | .14 | 1.1 |
| 97 | .177 | 2.10 | 11.9 |
| 99 | .183 | 1.96 | 10.7 |
| 113 | .217 | 2.03 | 9.4 |
| 135 | .190 | 1.42 | 7.5 |
| 137 | .242 | 2.03 | 8.4 |
| 175 | .175 | 1.22 | 7.1 |
| 177 | .270 | 2.03 | 7.5 |
| 179 | .303 | 2.03 | 6.7 |
| 193 | .246 | 1.83 | 7.4 |
| 206 | .233 | 1.83 | 7.8 |
| 208 | .316 | 2.43 | 7.7 |
| 210 | .362 | 2.57 | 7.1 |
| 219 | .304 | 2.57 | 8.5 |
| 229 | .310 | 2.70 | 8.7 |
| 231 | .384 | 2.84 | 7.4 |

Table 6.9: Numerical and Photogrammetric Displacements for Model VII.

all respects.

The model configuration after the initial stabilising loads had been applied is shown in Figure 6.59. The initial loading yielded a Fv/Fh ratio of 1.70, the vertical and horizontal pressures being .190 MPa and .112 MPa respectively. The subsequent increased loading was applied in a similar manner to Model VII, whereby the vertical pressure was raised until movements of blocks surrounding the openings were observed or detected. This latter loading was accomplished under the constant initial

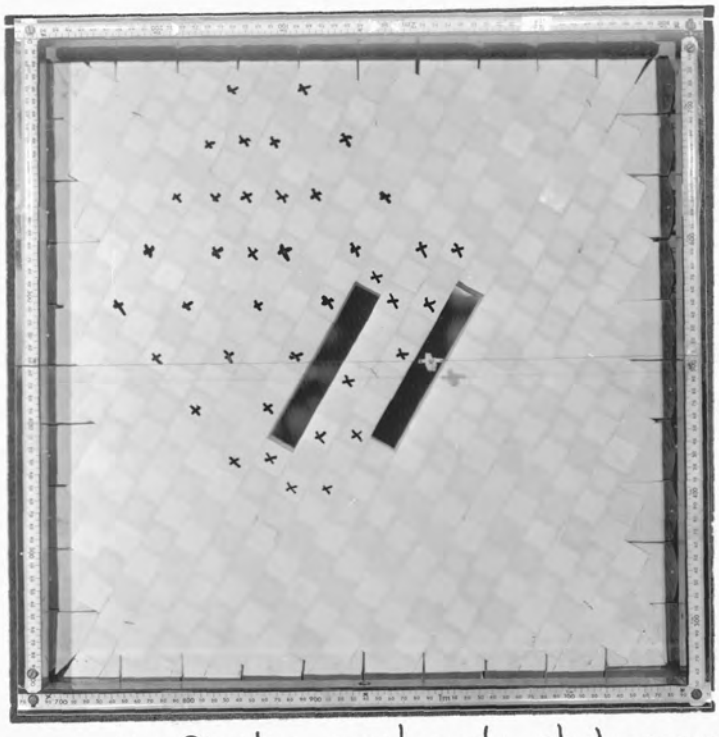



Figure 6.59: Model VIII under initial loading.

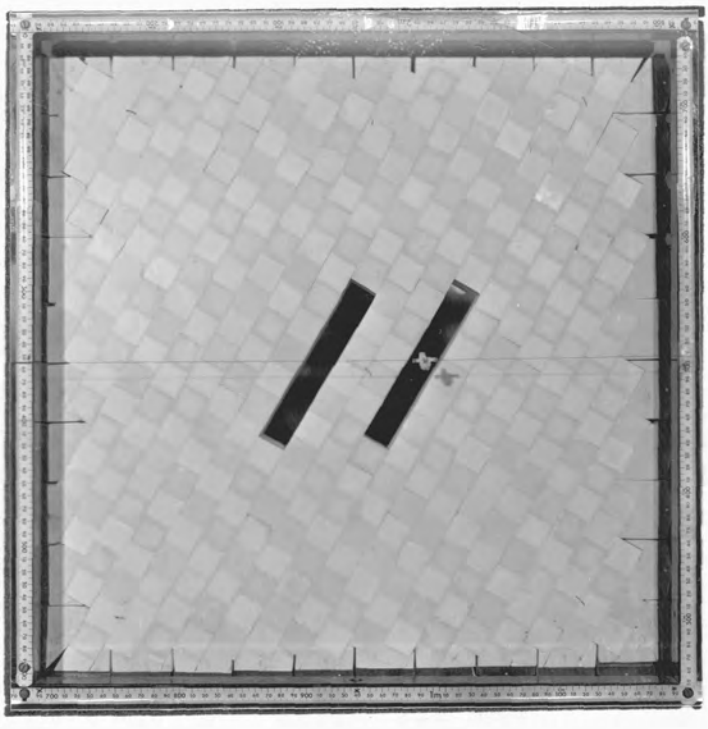


Figure 6.60: Model VIII - Pv/Ph = 4.2.

horizontal pressure.

Photogrammetry was utilized for the configuration shown in Figure 6.60, where the vertical pressure has been increased to .466 MPa, representing a Fv/Fh ratio of 4.2 (c.f. 4.4 for Model VII). The development of a symmetrical failure pattern about the two openings is illustrated in Figure 6.60. This is in contrast to that observed for Model VII, however, in that the location of one of the hinge zones in both the footwall and hangingwall appears to be primarily a result of the pillar behaviour.

For the hangingwall, this hinging zone initiates from beaming of the up-dip joints intersecting the footwall opening and propagates along a stepped path traversing the crown abutment of the second opening. Rotations of blocks are reflected by the widespread separations along discontinuous joints with quite extensive slabbing present along the down-dip hinge zone intersecting the face of the opening.

When subjected to loading conditions similar to those in Model VII, the pillar behaviour of Model VIII indicates a much more stable condition. Separation of the discontinuous joints at the pillar extremities results in a two-hinged beaming action for the pillar rows. Also, there is a noticeable absence of any shear sliding along the discontinuous joints located in the central pillar region. By decreasing the pillar thickness, the amount of material available for load transmittal at each pillar abutment has been substantially reduced in Model VIII. This implies that under equivalent loading conditions the loads causing pillar movements and ultimate failure are smaller for the model with the decreased pillar thickness.

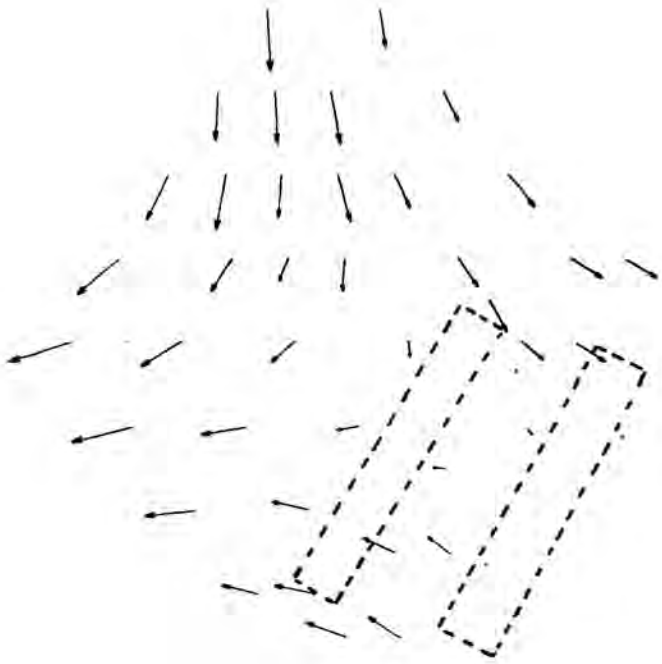
The photogrammetric displacement vectors are plotted to scale in Figure 6.61. The flow field for Model VIII displays similar characteristics to that of Model VII

RESULTS FOR EXPERIMENTAL MODEL STUDY NUMBER 8

CONT.JOINTS AT 60 DEGS.TO HORIZ. TWO OPENINGS WITH PILLAR 50MM WIDE. PV.GT.PH.

PLOT OF TRANSLATIONAL BLOCK DISPLACEMENTS

NUMBER OF PROBLEM UNITS PER INCH = 0.00224 METRES. SCALE IS 1 INCH = _____



RESULTS FOR EXPERIMENTAL MODEL STUDY NUMBER 8

CONT.JOINTS AT 60 DEGS.TO HORIZ. TWO OPENINGS WITH PILLAR 50MM WIDE. PV.GT.PH.

PLOT OF TRANSLATIONAL AND ROTATIONAL BLOCK DISPLACEMENTS-ROT.PRINTED IN RADIANS

NUMBER OF PROBLEM UNITS PER INCH = 0.00224 METRES. SCALE IS 1 INCH = _____




Figure 6.61.



Figure 6.62: Model VIII - Pv/Ph = 5.0.

(Figure 6.54). Again, the central pillar region has remained relatively undisturbed while displacements of equal magnitude but opposite direction are located around opposing pillar extremities. The failure state for a Fv/Fh ratio of 5.0 is shown in Figure 6.62, and the hinging zones delineating stable and unstable regions are clearly seen. Also, the independent behaviour of the two pillar rows is pronounced with separation along the entire continuous joint between them.

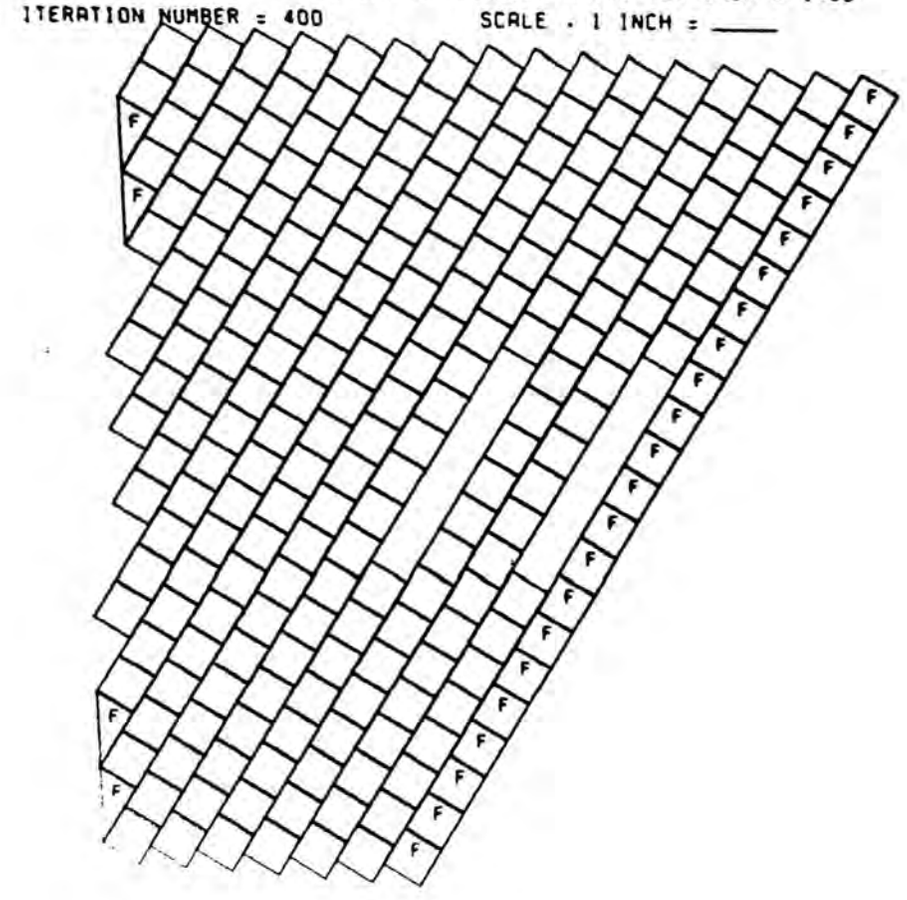
The extent of tensile slabbing along primary hinge zones and secondary hinge formation is also evident from Figure 6.62.

Numerical Analysis of Model VIII:

The sole difference between the numerical representations of Models VII and VIII was that, for the latter model, the hangingwall opening had been displaced one row towards the footwall opening, thus leaving a pillar consisting of two rows of blocks between excavations. The numerical geometry was considered to be an adequate approximation to the jointing configuration used in the physical model with the discontinuous joints offset to intersect the mid-point of block edges.

The arrangement of square blocks used in the computer model is shown in Figure 6.63 and a comparison with the experimental geometry (Figure 6.59) shows that this is not an exact simulation but was selected for convenience since a routine for automatically generating a system of blocks could be incorporated. Otherwise, the tedious task of inputting individual block co-ordinates would be required.

This slightly modified geometry necessitated an independent initial loading phase which again consisted of 400 iterations. The initial Fv/Fh ratio deviated somewhat from that applied in Model VII, the vertical pressure being 30% higher while the horizontal pressure was identical


INITIAL LOADING FOR MODEL EXPERIMENT 8. 0-400 CYCLES
BLOCK PLOT
NUMBER OF PROBLEM UNITS PER INCH = 1.56
ITERATION NUMBER = 400
SCALE . 1 INCH = _____

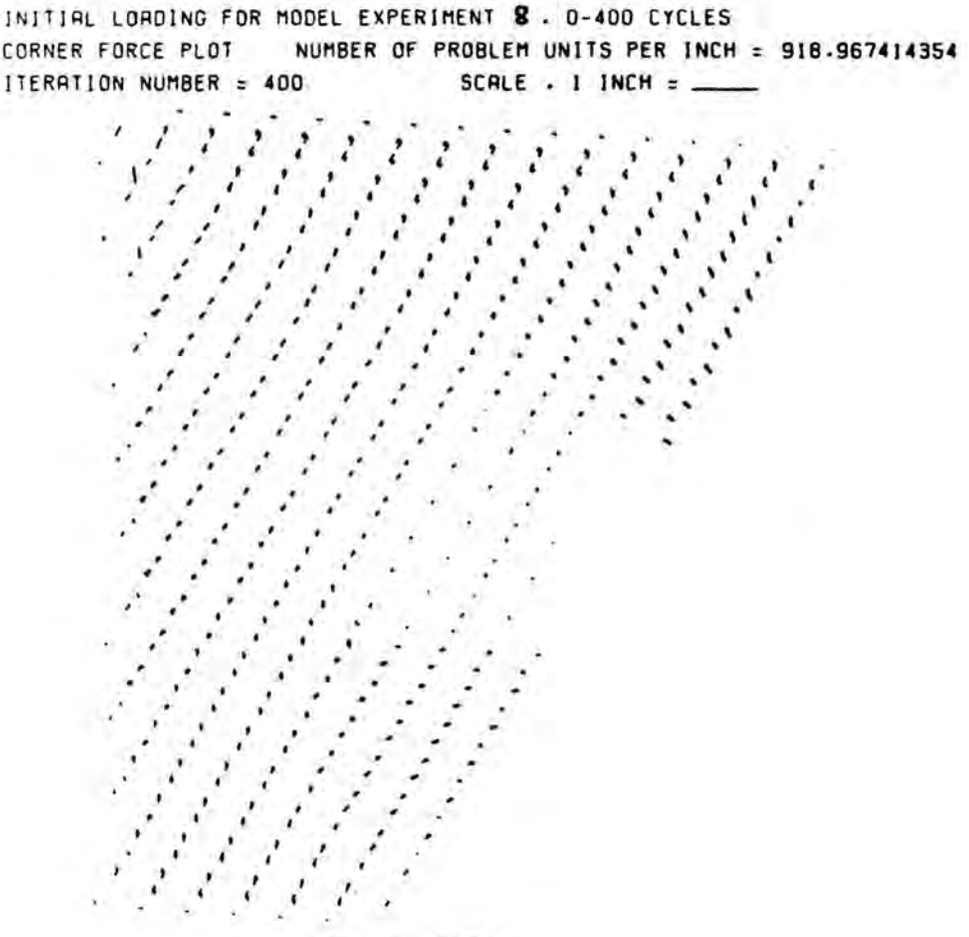
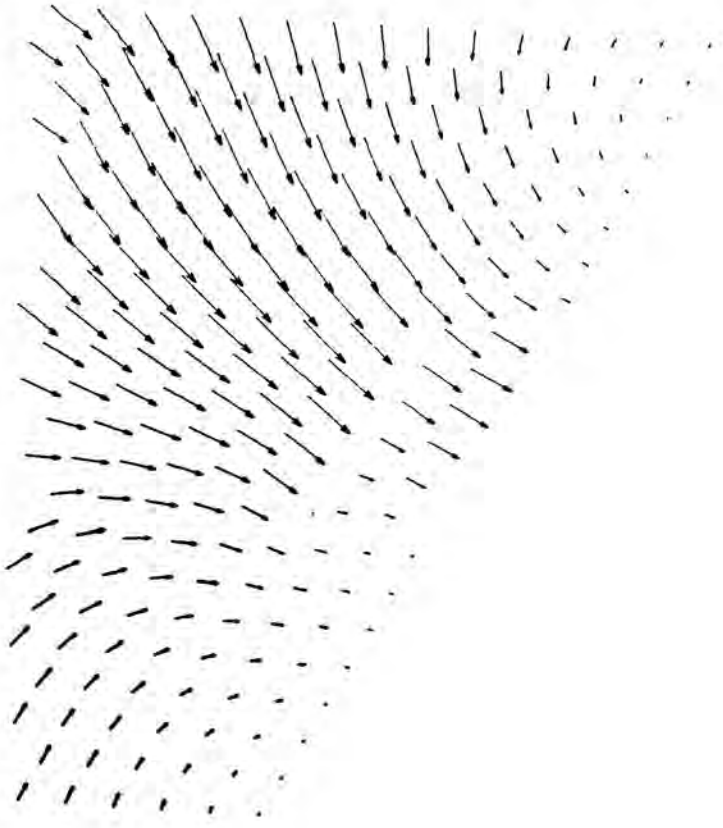

INITIAL LOADING FOR MODEL EXPERIMENT 8. 0-400 CYCLES
CORNER FORCE PLOT
NUMBER OF PROBLEM UNITS PER INCH = 918.967414354
ITERATION NUMBER = 400
SCALE . 1 INCH = _____

Figure 6.63

INITIAL LOADING FOR MODEL EXPERIMENT 8 . 0-400 CYCLES
INCREM.DISPL PLOT NUMBER OF PROBLEM UNITS PER INCH = 0.000000001
ITERATION NUMBER = 400 SCALE . 1 INCH = _____



INITIAL LOADING FOR MODEL EXPERIMENT 8 . 0-400 CYCLES
TOTAL DISPL PLOT NUMBER OF PROBLEM UNITS PER INCH = 0.000000849
ITERATION NUMBER = 400 SCALE . 1 INCH = _____

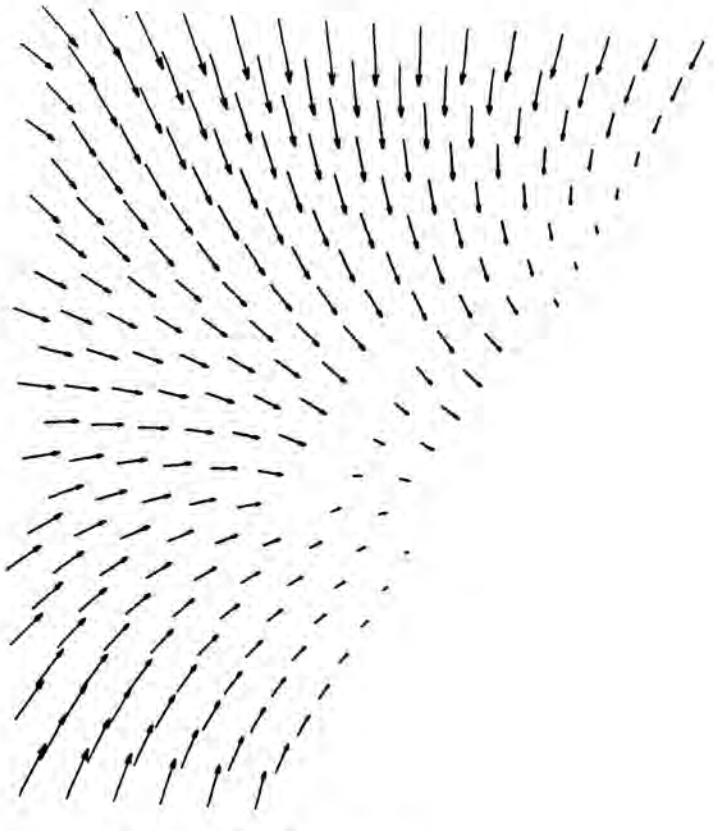


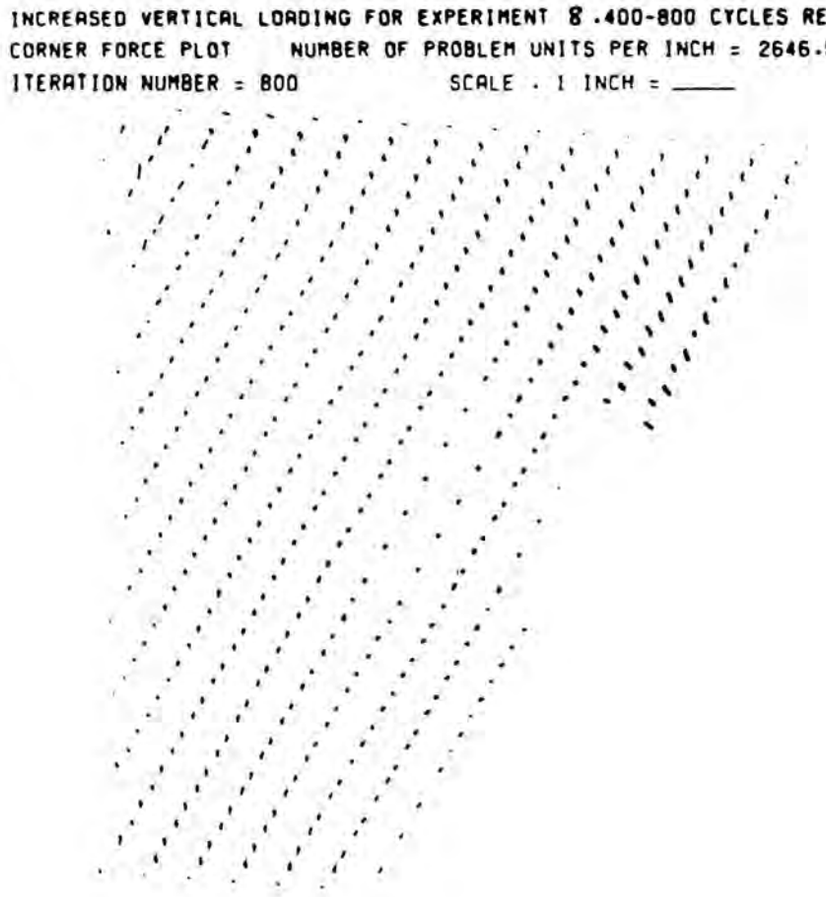
Figure 6.63 contd.

for both models. The resulting contact forces and block displacement vectors prior to increasing the vertical load are presented in Figure 6.63. The attainment of a satisfactory equilibrium state is indicated by the fact that incremental block movements have diminished to less than 1% of their maximum valves while out-of-balance forces are between 3% and 4% of typical boundary loads.

The force distribution of Figure 6.63 shows similar characteristics to that for Model VII (Figure 6.56), with load arching surrounding the floor and roof of each opening and independent behaviour of rows in both the pillar and overlying hangingwall material. It is interesting to note that at this stage the independent behaviour of pillar and hangingwall rows is more pronounced for Model VIII, this being a direct consequence of the increased initial vertical loading. Pre-failure separation along the continuous joints within the pillar and immediate hangingwall is indicated by the contact force printout and again slip has been inhibited along any of the discontinuous joints traversing the opening faces.

A further 400 iterations of increased vertical loading corresponding to a Fv/Fh ratio of 4.2 followed the preliminary sequence. The ensuing behaviour after a cumulative total of 800 iterations is illustrated in Figure 6.64. As expected, there is a marked similarity between the force plots for both models VII and VIII after increased loading. Tensile separation of the continuous jointing between the overlying hangingwall rows has propagated to the boundaries in much the same fashion as that illustrated for Model VII (Figure 6.58).

The development of upper and lower stepped hinge zones in the hangingwall is indicated from the magnitude of the normal contact forces across discontinuous joints. Although tensile separation has not occurred along these joints after the specified loading, the location and nature


INCREASED VERTICAL LOADING FOR EXPERIMENT 8 .400-800 CYCLES RESTART
CORNER FORCE PLOT NUMBER OF PROBLEM UNITS PER INCH = 2646.573443314
ITERATION NUMBER = 800 SCALE . 1 INCH = ____

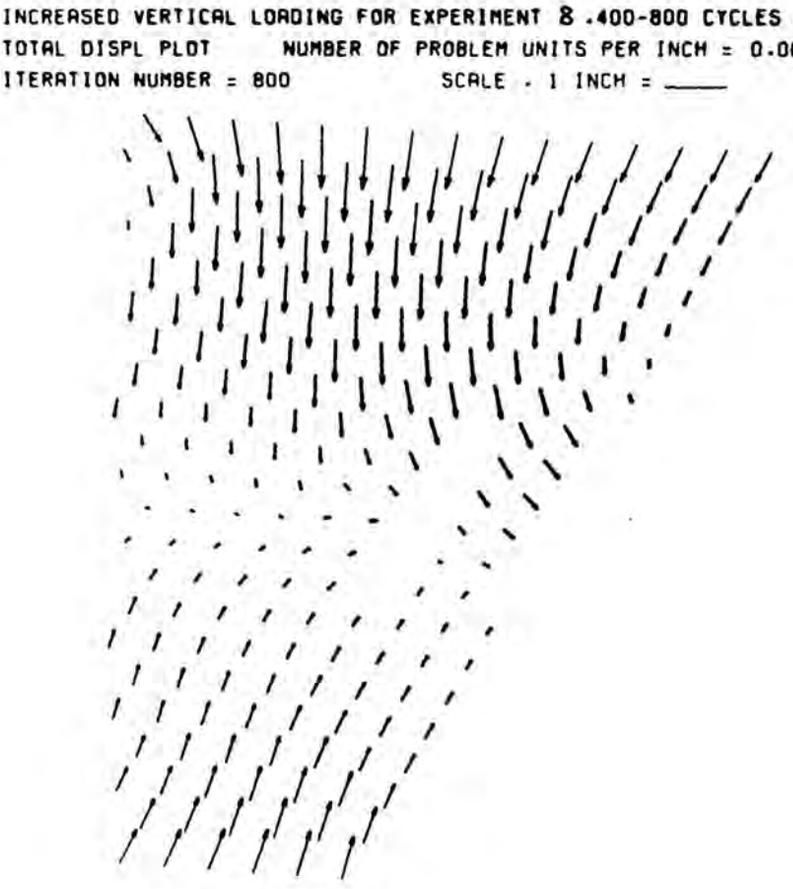

INCREASED VERTICAL LOADING FOR EXPERIMENT 8 .400-800 CYCLES RESTART
TOTAL DISPL PLOT NUMBER OF PROBLEM UNITS PER INCH = 0.000001684
ITERATION NUMBER = 800 SCALE . 1 INCH = ____

Figure 6.64.

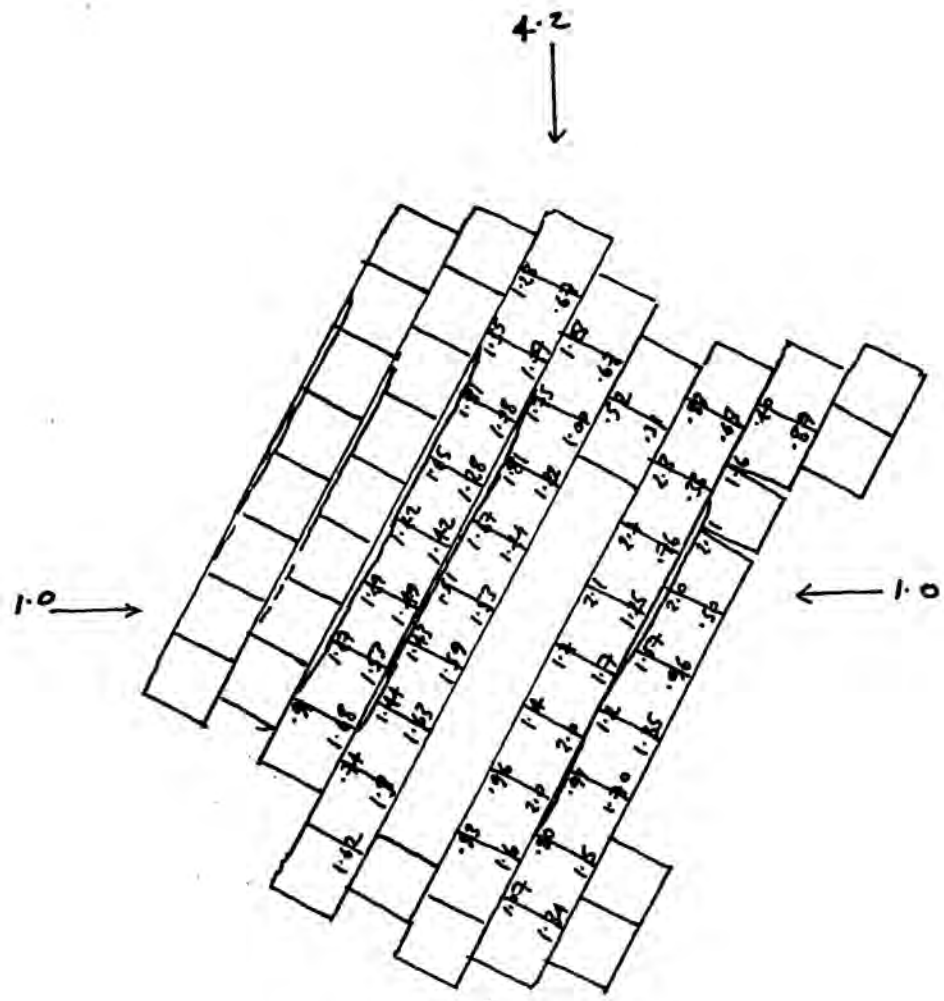



Figure 6.65: Model VIII - PV/PH = 4.2 showing normal force magnitudes.

of block rotations and force magnitudes calculated numerically was such as to suggest that hinge formation and joint separation compatible with the physical model was imminent.

The joint separations and normal force magnitudes within the pillar are depicted in Figure 6.65. The pillar deformations resemble closely those observed experimentally, particularly at the up-dip end. Although the Fv/Fh ratios for Models VII and VIII differ (4.4 and 4.2 respectively), a comparison of the pillar forces for both models indicates that as the thickness of the pillar is decreased the load intensity in the pillar increases. However, as Chappell (1972) points out, this does not affect the mechanistic modes causing the load distributions.

Table 6.10 presents a comparison between photogrammetrically measured and numerically calculated rigid body displacements for the blocks indicated in Figure 6.59. It is again apparent that the numerical displacements are several times smaller than those determined photogrammetrically. Also, the numerical displacements for Model VIII are approximately 20% less than those for corresponding blocks in Model VII. Extensive slabbing was visible along the down-dip hangingwall hinge zone for the Fv/Fh ratio of 4.2 and this most probably accounts for the deviation between the two sets of displacements.

### 6.3.9. Summary:

Numerous model studies of rectangular openings in discontinuous media were analysed using both physical and numerical modelling techniques. The purpose of these studies was to examine the load distributing mechanisms generated in each model under various loading conditions. On this basis, an assessment of the applicability of the numerical model in analysing the influence of critically oriented joints on the stability of rectangular openings was possible. Also, by examining modes of failure, insight into the stability of underground openings is better

| Block Number | Numerical Displ.Dn(mm) | Photogrammetric Displ.Dp(mm) | Ratio Dp/Dn |
|---|---|---|---|
| 50 | .102 | .27 | 2.6 |
| 52 | .124 | 1.17 | 9.4 |
| 54 | .090 | 1.25 | 13.9 |
| 74 | .141 | .99 | 7.0 |
| 76 | .132 | 1.30 | 9.8 |
| 91 | .174 | 1.30 | 7.5 |
| 112 | .143 | .54 | 3.8 |
| 114 | .188 | 1.30 | 6.9 |
| 116 | .191 | 1.52 | 8.0 |
| 157 | .213 | 1.17 | 5.5 |
| 159 | .235 | 1.30 | 5.5 |
| 161 | .248 | 1.21 | 4.9 |
| 176 | .213 | .85 | 4.0 |
| 178 | .246 | 1.70 | 6.9 |
| 194 | .252 | 1.48 | 5.9 |
| 196 | .283 | 1.93 | 6.8 |
| 198 | .308 | 1.39 | 4.5 |
| 207 | .244 | 1.97 | 8.1 |
| 209 | .287 | 1.88 | 6.6 |
| 220 | .281 | 1.70 | 6.0 |
| 222 | .326 | 2.24 | 6.9 |

Table 6.10: Numerical and Photogrammetric Displacements for Model VIII.

appreciated.

Rigid block displacements were selected as the control when comparisons between techniques were made. The numerical models were chosen so as to be as representative as possible with input parameters (joint stiffnesses, friction coefficient) accurately determined and boundary conditions compatible. A wide variation of joint orientations was selected so that there was no loss of generality in the final conclusions. The loading was applied in such a manner as to induce failure in the models

and not necessarily to simulate prototype conditions.

The results of the physical modelling studies showed in general that the basic load distributing mechanisms were present in all models, the differences between models depending upon the extent to which the various mechanisms were mobilised. These mechanisms were slip, rotation and tension with associated tensile block fracture phenomena such as slabbing of corners and axial splitting. Unfortunately, the numerical algorithm was limited in the mechanisms which it could simulate and the fracture mechanisms were not able to be accurately assessed in the numerical modelling. The numerical results showed, however, that the primary mechanisms of slip, rotation and tension were all predicted and were compatible with the corresponding physical model behaviour. The other limitation of the numerical model was the inability to allow blocks to deform; to overcome this, experimental loading was kept as low as practically possible so as to minimise elastic deformations of the plaster blocks.

Comparisons between rigid body displacements determined from both modelling techniques often showed substantial discrepancies in actual magnitudes even though relative displacements were generally in satisfactory agreement. The correlation between displacement magnitudes was closest when tensile block failures were absent or of minimal extent. Discrepancies in displacements could arise from a combination of many factors, such as

i) incorrect normal and shear stiffnesses modelled numerically for a particular jointing configuration;

ii) disturbed boundary conditions in the physical model due to the zone of influence of the opening extending to the loaded boundaries (depending on Fv/Fh ratio);

iii) the presence of effects in the physical model such as tensile slabbing and block fracture, which cannot at

present be accounted for numerically;

iv) the limitation on problem execution time for the numerically analysed models.

Therefore, it may be concluded that the basic load distributing mechanisms mobilised for all of the jointed models examined were similar, each model differing only in the extent to which individual mechanisms were present. These mechanisms, together with general load-displacement behaviour of openings in jointed media, were satisfactorily predicted by the numerical modelling technique.

# CHAPTER 7

# *SUMMARY AND CONCLUSIONS*

## CHAPTER 7:

## SUMMARY AND CONCLUSIONS:

The philosophy adopted for the investigations into the behaviour of jointed media reported in this dissertation was to develop and utilize complementary methods of approach. In this way, maximum benefit could derive from the studies since one method was able to expose the limitations or advantages of the other. The first portion of the dissertation was concerned with the development of a numerical model, based on conventional relaxation, which allowed for slip, separation and other rigid body motion in the rock medium. The method differs from others in that it seeks a direct force-displacement path to the equilibrium position, whereas most existing codes operate through time-dependent displacement steps. The major limitation on the method at present is that all constituent elements are considered as rigid entities.

The static relaxation method developed for the two-dimensional analyses of underground excavations in discontinuous rock masses was compared to solutions commonly used to describe the behaviour of jointed rock masses. In the comparisons presented in Chapter 3, the behaviour predicted by the numerical model was shown to be in satisfactory agreement with the theoretical solutions. Advantages of the technique when compared with dynamic relaxation methods are the elimination of the time-step and damping parameters and a favourable reduction in the demands placed on computing resources for many similar problems, especially as far as execution times are concerned.

The original computer program was limited as to the size of the problem that could be investigated. This was a serious limitation where realistic problem geometries required examination since simplified, idealised models may prevent the generation of actual failure modes and mechanisms of failure. The original program was modified to allow for an increase in the number of rock units constituting a jointed rock assemblage, by storage of the problem data during job execution on mass storage

files. This enabled investigative studies of typical excavation geometries to be performed in which the action of pertinent variables could be identified.

The second portion of the dissertation was concerned with how well the static relaxation approach, together with other numerical methods (e.g. dynamic relaxation), model the performance of real jointed systems. The requirement for the precise measurement of the displacements of the discontinuous model constituents in the programme of experiments highlighted the need for an accurate and predictable loading system. A biaxial loading apparatus was designed and constructed by the author for the purposes of this project. In the controlled physical modelling, a wide variation of joint orientations was selected so that there was no loss of generality in the final conclusions. In general, the results of the physical modelling showed that the basic load distributing mechanisms of slip, rotation and separation were present in all models. the differences between models depending upon the extent to which the various mechanisms were mobilised. However, other mechanisms such as tensile slabbing of block corners and axial splitting which were not incorporated in the numerical model were present and were the cause of substantial discrepancies between the rigid body displacements determined from both modelling techniques. In view of the lack of correlation between predicted and measured displacements , the model studies must be regarded as a failure. However, the failure mode and mechanisms of failure predicted physically and numerically were in close agreement.

Several directions for further research have been identified as a result of this work. They are:

i) the need to incorporate block deformability and, perhaps more importantly, slabbing of block edges and splitting of blocks as evidenced in the physical modelling tests. The author crudely simulated some of these effects by incorporating variable stiffnesses along block edges, but a properly validated failure criterion for blocks is needed in the numerical algorithm if realistic behaviour is to be modelled;

ii) the coupling of elastic programs (e.g. boundary element) with the static relaxation method. This has the major advantage in that for many problems the elastic pre-mining stresses can be determined in a very short solution time and could be input to the block program at the stage where large scale displacements were likely. This is not fundamentally difficult with the present program structure;

iii) associated with ii) above is the idea that blocks removed from the areas of largest displacement need not be analysed exactly to determine their incremental displacements each iteration. A displacement criterion based on the magnitude of the resultant forces and moments could lead to favourable computing economies, especially for large sized problems;

iv) most of the geometries analysed throughout this dissertation have involved highly idealised configurations involving smooth, planar joints and regularly shaped blocks. Generalised model studies involving random distributions of block sizes and shapes are required if maximum benefit is to be derived from both the physical and numerical modelling. The author hopes that the biaxial loading apparatus will be subsequently used to perform such studies;

v) to accurately simulate prototype behaviour, more realistic joint characteristics are necessary. The incorporation of non-linear normal joint stiffnesses as a function of the applied loading was discussed in Chapter 6. The implementation of arbitrary joint characteristics in the numerical model is a relatively straightforward procedure - the difficulty lies in specifying the exact nature of the characteristics whether they be for controlled physical modelling or for actual field behaviour. Joint dilatancy, in which the normal force becomes a function of shear slip along joints, is the other important feature not presently incorporated in the numerical model. Again, this is not fundamentally difficult to model and the author sees this as being another fruitful avenue for research with closely controlled experiments performed on the loading apparatus complementing the numerical results.

# *REFERENCES*

REFERENCES

ATKINSON, K.B. (1972). The measurement of models with particular reference to a suspended roof structure. Photogrammetric Record, 7 (39), pp. 334-337.

BACZYNSKI, N.R. (1977). Geological characteristics of the rock-mass: Dolomitic shales: Mount Isa Mine, Qld. Internal Report, Dept. of Mining, University of Melbourne.

BARRON, K. & LAROCQUE, G.E. (1962). Development of a model for a mine structure. Proc. Rock Mech. Symp., McGill University, Montreal, pp.145-189.

BARTON, N.R. (1970). A low strength material for simulation of the mechanical properties of intact rock in rock mechanics models. 12 p. Proc. of 2nd Cong. Int. Soc. Rock Mech., Belgrade, Vol. 2, paper 3-15.

BRADY, B.H.G. (1977). An analysis of rock behaviour in an experimental stoping block at the Mount Isa Mine, Australia. Int. J. Rock Mech.Min.Sci. & Geomech. Austr., Vol. 14, pp.59-66.

BRADY, B.H.G. (1979). Boundary element methods for mine design. Ph.D. Thesis, University of London.

BRAY, J.W. (1967). A study of jointed and fractured rock. Part I: "Fracture patterns and their failure characteristics". Rock Mech. & Eng. Geol., Vol. 5, No.4, pp.117-136.

BRAY, J.W. (1978). Unpublished work.

BRAY, J.W. (1981). Personal communication.

BRIDGES, M.C. (1980). M662-665-667 Stope Triplet 8 Orebody. Mount Isa Mines Ltd. Internal Report.

BROWN, E.T. (1968). The influence of planar discontinuities on the shear strengt of a rock-like material. Ph.D. Thesis, James Cook University of N. Queensland, Townsville, Australia.

BROWN, E.T. (1970). Modes of failure in jointed rock masses. Proc. 2nd Cong. I.S.R.M., Vol. 2, paper 3-42.

BROWN, E.T. & GONANO, L.P. (1974). Improved compression testing techniques for soft rock. J. Geotech. Eng. Div., Am. Soc. Civ. Engrs., Vol. 100, pp.196-199.

BROWN, E.T. & HUDSON, J.A. (1972). Progressive collapse of simple block-jointed systems. Aust. Geomechanics Jour., Vol. G2, No. 1, pp.49-54.

BROWN, E.T. & TROLLOPE, D.H. (1967). The failure of linear brittle materials under effective tensile stress. Rock Mech. and Eng. Geol., Vol. 5, pp.229-241.

BURMAN, B.C. (1972). A numerical approach to the mechanics of discontinua. Ph.D. Thesis, James Cook University of N. Queensland, Townsville, Australia

BUTTERFIELD, R., HARKNESS, R.M. & ANDRAWES, K.Z. (1970). A stereo-photogrammetric method for measuring displacement fields. Geotechnique, 20, No. 3, pp.308-314.

CHAPPELL, B.A. (1972). The mechanics of blocky material. Ph.D. Thesis, Australian National University, Canberra.

CHIAT, B., GURR, J. & ROBINSON, S.J. (1979). The application of photogrammetry to current determination in an hydraulic model. Photogrammetric Record, 9(53), pp.659-667.

CROSS,HARDY (1932). Analysis of continuous frames by distributing fixed-end moments. Paper No. 1793, Trans. Amer. Soc. Civ. Eng., 96, pp.1-10.

CUNDALL, P.A. (1971). The measurement and analysis of acceleration in rock slopes. Ph.D. Thesis, University of London.

CUNDALL, P.A. (1971a). A computer model for simulating progressive large scale movements in blocky rock systems. Proc. Int. Symp. on Rock Fracture, Nancy (ISRM), paper 2-8.

CUNDALL, P.A. (1971b). Contribution to Symposium on Rock Fracture, Nancy, France; published in volume 2 of Proceedings, pp.129-132.

CUNDALL, P.A. (1974). A computer model for rock mass behaviour using interactive graphics. U.S. Army, Corps of Engineers, Technical Report MRD 2-74 (Missouri River Division).

CUNDALL, P.A., VOEGELE, M.D. & FAIRHURST, C. (1975). Computerized design of rock slopes using interactive graphics for the input and output of geometrical data. Proc. 16th Symp. on Rock Mech., University of Minnesota, Minneapolis.

CUNDALL, P.A. (1976). Explicit finite-difference methods of geomechanics. Proc. of ASCE Engineering Foundation Conference on Numerical Methods in Geomechanics, Virginia, pp.132-150.

CUNDALL, P.A., SHILLABEER, J.H. & HERGET, G. (1978). Modelling to predict back-fill stability in pillar extraction. Proceedings 12th Canadian Symp. Rock Mech., pp.92-99.

CUNDALL, P.A. & MARTI, J. (1979). Some new developments in discrete numerical methods for dynamic modelling of jointed rock masses. Rapid Excavation and Tunneling Conference, Atlanta, Georgia.

CUNDALL, P.A. & STRACK, O.D.L. (1979). A discrete numerical model for granular assemblies. Geotechniques, 29, No. 1, pp.47-65.

EISSA, E.A. (1974). Joint roughness measured on small and large scales. M.Sc. Dissertation, University of London.

EISSA, E.A. (1980). Stress analysis of underground excavations in isotropic and stratified rock using the boundary element method. Ph.D. Thesis, University of London.

ELSWORTH, D. (1980). A boundary element analysis for slip on planes of weakness traversing an underground opening. M.Sc. Dissertation, University of London.

ERGUN, I. (1970). Stability of underground openings in jointed media. Ph.D. Thesis, University of London.

ERGUVANLI, K.A. & GOODMAN, R.E. (1972). Applications of models to engineering geology for rock excavations. Bulletin of the Assoc. of Engng. Geologists, Vol. IX, No. 2, pp.89-104.

EVERLING, G. (1964). Model tests concerning the interaction of ground and roof support in gate-roads. Int. J. Rock Mech. Min. Sci., Vol. 1, pp.319-326.

FABJANCZYK, M. (1978). M662-665-667 Stope Triplet 8 Orebody. Mount Isa Mines Ltd., Internal Report.

FAIG, W. (1975). Photogrammetric equipment systems with non-metric cameras. Proceedings of ASP-ISP Symposium on Close-Range Photogrammetric Systems, Urbana, Illinois.

GONANO, L.P. (1974). Stress gradient and size effect phenomena in brittle materials. Ph.D. Thesis, James Cook University of N. Queensland, Townsvill Australia.

GOODMAN, R.E. (1970). The deformability of joints. ASTM Spec. Tech. Publ. 477, pp.174-196.

GOODMAN, R.E. (1974). The mechanical properties of joints. Proc. 3rd Congr. I.S.R.M., Denver, Vol. 1-A, pp.127-140.

GOODMAN, R.E. (1976). Methods of geological engineering in discontinuous rocks. West Publishing Co., New York.

GOODMAN, R.E., TAYLOR, R.L. & BREKKE, T. (1968). A model for the mechanics of jointed rock. Journal of the Soil Mechanics and Foundation Division, Procs. ASCE, Vol. 94, No. SM3, pp.637-658.

GOODMAN, R.E. & BRAY, J.W. (1976). Toppling of rock slopes. Paper in "Rock engineering for foundations and slopes", Vol II, Proc. ASCE Speciality Conference, Boulder, pp.201-234.

HAMMETT, R.D. (1974). A study of the behaviour of discontinuous rock masses. Ph.D. Thesis, James Cook University of N. Queensland, Townsville, Australia

HEUER, R.E. (1971). Geomechanical model study of the behaviour of underground openings in rock subject to static loads. Ph.D. Thesis, University of Illinois, Urbana.

HEUER, R.E. & HENDRON, A.J. (1971). Geomechanical model study of the behaviour of underground openings in rock subjected to static loads. Technical Report N-69-1, U.S. Army Engineer Waterways, University of Illinois.

HITTINGER, M. & GOODMAN, R.E. (1978). A computer program for stress analysis of two-dimensional discontinuous rock masses. Report No. UCB/GT/78-04, Dept. of Civil Engineering, University of California, Berkeley.

HIRVONEN, R.A. (1971). Adjustment by least squares in geodesy and photogrammetry. F. Ungar Publishing Co., New York.

HOBBS, D.W. (1966). Scale model studies of strata movement around mine roadways - apparatus, technique and some preliminary results. Int. J. Rock Mech. Min. Sco., Vol. 3, No. 2, pp.101-127.

HOCKING, G. (1977). Development and application of the boundary integral and rigid block methods for geotechnics. Ph.D. Thesis, University of Londo

HOEK, E. (1965). Rock fracture under static stress conditions. CSIR Report. MEG 383, 159 pp.

HOEK, E. (1970). The influence of structure upon the stability of rock slopes. Proc. 1st Symposium on Stability in Open Pit Mining, Vancouver. Published by A.I.M.E., New York, pp.49-63.

JAEGER, J.C. & COOK, N.G.W. (1976). Fundamentals of Rock Mechanics. 2nd Edition, Chapman and Hall, London.

JAGGER, F. (1967). Designing and loading of models of underground structures. Proceedings, Symposium on Stress and Failure around Underground Openings, University of Sydney, Australia.

JOHN, K.W. (1969). Civil engineering approach to evaluate strength and deformability of regularly jointed rock. Rock Mechanics - Theory and Practice. Procs. 11th Symp. Rock Mech., Berkeley, pp.69-82.

KARARA, H.M. (1975). Non-topographic photogrammetry. Int. Symp. on Industrial Photogrammetry, Photogrammetric Society, Birmingham.

KRSMANOVIC, D. & MILIC, S. (1964). Model experiments on pressure distributions in some cases of a discontinuum. Rock Mech. and Eng. Geol., 14th Symp., Austrian Regional Group of Int. Soc. Rock Mech.

LANG, A.M. (1979). Monitoring Report - L685 Stope, 5 Orebody. Mount Isa Mines Ltd. Internal Report.

LIVESLEY, R.K. (1978). Limit analysis of structures formed from rigid blocks. Int. J. for Num. Methods in Engng., Vol. 12, pp.1853-1871.

MAINI, T., CUNDALL, P.A., MARTI, J., BERESFORD, P., LAST, N. & ASGIAN, M. (1978). Computer modelling of jointed rock masses. U.S. Army Corps of Engineers, Technical Report N-78-4.

MAY, R.E. (1979). The behaviour of underground excavations in discontinuous rock strata. B.Sc. (Eng.). Dissertation, King's College, University of London.

MOORE, J.F.A. (1965). The behaviour of discontinuous ground. Ph.D. Thesis, University of London.

MOORE, J.F.A. (1966). Experimental tests on models of discontinuous ground. Proc. 1st Cong. Int. Soc. Rock Mech., Lisbon, pp.307-312.

MORGAN, G.A. (1979). A boundary element analysis of slip on a plane of weakness near an excavation. M.Sc. Dissertation, University of London.

MULLER, L. & HOFMANN, H.(1970). Selection, compilation and assessment of geological data for the slope problem. Proc. Symp. on Planning of Open Pit Mines, Johannesburg, S. Afr. Inst. Min. Met.

MULLER, L. & PACHER, F. (1965). Model tests to investigate the danger of failure of jointed media. Rock Mech. & Eng. Geol., Suppl.II, pp.7-24.

OTTER, J.R.H., CASSELL, A.C. & HOBBS, R.E. (1966). Dynamic relaxation. Proc. Inst. Civil Engrs., Vol. 35, pp.633-365.

OZGENOGLU, A. (1978). The analysis of toppling failure using models and numerical methods. M.Phil. Dissertation, University of London.

PAREKH, C.J. (1976). Dynamic relaxation solution of seepage problems. Proc. of ASCE Engineering Foundation Conference on Numerical Methods in Geomechanics, Virginia, pp.1133-1144.

POULOS, H.G. & DAVIS, E.H. (1974). Elastic solutions for soil and rock mechanics. John Wiley & Sons, Inc., New York.

RAPHAEL, J.M. (1960). Structural model investigations for Oroville Dam. Final Report to Dept. of Water Resources, University of California, Berkeley, Ser.100, Issue 6.

ROBINSON, S.J. (1979). Hydraulic modelling of circulation in reservoirs. M.Phil. Dissertation, University of London.

ROBINSON, S.J. & MINTON, P. (1979). A method of measuring low velocities in large hydraulic models. Procs. of Inst. of Civil Engrs., 67(2), pp.203-211.

ROSENBLAD, J.L. (1968). Development of a rock-like model material. Preprint, 10th Symp. Rock Mech., University of Texad, Austin.

ROSENBLAD, J.L. (1969). Development of equipment for testing models of jointed rock masses. Rock Mechanics - Theory and Practice, Proc. 11th Symp. Rock Mech., Berkeley, Paper No. 8, pp.127-146.

RUSSELL, J.J. & BLAKEY, F.A. (1956). Physical and mechanical properties of one-case gypsum plaster: plaster AB/2. Aust. J. Appl. Sci., 7, pp.176-190.

SOUTHWELL, R.V. (1940). Relaxation methods in engineering science. Oxford University Press. First Edition.

STIMPSON, B. (1970). Modelling materials for engineering rock mechanics. Int. J. Rock Mech. Min. Sci., Vol. 7, pp.77-121.

TERZAGHI, K. (1946). Introduction to tunnel geology. In "Rock Tunnelling with Steel Supports" by Proctor and White (Commercial Shearing and Stamping Co., Youngstown, Ohio).

THEOCARIS, P.S. (1962). Moire fringes: a powerful measuring device. Applied Mechanics Reviews, Vol. 15, No. 5, pp.333-339.

TOWNSEND, P. (1980). An investigation of the effects of tensile failures on planes of weakness near an underground opening. M.Sc. Dissertation, University of London.

TROLLOPE, D.H. (1966). The stability of trapezoidal openings in rock masses. Rock Mech. & Eng. Geol., Vol. 4, No. 3, pp.232-241.

TROLLOPE, D.H. (1968). The mechanics of discontinua or clastic mechanics in rock problems. Chapter 9 in "Rock Mechanics in Engineering Practice", K.G. Stagg and O.C. Zienkiewicz (eds.), London, Wiley, 1968.

TROLLOPE, D.H. & BROWN, E.T. (1965). Pressure distributions in some discontinua. Water Power, August, pp.310-313.

VARGAS, E.A. (1981). Ph.D. Thesis, University of London (in preparation).

VOEGELE, M.D. (1978). An interactive graphics based analysis of the support requirements of excavations in jointed rock masses. Ph.D. Thesis, University of Minnesota, Minneapolis.

WARNER, M.F. (1979). The effects of certain boundary conditions and physical properties on the stability of an underground opening in a jointed rock mass. M.Sc. Dissertation, University of London.

WICKENS, E.H. & BARTON, N.R. (1971). The application of photogrammetry to the stability of excavated rock slopes. Photogrammetric Record, 7(37), pp.46-54.

# *APPENDICES*

APPENDIX I:

A. Rigid Block Displacement Transformation:

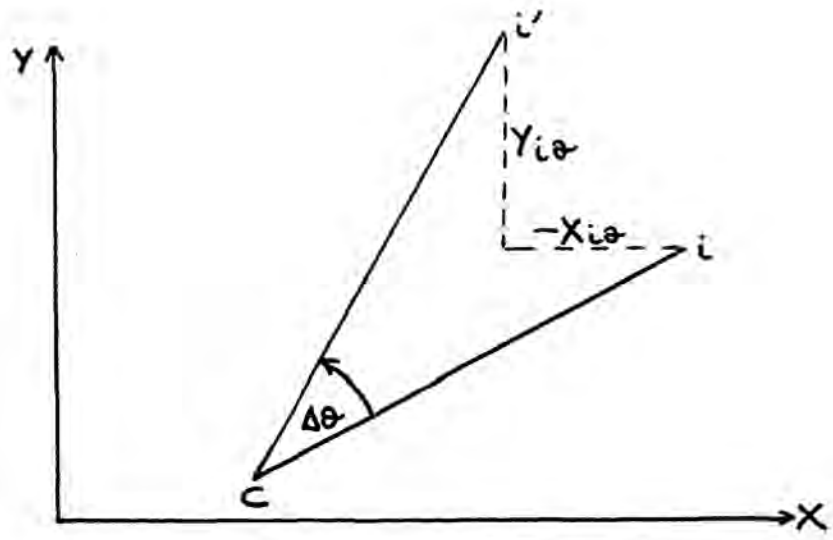



Figure A.1: Rigid Block Displacement Transform

Since the blocks are rigid, the complete motion of any point within a block may be defined by the motion relative to some other point. In particular, the displacements of the block corners can be defined in terms of the displacements of the block centroid. If the centroid C undergoes translation $\Delta X$, $\Delta Y$ and a rotation $\Delta\theta$ as shown in Figure A.1, then the displacements of corner point i can be described as

$$\Delta X_i = \Delta X + X_{i\theta}$$

$$\Delta Y_i = \Delta Y + Y_{i\theta}$$

where $X_{i\theta}$ , $Y_{i\theta}$ represent the displacement components of point i due to the rotation of the block about C.

Using trigonometry, it can be shown that

$$X_{i\theta} = (X_i - X_c)(\cos\Delta\theta - 1) - (Y_i - Y_c)\sin\Delta\theta$$

$$Y_{i\theta} = (X_i - X_c)\sin\Delta\theta + (Y_i - Y_c)(\cos\Delta\theta - 1)$$

Using truncated power series expansions for the sine and

cosine functions yields

$$\sin\Delta\theta = \Delta\theta - \Delta\theta^3/3!$$

$$\cos\Delta\theta = 1 - \Delta\theta^2/2!$$

it can be shown that:

$$\Delta X_i = \Delta X - (Y_i - Y_c)\Delta\theta - (X_i - X_c)\Delta\theta^2/2 + (Y_i - Y_c)\Delta\theta^3/6$$

$$\Delta Y_i = \Delta Y + (X_i - X_c)\Delta\theta - (Y_i - Y_c)\Delta\theta^2/2 - (X_i - X_c)\Delta\theta^3/6$$

The transformation reduces to a linear version for small values of rotation $\Delta\theta$, for which second and higher order terms can be neglected. Thus

$$\Delta X_i = \Delta X - (Y_i - Y_c)\Delta\theta$$

$$\Delta Y_i = \Delta Y + (X_i - X_c)\Delta\theta$$

B. Calculation of Rigid Block Displacements:

The three components of rigid body displacement (rotation $\Delta\theta$ and translation $\Delta X$ and $\Delta Y$) could be calculated from a knowledge of the initial and final global corner co-ordinates. The co-ordinates of three block corners were required.

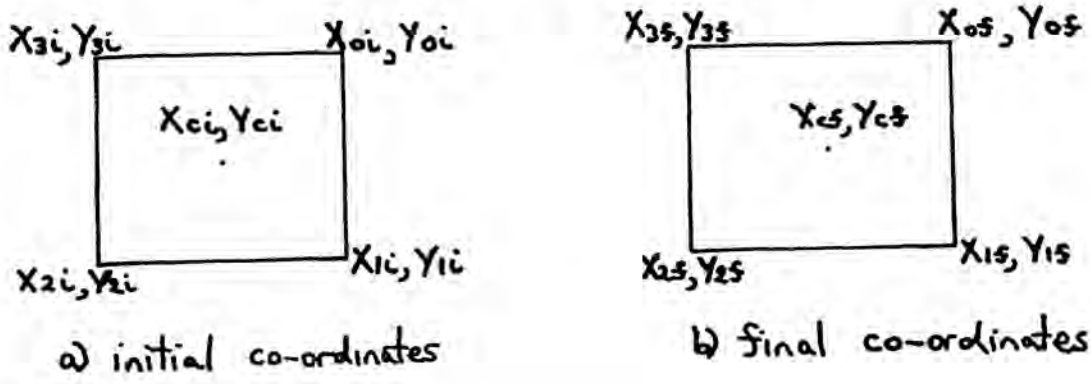



Figure A.2: Global block corner co-ordinates

Considering corners 0 and 3, one of four possible combinations is as follows:

$$(X_{of} - X_{oi}) = \Delta X + \Delta\theta(Y_{ci} - Y_{oi})$$

$$(Y_{of} - Y_{oi}) = \Delta Y + \Delta\theta\,(X_{oi} - X_{ci})$$

$$(X_{3f} - X_{3i}) = \Delta X + \Delta\theta\,(Y_{ci} - Y_{3i})$$

Thus, the three equations can be solved for the three unknowns ( $\Delta X$, $\Delta Y$, $\Delta\theta$), and a similar procedure can be carried out for the other combinations. When calculating $\Delta X$, $\Delta Y$ and $\Delta\theta$, all possible combinations of block corners were considered and average values obtained for the unknowns.

APPENDIX II:

Derivation of simultaneous equations for static relaxation method:

Consider the rigid block in Figure 2.12 which is surrounded by 4 other blocks such that there are 6 corner-edge contacts generated.

The problem is to determine the incremental displacements and rotations of the block ($\Delta X^a$, $\Delta Y^a$, $\Delta\theta^a$) for the $(N+1)^{th}$ iteration due to out-of-balance forces and moments acting on the block after the completion of the $N^{th}$ iteration.

The unit problem for the solution procedure is based on the block displacing in such a manner so as to liquidate completely the residual forces and moments i.e. to satisfy equilibrium.

Thus, for this block, the following equations must be satisfied during any one iteration

i) $$\sum_{i=1}^{6} FX^a{}_i + \sum_{i=1}^{6} \Delta FX^a{}_i + FX_{load} = 0$$

ii) $$\sum_{i=1}^{6} FY^a{}_i + \sum_{i=1}^{6} \Delta FY^a{}_i + W^a + FY_{load} = 0$$

iii) $$\sum_{i=1}^{6} (FY^a{}_i + \Delta FY^a{}_i)(X_i - \Delta\theta^a (Y_i - Y^a{}_c) - X^a{}_c) - \sum_{i=1}^{6} (FX^a{}_i + \Delta FX^a{}_i)(Y_i + \Delta\theta^a (X_i - X^a{}_c) - Y^a{}_c) + M_{load} = 0$$

where

$$\sum_i FX^a{}_i,\ \sum_i FY^a{}_i,\ FX_{load},\ FY_{load},\ M_{load},\ W^a,\ X_i,\ X^a{}_c,\ Y_i,\ Y^a{}_c$$

are all known; and

$FX^a{}_i$ $FY^a{}_i$ are the global contact forces for the $i^{th}$ contact after iteration N;

$\Delta FX^a{}_i, \Delta FY^a{}_i$ are the incremental global contact forces for the $i^{th}$ contact due to the block moving under the influence of residual forces during the $(N+1)^{th}$ iteration;

$W^a$ is the self weight of block 'a';

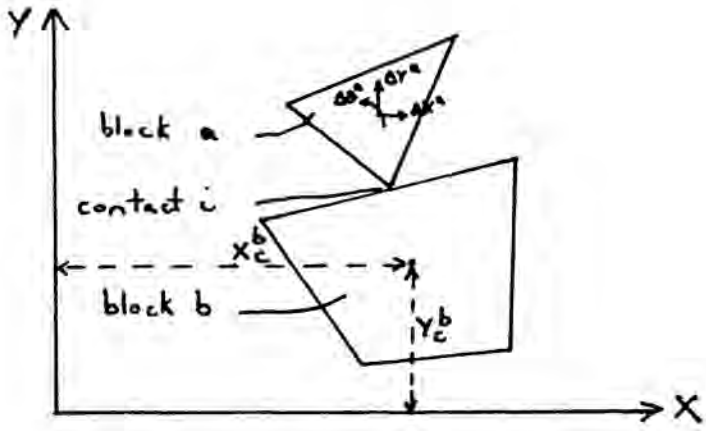
$FX_{load}$, $FY_{load}$, $M_{load}$ are the resultant global X, Y, and

moment external loads acting on the block after the $N^{th}$ iteration;

$X_i$, $Y_i$ are the global contact point co-ordinates;

$X^a_c$, $Y^a_c$ are the global block centroid co-ordinates.

Now. consider a single corner-edge contact as shown below, and assume that the constraints on block 'a' have been relaxed.




Since all blocks are considered to be rigid, the incremental global displacements at the contact point i can be defined in terms of the global centroidal co-ordinates ($X^a_c$, $Y^a_c$), the global contact point co-ordinates ($X_i$, $Y_i$) and the global incremental centroidal displacements ($\Delta X^a, \Delta Y^a, \Delta \theta^a$). Thus, to a first order approximation (see Appendix I).

$$\Delta Y^a_i = \Delta Y^a + \Delta \theta^a (X_i - X^a_c)$$

and

$$\Delta X^a_i = \Delta X^a - \Delta \theta^a (Y_i - Y^a_c)$$

$\Delta X^a_i$ and $\Delta Y^a_i$ are the relative incremental displacements of block 'a' relative to block 'b' since the solution procedure assumes that only block 'a' is free to move, all other blocks being fixed in position by the constraints. The global force increments due to these relative displacements can be evaluated via the constitutive relationship for the contact. Therefore

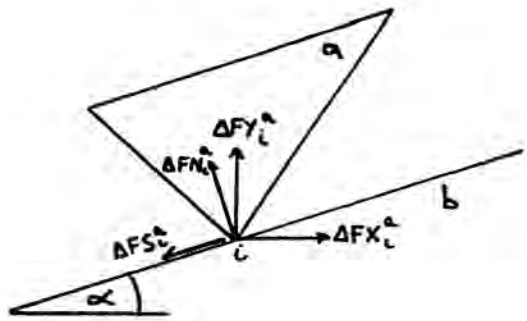
$$\Delta FY^a_i = KY_i * \Delta Y^a_i$$

and

$$\Delta FX^a_i = KX_i * \Delta X^a_i$$

where $KY_i$. $KX_i$ are the global joint stiffnesses.

· These global force increments can be resolved into local normal and shear components perpendicular and parallel respectively to the edge of the contact.



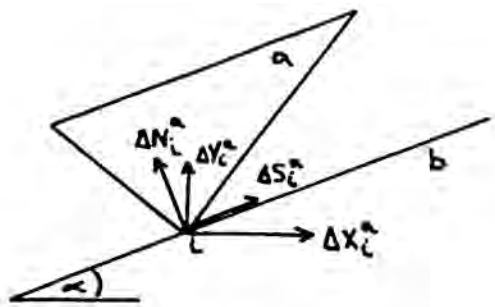

all forces and angles shown acting in positive directions

Thus

$$\Delta FX^a_i = - \Delta FS^a_i * \cos \alpha - \Delta FN^a_i * \sin \alpha$$

$$\Delta FY^a_i = - \Delta FS^a_i * \sin \alpha + \Delta FN^a_i * \cos \alpha$$

These normal and shear incremental force components are due to the relative incremental normal and shear displacements ($\Delta N^a_i$, $\Delta S^a_i$) at contact i.



Also, $\Delta FN^a_i = - \Delta N^a_i * KN_i$ (since $N^a_i$ is negative for an overlap)

and

$$\Delta FS^a_i = + \Delta S^a_i * KS_i$$

where

$KN_i$ and $KS_i$ are the normal and shear joint stiffnesses.

The normal and shear displacements $\Delta N^a_i$ and $\Delta S^a_i$ are related to the relative global incremental displacements $\Delta X^a_i$ and $\Delta Y^a_i$ by the following transformation equations.

$$\Delta S^a_i = \Delta X^a_i * \cos \alpha + \Delta Y^a_i * \sin \alpha$$

$$\Delta N^a_i = \Delta Y^a_i * \cos \alpha - \Delta X^a_i * \sin \alpha$$

Therefore

$$\Delta FX^a_i = -\Delta FS^a_i * \cos \alpha - \Delta FN^a_i * \sin \alpha$$

$$= -\Delta S^a_i * KS_i * \cos \alpha + \Delta N^a_i * KN_i * \sin \alpha$$

$$= -[\Delta X^a - \Delta \theta^a (Y_i - Y^a_c)] * KS_i * \cos^2 \alpha$$

$$-[\Delta Y^a + \Delta \theta^a (X_i - X^a_c)] * KS_i * \cos \alpha \sin \alpha$$

$$+[\Delta Y^a + \Delta \theta^a (X_i - X^a_c)] * KN_i * \cos \alpha \sin \alpha$$

$$-[\Delta X^a - \Delta \theta^a (Y_i - Y^a_c)] * KN_i * \sin^2 \alpha$$

The coefficients of the incremental global centroidal displacements ($\Delta X^a$, $\Delta Y^a$, $\Delta \theta^a$) due to the global contact force increments in the X direction can therefore be summed over all contacts. These are as follows:

| coefficients of | |
|---|---|
| $\Delta X^a$ (XCOX) | $\sum (- KS_i * \cos^2 \alpha - KN_i * \sin^2 \alpha )$ |
| $\Delta Y^a$ (XCOY) | $\sum (- KS_i * \cos \alpha \sin \alpha + KN_i * \cos \alpha \sin \alpha )$ |
| $\Delta \theta^a$ (XCOM) | $\sum (KS_i (\cos^2 \alpha * (Y_i - Y^a_c) - \sin \alpha \cos \alpha * (X_i - X^a_c))$ $+ KN_i (\cos \alpha \sin \alpha * (X_i - X^a_c) + \sin^2 \alpha * (Y_i - Y^a_c))]$ |

where $\sum$ implies the summation over all contact points for block 'a'. The variables XCOX, XCOY, XCOM are used to store these summations in the Fortran implementation.

Likewise, the coefficients of $\Delta X^a$, $\Delta Y^a$ and $\Delta\theta^a$ due to the global contact force increments in the Y direction and the incremental moments about the centroid can be determined. These are tabulated as follows:

| coefficients of | |
|---|---|
| $\Delta X^a$ (YCOX) | $\sum(-KS_i * \cos\alpha \sin\alpha + KN_i * \cos\alpha \sin\alpha)$ |
| $\Delta Y^a$ (YCOY) | $\sum(-KS_i * \sin^2\alpha - KN_i * \cos^2\alpha)$ |
| $\Delta\theta^a$ (YCOM) | $\sum[KS_i(\cos\alpha \sin\alpha * (Y_i - Y^a_c) - \sin^2\alpha * (X_i - X^a_c)) - KN_i(\cos^2\alpha * (X_i - X^a_c) + \cos\alpha \sin\alpha * (Y_i - Y^a_c))]$ |
| $\Delta X^a$ (MCOX) | $\sum(YCOX * (X_i - X^a_c) - XCOX * (Y_i - Y^a_c))$ |
| $\Delta Y^a$ (MCOY) | $\sum(YCOY * (X_i - X^a_c) - XCOY * (Y_i - Y^a_c))$ |
| $\Delta\theta^a$ (MCOM) | $\sum[YCOM * (X_i - X^a_c) - XCOM * (Y_i - Y^a_c) - FY^a_i * (Y_i - Y^a_c) - FX^a_i (X_i - X^a_c)]$ |

where YCOX, YCOY, YCOM are the variables relating to the global contact force increments in the Y direction and MCOX, MCOY, MCOM are the variables relating to the incremental moments about the centroid.

Therefore, the three equations of equilibrium can be expressed in terms of the three unknowns $\Delta X^a$, $\Delta Y^a$ and $\Delta\theta^a$ as follows:

$$XCOX * \Delta X^a + XCOY * \Delta Y^a + XCOM * \Delta\theta^a + XLOAD = 0$$

$$YCOX * \Delta X^a + YCOY * \Delta Y^a + YCOM * \Delta\theta^a + YLOAD = 0$$

$$MCOX * \Delta X^a + MCOY * \Delta Y^a + MCOM * \Delta\theta^a + MLOAD = 0$$

where

$$XLOAD = \sum_i FX_i + FX_{load}$$

$$YLOAD = \sum_i FY_i + W + FY_{load}$$

$$MLOAD = \sum_i FY_i (X_i - X^a_c) - \sum_i FX_i (Y_i - Y^a_c) + M_{load}$$

Note that the matrix of coefficients is symmetric.

APPENDIX III:

Representing a Continuum by the Rigid Block Model:

In the following it is shown the way in which model stiffnesses should be chosen so as to adequately simulate the elasticity of the system.

A. Normal Stiffnesses in an Infinite Continuum:

Consider an infinite rectangular array of blocks set up to represent an infinite continuum (Figure A.3). A single unit of this array is selected, which consists of one block with half-springs attached to the edges (Figure A.3). Each half-spring has double the stiffness of the original complete spring.

If normal loads $F_x$, $F_z$ are applied as shown then only normal stiffnesses need be considered.

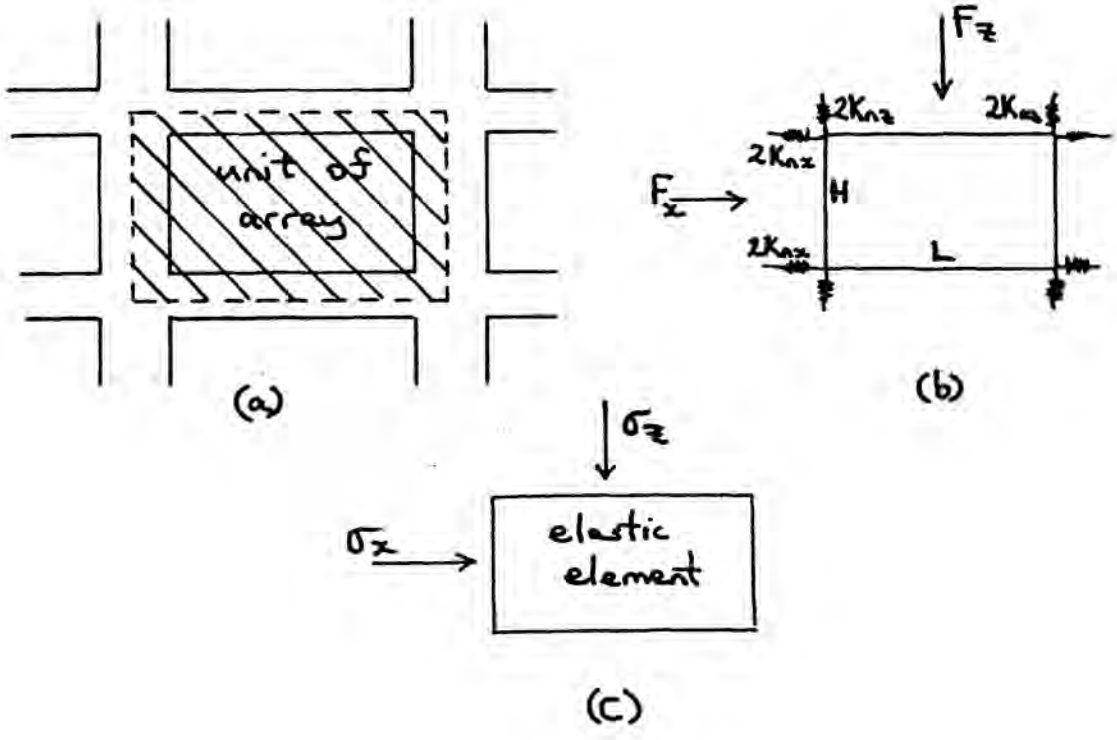



Figure A.3: Representing a Continuum by Rigid Blocks - Normal Stiffness.

The vertical contraction for the unit element is

$$F_z \left( \frac{1}{4K_{nz}} + \frac{1}{4K_{nz}} \right) = \frac{F_z}{2K_{nz}}$$

Similarly, overall horizontal contraction is

$$\frac{F_x}{2K_{nx}}$$

The element is assumed to represent an element of an isotropic elastic continuum of the same dimensions (H,L) and of unit thickness, subjected to the same applied loads ($F_x$, $F_z$) - see Figure A.3.

Thus, vertical contraction $\epsilon_z H = \frac{H}{E} (\sigma_z - \nu\sigma_x)$

$$= \frac{H}{E} \left(\frac{F_z}{L} - \nu \frac{F_x}{H}\right)$$

Similarly, horizontal contraction $= \frac{L}{E} \left(\frac{F_x}{H} - \nu \frac{F_z}{L}\right)$

Therefore, combining with previous expressions gives

$$\nu = 0$$

$$K_{nz} = \frac{EL}{2H}$$

$$K_{nx} = \frac{EH}{2L}$$

showing that the model cannot allow for the Poisson effect. Jaegar and Cook (1976) conclude that $\nu$ ROCK MASS is less than $\nu$ INTRINSIC if the rock mass contains equidimensional cavities or very flat, open cracks. The Poisson effect is likely to be small when compared with normal deformation and slip movements and may be ignored.

B. Shear Stiffnesses in an Infinite Continuum:

Shear forces $S_x$, $S_z$ are applied to the element so as to represent a state of pure shear and only shear stiffnesses $K_{sx}$, $K_{sz}$ are considered.

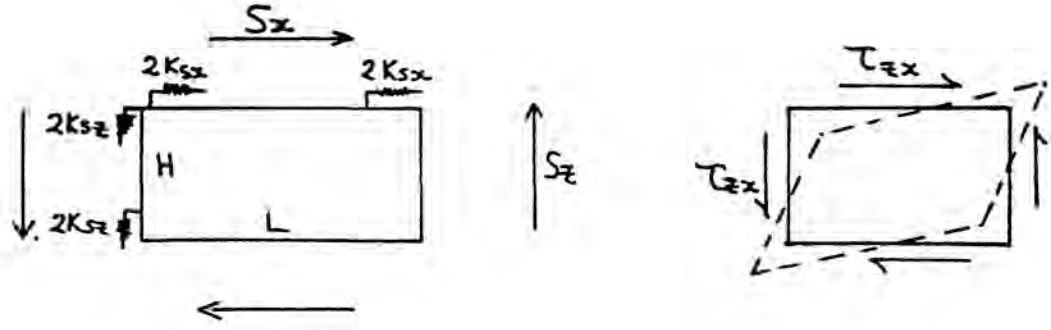



Figure A.4: Representing a Continuum by Rigid Blocks - Shear Stiffness.

The relative horizontal displacement between the top and bottom of the element, $U_x = S_x/2K_{sx}$. The relative vertical displacement between the sides of the element, $U_z = S_z/2K_{sz}$. Comparison with the continuum gives

$$S_z = \tau_{zx} \cdot H$$

$$S_x = \tau_{zx} \cdot L$$

$$\gamma_{zx} = \frac{U_z}{L} + \frac{U_x}{H} = \frac{S_z}{2K_{sz}L} + \frac{S_x}{2K_{sx}H} = \frac{\tau_{zx}}{2}\left(\frac{H}{K_{sz}L} + \frac{L}{K_{sx}H}\right)$$

Now $\gamma_{zx} = \tau_{zx}/G$

$$\therefore \tfrac{1}{2}\left(\frac{H}{K_{sz}L} + \frac{L}{K_{sx}H}\right) = \frac{1}{G}$$

Since $\nu = 0$, $G = E/2$

$$\therefore \quad \frac{H}{K_{sz}L} + \frac{L}{K_{sx}H} = \frac{4}{E}$$

This equation is satisfied by various combinations of $K_{sz}$ and $K_{sx}$. One choice may be

$$K_{sz} = EH/2L$$

$$K_{sx} = EL/2H$$

C. Representing a Bounded Continuum:

Providing that all boundary blocks which carry an external load are provided with external half-springs of double the complete spring stiffness, then the above relationships between spring stiffness and elastic constants will still apply. If these boundary springs are omitted, then the block model represents a continuum bounded by an infinitely stiff edge.

## APPENDIX IV

### A. Summary of Photogrammetric Process:

The purpose of the photogrammetry was to enable the rigid body components of translation and rotation for selected model bricks to be determined. The following steps summarize the photogrammetric process described in Chapter 5 (also see Robinson, 1979).

1) After the model had been positioned ready for testing and the photogrammetric control established, the model was photographed to determine the initial ('zero') positions of the bricks;

2) the model was next photographed when the loading ratio was such that movement of the model material surrounding the excavation(s) had been induced. This enabled the deflected positions of the model bricks to be determined;

3) the relevant co-ordinates (x and y) on each negative were measured relative to the travelling microscope axes. The corners of the plaster bricks, the required number of photogrammetric control points and the 8 edge points were all recorded;

4) the co-ordinates of the centre of each negative relative to the analyzer axes were calculated using the 8 edge point measurements;

5) the space co-ordinates of the corners of the model elements in each negative were determined by inputting the control point measurements, their known space co-ordinates from the triangulation survey and the negative centre co-ordinates into the computer program listed in Section B. In this way, the computer program was used in calibration mode;

6) the absolute displacement components in the global x and y directions of each brick corner were found by subtracting the global co-ordinates of each brick corner as determined for the initial 'unloaded' condition from the global co-ordinates for the same brick corner as determined for the 'loaded' condition;

7) knowing the global X and Y displacements of at least 3 corners of each brick enabled the components of rigid body translation and rotation to be determined. This is outlined in Appendix I. Since global co-ordinates for all 4 corners of each brick were determined, all possible combinations involving three sets of corner co-ordinates enabled the average rigid body centroidal displacements to be calculated;

8) the rigid body displacements for selected bricks in each model experiment were plotted as vectors, using the computer, where the length of each vector represented the magnitude of the resultant translation while the magnitude of rotation was printed out (in radians) alongside each vector. These plots are presented in Chapter 6.

B. PROGRAM GIRDER - conversion of photo co-ordinates to planimetric rectangular co-ordinates.

```
      PROGRAM GIRDER(INPUT,OUTPUT,TMIC23,TAPE5=INPUT,TAPE6=OUTPUT,
     *TAPE7=TMIC23,TAPE1)
      DIMENSION PHOTX(300),PHOTY(300),ZE(300),XN(300),YH(300),
     1RHS(9),X(300),Y(300),DX(300),DY(300),DH(300),CPHOTX(300),
     2CPHOTY(300),EQNM(45),VCV(45),EQOB(9),XRDNG(300),YRDNG(300),
     3IDENT(300)
      COMMON ROT(3,3),PI,SINPHI,SINW,SINKAP
      DATA NKNWNS/6/
      DATA PHI,OMEGA,CAPPA/ 0.00, 0.00, 0.00/
      INDEX(NROW,NCOL)=NCOL*(1+2*NKNWNS-NCOL)/2-NKNWNS+NROW
      PI=4.*ATAN(1.)
      RADN=45./ATAN(1.)
      SINPHI=SIN(PHI)
      SINW=SIN(OMEGA)
      SINKAP=SIN(CAPPA)
      READ(5,27) CENTRX,CENTRY
   27 FORMAT(2F10.2)
      READ(5,10) NPTS,KNTROL,ITERTN
   10 FORMAT(3I5)
      READ(5,63)PD,PPX,PPY
   63 FORMAT(3F10.2)
      IF(ITERTN.EQ.0) ITERTN=3
      WRITE(6,108)
  108 FORMAT(1H1)
      WRITE(6,109) PPX,PPY
  109 FORMAT(*0CO-ORDINATES OF PRINCIPAL POINT RELATIVE TO PLATE CENTRE
     1AS ORIGIN*//11X,*X =*,F8.6,*Y =*,F8.6,/)
      WRITE(6,110) CENTRX,CENTRY
  110 FORMAT(/* PLATE CENTRE CO-ORDINATES   X =*,F9.6,*  Y =*,F9.6,* MM*
     1//)
      WRITE(6,111)
  111 FORMAT(1HO,14X,*PHOTO CO-ORDINATES*,17X,*SPACE CO-ORDINATES*//
     117X,*X*,10X,*Y*,16X,*Z*,10X,*X*,10X,*Y*/)
      READ(5,11)H,XNPC,YZPC,(IDENT(I),ZE(I),XN(I),YH(I),I=1,KNTROL)
   11 FORMAT(3F10.1,/(A10,3F10.2))
      KNTPLO=KNTROL+1
      DO 226 I=KNTPLO,NPTS
      ZE(I)=-20.0000
  226  CONTINUE
      DO 221 I=1,NPTS
      READ(7,220)XRDNG(I),YRDNG(I)
  220 FORMAT(2F7.2)
      XRDNG(I)=XRDNG(I)/1000.
      YRDNG(I)=YRDNG(I)/1000.
  221 CONTINUE
      SUM=0.
      DO 18 I=1,NPTS
      SUM=SUM+ZE(I)
      PHOTX(I)=XRDNG(I)-CENTRX-PPX
   18 PHOTY(I)=YRDNG(I)-CENTRY-PPY
      ZMEAN=SUM/FLOAT(NPTS)
      DO 19 I=1,NPTS
   19 ZE(I)=ZE(I)-ZMEAN
      H=H-ZMEAN
      WRITE(6,13) XNPC,YZPC
   13 FORMAT(/* PERSPECTIVE CENTRE CO-ORDINATES  X =*,F8.5,*  Y =*,F9.5)
      CALL ENZXY
      DO 12 I=1,NPTS
      DH(I)=H-ZE(I)
      SCALE=(ROT(1,3)*PHOTX(I)+ROT(2,3)*PHOTY(I)+ROT(3,3)*PD)/DH(I)
      X(I)=XNPC+(ROT(1,1)*PHOTX(I)+ROT(2,1)*PHOTY(I)+ROT(3,1)*PD)/SCALE
      Y(I)=YZPC+(ROT(1,2)*PHOTX(I)+ROT(2,2)*PHOTY(I)+ROT(3,2)*PD)/SCALE
      DX(I)= X(I)-XNPC
      DY(I)= Y(I)-YZPC
      IF(I.LE.KNTROL) DX(I)=XN(I)-XNPC
      IF(I.LE.KNTROL) DY(I)=YH(I)-YZPC
   12 CONTINUE
      WRITE(6,112)
  112 FORMAT(//14X,*PHOTO CO-ORDINATES*,12X,*SPACE CO-ORDINATES*,
     1//17X,*X*,10X,*Y*,16X,*X*,10X,*Y*/)
      DO 4 LOOP=1,ITERTN
      NOTCH=0
      WRITE(6,101) LOOP
  101 FORMAT(//61X,*ITERATION NO.*,I2//)
      P=PHI/RADN
      DO 3 I=1,KNTROL
      SCALE=(ROT(1,3)*PHOTX(I)+ROT(2,3)*PHOTY(I)+ROT(3,3)*PD)/DH(I)
      XBYF=PHOTX(I)/PD
      YBYF=PHOTY(I)/PD
      EQOB(1)=SCALE*(ROT(1,1)-ROT(3,1)*XBYF)
      EQOB(2)=SCALE*(ROT(1,2)-ROT(3,2)*XBYF)
      EQOB(3)=-SCALE*(ROT(1,3)-ROT(3,3)*XBYF )
      EQOB(4)=PHOTY(I)*(ROT(3,3)+ROT(1,3)*XBYF)-ROT(2,3)*(PD+PHOTX(I)*
     1XBYF)
      EQOB(5)=-PHOTY(I)*(SIN(P)+XBYF*COS(P))
      EQOB(6)=-(PD+PHOTX(I)*XBYF)
      IF(NKNWNS.EQ.6) GO TO 23
      EQOB(7)= DX(I)/DH(I)
      EQOB(8)=1.
      EQOB(9)=0.
   23 ARITHC=PHOTX(I)-(ROT(1,1)*DX(I)+ROT(1,2)*DY(I)+ROT(1,3)*DH(I))*
     1SCALE
      CALL INDOBS(EQNM,VCV,RHS,EQOB ,ARITHC,NOTCH,KNTROL,NKNWNS)
      EQOB(1)=SCALE*(ROT(2,1)-ROT(3,1)*YBYF)
      EQOB(2)=SCALE*(ROT(2,2)-ROT(3,2)*YBYF)
      EQOB(3)=-SCALE*(ROT(2,3)-ROT(3,3)*YBYF)
      EQOB(4)=-PHOTX(I)*(ROT(3,3)+ROT(2,3)*YBYF)+ROT(1,3)*(PD+PHOTY(I)*
     1YBYF)
      EQOB(5)=PHOTX(I)*SIN(P)-(PD+PHOTY(I)*YBYF)*COS(P)
      EQOB(6)=-PHOTX(I)*YBYF
      IF(NKNWNS.EQ.6) GO TO 24
      EQOB(7)= DY(I)/DH(I)
      EQOB(8)=0.
      EQOB(9)=1.
   24 ARITHC=PHOTY(I)-(ROT(2,1)*DX(I)+ROT(2,2)*DY(I)+ROT(2,3)*DH(I))*
     1SCALE
      NOTCH=NOTCH+1
    3 CALL INDOBS(EQNM,VCV,RHS,EQOB ,ARITHC,NOTCH,KNTROL,NKNWNS)
      XNPC=XNPC-RHS(1)
      YZPC=YZPC-RHS(2)
      H=H-RHS(3)+ZMEAN
      SINKAP=SINKAP+RHS(4)
      SINW=SINW+RHS(5)
      SINPHI=SINPHI+RHS(6)
      IF(NKNWNS.EQ.6) GO TO 25
      PD=PD+RHS(7)
      PPX=PPX+RHS(8)
      PPY=PPY+RHS(9)
   25 CAPPA=ASIN(SINKAP)*RADN
      PHI=ASIN(SINPHI)*RADN
      OMEGA=ASIN(SINW)*RADN
   21 FORMAT(* PRINCIPAL DISTANCE =*,F7.5,* MM      DISTANCE FROM DATUM
     1PLANE ("FLYING HEIGHT") =*,F9.5//* TILTS IN DEGREES  / PHI =*,
     2F10.4,*  / OMEGA =*,F10.4,*  / KAPPA =*,F10.4,*  /*)
      WRITE(6,21) PD,H,PHI,OMEGA,CAPPA
      WRITE(6,13) XNPC,YZPC
      WRITE(6,109)PPX,PPY
      H=H-ZMEAN
```

```
      CALL ENZXY
      DO 22 I=1,NPTS
      DH(I)=H-ZE(I)
      DX(I)= X(I)-XNPC
      DY(I)= Y(I)-YZPC
      IF(I.LE.KNTROL) DX(I)=XN(I)-XNPC
      IF(I.LE.KNTROL) DY(I)=YH(I)-YZPC
      IF(NKNWNS.EQ.6) GO TO 26
      PHOTX(I)=PHOTX(I)-RHS(8)
      PHOTY(I)=PHOTY(I)-RHS(9)
   26 SF=DH(I)/(ROT(1,3)*PHOTX(I)+ROT(2,3)*PHOTY(I)+ROT(3,3)*PD)
      X(I)=XNPC+(ROT(1,1)*PHOTX(I)+ROT(2,1)*PHOTY(I)+ROT(3,1)*PD)*SF
   22 Y(I)=YZPC+(ROT(1,2)*PHOTX(I)+ROT(2,2)*PHOTY(I)+ROT(3,2)*PD)*SF
      IF(LOOP.NE.ITERTN)GO TO 235
      WRITE(6,112)
      WRITE(6,16)(IDENT(I),XRDNG(I),YRDNG(I),X(I),Y(I),I=1,KNTROL)
   16 FORMAT(1X,A10,2F10.6,10X,2F15.5)
      DO 229 I=KNTPLO,NPTS
      WRITE(6,502)I,XRDNG(I),YRDNG(I),X(I),Y(I)
  502 FORMAT(1X,I10,2F10.6,10X,2F15.5)
  229 CONTINUE
  235 CONTINUE
    4 CONTINUE
      DO 236 I=1,NPTS
      WRITE(1,503)X(I),Y(I)
  503 FORMAT(2F15.5)
  236 CONTINUE
      SUM=0.
      DO 44 I=1,NPTS
      SF=DH(I)/(ROT(1,3)*PHOTX(I)+ROT(2,3)*PHOTY(I)+ROT(3,3)*PD)
      PHOTX(I)=(ROT(1,1)*DX(I)+ROT(1,2)*DY(I)+ROT(1,3)*DH(I))/SF
      PHOTY(I)=(ROT(2,1)*DX(I)+ROT(2,2)*DY(I)+ROT(2,3)*DH(I))/SF
C
C    THE RESIDUALS ARE STORED IN THE ARRAYS CPHOTX AND CPHOTY.
C
      CPHOTX(I)=PHOTX(I)+CENTRX+PPX-XRDNG(I)
      CPHOTY(I)=PHOTY(I)+CENTRY+PPY-YRDNG(I)
      SUM=SUM+CPHOTX(I)*CPHOTX(I)+CPHOTY(I)*CPHOTY(I)
   44 CONTINUE
      WRITE(6,113)
  113 FORMAT(/14X,*PHOTO CO-ORDINATES     CALCULATED PHOTO CO-ORDINATES*
     1,10X,*RESIDUALS*//31X,*RELATIVE TO PRINCIPAL POINT AS ORIGIN*//
     216X,*X*,9X,*Y*,17X,*X*,9X,*Y*,20X,*X*,9X,*Y*/)
      WRITE(6,47)(IDENT(I),XRDNG(I),YRDNG(I),PHOTX(I),PHOTY(I),CPHOTX(I)
     1,CPHOTY(I),I=1,KNTROL)
   47 FORMAT(1X,A10,2F10.6,6X,2F10.6,11X,2F10.6)
      DO 239 I=KNTPLO,NPTS
      WRITE(6,48)I,XRDNG(I),YRDNG(I),PHOTX(I),PHOTY(I),
     1CPHOTX(I),CPHOTY(I)
   48   FORMAT(1X,I10,2F10.6,6X,2F10.6,11X,2F10.6)
  239   CONTINUE
      SEUNIT=SQRT(SUM/FLOAT(2*KNTROL-NKNWNS))
      WRITE(6,102) SEUNIT
  102 FORMAT(//* STANDARD ERROR OF PHOTO CO-ORDINATE READING=*,F9.6)
      DO 46 I=1,NKNWNS
      J=INDEX(I,I)
   46 RHS(I)=SEUNIT*SQRT(VCV(J))
      WRITE(6,103) RHS(1),RHS(2),RHS(3)
  103 FORMAT(/* S.E. OF PERSPECTIVE CENTRE CO-ORDINATES*,2F8.6//* S.E. O
     1F "FLYING HEIGHT"*,F8.6/)
      IF(NKNWNS.EQ.6) STOP
      WRITE(6,104) RHS(7),RHS(8),RHS(9)
  104 FORMAT(* S.E. OF PRINCIPAL DISTANCE*,F9.6//* S.E. OF PRINCIPAL POI
     INT CO-ORDINATES*,2F9.6/)
      STOP
      END
      SUBROUTINE ENZXY
      COMMON ROT(3,3),PI,SINPHI,SINW,SINKAP
      STCOS(A,B,C)=COS(A)*COS(B)+SIN(A)*SIN(B)*COS(C)
      STSIN(A,B)=SIN(A)*SIN(B)
      P=ASIN(SINPHI)
      COMP=PI/2.-P
      PRA=PI/2.+P
      COMW=PI/2.-ASIN(SINW)
      CAP=ASIN(SINKAP)
      COMK=PI/2.-CAP
      CAPRA=PI/2.+CAP
      ROT(1,1)=STCOS(P,CAP,COMW)
      ROT(1,2)=-STCOS(P,CAPRA,COMW)
      ROT(1,3)=-STSIN(P,COMW)
      ROT(2,1)=-STSIN(CAP,COMW)
      ROT(2,2)=STSIN(COMK,COMW)
      ROT(2,3)=-SINW
      ROT(3,1)=-STCOS(PRA,CAP,COMW)
      ROT(3,2)=STCOS(COMP,COMK,COMW)
      ROT(3,3)=STSIN(COMP,COMW)
      RETURN
      END
      SUBROUTINE INDOBS(EQNM,VCV,RHS,EQOB,ARITHC,NOTCH,KNTROL,NKNWNS)
      DIMENSION EQNM(45),VCV(45),RHS(9),EQOB(9)
      INDEX(NROW,NCOL)=NCOL*(1+2*NKNWNS-NCOL)/2-NKNWNS+NROW
      LMNTS=NKNWNS*(NKNWNS+1)/2
      IF(NOTCH.GT.0) GO TO 12
      DO 20 I=1,NKNWNS
   20 RHS(I)=0.
      DO 21 I=1,LMNTS
   21 EQNM(I)=0.
C
C THE CONTRIBUTIONS OF THE OBSERVATION EQUATIONS TAKEN ONE AT A TIME ARE
C ACCUMULATED IN ARRAY "EQNM" AND THE FIRST COLUMN OF ARRAY "RHS" TO FORM THE
C ELEMENTS OF THE L.H.S. MATRIX AND R.H.S. COLUMN VECTOR RESPECTIVELY OF THE
C NORMAL EQUATIONS.
C
   12 DO 1 K=1,NKNWNS
      RHS(K)=RHS(K)+EQOB(K)*ARITHC
      DO 2 L=1,K
      IM=INDEX(K,L)
      EQNM(IM)=EQNM(IM)+EQOB(K)*EQOB(L)
    2 CONTINUE
    1 CONTINUE
      IF(NOTCH.EQ.  KNTROL)CALLCHTRSI(EQNM,RHS,VCV,NKNWNS,LMNTS)
      RETURN
      END
      SUBROUTINE CHTRSI(A,R,V,N,LMNTS)
      DIMENSION A(45),V(45),R(9)
      INDEX(I,J)=J*(1+2*N-J)/2-N+I
      DO 1 I=1,LMNTS
    1 V(I)=0.
      INITL=1
      DO 2 I=1,N
      V(INITL)=1.
    2 INITL=INITL+N+1-I
C
C SYMMETRIC DECOMPOSITION
C
      A(1)=SQRT(A(1))
      DO  8 I=2,N
    8 A(I)=A(I)/A(1)
```

```
      DO 11 J=2,N
      JJ=INDEX(J,J)
      JLESS1=J-1
      DO 9 K=1,JLESS1
      JK=INDEX(J,K)
    9 A(JJ)=A(JJ)-A(JK)*A(JK)
      A(JJ)=SQRT(A(JJ))
      IF(J.EQ.N) GO TO 12
      JPLUS1=J+1
      DO 11 M=JPLUS1,N
      MJ=INDEX(M,J)
      DO 10 K=1,JLESS1
      JK=INDEX(J,K)
      MK=INDEX(M,K)
   10 A(MJ)=A(MJ)-A(JK)*A(MK)
   11 A(MJ)=A(MJ)/A(JJ)
C
C FORWARD SUBSTITUTION
C
   12 R(1)=R(1)/A(1)
      V(1)=V(1)/A(1)
      DO 22 I=2,N
      II=INDEX(I,I)
      ILESS1=I-1
      DO 21 J=1,ILESS1
      IJ=INDEX(I,J)
      DO 20 M=1,I
      IF(J.LT.M) GO TO 20
      IM=INDEX(I,M)
      JM=INDEX(J,M)
      V(IM)=V(IM)-A(IJ)*V(JM)
   20 CONTINUE
   21 R(I)=R(I)-A(IJ)*R(J)
      DO 23 M=1,I
      IM=INDEX(I,M)
   23 V(IM)=V(IM)/A(II)
   22 R(I)=R(I)/A(II)
C
C BACK SUBSTITUTION
C
      R(N)=R(N)/A(LMNTS)
      DO 30 J=1,N
      NJ=INDEX(N,J)
   30 V(NJ)=V(NJ)/A(LMNTS)
      DO 32 I=2,N
      K=N+1-I
      KK=INDEX(K,K)
      KPLUS1=K+1
      DO 31 J=KPLUS1,N
      JK=INDEX(J,K)
      DO 28 M=1,K
      KM=INDEX(K,M)
      JM=INDEX(J,M)
   28 V(KM)=V(KM)-A(JK)*V(JM)
   31 R(K)=R(K)-A(JK)*R(J)
      DO 29 M=1,K
      KM=INDEX(K,M)
   29 V(KM)=V(KM)/A(KK)
   32 R(K)=R(K)/A(KK)
      RETURN
      END
```

APPENDIX V

Preparation of Modelling Material:

The importance of manufacturing the plaster model bricks to obtain very accurate dimensions and reproducible material properties has been highlighted in Chapter 5. These and additional requirements specified for the model material indicated that a routine and carefully controlled preparation procedure must be adopted if quality control was to be achieved throughout the manufacturing process.

Some of the physical variables which may influence the resultant properties of the cured plaster specimens are the type of plaster and storage conditions under which it has been kept, the preparation and curing procedure, and the age of the plaster when testing is undertaken. Due to the large variation of these and other physical parameters throughout the world, it has not been possible for a standard manufacturing procedure to be adopted and this has generally led to each investigator establishing his own manufacturing criterion and material calibration. The steps involved in the casting procedure adopted in this study are listed as follows:

1) plaster and water in the proportions of 2.25 : 1 by weight were mixed together, the plaster being gradually added to the water during the mixing process. For those samples including a diatomaceous earth filler, the plaster and filler were thoroughly mixed before being added to the water;

2) mixing would occur slowly, by hand, for a period of between 5 and 10 minutes, depending on the mix quantities and setting times, with care being taken not to produce a vortex, so entrapping air in the mixture. The mixing time must be sufficient to ensure that bleeding is eliminated;

3) the thick and creamy mix was poured into the moulds immediately after mixing with the occasional tapping of the sides of the pouring container to drive entrapped air bubbles to the surface;

4) after pouring, the moulds were left to sit on glass plates without vibration until the hydration process was completed. During this process excess water would either drain from underneath the mould and onto the glass plates or would rise to the surface. It was usually necessary to displace this free surface water with additional plaster slurry;

5) when the mixture had almost set, the excess plaster on the surface was wiped off using a sharp edge. The bleeding of water from the mix during and after such screeding was kept to a minimum;

6) without further disturbance, the bricks within the moulds were left to cure for a period of between 30 and 60 minutes;

7) when the bricks had achieved sufficient integrity, the moulds were placed in an oven and heated to between 35 and 40 degrees C. for a period of 10 to 15 minutes. The moulds were then removed from the oven and the plaster bricks were removed from the moulds by applying light finger pressure to the base of each brick;

8) the bricks were placed on glass trays and left to cure at room temperature for at least three weeks. The bricks were cured to constant unit weight with the maximum variation in unit weight being less than 3%.

The resulting mix had a setting time which allowed for the mixing and pouring of a batch sufficient to fill three complete moulds i.e. 108 plaster bricks. It was found unnecessary to vibrate the moulds during and after pouring since vibration introduced further air bubbles into the mixture and also induced segregation of the constituents. After each batch, the rubber moulds were washed in water and thoroughly dried before reuse. The moulds were graded as to the size of brick they each produced, the slight variations in size between moulds being a function of the mould manufacture process. Bricks were carefully sorted during curing to ensure uniformity in dimensions, the maximum variation between brick dimensions being within $\pm$.025 mm for any one batch of bricks. There was found to be no significant variation between the properties of a brick and its position in the mould.

APPENDIX VI:

Listings of dynamic relaxation programs:

A. PROGRAM TEST - rigid block formulation developed by Hocking (1977)

```
*COMDECK,GENALL
      COMMON /GENALL/CX(20),CY(20),ANT(20),DIPA,DIPB,A,B,AA,BB,RHO,
     *                 BNN,BMASS,BMOI,NBASE,NROW,FF,HH,IAXIS,NON,SN,GRAV,
     *                 RATIO,SCAL,PI,SCALT,ANN,ITR,IZCYC,TITLE(20)
*COMDECK,MAIN
      COMMON /MAIN/FXX(20),FYY(20),SMM(20),BVLN(20,12),BVLS(20,12),
     *             SF(20,12),VXN(20),VYN(20),AVN(20),FPCYC(20),
     *             SMPCYC(20)
*COMDECK,CNEIGH
      COMMON /CNEIGH/NEIGH(20,8),N(4,3),NREMBV(30),NREM
*COMDECK,CCBBR
      COMMON /CCBBR/DMBVE(20),WEIGHT,BETA1,BETA2,XBRIG,YBRIG,
     *              IFIXED,IFIX(50)
*DECK,TEST
      PROGRAM TEST(INPUT=1002,OUTPUT,TAPE5=INPUT,TAPE6=1002,TAPE62,     MAINL
     *TAPE4=1002)                                                       MAINL
*CALL GENALL
*CALL MAIN
*CALL CNEIGH
*CALL CCBBR
      DIMENSION GEN(105),AMAI(880),CNE(203),CIG(76),REMBV(7)
      EQUIVALENCE (CX,GEN),(FXX,AMAI),(NEIGH,CNE),(DMBVE,CIG)           MAINL
      DATA DEGREE,PI/0.0174532925199E3,3.1415926535897B/                MAINL
      READ(5,198)(TITLE(I),I=1,8)                                       MAINL
      ITR=0                                                             MAINL
198   FORMAT(8A10)                                                      MAINL
      READ(5,700)DUM,RREST                                              MAINL
700   FORMAT(A5,F10.0)                                                  MAINL
      NRREST=RREST                                                      MAINL
      IF(NRREST.NE.2)GB TB 703                                          MAINL
      READ(4)  (GEN(I),I=1,105),(AMAI(I),I=1,880),(CNE(I),I=1,203),
     *(CIG(I),I=1,76)
703   CONTINUE                                                          MAINL
      WRITE(6,197)(TITLE(I),I=1,8)                                      MAINL
197   FORMAT(1H ,8A10)                                                  MAINL
      WRITE(6,399)                                                      MAINL
399   FORMAT(*  CARD        FIELD 1        FIELD 2        FIELD 3
     * FIELD 4        FIELD 5        FIELD 6        FIELD 7*,//)       MAINL
      WRITE(6,701)DUM,RREST                                             MAINL
701   FORMAT(1H ,A5,E15.8)                                              MAINL
      READ(5,100)NC,A,B,DIPA,DIPB,ANROW,ANBASE                          MAINL
      NROW=ANROW                                                        MAINL
      NBASE=ANBASE                                                      MAINL
      WRITE(6,101)NC,A,B,DIPA,DIPB,ANROW,ANBASE                         MAINL
      READ(5,100)NC,DT,FAC,CYCLES,PRINT,WHEN,ZCYCLE,WREST               MAINL
      NWREST=WREST                                                      MAINL
      READ(5,100)NC,SN,RSD,DMU,RHO,GRAV                                 MAINL
      NCYCLE=CYCLES                                                     MAINL
      IWHEN=WHEN                                                        MAINL
      IZCYC=ZCYCLE                                                      MAINL
      IPRINT=PRINT                                                      MAINL
      WRITE(6,101)NC,DT,FAC,CYCLES,PRINT,WHEN,ZCYCLE,WREST              MAINL
      READ(5,100)NC,SCAL,SCALT,VECL,XBRIG,YBRIG,ANEIB                   MAINL
      NEIB=ANEIB                                                        MAINL
      WRITE(6,101)NC,SCAL,SCALT,VECL,XBRIG,YBRIG,ANEIB                  MAINL
100   FORMAT(I5,7F10.0)                                                 MAINL
      WRITE(6,101)NC,SN,RSD,DMU,RHO,GRAV                                MAINL
101   FORMAT(1H ,I5,7E15.8/)                                            MAINL
      READ(5,100)NC,(REMBV(I),I=1,7)                                    MAINL
      WRITE(6,101)NC,(REMBV(I),I=1,7)                                   MAINL
      NREM=REMBV(1)                                                     MAINL
      DB 713 I=2,7                                                      MAINL
713   NREMBV(I-1)=REMBV(I)                                              MAINL
      IF(NREM.LE.6)GB TB 714                                            MAINL
      J=6                                                               MAINL
      DB 711 IIJ=1,10                                                   MAINL
      READ(5,100)NC,(REMBV(I),I=1,7)                                    MAINL
      WRITE(6,101)NC,(REMBV(I),I=1,7)                                   MAINL
      IF(NC.EQ.99)GB TB 714                                             MAINL
      DB 711 IJ=1,7                                                     MAINL
      J=J+1                                                             MAINL
711   NREMBV(J)=REMBV(IJ)                                               MAINL
714   CONTINUE                                                          MAINL
      IPCBN=1                                                           MAINL
      CALL PL(IPCBN)                                                    MAINL
      RSD=TAN(RSD*PI/180.)                                              MAINL
      DMU=TAN(DMU*PI/180.)                                              MAINL
      NTILT=0.                                                          MAINL
      VV=0.01                                                           MAINL
      PII=PI*2.                                                         MAINL
      RATIB=0.                                                          MAINL
      DIPA=DIPA*PI/180.                                                 MAINL
      DIPB=DIPB*PI/180.                                                 MAINL
      DELTA=DIPA                                                        MAINL
      FF=A/SIN(DIPA+DIPB)                                               MAINL
      HH=B/SIN(DIPA+DIPB)                                               MAINL
      ST=SN                                                             MAINL
      DISMAX=0.01                                                       MAINL
      IF(NRREST.EQ.2)GB TB 501                                          MAINL
      CALL CBBRDS                                                       MAINL
501   WEIGHT=BMASS*GRAV                                                 MAINL
      CALL NEIGHB                                                       MAINL
      IF(NRREST.EQ.2)GB TB 502                                          MAINL
      CALL CBNSBL                                                       MAINL
502   CONTINUE                                                          MAINL
      DSST=DT/BMASS                                                     MAINL
      DBIT=DT/BMBI                                                      MAINL
      DAMPN=(FAC*2.*SQRT(SN*BMASS))/DT                                  MAINL
      DAMPS=(FAC*2.*SQRT(ST*BMASS))/DT                                  MAINL
      IF(NRREST.EQ.2)GB TB 500                                          MAINL
      DB 206 I=1,NBN                                                    MAINL
      FXX(I)=0.                                                         MAINL
      FYY(I)=0.                                                         MAINL
      SMM(I)=0.                                                         MAINL
      VXN(I)=0.0                                                        MAINL
      VYN(I)=0.0                                                        MAINL
      AVN(I)=0.0                                                        MAINL
      DB 206 J=1,12                                                     MAINL
      BVLN(I,J)=0.                                                      MAINL
      BVLS(I,J)=0.                                                      MAINL
206   SF(I,J)=0.                                                        MAINL
500   ITR=ITR+1                                                         MAINL
      DB 44 I=1,NBN                                                     MAINL
      FXX(I)=0.                                                         MAINL
      FYY(I)=0.                                                         MAINL
      SMM(I)=0.                                                         MAINL
   44 CBNTINUE                                                          MAINL
      DB 68 I=1,NBN                                                     MAINL
      IF(NREM.EQ.0)GB TB 256                                            MAINL
      DB 156 J=1,NREM                                                   MAINL
      IF(NREMBV(J).EQ.I)GB TB 68                                        MAINL
156   CBNTINUE                                                          MAINL
256   CBNTINUE                                                          MAINL
      K=1.                                                              MAINL
      ANTI=ANT(I)                                                       MAINL
      SI=SIN(ANTI)                                                      MAINL
      CB=CBS(ANTI)                                                      MAINL
      IF(IAXIS.EQ.1)GB TB 40                                            MAINL
```

```
      ANTIC=DIPA+DIPB+ANTI                                                  MAINL
      SS=SIN(ANTIC)                                                         MAINL
      CC=COS(ANTIC)                                                         MAINL
      ANTII=DIPA+DIPB+ANTI-PI/2.                                            MAINL
      SOI=SIN(ANTII)                                                        MAINL
      COI=COS(ANTII)                                                        MAINL
      GO TO 41                                                              MAINL
   40 ANTIC=ANTI+PI-DIPA-DIPB                                               MAINL
      SS=SIN(ANTIC)                                                         MAINL
      CC=COS(ANTIC)                                                         MAINL
      ANTII=ANTI+PI/2.-DIPA-DIPB                                            MAINL
      SOI=SIN(ANTII)                                                        MAINL
      COI=COS(ANTII)                                                        MAINL
   41 CONTINUE                                                              MAINL
      UAA=AA*CO                                                             MAINL
      VAA=AA*SI                                                             MAINL
      UBB=BB*CC                                                             MAINL
      VBB=BB*SS                                                             MAINL
      DO 65 IL=1,4                                                          MAINL
      LL=2*IL                                                               MAINL
      GO TO (1,2,3,4) IL                                                    MAINL
    1 XX=CX(I)+UAA+UBB                                                      MAINL
      YY=CY(I)+VAA+VBB                                                      MAINL
      GO TO 52                                                              MAINL
    2 XX=CX(I)+UAA-UBB                                                      MAINL
      YY=CY(I)+VAA-VBB                                                      MAINL
      GO TO 52                                                              MAINL
    3 XX=CX(I)-UAA-UBB                                                      MAINL
      YY=CY(I)-VAA-VBB                                                      MAINL
      GO TO 52                                                              MAINL
    4 XX=CX(I)-UAA+UBB                                                      MAINL
      YY=CY(I)-VAA+VBB                                                      MAINL
   52 J=NEIGH(I,LL-1)                                                       MAINL
      GO TO 60                                                              MAINL
   54 J=NEIGH(I,LL+1)                                                       MAINL
      GO TO 60                                                              MAINL
   55 J=NEIGH(I,1)                                                          MAINL
      GO TO 60                                                              MAINL
   53 J=NEIGH(I,LL)                                                         MAINL
   60 CONTINUE                                                              MAINL
      LTOUCH=1                                                              MAINL
      L=K                                                                   MAINL
      IF(J.EQ.0)GO TO 66                                                    MAINL
      KONTER=0.                                                             MAINL
      KONTEJ=0.                                                             MAINL
      KHECKS=0.                                                             MAINL
      XD=XX-CX(J)                                                           MAINL
      YD=YY-CY(J)                                                           MAINL
      ALPHAJ=ANT(J)                                                         MAINL
      SSI=SIN(ALPHAJ)                                                       MAINL
      CCO=COS(ALPHAJ)                                                       MAINL
      IF(IAXIS.EQ.1)GO TO 69                                                MAINL
      ALPHAI=DIPA+DIPB+ALPHAJ-PI/2.                                         MAINL
      SII=SIN(ALPHAI)                                                       MAINL
      COO=COS(ALPHAI)                                                       MAINL
      ALPHII=DIPA+DIPB+ALPHAJ                                               MAINL
      SOJ=SIN(ALPHII)                                                       MAINL
      COJ=COS(ALPHII)                                                       MAINL
      GO TO 70                                                              MAINL
   69 ALPHAI=ALPHAJ+PI/2.-DIPA-DIPB                                         MAINL
      SII=SIN(ALPHAI)                                                       MAINL
      COO=COS(ALPHAI)                                                       MAINL
      ALPHII=ALPHAJ+PI-DIPA-DIPB                                            MAINL
      SOJ=SIN(ALPHII)                                                       MAINL
      COJ=COS(ALPHII)                                                       MAINL
   70 CONTINUE                                                              MAINL
      AJJ=-XD*SSI+YD*CCO                                                    MAINL
      TJJ=XD*CCO+YD*SSI                                                     MAINL
      AII=XD*COO+YD*SII                                                     MAINL
      TII=XD*SII-YD*COO                                                     MAINL
      ANI=ABS(AII)                                                          MAINL
      ANJ=ABS(AJJ)                                                          MAINL
      IF(ANI.GT.ANN.OR.ANJ.GT.BNN)GO TO 66                                  MAINL
C  WHEN IF STATEMENT CORRECT NO CONTACT EXSTS BETWEEN I AND J               MAINL
C  FIND WHAT FACE CORNER PENERTRATES BY THE USE OF ANGLES.  CORNER ONE       MAINL
C  HAS ANGLE OF ZERO.                                                       MAINL
      IF(ALPHAJ.GT.PII)GO TO 88                                             MAINL
      ALP=ALPHAJ                                                            MAINL
      GO TO 89                                                              MAINL
   88 KALP=ALPHAJ/PII                                                       MAINL
      ALP=ALPHAJ-KALP*PII                                                   MAINL
   89 ALPP=ALP+BETA1                                                        MAINL
      IF(ALPP.GT.PII)ALPP=ALPP-PII                                          MAINL
      ALP1=0.                                                               MAINL
      ALP4=PI-BETA1-BETA2                                                   MAINL
      ALP3=PI                                                               MAINL
      ALP2=PI+ALP4                                                          MAINL
      UCC=AA*CCO                                                            MAINL
      VCC=AA*SSI                                                            MAINL
      UDD=BB*COJ                                                            MAINL
      VDD=BB*SOJ                                                            MAINL
C  FINDS WHICH FACE OF BLOCK J, THE CORNER PENERTRATES                      MAINL
      KONTER=1.                                                             MAINL
      KONTEJ=1                                                              MAINL
      K1=0                                                                  MAINL
      K2=0                                                                  MAINL
      KA=0                                                                  MAINL
      GM=ABS(CCO)                                                           MAINL
      IF(GM.LE.1E-5)GO TO 94                                                MAINL
      AF1=SSI/CCO                                                           MAINL
  121 GM=ABS(COJ)                                                           MAINL
      IF(GM.LE.1E-5)GO TO 95                                                MAINL
      AF2=SOJ/COJ                                                           MAINL
      GO TO 86                                                              MAINL
   94 K1=1                                                                  MAINL
      GO TO 121                                                             MAINL
   95 K2=1                                                                  MAINL
   86 XO=XX-CX(I)                                                           MAINL
      YO=YY-CY(I)                                                           MAINL
      GM=ABS(XO)                                                            MAINL
      IF(GM.LE.1.E-5)XO=1.E-5                                               MAINL
      ACTOC=YO/XO                                                           MAINL
      BCTOC=YD-XD*ACTOC                                                     MAINL
      KTOUCH=0.                                                             MAINL
      KFF=0.                                                                MAINL
      DO 87 KF=1,4                                                          MAINL
      GO TO (96,97,98,99)KF                                                 MAINL
   96 UU=UCC+UDD                                                            MAINL
      VV=VCC+VDD                                                            MAINL
      AF=AF1                                                                MAINL
      AP1=0                                                                 MAINL
      AP2=ALP4                                                              MAINL
      KA=K1                                                                 MAINL
      GO TO 106                                                             MAINL
   97 UU=UCC-UDD                                                            MAINL
      VV=VCC-VDD                                                            MAINL
      AF=AF1                                                                MAINL
      AP1=ALP3                                                              MAINL
```

```
      AP2=ALP2                                                          MAINL
      KA=K1                                                             MAINL
      GO TO 106                                                         MAINL
   98 UU=UCC-UDD                                                        MAINL
      VV=VCC-VDD                                                        MAINL
      AF=AF2                                                            MAINL
      AP1=ALP2                                                          MAINL
      AP2=PII                                                           MAINL
      KA=K2                                                             MAINL
      GO TO 106                                                         MAINL
   99 UU=-UCC-UDD                                                       MAINL
      VV=-VCC-VDD                                                       MAINL
      AF=AF2                                                            MAINL
      AP1=ALP4                                                          MAINL
      AP2=ALP3                                                          MAINL
      KA=K2                                                             MAINL
106    IF(KA.EQ.1)GO TO 126                                             MAINL
      BF=VV-UU*AF                                                       MAINL
      XF=(BCTOC-BF)/(AF-ACTOC)                                          MAINL
      YF=BF+XF*AF                                                       MAINL
      GO TO 127                                                         MAINL
126   XF=UU                                                             MAINL
      YF=BCTOC+XF*ACTOC                                                 MAINL
127   GM=ABS(XF)                                                        MAINL
      RG=SQRT((XF+CX(J)-CX(I))**2+(YF+CY(J)-CY(I))**2)                  MAINL
      RGI=SQRT(XO**2+YO**2)                                             MAINL
      IF(RG.GT.RGI)GOTO 87                                              MAINL
      IF(GM.LE.1E-5)  XF=1E-5                                           MAINL
      AG=ATAN2(YF,XF)                                                   MAINL
      IF(AG.LT.0)AG=PII+AG                                              MAINL
      AG=AG-ALPP                                                        MAINL
      IF(AG.LT.0)AG=AG+PII                                              MAINL
      IF(AG.LE.AP2.AND.AG.GE.AP1)GO TO 107                              MAINL
      GO TO 87                                                          MAINL
  107 IF(KFF.NE.0)GO TO 102                                             MAINL
      KFF=KF                                                            MAINL
      XFF=XF                                                            MAINL
      YFF=YF                                                            MAINL
      KTOUCH=1.                                                         MAINL
      GO TO 87                                                          MAINL
  102 KFO=KF                                                            MAINL
      XFO=XF                                                            MAINL
      YFO=YF                                                            MAINL
      KTOUCH=2.                                                         MAINL
      GO TO 103                                                         MAINL
   87 CONTINUE                                                          MAINL
      IF(KTOUCH.EQ.0)GOTO 66                                            MAINL
      GO TO (56,77,73,72)KFF                                            MAINL
  103 XGF=XFF+CX(J)-CX(I)                                               MAINL
      YGF=YFF+CY(J)-CY(I)                                               MAINL
*     DGF=SQRT(XGF*XGF+YGF*YGF)                                         MAINL
      XGF=XFO+CX(J)-CX(I)                                               MAINL
      YGF=YFO+CY(J)-CY(I)                                               MAINL
      DGO=SQRT(XGF*XGF+YGF*YGF)                                         MAINL
      IF(DGF.GT.DGO)KFF=KFO                                             MAINL
      GO TO (56,77,73,72)KFF                                            MAINL
   77 KONTER=-1.                                                        MAINL
      GO TO 79                                                          MAINL
   56 CONTINUE                                                          MAINL
C  CORNER PENERTRATES A FACE PARALLEL TO A MAJOR AXIS (MAJOR FACE)      MAINL
   79 FFJ=SN*(BNN-ANJ)                                                  MAINL
      IF(FFJ.LT.0.0)GOTO 66                                             MAINL
      OVLNO=OVLN(I,L)                                                   MAINL
      IF(OVLNO.EQ.0)  OVLNO=ANJ                                         MAINL
      DNF=FFJ+DAMPN*(OVLNO-ANJ)                                         MAINL
      DSF=0.                                                            MAINL
C  DSF EQUALS ZERO, BECAUSE ONLY NORMAL FORCES ARE INVOLVED IN COMMON    MAINL
C  BLOCK INTERACTIONS, SINCE THERE IS NO SLIDING PLANE INVOLVED          MAINL
      OVLSO=OVLS(I,L)                                                   MAINL
      IF(OVLSO.EQ.0)  OVLSO=TJJ                                         MAINL
      SHDJ=TJJ-OVLSO                                                    MAINL
C  SHDJ=DISTANCE OF SHEARING MOTION ALONG A MAJOR FACE                  MAINL
      FSJ=SF(I,L)+SHDJ*ST                                               MAINL
      DSF=FSJ+SHDJ*DAMPS                                                MAINL
      XSF=ABS(DMU*FFJ)                                                  MAINL
      IF(ABS(FSJ).GT.XSF)  DSF=RSD*ABS(FFJ)*FSJ/ABS(FSJ)                MAINL
      OVLN(I,L)=ANJ                                                     MAINL
      OVLS(I,L)=TJJ                                                     MAINL
   51 HOR=(-DNF*SSI)*KONTER-DSF*CCO                                     MAINL
      VER=(DNF*CCO)*KONTER-DSF*SSI                                      MAINL
   64 CONTINUE                                                          MAINL
      FXX(I)=FXX(I)+HOR                                                 MAINL
      FYY(I)=FYY(I)+VER                                                 MAINL
      FXX(J)=FXX(J)-HOR                                                 MAINL
      FYY(J)=FYY(J)-VER                                                 MAINL
      SMM(J)=SMM(J)+HOR*YO-VER*XO                                       MAINL
      SMM(I)=SMM(I)-HOR*YO+VER*XO                                       MAINL
      SF(I,L)=DSF                                                       MAINL
   57 CONTINUE                                                          MAINL
      LTOUCH=2.                                                         MAINL
      GO TO 66                                                          MAINL
104   CONTINUE                                                          MAINL
      WRITE(6,201)                                                      MAINL
201   FORMAT(* ERROR IN BLOCK INTERACTION*)                             MAINL
      GO TO 66                                                          MAINL
   72 KONTEJ=-1.                                                        MAINL
      GO TO 74                                                          MAINL
73    CONTINUE                                                          MAINL
C C  CORNER PENERTRATES A FACE PARALLEL TO A MINOR AXIS (MINOR FACE)    MAINL
   74 FFI=SN*(ANN-ANI)                                                  MAINL
      IF(FFI.LT.0.0)GOTO 66                                             MAINL
      OVLNO=OVLN(I,L)                                                   MAINL
      IF(OVLNO.EQ.0)  OVLNO=ANI                                         MAINL
      DNF=FFI+DAMPN*(OVLNO-ANI)                                         MAINL
      DSF=0.                                                            MAINL
      OVLSO=OVLS(I,L)                                                   MAINL
      IF(OVLSO.EQ.0)  OVLSO=TII                                         MAINL
      SHDI=TII-OVLSO                                                    MAINL
      FSI=SF(I,L)+SHDI*ST                                               MAINL
      DSF=FSI+SHDI*DAMPS                                                MAINL
      XSF=ABS(DMU*FFI)                                                  MAINL
      IF(ABS(FSI).GT.XSF)  DSF=RSD*ABS(FFI)*FSI/ABS(FSI)                MAINL
      OVLN(I,L)=ANI                                                     MAINL
      OVLS(I,L)=TII                                                     MAINL
      HOR=(DNF*COO)*KONTEJ-DSF*SII                                      MAINL
      VER=(DNF*SII)*KONTEJ+DSF*COO                                      MAINL
      GO TO 64                                                          MAINL
   66 CONTINUE                                                          MAINL
      IF(LTOUCH.EQ.2)GO TO 67                                           MAINL
      SF(I,L)=0.                                                        MAINL
      OVLN(I,L)=0.                                                      MAINL
      OVLS(I,L)=0.                                                      MAINL
67    K=K+1                                                             MAINL
      GO TO (65,54,53,65,54,53,65,54,53,65,55,53,65)K                   MAINL
65    CONTINUE                                                          MAINL
   68 CONTINUE                                                          MAINL
      DO 71 I=1,NON                                                     MAINL
      FYY(I)=FYY(I)-WEIGHT                                              MAINL
```

```
      VXN(I)=VXN(I)+FXX(I)*DSST
      VYN(I)=VYN(I)+FYY(I)*DSST
      AVN(I)=AVN(I)+SMM(I)*DOIT
   71 CONTINUE
C  THIS SUBROUTINE SETS FIXED BLOCKS VELOCITIES TO ZERO
      DO 10 I=1,IFIXED
      J=IFIX(I)
      VXN(J)=0.
      VYN(J)=0.
      AVN(J)=0.
   10 CONTINUE
      DO 26 I=1,NON
      CX(I)=CX(I)+VXN(I)*DT
      CY(I)=CY(I)+VYN(I)*DT
      ANT(I)=ANT(I)+AVN(I)*DT
   26 CONTINUE
      IP=ITR/IPRINT
      IP=IP*IPRINT
      IF(IP.EQ.ITR)CALL PRIN
      IT=ITR/ILWHEN
      IT=IT*ILWHEN
      IF(IT.EQ.ITR)CALL BLOCK
      IF(IT.EQ.ITR.AND.VECL.GE..0001)CALL VELOC(VECL)
      IT=ITR/NEIB
      IT=IT*NEIB
      IF(IT.EQ.ITR)CALL NEIGHB
      IF(ITR.NE.NCYCLE )GO TO 500
   50 CONTINUE
      IF(NWREST.NE.1)GO TO 704
      REWIND 4
      WRITE(4)  (GEN(I),I=1,105),(AMAI(I),I=1,880),(CNE(I),I=1,203),
     *(CIG(I),I=1,76)
  704 CONTINUE
  999 IPCON=2
      CALL PL(IPCON)
      STOP
      END
*DECK,COORDS
      SUBROUTINE COORDS
*CALL GENALL
*CALL CCOOR
      XCC=COS(DIPA)*HH
      YCC=SIN(DIPA)*HH
C  HH IS DISTANCE BETWEEN CENTROIDS OF BLOCKS IN SAME ROW
      XFF=COS(DIPB)*FF
      YFF=SIN(DIPB)*FF
C  FF IS DISTANCE BETWEEN CENTROIDS OF BLOCKS IN SAME COLUMN
      DD=HH/2.
      EE=FF/2.
C  DD AND EE ARE HALF LENGTHS OF AXES
      IF(EE.GT.DD)GO TO 80
C  IAXIS IS EQUAL TO ONE WHEN THE MAJOR AXIS IS PARALLEL TO DIPA
C  EQUAL TO TWO WHEN PARALLEL TO DIPB
      AA=DD
      ANN=B/2.
      BB=EE
      BNN=A/2.
      AGG=DIPA
      IAXIS=1.
      GO TO 81
   80 AA=EE
      ANN=A/2.
      BB=DD
      BNN=B/2.
      AGG=PI-DIPB
      IAXIS=2.
   81 CONTINUE
C  AA=HALF LENGTH OF MAJOR AXIS    BB=HALF LENGTH OF MINOR AXIS
C  ANN=DISTANCE FROM CENTROID TO MINOR FACE
C  BNN=DISTANCE FROM CENTROID TO MAJOR FACE
C  AGG=ANGLE ANTICLOCKWISE POSITIVE BETWEEN X AXIS AND MAJOR AXIS
C  CALCULATE BETA SO THAT CORNER POSITIONS CAN BE FOUND
      PP=BB*(COS(PI-DIPA-DIPB))
      IF(IAXIS.EQ.1)GO TO 82
      AG=AA-PP
      AH=AA+PP
      GO TO 83
   82 AG=AA+PP
      AH=AA-PP
   83 CONTINUE
      BETA1=ATAN(BNN/AG)
      BETA2=ATAN(BNN/AH)
C
      BMASS=HH*A*RHO
      BE=ABS(FF*COS(DIPA+DIPB))
      BC=(HH-BE)/2.
      BMOI1=HH*(A**3.)/12.
      BMOI2=2.*A*((BC**3)/3.+(BE**3)/36.+BE*(BC+BE/3.)*(BC+BE/3.)/2.)
      BMOI=(BMOI1+BMOI2)*RHO
C  THIS IS A SIMPLE CASE OF NINE BLOCKS STACKED IN THREE ROW AND THREE
      CALL GEN
      DO 30 I=1,NON
      AMT(I)=AGG
   30 CONTINUE
      IF(IZCYC.EQ.1)CALL BLOCK
      RETURN
      END
*DECK,NEIGHB
      SUBROUTINE NEIGHB
*CALL GENALL
*CALL CNEIGH
      DIMENSION NEIG(30)
C  THIS SUBROUTINE FINDS A MAXIMUM OF EIGHT NEIGHBOURING BLOCKS AND
C  ARRANGES THEM IN AN ANTI-CLOCKWISE ORDER SO THAT EACH CORNER OF
C  THE BLOCK HAS A MAXIMUM OF THREE NEIGHBOURING BLOCKS
      XNN=COS(DIPA)*HH+COS(DIPB)*FF
      YNN=SIN(DIPA)*HH+SIN(DIPB)*FF
      RES=SQRT(XNN*XNN+YNN*YNN)
      DIF=1.1*RES
      DO 136 I=1,NON
      DO 136 J=1,8
  136 NEIGH(I,J)=0
      DO 41 I=1,NON
      IF(NREM.EQ.0)GO TO 235
      DO 135 J=1,NREM
      IF(NREMOV(J).EQ.I)GO TO 41
  135 CONTINUE
  235 CONTINUE
      NEX=0.
      DO 33 L=1,4
      DO 33 M=1,3
      N(L,M)=0.
   33 CONTINUE
      DO 32 J=1,30
   32 NEIG(J)=0.
      XG=CX(I)+DIF
      XL=CX(I)-DIF
      YG=CY(I)+DIF
```

```
      YL=CY(I)-DIF
      DO 24 J=1,NON
      IF(NREM.EQ.0)GO TO 237
      DO 137 IJ=1,NREM
      IF(NREMOV(IJ).EQ.J)GO TO 24
  137 CONTINUE
  237 CONTINUE
      IF(J.EQ.I)GO TO 24
      IF(CY(J).GT.YG.OR.CY(J).LT.YL)GO TO 24
      IF(CX(J).GT.XG.OR.CX(J).LT.XL)GO TO 24
      NEX=NEX+1.
      NEIG(NEX)=J
   24 CONTINUE
      SI=SIN(ANT(I))
      CO=COS(ANT(I))
      IF(IAXIS.EQ.1)GO TO 34
      SS=SIN(DIPA+DIPB+ANT(I))
      CC=COS(DIPA+DIPB+ANT(I))
      GO TO 38
   34 SS=SIN(ANT(I)+PI-DIPA-DIPB)
      CC=COS(ANT(I)+PI-DIPA-DIPB)
   38 CONTINUE
      UAA=AA*CO
      VAA=AA*SI
      UBB=BB*CC
      VBB=BB*SS
      AAN=ANN+0.9*BNN
      BBN=1.9*BNN
      DO 25 K=1,4
      GO TO (1,2,3,4)K
    1 XX=CX(I)+UAA+UBB
      YY=CY(I)+VAA+VBB
      GO TO 26
    2 XX=CX(I)+UAA-UBB
      YY=CY(I)+VAA-VBB
      GO TO 26
    3 XX=CX(I)-UAA-UBB
      YY=CY(I)-VAA-VBB
      GO TO 26
    4 XX=CX(I)-UAA+UBB
      YY=CY(I)-VAA+VBB
   26 CONTINUE
      MM=0.
      DO 25 J=1,NEX
      JJ=NEIG(J)
      SSI=SIN(ANT(JJ))
      COO=COS(ANT(JJ))
      IF(IAXIS.EQ.1)GO TO 39
      SII=SIN(DIPA+DIPB+ANT(JJ)-PI/2.)
      CCO=COS(DIPA+DIPB+ANT(JJ)-PI/2.)
      GO TO 40
   39 SII=SIN(ANT(JJ)+PI/2.-DIPA-DIPB)
      CCO=COS(ANT(JJ)+PI/2.-DIPA-DIPB)
   40 CONTINUE
      XD=XX-CX(JJ)
      YD=YY-CY(JJ)
      AJJ=ABS(-XD*SSI+YD*COO)
      AII=ABS(XD*CCO+YD*SII)
      IF(AJJ.GE.BBN.OR.AII.GE.AAN)GO TO 25
      MM=MM+1.
      N(K,MM)=JJ
   25 CONTINUE
      DO 23 J=1,3
      DO 23 K=1,3
      DO 23 L=1,3
      DO 23 M=1,3
      L1=N(1,J)
      L2=N(2,K)
      L3=N(3,L)
      L4=N(4,M)
      IF(L1.EQ.L2)GO TO 27
      IF(L2.EQ.L3)GO TO 28
   42 IF(L3.EQ.L4)GOTO 29
   43 IF(L4.EQ.L1)GOTO 30
      GO TO 23
   27 IF(L1.EQ.0)GOTO 42
      NEIGH(I,3)=L1
      GOTO 42
   28 IF(L2.EQ.0)GOTO 43
      NEIGH(I,5)=L2
      GOTO 43
   29 IF(L3.EQ.0)GOTO 23
      NEIGH(I,7)=L3
      GO TO 23
   30 IF(L4.EQ.0)GOTO 23
      NEIGH(I,1)=L4
   23 CONTINUE
      DO 35 M=1,3
      L1=N(1,M)
      L2=N(2,M)
      L3=N(3,M)
      L4=N(4,M)
      IF(L1.EQ.NEIGH(I,1).OR.L1.EQ.NEIGH(I,3))GO TO 31
      IF(L1.EQ.0)GOTO 31
      NEIGH(I,2)=L1
   31 CONTINUE
      IF(L2.EQ.NEIGH(I,3).OR.L2.EQ.NEIGH(I,5))GO TO 36
      IF(L2.EQ.0)GOTO 36
   36 CONTINUE
      IF(L3.EQ.NEIGH(I,5).OR.L3.EQ.NEIGH(I,7))GO TO 37
      IF(L3.EQ.0)GOTO 37
      NEIGH(I,6)=L3
   37 CONTINUE
      IF(L4.EQ.NEIGH(I,7).OR.L4.EQ.NEIGH(I,1))GO TO 35
      IF(L4.EQ.0)GOTO 35
      NEIGH(I,8)=L4
   35 CONTINUE
   41 CONTINUE
      RETURN
      END
*DECK,CONSOL
      SUBROUTINE CONSOL
C   THIS IS A DUMMY CONSOLIDATION SUBROUTINE
C   REMEMBER TO INCLUDE COMMON BLOCKS
      RETURN
      END
*DECK,GEN
      SUBROUTINE GEN
C  THIS IS A DUMMY SUBROUTINE , YOU SHOULD DELETE AND INSERT YOUR
C  PARTICULAR BLOCK GENERATION ROUTINE INCLUDING BLOCK FIXING
C  REMEMBER THAT COMMON BLOCKS GENALL AND CCOOR ARE TO BE CALLED.
*CALL GENALL
*CALL CCOOR
      NON=5
      READ(5,10)(CX(I),CY(I),I=1,NON)
   10 FORMAT(4F20.0)
      IFIXED=4
      READ(5,20)(IFIX(I),I=1,IFIXED)
```

```
 20   FORMAT(2014)                                                          
      RETURN                                                          GEN   
      END                                                             GEN   
*DECK,PL                                                                    
      SUBROUTINE PL(IPCON)                                            PL    
      GO TO (10,20) IPCON                                             PL    
10    CALL START (2)                                                  PL    
      CALL PEN (1)                                                    PL    
      RETURN                                                          PL    
20    CALL ENPLOT                                                     PL    
      RETURN                                                          PL    
      END                                                             PL    
*DECK,BLOCK                                                                 
      SUBROUTINE BLOCK                                                BLOCK 
*CALL GENALL                                                                
*CALL CNEIGH                                                                
*CALL CCOOR                                                                 
C  THIS SUBROUTINE PLOTS ALL BLOCKS WITH THEIR RESPECTIVE NUMBER        BLOCK 
C  SCAL= NUMBER OF PROBLEM UNITS TO THE INCH AND DEPENDS ON SIZE OF NUM BLOCK 
C  AND PAPER SIZE AI  (AO=LARGE  A1=MEDIUM  A2=SMALL)                   BLOCK 
C**************                                  **************        BLOCK 
C**************                                  **************        BLOCK 
      CALL TITLES(1,SCAL)                                             BLOCK 
      DO 10 I=1,NON                                                   BLOCK 
      IF(NREM.EQ.0)GO TO 150                                          BLOCK 
      DO 50 IJ=1,NREM                                                 BLOCK 
      IF(NREMOV(IJ).EQ.I)GO TO 10                                     BLOCK 
50    CONTINUE                                                        BLOCK 
150   CONTINUE                                                        BLOCK 
      SI=SIN(ANT(I))                                                  BLOCK 
      CO=COS(ANT(I))                                                  BLOCK 
      IF(IAXIS.EQ.1)GO TO 20                                          BLOCK 
      SS=SIN(DIPA+DIPB+ANT(I))                                        BLOCK 
      CC=COS(DIPA+DIPB+ANT(I))                                        BLOCK 
      GO TO 21                                                        BLOCK 
   20 SS=SIN(ANT(I)+PI-DIPA-DIPB)                                     BLOCK 
      CC=COS(ANT(I)+PI-DIPA-DIPB)                                     BLOCK 
   21 CONTINUE                                                        BLOCK 
      UAA=AA*CO/SCAL                                                  BLOCK 
      VAA=AA*SI/SCAL                                                  BLOCK 
      UBB=BB*CC/SCAL                                                  BLOCK 
      VBB=BB*SS/SCAL                                                  BLOCK 
      XX=CX(I)/SCAL                                                   BLOCK 
      YY=CY(I)/SCAL                                                   BLOCK 
      XX1=XX+UAA+UBB                                                  BLOCK 
      YY1=YY+VAA+VBB                                                  BLOCK 
      XX2=XX+UAA-UBB                                                  BLOCK 
      YY2=YY+VAA-VBB                                                  BLOCK 
      XX3=XX-UAA-UBB                                                  BLOCK 
      YY3=YY-VAA-VBB                                                  BLOCK 
      XX4=XX-UAA+UBB                                                  BLOCK 
      YY4=YY-VAA+VBB                                                  BLOCK 
      AAA=I                                                           BLOCK 
      CALL PLOT(XX1,YY1,3)                                            BLOCK 
      CALL PLOT(XX2,YY2,2)                                            BLOCK 
      CALL PLOT(XX3,YY3,2)                                            BLOCK 
      CALL PLOT(XX4,YY4,2)                                            BLOCK 
      CALL PLOT(XX1,YY1,2)                                            BLOCK 
      H=0.07                                                          BLOCK 
      IF(I.GT.9)GO TO 22                                              BLOCK 
      XC=XX-H/2.                                                      BLOCK 
      YC=YY-H/2.                                                      BLOCK 
      GO TO 24                                                        BLOCK 
   22 IF(I.GT.99)GO TO 23                                             BLOCK 
      XC=XX-H                                                         BLOCK 
      YC=YY-H                                                         BLOCK 
      GO TO 24                                                        BLOCK 
   23 XC=XX-1.5*H                                                     BLOCK 
      YC=YY-1.5*H                                                     BLOCK 
   24 CONTINUE                                                        BLOCK 
      CALL NUMBER(XC,YC,H,AAA,0.0,-1)                                 BLOCK 
      DO 26 K=1,IFIXED                                                BLOCK 
      J=IFIX(K)                                                       BLOCK 
      IF(I.EQ.J)GO TO 27                                              BLOCK 
26    CONTINUE                                                        BLOCK 
      GO TO 10                                                        BLOCK 
27    YCA=YC-0.28                                                     BLOCK 
      CALL SYMBOL(XC,YCA,H,1HF,0.0,1)                                 BLOCK 
   25 CONTINUE                                                        BLOCK 
   10 CONTINUE                                                        BLOCK 
      CALL NEWPAGE                                                    BLOCK 
      RETURN                                                          BLOCK 
      END                                                             BLOCK 
*DECK,PRIN                                                                  
      SUBROUTINE PRIN                                                 PRIN  
C    COMMON PRINT FOR NOMINATED CYCLES                                PRIN  
*CALL GENALL                                                                
*CALL MAIN                                                                  
*CALL CNEIGH                                                                
*CALL CCOOR                                                                 
      WRITE(6,10) ITR                                                 PRIN  
 10   FORMAT(1H1,*CYCLE NUMBER*,I5)                                          
      WRITE(6,20)                                                     PRIN  
20    FORMAT(* BLOCK        X                Y                ANG          V PRIN
     *X              VY             OMEGA      *)                   PRIN  
      DO 30 I=1,NON                                                   PRIN  
      WRITE(6,40)   I,CX(I),CY(I),ANT(I),VXN(I),VYN(I),AVN(I)         PRIN  
40    FORMAT(I5,7E15.6)                                               PRIN  
30    CONTINUE                                                        PRIN  
      RETURN                                                          PRIN  
      END                                                             PRIN  
*DECK,VELOC                                                                 
      SUBROUTINE VELOC(VECL)                                          VELOC 
C  PLOTS VELOCITIES AS VECTORS WITH MAXIMUM VELOCITY EQUAL TO VECL INCHE VELOC 
*CALL GENALL                                                                
*CALL MAIN                                                                  
*CALL CNEIGH                                                                
*CALL CCOOR                                                                 
      V0=0.                                                           VELOC 
      DO 10 I=1,NON                                                   VELOC 
      IF(NREM.EQ.0)GO TO 30                                           VELOC 
      DO 40 IJ=1,NREM                                                 VELOC 
      IF(NREMOV(IJ).EQ.I)GO TO 10                                     VELOC 
40    CONTINUE                                                        VELOC 
30    CONTINUE                                                        VELOC 
      VN=SQRT(VXN(I)*VXN(I)+VYN(I)*VYN(I))                            VELOC 
      IF(VN.LE.V0)GO TO 10                                            VELOC 
      V0=VN                                                           VELOC 
   10 CONTINUE                                                        VELOC 
      FG=VECL/V0                                                      VELOC 
C  VECL IS LENGTH OF MAXIMUM VELOCITY IN INCHES                       VELOC 
      GG=1./FG                                                        VELOC 
      CALL TITLES(2,GG)                                               VELOC 
      DO 20 I=1,NON                                                   VELOC 
      IF(NREM.EQ.0)GO TO 50                                           VELOC 
      DO 60 IJ=1,NREM                                                 VELOC 
      IF(NREMOV(IJ).EQ.I)GO TO 20                                     VELOC 
60    CONTINUE                                                        VELOC 
```

```
 50     CONTINUE                                                        VELOC
    15  X=CX(I)/SCAL                                                   VELOC
        Y=CY(I)/SCAL                                                    VELOC
        VX=VXN(I)*FG                                                    VELOC
        VY=VYN(I)*FG                                                    VELOC
        CALL VECTOR(X,Y,VX,VY)                                          VELOC
    20  CONTINUE                                                        VELOC
        CALL NEWPAGE                                                    VELOC
        RETURN                                                          VELOC
        END                                                             VELOC
*DECK,VECTOR
        SUBROUTINE VECTOR(X,Y,XV,YV)                                    VECTOR
*CALL GENALL
        CALL PLOT(X,Y,3)                                                VECTOR
        X=X+XV                                                          VECTOR
        Y=Y+YV                                                          VECTOR
        CALL PLOT(X,Y,2)                                                VECTOR
        VT=(SQRT(XV*XV+YV*YV))/5.                                       VECTOR
        GM=ABS(XV)                                                      VECTOR
        IF(GM.LE.1.E-5) XV=1.E-5                                        VECTOR
        ABA=ATAN2(YV,XV)                                                VECTOR
        IF(ABA.LT.0) ABA=2.*PI+ABA                                      VECTOR
        ABA1=PI+ABA-0.25                                                VECTOR
        ABA2=ABA1+0.5                                                   VECTOR
        XA=X+VT*(COS(ABA1))                                             VECTOR
        YA=Y+VT*(SIN(ABA1))                                             VECTOR
        CALL PLOT(XA,YA,2)                                              VECTOR
        CALL PLOT(X,Y,3)                                                VECTOR
        XA=X+VT*(COS(ABA2))                                             VECTOR
        YA=Y+VT*(SIN(ABA2))                                             VECTOR
        CALL PLOT(XA,YA,2)                                              VECTOR
        RETURN                                                          VECTOR
        END                                                             VECTOR
*DECK,TITLES
        SUBROUTINE TITLES(IPLOT,DIS)                                    TITLES
*CALL GENALL
*CALL CCOOR
        CALL SYMBOL(0.5,12.0,0.21,TITLE,0.,80)                          TITLES
        GO TO (10,11,12,13,14) IPLOT                                    TITLES
    10  CONTINUE                                                        TITLES
C   THIS IS FOR A BLOCK PLOT                                            TITLES
        CALL SYMBOL(0.5,11.25,0.21,10HBLOCK PLOT,0.,10)                 TITLES
        GO TO 15                                                        TITLES
    11  CONTINUE                                                        TITLES
C   THIS IS FOR A LINEAR VELOCITY PLOT                                  TITLES
        CALL SYMBOL(0.5,11.25,0.21,13HVELOCITY PLOT,0.,13)              TITLES
        GO TO 15                                                        TITLES
    12  CONTINUE                                                        TITLES
        CALL SYMBOL(0.5,11.25,0.21,17HCORNER FORCE PLOT,0.,17)          TITLES
        GO TO 15                                                        TITLES
    13  CONTINUE                                                        TITLES
C   THIS IS FOR A DISPLACEMENT PLOT                                     TITLES
        GO TO 15                                                        TITLES
    14  CONTINUE                                                        TITLES
C   THIS IS FOR A STRESS PLOT                                           TITLES
    15  CONTINUE                                                        TITLES
        CALL SYMBOL(5.0,11.25,0.21,34HNUMBER OF PROBLEM UNITS PER INCH =,0 TITLES
       *,.34)                                                           TITLES
        CALL NUMBER(12.4,11.25,0.21,DIS,0.,2)                           TITLES
        FL=ITR                                                          TITLES
        CALL SYMBOL(14.3,11.25,0.21,14HCYCLE NUMBER =,0.,14)            TITLES
        CALL NUMBER(17.5,11.25,0.21,FL,0.,-1)                           TITLES
        CALL PLOT(XORIG,YORIG,-3)                                       TITLES
        RETURN                                                          TITLES
```

END

TITLES

B. PROGRAM RBM - generalised rigid block formulation (Maini et. al., 1978)

```
      PROGRAM RBM(INPUT,OUTPUT,TAPE5=INPUT,TAPE6=OUTPUT,TAPE1,TAPE2,
     *                TAPE62)
C
C-----------------------------------------------------------------
C-------------DYNAMIC RELAXATION RIGID BLOCK MODEL----------------
C-----------------BASED ON ORIGINAL PROGRAM WRITTEN---------------------
C-------------BY P.A.CUNDALL. UPDATED BY I.J.STEWART.---------------
C-----------------------------------------------------------------
C
      COMMON/CBLOCK/HED(8),NBLOKM,NBOXES,M1,M2,M3,M4,M5,M6,M7,
     .                    NBLOKS,NCYC,MCYCLE,NEMPT,RFLAG,UFLAG,EFLAG,
     .                    TFRAC,TDEL,IBOXES,JBOXES,BSIZE,XSIZE,YSIZE,
     .                    UDMAX,UMOST,STIFN,STIFS,FRIC,ALPHA,BETA,BDT,
     .                    CON1,CON2,NVARB,NFRAG,NBR,NPR,
     *                    GRAVX,GRAVY,LOC1,LOC2,NUPDAT,
     *              NBCODD,NDCON(76),DISPL,THMOST,THMAX,
     *                   IBPLT,IFPLT,IDPLT,ICONDA,IBLKDA,IBOXDA,
     *                    XYL,THL,LGNEIB,ITDPLT,IRFPO,COHES,
     *                   SCREEN,FORCL,VECL,NREM,NBNREM(60),LBLOCK
      LOGICAL RFLAG,UFLAG,EFLAG
      COMMON A(30000)
      DIMENSION IA(1)
      EQUIVALENCE (A,IA)
      COMMON/INEIG/IN(111),NEIGHB(111,15)
      DIMENSION INEI(1887)
      EQUIVALENCE(IN,INEI)
C
      DATA STIFN,STIFS,FRIC,BETA/2*1.0E8,0.0,0.0/
      DATA GRAVY,GRAVX/-9.81,0.0/
      DATA M7,MCYCLE,NUPDAT,LBLOCK/5000,0,0,206/
      DATA RFLAG,UFLAG,EFLAG/.FALSE.,.TRUE.,.FALSE./
      DATA SCREEN,FORCL,VECL/20.0,1.0,1.0/
      DATA DISPL/1./
      DATA NREM/0/
      DATA LGNEIB,NBCODD/1887,0/
      DATA COHES/0.0/
C
      IPCON=1
      CALL PL(IPCON)
      CALL SETUP
   10 CALL NEXT
      CALL CYCLE
      GOTO 10
C
      END
      SUBROUTINE SETUP
C
      COMMON/CBLOCK/HED(8),NBLOKM,NBOXES,M1,M2,M3,M4,M5,M6,M7,
     .                    NBLOKS,NCYC,MCYCLE,NEMPT,RFLAG,UFLAG,EFLAG,
     .                    TFRAC,TDEL,IBOXES,JBOXES,BSIZE,XSIZE,YSIZE,
     .                    UDMAX,UMOST,STIFN,STIFS,FRIC,ALPHA,BETA,BDT,
     .                    CON1,CON2,NVARB,NFRAG,NBR,NPR,
     *                    GRAVX,GRAVY,LOC1,LOC2,NUPDAT,
     *              NBCODD,NDCON(76),DISPL,THMOST,THMAX,
     *                   IBPLT,IFPLT,IDPLT,ICONDA,IBLKDA,IBOXDA,
     *                    XYL,THL,LGNEIB,ITDPLT,IRFPO,COHES,
     *                   SCREEN,FORCL,VECL,NREM,NBNREM(60),LBLOCK
      LOGICAL RFLAG,UFLAG,EFLAG
      COMMON A(30000)
      DIMENSION IA(1)
      EQUIVALENCE (A,IA)
      COMMON/INEIG/IN(111),NEIGHB(111,15)
      DIMENSION INEI(1887)
      EQUIVALENCE(IN,INEI)
C
      WRITE(6,2003)
 2003 FORMAT(1H1)
C
      WRITE(6,2000)
      READ(5,1000) WORD
C
      IF(WORD.EQ.4HSTAR) GOTO 20
      IF(WORD.EQ.4HREST) GOTO 10
C
      WRITE(6,3000)
      STOP
C
C---------- 'RESTART' RUN ----
   10 READ(1) (HED(I),I=1,LBLOCK)
      READ(1) (INEI(I),I=1,LGNEIB)
      READ(1) (A(I),I=1,M7)
      REWIND 1
      READ(5,1005)HED
 1005 FORMAT(8A10)
      WRITE(6,2001) HED,MCYCLE
      RETURN
C
C---------- 'START' RUN ----
   20 READ(5,1001) HED,NBLOKM,IBOXES,JBOXES,IBSIZE,TFRAC
C
      NBOXES=IBOXES*JBOXES
      BSIZE=IBSIZE
      XSIZE=IBOXES*BSIZE
      YSIZE=JBOXES*BSIZE
C
      WRITE(6,2002) HED,NBLOKM,IBOXES,JBOXES,NBOXES,
     .                    IBSIZE,XSIZE,YSIZE,TFRAC
C-----------INTERVALS FOR PLOTTING AND PRINTING RESULTS---------
      READ(5,1002) IBPLT,IFPLT,IDPLT,ITDPLT,ICONDA,IBLKDA,IBOXDA,IRFPO
 1002 FORMAT(8I10)
      WRITE(6,2004) IBPLT,IFPLT,IDPLT,ITDPLT,ICONDA,IBLKDA,IBOXDA,IRFPO
 2004 FORMAT(10X,21HBLOCK PLOT INTERVAL =,I4,  10HITERATIONS,/,
     *       10X,29HCONTACT FORCE PLOT INTERVAL =,I4,10HITERATIONS,/,
     *      10X,28HDISPL. + VEL.PLOT INTERVAL =,I4,10HITERATIONS,/,
     *    10X,34HTOTAL DISPLACEMENT PLOT INTERVAL =,I4,10HITERATIONS,//,
     *       10X,29HCONTACT DATA PRINT INTERVAL =,I4,10HITERATIONS,/,
     *       10X,27HBLOCK DATA PRINT INTERVAL =,I4,10HITERATIONS,/,
     *       10X,25HBOX DATA PRINT INTERVAL =,I4,10HITERATIONS,/,
     *       10X,32HRESULTANT FORCE PRINT INTERVAL =,I4,10HITERATIONS//)
C-----------THRESHOLDS FOR UPDATING CONTACTS----------
      READ(5,1003) XYL,THL
 1003 FORMAT(2F10.2)
      WRITE(6,2005) XYL,THL
 2005 FORMAT(1X, 36HTHRESHOLDS FOR UPDATING CONTACTS ARE,F10.5,3HAND,
     *       F10.5,58HFOR THE TRANSLATIONAL AND ROTATIONAL MOVEMENT RESP
     *ECTIVELY,//)
C-----------SIZE OF MEMORY----------
      READ(5,1004) M7D
 1004 FORMAT(I10)
      M7=MAXO(M7,M7D)
      WRITE(6,2006) M7
 2006 FORMAT(10X,16HSIZE OF MEMORY =,I10,//)
C
C---------- INITIALISE SOME VARIABLES ----
      UMOST=0.0
      THMOST=0.0
      NBLOKS=0
      M1=1
```

```
      M2=M1+NBLOKM
      M3=M2
      RETURN
C
 1000 FORMAT(A4)
 1001 FORMAT(8A10/4I10,F10.0)
 2000 FORMAT(30X,25H RBM - RIGID BLOCK MODEL./
     .       30X,25H ----------------------/)
 2001 FORMAT(1X,8A10//30X,30HRESTART RUN. CURRENT CYCLES ...,I10//)
 2002 FORMAT(1X,8A10//
     .       30X,24HMAXIMUM NUMBER OF BLOCKS,I5//
     .       30X,24HBOXES IN X-DIRECTION    ,I5/
     .       30X,24HBOXES IN Y-DIRECTION    ,I5/
     .       30X,24HTOTAL NUMBER OF BOXES   ,I5//
     .       30X,24HSIZE OF SINGLE BOX      ,I5/
     .       30X,24HPROBLEM SIZE IN X-DIRN  ,F6.0/
     .       30X,24HPROBLEM SIZE IN Y-DIRN  ,F6.0//
     .       30X,24HTIMESTEP MULTIPLIER     ,F6.3//)
 3000 FORMAT(48H *** ERROR O 'START' OR 'RESTART' CARD NOT FOUND)
C
      END
      SUBROUTINE NEXT
C
      COMMON/CBLOCK/HED(8),NBLOKM,NBOXES,M1,M2,M3,M4,M5,M6,M7,
     .                  NBLOKS,NCYC,MCYCLE,NEMPT,RFLAG,UFLAG,EFLAG,
     .                  TFRAC,TDEL,IBOXES,JBOXES,BSIZE,XSIZE,YSIZE,
     .                  UDMAX,UMOST,STIFN,STIFS,FRIC,ALPHA,BETA,BDT,
     .                  CON1,CON2,NVARB,NFRAG,NBR,NPR,
     *                  GRAVX,GRAVY,LOC1,LOC2,NUPDAT,
     *            NBCODD,NDCON(76),DISPL,THMOST,THMAX,
     *                 IBPLT,IFPLT,IDPLT,ICONDA,IBLKDA,IBOXDA,
     *                  XYL,THL,LGNEIB,ITDPLT,IRFPO,COMES,
     *                SCREEN,FORCL,VECL,NREM,NBNREM(60),LBLOCK
      LOGICAL RFLAG,UFLAG,EFLAG
      COMMON A(30000)
      DIMENSION IA(1)
      EQUIVALENCE (A,IA)
C
      DIMENSION CARD(8),WORD(20),X(50),Y(50),BNREM(18)
C
      DATA WORD /10HCREATE    ,10HDELETE    ,10HDUMP      ,10HCYCLE
     *          ,10HSTOP      ,10HPLOT      ,10HCOMN      ,10HRSET
     *          ,10HISET      ,10HCHECK     ,10HRINV      ,10HSTIFFNESS
     *          ,10HDAMPING   ,10HFRICTION  ,10HZERO      ,10HLOAD
     *          ,10HMOFY      ,10HUPDA      ,10HDCON      ,10HZTOP
     *          /
C
C-------------------- READ NEXT CARD ---
   10 READ(5,1000) CARD
      WRITE(6,2000) CARD
      DO 20 I=1,20
      IF(CARD(1).EQ.WORD(I)) GOTO 30
   20 CONTINUE
      WRITE(6,3000)
      GOTO 10
C-------------------- JUMP TO APPROPRIATE CODE ---
   30 GOTO (100,150,200,250,300,
     .      350,400,450,500,550,
     .      600,650,700,750,800,
     *      850,900,910,920,930),I
C
   40 WRITE(6,3001)
      GOTO 10
C-------------------- CREATE A NEW BLOCK ---
  100 NBLOKS=NBLOKS+1
      DECODE(40,1001,CARD) NC,RHO,JFIX
      READ(5,1002)  (X(I),Y(I),I=1,NC)
      WRITE(6,2001)  (X(I),Y(I),I=1,NC)
      I2=M3
      IA(NBLOKS)=I2
C
C  INITIALISE SOME VARIABLES
C
      IA(I2)=0
      A(I2+4)=0.
      A(I2+5)=0.
      A(I2+6)=0.
      A(I2+7)=0.
      A(I2+8)=0.
      A(I2+9)=0.
      A(I2+10)=0.
      A(I2+13)=0.
      A(I2+14)=0.
      A(I2+15)=0.
      A(I2+16)=0.
      A(I2+17)=0.
      IF(JFIX.NE.0)  IA(I2)=1
      IA(I2+1)=NC
      A(I2+18)=1.0
      A(I2+19)=0.0
      A(I2+20)=0.0
      A(I2+21)=0.0
      A(I2+22)=0.0
C-------------------- AREA AND CENTROID OF THIS BLOCK ---
      AREA=(X(1)-X(NC))*(Y(1)+Y(NC))
      YC=(X(1)-X(NC))*((Y(1)-Y(NC))*(Y(1)+2.0*Y(NC))+3.0*Y(NC)**2)
      XC=(Y(1)-Y(NC))*((X(1)-X(NC))*(X(1)+2.0*X(NC))+3.0*X(NC)**2)
      DO 110 I=2,NC
      AREA=AREA+(X(I)-X(I-1))*(Y(I)+Y(I-1))
      YC=YC+(X(I)-X(I-1))*((Y(I)-Y(I-1))*(Y(I)+2.0*Y(I-1))
     .     +3.0*Y(I-1)**2)
      XC=XC+(Y(I)-Y(I-1))*((X(I)-X(I-1))*(X(I)+2.0*X(I-1))
     .     +3.0*X(I-1)**2)
  110 CONTINUE
      AREA=0.5*AREA
      YC=YC/(6.0*AREA)
      XC=-XC/(6.0*AREA)
      A(I2+2)=XC
      A(I2+3)=YC
      A(I2+11)=AREA*RHO
C-------------------- LOCAL COORDINATES FOR THIS BLOCK ---
      M3=M3+23
      A(M3)=X(1)-XC
      A(M3+1)=Y(1)-YC
      DO 120 I=2,NC
      A(M3+3)=X(I)-XC
      A(M3+4)=Y(I)-YC
      A(M3+2)=SQRT((A(M3+3)-A(M3))**2+(A(M3+4)-A(M3+1))**2)
  120 M3=M3+3
      A(M3+2)=SQRT((A(I2+23)-A(M3))**2+(A(I2+24)-A(M3+1))**2)
      M3=M3+3
C-------------------- MOMENT OF INERTIA ---
      RMOI=0.0
      IC=I2+23
      DO 130 NP=2,NC
      AREA=A(IC)*A(IC+1)  +  (A(IC+3)-A(IC))*(A(IC+4)+A(IC+1))
     .     - A(IC+3)*A(IC+4)
      AREA=0.5*AREA
```

```
      TEMP=A(IC)**2+A(IC+1)**2+A(IC+3)**2+A(IC+4)**2
     .     +A(IC)*A(IC+3)+A(IC+1)*A(IC+4)
      RMOI=RMOI+AREA*TEMP/6.0
  130 IC=IC+3
      AREA=A(IC)*A(IC+1)+(A(I2+23)-A(IC))*(A(I2+24)+A(IC+1))
     *     -A(I2+23)*A(I2+24)
      AREA=0.5*AREA
      TEMP=A(I2+23)**2+A(I2+24)**2+A(IC)**2+A(IC+1)**2
     *     +A(I2+23)*A(IC)+A(I2+24)*A(IC+1)
      RMOI=RMOI+AREA*TEMP/6.0
      A(I2+12)=RMOI*RHO
C
      WRITE(6,2002) XC,YC,A(I2+11),A(I2+12)
      GOTO 10
C-------------------- DELETE A BLOCK ---
C REMOVE NREM BLOCKS
  150 CONTINUE
      READ(5,1007)NREM
 1007 FORMAT(I4)
      WRITE(6,2003)NREM
 2003 FORMAT(1X, 32H THE NUMBER OF BLOCKS REMOVED IS,I4,
     * 29H THEIR NUMBERS ARE----------)
      READ(5,1008)NBC,(BNREM(K),K=1,19)
 1008 FORMAT(I4,19F4.0)
      WRITE(6,2004)(BNREM(K),K=1,19)
 2004 FORMAT(1X,19F4.0)
      DO 151 K=1,19
      IF(BNREM(K).EQ.0.)GO TO 151
      NBNREM(K)=BNREM(K)
  151 CONTINUE
      IF(NREM.LE.19)GO TO 152
      JJ=19
      DO 153 IIJ=1,10
      READ(5,1008)NBC,(BNREM(K),K=1,19)
      IF(NBC.EQ.999)GO TO 152
      WRITE(6,2004)(BNREM(K),K=1,19)
      DO 153 IJ=1,19
      JJ=JJ+1
      IF(BNREM(IJ).EQ.0.)GO TO 153
      NBNREM(JJ)=BNREM(IJ)
  153 CONTINUE
  152 CONTINUE
      UFLAG=.TRUE.
      GO TO 10
C-------------------- DUMP MEMORY AS REQUESTED ---
  200 CALL DUMP(1)
      CALL DUMP(2)
      CALL DUMP(3)
      GOTO 10
C-------------------- CYCLE ROUND MOTION AND FORD ---
  250 DECODE(20,1001,CARD) NCYC
      WRITE(6,2030)NCYC
 2030 FORMAT(1X,19H NUMBER OF CYCLES =,I10)
      IF(NCYCLE.EQ.0) CALL BOX
      RETURN
C-------------------- STOP COMMAND ---
  300 CALL FINISH
C-------------------- PLOT COMMAND ---
  350 CALL BPLOT
      GOTO 10
  400 CONTINUE
C-------JOINT COHESION--------
      READ(5,1060)COHES
 1060 FORMAT(F10.0)
      WRITE(6,2031)COHES
 2031 FORMAT(10X,16HJOINT COHESION =,F10.2,/)
      GOTO 10
C-------------------- SET REAL DATA ---
  450 DECODE(30,1004,CARD) IADR,VAL
      IF(IADR.LE.0.OR.IADR.GT.M7) GOTO 480
      A(IADR)=VAL
      GOTO 10
  480 WRITE(6,3002)
      GOTO 10
C-------------------- SET INTEGER DATA ---
  500 DECODE(30,1003,CARD) IADR,IVAL
      IF(IADR.LE.0.OR.IADR.GT.M7) GOTO 480
      IA(IADR)=IVAL
      GOTO 10
C-------------------- MOMENTUM & ENERGY CHECK ---
  550 CALL CHECK
      GOTO 10
  600 CONTINUE
C-------PLOT AND PRINT INTERVALS--------
      READ(5,1011)IBPLT,IFPLT,IDPLT,ITDPLT,ICONDA,IBLKDA,IBOXDA,IRFPO
 1011 FORMAT(8I10)
      WRITE(6,2007)IBPLT,IFPLT,IDPLT,ITDPLT,ICONDA,IBLKDA,IBOXDA,IRFPO
 2007 FORMAT(10X,21HBLOCK PLOT INTERVAL =,I4,  10HITERATIONS,/,
     *       10X,29HCONTACT FORCE PLOT INTERVAL =,I4,10HITERATIONS,/,
     *     10X,28HDISPL. + VEL.PLOT INTERVAL =,I4,10HITERATIONS,/,
     *    10X,34HTOTAL DISPLACEMENT PLOT INTERVAL =,I4,10HITERATIONS,//,
     *       10X,29HCONTACT DATA PRINT INTERVAL =,I4,10HITERATIONS,/,
     *       10X,27HBLOCK DATA PRINT INTERVAL =,I4,10HITERATIONS,/,
     *       10X,25HBOX DATA PRINT INTERVAL =,I4,10HITERATIONS,/,
     *       10X,32HRESULTANT FORCE PRINT INTERVAL =,I4,10HITERATIONS//)
      READ(5,1012)M7O
 1012 FORMAT(I10)
      M7=M7O
      WRITE(6,2008)M7
 2008 FORMAT(10X,22HMODIFIED MEMORY SIZE =,I10,//)
      GOTO 10
C-------------------- CONTACT STIFFNESSES ---
  650 DECODE(30,1005,CARD) STIFN,STIFS
      WRITE(6,2009)STIFN,STIFS
 2009 FORMAT(10X,24HJOINT NORMAL STIFFNESS =,E10.4,/,
     *       10X,23HJOINT SHEAR STIFFNESS =,E10.4,/)
      GOTO 10
C-------------------- RAYLEIGH DAMPING ---
  700 DECODE(50,1006,CARD) FRAC,FREQ,IF1,IF2
      WRITE(6,2025)FRAC,FREQ
 2025 FORMAT(10X,26HDAMPING TERMS ARE . FRAC =,F5.2,10HAND FREQ =,F10.1)
      PI2=8.0*ATAN(1.0)
      ALPHA=PI2*FRAC*FREQ
      BETA=FRAC/(PI2*FREQ)
      IF(IF1.EQ.0) GO TO 710
      ALPHA=0.0
      WRITE(6,3003)
  710 IF(IF2.EQ.0) GO TO 720
      BETA=0.0
      WRITE(6,3004)
  720 IF(MCYCLE.EQ.0) GO TO 10
      BDT=BETA/TDEL
      CON1=1.0-ALPHA*TDEL/2.0
      CON2=1.0/(1.0+ALPHA*TDEL/2.0)
      GOTO 10
C-------------------- FRICTION COEFFICIENT ---
  750 DECODE(20,1005,CARD) FRIC
      WRITE(6,2011)FRIC
```

```
 2011 FORMAT(10X,28HJOINT FRICTION COEFFICIENT =,F10.3,/)
      GOTO 10
C------------------ ZERO ALL VELOCITIES ---
  800 DO 820 NB=1,NBLOKS
      I2=IA(NB)
      A(I2+5)=0.0
      A(I2+6)=0.0
      A(I2+7)=0.0
  820 CONTINUE
      GOTO 10
C------------------ SET BLOCK LOADS ---
  850 DECODE(40,1006,CARD) FX,FY,NB
      I2=IA(NB)
      A(I2+16)=FX
      A(I2+17)=FY
      GOTO 10
  900 CONTINUE
      READ(5,1016)XYL,THL
 1016 FORMAT(2F10.2)
      WRITE(6,2015)XYL,THL
 2015 FORMAT(10X,8HNEW XYL =,F10.5,8HNEW THL =,F10.5)
      GO TO 10
  910 CONTINUE
      CALL UPDAT
      GO TO 10
  920 CONTINUE
C----BLOCK NUMBERS FOR WHICH CONTACT DATA TO BE DUMPED-------
      READ(5,1007)NBCODD
      READ(5,1008)NBCC,(BNREM(K),K=1,19)
      WRITE(6,2014)NBCODD
 2014 FORMAT(10X,55HNUMBER OF BLOCKS FOR WHICH CONTACT DATA TO BE DUMPED
     * IS,I4,/,  26HTHEIR NUMBERS ARE----------)
      WRITE(6,2004)(BNREM(K),K=1,19)
      DO 951 K=1,19
      IF(BNREM(K).EQ.0.)GO TO 951
      NDCON(K)=BNREM(K)
  951 CONTINUE
      IF(NBCODD.LE.19)GO TO 952
      JJ=19
      DO 953 IIJ=1,10
      READ(5,1008)NBCC,(BNREM(K),K=1,19)
      IF(NBCC.EQ.999)GO TO 952
      WRITE(6,2004)(BNREM(K),K=1,19)
      DO 953 IJ=1,19
      JJ=JJ+1
      IF(BNREM(IJ).EQ.0.)GO TO 953
      NDCON(JJ)=BNREM(IJ)
  953 CONTINUE
  952 CONTINUE
      GO TO 10
  930 CONTINUE
C-----ZEROISE TOTAL DISPLACEMENTS----------
      DO 931 NB=1,NBLOKS
      I2=IA(NB)
      A(I2+20)=0.0
      A(I2+21)=0.0
      A(I2+22)=0.0
  931 CONTINUE
      WRITE(6,932)MCYCLE
  932 FORMAT(10X,43HTOTAL DISPL. PLOT HAS BEEN ZEROED AT CYCLE ,I4)
      GO TO 10
C
 1000 FORMAT(8A10)
 1001 FORMAT(10X,I10,F10.0,I10)
 1002 FORMAT(8F10.0)
 1003 FORMAT(10X,2I10)
 1004 FORMAT(10X,I10,F10.0)
 1005 FORMAT(10X,2F10.0)
 1006 FORMAT(10X,2F10.0,2I10)
 2000 FORMAT(1X,4H+++ ,8A10,4H +++)
 2001 FORMAT(1X,4(1H(,E12.4,1H,,E12.4,3H ) ))
 2002 FORMAT(18H XC,YC,MASS,RMOI 0,1P4E12.3)
 3000 FORMAT(28H !!! ERROR 0 ILLEGAL COMMAND)
 3001 FORMAT(34H !!! ERROR 0 COMMAND NOT AVAILABLE)
 3002 FORMAT(33H !!! ERROR 0 ADDRESS OUT OF RANGE)
 3003 FORMAT(10X,29HMASS DAMPING TERM SET TO ZERO)
 3004 FORMAT(10X,34HSTIFFNESS DAMPING TERM SET TO ZERO)
C
      END
      SUBROUTINE BOX
C
C------------------ ALL BLOCKS HAVE BEEN CREATED,
C------------------ BLOCKS CAN NOW BE BOXED -----
C
      COMMON/CBLOCK/HED(8),NBLOKM,NBOXES,M1,M2,M3,M4,M5,M6,M7,
     .                    NBLOKS,NCYC,MCYCLE,NEMPT,RFLAG,UFLAG,EFLAG,
     .                    TFRAC,TDEL,IBOXES,JBOXES,BSIZE,XSIZE,YSIZE,
     .                    UDMAX,UMOST,STIFN,STIFS,FRIC,ALPHA,BETA,BDT,
     .                    CON1,CON2,NVARB,NFRAG,NBR,NPR,
     *                    GRAVX,GRAVY,LOC1,LOC2,NUPDAT,
     *             NBCODD,NDCON(76),DISPL,THMOST,THMAX,
     *                    IBPLT,IFPLT,IDPLT,ICONDA,IBLKDA,IBOXDA,
     *                    XYL,THL,LGNEIB,ITDPLT,IRFPO,COMES,
     *                   SCREEN,FORCL,VECL,NREM,NBNREM(60),LBLOCK
      LOGICAL RFLAG,UFLAG,EFLAG
      COMMON A(30000)
      DIMENSION IA(1)
      EQUIVALENCE (A,IA)
C
      M4=M3+NBOXES
      M5=M4
C------------------ INITIALISE BOX POINTERS ---
      I1=M4-1
      DO 10 I=M3,I1
   10 IA(I)=0
C------------------ LOOP ON EACH BLOCK ---
      DO 50 NB=1,NBLOKS
      I2=IA(NB)
      NC=IA(I2+1)
      IC=I2+23
C------------------ LOOP ON EACH CORNER ---
      DO 40 NP=1,NC
      X=A(I2+2)+A(IC)
      Y=A(I2+3)+A(IC+1)
      IBOX=MIND(IFIX(X/BSIZE)+1,IBOXES)
      JBOX=MIND(IFIX(Y/BSIZE),JBOXES-1)
      NBOX=JBOX*IBOXES+IBOX
      I3=M3+NBOX-1
      IA(M5+2)=IA(I3)
      IA(I3)=M5
      IA(M5)=NP
      IA(M5+1)=NB
      M5=M5+3
      IC=IC+3
   40 CONTINUE
C
   50 CONTINUE
C
```

```
      M6=M5+NBLOKM
      DO 60 I=M5,M6
   60 IA(I)=0
C------------------- CREATE EMPTY LIST TO END OF MEMORY ---
      NEMPT=M5
      I6=M6+4
      DO 80 I=I6,M7,13
      J=I
      IA(I)=I+9
   80 CONTINUE
      IA(J)=0
      WRITE(6,2001)M2,M3,M4,M5,M6
 2001 FORMAT(1X,16H M2,M3,M4,M5,M6..,5I10)
C------------------- DETERMINE TIMESTEP ---
      TDEL=1.0E20
      DO 100 NB=1,NBLOKS
      I2=IA(NB)+11
      TN=2.0*SQRT(A(I2)/STIFN)
      TS=2.0*SQRT(A(I2)/STIFS)
      TDEL=AMIN1(TDEL,TN,TS)
  100 CONTINUE
      TDEL=TDEL*TFRAC
      WRITE(6,2000) TDEL
C------------------- SET UP DAMPING TERMS ---
      BDT=BETA/TDEL
      CON1=1.0-ALPHA*TDEL/2.0
      CON2=1.0/(1.0+ALPHA*TDEL/2.0)
C
      RETURN
C
 2000 FORMAT(30X,17H TIME INCREMENT =,1PE12.4)
C
      END
      SUBROUTINE CYCLE
C
C------------------- DRIVER FOR ITERATIONS ---
C
      COMMON/CBLOCK/HED(8),NBLOKM,NBOXES,M1,M2,M3,M4,M5,M6,M7,
     .              NBLOKS,NCYC,MCYCLE,NEMPT,RFLAG,UFLAG,EFLAG,
     .              TFRAC,TDEL,IBOXES,JBOXES,BSIZE,XSIZE,YSIZE,
     .              UDMAX,UMOST,STIFN,STIFS,FRIC,ALPHA,BETA,BDT,
     .              CON1,CON2,NVARB,NFRAG,NBR,NPR,
     *              GRAVX,GRAVY,LOC1,LOC2,NUPDAT,
     *        NBCODD,NDCON(76),DISPL,THMOST,THMAX,
     *             IBPLT,IFPLT,IDPLT,ICONDA,IBLKDA,IBOXDA,
     *              XYL,THL,LGNEIB,ITDPLT,IRFPO,COMES,
     *             SCREEN,FORCL,VECL,NREM,NBNREM(60),LBLOCK
      LOGICAL RFLAG,UFLAG,EFLAG
      COMMON A(30000)
      DIMENSION IA(1)
      EQUIVALENCE (A,IA)
      COMMON/INEIG/IN(111),NEIGHB(111,16)
      DIMENSION INEI(1887)
      EQUIVALENCE(IN,INEI)
C
      DO 100 NCYCLE=1,NCYC
      MCYCLE=MCYCLE+1
C------------------- UPDATE IF NECESSARY ---
      IF(UFLAG) CALL UPDAT
C------------------- SCAN ALL BLOCKS ---
      UDMAX=0.0
      THMAX=0.0
      DO 20 NB=1,NBLOKS
C
C CHECK IF BLOCK REMOVED
C
      IF(NREM.EQ.0)GO TO 120
      DO 130 K=1,NREM
      IF(NB.EQ.NBNREM(K))GO TO 20
  130 CONTINUE
  120 CONTINUE
      IB=IA(NB)
C------------------- IS THIS BLOCK FIXED ? ---
      IF(IA(IB).NE.0)GO TO 20
C------------------- NO ---
      CALL MOTION(A,IA,IB,NB)
      IF(RFLAG) CALL REBOX(NB)
   20 CONTINUE
C------------------- EXIT IF NOTHING MOVED ---
      IF(UDMAX.EQ.0.0) GOTO 110
C------------------- UPDATE CONTACTS ? ---
      TRANS=UDMAX*TDEL
      ROTN=THMAX*TDEL
      UMOST=UMOST+TRANS
      THMOST=THMOST+ROTN
      IF(UMOST.GT.XYL.OR.THMOST.GT.THL)GO TO 30
      GO TO 40
   30 UFLAG=.TRUE.
      UMOST=0.0
      THMOST=0.0
   40 CONTINUE
      WRITE(6,1001)MCYCLE,TRANS,ROTN
 1001 FORMAT(1X,61HMAXIMUM BLOCK TRANSLATIONAL AND ROTATIONAL MOVEMENT F
     *OR CYCLE,I5,3HWAS,F10.8,4H AND,F10.8,13H RESPECTIVELY)
      GO TO 250
  110 WRITE(6,2001)MCYCLE
 2001 FORMAT(1X,29HBLOCKS DID NOT MOVE FOR CYCLE,I5)
      GO TO 111
  250 CONTINUE
      DO 50 NB=1,NBLOKS
C
C CHECK IF BLOCK REMOVED
C
      IF(NREM.EQ.0)GO TO 140
      DO 150 K=1,NREM
      IF(NB.EQ.NBNREM(K))GO TO 50
  150 CONTINUE
  140 CONTINUE
      IBE=IA(NB)
      J6=M5+NB-1
   60 I6=IA(J6)
      IF(I6.EQ.0) GOTO 50
      JBC=IA(I6+3)
      IBC=IA(JBC)
      CALL FORD(A(I6),A(IBC),A(IBE))
      J6=I6+4
      GO TO 60
   50 CONTINUE
C
C------------------- END CYCLE LOOP ---
C
      JPLOT1=(MCYCLE/IBPLT)*IBPLT
      IF(JPLOT1.NE.MCYCLE)GO TO 152
      CALL BPLOT
  152 JPLOT2=(MCYCLE/IFPLT)*IFPLT
      IF(JPLOT2.NE.MCYCLE)GO TO 153
      CALL FORPLT
  153 JPLOT3=(MCYCLE/IDPLT)*IDPLT
```

```
      IF(JPLOT3.NE.MCYCLE)GO TO 151
      CALL DISPLT
      CALL VELOC
  151 JPLOT4=(MCYCLE/ITDPLT)*ITDPLT
      IF(JPLOT4.NE.MCYCLE)GO TO 154
      CALL TDISPL
  154 CONTINUE
      IPRIN1=(MCYCLE/ICONDA)*ICONDA
      IF(IPRIN1.NE.MCYCLE)GO TO 751
      CALL DUMP(1)
  751 IPRIN2=(MCYCLE/IBLKDA)*IBLKDA
      IF(IPRIN2.NE.MCYCLE)GO TO 752
      CALL DUMP(2)
  752 IPRIN3=(MCYCLE/IBOXDA)*IBOXDA
      IF(IPRIN3.NE.MCYCLE)GO TO 750
      CALL DUMP(3)
  750 CONTINUE
  100 CONTINUE
C
  111 CONTINUE
C
      RETURN
C
      END
      SUBROUTINE MOTION(A,IA,IB,NB)
C
C------------------- LAW OF MOTION FOR A SINGLE BLOCK ---
C
      COMMON/CBLOCK/HED(8),NBLOKM,NBOXES,M1,M2,M3,M4,M5,M6,M7,
     .                  NBLOKS,NCYC,MCYCLE,NEMPT,RFLAG,UFLAG,EFLAG,
     .                  TFRAC,TDEL,IBOXES,JBOXES,BSIZE,XSIZE,YSIZE,
     .                  UDMAX,UMOST,STIFN,STIFS,FRIC,ALPHA,BETA,BDT,
     .                  CON1,CON2,NVARB,NFRAG,NBR,NPR,
     *                  GRAVX,GRAVY,LOC1,LOC2,NUPDAT,
     *            NBCODD,NDCON(76),DISPL,THMOST,THMAX,
     *                  IBPLT,IFPLT,IDPLT,ICONDA,IBLKDA,IBOXDA,
     *                   XYL,THL,LGNEIB,ITDPLT,IRFPO,COMES,
     *                  SCREEN,FORCL,VECL,NREM,NBNREM(60),LBLOCK
      LOGICAL RFLAG,UFLAG,EFLAG
      COMMON/INEIG/IN(111),NEIGHB(111,16)
      DIMENSION INEI(1887)
      EQUIVALENCE(IN,INEI)
      DIMENSION A(1),IA(1)
      DIMENSION XCON(50),YCON(50),NBCON(50),NEIG(20)
      DO 300 J=1,50
      XCON(J)=0.0
      YCON(J)=0.0
      NBCON(J)=0
  300 CONTINUE
      J=0
      J6=M6+NB-1
  100 I6=IA(J6)
      IF(I6.EQ.0)GO TO 90
      J=J+1
      XCON(J)=A(I6+11)
      YCON(J)=A(I6+12)
      NBCON(J)=IA(I6+3)
      A(IB+13)=A(IB+13)+A(I6+6)
      A(IB+14)=A(IB+14)+A(I6+5)
      A(IB+15)=A(IB+15)+(A(I6+5)*(A(I6+11)-A(IB+2))
     *         -A(I6+6)*(A(I6+12)-A(IB+3)))
      J6=I6+4
      GO TO 100
   90 CONTINUE
      IXX=0
      INNB=IN(NB)
      DO 650 JX=1,INNB
      NBB=NEIGHB(NB,JX)
      IF(NBB.EQ.0)GO TO 650
      IF(NBB.EQ.NB)GO TO 700
      GO TO 710
  700 WRITE(6,1010)
 1010 FORMAT(1X,32HERRORS IN NEIGHB ARRAY IN MOTION)
      EFLAG=.TRUE.
      CALL FINISH
  710 IF(IXX.EQ.0)GO TO 660
      DO 670 JXX=1,IXX
      IF(NEIG(JXX).EQ.NBB)GO TO 650
  670 CONTINUE
  660 CONTINUE
      IXX=IXX+1
      NEIG(IXX)=NBB
      N6=M6+NBB-1
      I6=IA(N6)
  120 CONTINUE
      IF(I6.EQ.0)GO TO 650
      IF(IA(I6+3).EQ.NB)GO TO 130
  180 N6=I6+4
      I6=IA(N6)
      GO TO 120
  130 CONTINUE
      I2B=IA(NBB)
      XX=A(I6+11)
      YY=A(I6+12)
      RLENG=(A(I2B+22+IA(I6+1)*3))/20.
      DO 600 I=1,J
      IF(NBCON(I).EQ.NBB)GO TO 610
      GO TO 620
  610 XDIF=ABS(XX-XCON(I))
      YDIF=ABS(YY-YCON(I))
      IF(XDIF.LT.RLENG.AND.YDIF.LT.RLENG)GO TO 180
  620 CONTINUE
  600 CONTINUE
      A(IB+13)=A(IB+13)-A(I6+6)
      A(IB+14)=A(IB+14)-A(I6+5)
      A(IB+15)=A(IB+15)-(A(I6+5)*(A(I6+11)-A(IB+2))
     *         -A(I6+6)*(A(I6+12)-A(IB+3)))
      GO TO 180
  650 CONTINUE
C-------PRINT OUT RESULTANT FORCES ON BLOCK---------
      IPOOF=(MCYCLE/IRFPO)*IRFPO
      IF(IPOOF.NE.MCYCLE)GO TO 951
      WRITE(6,1020)A(IB+13),A(IB+14),A(IB+15)
 1020 FORMAT(10X,E10.4,5X,E10.4,5X,E10.4)
  951 CONTINUE
C-------------------VELOCITIES FROM ACCELERATIONS----------------
      A(IB+5)=(A(IB+5)*CON1+(A(IB+13)/A(IB+11)+GRAVX)*TDEL)*CON2
      UDMAX=AMAX1(UDMAX,ABS(A(IB+5)))
      A(IB+6)=(A(IB+6)*CON1+(A(IB+14)/A(IB+11)+GRAVY)*TDEL)*CON2
      UDMAX=AMAX1(UDMAX,ABS(A(IB+6)))
      A(IB+7)=(A(IB+7)*CON1+(A(IB+15)/A(IB+12))*TDEL)*CON2
      THMAX=AMAX1(THMAX,ABS(A(IB+7)))
      A(IB+13)=A(IB+16)
      A(IB+14)=A(IB+17)
      A(IB+15)=0.0
C-------------DISPLACEMENTS FROM VELOCITIES--------------
      IBX=A(IB+2)
      IBY=A(IB+3)
```

```
      A(IB+8)=A(IB+5)*TDEL
      A(IB+9)=A(IB+6)*TDEL
      A(IB+10)=A(IB+7)*TDEL
      A(IB+2)=A(IB+2)+A(IB+8)
      A(IB+3)=A(IB+3)+A(IB+9)
      A(IB+4)=A(IB+4)+A(IB+10)
      A(IB+20)=A(IB+20)+A(IB+8)
      A(IB+21)=A(IB+21)+A(IB+9)
      A(IB+22)=A(IB+22)+A(IB+10)
C-----------DO WE NEED TO REBOX----------
      IF(IBX.EQ.IFIX(A(IB+2)).AND.IBY.EQ.IFIX(A(IB+3)).AND.
     *   ABS(A(IB+4)).LT.0.01)GO TO 150
C-----------YES----------
      RFLAG=.TRUE.
      A(IB+4)=0.0
C-----------UPDATE COS AND SINE FOR THIS BLOCK----------
  150 TEMP=A(IB+18)
      A(IB+18)=A(IB+18)-A(IB+10)*A(IB+19)
      A(IB+19)=A(IB+19)+A(IB+10)*TEMP
      RETURN
C
      END
      SUBROUTINE FORD(C,BC,BE)
C
C---------- FORCE DISPLACEMENT LAW FOR SINGLE CONTACT ---
C
      COMMON/CBLOCK/HED(8),NBLOKM,NBOXES,M1,M2,M3,M4,M5,M6,M7,
     .                    NBLOKS,NCYC,MCYCLE,NEMPT,RFLAG,UFLAG,EFLAG,
     .                    TFRAC,TDEL,IBOXES,JBOXES,BSIZE,XSIZE,YSIZE,
     .                    UDMAX,UMOST,STIFN,STIFS,FRIC,ALPHA,BETA,BDT,
     .                    CON1,CON2,NVARB,NFRAG,NBR,NPR,
     *                    GRAVX,GRAVY,LOC1,LOC2,NUPDAT,
     *             NBCODD,NDCON(76),DISPL,THMOST,THMAX,
     *                   IBPLT,IFPLT,IDPLT,ICONDA,IBLKDA,IBOXDA,
     *                    XYL,THL,LGNEIB,ITDPLT,IRFPO,COHES,
     *                  SCREEN,FORCL,VECL,NREM,NBNREM(60),LBLOCK
      LOGICAL RFLAG,UFLAG,EFLAG
      DIMENSION C(1),BC(1),BE(1)
C
C---------- INCREMENTAL GLOBAL DISPLACEMENTS ---
      DUY=BC(10)-BE(10)+BC(11)*(C(12)-BC(3))-BE(11)*(C(12)-BE(3))
      DUX=BC( 9)-BE( 9)-BC(11)*(C(13)-BC(4))+BE(11)*(C(13)-BE(4))
C---------- NORMAL COORDINATES ---
      DUS=DUX*C(11)+DUY*C(10)
      DUN=DUY*C(11)-DUX*C(10)
C---------- NORMAL FORCE ---
      DFN=-DUN*STIFN
      C(8)=C(8)+DFN
C---------- TEST FOR TENSION ---
      IF(C(8).GE.0.0) GOTO 20
      C(8)=0.0
      C(9)=0.0
      DN=0.0
      DS=0.0
      GOTO 60
C---------- SHEAR FORCE ---
   20 DFS=DUS*STIFS
      C(9)=C(9)+DFS
      FRICF=FRIC*C(8)+COHES
      IF(ABS(C(9)).LE.FRICF) GOTO 40
      C(9)=SIGN(FRICF,C(9))
      DS=0.0
      GOTO 50
C---------- DASHPOT FORCES ---
   40 DS=BDT*DFS
   50 DN=BDT*DFN
C---------- GLOBAL CONTACT FORCES ---
   60 FYC=(C(9)+DS)*C(10)-(C(8)+DN)*C(11)
      FXC=(C(9)+DS)*C(11)+(C(8)+DN)*C(10)
C---------- ADD CONTRIBUTION TO BLOCK FORCES ---
      C(6)=FYC
      C(7)=FXC
C
      RETURN
C
      END
      SUBROUTINE UPDAT
C
C---------- UPDATE ALL CONTACTS ---
C
      COMMON/CBLOCK/HED(8),NBLOKM,NBOXES,M1,M2,M3,M4,M5,M6,M7,
     .                    NBLOKS,NCYC,MCYCLE,NEMPT,RFLAG,UFLAG,EFLAG,
     .                    TFRAC,TDEL,IBOXES,JBOXES,BSIZE,XSIZE,YSIZE,
     .                    UDMAX,UMOST,STIFN,STIFS,FRIC,ALPHA,BETA,BDT,
     .                    CON1,CON2,NVARB,NFRAG,NBR,NPR,
     *                    GRAVX,GRAVY,LOC1,LOC2,NUPDAT,
     *             NBCODD,NDCON(76),DISPL,THMOST,THMAX,
     *                   IBPLT,IFPLT,IDPLT,ICONDA,IBLKDA,IBOXDA,
     *                    XYL,THL,LGNEIB,ITDPLT,IRFPO,COHES,
     *                  SCREEN,FORCL,VECL,NREM,NBNREM(60),LBLOCK
      LOGICAL RFLAG,UFLAG,EFLAG
      COMMON A(30000)
      DIMENSION IA(1)
      EQUIVALENCE (A,IA)
      COMMON/INEIG/IN(111),NEIGHB(111,16)
      DIMENSION INEI(1887)
      EQUIVALENCE(IN,INEI)
C
      LOGICAL FIRST
      DO 600 IX=1,NBLOKS
      IN(IX)=0
      DO 610 JX=1,16
      NEIGHB(IX,JX)=0
  610 CONTINUE
  600 CONTINUE
      DATA TOL,TOLB /1.0,-0.01/
C
C---------- SCAN EACH BLOCK ---
      DO 500 NB=1,NBLOKS
C
C CHECK IF BLOCK REMOVED
C
      IF(NREM.EQ.0)GO TO 110
      DO 100 K=1,NREM
      IF(NB.EQ.NBNREM(K))GO TO 405
  100 CONTINUE
  110 CONTINUE
      I2=IA(NB)
      NC=IA(I2+1)
C---------- SCAN EACH EDGE OF BLOCK ---
      IEND2=I2+23
      DO 400 NP=1,NC
      FIRST=.TRUE.
      IEND1=IEND2
      IEND2=IEND1+3
      IF(NP.EQ.NC) IEND2=I2+23
C---------- DETERMINE BOXES TO BE SEARCHED ---
      X11=GLX(A(I2),IEND1)
```

```
      X22=GLX(A(I2),IEND2)
      Y11=GLY(A(I2),IEND1)
      Y22=GLY(A(I2),IEND2)
      TEMP=AMAX1(X11,X22)
      X1=AMIN1(X11,X22)
      X2=TEMP
      TEMP=AMAX1(Y11,Y22)
      Y1=AMIN1(Y11,Y22)
      Y2=TEMP
      NXL=IFIX((X1-XYL)/BSIZE)+1
      NXU=MINO(IFIX((X2+XYL)/BSIZE)+1,IBOXES)
      NYL=IFIX((Y1-XYL)/BSIZE)+1
      NYU=MINO(IFIX((Y2+XYL)/BSIZE)+1,JBOXES)
C---------------- SEARCH EACH CANDIDATE BOX ---
      DO 350 JBOX=NYL,NYU
      NBOX=(JBOX-1)*IBOXES+NXL-1
      DO 300 IBOX=NXL,NXU
      NBOX=NBOX+1
      I4=IA(M3+NBOX-1)
C---------------- END OF BOX LIST ? ---
  210 CONTINUE
      IF(I4.EQ.0) GOTO 300
C
C CHECK IF BLOCK REMOVED
C
      IF(NREM.EQ.0)GO TO 120
      DO 130 K=1,NREM
      IF(IA(I4+1).EQ.NBNREM(K))GO TO 215
  130 CONTINUE
  120 CONTINUE
C---------------- NO, IS THIS BLOCK NB ? ---
      IF(IA(I4+1).NE.NB) GOTO 220
C---------------- YES ---
C---------------- GET NEXT ENTRY IN THIS BOX ---
  215 I4=IA(I4+2)
      GOTO 210
C---------------- FIRST TIME THROUGH ? ---
  220 IF(.NOT.FIRST) GOTO 230
C---------------- YES, COMPUTE COS AND SIN FOR THIS EDGE ---
      FIRST=.FALSE.
      COSA=(X22-X11)/A(IEND1+2)
      SINA=(Y22-Y11)/A(IEND1+2)
C---------------- COMPUTE CORNER COORDINATES RELATIVE TO EDGE ---
  230 I2C=IA(I4+1)
      I2C=IA(I2C)
      IC=I2C+IA(I4)*3+20
      X1C=GLX(A(I2C),IC)
      Y1C=GLY(A(I2C),IC)
      YT=(Y1C-Y11)*COSA-(X1C-X11)*SINA
      IF(YT.GT.XYL)GO TO 215
      COF=-3.0*XYL
      IF(YT.LE.COF)GO TO 215
      XT=(X1C-X11)*COSA+(Y1C-Y11)*SINA
      CHEKFL=(X22-X11)*COSA+(Y22-Y11)*SINA
      CHEK2=1.E-10+CHEKFL
      IF(XT.GT.CHEK2)GO TO 215
      IF(XT.LT.-1.E-10)GO TO 215
C---------------- CONTACT LIST FOR BLOCK NB ---
      J6=M5+NB-1
      I6=IA(J6)
C---------------- END OF LIST ? ---
  235 CONTINUE
      IF(I6.EQ.0) GOTO 250
C---------------- NO, SAME CORNER AND EDGE ? ---
      IF(IA(I4).EQ.IA(I6+2).AND.IA(I4+1).EQ.IA(I6+3)
     .   .AND.NP.EQ.IA(I6+1)) GOTO 240
C---------------- NO, GET NEXT ENTRY IN CONTACT LIST ---
      J6=I6+4
      I6=IA(J6)
      GOTO 235
  240 A(I6+9)=SINA
      A(I6+10)=COSA
      A(I6+11)=GLX(A(I2C),IC)
      A(I6+12)=GLY(A(I2C),IC)
      IA(I6)=1
      LMARK=IA(I4+1)
      CHEK3=CHEKFL-1.E-10
      IF(XT.LE.1.E-10)GO TO 620
      IF(XT.GE.CHEK3)GO TO 620
      IN(LMARK)=IN(LMARK)+1
      IF(IN(LMARK).GT.16)GO TO 619
      NEIGHB(LMARK,IN(LMARK))=NB
      GO TO 620
  619 WRITE(6,1000)LMARK
 1000 FORMAT(1X,61HGREATER THAN 16 NEIGHBOURING BLOCKS IN NEIGHB ARRAY F
     *OR BLOCK,I5)
  620 CONTINUE
      GOTO 215
C---------------- NEW CONTACT ? ---
  250 CONTINUE
      IF(YT.GT.1.E-10)GO TO 215
C---------------- YES ---
      I6=NEMPT
      ICR=IC-3
      IF(IA(I4).EQ.1)  ICR=IC+3*(IA(I2C+1)-1)
      YTR=(GLY(A(I2C),ICR)-Y11)*COSA
     *     -(GLX(A(I2C),ICR)-X11)*SINA
      COFF=-2.0*XYL
      IF(YTR.LE.COFF)GO TO 215
      ICL=IC+3
      IF(IA(I4).EQ.IA(I2C+1))ICL=I2C+23
      YTL=(GLY(A(I2C),ICL)-Y11)*COSA
     *     -(GLX(A(I2C),ICL)-X11)*SINA
      IF(YTL.LE.COFF)GO TO 215
C---------------- ANY SPACE AVAILABLE IN EMPTY LIST ? ---
      IF(IA(NEMPT+4).NE.0) GOTO 260
      WRITE(6,3001)
      CALL FINISH
C---------------- NEW CONTACT ---
  260 A(I6+5)=0.0
      A(I6+6)=0.0
      A(I6+7)=0.0
      A(I6+8)=0.0
      IA(I6+1)=NP
      IA(I6+2)=IA(I4)
      IA(I6+3)=IA(I4+1)
      NEMPT=IA(I6+4)
      IA(J6)=I6
      IA(I6+4)=0
      GO TO 240
C---------------- END OF BOX SCAN ---
  300 CONTINUE
  350 CONTINUE
C---------------- END OF EDGE SCAN ---
  400 CONTINUE
  405 CONTINUE
C---------------- SCAN CONTACT LIST FOR PRESERVE FLAGS ---
      J6=M5+NB-1
```

```
      I6=IA(J6)
C------------------- END-OF LIST ? ---
  410 IF(I6.EQ.0) GOTO 490
C------------------- NO ---
C------------------- IS THE PRESERVE FLAG SET ? ---
      IF(IA(I6).EQ.0) GOTO 420
C------------------- YES ---
      IA(I6)=0
      J6=I6+4
      GOTO 430
C------------------- NO ---
  420 IA(J6)=IA(I6+4)
      IA(I6+4)=NEMPT
      NEMPT=I6
C------------------- GET NEXT CONTACT ---
  430 I6=IA(J6)
      GOTO 410
C------------------- END OF BLOCK SCAN ---
  490 CONTINUE
  500 CONTINUE
C
      NUPDAT=NUPDAT+1
      UFLAG=.FALSE.
      RETURN
C
 3001 FORMAT(30X,32H NO MORE MEMORY FOR CONTACT LIST)
C
      END
      SUBROUTINE REBOX(NB)
C
C------------------- ROUTINE TO REBOX A SINGLE BLOCK ---
C
      COMMON/CBLOCK/HED(8),NBLOKM,NBOXES,M1,M2,M3,M4,M5,M6,M7,
     .                  NBLOKS,NCYC,MCYCLE,NEMPT,RFLAG,UFLAG,EFLAG,
     .                  TFRAC,TDEL,IBOXES,JBOXES,BSIZE,XSIZE,YSIZE,
     .                  UDMAX,UMOST,STIFN,STIFS,FRIC,ALPHA,BETA,BDT,
     .                  CON1,CON2,NVARB,NFRAG,NBR,NPR,
     *                  GRAVX,GRAVY,LOC1,LOC2,NUPDAT,
     *            NBCODD,NDCON(76),DISPL,THMOST,THMAX,
     *                 IBPLT,IFPLT,IDPLT,ICONDA,IBLKDA,IBOXDA,
     *                  XYL,THL,LGNEIB,ITDPLT,IRFPO,COMES,
     *                 SCREEN,FORCL,VECL,NREM,NBNREM(60),LBLOCK
      LOGICAL RFLAG,UFLAG,EFLAG
      COMMON A(30000)
      DIMENSION IA(1)
      EQUIVALENCE (A,IA)
C
      IB=IA(NB)
      NC=IA(IB+1)
C------------------- SCAN EACH CORNER OF THE BLOCK ---
      IC=IB+23
      DO 100 NP=1,NC
C------------------- ARE WE AT EDGE OF DOMAIN ? ---
      IF(GLX(A(IB),IC).GT.0.0.AND.GLX(A(IB),IC).LT.XSIZE.AND.
     .   GLY(A(IB),IC).GT.0.0.AND.GLY(A(IB),IC).LT.YSIZE) GOTO 20
C------------------- YES. SET MASTER FIX FLAG ---
      WRITE(6,2000)NP,NB
 2000 FORMAT(1X,7H CORNER,I4,9H OF BLOCK,I4,21H IS AT EDGE OF DOMAIN)
      IA(IB)=2
      A(IB+5)=0.0
      A(IB+6)=0.0
      A(IB+7)=0.0
      A(IB+8)=0.0
      A(IB+9)=0.0
      A(IB+10)=0.0
      GOTO 900
C------------------- NO, WHICH BOX SHOULD CORNER BE IN ? ---
   20 NBOX=IFIX(GLX(A(IB),IC)/BSIZE)+IFIX(GLY(A(IB),IC)/BSIZE)*IBOXES+1
C------------------- SEARCH THIS BOX ---
      J4N=M3+NBOX-1
   30 I4N=IA(J4N)
      IF(I4N.EQ.0) GOTO 40
      IF(NB.EQ.IA(I4N+1).AND.NP.EQ.IA(I4N)) GOTO 100
      J4N=I4N+2
      GOTO 30
C------------------- SEARCH THE SURROUNDING BOXES ---
   40 NXL=MAXO(MOD(NBOX-1,IBOXES),1)
      NXU=MINO(NXL+2,IBOXES)
      NYL=MAXO((NBOX-1)/IBOXES,1)
      NYU=MINO(NYL+2,JBOXES)
      DO 80 JBOX=NYL,NYU
      MBOX=(JBOX-1)*IBOXES+NXL-1
      DO 70 IBOX=NXL,NXU
      MBOX=MBOX+1
      IF(MBOX.EQ.NBOX) GOTO 70
      J4M=M3+MBOX-1
   50 I4M=IA(J4M)
      IF(I4M.EQ.0) GOTO 70
      IF(NB.EQ.IA(I4M+1).AND.NP.EQ.IA(I4M)) GOTO 60
      J4M=I4M+2
      GOTO 50
C------------------- SWAP ENTRIES FOR THIS CORNER ---
   60 IA(J4M)=IA(I4M+2)
      IA(J4N)=I4M
      IA(I4M+2)=0
      GOTO 100
C------------------- END OF SURROUNDING BOXES SCAN ---
   70 CONTINUE
   80 CONTINUE
      WRITE(6,3000) NP,NB
      EFLAG=.TRUE.
      CALL FINISH
C------------------- END OF CORNERS SCAN ---
  100 IC=IC+3
C
C------------------- EXIT ---
  900 RFLAG=.FALSE.
      RETURN
C
 3000 FORMAT(24H ERROR IN REBOX O CORNER,I3,
     .       9H OF BLOCK,I4,20H NOT IN ADJACENT BOXO
C
      END
      SUBROUTINE DUMP(IDF)
C
C------------------- ROUTINE TO PRINT MEMORY ALLOCATION AND CONTENTS ---
C
      COMMON/CBLOCK/HED(8),NBLOKM,NBOXES,M1,M2,M3,M4,M5,M6,M7,
     .                  NBLOKS,NCYC,MCYCLE,NEMPT,RFLAG,UFLAG,EFLAG,
     .                  TFRAC,TDEL,IBOXES,JBOXES,BSIZE,XSIZE,YSIZE,
     .                  UDMAX,UMOST,STIFN,STIFS,FRIC,ALPHA,BETA,BDT,
     .                  CON1,CON2,NVARB,NFRAG,NBR,NPR,
     *                  GRAVX,GRAVY,LOC1,LOC2,NUPDAT,
     *            NBCODD,NDCON(76),DISPL,THMOST,THMAX,
     *                 IBPLT,IFPLT,IDPLT,ICONDA,IBLKDA,IBOXDA,
     *                  XYL,THL,LGNEIB,ITDPLT,IRFPO,COMES,
     *                 SCREEN,FORCL,VECL,NREM,NBNREM(60),LBLOCK
      LOGICAL RFLAG,UFLAG,EFLAG
```

```
      COMMON A(30000)
      DIMENSION IA(1)
      EQUIVALENCE (A,IA)
C
      IF(IDF.EQ.3)GO TO 100
      IF(IDF.EQ.2)GO TO 200
      IF(IDF.EQ.1)GO TO 300
      WRITE(6,3000)
 3000 FORMAT(1X,27H****ERROR IN DUMP CALL ****)
      RETURN
C
C------------------ DUMP BY BOX ---
  100 WRITE(6,2002)
      DO 120 NBOX=1,NBOXES
      I3=IA(M3+NBOX-1)
C------------------ ANY MORE ENTRIES ? ---
  110 IF(I3.EQ.0) GOTO 120
C------------------ NO, PRINT BLOCK,CORNER ---
      WRITE(6,2008) NBOX,IA(I3+1),IA(I3)
      I3=IA(I3+2)
      GOTO 110
  120 CONTINUE
C------------------ CONTENTS OF EACH BLOCK ---
      RETURN
  200 WRITE(6,2006)
      DO 130 NB=1,NBLOKS
C
C CHECK IF BLOCK REMOVED
C
      IF(NREM.EQ.0)GO TO 170
      DO 160 K=1,NREM
      IF(NB.EQ.NBNREM(K))GO TO 130
  160 CONTINUE
  170 CONTINUE
      IF=IA(NB)
      IL=IF+22+3*IA(IF+1)
      IF2=IF+2
      WRITE(6,2003)NB,IA(IF),IA(IF+1),(A(I),I=IF2,IL)
  130 CONTINUE
C------------------ DUMP CONTACT DATA ---
      RETURN
  300 IF(M5.EQ.0)GO TO 500
      WRITE(6,2007)
      DO 150 NB=1,NBLOKS
C
C CHECK IF BLOCK REMOVED
C
      IF(NREM.EQ.0)GO TO 180
      DO 190 K=1,NREM
      IF(NB.EQ.NBNREM(K))GO TO 150
  190 CONTINUE
  180 CONTINUE
      IF(NBCODD.EQ.0)GO TO 653
      DO 654 K=1,NBCODD
      IF(NB.EQ.NDCON(K))GO TO 653
  654 CONTINUE
      GO TO 150
  653 CONTINUE
      J6=M5+NB-1
  140 I6=IA(J6)
      IF(I6.EQ.0) GOTO 150
      I64=I6+4
      I65=I6+5
      I612=I6+12
      WRITE(6,2004)NB,(IA(I),I=I6,I64),
     *                (A(I),I=I65,I612)
      J6=I6+4
      GOTO 140
  150 CONTINUE
C------------------
  500 WRITE(6,2000)
C
      RETURN
C
 2000 FORMAT(1X,130(1H-))
 2001 FORMAT(1X,10012,I6)
 2002 FORMAT(10X,3HBOX,7X,5HBLOCK,6X,6HCORNER)
 2003 FORMAT(/1X,3I3,1P11E10.2/(10X,1P11E10.2))
 2004 FORMAT(/1X,6I10/1X,1P8E10.2)
 2005 FORMAT(9X,2HM1,8X,2HM2,8X,2HM3,8X,2HM4,8X,2HM5,8X,2HM6,
     .       8X,2HM7,4X,6HNBLOKS,6X,4HNCYC,5X,5HNEMPT,4X,6HMCYCLE/
     .       1X,11I10)
 2006 FORMAT(11H BLOCK DATA,10(1H-)/1X,9H NB IF NC,8X,2HXC,8X,2HYC,
     .       5X,5HTHETA,6X,4HXDOT,6X,4HYDOT,6X,4HTDOT,
     .       8X,2HDX,8X,2HDY,4X,6HDTHETA,6X,4HAREA,3X,7HINERTIA/
     .       15X,5HXFSUM,5X,5HYFSUM,6X,4HMSUM,5X,5HXLOAD,5X,5HYLOAD,
     *       7X,3HCOS,7X,3HSIN,5X,5HTOTLX,5X,5HTOTLY,5X,4HTMOM)
 2007 FORMAT(13H CONTACT DATA,10(1H-)/8X,3HNBE,7X,3HPRE,7X,3HNPE,7X,
     .       3HNPC,7X,3HNBC,6X,4HLINK/10X,1HS,9X,1HN,8X,2HFN,8X,2HFS,
     .       7X,3HSIN,7X,3HCOS,7X,3HXCP,7X,3HYCP)
 2008 FORMAT(1X,3I12)
 2009 FORMAT(1X,30(1H*),19HVALUES ARE IN OCTAL,30(1H*))
C
      END
      SUBROUTINE CHECK
C
C------------------ MOMENTUM AND ENERGY CHECK ---
C
      COMMON/CBLOCK/HED(8),NBLOKM,NBOXES,M1,M2,M3,M4,M5,M6,M7,
     .                    NBLOKS,NCYC,MCYCLE,NEMPT,RFLAG,UFLAG,EFLAG,
     .                    TFRAC,TDEL,IBOXES,JBOXES,BSIZE,XSIZE,YSIZE,
     .                    UDMAX,UMOST,STIFN,STIFS,FRIC,ALPHA,BETA,BDT,
     .                    CON1,CON2,NVARB,NFRAG,NBR,NPR,
     *                    GRAVX,GRAVY,LOC1,LOC2,NUPDAT,
     *             NBCODD,NDCON(76),DISPL,THMOST,THMAX,
     *                    IBPLT,IFPLT,IDPLT,ICONDA,IBLKDA,IBOXDA,
     *                    XYL,THL,LGNEIB,ITDPLT,IRFPO,COHES,
     *                   SCREEN,FORCL,VECL,NREM,NBNREM(60),LBLOCK
      LOGICAL RFLAG,UFLAG,EFLAG
      COMMON A(30000)
      DIMENSION IA(1)
      EQUIVALENCE (A,IA)
C
      XMOM=0.0
      YMOM=0.0
      TMOM=0.0
      TARM=0.0
      XKE=0.0
      YKE=0.0
      TKE=0.0
      DO 100 NB=1,NBLOKS
C
C CHECK IF BLOCK REMOVED
C
      IF(NREM.EQ.0)GO TO 110
      DO 120 K=1,NREM
      IF(NB.EQ.NBNREM(K))GO TO 100
  120 CONTINUE
```

```
  110  CONTINUE
       I2=IA(NB)
       XMOM=XMOM+A(I2+11)*A(I2+5)
       YMOM=YMOM+A(I2+11)*A(I2+6)
       TMOM=TMOM+A(I2+12)*A(I2+7)
       TARM=TARM+A(I2+11)*(A(I2+2)*A(I2+6)-A(I2+3)*A(I2+5))
       XKE=XKE+0.5*A(I2+11)*A(I2+5)**2
       YKE=YKE+0.5*A(I2+11)*A(I2+6)**2
       TKE=TKE+0.5*A(I2+12)*A(I2+7)**2
       WRITE(6,2001)  XMOM,YMOM,TMOM,TARM,XKE,YKE,TKE
    100 CONTINUE
C
       ESUM=XKE+YKE+TKE
       TSUM=TMOM+TARM
C
       WRITE(6,2000)  XMOM,YMOM,TMOM,TARM,TSUM,XKE,YKE,TKE,ESUM
C
       RETURN
C
  2000 FORMAT(9H MOMENTUM,11X,1HX,11X,1HY,2X,10HROTATIONAL/
     .        9X,1P5E12.4//
     .        9H ENERGY  ,11X,1HX,11X,1HY,2X,10HROTATIONAL,7X,5HTOTAL/
     .        9X,1P4E12.4)
  2001 FORMAT(1X,1P7E12.4)
C
       END
       FUNCTION GLX(B,IC)
C
C------------------- LOCAL-GLOBAL X-COORDINATE TRANSFORMATION ---
C
       COMMON A(30000)
       DIMENSION IA(1)
       EQUIVALENCE (A,IA)
       DIMENSION B(1)
C
       GLX=B(3)+A(IC)*B(19)-A(IC+1)*B(20)
C
       RETURN
C
       END
       FUNCTION GLY(B,IC)
C
C------------------- LOCAL-GLOBAL Y-COORDINATE TRANSFORMATION ---
C
       COMMON A(30000)
       DIMENSION IA(1)
       EQUIVALENCE (A,IA)
       DIMENSION B(1)
C
       GLY=B(4)+A(IC)*B(20)+A(IC+1)*B(19)
C
       RETURN
C
       END
       SUBROUTINE PL(IPCON)
       GO TO (10,20) IPCON
   10  CALL START(2)
       CALL PEN(1)
       RETURN
   20  CALL ENPLOT
       RETURN
       END
       SUBROUTINE BPLOT
C
C------------------- PLOT A SNAPSHOT OF THE GEOMETRY ---
C
       COMMON/CBLOCK/HED(8),NBLOKM,NBOXES,M1,M2,M3,M4,M5,M6,M7,
      .              NBLOKS,NCYC,MCYCLE,NEMPT,RFLAG,UFLAG,EFLAG,
      .              TFRAC,TDEL,IBOXES,JBOXES,BSIZE,XSIZE,YSIZE,
      .              UDMAX,UMOST,STIFN,STIFS,FRIC,ALPHA,BETA,BDT,
      .              CON1,CON2,NVARB,NFRAG,NBR,NPR,
      *              GRAVX,GRAVY,L0C1,L0C2,NUPDAT,
      *          NBCODD,NDCON(76),DISPL,THMOST,THMAX,
      *              IBPLT,IFPLT,IDPLT,ICONDA,IBLKDA,IBOXDA,
      *               XYL,THL,LGNEIB,ITDPLT,IRFP0,COMES,
      *              SCREEN,FORCL,VECL,NREM,NBNREM(60),LBLOCK
       LOGICAL RFLAG,UFLAG,EFLAG
       COMMON A(30000)
       DIMENSION IA(1)
       EQUIVALENCE (A,IA)
C
       FACT=SCREEN/AMAX1(XSIZE,YSIZE)
       FACTIV=1./FACT
       CALL TITLES(1,FACTIV)
C------------------- PLOT EACH BLOCK ---
       DO 100 NB=1,NBLOKS
C
C CHECK IF BLOCK REMOVED
C
       IF(NREM.EQ.0)GO TO 200
       DO 210 K=1,NREM
       IF(NB.EQ.NBNREM(K))GO TO 100
  210  CONTINUE
  200  CONTINUE
       I2=IA(NB)
       NC=IA(I2+1)
       XC=FACT*A(I2+2)
       YC=FACT*A(I2+3)
C------------------- FIXED ? ---
       IF(IA(I2).EQ.0)  GOTO 20
       CALL SYMBOL(XC,YC,0.1,1HF,0.0,1)
   20  IC=I2+23
       X=FACT*GLX(A(I2),IC)
       Y=FACT*GLY(A(I2),IC)
       CALL PLOT(X,Y,3)
       DO 50 NP=2,NC
       IC=IC+3
       X=FACT*GLX(A(I2),IC)
       Y=FACT*GLY(A(I2),IC)
       CALL PLOT(X,Y,2)
    50 CONTINUE
       X=FACT*GLX(A(I2),I2+23)
       Y=FACT*GLY(A(I2),I2+23)
       CALL PLOT(X,Y,2)
C------------------- END OF BLOCK LOOP ---
   100 CONTINUE
C
       CALL PLOT(X,Y,3)
       CALL PLOT(0.0,0.0,3)
       CALL NEWPAGE
C
       RETURN
C
       END
       SUBROUTINE FORPLT
       COMMON A(30000)
       DIMENSION IA(1)
       EQUIVALENCE (A,IA)
```

```
      COMMON/CBLOCK/HED(8),NBLOKM,NBOXES,M1,M2,M3,M4,M5,M6,M7,
     .                  NBLOKS,NCYC,MCYCLE,NEMPT,RFLAG,UFLAG,EFLAG,
     .                  TFRAC,TDEL,IBOXES,JBOXES,BSIZE,XSIZE,YSIZE,
     .                  UDMAX,UMOST,STIFN,STIFS,FRIC,ALPHA,BETA,BDT,
     .                  CON1,CON2,NVARB,NFRAG,NBR,NPR,
     *                  GRAVX,GRAVY,LOC1,LOC2,NUPDAT,
     *            NBCODD,NDCON(76),DISPL,THMOST,THMAX,
     *                 IBPLT,IFPLT,IDPLT,ICONDA,IBLKDA,IBOXDA,
     *                  XYL,THL,LGNEIB,ITDPLT,IRFPO,COMES,
     *                SCREEN,FORCL,VECL,NREM,NBNREM(60),LBLOCK
      LOGICAL RFLAG,UFLAG,EFLAG
      FO=0.
      DO 100 NB=1,NBLOKS
C
C CHECK IF BLOCK REMOVED
C
      IF(NREM.EQ.0)GO TO 110
      DO 120 K=1,NREM
      IF(NB.EQ.NBNREM(K))GO TO 100
  120 CONTINUE
  110 CONTINUE
      J6=M5+NB-1
  300 I6=IA(J6)
      IF(I6.EQ.0)GO TO 100
      FN=SQRT(A(I6+5)**2+A(I6+6)**2)
      IF(FN.LE.FO)GO TO 200
      FO=FN
  200 J6=I6+4
      GO TO 300
  100 CONTINUE
      IF(FO.EQ.0.0)FO=1.E-05
      FG=FORCL/FO
      GG=1./FG
      FACT=SCREEN/AMAX1(XSIZE,YSIZE)
      CALL TITLES(2,GG)
      DO 500 NB=1,NBLOKS
C
C CHECK IF BLOCK REMOVED
C
      IF(NREM.EQ.0)GO TO 130
      DO 140 K=1,NREM
        IF(NB.EQ.NBNREM(K))GO TO 500
  140 CONTINUE
  130  CONTINUE
      J6=M5+NB-1
  600 I6=IA(J6)
      IF(I6.EQ.0)GO TO 500
      X=A(I6+11)*FACT
      Y=A(I6+12)*FACT
      FX=A(I6+6)*FG
      FY=A(I6+5)*FG
      CALL PLOT(X,Y,3)
      X=X+FX
      Y=Y+FY
      CALL PLOT(X,Y,2)
      J6=I6+4
      GO TO 600
  500 CONTINUE
      CALL NEWPAGE
      RETURN
      END
      SUBROUTINE DISPLT
C     ROUTINE FOR PLOTTING INCREMENTAL BLOCK DISPLACEMENTS
      COMMON/CBLOCK/HED(8),NBLOKM,NBOXES,M1,M2,M3,M4,M5,M6,M7,
     .                  NBLOKS,NCYC,MCYCLE,NEMPT,RFLAG,UFLAG,EFLAG,
     .                  TFRAC,TDEL,IBOXES,JBOXES,BSIZE,XSIZE,YSIZE,
     .                  UDMAX,UMOST,STIFN,STIFS,FRIC,ALPHA,BETA,BDT,
     .                  CON1,CON2,NVARB,NFRAG,NBR,NPR,
     *                  GRAVX,GRAVY,LOC1,LOC2,NUPDAT,
     *            NBCODD,NDCON(76),DISPL,THMOST,THMAX,
     *                 IBPLT,IFPLT,IDPLT,ICONDA,IBLKDA,IBOXDA,
     *                  XYL,THL,LGNEIB,ITDPLT,IRFPO,COMES,
     *                SCREEN,FORCL,VECL,NREM,NBNREM(60),LBLOCK
      LOGICAL RFLAG,UFLAG,EFLAG
      COMMON A(30000)
      DIMENSION IA(1)
      EQUIVALENCE (A,IA)
      DO=0.
      DO 100 NB=1,NBLOKS
      IF(NREM.EQ.0)GO TO 110
      DO 120 K=1,NREM
      IF(NB.EQ.NBNREM(K))GO TO 100
  120 CONTINUE
  110 CONTINUE
      I2=IA(NB)
      DN=SQRT(A(I2+8)**2+A(I2+9)**2)
      IF(DN.LE.DO)GO TO 100
      DO=DN
  100 CONTINUE
      IF(DO.EQ.0.0)DO=1.E-05
      DG=DISPL/DO
      GG=1./DG
      FACT=SCREEN/AMAX1(XSIZE,YSIZE)
      CALL TITLES(4,GG)
      DO 200  NB=1,NBLOKS
      IF(NREM.EQ.0)GO TO 130
      DO 140 K=1,NREM
      IF(NB.EQ.NBNREM(K))GO TO 200
  140 CONTINUE
  130 CONTINUE
      I2=IA(NB)
      X=A(I2+2)*FACT
      Y=A(I2+3)*FACT
      DX=A(I2+8)*DG
      DY=A(I2+9)*DG
      CALL VECTOR(X,Y,DX,DY)
  200 CONTINUE
      CALL NEWPAGE
      RETURN
      END
      SUBROUTINE TDISPL
C     ROUTINE FOR PLOTTING TOTAL BLOCK DISPLACEMENTS
      COMMON/CBLOCK/HED(8),NBLOKM,NBOXES,M1,M2,M3,M4,M5,M6,M7,
     .                  NBLOKS,NCYC,MCYCLE,NEMPT,RFLAG,UFLAG,EFLAG,
     .                  TFRAC,TDEL,IBOXES,JBOXES,BSIZE,XSIZE,YSIZE,
     .                  UDMAX,UMOST,STIFN,STIFS,FRIC,ALPHA,BETA,BDT,
     .                  CON1,CON2,NVARB,NFRAG,NBR,NPR,
     *                  GRAVX,GRAVY,LOC1,LOC2,NUPDAT,
     *            NBCODD,NDCON(76),DISPL,THMOST,THMAX,
     *                 IBPLT,IFPLT,IDPLT,ICONDA,IBLKDA,IBOXDA,
     *                  XYL,THL,LGNEIB,ITDPLT,IRFPO,COMES,
     *                SCREEN,FORCL,VECL,NREM,NBNREM(60),LBLOCK
      LOGICAL RFLAG,UFLAG,EFLAG
      COMMON A(30000)
      DIMENSION IA(1)
      EQUIVALENCE (A,IA)
      DT=0.0
      DO 100 NB=1,NBLOKS
```

```
      IF(NREM.EQ.0)GO TO 110
      DO 120 K=1,NREM
      IF(NB.EQ.NBNREM(K))GO TO 100
  120 CONTINUE
  110 CONTINUE
      I2=IA(NB)
      DN=SQRT(A(I2+20)**2+A(I2+21)**2)
      IF(DN.LE.DT)GO TO 100
      DT=DN
  100 CONTINUE
      IF(DT.EQ.0.0)DT=1.E-05
      DG=DISPL/DT
      GG=1./DG
      FACT=SCREEN/AMAX1(XSIZE,YSIZE)
      CALL TITLES(5,GG)
      DO 200 NB=1,NBLOKS
      IF(NREM.EQ.0)GO TO 130
      DO 140 K=1,NREM
      IF(NB.EQ.NBNREM(K))GO TO 200
  140 CONTINUE
  130 CONTINUE
      I2=IA(NB)
      X=A(I2+2)*FACT
      Y=A(I2+3)*FACT
      DX=A(I2+20)*DG
      DY=A(I2+21)*DG
      CALL VECTOR(X,Y,DX,DY)
  200 CONTINUE
      CALL NEWPAGE
      RETURN
      END
      SUBROUTINE TITLES(IPLOT,DIS)
      COMMON/CBLOCK/HED(8),NBLOKM,NBOXES,M1,M2,M3,M4,M5,M6,M7,
     .                  NBLOKS,NCYC,MCYCLE,NEMPT,RFLAG,UFLAG,EFLAG,
     .                  TFRAC,TDEL,IBOXES,JBOXES,BSIZE,XSIZE,YSIZE,
     .                  UDMAX,UMOST,STIFN,STIFS,FRIC,ALPHA,BETA,BDT,
     .                  CON1,CON2,NVARB,NFRAG,NBR,NPR,
     *                  GRAVX,GRAVY,LOC1,LOC2,NUPDAT,
     *           NBCODD,NDCON(76),DISPL,THMOST,THMAX,
     *                IBPLT,IFPLT,IDPLT,ICONDA,IBLKDA,IBOXDA,
     *                 XYL,THL,LGNEIB,ITDPLT,IRFPO,COHES,
     *               SCREEN,FORCL,VECL,NREM,NBNREM(60),LBLOCK
      LOGICAL RFLAG,UFLAG,EFLAG
      CALL SYMBOL(0.5,14.0,0.21,HED,0.,80)
      GO TO (100,200,300,320,340) IPLOT
  100 CONTINUE
C THIS IS A BLOCK GEOMETRY PLOT
      CALL SYMBOL(0.5,13.25,0.21,10HBLOCK PLOT,0.,10)
      GO TO 390
  200 CONTINUE
C THIS IS A CORNER FORCE PLOT
      CALL SYMBOL(0.5,13.25,0.21,17HCORNER FORCE PLOT,0.,17)
      GO TO 400
  300 CONTINUE
C THIS IS A VELOCITY PLOT
      CALL SYMBOL(0.5,13.25,0.21,13HVELOCITY PLOT,0.,13)
      GO TO 400
  320 CONTINUE
C     THIS IS AN INCREMENTAL DISPL. PLOT
      CALL SYMBOL(0.5,13.25,0.21,17HINCREM.DISPL.PLOT,0.,17)
      GO TO 400
  340 CONTINUE
C     THIS IS AN TOTAL DISPL. PLOT
      CALL SYMBOL(0.5,13.25,0.21,16HTOTAL DISPL.PLOT,0.,16)
      GO TO 400
  390 CONTINUE
      CALL SYMBOL(5.0,13.25,0.21,34HNUMBER OF PROBLEM UNITS PER INCH =,
     *0.,34)
      CALL NUMBER(12.4,13.25,0.21,DIS,0.,2)
      GO TO 500
  400 CONTINUE
      CALL SYMBOL(5.0,13.25,0.21,34HNUMBER OF PROBLEM UNITS PER INCH =,
     *  0.,34)
      CALL NUMBER(12.4,13.25,0.21,DIS,0.,8)
  500 FL=MCYCLE
      CALL SYMBOL(0.5,12.5,0.21,14HCYCLE NUMBER =,0.,14)
      CALL NUMBER(4.5,12.5,0.21,FL,0.,-1)
      CALL SYMBOL(7.5,12.5,0.21,16HSCALE . 1 INCH =,0.,16)
      CALL PLOT(11.0,12.5,3)
      CALL PLOT(12.0,12.5,2)
      RETURN
      END
      SUBROUTINE VELOC
      COMMON/CBLOCK/HED(8),NBLOKM,NBOXES,M1,M2,M3,M4,M5,M6,M7,
     .                  NBLOKS,NCYC,MCYCLE,NEMPT,RFLAG,UFLAG,EFLAG,
     .                  TFRAC,TDEL,IBOXES,JBOXES,BSIZE,XSIZE,YSIZE,
     .                  UDMAX,UMOST,STIFN,STIFS,FRIC,ALPHA,BETA,BDT,
     .                  CON1,CON2,NVARB,NFRAG,NBR,NPR,
     *                  GRAVX,GRAVY,LOC1,LOC2,NUPDAT,
     *           NBCODD,NDCON(76),DISPL,THMOST,THMAX,
     *                IBPLT,IFPLT,IDPLT,ICONDA,IBLKDA,IBOXDA,
     *                 XYL,THL,LGNEIB,ITDPLT,IRFPO,COHES,
     *               SCREEN,FORCL,VECL,NREM,NBNREM(60),LBLOCK
      LOGICAL RFLAG,UFLAG,EFLAG
      COMMON A(30000)
      DIMENSION IA(1)
      EQUIVALENCE (A,IA)
      V0=0.
      DO 100 NB=1,NBLOKS
C
C CHECK IF BLOCK REMOVED
C
      IF(NREM.EQ.0)GO TO 110
      DO 120 K=1,NREM
      IF(NB.EQ.NBNREM(K))GO TO 100
  120 CONTINUE
  110 CONTINUE
      I2=IA(NB)
      VN=SQRT(A(I2+5)**2+A(I2+6)**2)
      IF(VN.LE.V0)GO TO 100
      V0=VN
  100 CONTINUE
      FG=VECL/V0
      GG=1./FG
      FACT=SCREEN/AMAX1(XSIZE,YSIZE)
      CALL TITLES(3,GG)
      DO 200 NB=1,NBLOKS
C
C CHECK IF BLOCK REMOVED
C
      IF(NREM.EQ.0)GO TO 130
      DO 140 K=1,NREM
      IF(NB.EQ.NBNREM(K))GO TO 200
  140 CONTINUE
  130 CONTINUE
      I2=IA(NB)
      X=A(I2+2)*FACT
      Y=A(I2+3)*FACT
```

```
      VX=A(I2+5)*FG
      VY=A(I2+6)*FG
      CALL VECTOR(X,Y,VX,VY)
  200 CONTINUE
      CALL NEWPAGE
       RETURN
       END
      SUBROUTINE VECTOR(X,Y,XV,YV)
      PI=4.0*ATAN(1.0)
      CALL PLOT(X,Y,3)
      X=X+XV
      Y=Y+YV
      CALL PLOT(X,Y,2)
      VT=(SQRT(XV**2+YV**2))/5.
      GM=ABS(XV)
      IF(GM.LE.1.E-5) XV=1.E-5
      ABA=ATAN2(YV,XV)
      IF(ABA.LT.0.)ABA=2.*PI+ABA
      ABA1=PI+ABA-0.25
       ABA2=ABA1+0.5
      XA=X+VT*(COS(ABA1))
      YA=Y+VT*(SIN(ABA1))
      CALL PLOT(XA,YA,2)
      CALL PLOT(X,Y,3)
      XA=X+VT*(COS(ABA2))
      YA=Y+VT*(SIN(ABA2))
      CALL PLOT(XA,YA,2)
      RETURN
      END
      SUBROUTINE FINISH
C
C------------------- TIDY UP AND STOP ---
C
      COMMON/CBLOCK/HED(8),NBLOKM,NBOXES,M1,M2,M3,M4,M5,M6,M7,
     .                  NBLOKS,NCYC,MCYCLE,NEMPT,RFLAG,UFLAG,EFLAG,
     .                  TFRAC,TDEL,IBOXES,JBOXES,BSIZE,XSIZE,YSIZE,
     .                  UDMAX,UMOST,STIFN,STIFS,FRIC,ALPHA,BETA,BDT,
     .                  CON1,CON2,NVARB,NFRAG,NBR,NPR,
     *                  GRAVX,GRAVY,LOC1,LOC2,NUPDAT,
     *           NBCODD,NDCON(76),DISPL,THMOST,THMAX,
     *                  IBPLT,IFPLT,IDPLT,ICONDA,IBLKDA,IBOXDA,
     *                  XYL,THL,LGNEIB,ITDPLT,IRFPO,COMES,
     *                 SCREEN,FORCL,VECL,NREM,NBNREM(60),LBLOCK
      LOGICAL RFLAG,UFLAG,EFLAG
      COMMON A(30000)
      DIMENSION IA(1)
      EQUIVALENCE (A,IA)
      COMMON/INEIG/IN(111),NEIGHB(111,16)
      DIMENSION INEI(1887)
      EQUIVALENCE(IN,INEI)
C
      CALL BPLOT
      CALL FORPLT
      CALL VELOC
      CALL DISPLT
      CALL TDISPL
      IPCON=2
      CALL PL(IPCON)
      WRITE(6,2000) MCYCLE,NUPDAT
C
C------------------- WRITE RESTART FILE IF NO ERRORS ---
      IF(EFLAG) GOTO 100
      REWIND 2
      WRITE(2) (HED(I),I=1,LBLOCK)
      WRITE(2) (INEI(I),I=1,LGNEIB)
      WRITE(2) (A(I),I=1,M7)
      WRITE(6,1002)
 1002 FORMAT(30X,43H A RESTART FILE HAS BEEN WRITTEN ONTO TAPE2)
  100 CONTINUE
      STOP
C
 2000 FORMAT(30X,13H TOTAL CYCLES,I10/
     .       30X,13H NO. UPDATES ,I10)
C
      END
```

APPENDIX VII:

User information, input specifications and listings for static relaxation programs:

A. PROGRAM BLOCK - baseline static relaxation program

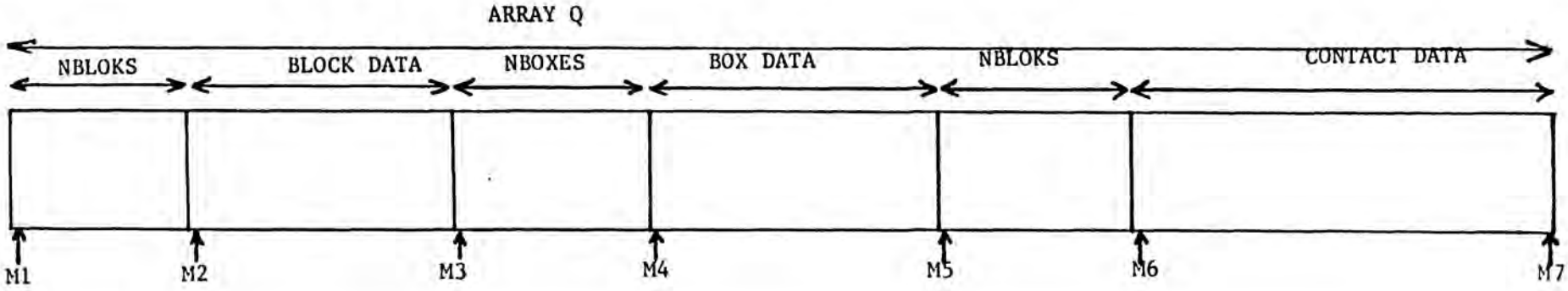
1) The program is the algorithm for the static relaxation formulation for rigid blocks described in Chapter 2. General shaped rock blocks may be defined and arbitrary physical properties assigned to any edge of any block.

2) Several features of a general rigid block dynamic relaxation program (Maini et. al., 1978) have been implemented in PROGRAM BLOCK. The allocation of memory is via linked list arrays stored in one large, singly-subscripted array Q, all storage locations being held simultaneously in core. By the use of memory pointers occupying fixed locations throughout the array, any selected information can be economically referenced. The memory partition of array Q is shown in Figure A.5. The data structures for the block information, box array, corner list and contact array and list are shown in Figures A.6, A.7 and A.8.

3) The same boxing technique as developed by Cundall (1974) for storing block corners in a coarse box mesh which overlies the problem area was adopted to assist in the updating of block interactions. The specification of the variables necessary to perform this boxing of corners is described in the first set of data input. (For further information, see Section 2.4, Maini et. al., 1978).

4) The subroutine UPDATE for updating the block interactions at specified intervals is also very similar to that used in the dynamic relaxation program RBM (listing in Appendix VI).

5) The following tree illustrates the manner in which the different routines are called:



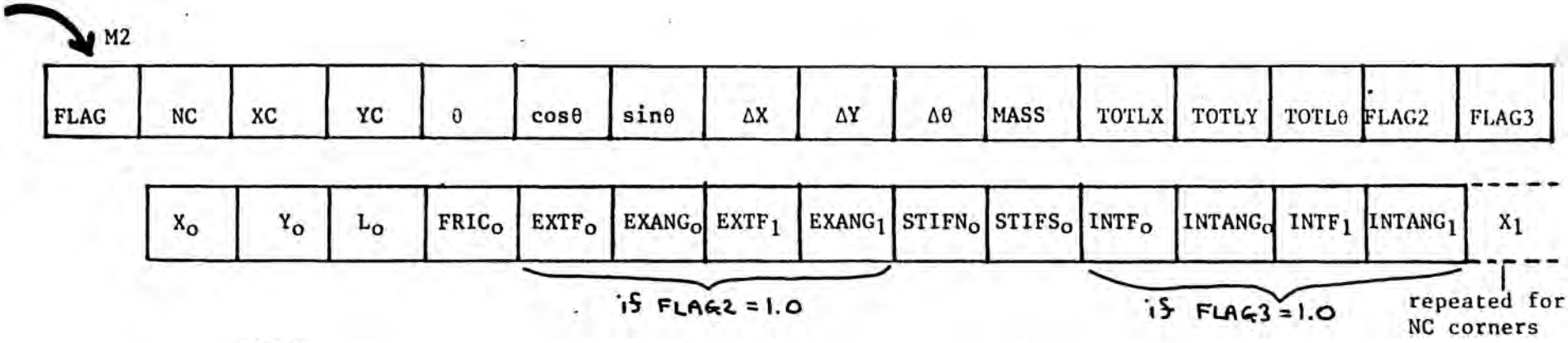

CODE

NBLOKS - no. of blocks

NBOXES - no. of boxes

M1,M2...M7 - memory pointers

Figure A.5: Schematic layout of computer memory

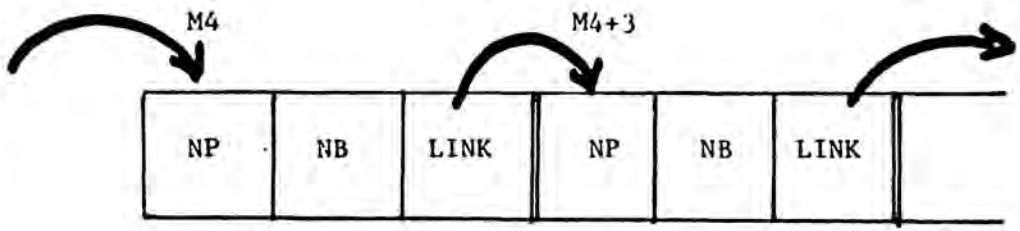



CODE

NC - no. of corners
XC), YC) - centroidal block co-ordinates
θ - angle of local block axes
ΔX), ΔY), Δθ) - incremental block movements
TOTLX, TOTLY, TOTLθ - total block movements

$X_o$), $Y_o$) - local co-ordinates of block corner
$L_o$ - length of edge
FRIC - coeff. of friction
EXTF ), EXANG) - external forces and direction
STIFN), STIFS) - normal and shear stiffness
INTF ), INTANG) - internal forces and direction

Figure A.6: Layout of information stored in block data array

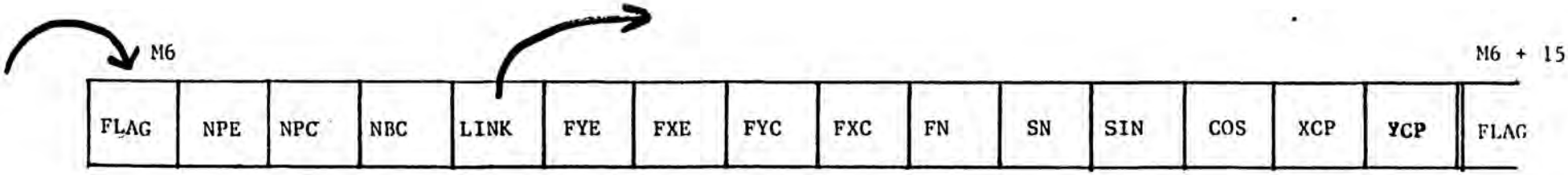



CODE

NP) - corner and block number
NB) of corner in box

LINK - address of next corner in box

Figure A.7: Layout and information stored in box data array

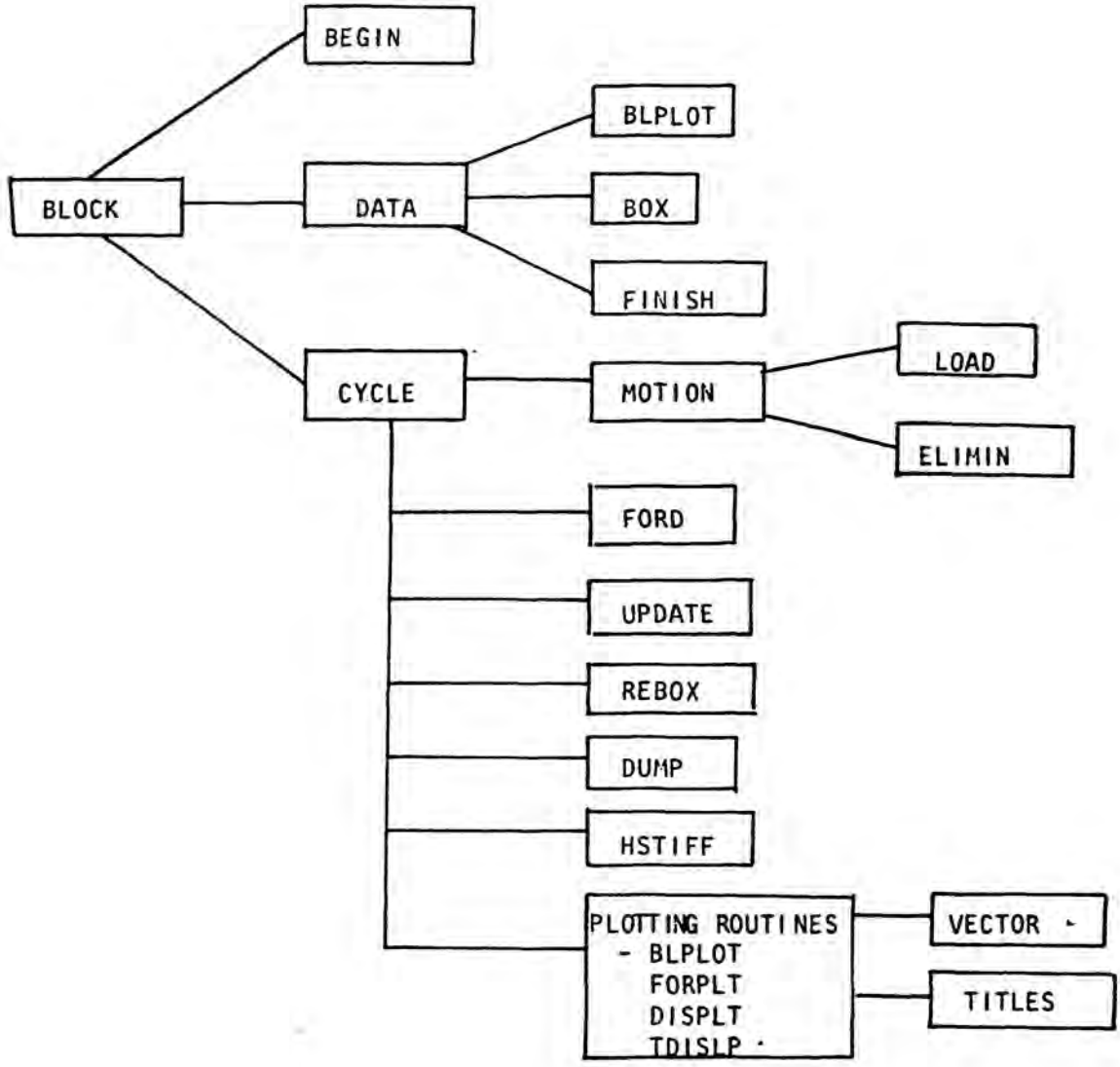



CODE

NPE - edge no. of contact
NPC) - corner and block numbers
NBC) of corner in contact
LINK - address of next contact data
FYE) - global X and Y forces acting
FXE) on edge

FYC) - global X and Y forces
FXC) acting on corner
FN) - normal and shear force
SN)
SIN) - sine and cosine of edge
COS)
XCP) - global co-ordinates of contact
YCP) point

Figure A.8: Layout of information stored in contact data array.




6) A brief description of each subroutine follows:

BLOCK - Main program. Calls BEGIN, DATA and CYCLE.

BEGIN - If start run: reads title, initial problem definition, plotting and printing intervals, updating and memory data and initialises data.
If restart run: reads saved information from a previous run off logical unit 1.

| | | |
|---|---|---|
| DATA | - | Reads in keywords and jumps to appropriate code. For further information see input data format section. Returns control to BLOCK when ready for job execution. |
| BOX | - | Once blocks have been created and before job execution, BOX is called to perform the initial classification of block corners into boxes. |
| CYCLE | - | This is the driving routine for the relaxation algorithm. Controls calls to most of the remaining routines. |
| MOTION | - | Calculates incremental rigid body displacements for relaxation of a single block. Calls LOAD and ELIMIN. |
| LOAD | - | Routine to calculate resultant surface forces on block. |
| ELIMIN | - | The equation solver solves the simultaneous linear equations by Gaussian elimination with partial pivoting. Writes out appropriate message if equations singular or ill-conditioned. |
| FORD | - | Applies the constitutive laws for a single block. Contact forces between blocks are determined from their position in space. |
| REBOX | - | Routine to rebox a single block's corners. Reboxing is triggered when a block centroid exceeds specified displacements. |
| UPDATE | - | Updates all contacts between blocks. UPDATE is called either at regular intervals or when the maximum cumulative block displacements exceed a specified limit. |
| DUMP | - | Prints out information in memory. |

| | | |
|---|---|---|
| HSTIFF | - | Routine to calculate displacements on boundary blocks carrying external loads with external half-springs of double stiffness. |
| BLPLOT | - | Plots block geometry. All plotting intervals specified on input. |
| FORPLT | - | Plots inter-block contact forces. |
| DISPLT | - | Plots incremental block displacements. |
| TDISPL | - | Plots cumulative block displacements. |
| VECTOR | - | Draws vector. |
| TITLES | - | Prints headings on plots. |
| FINISH | - | Terminates the program and writes restart file on logical unit 2. |

7) The number of storage locations of array Q required by a problem depends on the number of blocks and the nature of the properties for each block. For efficient use of computing resources, it is essential to have some knowledge of the maximum amount of storage locations required. This can be estimated by the following formula:

$$M = (NBLOKS * 2) + (16 + 6 * NC) * NBLOKSI + (16 + 10 * NC) * NBLOKS2 + (16 + 14 * NC) * NBLOKS3 + NBOXES + \sum_{i=1}^{NBLOKS} (NC * 3) + \sum_{i=1}^{NBLOKS} (NCONT * 15)$$

where

M is the maximum storage required;
NBLOKS is the total number of blocks;
NC is the number of corners per block;
NBLOKSI is the number of blocks with no external or internal forces on edges;
NBLOKS2 is the number of blocks with either external forces or internal forces on edges;
NBLOKS3 is the number of blocks with both external and internal forces on edges;
NBOXES is the number of grid boxes;

NCONT is the maximum number of contacts per block.

Once M is evaluated, the array Q can be suitably dimensioned.

8) The input data format for job execution which follows should be read in conjunction with the Fortran implementation discussed in Section 2.4.2. The specification of data requires two data sets - the first defining the general problem area and control variables while the second set relates to the properties of the problem. The input format is in fixed columns. The first command must be either STAR(T) or REST(ART), as shown below:

DATA SET 1:

Card 1: (A4) run type identifiers.

Cols 1-4: WORD [ either STAR(T) or REST(ART)]
If STAR ⇒ start a new run. This card must be followed by the five following cards:

If REST ⇒ restart from a preceding run. Program reads an existing restart file off logical unit 1 and reads new title. Then jumps to data set number two.

Card 2: (8A10) heading card - any alphanumeric characters may be used. Read for both STAR(T) and REST(ART) commands.

Cols 1-80: HED(8) title of problem.

The following cards are only read for a STAR(T) command:

Card 3: (4I10) problem identifier.

Cols 1-10 NBLOKM maximum number of blocks
Cols 11-20 IBOXES number of boxes in X-direction
Cols 21-30 JBOXES number of boxes in Y-direction
Cols 31-40 IBSIZE size of single box (boxes are square)

Card 4: (8I10) intervals for plotting and printing results

Cols 1-10 IBPLT block plot interval

Cols 11-20 IFPLT contact force plot interval

Cols 21-30 IDPLT incremental displacement plot interval

Cols 31-40 ITDPLT cumulative displacement plot interval

Cols 41-50 ICONDA contact data arrays print interval

Cols 51-60 IBLKDA block data arrays print interval

Cols 61-70 IBOXDA box data arrays print interval

Cols 71-80 IRFPO resultant force print interval

Card 5: (2F10.0) thresholds for updating contacts

Cols 1-10 XYL translation threshold

Cols 11-20 THL rotation threshold

Card 6: (I10) storage locations for array Q (default value 6000)

Cols 1-10 M7D number of storage locations.

DATA SET 2:

Card 1: (A4) keyword for type of information to be read

Cols 1-4 CARD

After reading the keyword, the program then jumps to the appropriate segment of code to read in the relevant data:

Keyword CREA(TE):

Card 2: (I10,F10.0,3I10) single block properties

Cols 1-10 NC number of corners. Must be $\leqslant 50$.

Cols 11-20 RHO block density

Cols 21-30 JFIX fix/free flag

JFIX = 0 block free to move

JFIX = 1 block fixed

Cols 31-40 JBOUND external load flag

JBOUND = 0 no external loads on block edges

JBOUND = 1 external loads applied to block edges

Cols 41-50 JINT internal load flag

JINT = 0 no internal loads on block edges

JINT = 1 internal loads applied to block edges

Card 3: (8F10.0) block corner co-ordinates given in clockwise direction (starting from any corner). May need more than one card if NC > 4.

Cols 1-80 X(I), Y(I), I = 1, NC
X and Y co-ordinates

A CREA(TE) command must not be given after a CYCL(E) command has been given. For problem geometries with a large number of blocks, a mesh generator may be written in place of cards 2 and 3. Blocks are numbered consecutively in the order created.

Keyword DELE(TE):

Card 2: (I4) removal of blocks (to simulate excavation)

Cols 1-4 NREM number of blocks removed

Card 3: (I4,19F4.0) block numbers of blocks removed. May need more than one card if NREM > 19.

Cols 1-4 NBC identifying flag
NBC = 999 no more blocks to be removed (used only if greater than 19 blocks removed).

Cols 5-80 BNREM(K), K = 1, 19 numbers of the blocks removed.

Keyword DUMP: dumps contact force, block and box data arrays.
no data cards follow keyword

Keyword CYCL(E):

Card 2: (I10) commences job execution

Cols 1-10 NCYC number of iterations

Keyword STOP: stops the program. Writes a restart file.
no data cards follow keyword

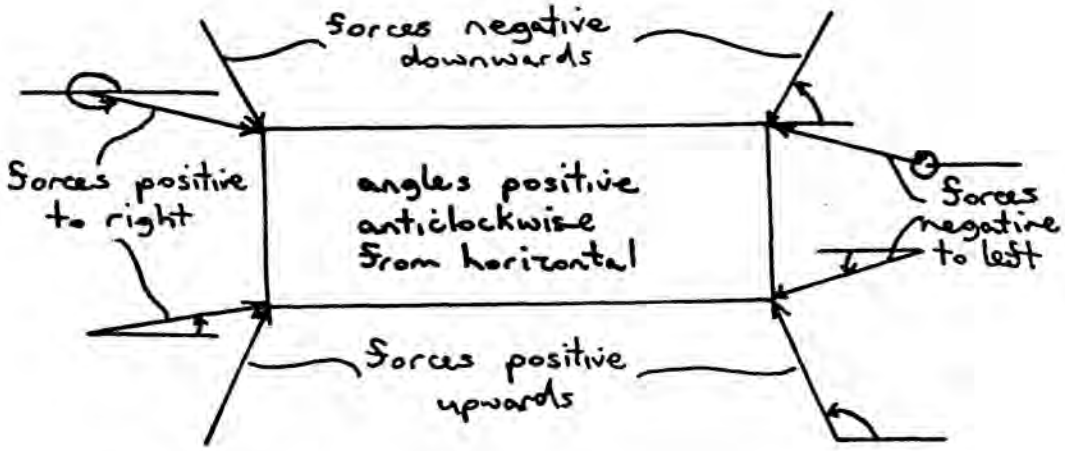
Keyword PLOT: plots the block geometry
no data cards follow keyword

Keyword INTF:

Card 2 : (2I10,4F10.0) apply internal forces to edge NE of block NB

| | | |
|---|---|---|
| Cols 1-10 | NB | block number |
| Cols 11-20 | NE | edge number |
| Cols 21-30 | INFL | force applied to lower corner |
| Cols 31-40 | INANGL | angle of lower corner force |
| Cols 41-50 | INFU | force applied to upper corner |
| Cols 51-60 | INANGU | angle of upper corner force |

The sign convention for forces applied to block edges is shown below:




Keyword RSET:

Card 2 : (I10,F10.0) set real data

| | | |
|---|---|---|
| Cols 1-10 | IADR | storage location in array Q |
| Cols 11-20 | VAL | value set i.e. Q(IADR) = VAL |

Keyword ISET:

Card 2 : (2I10) set integer data

Cols 1-10 IADR storage location in array Q

Cols 11-20 IVAL value set i.e. IQ(IADR) = IVAL

Keyword EXTF:

Card 2 : (2I10,4F10.0) apply external forces to edge NE of block NB

data input as with Keyword INTF
except EXFL, EXANGL, EXFU, EXANGU
replace INFL, INANGL, INFU, INANGU.

Keyword STIF:

Card 2 : (2E10.4) normal and shear stiffness

Cols 1-10 STIFN normal stiffness
Cols 11-20 STIFS shear stiffness

Keyword COHN:

Card 2 : (F10.0) joint cohesion

Cols 1-10 COHES joint cohesion

Keyword FRIC:

Card 2 : (F10.0) friction coefficient

Cols 1-10 FRIC joint friction coefficient

Keyword RINV:

Card 2 : (8I10) reset intervals for plotting and printing and reset size of memory

Card 3 (I10)

data input as for Cards 4 and 6, data set 1.

Keyword MDFY:

Card 2 : (2F10.0) reset displacement thresholds for updating

data input as for Card 5, data set 1.

Keyword UPDA(TE): calls routine UPDATE
no data cards follow keyword

Keyword DCON:

Card 2 : (I4) block numbers for which contact data to be dumped. If DCON not used, contact data for all blocks is dumped when DUMP called.

Cols 1-4 NBCODD number of blocks for dumping of contact data

| | |
|---|---|
| Card 3 | data input as with card 3, keyword |
| (I4,19F4.0) | DELE(TE) |

Keyword ZTDP: zeroises total block displacements
no data cards follow keyword

Keywords STIF and FRIC assign the values STIFN, STIFS, and FRIC to each edge of each block. Different values may be assigned by using the RSET command.

9) The following variables are specified via Fortran DATA statements:

| VARIABLE NAME | VALUE | DESCRIPTION |
|---|---|---|
| GRAVY | - 9.81 | gravity in Y-direction |
| M7 | 6000 | default storage limit for array Q |
| MCYCLE | 0 | current cycle number |
| NUPDAT | 0 | number of updates performed |
| LBLOCK | 177 | length of labelled COMMON block CBLOCK |
| RFLAG | . FALSE . | rebox flag |
| UFLAG | . TRUE . | update flag |
| EFLAG | . FALSE . | error flag |
| SCREEN | 20 . | scales for block, |
| FORCL | 1 . | force and displacement |
| DISPL | 1 . | plots |
| NREM | 0 | default value for number of blocks removed |
| NBCODD | 0 | default value for number of blocks requiring contact data to be dumped |
| RESTFL | 0.0 | flag used in MOTION |
| LGNEIB | 1887 | value calculated is: NBLOKS + NBLOKS * 16 (value shown is for 111 blocks) |
| COHES | 0.0 | default value for joint cohesion |

10) In addition to the above data requirements, the following arrays must be appropriately dimensioned before problem execution.

Q (dimensioned to maximum number of storage locations)
IN (dimensioned to NBLOKS)
NEIGHB (2D array dimensioned to NBLOKS, 16)
INEI (dimensioned to LGNEIB)

11) Output from Program:

a) each input line is echoed on output;
b) maximum translational and rotational displacement each iteration;
c) plots of block geometry, contact force magnitudes and distribution and incremental and cumulative displacement magnitudes;
d) print-out of contact force data arrays, block data arrays, box data arrays and resultant forces on blocks.

12) Listing of PROGRAM BLOCK:

```
      PROGRAM BLOCK(INPUT,OUTPUT,TAPE5=INPUT,TAPE6=OUTPUT,TAPE1,TAPE2,
     *                TAPE62)
C
C  RIGID BLOCK PROGRAM USING CONVENTIONAL RELAXATION TECHNIQUE
C
      COMMON/CBLOCK/HED(8),NBLOKM,NBOXES,M1,M2,M3,M4,M5,M6,M7,
     *              NBLOKS,NCYC,MCYCLE,NEMPT,RFLAG,UFLAG,EFLAG,NBCBOD,
     *              IBOXES,JBOXES,BSIZE,XSIZE,YSIZE,GRAVY,NOCBN(100),
     *              NUPDAT,UMBST,THMBST,SCREEN,FORCL,DISPL,NREM,
     *              NBNREM(20),IBPLT,IFPLT,IDPLT,ICBNDA,IBLKDA,
     *              IBOXDA,XYL,THL,RESTFL,XBLD,YBLD,RMBLD,XBLDF,YBLDF,
     *              RMBLDF,LGNEIB,CONES,IRFPB,ITDPLT,LBLBCK
      LOGICAL RFLAG,UFLAG,EFLAG
      COMMON Q(6000)
      DIMENSION IQ(1)
      EQUIVALENCE(Q,IQ)
      COMMON/INEIG/IN(6),NEIGHB(6,16)
      DIMENSION INEI(102)
      EQUIVALENCE(IN,INEI)
      COMMON/CLOCK/SEC(30),ISEC(30)
C
      DATA GRAVY/-9.81/
      DATA M7,MCYCLE,NUPDAT,LBLBCK/6000,0,0,177/
      DATA RFLAG,UFLAG,EFLAG/.FALSE.,.TRUE.,.FALSE./
      DATA SCREEN,FORCL,DISPL/20.,1.,1./
      DATA NREM,NBCBOD/0,0/
      DATA RESTFL/0.0/
      DATA LGNEIB/102/
      DATA CONES/0.0/
C
      IPCBN=1
      CALL PL(IPCBN)
      CALL PTIME(0)
      CALL BEGIN
   10 CALL DATA
      CALL CYCLE
      GO TO 10
      END
C
C
      SUBROUTINE BEGIN
C
C   ROUTINE TO DETERMINE WHETHER START OR RESTART RUN
C
      COMMON Q(6000)
      DIMENSION IQ(1)
      EQUIVALENCE(Q,IQ)
      COMMON/CBLOCK/HED(8),NBLOKM,NBOXES,M1,M2,M3,M4,M5,M6,M7,
     *              NBLOKS,NCYC,MCYCLE,NEMPT,RFLAG,UFLAG,EFLAG,NBCBOD,
     *              IBOXES,JBOXES,BSIZE,XSIZE,YSIZE,GRAVY,NOCBN(100),
     *              NUPDAT,UMBST,THMBST,SCREEN,FORCL,DISPL,NREM,
     *              NBNREM(20),IBPLT,IFPLT,IDPLT,ICBNDA,IBLKDA,
     *              IBOXDA,XYL,THL,RESTFL,XBLD,YBLD,RMBLD,XBLDF,YBLDF,
     *              RMBLDF,LGNEIB,CONES,IRFPB,ITDPLT,LBLBCK
      LOGICAL RFLAG,UFLAG,EFLAG
      COMMON/INEIG/IN(6),NEIGHB(6,16)
      DIMENSION INEI(102)
      EQUIVALENCE(IN,INEI)
      WRITE(6,2003)
 2003 FORMAT(1H1)
      WRITE(6,2000)
 2000 FORMAT(30X,52H----RIGID BLOCK PROGRAM USING RELAXATION METHOD.----
     *      /,30X,48H------------------------------------------------/)
      READ(5,1000) WORD
 1000 FORMAT(A4)
C
      IF(WORD.EQ.4HSTAR) GOTO 20
      IF(WORD.EQ.4HREST) GOTO 10
C
      WRITE(6,3000)
 3000 FORMAT(1X, 39H*** ERROR . NO START OR RESTART CARD***)
      STOP
C
C-------RESTART RUN--------
   10 READ(1)  (HED(I),I=1,LBLBCK)
      READ(1) (INEI(I),I=1,LGNEIB)
      READ(1) (Q(I),I=1,M7)
      REWIND 1
      READ(5,1005) HED
 1005 FORMAT(8A10)
      WRITE(6,2001)  HED,MCYCLE
 2001 FORMAT(1X,8A10//30X,30HRESTART RUN . CURRENT CYCLES =,I10//)
      RETURN
C
C-------START RUN--------
   20 READ(5,1001) HED,NBLOKM,IBOXES,JBOXES,IBSIZE
 1001 FORMAT(8A10/4I10)
C
      NBOXES=IBOXES*JBOXES
      BSIZE=IBSIZE
      XSIZE=IBOXES*BSIZE
      YSIZE=JBOXES*BSIZE
C
      WRITE(6,2002) HED,NBLOKM,IBOXES,JBOXES,NBOXES,IBSIZE,XSIZE,YSIZE
 2002 FORMAT(1X,8A10//
     .       30X,24HMAXIMUM NUMBER OF BLOCKS,I5//
     .       30X,24HBOXES IN X-DIRECTION    ,I5/
     .       30X,24HBOXES IN Y-DIRECTION    ,I5/
     .       30X,24HTOTAL NUMBER OF BOXES   ,I5//
     .       30X,24HSIZE OF SINGLE BOX      ,I5/
     .       30X,24HPROBLEM SIZE IN X-DIRN  ,F6.0/
     $       30X,24HPROBLEM SIZE IN Y-DIRN  ,F6.0//)
C
C-----------INTERVALS FOR PLOTTING AND PRINTING RESULTS----------
C
      READ(5,1002) IBPLT,IFPLT,IDPLT,ITDPLT,ICBNDA,IBLKDA,IBOXDA,IRFPB
 1002 FORMAT(8I10)
      WRITE(6,2004) IBPLT,IFPLT,IDPLT,ITDPLT,ICBNDA,IBLKDA,IBOXDA,IRFPB
 2004 FORMAT(10X,21HBLOCK PLOT INTERVAL =,I4,  10HITERATIONS./,
     *       10X,29HCONTACT FORCE PLOT INTERVAL =,I4,10HITERATIONS./,
     *       10X,28HDISPLACEMENT PLOT INTERVAL =,I4,10HITERATIONS./,
     *     10X,34HTOTAL DISPLACEMENT PLOT INTERVAL =,I4,10HITERATIONS.//,
     *       10X,29HCONTACT DATA PRINT INTERVAL =,I4,10HITERATIONS./,
     *       10X,27HBLOCK DATA PRINT INTERVAL =,I4,10HITERATIONS./,
     *       10X,25HBOX DATA PRINT INTERVAL =,I4,10HITERATIONS./,
     *       10X,32HRESULTANT FORCE PRINT INTERVAL =,I4,10HITERATIONS//)
C
C-----------THRESHOLDS FOR UPDATING CONTACTS----------
C
      READ(5,1003) XYL,THL
 1003 FORMAT(2F10.2)
      WRITE(6,2005) XYL,THL
 2005 FORMAT(1X, 36HTHRESHOLDS FOR UPDATING CONTACTS ARE,F10.5,3HAND,
     *       F10.5,58HFOR THE TRANSLATIONAL AND ROTATIONAL MOVEMENT RESP
     *ECTIVELY.//)
C
C-----------SIZE OF MEMORY----------
C
```

```
      READ(5,1004)M7D
 1004 FORMAT(I10)
      M7=MAXO(M7,M7D)
      WRITE(6,2006)M7
 2006 FORMAT(1X,16HSIZE OF MEMORY =,I10,//)
C
C------------------ INITIALISE SOME VARIABLES --
      NBLOKS=0
      M1=1
      M2=M1+NBLOKM
      M3=M2
      XBLDF=0.0
      YBLDF=0.0
      RMBLDF=0.0
      RETURN
      END
C
C
      SUBROUTINE DATA
C
C  RBUTINE TO ASSEMBLE SOME BLOCK DATA
C
      COMMON Q(6000)
      DIMENSION IQ(1)
      EQUIVALENCE(Q,IQ)
      COMMON/CBLOCK/HED(8),NBLOKM,NBOXES,M1,M2,M3,M4,M5,M6,M7,
     *              NBLOKS,NCYC,MCYCLE,NEMPT,RFLAG,UFLAG,EFLAG,NBCODD,
     *              IBOXES,JBOXES,BSIZE,XSIZE,YSIZE,GRAVY,NDCON(100),
     *              NUPDAT,UMOST,THMOST,SCREEN,FORCL,DISPL,NREM,
     *              NBNREM(20),IBPLT,IFPLT,IDPLT,ICOMDA,IBLKDA,
     *              IBOXDA,XYL,THL,RESTFL,XBLD,YBLD,RMBLD,XBLDF,YBLDF,
     *              RMBLDF,LGNEIB,CBHES,IRFPO,ITDPLT,LBLOCK
      LOGICAL RFLAG,UFLAG,EFLAG
      REAL INFL,INANGL,INFU,INANGU
      DIMENSION WORD(20),X(50),Y(50),BNREM(18)
      DATA PI/3.1415926358979/
      DATA WORD /4HCREA,4HDELE,4HDUMP,4HCYCL,4HSTOP,
     *           4HPLOT,4HINTF,4HRSET,4HISET,4HEXTF,
     *           4HGRAV,4HSTIF,4HCOHN,4HFRIC,4HRINV,
     *           4HMDFY,4HUPDA,4HDCON,4HZTOP,4HSTCH/
C
C------------------ READ NEXT CARD --
   10 READ(5,1000) CARD
 1000 FORMAT(A4)
      WRITE(6,2000) CARD
 2000 FORMAT(1X,4H++++ ,A4,4H ++++)
      DO 20 I=1,20
      IF(CARD.EQ.WORD(I))GO TO 30
   20 CONTINUE
      WRITE(6,3000)
 3000 FORMAT(1X, 29H***ERROR . ILLEGAL COMMAND***)
      GOTO 10
C------------------ JUMP TO APPROPRIATE CODE --
   30 GOTO (100,150,200,250,300,
     .       350,400,450,500,550,
     .       600,650,700,750,800,
     *       850,900,950,970,980),I
C
   40 WRITE(6,3001)
 3001 FORMAT(1X, 37H*** ERROR . COMMAND NOT AVAILABLE ***)
      GO TO 10
C
C-------------CREATE A NEW BLOCK----------
C
  100 NBLOKS=NBLOKS+1
      READ(5,1001)NC,RHO,JFIX,JBOUND,JINT
 1001 FORMAT(I10,F10.0,3I10)
      WRITE(6,2006)NBLOKS,NC,RHO,JFIX,JBOUND,JINT
 2006 FORMAT(10X,12HBLOCK NO. = ,I3, 17HNO. OF CORNERS = ,I2,
     *       10HDENSITY = ,E10.4,11HFIX FLAG = ,I2,
     *       15HBOUNDARY FLAG =,I2,16HINT.FORCE FLAG =,I2)
      READ(5,1002)  (X(I),Y(I),I=1,NC)
 1002 FORMAT(8F10.0)
      WRITE(6,2001)  (X(I),Y(I),I=1,NC)
 2001 FORMAT(1X,4(1H(,E12.4,1H,,E12.4,3H ) ))
      I2=M3
      IQ(NBLOKS)=I2
      IQ(I2)=0
      Q(I2+4)=0.0
      Q(I2+7)=0.0
      Q(I2+8)=0.0
      Q(I2+9)=0.0
      Q(I2+11)=0.0
      Q(I2+12)=0.0
      Q(I2+13)=0.0
      Q(I2+14)=0.0
      Q(I2+15)=0.0
      IF(JFIX.NE.0)IQ(I2)=1
      IF(JBOUND.NE.0)Q(I2+14)=1.0
      IF(JINT.NE.0)Q(I2+15)=1.0
      IQ(I2+1)=NC
      Q(I2+5)=1.0
      Q(I2+6)=0.0
C------------------ AREA AND CENTROID OF THIS BLOCK --
      AREA=(X(1)-X(NC))*(Y(1)+Y(NC))
      YC=(X(1)-X(NC))*((Y(1)-Y(NC))*(Y(1)+2.0*Y(NC))+3.0*Y(NC)**2)
      XC=(Y(1)-Y(NC))*((X(1)-X(NC))*(X(1)+2.0*X(NC))+3.0*X(NC)**2)
      DO 110 I=2,NC
      AREA=AREA+(X(I)-X(I-1))*(Y(I)+Y(I-1))
      YC=YC+(X(I)-X(I-1))*((Y(I)-Y(I-1))*(Y(I)+2.0*Y(I-1))
     .      +3.0*Y(I-1)**2)
      XC=XC+(Y(I)-Y(I-1))*((X(I)-X(I-1))*(X(I)+2.0*X(I-1))
     .      +3.0*X(I-1)**2)
  110 CONTINUE
      AREA=0.5*AREA
      YC=YC/(6.0*AREA)
      XC=-XC/(6.0*AREA)
      Q(I2+2)=XC
      Q(I2+3)=YC
      Q(I2+10)=AREA*RHO
C------------------ LOCAL COORDINATES FOR THIS BLOCK --
      M3=M3+16
      Q(M3)=X(1)-XC
      Q(M3+1)=Y(1)-YC
      DO 120 I=2,NC
      Q(M3+3)=0.0
      Q(M3+4)=0.0
      Q(M3+5)=0.0
      NBARRY=6
      IF(Q(I2+14).EQ.0.0)GO TO 111
      M3TEMP=M3+NBARRY
      Q(M3TEMP)=0.0
      Q(M3TEMP+1)=0.0
      Q(M3TEMP+2)=0.0
      Q(M3TEMP+3)=0.0
      NBARRY=NBARRY+4
  111 CONTINUE
      IF(Q(I2+15).EQ.0.0)GO TO 112
```

```
      M3TEMP=M3+NBARRY
      Q(M3TEMP)=0.0
      Q(M3TEMP+1)=0.0
      Q(M3TEMP+2)=0.0
      Q(M3TEMP+3)=0.0
      NBARRY=NBARRY+4
  112 CONTINUE
      M3TEMP=M3+NBARRY
      Q(M3TEMP)=X(I)-XC
      Q(M3TEMP+1)=Y(I)-YC
      Q(M3+2)=SQRT((Q(M3TEMP)-Q(M3))**2+(Q(M3TEMP+1)-Q(M3+1))**2)
  120 M3=M3TEMP
      Q(M3+2)=SQRT((Q(I2+16)-Q(M3))**2+(Q(I2+17)-Q(M3+1))**2)
      Q(M3+3)=0.0
      Q(M3+4)=0.0
      Q(M3+5)=0.0
      NBARRY=6
      IF(Q(I2+14).EQ.0.0)GO TO 113
      M3TEMP=M3+NBARRY
      Q(M3TEMP)=0.0
      Q(M3TEMP+1)=0.0
      Q(M3TEMP+2)=0.0
      Q(M3TEMP+3)=0.0
      NBARRY=NBARRY+4
  113 CONTINUE
      IF(Q(I2+15).EQ.0.0)GO TO 114
      M3TEMP=M3+NBARRY
      Q(M3TEMP)=0.0
      Q(M3TEMP+1)=0.0
      Q(M3TEMP+2)=0.0
      Q(M3TEMP+3)=0.0
      NBARRY=NBARRY+4
  114 CONTINUE
      M3=M3+NBARRY
      WRITE(6,2002)XC,YC,Q(I2+10)
 2002 FORMAT(1X,13H XC,YC,MASS ,3E12.3)
      GOTO 10
C
C-----------REMOVE BLOCKS-----------
C
  150 CONTINUE
      READ(5,1006)NREM
 1006 FORMAT(I4)
      WRITE(6,2004)NREM
 2004 FORMAT(1X,32H THE NUMBER OF BLOCKS REMOVED IS,I4,
     * 29H THEIR NUMBERS ARE----------)
      READ(5,1007)NBC,(BNREM(K),K=1,19)
 1007 FORMAT(I4,19F4.0)
      WRITE(6,2005)(BNREM(K),K=1,19)
 2005 FORMAT(1X,19F4.0)
      DO 151 K=1,19
      NBNREM(K)=BNREM(K)
  151 CONTINUE
      IF(NREM.LE.19)GO TO 152
      JJ=19
      DO 153 II=1,10
      READ(5,1007)NBC,(BNREM(K),K=1,19)
      IF(NBC.EQ.999)GO TO 152
      WRITE(6,2005)(BNREM(K),K=1,19)
      DO 153 IJ=1,19
      JJ=JJ+1
      NBNREM(JJ)=BNREM(IJ)
  153 CONTINUE
  152 CONTINUE
      UFLAG=.TRUE.
      RESTFL=1.0
      GO TO 10
C
C-----------PRINT OUT DATA-----------
C
  200 CALL DUMP(1)
      CALL DUMP(2)
      CALL DUMP(3)
      GO TO 10
C
C-----------COMMENCE ITERATIONS-----------
C
  250 READ(5,1003)NCYC
 1003 FORMAT(I10)
      WRITE(6,2003)NCYC
 2003 FORMAT(1X,19H NUMBER OF CYCLES =,I10)
      IF(NCYCLE.EQ.0)CALL SOX
      RETURN
C
C-----------STOP THE PROGRAM-----------
C
  300 CALL FINISH
C
C-----------PLOT THE PROBLEM GEOMETRY-----------
C
  350 CALL BLPLOT
      GO TO 10
C
C-----------APPLY INTERNAL FORCES TO EDGE NE OF BLOCK NB-----------
C
  400 READ(5,1010)NB,NE,INFL,INANGL,INFU,INANGU
 1010 FORMAT(2I10,4F10.0)
      WRITE(6,2012)NB,NE,INFL,INANGL,INFU,INANGU
 2012 FORMAT(14X,5HNB      NE        INFL      INANGL      INFU      INAN
     *GU,/,6X,2I10,3X,4(E10.4,1X))
      I2=IQ(NB)
      Q(I2+15)=1.0
      J3=I2+12+NE*14
      IF(Q(I2+14).EQ.0.0)J3=I2+12+NE*10
      Q(J3)=INFL
      Q(J3+1)=INANGL*PI/180.
      Q(J3+2)=INFU
      Q(J3+3)=INANGU*PI/180.
      GO TO 10
C
C-----------SET REAL DATA-----------
C
  450 READ(5,1008)IADR,VAL
 1008 FORMAT(I10,F10.0)
      IF(IADR.LE.0.OR.IADR.GT.M7)GO TO 480
      Q(IADR)=VAL
       GO TO 10
C
C-----------SET INTEGER DATA-----------
C
  500 READ(5,1009)IADR,IVAL
 1009 FORMAT(2I10)
      IF(IADR.LE.0.OR.IADR.GT.M7)GO TO 480
      IQ(IADR)=IVAL
      GO TO 10
  480 WRITE(6,3002)
 3002 FORMAT(1X,38H***** ERROR . ADDRESS OUT OF RANGE *****)
      GO TO 10
```

```
C
C----------APPLY EXTERNAL FORCES TO EDGE NE OF BLOCK NB----------
C
 550  READ(5,1010) NB,NE,EXFL,EXANGL,EXFU,EXANGU
      WRITE(6,2013) NB,NE,EXFL,EXANGL,EXFU,EXANGU
 2013 FORMAT(14X,5HNB          NE        EXFL      EXANGL      EXFU      EXAN
     *GU,/,6X,2I10,3X,4(E10.4,1X))
      I2=IQ(NB)
      Q(I2+14)=1.0
      J3=I2+8+NE*14
      IF(Q(I2+15).EQ.0.0) J3=I2+12+NE*10
      Q(J3)=EXFL
      Q(J3+1)=EXANGL*PI/180.
      Q(J3+2)=EXFU
      Q(J3+3)=EXANGU*PI/180.
      GO TO 10
 600  GO TO 40
C ----------NORMAL AND SHEAR STIFFNESS----------
 650  CONTINUE
      READ(5,1014) STIFN,STIFS
 1014 FORMAT(2E10.4)
      WRITE(6,2009) STIFN,STIFS
 2009 FORMAT(10X,24HJOINT NORMAL STIFFNESS =,E10.4,/,
     *       10X,23HJOINT SHEAR STIFFNESS =,E10.4,/)
      DO 651 NB=1,NBLOKS
      I2=IQ(NB)
      NC=IQ(I2+1)
      IC=I2+20
      Q(IC)=STIFN
       Q(IC+1)=STIFS
      DO 652 NP=2,NC
      IC=IC+6
      IF(Q(I2+14).EQ.1.0) IC=IC+4
      IF(Q(I2+15).EQ.1.0) IC=IC+4
      Q(IC)=STIFN
      Q(IC+1)=STIFS
 652  CONTINUE
 651  CONTINUE
      GO TO 10
 700  CONTINUE
C----------JOINT COHESION----------
      READ(5,1015) COHES
 1015 FORMAT(F10.0)
      WRITE(6,2010) COHES
 2010 FORMAT(10X,16HJOINT COHESION =,F10.2,/)
      GO TO 10
C----------FRICTION COEFFICIENT----------
 750  CONTINUE
      READ(5,1013) FRIC
 1013 FORMAT(F10.0)
      WRITE(6,2011) FRIC
 2011 FORMAT(10X,28HJOINT FRICTION COEFFICIENT =,F10.3,/)
      DO 751 NB=1,NBLOKS
      I2=IQ(NB)
      NC=IQ(I2+1)
      IC=I2+19
      Q(IC)=FRIC
      DO 752 NP=2,NC
      IC=IC+6
      IF(Q(I2+14).EQ.1.0) IC=IC+4
      IF(Q(I2+15).EQ.1.0) IC=IC+4
      Q(IC)=FRIC
 752  CONTINUE
 751  CONTINUE
      GO TO 10
 800  READ(5,1011) IBPLT,IFPLT,IDPLT,ITDPLT,ICONDA,IBLKDA,IBOXDA,IRFPO
 1011 FORMAT(8I10)
      WRITE(6,2007) IBPLT,IFPLT,IDPLT,ITDPLT,ICONDA,IBLKDA,IBOXDA,IRFPO
 2007 FORMAT(10X,21HBLOCK PLOT INTERVAL =,I4,  1OHITERATIONS,/,
     *       10X,29HCONTACT FORCE PLOT INTERVAL =,I4,1OHITERATIONS,/,
     *       10X,29HDISPLACEMENT PLOT INTERVAL =,I4,1OHITERATIONS,/,
     *    10X,34HTOTAL DISPLACEMENT PLOT INTERVAL =,I4,1OHITERATIONS,//,
     *       10X,29HCONTACT DATA PRINT INTERVAL =,I4,1OHITERATIONS,/,
     *       10X,27HBLOCK DATA PRINT INTERVAL =,I4,1OHITERATIONS,/,
     *       10X,25HBOX DATA PRINT INTERVAL =,I4,1OHITERATIONS,/,
     *       10X,32HRESULTANT FORCE PRINT INTERVAL =,I4,1OHITERATIONS//)
      READ(5,1012) M7O
 1012 FORMAT(I10)
      M7=M7O
      WRITE(6,2008) M7
 2008 FORMAT(1X,22HMODIFIED MEMORY SIZE =,I10,//)
      GO TO 10
C
C
 850  CONTINUE
      READ(5,1016) XYL,THL
 1016 FORMAT(2F10.2)
      WRITE(6,2015) XYL,THL
 2015 FORMAT(10X,8HNEW XYL =,F10.5,8HNEW THL =,F10.5)
      GO TO 10
C
C----------UPDATE ALL BLOCK CONTACTS----------
C
 900  CALL UPDATE
      GO TO 10
C
C----------BLOCK NUMBERS FOR WHICH CONTACT DATA TO BE  DUMPED
C
 950  CONTINUE
      READ(5,1006) NBCODD
      READ(5,1007) NBCC,(BNREM(K),K=1,19)
      WRITE(6,2014) NBCODD
 2014 FORMAT(1OX,55HNUMBER OF BLOCKS FOR WHICH CONTACT DATA TO BE DUMPED
     * IS,I4,/,  26HTHEIR NUMBERS ARE----------)
      WRITE(6,2005) (BNREM(K),K=1,19)
      DO 951 K=1,19
      NDCBN(K)=BNREM(K)
 951  CONTINUE
      IF(NBCODD.LE.19) GO TO 952
      JJ=19
      DO 953 IIJ=1,10
      READ(5,1007) NBCC,(BNREM(K),K=1,19)
      IF(NBCC.EQ.999) GO TO 952
      WRITE(6,2005) (BNREM(K),K=1,19)
      DO 953 IJ=1,19
      JJ=JJ+1
      NDCBN(JJ)=BNREM(IJ)
 953  CONTINUE
 952  CONTINUE
      GO TO 10
C ZEROISE TOTAL BLOCK DISPLACEMENTS
 970  CONTINUE
      DO 971 NB=1,NBLOKS
      IB=IQ(NB)
      Q(IB+11)=0.0
      Q(IB+12)=0.0
      Q(IB+13)=0.0
 971  CONTINUE
```

```
      WRITE(6,1019)
 1019 FORMAT(1X,32HTOTAL BLOCK DISPLACEMENTS ZEROED)
      GO TO 10
  980 CONTINUE
      GO TO 10
      END
C
C
      SUBROUTINE BOX
C
C  ROUTINE TO BOX ALL BLOCK CORNERS ONCE BLOCKS HAVE BEEN CREATED
C
      COMMON/CBLOCK/HED(8),NBLOKM,NBOXES,M1,M2,M3,M4,M5,M6,M7,
     *              NBLOKS,NCYC,MCYCLE,NEMPT,RFLAG,UFLAG,EFLAG,NBCODD,
     *              IBOXES,JBOXES,BSIZE,XSIZE,YSIZE,GRAVY,NDCON(100),
     *              NUPDAT,UMBST,THMBST,SCREEN,FORCL,DISPL,NREM,
     *              NBNREM(20),IBPLT,IFPLT,IDPLT,ICONDA,IBLKDA,
     *              IBOXDA,XYL,THL,RESTFL,XBLD,YBLD,RMBLD,XBLDF,YBLDF,
     *              RMBLDF,LGNEIB,COMES,IRFPO,ITDPLT,LBLOCK
      LOGICAL RFLAG,UFLAG,EFLAG
      COMMON Q(6000)
      DIMENSION IQ(1)
      EQUIVALENCE(Q,IQ)
      M4=M3+NBOXES
      M5=M4
C------------------ INITIALISE BOX POINTERS ---
      I1=M4-1
      DO 10 I=M3,I1
   10 IQ(I)=0
C------------------ LOOP ON EACH BLOCK ---
      DO 50 NB=1,NBLOKS
      I2=IQ(NB)
      NC=IQ(I2+1)
      IC=I2+16
C------------------ LOOP ON EACH CORNER ---
      DO 40 NP=1,NC
      X=Q(I2+2)+Q(IC)
      Y=Q(I2+3)+Q(IC+1)
      IBOX=MIND(IFIX(X/BSIZE)+1,IBOXES)
      JBOX=MIND(IFIX(Y/BSIZE),JBOXES-1)
      NBOX=JBOX*IBOXES+IBOX
      I3=M3+NBOX-1
      IQ(M5+2)=IQ(I3)
      IQ(I3)=M5
      IQ(M5)=NP
      IQ(M5+1)=NB
      M5=M5+3
      IC=IC+6
      IF(Q(I2+14).EQ.1.0)IC=IC+4
      IF(Q(I2+15).EQ.1.0)IC=IC+4
   40 CONTINUE
C
   50 CONTINUE
C
      M5=M5+NBLOKM
      DO 60 I=M5,M6
   60 IQ(I)=0
C------------------ CREATE EMPTY LIST TO END OF MEMORY ---
      NEMPT=M5
      I6=M5+4
      DO 80 I=I6,M7,15
      J=I
      IQ(I)=I+11
   80 CONTINUE
      IQ(J)=0
      WRITE(6,2000)M2,M3,M4,M5,M6
 2000 FORMAT(1X, 16H M2,M3,M4,M5,M6,,5I10)
C
      RETURN
      END
C
C
      SUBROUTINE CYCLE
C
      COMMON Q(6000)
      DIMENSION IQ(1)
      EQUIVALENCE(Q,IQ)
      COMMON/CBLOCK/HED(8),NBLOKM,NBOXES,M1,M2,M3,M4,M5,M6,M7,
     *              NBLOKS,NCYC,MCYCLE,NEMPT,RFLAG,UFLAG,EFLAG,NBCODD,
     *              IBOXES,JBOXES,BSIZE,XSIZE,YSIZE,GRAVY,NDCON(100),
     *              NUPDAT,UMBST,THMBST,SCREEN,FORCL,DISPL,NREM,
     *              NBNREM(20),IBPLT,IFPLT,IDPLT,ICONDA,IBLKDA,
     *              IBOXDA,XYL,THL,RESTFL,XBLD,YBLD,RMBLD,XBLDF,YBLDF,
     *              RMBLDF,LGNEIB,COMES,IRFPO,ITDPLT,LBLOCK
      LOGICAL RFLAG,UFLAG,EFLAG
      TRANS=0.0
      ROTN=0.0
      DO 100 NCYCLE=1,NCYC
      MCYCLE=MCYCLE+1
      UMBST=0.0
      THMBST=0.0
      XBLD=0.0
      YBLD=0.0
      RMBLD=0.0
      CALL PTICK(1)
      IF(UFLAG)CALL UPDATE
      CALL PTBCK(1)
C SCAN EACH BLOCK
      DO 50 NB=1,NBLOKS
C
C CHECK IF BLOCK REMOVED
C
      IF(NREM.EQ.0)GO TO 140
      DO 150 K=1,NREM
      IF(NB.EQ.NBNREM(K))GO TO 50
  150 CONTINUE
  140 CONTINUE
      IB=IQ(NB)
       J6=M5+NB-1
   60 I6=IQ(J6)
      IF(I6.EQ.0)GO TO 50
      JBC=IQ(I6+3)
      IBC=IQ(JBC)
      CALL FORD(Q,IQ,I6,IBC,IB)
      J6=I6+4
      GO TO 60
   50 CONTINUE
      DO 20 NB=1,NBLOKS
C
C CHECK IF BLOCK REMOVED
C
      IF(NREM.EQ.0)GO TO 120
      DO 130 K=1,NREM
      IF(NB.EQ.NBNREM(K))GO TO 20
  130 CONTINUE
  120 CONTINUE
      IB=IQ(NB)
C IS BLOCK FIXED
```

```
      IF(IQ(I8).NE.0)GO TO 20
C NO.BLOCK NOT FIXED
      CALL PTICK(2)
      CALL MOTION(Q,IQ,I8,N8)
      CALL PTOCK(2)
      CALL PTICK(3)
      IF(RFLAG)CALL REBOX(N8)
      CALL PTOCK(3)
 20   CONTINUE
      XBLDF=XBLD
      YBLDF=YBLD
      RMBLDF=RMBLD
      JPLOT1=(MCYCLE/IOPLT)*IOPLT
      IF(JPLOT1.NE.MCYCLE)GO TO 152
      CALL OLPLOT
 152  JPLOT2=(MCYCLE/IFPLT)*IFPLT
      IF(JPLOT2.NE.MCYCLE)GO TO 153
      CALL FORPLT
 153  JPLOT3=(MCYCLE/IDPLT)*IDPLT
      IF(JPLOT3.NE.MCYCLE)GO TO 151
      CALL DISPLT
 151  JPLOT4=(MCYCLE/ITDPLT)*ITDPLT
      IF(JPLOT4.NE.MCYCLE)GO TO 154
      CALL TDISPL
 154  CONTINUE
      IPRIN1=(MCYCLE/ICONDA)*ICONDA
      IF(IPRIN1.NE.MCYCLE)GO TO 751
      CALL DUMP(1)
 751  IPRIN2=(MCYCLE/IBLKDA)*IBLKDA
      IF(IPRIN2.NE.MCYCLE)GO TO 752
      CALL DUMP(2)
 752  IPRIN3=(MCYCLE/IBOXDA)*IBOXDA
      IF(IPRIN3.NE.MCYCLE)GO TO 750
      CALL DUMP(3)
 750  CONTINUE
C EXIT IF BLOCKS HAVEN"T MOVED
      IF(UMOST.LE.1.E-20.AND.THMOST.LE.1.E-20)GO TO 110
      TRANS=TRANS+UMOST
      ROTN=ROTN+THMOST
      IF(TRANS.GT.XYL.OR.ROTN.GT.THL)GO TO 30
      GO TO 40
 30   UFLAG=.TRUE.
      TRANS=0.0
      ROTN=0.0
 40   CONTINUE
      WRITE(6,1001)MCYCLE,UMOST,THMOST
 1001 FORMAT(1X, 65HMAXIMUM BLOCK TRANSLATIONAL AND ROTATIONAL MOVEMENT
     *FOR ITERATION,I5,3HWAS,E10.4,4H AND,E10.4,13H RESPECTIVELY)
      GO TO 100
 110  WRITE(6,2001)MCYCLE
 2001 FORMAT(1X, 42HUMOST AND THMOST BELOW THRESHOLD FOR CYCLE,I5)
      GO TO 111
 100  CONTINUE
 111  CONTINUE
      CALL HSTIFF
      RETURN
      END
C
C
      SUBROUTINE MOTION(Q,IQ,I8,N8)
C
      DIMENSION Q(5000)
      DIMENSION IQ(1)
      COMMON/CBLOCK/HED(8),NBLOKM,NBOXES,M1,M2,M3,M4,M5,M6,M7,
     *             NBLOKS,NCYC,MCYCLE,NEMPT,RFLAG,UFLAG,EFLAG,NBCOOD,
     *             IBOXES,JBOXES,BSIZE,XSIZE,YSIZE,GRAVY,NDCON(100),
     *             NUPDAT,UMOST,THMOST,SCREEN,FORCL,DISPL,NREM,
     *             NBNREM(20),IBPLT,IFPLT,IDPLT,ICONDA,IBLKDA,
     *             IBOXDA,XYL,THL,RESTFL,XBLD,YBLD,RMBLD,XBLDF,YBLDF,
     *             RMBLDF,LGNEIB,CONES,IRFPB,ITDPLT,LBLOCK
      LOGICAL RFLAG,UFLAG,EFLAG
      COMMON/INEIG/IN(8),NEIGHB(8,16)
      DIMENSION INEI(102)
      EQUIVALENCE(IN,INEI)
      DIMENSION A(3,4),X(3),NEIG(20),XCON(50),YCON(50),NBCON(50)
      REAL MSUM,MCBX,MCBY,MCBM,MLOAD
      ICOUNT=0
      XFSUM=0.0
      YFSUM=0.0
      MSUM=0.0
      XCBX=0.0
      XCBY=0.0
      XCBM=0.0
      YCBX=0.0
      YCBY=0.0
      YCBM=0.0
      MCBX=0.0
      MCBY=0.0
      MCBM=0.0
      XLOAD=0.0
      YLOAD=0.0
      MLOAD=0.0
      DO 300 J=1,50
      XCON(J)=0.0
      YCON(J)=0.0
      NBCON(J)=0
 300  CONTINUE
C DETERMINE COEFFICIENTS FOR EQUILIBRIUM EQUATIONS
      I2=I8
      J6=M6+N8-1
      J=0
 100  I6=IQ(J6)
      IF(I6.EQ.0)GO TO 90
      J=J+1
      XCON(J)=Q(I6+13)
      YCON(J)=Q(I6+14)
      NBCON(J)=IQ(I6+3)
      IF(Q(I6+9).EQ.0.0.AND.Q(I6+10).EQ.0.0)GO TO 10
      XFSUM=XFSUM+Q(I6+6)
       YFSUM=YFSUM+Q(I6+5)
      MSUM=MSUM+Q(I6+5)*(Q(I6+13)-Q(I2+2))
     *          -Q(I6+6)*(Q(I6+14)-Q(I2+3))
      GO TO 11
 10   IF(RESTFL.EQ.1.0)GO TO 12
 11   ICOUNT=ICOUNT+1
      XDIF=Q(I6+13)-Q(I2+2)
      YDIF=Q(I2+3)-Q(I6+14)
      IF(Q(I2+14).EQ.0.0.AND.Q(I2+15).EQ.0.0)GO TO 702
      IF(Q(I2+14).EQ.1.0.AND.Q(I2+15).EQ.1.0)GO TO 701
      IARG1=I2+11+IQ(I6+1)*10
      IARG2=I2+10+IQ(I6+1)*10
      GO TO 704
 701  IARG1=I2+7+IQ(I6+1)*14
      IARG2=I2+6+IQ(I6+1)*14
      GO TO 704
 702  IARG1=I2+15+IQ(I6+1)*8
      IARG2=I2+14+IQ(I6+1)*8
 704  CONTINUE
```

```
      AAA=Q(IARG1)*Q(I6+12)
      AAB=Q(IARG2)*Q(I6+11)
      BBA=Q(IARG1)*Q(I6+11)
      BBB=Q(IARG2)*Q(I6+12)
      XC8X=XC8X-AAA*Q(I6+12)-AAB*Q(I6+11)
      XC8Y=XC8Y-AAA*Q(I6+11)+AAB*Q(I6+12)
      XC8M=XC8M-AAA*YDIF*Q(I6+12)-AAA*XDIF*Q(I6+11)
     *          +AAB*XDIF*Q(I6+12)-AAB*YDIF*Q(I6+11)
      YC8X=YC8X-BBA*Q(I6+12)+BBB*Q(I6+11)
      YC8Y=YC8Y-BBA*Q(I6+11)-BBB*Q(I6+12)
      YC8M=YC8M-BBA*YDIF*Q(I6+12)-BBA*XDIF*Q(I6+11)
     *          -BBB*XDIF*Q(I6+12)+BBB*YDIF*Q(I6+11)
      MC8X=MC8X+XDIF*(-BBA*Q(I6+12)+BBB*Q(I6+11))
     *          +YDIF*(-AAA*Q(I6+12)-AAB*Q(I6+11))
      MC8Y=MC8Y+XDIF*(-BBA*Q(I6+11)-BBB*Q(I6+12))
     *          +YDIF*(-AAA*Q(I6+11)+AAB*Q(I6+12))
      MC8M=MC8M+XDIF*(-BBA*YDIF*Q(I6+12)-BBA*XDIF*Q(I6+11)
     *                -BBB*XDIF*Q(I6+12)+BBB*YDIF*Q(I6+11))
     *          +YDIF*(-AAA*YDIF*Q(I6+12)-AAA*XDIF*Q(I6+11)
     *                +AAB*XDIF*Q(I6+12)-AAB*YDIF*Q(I6+11))
  12  CONTINUE
      J6=I6+4
      GO TO 100
  90  CONTINUE
C ADD FORCES AND DETERMINE EQUILIBRIUM EQUATION COEFFICIENTS BETWEEN
C CONTACTS OF CORNERS OF NB AND SURROUNDING BLOCKS
      IXX=0
      INNB=IN(NB)
      DO 650 JX=1,INNB
      NBB=NEIGHB(NB,JX)
      IF(NBB.EQ.0)GO TO 650
      IF(NBB.EQ.NB)GO TO 700
      GO TO 710
  700 WRITE(6,1010)
 1010 FORMAT(1X,32HERRORS IN NEIGHB ARRAY IN MOTION)
      EFLAG=.TRUE.
      CALL FINISH
C
C CHECK IF BLOCK NBB ALREADY EVALUATED
C
  710 IF(IXX.EQ.0)GO TO 660
      DO 670 JXX=1,IXX
      IF(NEIG(JXX).EQ.NBB)GO TO 650
  670 CONTINUE
  660 CONTINUE
      IXX=IXX+1
      NEIG(IXX)=NBB
      N6=I6+NBB-1
      I6=IQ(N6)
  120 CONTINUE
      IF(I6.EQ.0)GO TO 650
      IF(IQ(I6+3).EQ.NB)GO TO 130
  180 N6=I6+4
      I6=IQ(N6)
      GO TO 120
C-----------N6 IS A CORNER CONTACT OF NBB----------
  130 CONTINUE
      I2B=IQ(N6B)
      XX=Q(I6+13)
        YY=Q(I6+14)
      IF(Q(I2B+14).EQ.0.0.AND.Q(I2B+15).EQ.0.0)GO TO 712
      IF(Q(I2B+14).EQ.1.0.AND.Q(I2B+15).EQ.1.0)GO TO 711
      RLENG=(Q(I2B+6+IQ(I6+1)*10))/20.
      GO TO 714
  711 RLENG=(Q(I2B+4+IQ(I6+1)*14))/20.
      GO TO 714
  712 RLENG=(Q(I2B+12+IQ(I6+1)*8))/20.
  714 CONTINUE
C
C SEARCH J CORNER CONTACTS OF NB ELIMINATING DIAGONAL CORNER-CORNER
C CONTACTS
C
      DO 600 I=1,J
      IF(N8CON(I).EQ.NBB)GO TO 610
      GO TO 620
  610 XDIF=ABS(XX-XCON(I))
      YDIF=ABS(YY-YCON(I))
      IF(XDIF.LT.RLENG.AND.YDIF.LT.RLENG)GO TO 180
  620 CONTINUE
  600 CONTINUE
      IF(Q(I6+8).EQ.0.0.AND.Q(I6+10).EQ.0.0)GO TO 13
      XFSUM=XFSUM+Q(I6+8)
      YFSUM=YFSUM+Q(I6+7)
      MSUM=MSUM+Q(I6+7)*(Q(I6+13)-Q(I2+2))
     *          -Q(I6+8)*(Q(I6+14)-Q(I2+3))
      GO TO 14
  13  IF(RESTFL.EQ.1.0)GO TO 15
  14  ICOUNT=ICOUNT+1
      XDIF=Q(I6+13)-Q(I2+2)
      YDIF=Q(I2+3)-Q(I6+14)
      IF(Q(I2B+14).EQ.0.0.AND.Q(I2B+15).EQ.0.0)GO TO 722
      IF(Q(I2B+14).EQ.1.0.AND.Q(I2B+15).EQ.1.0)GO TO 721
      IARG3=I2B+11+IQ(I6+1)*10
      IARG4=I2B+10+IQ(I6+1)*10
      GO TO 724
  721 IARG3=I2B+7+IQ(I6+1)*14
      IARG4=I2B+6+IQ(I6+1)*14
      GO TO 724
  722 IARG3=I2B+15+IQ(I6+1)*8
      IARG4=I2B+14+IQ(I6+1)*8
  724 CONTINUE
      AAA=Q(IARG3)*Q(I6+12)
      AAB=Q(IARG4)*Q(I6+11)
      BBA=Q(IARG3)*Q(I6+11)
      BBB=Q(IARG4)*Q(I6+12)
      XC8X=XC8X-AAA*Q(I6+12)-AAB*Q(I6+11)
      XC8Y=XC8Y-AAA*Q(I6+11)+AAB*Q(I6+12)
      XC8M=XC8M-AAA*YDIF*Q(I6+12)-AAA*XDIF*Q(I6+11)
     *          +AAB*XDIF*Q(I6+12)-AAB*YDIF*Q(I6+11)
      YC8X=YC8X-BBA*Q(I6+12)+BBB*Q(I6+11)
      YC8Y=YC8Y-BBA*Q(I6+11)-BBB*Q(I6+12)
      YC8M=YC8M-BBA*YDIF*Q(I6+12)-BBA*XDIF*Q(I6+11)
     *          -BBB*XDIF*Q(I6+12)+BBB*YDIF*Q(I6+11)
      MC8X=MC8X+XDIF*(-BBA*Q(I6+12)+BBB*Q(I6+11))
     *          +YDIF*(-AAA*Q(I6+12)-AAB*Q(I6+11))
      MC8Y=MC8Y+XDIF*(-BBA*Q(I6+11)-BBB*Q(I6+12))
     *          +YDIF*(-AAA*Q(I6+11)+AAB*Q(I6+12))
      MC8M=MC8M+XDIF*(-BBA*YDIF*Q(I6+12)-BBA*XDIF*Q(I6+11)
     *                -BBB*XDIF*Q(I6+12)+BBB*YDIF*Q(I6+11))
     *          +YDIF*(-AAA*YDIF*Q(I6+12)-AAA*XDIF*Q(I6+11)
     *                +AAB*XDIF*Q(I6+12)-AAB*YDIF*Q(I6+11))
  15  CONTINUE
      N6=I6+4
      I6=IQ(N6)
      GO TO 120
  650 CONTINUE
      IF(NCYCLE.EQ.1)GO TO 500
      IF(XFSUM.EQ.0.0.AND.YFSUM.EQ.0.0.AND.MSUM.EQ.0.0)GO TO 530
```

```
      GO TO 500
  530 WRITE(6,1006)NB,MCYCLE
 1006 FORMAT(1X, 57HNO FORCES FROM CONTACTS WITH SURROUNDING BLOCKS FOR
     *BLOCK,I5,  19HAT ITERATION NUMBER,I10)
  500 WEIGHT=Q(I2+10)*GRAVY
      XSURL=0.0
      YSURL=0.0
      RMSURL=0.0
      IF(Q(I2+14).EQ.0.0.AND.Q(I2+15).EQ.0.0)GO TO 950
      CALL LOAD(I2,XSURL,YSURL,RMSURL)
  950 XLOAD=XFSUM+XSURL
      YLOAD=YFSUM+YSURL+WEIGHT
      MLOAD=MSUM+RMSURL
C
C PRINT OUT RESULTANT FORCES ACTING ON BLOCK IF AT REQUIRED ITERATION
C
      IPOOF=(MCYCLE/IRFPO)*IRFPO
      IF(IPOOF.NE.MCYCLE)GO TO 951
      WRITE(6,1020)XLOAD,YLOAD,MLOAD
 1020 FORMAT(10X,E10.4,5X,E10.4,5X,E10.4)
  951 CONTINUE
      IF(ICOUNT.LE.1)GO TO 510
      A(1,1)=XCOX
      A(1,2)=XCOY
      A(1,3)=XCOM
      A(2,1)=YCOX
      A(2,2)=YCOY
      A(2,3)=YCOM
      A(3,1)=MCOX
      A(3,2)=MCOY
      A(3,3)=MCOM
      A(1,4)=-XLOAD
      A(2,4)=-YLOAD
      A(3,4)=-MLOAD
C
C SOLUTION OF SIMULTANEOUS LINEAR EQUATIONS BY GAUSSIAN ELIMINATION
C
      NEQN=3
C
C APPLY GAUSSIAN ELIMINATION
      CALL ELIMIN(A,X,NEQN,3,4,DETA,RATIO)
      IF(DETA.EQ.0.0.OR.ABS(RATIO).LT.1.E-05)GO TO 510
C SOLUTIONS CONTAINED IN VECTOR X
  520 UMOST=AMAX1(UMOST,ABS(X(1)))
      UMOST=AMAX1(UMOST,ABS(X(2)))
      THMOST=AMAX1(THMOST,ABS(X(3)))
      XOLD=AMAX1(XOLD,ABS(X(1)))
      YOLD=AMAX1(YOLD,ABS(X(2)))
      RMOLD=AMAX1(RMOLD,ABS(X(3)))
      LBX=Q(I2+2)
      LBY=Q(I2+3)
      Q(I2+7)=X(1)
      Q(I2+8)=X(2)
      Q(I2+9)=X(3)
      Q(I2+11)=Q(I2+11)+X(1)
      Q(I2+12)=Q(I2+12)+X(2)
      Q(I2+13)=Q(I2+13)+X(3)
C UPDATE BLOCK CENTROIDAL CO-ORDINATES
      Q(I2+2)=Q(I2+2)+X(1)
      Q(I2+3)=Q(I2+3)+X(2)
      Q(I2+4)=Q(I2+4)+X(3)
      TEMP=Q(I2+5)
      Q(I2+5)=Q(I2+5)-Q(I2+9)*Q(I2+6)
      Q(I2+6)=Q(I2+6)+Q(I2+9)*TEMP
      IF(LBX.EQ.IFIX(Q(I2+2)).AND.LBY.EQ.IFIX(Q(I2+3)).AND.
     *   ABS(Q(I2+4)).LT.0.01)GO TO 545
      RFLAG=.TRUE.
      Q(I2+4)=0.0
  545 CONTINUE
      RETURN
  510 CONTINUE
C
C SINCE EQUATIONS ARE SINGULAR OR VERY ILL-CONDITIONED LET BLOCK
C DISPLACE A SPECIFIED AMOUNT IN DIRECTION OF RESULTANT FORCES
C
      WRITE(6,1005)NB,MCYCLE
 1005 FORMAT(1X, 60HTHE EQUATIONS ARE SINGULAR OR VERY ILL-CONDITIONED F
     *OR BLOCK,I5,19HAT ITERATION NUMBER,I5)
      IF(XLOAD.EQ.0.0)GO TO 511
      GXD=XBLDF
      X(1)=SIGN(GXD,XLOAD)
      GO TO 512
  511 X(1)=0.0
  512 IF(YLOAD.EQ.0.0)GO TO 515
      GYD=YBLDF
      X(2)=SIGN(GYD,YLOAD)
      GO TO 516
  515 X(2)=0.0
  516 IF(MLOAD.EQ.0.0)GO TO 513
      GMD=RMBLDF
      X(3)=SIGN(GMD,MLOAD)
      GO TO 514
  513 X(3)=0.0
  514 CONTINUE
      GO TO 520
      END
      SUBROUTINE ELIMIN(A,X,NEQN,NROW,NCOL,DET,RATIO)
C
C SUBROUTINE FOR SOLVING SIMULTANEOUS LINEAR EQUATIONS BY
C GAUSSIAN ELIMINATION WITH PARTIAL PIVOTING
C
      DIMENSION A(NROW,NCOL),X(NROW)
      NEQN=NEQN
      IF(NEQN.LE.NROW.AND.NEQN.LE.NCOL-1)GO TO 1
      WRITE(6,1000)
 1000 FORMAT(1X,31H STOP-DIMENSION ERROR IN ELIMIN)
      STOP
C FIND MEAN COEFFICIENT MAGNITUDE
    1 AMEAN=0.
      DO 2 I=1,NEQN
      DO 2 J=1,NEQN
    2 AMEAN=AMEAN+ABS(A(I,J))
      AMEAN=AMEAN/FLOAT(NEQN*NEQN)
C COMMENCE ELIMINATION PROCESS
      JMAX=NEQN+1
      NEQNM1=NEQN-1
      DO 6 IEQN=1,NEQNM1
C
C SEARCH LEADING COLUMN OF THE COEFFICIENT MATRIX FROM
C THE DIAGONAL DOWNWARDS FOR THE LARGEST ELEMENT AND MAKE
C THIS THE PIVOTAL ELEMENT
C
      IMIN=IEQN+1
      IMAX=IEQN
      DO 3 I=IMIN,NEQN
    3 IF(ABS(A(I,IEQN)).GT.ABS(A(IMAX,IEQN)))IMAX=I
      IF(IMAX.EQ.IEQN)GO TO 5
      DO 4 J=IEQN,JMAX
```

```
      AA=A(IEQN,J)
      A(IEQN,J)=A(IMAX,J)
    4 A(IMAX,J)=AA
C
C ELIMINATE X(IEQN) FROM EQUATIONS (IEQN+1) TO NEQN.
C FIRST TESTING FOR NON ZERO PIVOTAL ELEMENT
C
    5 IF(ABS(A(IEQN,IEQN)/AMEAN).LT.1.E-8)GO TO 10
      DO 6 I=IMIN,NEQN
      FACT=A(I,IEQN)/A(IEQN,IEQN)
      DO 6 J=IMIN,JMAX
    6 A(I,J)=A(I,J)-FACT*A(IEQN,J)
C
C SOLVE UPPER-TRIANGULAR SET OF EQUATIONS BY BACK SUBSTITUTION
C
      IF(ABS(A(NEQN,NEQN)/AMEAN).LT.1.E-8)GO TO 10
      X(NEQN)=A(NEQN,JMAX)/A(NEQN,NEQN)
      DO 8 L=2,NEQN
      I=NEQN+1-L
      SUM=A(I,JMAX)
      IP1=I+1
      DO 7 J=IP1,NEQN
    7 SUM=SUM-A(I,J)*X(J)
    8 X(I)=SUM/A(I,I)
C
C EVALUATE DETERMINANT OF COEFFICIENT MATRIX AND COMPARE WITH
C ORIGINAL COEFFICIENTS
C
      DETA=1.
      DO 9 I=1,NEQN
    9 DETA=DETA*A(I,I)
      DET=DETA
      RATIO=DETA/AMEAN**NEQN
      RETURN
   10 DET=0.
      RETURN
      END
C
C
      SUBROUTINE FORD(Q,IQ,I6,IBC,IB)
C
      DIMENSION Q(5000)
      DIMENSION IQ(1)
      COMMON/CBLOCK/HED(8),NBLOKM,NBOXES,M1,M2,M3,M4,M5,M6,M7,
     *              NBLOKS,NCYC,MCYCLE,NEMPT,RFLAG,UFLAG,EFLAG,NBCODD,
     *              IBOXES,JBOXES,BSIZE,XSIZE,YSIZE,GRAVY,NDCOM(100),
     *              NUPDAT,UMBST,THMBST,SCREEN,FORCL,DISPL,NREM,
     *              NBNREM(20),IBPLT,IFPLT,IDPLT,ICONDA,IBLKDA,
     *              IBOXDA,XYL,THL,RESTFL,XBLD,YBLD,RMBLD,XBLDF,YBLDF,
     *              RMBLDF,LGNEIB,CONES,IRFPO,ITDPLT,LBLOCK
      LOGICAL RFLAG,UFLAG,EFLAG
C ROUTINE TO DETERMINE A SINGLE CONTACT FORCE BETWEEN TWO BLOCKS
C FROM THEIR POSITION IN SPACE
C
C RELATIVE INCREMENTAL GLOBAL DISPLACEMENTS OF CORNER RELATIVE TO EDGE
      DUY=Q(IBC+6)-Q(IB+6)+Q(IBC+9)*(Q(I6+13)-Q(IBC+2))
     *                    -Q(IB+9)*(Q(I6+13)-Q(IB+2))
      DUX=Q(IBC+7)-Q(IB+7)-Q(IBC+9)*(Q(I6+14)-Q(IBC+3))
     *                    +Q(IB+9)*(Q(I6+14)-Q(IB+3))
C RELATIVE INCREMENTAL NORMAL AND SHEAR DISPLACEMENTS OF CORNER
C RELATIVE TO EDGE
      DUS=DUX*Q(I6+12)+DUY*Q(I6+11)
      DUN=DUY*Q(I6+12)-DUX*Q(I6+11)
C NORMAL FORCE
      IF(Q(IB+14).EQ.0.0.AND.Q(IB+15).EQ.0.0)GO TO 102
      IF(Q(IB+14).EQ.1.0.AND.Q(IB+15).EQ.1.0)GO TO 101
      IARG1=IB+10+IQ(I6+1)*10
      IARG2=IB+11+IQ(I6+1)*10
      IARG3=IB+9+IQ(I6+1)*10
      GO TO 104
  101 IARG1=IB+6+IQ(I6+1)*14
      IARG2=IB+7+IQ(I6+1)*14
      IARG3=IB+5+IQ(I6+1)*14
      GO TO 104
  102 IARG1=IB+14+IQ(I6+1)*6
      IARG2=IB+15+IQ(I6+1)*6
      IARG3=IB+13+IQ(I6+1)*6
  104 CONTINUE
      DFN=-DUN*Q(IARG1)
      Q(I6+9)=Q(I6+9)+DFN
C TEST FOR TENSION
      IF(Q(I6+9).GE.0.0)GO TO 20
      Q(I6+9)=0.0
      Q(I6+10)=0.0
      GO TO 60
C SHEAR FORCE
   20 DFS=DUS*Q(IARG2)
      Q(I6+10)=Q(I6+10)+DFS
      FRICF=Q(I6+9)*Q(IARG3)+CONES
      IF(ABS(Q(I6+10)).LE.FRICF)GO TO 40
      Q(I6+10)=SIGN(FRICF,Q(I6+10))
   40 CONTINUE
C GLOBAL CONTACT FORCES
   60 Q(I6+5)=Q(I6+10)*Q(I6+11)-Q(I6+9)*Q(I6+12)
      Q(I6+6)=Q(I6+10)*Q(I6+12)+Q(I6+9)*Q(I6+11)
      Q(I6+7)=-Q(I6+5)
      Q(I6+8)=-Q(I6+6)
      RETURN
      END
      SUBROUTINE LOAD(I2,XSURL,YSURL,RMSURL)
C
C ROUTINE TO CALCULATE RESULTANT SURFACE FORCES ON BLOCK
C
      COMMON/CBLOCK/HED(8),NBLOKM,NBOXES,M1,M2,M3,M4,M5,M6,M7,
     *              NBLOKS,NCYC,MCYCLE,NEMPT,RFLAG,UFLAG,EFLAG,NBCODD,
     *              IBOXES,JBOXES,BSIZE,XSIZE,YSIZE,GRAVY,NDCOM(100),
     *              NUPDAT,UMBST,THMBST,SCREEN,FORCL,DISPL,NREM,
     *              NBNREM(20),IBPLT,IFPLT,IDPLT,ICONDA,IBLKDA,
     *              IBOXDA,XYL,THL,RESTFL,XBLD,YBLD,RMBLD,XBLDF,YBLDF,
     *              RMBLDF,LGNEIB,CONES,IRFPO,ITDPLT,LBLOCK
      LOGICAL RFLAG,UFLAG,EFLAG
      COMMON Q(5000)
      DIMENSION IQ(1)
      EQUIVALENCE(Q,IQ)
C
      IF(Q(I2+14).EQ.0.0)GO TO 70
       NC=IQ(I2+1)
      IC=I2+16
      DO 60 NP=1,NC
      IB=IC
      IC=IB+10
      IF(Q(I2+15).EQ.1.0)IC=IC+4
      IF(NP.EQ.NC)IC=I2+16
      XL=GLX(Q(I2),IB)
      YL=GLY(Q(I2),IB)
      XU=GLX(Q(I2),IC)
      YU=GLY(Q(I2),IC)
      XSURL=XSURL+Q(IB+6)*COS(Q(IB+7))+Q(IB+8)*COS(Q(IB+9))
```

```
      YSURL=YSURL+Q(IB+6)*SIN(Q(IB+7))+Q(IB+8)*SIN(Q(IB+9))
      RMSURL=RMSURL+Q(IB+6)*SIN(Q(IB+7))*(XL-Q(I2+2))
     *                    -Q(IB+8)*COS(Q(IB+7))*(YL-Q(I2+3))
     *                     +Q(IB+8)*SIN(Q(IB+9))*(XU-Q(I2+2))
     *                    -Q(IB+8)*COS(Q(IB+9))*(YU-Q(I2+3))
   60 CONTINUE
   70 CONTINUE
      IF(Q(I2+15).EQ.0.0)GO TO 50
      IC=I2+16
      DO 60 NP=1,NC
      IB=IC
      NBARRY=6
      IC=IB+10
      IF(Q(I2+14).EQ.1.0)IC=IC+4
      IF(NP.EQ.NC)IC=I2+16
      XL=GLX(Q(I2),IB)
      YL=GLY(Q(I2),IB)
      XU=GLX(Q(I2),IC)
      YU=GLY(Q(I2),IC)
      IF(Q(I2+14).EQ.1.0)NBARRY=10
      XSURL=XSURL+Q(IB+NBARRY)*COS(Q(IB+NBARRY+1))
     *                     +Q(IB+NBARRY+2)*COS(Q(IB+NBARRY+3))
      YSURL=YSURL+Q(IB+NBARRY)*SIN(Q(IB+NBARRY+1))
     *                     +Q(IB+NBARRY+2)*SIN(Q(IB+NBARRY+3))
      RMSURL=RMSURL+Q(IB+NBARRY)*SIN(Q(IB+NBARRY+1))*(XL-Q(I2+2))
     *          -Q(IB+NBARRY)*COS(Q(IB+NBARRY+1))*(YL-Q(I2+3))
     *                     +Q(IB+NBARRY+2)*SIN(Q(IB+NBARRY+3))*(XU-Q(I2+2))
     *          -Q(IB+NBARRY+2)*COS(Q(IB+NBARRY+3))*(YU-Q(I2+3))
   80 CONTINUE
   90 CONTINUE
      RETURN
      END
C
C
      SUBROUTINE UPDATE
C
C  UPDATES ALL CONTACTS BETWEEN BLOCKS
C
      COMMON/CBLOCK/NED(8),NBLOKM,NBOXES,M1,M2,M3,M4,M5,M6,M7,
     *              NBLOKS,NCYC,MCYCLE,NEMPT,RFLAG,UFLAG,EFLAG,NBCSOO,
     *              IBOXES,JBOXES,BSIZE,XSIZE,YSIZE,GRAVY,NDCSN(100),
     *              NUPDAT,UMBST,THMBST,SCREEN,FORCL,DISPL,NREM,
     *              NBNREM(20),IBPLT,IFPLT,IDPLT,ICSNDA,IBLKDA,
     *              IBOXDA,XYL,THL,RESTFL,XBLD,YBLD,RMBLD,XBLDF,YBLDF,
     *              RMBLDF,LGNEIB,CBNES,IRFPB,ITDPLT,LBLBCK
      LOGICAL RFLAG,UFLAG,EFLAG
      COMMON Q(8000)
      DIMENSION IQ(1)
      EQUIVALENCE(Q,IQ)
      COMMON/INEIG/IN(8),NEIGHB(8,16)
      DIMENSION INEI(102)
      EQUIVALENCE(IN,INEI)
      LOGICAL FIRST
      DO 600 IX=1,NBLOKS
      IN(IX)=0
      DO 610 JX=1,16
      NEIGHB(IX,JX)=0
  610 CONTINUE
  600 CONTINUE
C
C-------------------- SCAN EACH BLOCK --
      DO 500 NB=1,NBLOKS
C
C CHECK IF BLOCK REMOVED
C
      IF(NREM.EQ.0)GO TO 110
      DO 100 K=1,NREM
      IF(NB.EQ.NBNREM(K))GO TO 405
  100 CONTINUE
  110 CONTINUE
      I2=IQ(NB)
      NC=IQ(I2+1)
C-------------------- SCAN EACH EDGE OF BLOCK --
      IEND2=I2+16
      DO 400 NP=1,NC
      FIRST=.TRUE.
      IEND1=IEND2
      IEND2=IEND1+6
      IF(Q(I2+14).EQ.1.0)IEND2=IEND2+4
      IF(Q(I2+15).EQ.1.0)IEND2=IEND2+4
      IF(NP.EQ.NC)IEND2=I2+16
C-------------------- DETERMINE BOXES TO BE SEARCHED --
      X11=GLX(Q(I2),IEND1)
      X22=GLX(Q(I2),IEND2)
      Y11=GLY(Q(I2),IEND1)
      Y22=GLY(Q(I2),IEND2)
      TEMP=AMAX1(X11,X22)
      X1=AMIN1(X11,X22)
      X2=TEMP
      TEMP=AMAX1(Y11,Y22)
      Y1=AMIN1(Y11,Y22)
      Y2=TEMP
      NXL=IFIX((X1-XYL)/BSIZE)+1
      NXU=MIN0(IFIX((X2+XYL)/BSIZE)+1,IBOXES)
      NYL=IFIX((Y1-XYL)/BSIZE)+1
      NYU=MIN0(IFIX((Y2+XYL)/BSIZE)+1,JBOXES)
C-------------------- SEARCH EACH CANDIDATE BOX --
      DO 350 JBOX=NYL,NYU
      NBOX=(JBOX-1)*IBOXES+NXL-1
      DO 300 IBOX=NXL,NXU
      NBOX=NBOX+1
      I4=IQ(M3+NBOX-1)
C-------------------- END OF BOX LIST ? --
  210 CONTINUE
      IF(I4.EQ.0) GOTO 300
C
C CHECK IF BLOCK REMOVED
C
      IF(NREM.EQ.0)GO TO 120
      DO 130 K=1,NREM
      IF(IQ(I4+1).EQ.NBNREM(K))GO TO 215
  130 CONTINUE
  120 CONTINUE
C-------------------- NB, IS THIS BLOCK NB ? --
      IF(IQ(I4+1).NE.NB)GO TO 220
C-------------------- YES --
C-------------------- GET NEXT ENTRY IN THIS BOX --
  215 I4=IQ(I4+2)
      GOTO 210
C-------------------- FIRST TIME THROUGH ? --
  220 IF(.NOT.FIRST) GOTO 230
C-------------------- YES, COMPUTE COS AND SIN FOR THIS EDGE --
      FIRST=.FALSE.
      COSA=(X22-X11)/Q(IEND1+2)
      SINA=(Y22-Y11)/Q(IEND1+2)
C-------------------- COMPUTE CORNER COORDINATES RELATIVE TO EDGE --
  230 I2C=IQ(I4+1)
      I2C=IQ(I2C)
```

```
      IF (Q(I2C+14) .EQ.0.0.AND.Q(I2C+15) .EQ.0.0) GO TO 702
      IF (Q(I2C+14) .EQ.1.0.AND.Q(I2C+15) .EQ.1.0) GO TO 701
      IC=I2C+6+IQ(I4)*10
      GO TO 704
  701 IC=I2C+2+IQ(I4)*14
      GO TO 704
  702 IC=I2C+10+IQ(I4)*6
  704 CONTINUE
      X1C=GLX(Q(I2C),IC)
      Y1C=GLY(Q(I2C),IC)
      YT=(Y1C-Y11)*COSA-(X1C-X11)*SINA
      IF(YT.GT.XYL) GO TO 215
      CBF=-3.0*XYL
      IF(YT.LE.CBF) GO TO 215
      XT=(X1C-X11)*COSA+(Y1C-Y11)*SINA
      CHEKFL=(X22-X11)*COSA+(Y22-Y11)*SINA
      CHEK2=1.E-10+CHEKFL
      IF(XT.GT.CHEK2) GO TO 215
      IF(XT.LT.-1.E-10) GO TO 215
C------------------- CONTACT LIST FOR BLOCK NB ---
      J6=I6+NB-1
      I6=IQ(J6)
C------------------- END OF LIST ? ---
  235 CONTINUE
      IF(I6.EQ.0)  GOTO 250
C------------------- NB. SAME CORNER AND EDGE ? ---
      IF(IQ(I4) .EQ. IQ(I6+2) .AND. IQ(I4+1) .EQ. IQ(I6+3)
     *.AND.NP.EQ.IQ(I6+1)) GO TO 240
C------------------- NB. GET NEXT ENTRY IN CONTACT LIST ---
      J6=I6+4
      I6=IQ(J6)
      GOTO 235
C------------------- CONTACT ALREADY STORED ---
C------------------- UPDATE CONTACT DATA ---
  240 Q(I6+11)=SINA
      Q(I6+12)=COSA
      Q(I6+13)=X1C
      Q(I6+14)=Y1C
      IQ(I6)=1
      LMARK=IQ(I4+1)
      CHEK3=CHEKFL-1.E-10
      IF(XT.LE.1.E-10) GO TO 620
      IF(XT.GE.CHEK3) GO TO 620
      IN(LMARK)=IN(LMARK)+1
      IF(IN(LMARK).GT.16) GO TO 619
      NEIGHB(LMARK,IN(LMARK))=NB
      GO TO 620
  619 WRITE(6,1000) LMARK
 1000 FORMAT(1X,61HGREATER THAN 16 NEIGHBOURING BLOCKS IN NEIGHB ARRAY F
     *OR BLOCK,I5)
  620 CONTINUE
      GOTO 215
C------------------- NEW CONTACT ? ---
  250 CONTINUE
      IF(YT.GT.1.E-10) GO TO 215
C------------------- YES ---
      I6=NEMPT
      IF(IQ(I4).EQ.1) GO TO 710
      ICR=IC-6
      IF(Q(I2C+14).EQ.1.0) ICR=ICR-4
      IF(Q(I2C+15).EQ.1.0) ICR=ICR-4
      GO TO 711
  710 NBARRY=6
      IF(Q(I2C+14).EQ.1.0) NBARRY=NBARRY+4
      IF(Q(I2C+15).EQ.1.0) NBARRY=NBARRY+4
      ICR=IC+NBARRY*(IQ(I2C+1)-1)
  711 CONTINUE
      YTR=(GLY(Q(I2C),ICR)-Y11)*COSA-(GLX(Q(I2C),ICR)-X11)*SINA
      CBFF=-2.0*XYL
      IF(YTR.LE.CBFF) GO TO 215
      IF(IQ(I4).EQ.IQ(I2C+1)) GO TO 712
      ICL=IC+6
      IF(Q(I2C+14).EQ.1.0) ICL=ICL+4
      IF(Q(I2C+15).EQ.1.0) ICL=ICL+4
      GO TO 713
  712 ICL=I2C+16
  713 CONTINUE
      YTL=(GLY(Q(I2C),ICL)-Y11)*COSA-(GLX(Q(I2C),ICL)-X11)*SINA
      IF(YTL.LE.CBFF) GO TO 215
C------------------- ANY SPACE AVAILABLE IN EMPTY LIST ? ---
      IF(IQ(NEMPT+4).NE.0) GO TO 260
      WRITE(6,3001)
 3001 FORMAT(30X,32H NO MORE MEMORY FOR CONTACT LIST)
      CALL FINISH
C------------------- NEW CONTACT ---
  260 Q(I6+5)=0.0
      Q(I6+6)=0.0
      Q(I6+7)=0.0
      Q(I6+8)=0.0
      Q(I6+9)=0.0
      Q(I6+10)=0.0
      IQ(I6+1)=NP
      IQ(I6+2)=IQ(I4)
      IQ(I6+3)=IQ(I4+1)
      NEMPT=IQ(I6+4)
      IQ(J6)=I6
      IQ(I6+4)=0
      GO TO 240
C------------------- END OF BOX SCAN ---
  300 CONTINUE
  350 CONTINUE
C------------------- END OF EDGE SCAN ---
  400 CONTINUE
  405 CONTINUE
C------------------- SCAN CONTACT LIST FOR PRESERVE FLAGS ---
      J6=I6+NB-1
      I6=IQ(J6)
C------------------- END OF LIST ? ---
  410 IF(I6.EQ.0)  GOTO 490
C------------------- NB ---
C------------------- IS THE PRESERVE FLAG SET ? ---
      IF(IQ(I6).EQ.0) GO TO 420
C------------------- YES ---
      IQ(I6)=0
      J6=I6+4
      GOTO 430
C------------------- NB ---
  420 IQ(J6)=IQ(I6+4)
      IQ(I6+4)=NEMPT
      NEMPT=I6
C------------------- GET NEXT CONTACT ---
  430 I6=IQ(J6)
      GOTO 410
C------------------- END OF BLOCK SCAN ---
  490 CONTINUE
  500 CONTINUE
C
      NUPDAT=NUPDAT+1
```

```
      UFLAG=.FALSE.
      RETURN
      END
C
C
      SUBROUTINE REBOX(NB)
C
      COMMON Q(6000)
      DIMENSION IQ(1)
      EQUIVALENCE (Q,IQ)
      COMMON/CBLOCK/NED(8),NBLOKM,NBOXES,M1,M2,M3,M4,M5,M6,M7,
     *                NBLOKS,NCYC,MCYCLE,NEMPT,RFLAG,UFLAG,EFLAG,NBC800,
     *                IBOXES,JBOXES,BSIZE,XSIZE,YSIZE,GRAVY,NDC8N(100),
     *                NUPDAT,UMBST,THMBST,SCREEN,FORCL,DISPL,NREM,
     *                NBNREM(20),IBPLT,IFPLT,IDPLT,IC8NDA,IBLKDA,
     *                IB8XDA,XYL,THL,RESTFL,XBLD,YBLD,RMBLD,XBLDF,YBLDF,
     *                RMBLDF,LGNEIB,C8NES,IRFP8,ITDPLT,LBLOCK
      LOGICAL RFLAG,UFLAG,EFLAG
C SUBROUTINE TO REBOX A SINGLE BLOCK"S CORNERS
      IB=IQ(NB)
      NC=IQ(IB+1)
C SCAN EACH CORNER OF THE BLOCK
      IC=IB+16
      DO 100 NP=1,NC
C ARE WE AT EDGE OF DOMAIN
      IF(GLX(Q(IB),IC).GT.0.0.AND.GLX(Q(IB),IC).LT.XSIZE.AND.
     *  GLY(Q(IB),IC).GT.0.0.AND.GLY(Q(IB),IC).LT.YSIZE)GO TO 20
C YES,WE ARE AT EDGE OF DOMAIN.WRITE OUT ERROR MESSAGE
      WRITE(6,2000)NP,NB
 2000 FORMAT(1X,7H CORNER,I4,9H OF BLOCK,I4,21H IS AT EDGE OF DOMAIN)
C SET FIX FLAG
      IQ(IB)=1
      Q(IB+7)=0.0
      Q(IB+8)=0.0
      Q(IB+9)=0.0
      GO TO 900
C NO,NOT AT EDGE OF DOMAIN.DETERMINE WHICH BOX CORNER SHOULD BE IN
   20 NBOX=IFIX(GLX(Q(IB),IC)/BSIZE)+IFIX(GLY(Q(IB),IC)/BSIZE)*IBOXES+1
C SEARCH THIS BOX
      J4N=M3+NBOX-1
   30 I4N=IQ(J4N)
      IF(I4N.EQ.0)GO TO 40
      IF(NB.EQ.IQ(I4N+1).AND.NP.EQ.IQ(I4N))GO TO 200
      J4N=I4N+2
      GO TO 30
C SEARCH THE SURROUNDING BOXES
   40 NXL=MAXO(NBOX-1,IBOXES),1)
      NXU=MINO(NXL+2,IBOXES)
      NYL=MAXO((NBOX-1)/IBOXES,1)
      NYU=MINO(NYL+2,JBOXES)
      DO 60 JBOX=NYL,NYU
      NBOX=(JBOX-1)*IBOXES+NXL-1
      DO 70 IBOX=NXL,NXU
      NBOX=NBOX+1
      IF(NBOX.EQ.NBOX) GOTO 70
      J4N=M3+NBOX-1
   50 I4N=IQ(J4N)
      IF(I4N.EQ.0)GO TO 70
      IF(NB.EQ.IQ(I4N+1).AND.NP.EQ.IQ(I4N))GO TO 60
      J4N=I4N+2
      GO TO 50
C SWAP ENTRIES FOR THIS CORNER
   60 IQ(J4N)=IQ(I4N+2)
      IQ(J4N)=I4N
      IQ(I4N+2)=0
      GO TO 200
C END OF SURROUNDING BOXES SCAN
   70 CONTINUE
   80 CONTINUE
      WRITE(6,3000)NP,NB
 3000 FORMAT(1X,24H ERROR IN REBOX . CORNER,I3,
     *       9H OF BLOCK,I4,20H NOT IN ADJACENT BOX)
C END OF CORNERS SCAN
  200 IC=IC+6
      IF(Q(IB+14).EQ.1.0)IC=IC+4
      IF(Q(IB+15).EQ.1.0)IC=IC+4
  100 CONTINUE
C EXIT
  900 RFLAG=.FALSE.
      RETURN
      END
      SUBROUTINE DUMP(IDF)
C
C ROUTINE TO PRINT OUT INFORMATION IN MEMORY
C
      COMMON/CBLOCK/NED(8),NBLOKM,NBOXES,M1,M2,M3,M4,M5,M6,M7,
     *                NBLOKS,NCYC,MCYCLE,NEMPT,RFLAG,UFLAG,EFLAG,NBC800,
     *                IBOXES,JBOXES,BSIZE,XSIZE,YSIZE,GRAVY,NDC8N(100),
     *                NUPDAT,UMBST,THMBST,SCREEN,FORCL,DISPL,NREM,
     *                NBNREM(20),IBPLT,IFPLT,IDPLT,IC8NDA,IBLKDA,
     *                IB8XDA,XYL,THL,RESTFL,XBLD,YBLD,RMBLD,XBLDF,YBLDF,
     *                RMBLDF,LGNEIB,C8NES,IRFP8,ITDPLT,LBLOCK
      LOGICAL RFLAG,UFLAG,EFLAG
      COMMON Q(6000)
      DIMENSION IQ(1)
      EQUIVALENCE (Q,IQ)
      IF(IDF.EQ.1)GO TO 10
      IF(IDF.EQ.2)GO TO 20
      IF(IDF.EQ.3)GO TO 30
      WRITE(6,3000)
 3000 FORMAT(1X, 27H*****ERROR IN DUMP CALL *****)
      RETURN
C CONTACT DATA
   10 WRITE(6,2008)MCYCLE
 2008 FORMAT(1X,28H CURRENT CYCLE NUMBER IS =,I4)
      WRITE(6,2007)
 2007 FORMAT(1X,13H CONTACT DATA:10(1H-)/8X,3HNBE,7X,3HPRE,7X,3HNPE,7X,
     *       3HNPC,7X,3HNBC,6X,4HLINK/10X,3HFYE,9X,3HFXE,8X,3HFYC,8X,
     *       3HFXC,8X,2HFN,8X,2HSN,7X,3HSIN,7X,3HC8S,7X,3HXCP,7X,3HYCP)
      DO 650 NBN=1,NBLOKS
C
C CHECK IF BLOCK REMOVED
C
      IF(NREM.EQ.0)GO TO 651
      DO 652 K=1,NREM
      IF(NBN.EQ.NBNREM(K))GO TO 650
  652 CONTINUE
  651 CONTINUE
      IF(NBC800.EQ.0)GO TO 653
C
C BLOCK NUMBERS FOR WHICH CONTACT DATA TO BE PRINTED OUT
C CONTAINED IN ARRAY NDC8N
C
      DO 654 K=1,NBC800
      IF(NBN.EQ.NDC8N(K))GO TO 653
  654 CONTINUE
      GO TO 650
  653 CONTINUE
```

```
      JB=MB+NBN-1
  700 IB=IQ(JB)
      IF(IB.EQ.0)GO TO 650
      I64=I6+4
      I65=I6+5
      I614=I6+14
      WRITE(6,2004)NBN,(IQ(I),I=I6,I64),
     *(Q(I),I=I65,I614)
 2004 FORMAT(/1X,6I10/1X,10E10.4)
      JB=I6+4
      GO TO 700
  650 CONTINUE
      WRITE(6,2000)
 2000 FORMAT(1X,130(1H-))
      RETURN
C BLOCK DATA
   20 WRITE(6,2006)NBLOKS,NCYC,MCYCLE
 2006 FORMAT(1X,  6HNBLOKS,6X,4HNCYC,5X,6HMCYCLE/1X,I4,2I10)
      WRITE(6,2003)
 2003 FORMAT(1X,11H BLOCK DATA,10(1H-)/1X,9H NB IF NC,6X,2HXC,6X,2HYC,
     *       5X,5HTHETA,6X,4HCOST,6X,4HSINT,6X,2HDX,
     *       6X,2HDY,6X,4HDTHE,4X,4HRAS5,3X,5HTBTLX/
     *       15X,5HTBTLY,5X,5HTBTLM,6X,5HBFLAG,6X,5HIFLAG)
      DO 930 NB=1,NBLOKS
C
C CHECK IF BLOCK REMOVED
C
      IF(NREM.EQ.0)GO TO 931
      DO 932 K=1,NREM
      IF(NB.EQ.NBNREM(K))GO TO 930
  932 CONTINUE
  931 CONTINUE
      IF=IQ(IB)
      IF(Q(IF+14).EQ.0.0.AND.Q(IF+15).EQ.0.0)GO TO 952
      IF(Q(IF+14).EQ.1.0.AND.Q(IF+15).EQ.1.0)GO TO 951
      IL=IF+15+10*IQ(IF+1)
      GO TO 954
  951 IL=IF+15+14*IQ(IF+1)
      GO TO 954
  952 IL=IF+15+6*IQ(IF+1)
  954 CONTINUE
      IF2=IF+2
      WRITE(6,2005)NB,IQ(IF),IQ(IF+1),(Q(I),I=IF2,IL)
 2005 FORMAT(/1X,3I3,1P10E10.2/(10X,1P11E10.2))
  930 CONTINUE
      RETURN
C BBX DATA
   30 WRITE(6,2002)
 2002 FORMAT(10X,3HBBX,7X,5HBLOCK,6X,6HCORNER)
      DO 120 NBBX =1,NBBXES
      I3=IQ(M3+NBBX-1)
  110 IF(I3.EQ.0)GO TO 120
      WRITE(6,2009)NBBX,IQ(I3+1),IQ(I3)
 2009 FORMAT(1X,3I12)
      I3=IQ(I3+2)
      GO TO 110
  120 CONTINUE
      RETURN
      END
      SUBROUTINE HSTIFF
C
C SUBROUTINE TO CALCULATE DISPLACEMENTS ON BOUNDARY BLOCKS CARRYING EXTERNAL
C LOADS DUE TO EXTERNAL HALF-SPRINGS OF DOUBLE STIFFNESS
C
      COMMON/CBLOCK/HED(8),NBLOKM,NBBXES,M1,M2,M3,M4,M5,M6,M7,
     *              NBLOKS,NCYC,MCYCLE,NEMPT,RFLAG,UFLAG,EFLAG,NBC900,
     *              IBBXES,JBBXES,BSIZE,XSIZE,YSIZE,GRAVY,NDCOM(100),
     *              NUPDAT,UMBST,THMBST,SCREEN,FORCL,DISPL,NREM,
     *              NBNREM(20),IBPLT,IFPLT,IDPLT,ICOMDA,IBLKDA,
     *              IBBXDA,XYL,THL,RESTFL,XBLO,YBLO,RMBLO,XBLOF,YBLOF,
     *              RMBLOF,LGNEIB,COMES,IRFPO,ITDPLT,LBLOCK
      LOGICAL RFLAG,UFLAG,EFLAG
      COMMON Q(6000)
      DIMENSION IQ(1)
      EQUIVALENCE(Q,IQ)
      WRITE(6,1000)
 1000 FORMAT(20X,43H TABLE OF X AND Z EXTERNAL FORCE COMPONENTS,
     *      /,19X,44(1H-),/)
      WRITE(6,1001)
 1001 FORMAT(2X,2HNB,2X,2HNP,5X,3HFXL,9X,3HFZL,9X,3HFXU,9X,3HFZU,
     *       6X,6HDSTIFN,6X,6HDSTIFS,/)
      DO 100 NB=1,NBLOKS
      IB=IQ(NB)
C----------IS BLOCK FIXED----------
      IF(IQ(IB).NE.0)GO TO 100
C----------NO-BLOCK NOT FIXED----------
      IF Q(IB+14).NE.0.)GO TO 120
  110 IF(Q(IB+15).NE.0.)GO TO 130
      GO TO 100
C DISPLACEMENTS OF BOUNDARY BLOCKS UNDER EXTERNAL LOADS
  120 CONTINUE
      NC=IQ(IB+1)
      IC=IB+16
      DO 150 NP=1,NC
      IF(Q(IC+6).EQ.0..AND.Q(IC+8).EQ.0.)GO TO 140
C EXTERNAL FORCES PRESENT ALONG EDGE NP OF BLOCK NB
      FXL=Q(IC+6)*COS(Q(IC+7))
      FZL=Q(IC+6)*SIN(Q(IC+7))
      FXU=Q(IC+8)*COS(Q(IC+9))
      FZU=Q(IC+8)*SIN(Q(IC+9))
      DSTIFN=2.0*Q(IC+4)
      DSTIFS=2.0*Q(IC+5)
      WRITE(6,1002)NB,NP,FXL,FZL,FXU,FZU,DSTIFN,DSTIFS
 1002 FORMAT(1X,I3,I4,6E12.4)
  140 IC=IC+10
      IF(Q(IB+15).NE.0.)IC=IC+4
  150 CONTINUE
      GO TO 110
C CODE TO BE WRITTEN FOR DISPLACEMENTS DUE TO INTERNAL LOADS
  130 CONTINUE
  100 CONTINUE
      RETURN
      END
C
C
      FUNCTION GLX(B,IC)
C
C  LOCAL - GLOBAL X-COORDINATE TRANSFORMATION
C
      COMMON Q(6000)
      DIMENSION IQ(1)
      EQUIVALENCE(Q,IQ)
      DIMENSION B(1)
C
       GLX=B(3)+Q(IC)*B(5)-Q(IC+1)*B(7)
      RETURN
      END
C
```

```
C
      FUNCTION GLY(B,IC)
C
C  LOCAL - GLOBAL Y-COORDINATE TRANSFORMATION
C
      COMMON Q(6000)
      DIMENSION IQ(1)
      EQUIVALENCE(Q,IQ)
      DIMENSION B(1)
C
      GLY=B(4)+Q(IC)*B(7)+Q(IC+1)*B(8)
      RETURN
      END
      SUBROUTINE PTIME (JA)
C     SIMULTANEOUS TIMING OF UP TO LSEC SEGMENTS OF CODE
      COMMON/CLOCK/SEC(30),ISEC(30)
      DATA LSEC/30/
C     INITIALISATION
      CALL PZERO (SEC,LSEC)
      CALL PZERI (ISEC,LSEC)
      RETURN
      ENTRY PTICK
C     START CLOCK JA
      CALL SECOND (ELT)
      SEC(JA)=SEC(JA)-ELT
      RETURN
      ENTRY PTOCK
C     STOP CLOCK JA
      CALL SECOND (ELT)
      SEC(JA)=SEC(JA)+ELT
      ENTRY PCALL
C     COUNT HOW MANY TIMES SEGMENT JA IS EXECUTED
      ISEC(JA)=ISEC(JA)+1
      RETURN
      END
      SUBROUTINE PZERI(KA,JA)
C ZEROISES JA ELEMENTS OF KA
      DIMENSION KA(1)
      DO 1 IA=1,JA
      KA(IA)=0
 1    CONTINUE
      RETURN
      END
      SUBROUTINE PZERO(XA,JA)
C ZEROISES JA ELEMENTS OF XA
      DIMENSION XA(1)
      DO 1 IA=1,JA
      XA(IA)=0.0
 1    CONTINUE
      RETURN
      END
      SUBROUTINE BLPLOT
C ROUTINE FOR PLOTTING THE BLOCK GEOMETRY
      COMMON/CBLOCK/HED(8),NBLOKM,NBOXES,M1,M2,M3,M4,M5,M6,M7,
     *              NBLOKS,NCYC,MCYCLE,NEMPT,RFLAG,UFLAG,EFLAG,NBCOD,
     *              IBOXES,JBOXES,BSIZE,XSIZE,YSIZE,GRAVY,NDCOM(100),
     *              NUPDAT,UMBST,THMBST,SCREEN,FORCL,DISPL,NREM,
     *              NBNREM(20),IBPLT,IFPLT,IDPLT,ICBNDA,IBLKDA,
     *              IBOXDA,XYL,THL,RESTFL,XBLD,YBLD,RMBLD,XBLDF,YBLDF,
     *              RMBLDF,LGNEIB,CONES,IRFPB,ITDPLT,LBLOCK
      LOGICAL RFLAG,UFLAG,EFLAG
      COMMON Q(6000)
      DIMENSION IQ(1)
      EQUIVALENCE(Q,IQ)
      FACT=SCREEN/AMAX1(XSIZE,YSIZE)
      FACTIV=1./FACT
      CALL TITLES(1,FACTIV)
      DO 100 NB=1,NBLOKS
C
C CHECK IF BLOCK REMOVED
C
      IF(NREM.EQ.0)GO TO 200
      DO 210 K=1,NREM
      IF(NB.EQ.NBNREM(K))GO TO 100
 210  CONTINUE
 200  CONTINUE
      I2=IQ(NB)
      NC=IQ(I2+1)
      XC=FACT*Q(I2+2)
      YC=FACT*Q(I2+3)
C IS BLOCK FIXED
      IF(IQ(I2).EQ.0)GO TO 20
      CALL SYMBOL(XC,YC,0.2,1HF,0.0,1)
C
C BLOCK NOT FIXED
 20   IC=I2+16
      X=FACT*GLX(Q(I2),IC)
      Y=FACT*GLY(Q(I2),IC)
      CALL PLOT(X,Y,3)
      DO 50 NP=2,NC
      IC=IC+6
      IF(Q(I2+14).EQ.1.0)IC=IC+4
      IF(Q(I2+15).EQ.1.0)IC=IC+4
      X=FACT*GLX(Q(I2),IC)
      Y=FACT*GLY(Q(I2),IC)
      CALL PLOT(X,Y,2)
 50   CONTINUE
      X=FACT*GLX(Q(I2),I2+16)
      Y=FACT*GLY(Q(I2),I2+16)
      CALL PLOT(X,Y,2)
 100  CONTINUE
      CALL PLOT(X,Y,3)
      CALL PLOT(0.0,0.0,3)
      CALL NEWPAGE
      RETURN
      END
      SUBROUTINE FORPLT
C
C ROUTINE FOR PLOTTING INTER-BLOCK CONTACT FORCES
C
      COMMON/CBLOCK/HED(8),NBLOKM,NBOXES,M1,M2,M3,M4,M5,M6,M7,
     *              NBLOKS,NCYC,MCYCLE,NEMPT,RFLAG,UFLAG,EFLAG,NBCOD,
     *              IBOXES,JBOXES,BSIZE,XSIZE,YSIZE,GRAVY,NDCOM(100),
     *              NUPDAT,UMBST,THMBST,SCREEN,FORCL,DISPL,NREM,
     *              NBNREM(20),IBPLT,IFPLT,IDPLT,ICBNDA,IBLKDA,
     *              IBOXDA,XYL,THL,RESTFL,XBLD,YBLD,RMBLD,XBLDF,YBLDF,
     *              RMBLDF,LGNEIB,CONES,IRFPB,ITDPLT,LBLOCK
      LOGICAL RFLAG,UFLAG,EFLAG
      COMMON Q(6000)
      DIMENSION IQ(1)
      EQUIVALENCE(Q,IQ)
      FB=0.
      DO 100 NB=1,NBLOKS
C
C CHECK IF BLOCK REMOVED
C
      IF(NREM.EQ.0)GO TO 110
      DO 120 K=1,NREM
```

```
      IF (NB.EQ.NBNREM(K)) GO TO 100
  120 CONTINUE
  110 CONTINUE
      J6=I6+NB-1
  400 I6=IQ(J6)
      IF (I6.EQ.0) GO TO 100
      FN=SQRT(Q(I6+5)**2+Q(I6+6)**2)
      IF (FN.LE.F6) GO TO 200
      F6=FN
  200 J6=I6+4
      GO TO 400
  100 CONTINUE
C F6 IS MAXIMUM RESULTANT FORCE
      IF (F6.EQ.0.0) F6=1.E-05
      FG=FORCL/F6
      GG=1./FG
      FACT=SCREEN/AMAX1(XSIZE,YSIZE)
      CALL TITLES(2,GG)
      DO 500 NB=1,NBLOKS
C
C CHECK IF BLOCK REMOVED
C
      IF (NREM.EQ.0) GO TO 130
      DO 140 K=1,NREM
      IF (NB.EQ.NBNREM(K)) GO TO 500
  140 CONTINUE
  130 CONTINUE
      J6=I6+NB-1
  700 I6=IQ(J6)
      IF (I6.EQ.0) GO TO 500
      X=Q(I6+13)*FACT
      Y=Q(I6+14)*FACT
      FX=Q(I6+6)*FG
      FY=Q(I6+5)*FG
      CALL PLOT(X,Y,3)
      X=X+FX
      Y=Y+FY
      CALL PLOT(X,Y,2)
      J6=I6+4
      GO TO 700
  500 CONTINUE
      CALL NEWPAGE
      RETURN
      END
      SUBROUTINE DISPLT
C
C ROUTINE FOR PLOTTING INCREMENTAL BLOCK DISPLACEMENTS
C
      COMMON/COLOCK/HED(8),NBLOKM,NBOXES,M1,M2,M3,M4,M5,M6,M7,
     *                 NBLOKS,NCYC,MCYCLE,NEMPT,RFLAG,UFLAG,EFLAG,NBCOOD,
     *                 IBOXES,JBOXES,BSIZE,XSIZE,YSIZE,GRAVY,NDOFN(100),
     *                 NUPDAT,UMAST,THMAST,SCREEN,FORCL,DISPL,NREM,
     *                 NBNREM(20),IBPLT,IFPLT,IDPLT,ICONDA,IBLKDA,
     *                 IBOXDA,XYL,THL,RESTFL,XBLD,YBLD,RMBLD,XBLDF,YBLDF,
     *                 RMBLDF,LGNEIB,CONES,IRFPB,ITDPLT,LBLOCK
      LOGICAL RFLAG,UFLAG,EFLAG
      COMMON Q(6000)
      DIMENSION IQ(1)
      EQUIVALENCE(Q,IQ)
      D6=0.
      DO 100 NB=1,NBLOKS
C
C CHECK IF BLOCK REMOVED
C
      IF (NREM.EQ.0) GO TO 110
      DO 120 K=1,NREM
      IF (NB.EQ.NBNREM(K)) GO TO 100
  120 CONTINUE
  110 CONTINUE
      I2=IQ(NB)
      DN=SQRT(Q(I2+7)**2+Q(I2+8)**2)
      IF (DN.LE.D6) GO TO 100
      D6=DN
  100 CONTINUE
      IF (D6.EQ.0.0) D6=1.E-05
      DG=DISPL/D6
      GG=1./DG
      FACT=SCREEN/AMAX1(XSIZE,YSIZE)
      CALL TITLES(3,GG)
      DO 200  NB=1,NBLOKS
C
C CHECK IF BLOCK REMOVED
C
      IF (NREM.EQ.0) GO TO 130
      DO 140 K=1,NREM
      IF (NB.EQ.NBNREM(K)) GO TO 200
  140 CONTINUE
  130 CONTINUE
      I2=IQ(NB)
      X=Q(I2+2)*FACT
      Y=Q(I2+3)*FACT
      DX=Q(I2+7)*DG
      DY=Q(I2+8)*DG
      CALL VECTOR(X,Y,DX,DY)
  200 CONTINUE
      CALL NEWPAGE
      RETURN
      END
      SUBROUTINE TDISPL
C
C ROUTINE FOR PLOTTING TOTAL BLOCK DISPLACEMENTS
C
      COMMON/COLOCK/HED(8),NBLOKM,NBOXES,M1,M2,M3,M4,M5,M6,M7,
     *                 NBLOKS,NCYC,MCYCLE,NEMPT,RFLAG,UFLAG,EFLAG,NBCOOD,
     *                 IBOXES,JBOXES,BSIZE,XSIZE,YSIZE,GRAVY,NDOFN(100),
     *                 NUPDAT,UMAST,THMAST,SCREEN,FORCL,DISPL,NREM,
     *                 NBNREM(20),IBPLT,IFPLT,IDPLT,ICONDA,IBLKDA,
     *                 IBOXDA,XYL,THL,RESTFL,XBLD,YBLD,RMBLD,XBLDF,YBLDF,
     *                 RMBLDF,LGNEIB,CONES,IRFPB,ITDPLT,LBLOCK
      LOGICAL RFLAG,UFLAG,EFLAG
      COMMON Q(6000)
      DIMENSION IQ(1)
      EQUIVALENCE(Q,IQ)
      DT=0.0
      DO 100 NB=1,NBLOKS
C
C CHECK IF BLOCK REMOVED
C
      IF (NREM.EQ.0) GO TO 110
      DO 120 K=1,NREM
      IF (NB.EQ.NBNREM(K)) GO TO 100
  120 CONTINUE
  110 CONTINUE
      I2=IQ(NB)
      DN=SQRT(Q(I2+11)**2+Q(I2+12)**2)
      IF (DN.LE.DT) GO TO 100
      DT=DN
  100 CONTINUE
```

```
      IF (DT.EQ.0.0) DT=1.E-05
      DG=DISPL/DT
      GG=1./DG
      FACT=SCREEN/AMAX1 (XSIZE,YSIZE)
      CALL TITLES (4,GG)
      DO 200 NB=1,NBLOKS
C
C CHECK IF BLOCK REMOVED
C
      IF (NREM.EQ.0) GO TO 130
      DO 140 K=1,NREM
      IF (NB.EQ.NBNREM(K)) GO TO 200
  140 CONTINUE
  130 CONTINUE
      I2=IO(NB)
      X=Q(I2+2)*FACT
      Y=Q(I2+3)*FACT
      DX=Q(I2+11)*DG
      DY=Q(I2+12)*DG
      CALL VECTOR(X,Y,DX,DY)
  200 CONTINUE
      CALL NEWPAGE
      RETURN
      END
      SUBROUTINE VECTOR(X,Y,DX,DY)
C
      PI=4.0*ATAN(1.0)
      CALL PLOT(X,Y,3)
      X=X+DX
      Y=Y+DY
      CALL PLOT(X,Y,2)
      DT=(SQRT((DX**2+DY**2))/5.
      GM=ABS(DX)
      IF (GM.LE.1.E-5) DX=1.E-5
      ABA=ATAN2(DY,DX)
      IF (ABA.LT.0.) ABA=2.*PI+ABA
      ABA1=PI+ABA-.25
      ABA2=ABA1+.5
      XA=X+DT*(COS(ABA1))
      YA=Y+DT*(SIN(ABA1))
      CALL PLOT(XA,YA,2)
      CALL PLOT(X,Y,3)
      XA=X+DT*(COS(ABA2))
      YA=Y+DT*(SIN(ABA2))
      CALL PLOT(XA,YA,2)
      RETURN
      END
      SUBROUTINE TITLES(IPLOT,DIS)
      COMMON/COLOCK/HED(8),NBLOKM,NBOXES,M1,M2,M3,M4,M5,M6,M7,
     *                 NBLOKS,NCYC,NCYCLE,NEMPT,RFLAG,UFLAG,EFLAG,NBCOO,
     *                 IBOXES,JBOXES,BSIZE,XSIZE,YSIZE,GRAVY,NOCON(100),
     *                 NUPDAT,UMOST,THMOST,SCREEN,FORCL,DISPL,NREM,
     *                 NBNREM(20),IBPLT,IFPLT,IDPLT,ICONDA,IBLKDA,
     *                 IBOXDA,XYL,THL,RESTFL,XBLD,YBLD,RHBLD,XBLDF,YBLDF,
     *                 RHBLDF,LONEIB,CONES,IRFPB,ITDPLT,LBLOCK
      LOGICAL RFLAG,UFLAG,EFLAG
      CALL SYMBOL(0.5,14.0,0.21,HED,0.,80)
      GO TO (100,200,250,260) IPLOT
  100 CONTINUE
C THIS IS A BLOCK GEOMETRY PLOT
      CALL SYMBOL(0.5,13.25,0.21,10HBLOCK PLOT,0.,10)
      GO TO 300
  200 CONTINUE
C THIS IS A EDGE-CORNER CONTACT FORCE PLOT
      CALL SYMBOL(0.5,13.25,0.21,17HCORNER FORCE PLOT,0.,17)
      GO TO 400
  250 CONTINUE
C THIS IS A INCREMENTAL DISPLACEMENT PLOT
      CALL SYMBOL(0.5,13.25,0.21,17HINCREM.DISPL.PLOT,0.,17)
      GO TO 400
  260 CONTINUE
C THIS IS A TOTAL DISPLACEMENT PLOT
      CALL SYMBOL(0.5,13.25,0.21,16HTOTAL DISPL.PLOT,0.,16)
      GO TO 400
  300 CONTINUE
      CALL SYMBOL(5.0,13.25,0.21,34HNUMBER OF PROBLEM UNITS PER INCH =,
     *  0.,34)
      CALL NUMBER(12.4,13.25,0.21,DIS,0.,2)
      GO TO 500
  400 CONTINUE
      CALL SYMBOL(5.0,13.25,0.21,34HNUMBER OF PROBLEM UNITS PER INCH =,
     *            0.,34)
      CALL NUMBER(12.4,13.25,0.21,DIS,0.,8)
  500 FL=NCYCLE
      CALL SYMBOL(0.5,12.5,0.21,18HITERATION NUMBER =,0.,18)
      CALL NUMBER(4.5,12.5,0.21,FL,0.,-1)
      CALL SYMBOL(7.5,12.5,0.21,16HSCALE . 1 INCH =,0.,16)
      CALL PLOT(11.0,12.5,3)
       CALL PLOT(12.0,12.5,2)
      RETURN
      END
      SUBROUTINE PL(IPCON)
      GO TO (10,20) IPCON
   10 CALL START(2)
      CALL PEN(1)
      RETURN
   20 CALL ENPLOT
      RETURN
      END
      SUBROUTINE FINISH
      COMMON/COLOCK/HED(8),NBLOKM,NBOXES,M1,M2,M3,M4,M5,M6,M7,
     *                 NBLOKS,NCYC,NCYCLE,NEMPT,RFLAG,UFLAG,EFLAG,NBCOO,
     *                 IBOXES,JBOXES,BSIZE,XSIZE,YSIZE,GRAVY,NOCON(100),
     *                 NUPDAT,UMOST,THMOST,SCREEN,FORCL,DISPL,NREM,
     *                 NBNREM(20),IBPLT,IFPLT,IDPLT,ICONDA,IBLKDA,
     *                 IBOXDA,XYL,THL,RESTFL,XBLD,YBLD,RHBLD,XBLDF,YBLDF,
     *                 RHBLDF,LONEIB,CONES,IRFPB,ITDPLT,LBLOCK
      LOGICAL RFLAG,UFLAG,EFLAG
      COMMON Q(6000)
      DIMENSION IQ(1)
      EQUIVALENCE (Q,IQ)
      COMMON/INEIQ/IN(8),NEIGHB(8,16)
      DIMENSION INEI(102)
      EQUIVALENCE (IN,INEI)
      COMMON/CLOCK/SEC(30),ISEC(30)
C
      CALL BLPLOT
      CALL FORPLT
      CALL DISPLT
      CALL TDISPL
       WRITE(6,1000) SEC(1),SEC(2),SEC(3),ISEC(1),ISEC(2),ISEC(3)
 1000 FORMAT(1X,17H TIME IN UPDATE =,F10.5/
     *       1X,17H TIME IN MOTION =,F10.5/
     *       1X,16H TIME IN REBOX =,F10.5/
     *       1X,16H CALLS TO UPDATE =,I10/
     *       1X,16H CALLS TO MOTION =,I10/
     *       1X,17H CALLS TO REBOX =,I10)
      IPCON=2
```

```
      CALL PL(IPC8M)
      WRITE(6,1001)MCYCLE,NUPDAT
 1001 FORMAT(30X,15H TOTAL CYCLES =,I10/
     X       30X,17H NO. OF UPDATES =,I10)
C
C WRITE RESTART FILE IF NO ERRORS
C
      IF(EFLAG)GO TO 100
      REWIND 2
      WRITE(2)(HED(I),I=1,L8LBCK)
      WRITE(2)(IMEI(I),I=1,LONEIB)
      WRITE(2)(Q(I),I=1,M7)
      WRITE(6,1002)
 1002 FORMAT(30X,43H A RESTART FILE HAS BEEN WRITTEN ONTO TAPE2)
  100 CONTINUE
      STOP
      END
```

B. PROGRAM BLOCK - modified static relaxation program for large problems.

1) The program is the algorithm for the modified static relaxation formulation described in Chapter 4. The solution procedure is identical to that used in the baseline formulation but the program is designed for the handling of large amounts of data.

2) The memory allocation and data structures were different from those in the baseline formulation, the structure of the modified contact data array being shown in Figure A.9. Figures A.10 and A.11 show the layout of the memory in arrays Q and AO.

3) The input data format was the same as for the baseline program with two data sets being required. Additional keywords incorporated in data set 2 were as follows:

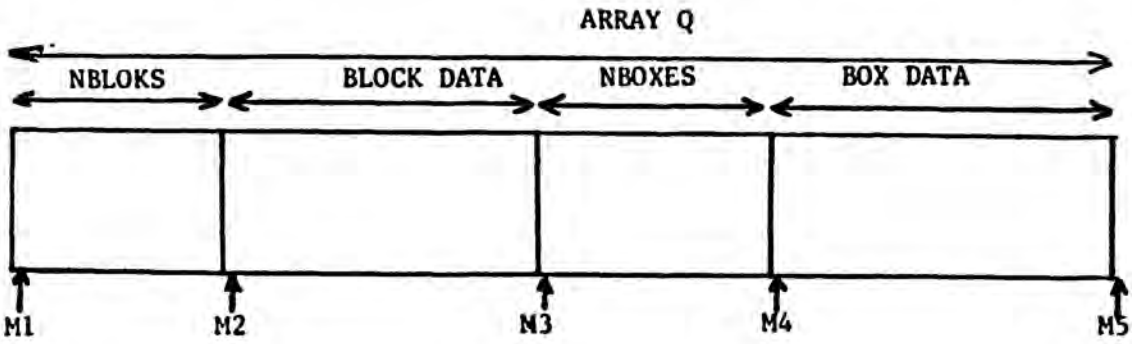
| FLAG | NPE | NPC | NBC | FYE | FXE | FYC | FXC | FN | SN | SIN | COS | XCP | YCP | FLAG |
|---|---|---|---|---|---|---|---|---|---|---|---|---|---|---|

CODE

NPE - edge no. of contact
NPC) corner and block numbers
NBC) of corner in contact
FYE) global X and Y forces acting
FXE) on edge

FYC) - global X and Y forces
FXC) acting on corner
FN) - normal and shear force
SN)
SIN) - sine and cosine of edge
COS)
XCP) - global co-ordinates of contact point
YCP)

Figure A.9: Layout of information stored in block of array AO.




CODE

NBLOKS - no. of blocks

NBOXES - no. of boxes

M1,M2...M5 - memory pointers

Figure A.10: Layout of memory in array Q

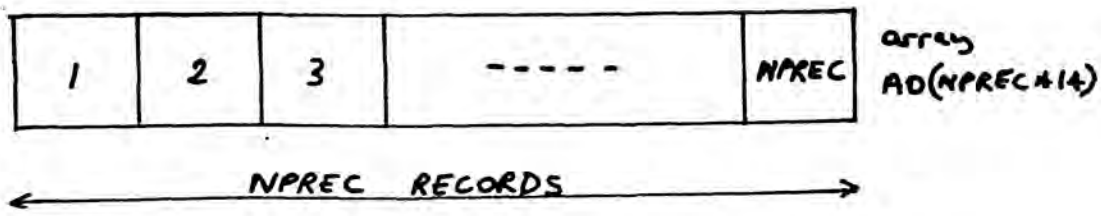



Figure A.11: Layout of memory in array AO.

Keyword RSTF:

Card 2 : (2I10.2E10.4) assign normal and shear stiffness to edge NE of block NB

| | | |
|---|---|---|
| Cols 1-10 | NB | block number |
| Cols 11-20 | NE | edge number |
| Cols 21-30 | STFN | normal stiffness |
| Cols 31-40 | STFS | shear stiffness |

Keyword RFRI:

Card 2 : (2I10,F10.0) assign friction coefficient to edge NE of block NB

| | | |
|---|---|---|
| Cols 1-10 | NB | block number |
| Cols 11-20 | NE | edge number |
| Cols 21-30 | FRIC | friction coefficient |

4) The additional variables specified via Fortran DATA statements are (see Section 4.2):

| VARIABLE | VALUE | DESCRIPTION |
|---|---|---|
| NBL | 100 | blocking factor |
| LBL | 14 | length of block |
| LUMO | 3 | logical unit numbers for scratch files |
| LUNO | 4 | |
| NPREC | 5 | number of records stored in array AO |
| LPFILE | 630 | value is NBLOKS * 2 + 2 (value shown is for 314 blocks) |

5) The following arrays, in addition to those specified for the baseline program, must be appropriately dimensioned:

AO (dimensioned to NBL * LBL * NPREC)
IPOINT (dimensioned to NBLOKS)
JPOINT (dimensioned to NBLOKS)
NEIGHB (dimensioned to NBLOKS, 8)

6) Listing of modified PROGRAM BLOCK:

```
      JPOINT(I)=JPOINT(I)-LREC
  255 CONTINUE
      IF(N2.EQ.NBLOKS)GO TO 200
      N1=NBMID(NPREC-1)+1
      N2=NBMID(NPREC)
      DO 260 I=N1,N2
      JPOINT(I)=IPOINT(I)+LREC*(NPREC-1)
  260 CONTINUE
  200 CONTINUE
      IB=IQ(NB)
C IS BLOCK FIXED
      IF(IQ(IB).NE.0)GO TO 50
C NO,BLOCK NOT FIXED
      CALL PTICK(2)
      CALL MOTION(Q,IQ,A0,IA0,IB,NB)
      CALL PTOCK(2)
      CALL PTICK(3)
      IF(RFLAG)CALL REBOX(NB)
      CALL PTOCK(3)
   50 CONTINUE
      REWIND LUM
C-------CALCULATE FORCES FOR CONTACT DATA RECORDS AND WRITE NEW FILE
C------- LUN OF UPDATED CONTACT DATA----------
      LREC1=1
      LREC2=LREC
      DO 102 KK=1,NPREC
      READ(LUMD (A0(I),I=LREC1,LREC2)
      LREC1=LREC1+LREC
      LREC2=LREC2+LREC
  102 CONTINUE
      NR=NPREC
      NBCHEK=LENG+1
  530 I6=1
  210 IF(I6.LT.NBCHEK)GO TO 510
      IF(NR.GE.JC00)GO TO 540
C-------WRITE OUT INFO TO FILE LUN-------
C-------READ IN MORE CONTACT DATA FROM LUM-------
      LREC1=1
      LREC2=LREC
      DO 103 KK=1,NPREC
      WRITE(LUN) (A0(I),I=LREC1,LREC2)
      LREC1=LREC1+LREC
      LREC2=LREC2+LREC
  103 CONTINUE
      JC00NR=JC00-NR
      IF(JC00NR.GE.NPREC)GO TO 520
      LREC1=1
      LREC2=LREC
      DO 106 KK=1,JC00NR
      READ(LUMD (A0(I),I=LREC1,LREC2)
      LREC1=LREC1+LREC
      LREC2=LREC2+LREC
  106 CONTINUE
      NR=NR+JC00NR
      NBCHEK=(JC00NR*LREC)+1
      GO TO 530
  520 LREC1=1
      LREC2=LREC
      DO 104 KK=1,NPREC
      READ(LUMD (A0(I),I=LREC1,LREC2)
      LREC1=LREC1+LREC
      LREC2=LREC2+LREC
  104 CONTINUE
      NR=NR+NPREC
      NBCHEK=LENG+1
      GO TO 530
  510 NB=IA0(I6)
      IB=IQ(NB)
      JBC=IA0(I6+3)
      IBC=IQ(JBC)
      CALL FORD(Q,IQ,A0,IA0,IB,IBC,IB)
      FN=SQRT(A0(I6+4)**2+A0(I6+5)**2)
      IF(FN.LE.F0)GO TO 270
      F0=FN
  270 I6=I6+LBL
      GO TO 210
  540 CONTINUE
      LREC1=1
      LREC2=LREC
      DO 107 KK=1,JC00NR
      WRITE(LUN) (A0(I),I=LREC1,LREC2)
      LREC1=LREC1+LREC
      LREC2=LREC2+LREC
  107 CONTINUE
      REWIND LUM
      REWIND LUN
      LUT=LUN
      LUN=LUM
      LUM=LUT
      XOLDF=XOLD
      YOLDF=YOLD
      RMOLDF=RMOLD
      JPLOT1=(MCYCLE/IBPLT)*IBPLT
      IF(JPLOT1.NE.MCYCLE)GO TO 152
      CALL BLPLOT
  152 JPLOT2=(MCYCLE/IFPLT)*IFPLT
      IF(JPLOT2.NE.MCYCLE)GO TO 153
      CALL FORPLT
  153 JPLOT3=(MCYCLE/IDPLT)*IDPLT
      IF(JPLOT3.NE.MCYCLE)GO TO 151
      CALL DISPLT
  151 JPLOT4=(MCYCLE/ITDPLT)*ITDPLT
      IF(JPLOT4.NE.MCYCLE)GO TO 154
      CALL TDISPL
  154 CONTINUE
      IPRIN1=(MCYCLE/ICONDA)*ICONDA
      IF(IPRIN1.NE.MCYCLE)GO TO 751
      CALL DUMP(1)
  751 IPRIN2=(MCYCLE/IBLKDA)*IBLKDA
      IF(IPRIN2.NE.MCYCLE)GO TO 752
      CALL DUMP(2)
  752 IPRIN3=(MCYCLE/IBOXDA)*IBOXDA
      IF(IPRIN3.NE.MCYCLE)GO TO 750
      CALL DUMP(3)
  750 CONTINUE
C EXIT IF BLOCKS HAVEN"T MOVED
      IF(UMOST.LE.1.E-10.AND.THMOST.LE.1.E-10)GO TO 110
      TRANS=TRANS+UMOST
      ROTN=ROTN+THMOST
      IF(TRANS.GT.XYL.OR.ROTN.GT.THL)GO TO 30
      GO TO 40
   30 UFLAG=.TRUE.
      TRANS=0.0
      ROTN=0.0
   40 CONTINUE
      WRITE(6,1001)MCYCLE,UMOST,THMOST
 1001 FORMAT(1X, 65HMAXIMUM BLOCK TRANSLATIONAL AND ROTATIONAL MOVEMENT
     *FOR ITERATION,I5, 3HWAS,F10.8,4H AND,F10.8,13H RESPECTIVELY)
```

```
      GO TO 100
  110 WRITE(6,2001)MCYCLE
 2001 FORMAT(1X, 42HUMOST AND THMOST BELOW THRESHOLD FOR CYCLE,I5)
      GO TO 111
  100 CONTINUE
  111 CONTINUE
      CALL HSTIFF
      RETURN
      END
C
C
      SUBROUTINE MOTION(Q,IQ,A0,IA0,IB,NB)
C
      DIMENSION Q(17435),A0(7000)
      DIMENSION IQ(17435),IA0(7000)
      COMMON/CBLOCK/HED(8),NBLOKM,NB0XES,M1,M2,M3,M4,M5,M6,M7,
     *              NBLOKS,NCYC,MCYCLE,NEMPT,RFLAG,UFLAG,EFLAG,NBC0DD,
     *              I80XES,J80XES,BSIZE,XSIZE,YSIZE,GRAVY,NDC0N(39),
     *              NUPDAT,UM0ST,THM0ST,SCREEN,F0RCL,DISPL,NREM,
     *              NBNREM(60),IBPLT,IFPLT,IDPLT,IC0NDA,IBLKDA,
     *              I80XDA,XYL,THL,RESTFL,X0LD,Y0LD,RM0LD,X0LDF,Y0LDF,
     *              RM0LDF,LUM0,LUN0,NBL,LBL,LREC,LGNEIB,NPREC,
     *              JC00,F0,ITDPLT,IRFP0,C0HES,LPFILE,LBL0CK
      LOGICAL RFLAG,UFLAG,EFLAG
      COMMON/INEIG/IN(314),NEIGHB(314,8)
      DIMENSION INEI(2826)
      EQUIVALENCE(IN,INEI)
      COMMON/PFILE/IP0INT(314),JP0INT(314),LUM,LUN
      DIMENSION A(3,4),X(3),NEIG(20),XC0N(50),YC0N(50),NBC0N(50)
      REAL MSUM,MC0X,MC0Y,MC0M,ML0AD
      IC0UNT=0
      XFSUM=0.0
      YFSUM=0.0
      MSUM=0.0
      XC0X=0.0
      XC0Y=0.0
      XC0M=0.0
      YC0X=0.0
      YC0Y=0.0
      YC0M=0.0
      MC0X=0.0
      MC0Y=0.0
      MC0M=0.0
      XL0AD=0.0
      YL0AD=0.0
      ML0AD=0.0
      DO 300 J=1,50
      XC0N(J)=0.0
      YC0N(J)=0.0
      NBC0N(J)=0
  300 CONTINUE
C DETERMINE COEFFICIENTS FOR EQUILIBRIUM EQUATIONS
      I2=IB
      J=0
      I6=JP0INT(NB)
  100 IF(IA0(I6).NE.NB)GO TO 90
C-------IA0(I6) IS EQUAL TO NB--------
      J=J+1
      XC0N(J)=A0(I6+12)
      YC0N(J)=A0(I6+13)
      NBC0N(J)=IA0(I6+3)
      IF(A0(I6+8).EQ.0.0.AND.A0(I6+9).EQ.0.0)GO TO 10
      XFSUM=XFSUM+A0(I6+5)
      YFSUM=YFSUM+A0(I6+4)
      MSUM=MSUM+A0(I6+4)*(A0(I6+12)-Q(I2+2))
     *         -A0(I6+5)*(A0(I6+13)-Q(I2+3))
      GO TO 11
   10 IF(RESTFL.EQ.1.0)GO TO 12
   11 IC0UNT=IC0UNT+1
      XDIF=A0(I6+12)-Q(I2+2)
      YDIF=Q(I2+3)-A0(I6+13)
      IF(Q(I2+14).EQ.0.0.AND.Q(I2+15).EQ.0.0)GO TO 702
      IF(Q(I2+14).EQ.1.0.AND.Q(I2+15).EQ.1.0)GO TO 701
      IARG1=I2+11+IA0(I6+1)*10
      IARG2=I2+10+IA0(I6+1)*10
      GO TO 704
  701 IARG1=I2+7+IA0(I6+1)*14
      IARG2=I2+6+IA0(I6+1)*14
      GO TO 704
  702 IARG1=I2+15+IA0(I6+1)*6
      IARG2=I2+14+IA0(I6+1)*6
  704 CONTINUE
      AAA=Q(IARG1)*A0(I6+11)
      AAB=Q(IARG2)*A0(I6+10)
      BBA=Q(IARG1)*A0(I6+10)
      BBB=Q(IARG2)*A0(I6+11)
      XC0X=XC0X-AAA*A0(I6+11)-AAB*A0(I6+10)
      XC0Y=XC0Y-AAA*A0(I6+10)+AAB*A0(I6+11)
      XC0M=XC0M-AAA*YDIF*A0(I6+11)-AAA*XDIF*A0(I6+10)
     *         +AAB*XDIF*A0(I6+11)-AAB*YDIF*A0(I6+10)
      YC0X=YC0X-BBA*A0(I6+11)+BBB*A0(I6+10)
      YC0Y=YC0Y-BBA*A0(I6+10)-BBB*A0(I6+11)
      YC0M=YC0M-BBA*YDIF*A0(I6+11)-BBA*XDIF*A0(I6+10)
     *         -BBB*XDIF*A0(I6+11)+BBB*YDIF*A0(I6+10)
      MC0X=MC0X+XDIF*(-BBA*A0(I6+11)+BBB*A0(I6+10))
     *         +YDIF*(-AAA*A0(I6+11)-AAB*A0(I6+10))
      MC0Y=MC0Y+XDIF*(-BBA*A0(I6+10)-BBB*A0(I6+11))
     *         +YDIF*(-AAA*A0(I6+10)+AAB*A0(I6+11))
      MC0M=MC0M+XDIF*(-BBA*YDIF*A0(I6+11)-BBA*XDIF*A0(I6+10)
     *               -BBB*XDIF*A0(I6+11)+BBB*YDIF*A0(I6+10))
     *         +YDIF*(-AAA*YDIF*A0(I6+11)-AAA*XDIF*A0(I6+10)
     *               +AAB*XDIF*A0(I6+11)-AAB*YDIF*A0(I6+10))
   12 CONTINUE
      I6=I6+LBL
      GO TO 100
   90 CONTINUE
C ADD FORCES AND DETERMINE EQUILIBRIUM EQUATION COEFFICIENTS BETWEEN
C CONTACTS OF CORNERS OF NB AND SURROUNDING BLOCKS
      IXX=0
      INNB=IN(NB)
      DO 650 JX=1,INNB
      NBB=NEIGHB(NB,JX)
      IF(NBB.EQ.0)GO TO 650
      IF(NBB.EQ.NB)GO TO 700
      GO TO 710
  700 WRITE(6,1010)
 1010 FORMAT(1X,32HERRORS IN NEIGHB ARRAY IN MOTION)
      EFLAG=.TRUE.
      CALL FINISH
C
C CHECK IF BLOCK NBB ALREADY EVALUATED
C
  710 IF(IXX.EQ.0)GO TO 660
      DO 670 JXX=1,IXX
      IF(NEIG(JXX).EQ.NBB)GO TO 650
  670 CONTINUE
  660 CONTINUE
      IXX=IXX+1
```

```
      NEIG(IXX)=NBB
      I6=JPOINT(NBB)
  120 CONTINUE.
      IF(IAB(I6).NE.NBB)GO TO 650
      IF(IAB(I6+3).EQ.NB)GO TO 130
  180 I6=I6+LBL
      GO TO 120
C-----------NB IS A CORNER CONTACT OF NBB-----------
  130 CONTINUE
      I2B=IQ(NBB)
      XX=AB(I6+12)
      YY=AB(I6+13)
      IF(Q(I2B+14).EQ.0.0.AND.Q(I2B+15).EQ.0.0)GO TO 712
      IF(Q(I2B+14).EQ.1.0.AND.Q(I2B+15).EQ.1.0)GO TO 711
      RLENG=(Q(I2B+8+IAB(I6+1)*10))/20.
      GO TO 714
  711 RLENG=(Q(I2B+4+IAB(I6+1)*14))/20.
      GO TO 714
  712 RLENG=(Q(I2B+12+IAB(I6+1)*6))/20.
  714 CONTINUE
C
C SEARCH J CORNER CONTACTS OF NB ELIMINATING DIAGONAL CORNER-CORNER
C CONTACTS
C
      DO 600 I=1,J
      IF(NBCON(I).EQ.NBB)GO TO 610
      GO TO 620
  610 XDIF=ABS(XX-XCON(I))
      YDIF=ABS(YY-YCON(I))
      IF(XDIF.LT.RLENG.AND.YDIF.LT.RLENG)GO TO 180
  620 CONTINUE
  600 CONTINUE
      IF(AB(I6+8).EQ.0.0.AND.AB(I6+9).EQ.0.0)GO TO 13
      XFSUM=XFSUM+AB(I6+7)
      YFSUM=YFSUM+AB(I6+6)
      MSUM=MSUM+AB(I6+6)*(AB(I6+12)-Q(I2+2))
     *          -AB(I6+7)*(AB(I6+13)-Q(I2+3))
      GO TO 14
   13 IF(RESTFL.EQ.1.0)GO TO 15
   14 ICOUNT=ICOUNT+1
      XDIF=AB(I6+12)-Q(I2+2)
      YDIF=Q(I2+3)-AB(I6+13)
      IF(Q(I2B+14).EQ.0.0.AND.Q(I2B+15).EQ.0.0)GO TO 722
      IF(Q(I2B+14).EQ.1.0.AND.Q(I2B+15).EQ.1.0)GO TO 721
      IARG3=I2B+11+IAB(I6+1)*10
      IARG4=I2B+10+IAB(I6+1)*10
      GO TO 724
  721 IARG3=I2B+7+IAB(I6+1)*14
      IARG4=I2B+6+IAB(I6+1)*14
      GO TO 724
  722 IARG3=I2B+15+IAB(I6+1)*6
      IARG4=I2B+14+IAB(I6+1)*6
  724 CONTINUE
      AAA=Q(IARG3)*AB(I6+11)
      AAB=Q(IARG4)*AB(I6+10)
      BBA=Q(IARG3)*AB(I6+10)
      BBB=Q(IARG4)*AB(I6+11)
      XC0X=XC0X-AAA*AB(I6+11)-AAB*AB(I6+10)
      XC0Y=XC0Y-AAA*AB(I6+10)+AAB*AB(I6+11)
      XC0M=XC0M-AAA*YDIF*AB(I6+11)-AAA*XDIF*AB(I6+10)
     *          +AAB*XDIF*AB(I6+11)-AAB*YDIF*AB(I6+10)
      YC0X=YC0X-BBA*AB(I6+11)+BBB*AB(I6+10)
      YC0Y=YC0Y-BBA*AB(I6+10)-BBB*AB(I6+11)
      YC0M=YC0M-BBA*YDIF*AB(I6+11)-BBA*XDIF*AB(I6+10)
      MC0X=MC0X+XDIF*(-BBA*AB(I6+11)+BBB*AB(I6+10))
     *          +YDIF*(-AAA*AB(I6+11)-AAB*AB(I6+10))
      MC0Y=MC0Y+XDIF*(-BBA*AB(I6+10)-BBB*AB(I6+11))
     *          +YDIF*(-AAA*AB(I6+10)+AAB*AB(I6+11))
      MC0M=MC0M+XDIF*(-BBA*YDIF*AB(I6+11)-BBA*XDIF*AB(I6+10)
     *          -BBB*XDIF*AB(I6+11)+BBB*YDIF*AB(I6+10))
     *          +YDIF*(-AAA*YDIF*AB(I6+11)-AAA*XDIF*AB(I6+10)
     *          +AAB*XDIF*AB(I6+11)-AAB*YDIF*AB(I6+10))
   15 CONTINUE
      I6=I6+LBL
      GO TO 120
  650 CONTINUE
      IF(MCYCLE.EQ.1)GO TO 500
      IF(XFSUM.EQ.0.0.AND.YFSUM.EQ.0.0.AND.MSUM.EQ.0.0)GO TO 530
      GO TO 500
  530 WRITE(6,1006)NB,MCYCLE
 1006 FORMAT(1X,'57HNO FORCES FROM CONTACTS WITH SURROUNDING BLOCKS FOR
     *BLOCK,I5,  19HAT ITERATION NUMBER,I10)
  500 WEIGHT=((Q(I2+10)*GRAVY)/1000000.)
      XSURL=0.0
      YSURL=0.0
      RMSURL=0.0
      IF(Q(I2+14).EQ.0.0.AND.Q(I2+15).EQ.0.0)GO TO 950
      CALL LOAD(I2,XSURL,YSURL,RMSURL)
  950 XLOAD=XFSUM+XSURL
      YLOAD=YFSUM+YSURL+WEIGHT
      MLOAD=MSUM+RMSURL
C
C PRINT OUT RESULTANT FORCES ACTING ON BLOCK IF AT REQUIRED ITERATION
C
      IPOOF=(MCYCLE/IRFPO)*IRFPO
      IF(IPOOF.NE.MCYCLE)GO TO 951
      WRITE(6,1020)XLOAD,YLOAD,MLOAD
 1020 FORMAT(10X,E10.4,5X,E10.4,5X,E10.4)
  951 CONTINUE
      IF(ICOUNT.LE.1)GO TO 510
      A(1,1)=XC0X
      A(1,2)=XC0Y
      A(1,3)=XC0M
      A(2,1)=YC0X
      A(2,2)=YC0Y
      A(2,3)=YC0M
      A(3,1)=MC0X
      A(3,2)=MC0Y
      A(3,3)=MC0M
      A(1,4)=-XLOAD
      A(2,4)=-YLOAD
      A(3,4)=-MLOAD
C
C SOLUTION OF SIMULTANEOUS LINEAR EQUATIONS BY GAUSSIAN ELIMINATION
C
      NEQN=3
C
C APPLY GAUSSIAN ELIMINATION
      CALL ELIMIN(A,X,NEQN,3,4,DETA,RATIO)
      IF(DETA.EQ.0.0.OR.ABS(RATIO).LT.1.E-05)GO TO 510
C SOLUTIONS CONTAINED IN VECTOR X
  520 UMOST=AMAX1(UMOST,ABS(X(1)))
      UMOST=AMAX1(UMOST,ABS(X(2)))
      THMOST=AMAX1(THMOST,ABS(X(3)))
      XBLD=AMAX1(XBLD,ABS(X(1)))
      YBLD=AMAX1(YBLD,ABS(X(2)))
      RMBLD=AMAX1(RMBLD,ABS(X(3)))
```

```
      LBX=Q(I2+2)
      LBY=Q(I2+3)
      Q(I2+7)=X(1)
      Q(I2+8)=X(2)
      Q(I2+9)=X(3)
      Q(I2+11)=Q(I2+11)+X(1)
      Q(I2+12)=Q(I2+12)+X(2)
      Q(I2+13)=Q(I2+13)+X(3)
C UPDATE BLOCK CENTROIDAL CO-ORDINATES
      Q(I2+2)=Q(I2+2)+X(1)
      Q(I2+3)=Q(I2+3)+X(2)
      Q(I2+4)=Q(I2+4)+X(3)
      TEMP=Q(I2+5)
      Q(I2+5)=Q(I2+5)-Q(I2+8)*Q(I2+6)
      Q(I2+6)=Q(I2+6)+Q(I2+9)*TEMP
      IF(LBX.EQ.IFIX(Q(I2+2)).AND.LBY.EQ.IFIX(Q(I2+3)).AND.
     *   ABS(Q(I2+4)).LT.0.01)GO TO 545
      RFLAG=.TRUE.
      Q(I2+4)=0.0
  545 CONTINUE
      RETURN
  510 CONTINUE
C
C SINCE EQUATIONS ARE SINGULAR OR VERY ILL-CONDITIONED LET BLOCK
C DISPLACE A SPECIFIED AMOUNT IN DIRECTION OF RESULTANT FORCES
C
      WRITE(6,1005)NB,MCYCLE
 1005 FORMAT(1X, 60HTHE EQUATIONS ARE SINGULAR OR VERY ILL-CONDITIONED F
     *OR BLOCK,I5,19HAT ITERATION NUMBER,I5)
      IF(XLOAD.EQ.0.0)GO TO 511
      GXD=XGLDF
      X(1)=SIGN(GXD,XLOAD)
      GO TO 512
  511 X(1)=0.0
  512 IF(YLOAD.EQ.0.0)GO TO 515
      GYD=YGLDF
      X(2)=SIGN(GYD,YLOAD)
      GO TO 516
  515 X(2)=0.0
  516 IF(MLOAD.EQ.0.0)GO TO 513
      GMD=RMGLDF
      X(3)=SIGN(GMD,MLOAD)
      GO TO 514
  513 X(3)=0.0
  514 CONTINUE
      GO TO 520
      END
      SUBROUTINE ELIMIN(A,X,MEQN,NROW,NCOL,DET,RATIO)
C
C SUBROUTINE FOR SOLVING SIMULTANEOUS LINEAR EQUATIONS BY
C GAUSSIAN ELIMINATION WITH PARTIAL PIVOTING
C
      DIMENSION A(NROW,NCOL),X(NROW)
      NEQN=MEQN
      IF(NEQN.LE.NROW.AND.NEQN.LE.NCOL-1)GO TO 1
      WRITE(6,1000)
 1000 FORMAT(1X,31H STOP-DIMENSION ERROR IN ELIMIN)
      STOP
C FIND MEAN COEFFICIENT MAGNITUDE
    1 AMEAN=0.
      DO 2 I=1,NEQN
      DO 2 J=1,NEQN
    2 AMEAN=AMEAN+ABS(A(I,J))
      AMEAN=AMEAN/FLOAT(NEQN*NEQN)
C COMMENCE ELIMINATION PROCESS
      JMAX=NEQN+1
      NEQNM1=NEQN-1
      DO 6 IEQN=1,NEQNM1
C
C SEARCH LEADING COLUMN OF THE COEFFICIENT MATRIX FROM
C THE DIAGONAL DOWNWARDS FOR THE LARGEST ELEMENT AND MAKE
C THIS THE PIVOTAL ELEMENT
C
      IMIN=IEQN+1
      IMAX=IEQN
      DO 3 I=IMIN,NEQN
    3 IF(ABS(A(I,IEQN)).GT.ABS(A(IMAX,IEQN)))IMAX=I
      IF(IMAX.EQ.IEQN)GO TO 5
      DO 4 J=IEQN,JMAX
      AA=A(IEQN,J)
      A(IEQN,J)=A(IMAX,J)
    4 A(IMAX,J)=AA
C
C ELIMINATE X(IEQN) FROM EQUATIONS (IEQN+1) TO NEQN.
C FIRST TESTING FOR NON ZERO PIVOTAL ELEMENT
C
    5 IF(ABS(A(IEQN,IEQN)/AMEAN).LT.1.E-8)GO TO 10
      DO 6 I=IMIN,NEQN
      FACT=A(I,IEQN)/A(IEQN,IEQN)
      DO 6 J=IMIN,JMAX
    6 A(I,J)=A(I,J)-FACT*A(IEQN,J)
C
C SOLVE UPPER-TRIANGULAR SET OF EQUATIONS BY BACK SUBSTITUTION
C
      IF(ABS(A(NEQN,NEQN)/AMEAN).LT.1.E-8)GO TO 10
      X(NEQN)=A(NEQN,JMAX)/A(NEQN,NEQN)
      DO 8 L=2,NEQN
      I=NEQN+1-L
      SUM=A(I,JMAX)
      IP1=I+1
      DO 7 J=IP1,NEQN
    7 SUM=SUM-A(I,J)*X(J)
    8 X(I)=SUM/A(I,I)
C
C EVALUATE DETERMINANT OF COEFFICIENT MATRIX AND COMPARE WITH
C ORIGINAL COEFFICIENTS
C
      DETA=1.
      DO 9 I=1,NEQN
    9 DETA=DETA*A(I,I)
      DET=DETA
      RATIO=DETA/AMEAN**NEQN
      RETURN
   10 DET=0.
      RETURN
      END
C
C
      SUBROUTINE FORD(Q,IQ,AO,IAO,I6,I8C,I8)
C
      DIMENSION Q(17435),AO(7000)
      DIMENSION IQ(17435),IAO(7000)
      COMMON/CBLOCK/HED(8),NBLOKM,NBOXES,M1,M2,M3,M4,M5,M6,M7,
     *              NBLOKS,NCYC,MCYCLE,NEMPT,RFLAG,UFLAG,EFLAG,NBCODD,
     *              IBOXES,JBOXES,BSIZE,XSIZE,YSIZE,GRAVY,NDCON(39),
     *              NUPDAT,UMOST,THMOST,SCREEN,FORCL,DISPL,NREM,
     *              NBNREM(60),IBPLT,IFPLT,IDPLT,ICONDA,IBLKDA,
     *              IBOXDA,XYL,THL,RESTFL,XGLD,YGLD,RMGLD,XGLDF,YGLDF,
```

```
     *              RMBLDF,LUMB,LUNB,NBL,LBL,LREC,LGNEIB,NPREC,
     *              JCBB,FB,ITDPLT,IRFPB,CBHES,LPFILE,LBLBCK
      LBGICAL RFLAG,UFLAG,EFLAG
C ROUTINE TB DETERMINE A SINGLE CONTACT FORCE BETWEEN TWB BLBCKS
C FROM THEIR PBSITIBN IN SPACE
C
C RELATIVE INCREMENTAL GLBBAL DISPLACEMENTS BF CBRNER RELATIVE TB EDGE
      DUY=Q(IBC+8)-Q(IB+8)+Q(IBC+9)*(AB(I6+12)-Q(IBC+2))
     *                    -Q(IB+9)*(AB(I6+12)-Q(IB+2))
      DUX=Q(IBC+7)-Q(IB+7)-Q(IBC+9)*(AB(I6+13)-Q(IBC+3))
     *                    +Q(IB+9)*(AB(I6+13)-Q(IB+3))
C RELATIVE INCREMENTAL NBRMAL AND SHEAR DISPLACEMENTS BF CBRNER
C RELATIVE TB EDGE
      DUS=DUX*AB(I6+11)+DUY*AB(I6+10)
      DUN=DUY*AB(I6+11)-DUX*AB(I6+10)
C NBRMAL FBRCE
      IF(Q(IB+14).EQ.B.B.AND.Q(IB+15).EQ.B.B)GB TB 102
      IF(Q(IB+14).EQ.1.B.AND.Q(IB+15).EQ.1.B)GB TB 101
      IARG1=IB+10+IAB(I6+1)*10
      IARG2=IB+11+IAB(I6+1)*10
      IARG3=IB+8+IAB(I6+1)*10
      GB TB 104
 101  IARG1=IB+6+IAB(I6+1)*14
      IARG2=IB+7+IAB(I6+1)*14
      IARG3=IB+5+IAB(I6+1)*14
      GB TB 104
 102  IARG1=IB+14+IAB(I6+1)*5
      IARG2=IB+15+IAB(I6+1)*5
      IARG3=IB+13+IAB(I6+1)*5
 104  CBNTINUE
      DFN=-DUN*Q(IARG1)
      AB(I6+8)=AB(I6+8)+DFN
C TEST FBR TENSIBN
      IF(AB(I6+8).GE.B.B)GB TB 20
      AB(I6+8)=B.B
      AB(I6+9)=B.B
      GB TB 60
C SHEAR FBRCE
 20   DFS=DUS*Q(IARG2)
      AB(I6+9)=AB(I6+9)+DFS
      FRICF=AB(I6+8)*Q(IARG3)+CBHES
      IF(ABS(AB(I6+9)).LE.FRICF)GB TB 40
      AB(I6+9)=SIGN(FRICF,AB(I6+9))
 40   CBNTINUE
C GLBBAL CBNTACT FBRCES
 60   AB(I6+4)=AB(I6+9)*AB(I6+10)-AB(I6+8)*AB(I6+11)
      AB(I6+5)=AB(I6+9)*AB(I6+11)+AB(I6+8)*AB(I6+10)
      AB(I6+6)=-AB(I6+4)
      AB(I6+7)=-AB(I6+5)
      RETURN
      END
      SUBRBUTINE LBAD(I2,XSURL,YSURL,RMSURL)
C
C RBUTINE TB CALCULATE RESULTANT SURFACE FBRCES BN BLBCK
C
      CBMMBN/CBLBCK/HED(8),NBLBKM,NBBXES,M1,M2,M3,M4,M5,M6,M7,
     *              NBLBKS,NCYC,MCYCLE,NEMPT,RFLAG,UFLAG,EFLAG,NBCBDD,
     *              IBBXES,JBBXES,BSIZE,XSIZE,YSIZE,GRAVY,NDCBN(39),
     *              NUPDAT,UMBST,THMBST,SCREEN,FBRCL,DISPL,NREM,
     *              NBNREM(6B),IBPLT,IFPLT,IDPLT,ICBNDA,IBLKDA,
     *              IBBXDA,XYL,THL,RESTFL,XBLD,YBLD,RMBLD,XBLDF,YBLDF,
     *              RMBLDF,LUMB,LUNB,NBL,LBL,LREC,LGNEIB,NPREC,
     *              JCBB,FB,ITDPLT,IRFPB,CBHES,LPFILE,LBLBCK
      LBGICAL RFLAG,UFLAG,EFLAG
      CBMMBN Q(17435)
      DIMENSIBN IQ(17435)
      EQUIVALENCE(Q,IQ)
      IF(Q(I2+14).EQ.B.B)GB TB 70
       NC=IQ(I2+1)
      IC=I2+16
      DB 60 NP=1,NC
      IB=IC
      IC=IB+10
      IF(Q(I2+15).EQ.1.B)IC=IC+4
      IF(NP.EQ.NC)IC=I2+16
      XL=GLX(Q(I2),IB)
      YL=GLY(Q(I2),IB)
      XU=GLX(Q(I2),IC)
      YU=GLY(Q(I2),IC)
      XSURL=XSURL+Q(IB+6)*CBS(Q(IB+7))+Q(IB+8)*CBS(Q(IB+9))
      YSURL=YSURL+Q(IB+6)*SIN(Q(IB+7))+Q(IB+8)*SIN(Q(IB+9))
      RMSURL=RMSURL+Q(IB+6)*SIN(Q(IB+7))*(XL-Q(I2+2))
     *                  -Q(IB+6)*CBS(Q(IB+7))*(YL-Q(I2+3))
     *                   +Q(IB+8)*SIN(Q(IB+9))*(XU-Q(I2+2))
     *                  -Q(IB+8)*CBS(Q(IB+9))*(YU-Q(I2+3))
 60   CBNTINUE
 70   CBNTINUE
      IF(Q(I2+15).EQ.B.B)GB TB 50
      IC=I2+16
      DB 80 NP=1,NC
      IB=IC
      NBARRY=6
      IC=IB+10
      IF(Q(I2+14).EQ.1.B)IC=IC+4
      IF(NP.EQ.NC)IC=I2+16
      XL=GLX(Q(I2),IB)
      YL=GLY(Q(I2),IB)
      XU=GLX(Q(I2),IC)
      YU=GLY(Q(I2),IC)
      IF(Q(I2+14).EQ.1.B)NBARRY=10
      XSURL=XSURL+Q(IB+NBARRY)*CBS(Q(IB+NBARRY+1))
     *                   +Q(IB+NBARRY+2)*CBS(Q(IB+NBARRY+3))
      YSURL=YSURL+Q(IB+NBARRY)*SIN(Q(IB+NBARRY+1))
     *                   +Q(IB+NBARRY+2)*SIN(Q(IB+NBARRY+3))
      RMSURL=RMSURL+Q(IB+NBARRY)*SIN(Q(IB+NBARRY+1))*(XL-Q(I2+2))
     *         -Q(IB+NBARRY)*CBS(Q(IB+NBARRY+1))*(YL-Q(I2+3))
     *                   +Q(IB+NBARRY+2)*SIN(Q(IB+NBARRY+3))*(XU-Q(I2+2))
     *         -Q(IB+NBARRY+2)*CBS(Q(IB+NBARRY+3))*(YU-Q(I2+3))
 80   CBNTINUE
 50   CBNTINUE
      RETURN
      END
C
C
      SUBRBUTINE UPDATE
C
C UPDATES ALL CBNTACTS BETWEEN BLBCKS
C
      CBMMBN/CBLBCK/HED(8),NBLBKM,NBBXES,M1,M2,M3,M4,M5,M6,M7,
     *              NBLBKS,NCYC,MCYCLE,NEMPT,RFLAG,UFLAG,EFLAG,NBCBDD,
     *              IBBXES,JBBXES,BSIZE,XSIZE,YSIZE,GRAVY,NDCBN(39),
     *              NUPDAT,UMBST,THMBST,SCREEN,FBRCL,DISPL,NREM,
     *              NBNREM(6B),IBPLT,IFPLT,IDPLT,ICBNDA,IBLKDA,
     *              IBBXDA,XYL,THL,RESTFL,XBLD,YBLD,RMBLD,XBLDF,YBLDF,
     *              RMBLDF,LUMB,LUNB,NBL,LBL,LREC,LGNEIB,NPREC,
     *              JCBB,FB,ITDPLT,IRFPB,CBHES,LPFILE,LBLBCK
      LBGICAL RFLAG,UFLAG,EFLAG
      CBMMBN Q(17435)
```

```
      DIMENSION IQ(17435)
      EQUIVALENCE(Q,IQ)
      COMMON/STORE/QC(1400),AQ(2800),JUNK(2800)
      EQUIVALENCE(QC,IQC),(AQ,IAQ)
      DIMENSION IQC(1400),IAQ(2800)
      COMMON/INEIG/IN(314),NEIGHB(314,8)
      DIMENSION INEI(2826)
      EQUIVALENCE(IN,INEI)
      COMMON/PFILE/IPOINT(314),JPOINT(314),LUM,LUN
      LOGICAL FIRST
      DO 600 IX=1,NBLOKS
      IN(IX)=0
      IPOINT(IX)=0
      DO 610 JX=1,8
      NEIGHB(IX,JX)=0
  610 CONTINUE
  600 CONTINUE
C
      LREC=NBL*LBL
      JA=1
      JB=1
      JCB=1
C------------------- SCAN EACH BLOCK ---
      DO 500 NB=1,NBLOKS
C
C CHECK IF BLOCK REMOVED
C
      IF(NREM.EQ.0)GO TO 110
      DO 100 K=1,NREM
      IF(NB.EQ.NBNREM(K))GO TO 500
  100 CONTINUE
  110 CONTINUE
      I2=IQ(NB)
      NC=IQ(I2+1)
C------------------- SCAN EACH EDGE OF BLOCK ---
      IEND2=I2+16
      DO 400 NP=1,NC
      FIRST=.TRUE.
      IEND1=IEND2
      IEND2=IEND1+6
      IF(Q(I2+14).EQ.1.0)IEND2=IEND2+4
      IF(Q(I2+15).EQ.1.0)IEND2=IEND2+4
      IF(NP.EQ.NC)IEND2=I2+16
C------------------- DETERMINE BOXES TO BE SEARCHED ---
      X11=GLX(Q(I2),IEND1)
      X22=GLX(Q(I2),IEND2)
      Y11=GLY(Q(I2),IEND1)
      Y22=GLY(Q(I2),IEND2)
      TEMP=AMAX1(X11,X22)
      X1=AMIN1(X11,X22)
      X2=TEMP
      TEMP=AMAX1(Y11,Y22)
      Y1=AMIN1(Y11,Y22)
      Y2=TEMP
      NXL=IFIX((X1-XYL)/BSIZE)+1
      NXU=MINO(IFIX((X2+XYL)/BSIZE)+1,IBOXES)
      NYL=IFIX((Y1-XYL)/BSIZE)+1
      NYU=MINO(IFIX((Y2+XYL)/BSIZE)+1,JBOXES)
C------------------- SEARCH EACH CANDIDATE BOX ---
      DO 350 JBOX=NYL,NYU
      NBOX=(JBOX-1)*IBOXES+NXL-1
      DO 300 IBOX=NXL,NXU
      NBOX=NBOX+1
      I4=IQ(M3+NBOX-1)
C------------------- END OF BOX LIST ? ---
  210 CONTINUE
      IF(JA.LE.NBL)GO TO 2
      WRITE(LUN)(QC(I),I=1,LREC)
      JA=1
      JB=1
      JCB=JCB+1
    2 CONTINUE
      IF(I4.EQ.0) GOTO 300
C
C CHECK IF BLOCK REMOVED
C
      IF(NREM.EQ.0)GO TO 120
      DO 130 K=1,NREM
      IF(IQ(I4+1).EQ.NBNREM(K))GO TO 215
  130 CONTINUE
  120 CONTINUE
C------------------- NB, IS THIS BLOCK NB ? ---
      IF(IQ(I4+1).NE.NB)GO TO 220
C------------------- YES ---
C------------------- GET NEXT ENTRY IN THIS BOX ---
  215 I4=IQ(I4+2)
      GOTO 210
C------------------- FIRST TIME THROUGH ? ---
  220 IF(.NOT.FIRST) GOTO 230
C------------------- YES, COMPUTE COS AND SIN FOR THIS EDGE ---
      FIRST=.FALSE.
      COSA=(X22-X11)/Q(IEND1+2)
      SINA=(Y22-Y11)/Q(IEND1+2)
C------------------- COMPUTE CORNER COORDINATES RELATIVE TO EDGE ---
  230 I2C=IQ(I4+1)
      I2C=IQ(I2C)
      IF(Q(I2C+14).EQ.0.0.AND.Q(I2C+15).EQ.0.0)GO TO 702
      IF(Q(I2C+14).EQ.1.0.AND.Q(I2C+15).EQ.1.0)GO TO 701
      IC=I2C+6+IQ(I4)*10
      GO TO 704
  701 IC=I2C+2+IQ(I4)*14
      GO TO 704
  702 IC=I2C+10+IQ(I4)*6
  704 CONTINUE
      X1C=GLX(Q(I2C),IC)
      Y1C=GLY(Q(I2C),IC)
      YT=(Y1C-Y11)*COSA-(X1C-X11)*SINA
      IF(YT.GT.XYL)GO TO 215
      COF=-3.0*XYL
      IF(YT.LE.COF)GO TO 215
      XT=(X1C-X11)*COSA+(Y1C-Y11)*SINA
      CHEKFL=(X22-X11)*COSA+(Y22-Y11)*SINA
      CHEK2=1.E-10+CHEKFL
      IF(XT.GT.CHEK2)GO TO 215
      IF(XT.LT.-1.E-10)GO TO 215
      IF(NUPDAT.EQ.0)GO TO 250
      IF(NB.EQ.1.AND.JB.EQ.1)GO TO 256
      GO TO 257
  256 REWIND LUM
      LREC2=2*LREC
      READ(LUM)(AQ(I),I=1,LREC)
      LREC1=LREC+1
      READ(LUM)(AQ(I),I=LREC1,LREC2)
      NR=2
      NBINIT=IAQ(1)
      NBMID=IAQ(LREC-LBL+1)
  257 IF(NB.GE.NBINIT.AND.NB.LE.NBMID)GO TO 258
C------EMPTY BOTTOM BUFFER AND REFILL TOP BUFFER-------
```

```
      PROGRAM BLOCK(INPUT,OUTPUT,TAPE5=INPUT,TAPE6=OUTPUT,TAPE1,TAPE2,
     *              TAPE3,TAPE4,TAPE62)
C
C  RIGID BLOCK PROGRAM USING CONVENTIONAL RELAXATION TECHNIQUE
C
      COMMON/CBLOCK/HED(8),NBLOKM,NBOXES,M1,M2,M3,M4,M5,M6,M7,
     *              NBLOKS,NCYC,MCYCLE,NEMPT,RFLAG,UFLAG,EFLAG,NBCODD,
     *              IBOXES,JBOXES,BSIZE,XSIZE,YSIZE,GRAVY,NDCON(38),
     *              NUPDAT,UMOST,THMOST,SCREEN,FORCL,DISPL,NREM,
     *              NBNREM(60),IBPLT,IFPLT,IDPLT,ICONDA,IBLKDA,
     *              IBOXDA,XYL,THL,RESTFL,XOLD,YOLD,RMOLD,XOLDF,YOLDF,
     *              RMOLDF,LUMO,LUNO,NBL,LBL,LREC,LGNEIB,NPREC,
     *              JCOO,FO,ITDPLT,IRFPO,COMES,LPFILE,LBLOCK
      LOGICAL RFLAG,UFLAG,EFLAG
      COMMON Q(17435)
      DIMENSION IQ(17435)
      EQUIVALENCE(Q,IQ)
      COMMON/STORE/AO(7000)
      EQUIVALENCE (AO,IAO)
      DIMENSION IAO(7000)
      COMMON/PFILE/IPOINT(314),JPOINT(314),LUM,LUN
      COMMON/INEIG/IN(314),NEIGHB(314,8)
      DIMENSION INEI(2826)
      EQUIVALENCE(IN,INEI)
      COMMON/CLOCK/SEC(30),ISEC(30)
C
      DATA GRAVY/-9.81/
      DATA M7,MCYCLE,NUPDAT,LBLOCK/6000,0,0,165/
      DATA RFLAG,UFLAG,EFLAG/.FALSE.,.TRUE.,.FALSE./
      DATA SCREEN,FORCL,DISPL/30.,.25,1./
      DATA NREM/0/
      DATA RESTFL/0.0/
      DATA NBL,LBL/100,14/
      DATA LUMO,LUNO/3,4/
      DATA LGNEIB,NPREC/2826,5/
      DATA LPFILE/630/
      DATA NBCODD/0/
      DATA COMES/0.0/
C
      IPCON=1
      CALL PL(IPCON)
      CALL PTIME(0)
      CALL BEGIN
 10   CALL DATA
      CALL CYCLE
      GO TO 10
      END
C
C
      SUBROUTINE BEGIN
C
C   ROUTINE TO DETERMINE WHETHER START OR RESTART RUN
C
      COMMON/CBLOCK/HED(8),NBLOKM,NBOXES,M1,M2,M3,M4,M5,M6,M7,
     *              NBLOKS,NCYC,MCYCLE,NEMPT,RFLAG,UFLAG,EFLAG,NBCODD,
     *              IBOXES,JBOXES,BSIZE,XSIZE,YSIZE,GRAVY,NDCON(39),
     *              NUPDAT,UMOST,THMOST,SCREEN,FORCL,DISPL,NREM,
     *              NBNREM(60),IBPLT,IFPLT,IDPLT,ICONDA,IBLKDA,
     *              IBOXDA,XYL,THL,RESTFL,XOLD,YOLD,RMOLD,XOLDF,YOLDF,
     *              RMOLDF,LUMO,LUNO,NBL,LBL,LREC,LGNEIB,NPREC,
     *              JCOO,FO,ITDPLT,IRFPO,COMES,LPFILE,LBLOCK
      LOGICAL RFLAG,UFLAG,EFLAG
      COMMON Q(17435)
      DIMENSION IQ(17435)
      EQUIVALENCE(Q,IQ)
      COMMON/STORE/AO(7000)
      EQUIVALENCE (AO,IAO)
      DIMENSION IAO(7000)
      COMMON/INEIG/IN(314),NEIGHB(314,8)
      DIMENSION INEI(2826)
      EQUIVALENCE(IN,INEI)
      COMMON/PFILE/IPOINT(314),JPOINT(314),LUM,LUN
      WRITE(6,2003)
 2003 FORMAT(1H1)
      WRITE(6,2000)
 2000 FORMAT(30X,52H----RIGID BLOCK PROGRAM USING RELAXATION METHOD.----
     *      /,30X,48H------------------------------------------------/)
      LUN=LUNO
      LUM=LUMO
      READ(5,1000) WORD
 1000 FORMAT(A4)
C
      IF(WORD.EQ.4HSTAR) GOTO 20
      IF(WORD.EQ.4HREST) GOTO 10
C
      WRITE(6,3000)
 3000 FORMAT(1X, 39H*** ERROR . NO START OR RESTART CARD***)
      STOP
C
C-------RESTART RUN--------
   10 READ(1)  (HED(I),I=1,LBLOCK)
      READ(1) (INEI(I),I=1,LGNEIB)
      READ(1) (IPOINT(I),I=1,LPFILE)
      LUM=LUMO
      LUN=LUNO
      M51=M5-1
      READ(1) (Q(I),I=1,M51)
C-------COPY REMAINING INFO ON TAPE1 ONTO SCRATCH FILE TAPE3---------
      DO 30 KK=1,JCOO
      READ(1) (AO(I),I=1,LREC)
      WRITE(3) (AO(I),I=1,LREC)
 30   CONTINUE
      REWIND 1
      REWIND 3
      READ(5,1005)HED
 1005 FORMAT(8A10)
      WRITE(6,2001)  HED,MCYCLE
 2001 FORMAT(1X,8A10//30X,30HRESTART RUN . CURRENT CYCLES =,I10//)
      RETURN
C
C-------START RUN--------
 20   READ(5,1001)HED,NBLOKM,IBOXES,JBOXES,IBSIZE
 1001 FORMAT(8A10/4I10)
C
      NBOXES=IBOXES*JBOXES
      BSIZE=IBSIZE
      XSIZE=IBOXES*BSIZE
      YSIZE=JBOXES*BSIZE
C
      WRITE(6,2002)HED,NBLOKM,IBOXES,JBOXES,NBOXES,IBSIZE,XSIZE,YSIZE
 2002 FORMAT(1X,8A10//
     .       30X,24HMAXIMUM NUMBER OF BLOCKS,I5//
     .       30X,24HBOXES IN X-DIRECTION    ,I5/
     .       30X,24HBOXES IN Y-DIRECTION    ,I5/
     .       30X,24HTOTAL NUMBER OF BOXES   ,I5//
     .       30X,24HSIZE OF SINGLE BOX      ,I5/
     .       30X,24HPROBLEM SIZE IN X-DIRN  ,F6.0/
     $       30X,24HPROBLEM SIZE IN Y-DIRN  ,F6.0//)
```

```
C
C------------INTERVALS FOR PLOTTING AND PRINTING RESULTS------------
C
      READ(5,1002) IBPLT,IFPLT,IDPLT,ITDPLT,ICONDA,IBLKDA,IBOXDA,IRFPO
 1002 FORMAT(8I10)
      WRITE(6,2004) IBPLT,IFPLT,IDPLT,ITDPLT,ICONDA,IBLKDA,IBOXDA,IRFPO
 2004 FORMAT(10X,21HBLOCK PLOT INTERVAL =,I4,  10HITERATIONS,/,
     *       10X,28HCONTACT FORCE PLOT INTERVAL =,I4,10HITERATIONS,/,
     *       10X,28HDISPLACEMENT PLOT INTERVAL =,I4,10HITERATIONS,/,
     *    10X,34HTOTAL DISPLACEMENT PLOT INTERVAL =,I4,10HITERATIONS,//,
     *       10X,29HCONTACT DATA PRINT INTERVAL =,I4,10HITERATIONS,/,
     *       10X,27HBLOCK DATA PRINT INTERVAL =,I4,10HITERATIONS,/,
     *       10X,25HBOX DATA PRINT INTERVAL =,I4,10HITERATIONS,/,
     *       10X,32HRESULTANT FORCE PRINT INTERVAL =,I4,10HITERATIONS//)
C
C------------THRESHOLDS FOR UPDATING CONTACTS------------
C
      READ(5,1003) XYL,THL
 1003 FORMAT(2F10.2)
      WRITE(6,2005) XYL,THL
 2005 FORMAT(1X, 36HTHRESHOLDS FOR UPDATING CONTACTS ARE,F10.5,3HAND,
     *       F10.5,58HFOR THE TRANSLATIONAL AND ROTATIONAL MOVEMENT RESP
     *ECTIVELY,//)
C
C------------SIZE OF MEMORY------------
C
      READ(5,1004) M7O
 1004 FORMAT(I10)
      M7=MAXO(M7,M7O)
      WRITE(6,2006) M7
 2006 FORMAT(10X,16HSIZE OF MEMORY =,I10,//)
C
C------------------- INITIALISE SOME VARIABLES ---
      NBLOKS=0
      M1=1
      M2=M1+NBLOKM
      M3=M2
      XOLDF=0.0
      YOLDF=0.0
      ROLDF=0.0
      RETURN
      END
C
C
      SUBROUTINE DATA
C
C  ROUTINE TO ASSEMBLE SOME BLOCK DATA
C
      COMMON/COBLOCK/HED(8),NBLOKM,NBOXES,M1,M2,M3,M4,M5,M6,M7,
     *               NBLOKS,NCYC,MCYCLE,NEMPT,RFLAG,UFLAG,EFLAG,NBCODD,
     *               IBOXES,JBOXES,BSIZE,XSIZE,YSIZE,GRAVY,NDCON(39),
     *               NUPDAT,UMOST,THMOST,SCREEN,FORCL,DISPL,NREM,
     *               NBNREM(60),IBPLT,IFPLT,IDPLT,ICONDA,IBLKDA,
     *               IBOXDA,XYL,THL,RESTFL,XOLD,YOLD,ROLD,XOLDF,YOLDF,
     *               ROLDF,LUMO,LUNO,NBL,LBL,LREC,LGNEIB,NPREC,
     *               JCOD,FO,ITDPLT,IRFPO,COKES,LPFILE,LBLOCK
      LOGICAL RFLAG,UFLAG,EFLAG
      COMMON Q(17435)
      DIMENSION IQ(17435)
      EQUIVALENCE(Q,IQ)
      REAL INFL,INANGL,INFU,INANGU
      DIMENSION WORD(25),X(50),Y(50),BNREM(19)
      DIMENSION CARD(8),XX(50),YY(50)
      DIMENSION NBLKI(18),NBLKF(18),NBLKE(28)
      DATA NBLKI/114,115,116,117,118,119,120,121,122,123,124,107,
     *95,83,71,59,47,35/
      DATA NBLKF/1,2,40,64,88,112,146,179,210,239,266,291,309,
     *310,311,312,313,314/
      DATA NBLKE/11,27,39,51,63,75,87,99,111,128,145,162,178,194,209,
     *224,238,252,265,278,290,302,308,310,311,312,313,314/
      DATA PI/3.1415926358979/
      DATA WORD /10HCREA      ,10HDELE      ,10HDUMP      ,10HCYCL
     *          ,10HSTOP      ,10HPLOT      ,10HINTF      ,10HRSET
     *          ,10HISET      ,10HEXTF      ,10HGRAV      ,10HSTIF
     *          ,10HCOMN      ,10HFRIC      ,10HRINV      ,10HMDFY
     *          ,10HUPDA      ,10HDCON      ,10HZTOP      ,10HRSTF
     *          ,10HRFRI      ,10HZZZZ      ,10HZZZZ      ,10HZZZZ
     *          ,10HZZZZ      /
C
C------------------- READ NEXT CARD ---
   10 READ(5,1000)  CARD
 1000 FORMAT(8A10)
      WRITE(6,2000) CARD
 2000 FORMAT(1X,4H+++ ,8A10,4H +++)
      DO 20 I=1,25
      IF(CARD(1).EQ.WORD(I))GO TO 30
   20 CONTINUE
      WRITE(6,3000)
 3000 FORMAT(1X, 29H***ERROR . ILLEGAL COMMAND***)
      GOTO 10
C------------------- JUMP TO APPROPRIATE CODE ---
   30 GOTO (100,150,200,250,300,
     .      350,400,450,500,550,
     .      600,650,700,750,800,
     *      850,900,950,970,980,
     *      990,10,10,10,10),I
C
   40 WRITE(6,3001)
 3001 FORMAT(1X, 37H*** ERROR . COMMAND NOT AVAILABLE ***)
      GO TO 10
C
C------------CREATE A NEW BLOCK------------
C
  100 NBLOKS=NBLOKS+1
      READ(5,1001)NC,RHO,JFIX,JBOUND,JINT
 1001 FORMAT(I10,F10.0,3I10)
      DO 125 I=1,18
      IF(NBLOKS.EQ.NBLKI(I))JINT=1
  125 CONTINUE
      DO 126 I=1,18
      IF(NBLOKS.EQ.NBLKF(I))JFIX=1
  126 CONTINUE
      DO 127 I=1,28
      IF(NBLOKS.EQ.NBLKE(I))JBOUND=1
  127 CONTINUE
      WRITE(6,2006)NBLOKS,NC,RHO,JFIX,JBOUND,JINT
 2006 FORMAT(10X,12HBLOCK NO. = ,I3, 17HNO. OF CORNERS = ,I2,
     *          10HDENSITY = ,F6.1, 11HFIX FLAG = ,I2,
     *       15HBOUNDARY FLAG =,I2,16HINT.FORCE FLAG =,I2)
      READ(5,1002)  (X(I),Y(I),I=1,NC)
      DIP=60.*PI/180.
      DO 19 I=1,NC
      XX(I)=X(I)
      YY(I)=Y(I)
      X(I)=XX(I)*COS(DIP)-YY(I)*SIN(DIP)
      Y(I)=XX(I)*SIN(DIP)+YY(I)*COS(DIP)
      X(I)=X(I)+125.
      Y(I)=Y(I)-200.
```

```
19    CONTINUE
1002 FORMAT(8F10.0)
     WRITE(6,2001)  (X(I),Y(I),I=1,NC)
2001 FORMAT(1X,4(1H(,E12.4,1H,,E12.4,3H ) ))
     I2=M3
     IQ(NBLOKS)=I2
     IQ(I2)=0
     Q(I2+4)=0.0
     Q(I2+7)=0.0
     Q(I2+8)=0.0
     Q(I2+9)=0.0
     Q(I2+11)=0.0
     Q(I2+12)=0.0
     Q(I2+13)=0.0
     Q(I2+14)=0.0
     Q(I2+15)=0.0
     IF(JFIX.NE.0)IQ(I2)=1
     IF(JBOUND.NE.0)Q(I2+14)=1.0
     IF(JINT.NE.0)Q(I2+15)=1.0
     IQ(I2+1)=NC
     Q(I2+5)=1.0
     Q(I2+6)=0.0
C--------------------- AREA AND CENTROID OF THIS BLOCK ---
     AREA=(X(1)-X(NC))*(Y(1)+Y(NC))
     YC=(X(1)-X(NC))*((Y(1)-Y(NC))*(Y(1)+2.0*Y(NC))+3.0*Y(NC)**2)
     XC=(Y(1)-Y(NC))*((X(1)-X(NC))*(X(1)+2.0*X(NC))+3.0*X(NC)**2)
     DO 110 I=2,NC
     AREA=AREA+(X(I)-X(I-1))*(Y(I)+Y(I-1))
     YC=YC+(X(I)-X(I-1))*((Y(I)-Y(I-1))*(Y(I)+2.0*Y(I-1))
    .      +3.0*Y(I-1)**2)
     XC=XC+(Y(I)-Y(I-1))*((X(I)-X(I-1))*(X(I)+2.0*X(I-1))
    .      +3.0*X(I-1)**2)
 110 CONTINUE
     AREA=0.5*AREA
     YC=YC/(6.0*AREA)
     XC=-XC/(6.0*AREA)
     Q(I2+2)=XC
     Q(I2+3)=YC
     Q(I2+10)=AREA*RHO
C--------------------- LOCAL COORDINATES FOR THIS BLOCK ---
     M3=M3+16
     Q(M3)=X(1)-XC
     Q(M3+1)=Y(1)-YC
     DO 120 I=2,NC
     Q(M3+3)=0.0
     Q(M3+4)=0.0
     Q(M3+5)=0.0
     NBARRY=6
     IF(Q(I2+14).EQ.0.0)GO TO 111
     M3TEMP=M3+NBARRY
     Q(M3TEMP)=0.0
     Q(M3TEMP+1)=0.0
     Q(M3TEMP+2)=0.0
     Q(M3TEMP+3)=0.0
     NBARRY=NBARRY+4
 111 CONTINUE
     IF(Q(I2+15).EQ.0.0)GO TO 112
     M3TEMP=M3+NBARRY
     Q(M3TEMP)=0.0
     Q(M3TEMP+1)=0.0
     Q(M3TEMP+2)=0.0
     Q(M3TEMP+3)=0.0
     NBARRY=NBARRY+4
 112 CONTINUE
     Q(M3TEMP+1)=Y(I)-YC
     Q(M3+2)=SQRT((Q(M3TEMP)-Q(M3))**2+(Q(M3TEMP+1)-Q(M3+1))**2)
 120 M3=M3TEMP
     NBARRY=6
     Q(M3+2)=SQRT((Q(I2+16)-Q(M3))**2+(Q(I2+17)-Q(M3+1))**2)
     Q(M3+3)=0.0
     Q(M3+4)=0.0
     Q(M3+5)=0.0
     IF(Q(I2+14).EQ.0.0)GO TO 113
     M3TEMP=M3+NBARRY
     Q(M3TEMP)=0.0
     Q(M3TEMP+1)=0.0
     Q(M3TEMP+2)=0.0
     Q(M3TEMP+3)=0.0
     NBARRY=NBARRY+4
 113 CONTINUE
     IF(Q(I2+15).EQ.0.0)GO TO 114
     M3TEMP=M3+NBARRY
     Q(M3TEMP)=0.0
     Q(M3TEMP+1)=0.0
     Q(M3TEMP+2)=0.0
     Q(M3TEMP+3)=0.0
     NBARRY=NBARRY+4
 114 CONTINUE
     M3=M3+NBARRY
     WRITE(6,2002)XC,YC,Q(I2+10)
2002 FORMAT(1X, 13H XC,YC,MASS .,3E12.3)
     GOTO 10
C
C-------------------REMOVE BLOCKS-------------------
C
 150 CONTINUE
     READ(5,1006)NREM
1006 FORMAT(I4)
     WRITE(6,2004)NREM
2004 FORMAT(1X, 32H THE NUMBER OF BLOCKS REMOVED IS,I4,
    * 29H THEIR NUMBERS ARE----------)
     READ(5,1007)NBC,(BNREM(K),K=1,19)
1007 FORMAT(I4,19F4.0)
     WRITE(6,2005)(BNREM(K),K=1,19)
2005 FORMAT(1X,19F4.0)
     DO 151 K=1,19
     NBNREM(K)=BNREM(K)
 151 CONTINUE
     IF(NREM.LE.19)GO TO 152
     JJ=19
     DO 153 IIJ=1,10
     READ(5,1007)NBC,(BNREM(K),K=1,19)
     IF(NBC.EQ.999)GO TO 152
     WRITE(6,2005)(BNREM(K),K=1,19)
     DO 153 IJ=1,19
     JJ=JJ+1
     NBNREM(JJ)=BNREM(IJ)
 153 CONTINUE
 152 CONTINUE
     UFLAG=.TRUE.
     RESTFL=1.0
     GO TO 10
C
C-------------------PRINT OUT DATA-------------------
C
 200 CALL DUMP(1)
```

```
      CALL DUMP(2)
      CALL DUMP(3)
      GO TO 10
C
C-----------COMMENCE ITERATIONS-----------
C
  250 READ(5,1003)NCYC
 1003 FORMAT(I10)
      WRITE(6,2003)NCYC
 2003 FORMAT(1X, 19H NUMBER OF CYCLES =,I10)
      IF(NCYCLE.EQ.0)CALL BOX
      RETURN
C
C-----------STOP THE PROGRAM-----------
C
  300 CALL FINISH
C
C-----------PLOT THE PROBLEM GEOMETRY-----------
C
  350 CALL BLPLOT
      GO TO 10
C
C-----------APPLY INTERNAL FORCES TO EDGE NE OF BLOCK NB-----------
C
  400 READ(5,1010)NB,NE,INFL,INANGL,INFU,INANGU
 1010 FORMAT(2I10,4F10.0)
      WRITE(6,2012)NB,NE,INFL,INANGL,INFU,INANGU
 2012 FORMAT(14X,54HNB         NE        INFL      INANGL      INFU      INAN
     *GU,/,6X,2I10,3X,4(E10.4,1X))
      I2=IQ(NB)
      Q(I2+15)=1.0
      J3=I2+12+NE*14
      IF(Q(I2+14).EQ.0.0)J3=I2+12+NE*10
      Q(J3)=INFL
      Q(J3+1)=INANGL*PI/180.
      Q(J3+2)=INFU
      Q(J3+3)=INANGU*PI/180.
      GO TO 10
C
C-----------SET REAL DATA-----------
C
  450 READ(5,1008)IADR,VAL
 1008 FORMAT(I10,F10.0)
      IF(IADR.LE.0.OR.IADR.GT.M7)GO TO 480
      Q(IADR)=VAL
       GO TO 10
C
C-----------SET INTEGER DATA-----------
C
  500 READ(5,1009)IADR,IVAL
 1009 FORMAT(2I10)
      IF(IADR.LE.0.OR.IADR.GT.M7)GO TO 480
      IQ(IADR)=IVAL
      GO TO 10
  480 WRITE(6,3002)
 3002 FORMAT(1X, 38H**** ERROR . ADDRESS OUT OF RANGE ****)
      GO TO 10
C
C-----------APPLY EXTERNAL FORCES TO EDGE NE OF BLOCK NB-----------
C
  550 READ(5,1010)NB,NE,EXFL,EXANGL,EXFU,EXANGU
      WRITE(6,2013)NB,NE,EXFL,EXANGL,EXFU,EXANGU
 2013 FORMAT(14X,54HNB         NE        EXFL      EXANGL      EXFU      EXAN
     *GU,/,6X,2I10,3X,4(E10.4,1X))
      I2=IQ(NB)
      Q(I2+14)=1.0
      J3=I2+8+NE*14
      IF(Q(I2+15).EQ.0.0)J3=I2+12+NE*10
      Q(J3)=EXFL
      Q(J3+1)=EXANGL*PI/180.
      Q(J3+2)=EXFU
      Q(J3+3)=EXANGU*PI/180.
      GO TO 10
  600 GO TO 40
C -----------NORMAL AND SHEAR STIFFNESS-----------
  650 CONTINUE
      READ(5,1014)STIFN,STIFS
 1014 FORMAT(2E10.4)
      WRITE(6,2009)STIFN,STIFS
 2009 FORMAT(10X,24HJOINT NORMAL STIFFNESS =,E10.4,/,
     *       10X,23HJOINT SHEAR STIFFNESS =,E10.4,/)
      DO 651 NB=1,NBLOKS
      I2=IQ(NB)
      NC=IQ(I2+1)
      IC=I2+20
      Q(IC)=STIFN
      Q(IC+1)=STIFS
      DO 652 NP=2,NC
      IC=IC+6
      IF(Q(I2+14).EQ.1.0)IC=IC+4
      IF(Q(I2+15).EQ.1.0)IC=IC+4
      Q(IC)=STIFN
      Q(IC+1)=STIFS
  652 CONTINUE
  651 CONTINUE
      GO TO 10
  700 CONTINUE
C-----------JOINT COHESION-----------
      READ(5,1015)COHES
 1015 FORMAT(F10.0)
      WRITE(6,2010)COHES
 2010 FORMAT(10X,16HJOINT COHESION =,F10.2,/)
      GO TO 10
C-----------FRICTION COEFFICIENT-----------
  750 CONTINUE
      READ(5,1013)FRIC
 1013 FORMAT(F10.0)
      WRITE(6,2011)FRIC
 2011 FORMAT(10X,28HJOINT FRICTION COEFFICIENT =,F10.3,/)
      DO 751 NB=1,NBLOKS
      I2=IQ(NB)
      NC=IQ(I2+1)
      IC=I2+19
      Q(IC)=FRIC
      DO 752 NP=2,NC
      IC=IC+6
      IF(Q(I2+14).EQ.1.0)IC=IC+4
      IF(Q(I2+15).EQ.1.0)IC=IC+4
      Q(IC)=FRIC
  752 CONTINUE
  751 CONTINUE
      GO TO 10
  800 READ(5,1011)IBPLT,IFPLT,IDPLT,ITDPLT,ICONDA,IBLKDA,IBOXDA,IRFPO
 1011 FORMAT(8I10)
      WRITE(6,2007)IBPLT,IFPLT,IDPLT,ITDPLT,ICONDA,IBLKDA,IBOXDA,IRFPO
 2007 FORMAT(10X,21HBLOCK PLOT INTERVAL =,I4,  10HITERATIONS,/,
     *       10X,29HCONTACT FORCE PLOT INTERVAL =,I4,10HITERATIONS,/,
     *       10X,28HDISPLACEMENT PLOT INTERVAL =,I4,10HITERATIONS,/,
```

```
     *    10X,34HTOTAL DISPLACEMENT PLOT INTERVAL =,I4,10HITERATIONS,//,
     *       10X,29HCONTACT DATA PRINT INTERVAL =,I4,10HITERATIONS,/,
     *       10X,27HBLOCK DATA PRINT INTERVAL =,I4,10HITERATIONS,/,
     *       10X,25HBOX DATA PRINT INTERVAL =,I4,10HITERATIONS,/,
     *       10X,32HRESULTANT FORCE PRINT INTERVAL =,I4,10HITERATIONS//)
      READ(5,1012)M7D
 1012 FORMAT(I10)
      M7=M7D
      WRITE(6,2008)M7
 2008 FORMAT(10X,22HMODIFIED MEMORY SIZE =,I10,//)
      GO TO 10
C
C
  850 CONTINUE
      READ(5,1016)XYL,THL
 1016 FORMAT(2F10.2)
      WRITE(6,2015)XYL,THL
 2015 FORMAT(10X,9HNEW XYL =,F10.5,9HNEW THL =,F10.5)
      GO TO 10
C
C---------UPDATE ALL BLOCK CONTACTS---------
C
  900 CALL UPDATE
      GO TO 10
C
C-------BLOCK NUMBERS FOR WHICH CONTACT DATA TO BE  DUMPED
C
  950 CONTINUE
      READ(5,1006)NBCODD
      READ(5,1007)NBCC,(BNREM(K),K=1,19)
      WRITE(6,2014)NBCODD
 2014 FORMAT(10X,55HNUMBER OF BLOCKS FOR WHICH CONTACT DATA TO BE DUMPED
     * IS,I4,/,  26HTHEIR NUMBERS ARE---------)
      WRITE(6,2005)(BNREM(K),K=1,19)
      DO 951 K=1,19
      NDCON(K)=BNREM(K)
  951 CONTINUE
      IF(NBCODD.LE.19)GO TO 952
      JJ=19
      DO 953 IIJ=1,10
      READ(5,1007)NBCC,(BNREM(K),K=1,19)
      IF(NBCC.EQ.999)GO TO 952
      WRITE(6,2005)(BNREM(K),K=1,19)
      DO 953 IJ=1,19
      JJ=JJ+1
      NDCON(JJ)=BNREM(IJ)
  953 CONTINUE
  952 CONTINUE
      GO TO 10
C
C--------- ZEROING TOTAL DISPL. PLOTS ----------
C
  970 CONTINUE
      DO 971 NB=1,NBLOKS
      I2=IQ(NB)
      Q(I2+11)=0.0
      Q(I2+12)=0.0
      Q(I2+13)=0.0
  971 CONTINUE
      WRITE(6,972)MCYCLE
  972 FORMAT(10X,43HTOTAL DISPL. PLOT HAS BEEN ZEROED AT CYCLE ,I4)
      GO TO 10
C
C---------CHANGE KN AND KS FOR EDGE NE OF BLOCK NB---------
C
  980 CONTINUE
      READ(5,981)NB,NE,STFN,STFS
  981 FORMAT(2I10,2E10.4)
      WRITE(6,982)NB,NE,STFN,STFS
  982 FORMAT(10X,5HBLOCK,I4,1X,4HEDGE,I4,1X,9HNORM STIF,1X,E10.4,
     *1X,10HSHEAR STIF,1X,E10.4)
      I2=IQ(NB)
      IC=I2+20
      IF(NE.NE.1)GO TO 983
      GO TO 988
  983 IF(Q(I2+14).NE.0.0)GO TO 985
      IF(Q(I2+15).NE.0.0)GO TO 986
      IC=I2+14+NE*6
      GO TO 988
  985 IF(Q(I2+15).NE.0.0)GO TO 987
  986 IC=I2+10+NE*10
      GO TO 988
  987 IC=I2+6+NE*14
  988 Q(IC)=STFN
      Q(IC+1)=STFS
      GO TO 10
C
C-------CHANGE FRICTION COEFF. FOR EDGE NE OF BLOCK NB---------
C
  990 CONTINUE
      READ(5,1018)NB,NE,FRIC
 1018 FORMAT(2I10,F10.0)
      WRITE(6,2017)NB,NE,FRIC
 2017 FORMAT(10X,31HRESET FRICTION COEFF. FOR BLOCK,I4,
     *       4HEDGE,I4,11HIS EQUAL TO,F10.4)
      I2=IQ(NB)
      IC=I2+19
      IF(NE.NE.1)GO TO 993
      GO TO 998
  993 IF(Q(I2+14).NE.0.0)GO TO 995
      IF(Q(I2+15).NE.0.0)GO TO 996
      IC=I2+13+NE*6
      GO TO 998
  995 IF(Q(I2+15).NE.0.0)GO TO 997
  996 IC=I2+9+NE*10
      GO TO 998
  997 IC=I2+5+NE*14
  998 Q(IC)=FRIC
      GO TO 10
      END
C
C
      SUBROUTINE BOX
C
C  ROUTINE TO BOX ALL BLOCK CORNERS ONCE BLOCKS HAVE BEEN CREATED
C
      COMMON/CBLOCK/HED(8),NBLOKM,NBOXES,M1,M2,M3,M4,M5,M6,M7,
     *              NBLOKS,NCYC,MCYCLE,NEMPT,RFLAG,UFLAG,EFLAG,NBCODD,
     *              IBOXES,JBOXES,BSIZE,XSIZE,YSIZE,GRAVY,NDCON(38),
     *              NUPDAT,UMOST,THMOST,SCREEN,FORCL,DISPL,NREM,
     *              NBNREM(60),IBPLT,IFPLT,IDPLT,ICONDA,IBLKDA,
     *              IBOXDA,XYL,THL,RESTFL,XOLD,YOLD,RMOLD,XOLDF,YOLDF,
     *              RMOLDF,LUMO,LUNO,NBL,LBL,LREC,LGNEIB,NPREC,
     *              JCOO,FO,ITDPLT,IRFPO,COMES,LPFILE,LBLOCK
      LOGICAL RFLAG,UFLAG,EFLAG
      COMMON Q(17435)
      DIMENSION IQ(17435)
      EQUIVALENCE(Q,IQ)
```

```
      M4=M3+NBOXES
      M5=M4
C------------------ INITIALISE BOX POINTERS ---
      I1=M4-1
      DO 10 I=M3,I1
 10   IQ(I)=0
C------------------ LOOP ON EACH BLOCK ---
      DO 50 NB=1,NBLOKS
      I2=IQ(NB)
      NC=IQ(I2+1)
      IC=I2+16
C------------------ LOOP ON EACH CORNER ---
      DO 40 NP=1,NC
      X=Q(I2+2)+Q(IC)
      Y=Q(I2+3)+Q(IC+1)
      IBOX=MINO(IFIX(X/BSIZE)+1,IBOXES)
      JBOX=MINO(IFIX(Y/BSIZE),JBOXES-1)
      NBOX=JBOX*IBOXES+IBOX
      I3=M3+NBOX-1
      IQ(M5+2)=IQ(I3)
      IQ(I3)=M5
      IQ(M5)=NP
      IQ(M5+1)=NB
      M5=M5+3
      IC=IC+6
      IF(Q(I2+14).EQ.1.0)IC=IC+4
      IF(Q(I2+15).EQ.1.0)IC=IC+4
   40 CONTINUE
C
   50 CONTINUE
C
      WRITE(6,2000)M2,M3,M4,M5
 2000 FORMAT(1X,13H M2,M3,M4,M5..4I10)
C
      RETURN
      END
C
C
      SUBROUTINE CYCLE
C
      COMMON/CBLOCK/HED(8),NBLOKM,NBOXES,M1,M2,M3,M4,M5,M6,M7,
     *              NBLOKS,NCYC,MCYCLE,NEMPT,RFLAG,UFLAG,EFLAG,NBCODD,
     *              IBOXES,JBOXES,BSIZE,XSIZE,YSIZE,GRAVY,NDCON(39),
     *              NUPDAT,UMOST,THMOST,SCREEN,FORCL,DISPL,NREM,
     *              NBNREM(60),IBPLT,IFPLT,IDPLT,ICONDA,IBLKDA,
     *              IBOXDA,XYL,THL,RESTFL,XOLD,YOLD,RMOLD,XOLDF,YOLDF,
     *              RMOLDF,LUMO,LUNO,NBL,LBL,LREC,LGNEIB,NPREC,
     *              JCOO,FO,ITDPLT,IRFPO,COMES,LPFILE,LBLOCK
      LOGICAL RFLAG,UFLAG,EFLAG
      COMMON Q(17435)
      DIMENSION IQ(17435)
      EQUIVALENCE(Q,IQ)
      COMMON/STORE/AO(7000)
      EQUIVALENCE (AO,IAO)
      DIMENSION IAO(7000)
      COMMON/PFILE/IPOINT(314),JPOINT(314),LUM,LUN
      DIMENSION NBMID(15)
      TRANS=0.0
      ROTN=0.0
      JCOONR=0
      DO 100 NCYCLE=1,NCYC
      MCYCLE=MCYCLE+1
      UMOST=0.0
      THMOST=0.0
      XOLD=0.0
      YOLD=0.0
      RMOLD=0.0
      CALL PTICK(1)
      IF(UFLAG)CALL UPDATE
      CALL PTOCK(1)
C-----------INITIAL READING OF NPREC RECORDS FROM SEQUENTIAL FILE LUM----------
      FO=0.0
      NX=NPREC/2+1
       LENG=LREC*NPREC
      LREC1=1
      LREC2=LREC
      DO 101 KK=1,NPREC
      READ(LUMO(AO(I),I=LREC1,LREC2)
      LREC1=LREC1+LREC
      LREC2=LREC2+LREC
 101  CONTINUE
      NR=NPREC
C----------POINTERS----------
      DO 105 I=1,NPREC
      NBMID(I)=IAO(LREC*I-LBL+1)
 105  CONTINUE
      NBCHEK=NBMID(NX)
      N2=NBMID(1)
      DO 115 I=1,N2
      JPOINT(I)=IPOINT(I)
 115  CONTINUE
      DO 120 NN=2,NPREC
      N1=N2+1
      N2=NBMID(NN)
      DO 125 I=N1,N2
      JPOINT(I)=IPOINT(I)+LREC*(NN-1)
 125  CONTINUE
 120  CONTINUE
      DO 50 NB=1,NBLOKS
C
C----------CHECK IF BLOCK REMOVED----------
C
      IF(NREM.EQ.0)GO TO 140
      DO 150 K=1,NREM
      IF(NB.EQ.NBNREM(K))GO TO 50
 150  CONTINUE
 140  CONTINUE
      IF(NB.LE.NBCHEK)GO TO 200
      IF(NR.GE.JCOO)GO TO 200
C----------EMPTY BOTTOM LREC WORDS AND SHUNT REMAINING WORDS TO CREATE
C ----------TOP END SPACE FOR NEW RECORD----------
      LLENG=LENG-LREC
      DO 240 KK=1,LLENG
      AO(KK)=AO(KK+LREC)
 240  CONTINUE
      LENGP1=LENG-LREC+1
      READ(LUMO(AO(I),I=LENGP1,LENG)
      NR=NR+1
C----------POINTERS----------
      DO 250 I=2,NPREC
      NBMID(I-1)=NBMID(I)
 250  CONTINUE
      NBMID(NPREC)=IAO(LENG-LBL+1)
      IF(NR.EQ.JCOO)NBMID(NPREC)=NBLOKS
      NBCHEK=NBMID(NX)
      N1=IAO(1)
      N2=NBMID(NPREC-1)
      DO 255 I=N1,N2
```

```
      IF(NR.GE.JC00)GO TO 258
      DO 255 KK=1,LREC
      A0(KK)=A0(KK+LREC)
  255 CONTINUE
      LREC1=LREC+1
      READ(LUM0 (A0(I),I=LREC1,LREC2)
      NR=NR+1
      NBINIT=IA0(1)
      NBMID=IA0(LREC-LBL+1)
  258 LLREC=LREC
      IF(NB.EQ.NBMID)LLREC=2*LREC
      IF(NR.GE.JC00)LLREC=2*LREC
      DO 260 IA=1,LLREC,LBL
      IF(IA0(IA).NE.NB)GO TO 260
      IF(IQ(I4).EQ.IA0(IA+2).AND.IQ(I4+1).EQ.IA0(IA+3).
     *AND.NP.EQ.IA0(IA+1))GO TO 245
  260 CONTINUE
      GO TO 250
C-----CONTACT ALREADY STORED-UPDATE CONTACT DATA--------
  245 QC(JB+4)=A0(IA+4)
      QC(JB+5)=A0(IA+5)
      QC(JB+6)=A0(IA+6)
      QC(JB+7)=A0(IA+7)
      QC(JB+8)=A0(IA+8)
      QC(JB+9)=A0(IA+9)
      IQC(JB+1)=IA0(IA+1)
      IQC(JB+2)=IA0(IA+2)
      IQC(JB+3)=IA0(IA+3)
  240 QC(JB+10)=SINA
      QC(JB+11)=COSA
      QC(JB+12)=X1C
      QC(JB+13)=Y1C
      IQC(JB)=NB
      IF(IPOINT(NB).NE.0)GO TO 251
      IPOINT(NB)=JB
  251 CONTINUE
      JA=JA+1
      JB=JB+LBL
      LMARK=IQ(I4+1)
      CHEK3=CHEKFL-1.E-10
      IF(XT.LE.1.E-10)GO TO 620
      IF(XT.GE.CHEK3)GO TO 620
      IN(LMARK)=IN(LMARK)+1
      IF(IN(LMARK).GT.8)GO TO 619
      NEIGHB(LMARK,IN(LMARK))=NB
      GO TO 620
  619 WRITE(6,1000)LMARK
 1000 FORMAT(1X,60HGREATER THAN 8 NEIGHBOURING BLOCKS IN NEIGHB ARRAY FO
     *R BLOCK,I5)
  620 CONTINUE
      GOTO 215
C-------------------- NEW CONTACT ? ---
  250 CONTINUE
      IF(YT.GT.1.E-10)GO TO 215
C-------------------- YES ---
      IF(IQ(I4).EQ.1)GO TO 710
      ICR=IC-6
      IF(Q(I2C+14).EQ.1.0)ICR=ICR-4
      IF(Q(I2C+15).EQ.1.0)ICR=ICR-4
      GO TO 711
  710 NBARRY=6
      IF(Q(I2C+14).EQ.1.0)NBARRY=NBARRY+4
      IF(Q(I2C+15).EQ.1.0)NBARRY=NBARRY+4
      ICR=IC+NBARRY*(IQ(I2C+1)-1)
  711 CONTINUE
      YTR=(GLY(Q(I2C),ICR)-Y11)*COSA-(GLX(Q(I2C),ICR)-X11)*SINA
      COFF=-2.0*XYL
      IF(YTR.LE.COFF)GO TO 215
      IF(IQ(I4).EQ.IQ(I2C+1))GO TO 712
      ICL=IC+6
      IF(Q(I2C+14).EQ.1.0)ICL=ICL+4
      IF(Q(I2C+15).EQ.1.0)ICL=ICL+4
      GO TO 713
  712 ICL=I2C+16
  713 CONTINUE
      YTL=(GLY(Q(I2C),ICL)-Y11)*COSA-(GLX(Q(I2C),ICL)-X11)*SINA
      IF(YTL.LE.COFF)GO TO 215
      QC(JB+4)=0.0
      QC(JB+5)=0.0
      QC(JB+6)=0.0
      QC(JB+7)=0.0
      QC(JB+8)=0.0
      QC(JB+9)=0.0
      IQC(JB+1)=NP
      IQC(JB+2)=IQ(I4)
      IQC(JB+3)=IQ(I4+1)
      GO TO 240
C-------------------- END OF BOX SCAN ---
  300 CONTINUE
  350 CONTINUE
C-------------------- END OF EDGE SCAN ---
  400 CONTINUE
  500 CONTINUE
      WRITE(LUN)(QC(I),I=1,LREC)
      REWIND LUN
      REWIND LUM
      JC00=JC0
      LUT=LUN
      LUN=LUM
      LUM=LUT
C
      NUPDAT=NUPDAT+1
      UFLAG=.FALSE.
      RETURN
      END
C
C
      SUBROUTINE REBOX(NB)
C
      COMMON/CBLOCK/HED(8),NBL0KM,NB0XES,M1,M2,M3,M4,M5,M6,M7,
     *                NBL0KS,NCYC,MCYCLE,NEMPT,RFLAG,UFLAG,EFLAG,NBC0DD,
     *                IB0XES,JB0XES,BSIZE,XSIZE,YSIZE,GRAVY,NDC0N(39),
     *                NUPDAT,UM0ST,THM0ST,SCREEN,F0RCL,DISPL,NREM,
     *                NBNREM(60),IBPLT,IFPLT,IDPLT,IC0NDA,IBLKDA,
     *                IB0XDA,XYL,THL,RESTFL,X0LD,Y0LD,RM0LD,X0LDF,Y0LDF,
     *                RM0LDF,LUM0,LUN0,NBL,LBL,LREC,LGNEIB,NPREC,
     *                JC00,F0,ITDPLT,IRFP0,C0HES,LPFILE,LBL0CK
      LOGICAL RFLAG,UFLAG,EFLAG
      COMMON Q(17435)
      DIMENSION IQ(17435)
      EQUIVALENCE(Q,IQ)
C SUBROUTINE TO REBOX A SINGLE BLOCK"S CORNERS
      IB=IQ(NB)
      NC=IQ(IB+1)
C SCAN EACH CORNER OF THE BLOCK
      IC=IB+16
      DO 100 NP=1,NC
C ARE WE AT EDGE OF DOMAIN
```

```
      IF(GLX(Q(IB),IC).GT.0.0.AND.GLX(Q(IB),IC).LT.XSIZE.AND.
     *  GLY(Q(IB),IC).GT.0.0.AND.GLY(Q(IB),IC).LT.YSIZE)GO TO 20
C YES,WE ARE AT EDGE OF DOMAIN.WRITE OUT ERROR MESSAGE
      WRITE(6,2000)NP,NB
 2000 FORMAT(1X,7H CORNER,I4,9H OF BLOCK,I4,21H IS AT EDGE OF DOMAIN)
C--------SET FIX FLAG--------
      IQ(IB)=1
      Q(IB+7)=0.0
      Q(IB+8)=0.0
      Q(IB+9)=0.0
      GO TO 900
C NO,NOT AT EDGE OF DOMAIN.DETERMINE WHICH BOX CORNER SHOULD BE IN
  20  NBOX=IFIX(GLX(Q(IB),IC)/BSIZE)+IFIX(GLY(Q(IB),IC)/BSIZE)*IBOXES+1
C SEARCH THIS BOX
      J4N=M3+NBOX-1
  30  I4N=IQ(J4N)
      IF(I4N.EQ.0)GO TO 40
      IF(NB.EQ.IQ(I4N+1).AND.NP.EQ.IQ(I4N))GO TO 200
      J4N=I4N+2
      GO TO 30
C SEARCH THE SURROUNDING BOXES
   40 NXL=MAXO(MOD(NBOX-1,IBOXES),1)
      NXU=MINO(NXL+2,IBOXES)
      NYL=MAXO((NBOX-1)/IBOXES,1)
      NYU=MINO(NYL+2,JBOXES)
      DO 80 JBOX=NYL,NYU
      MBOX=(JBOX-1)*IBOXES+NXL-1
      DO 70 IBOX=NXL,NXU
      MBOX=MBOX+1
      IF(MBOX.EQ.NBOX) GOTO 70
      J4M=M3+MBOX-1
  50  I4M=IQ(J4M)
      IF(I4M.EQ.0)GO TO 70
      IF(NB.EQ.IQ(I4M+1).AND.NP.EQ.IQ(I4M))GO TO 60
      J4M=I4M+2
      GO TO 50
C SWAP ENTRIES FOR THIS CORNER
  60  IQ(J4M)=IQ(I4M+2)
      IQ(J4N)=I4M
      IQ(I4M+2)=0
      GO TO 200
C END OF SURROUNDING BOXES SCAN
  70  CONTINUE
  80  CONTINUE
      WRITE(6,3000)NP,NB
 3000 FORMAT(1X,24H ERROR IN REBOX . CORNER,I3,
     *       9H OF BLOCK,I4,20H NOT IN ADJACENT BOX)
C END OF CORNERS SCAN
 200  IC=IC+6
      IF(Q(IB+14).EQ.1.0)IC=IC+4
      IF(Q(IB+15).EQ.1.0)IC=IC+4
 100  CONTINUE
C EXIT
 900  RFLAG=.FALSE.
      RETURN
      END
      SUBROUTINE DUMP(IDF)
C
C ROUTINE TO PRINT OUT INFORMATION IN MEMORY
C
      COMMON/COLOCK/HED(8),NBLOKM,NBOXES,M1,M2,M3,M4,M5,M6,M7,
     *              NBLOKS,NCYC,MCYCLE,NEMPT,RFLAG,UFLAG,EFLAG,NBCODD,
     *              IBOXES,JBOXES,BSIZE,XSIZE,YSIZE,GRAVY,NDCON(39),
     *              NUPDAT,UMOST,THMOST,SCREEN,FORCL,DISPL,NREM,
     *              NBNREM(60),IBPLT,IFPLT,IDPLT,ICONDA,IBLKDA,
     *              IBOXDA,XYL,THL,RESTFL,XOLD,YOLD,RMOLD,XOLDF,YOLDF,
     *              RMOLDF,LUMO,LUNO,NBL,LBL,LREC,LGNEIB,NPREC,
     *              JCOO,FO,ITDPLT,IRFPO,COMES,LPFILE,LBLOCK
      LOGICAL RFLAG,UFLAG,EFLAG
      COMMON Q(17435)
      DIMENSION IQ(17435)
      EQUIVALENCE(Q,IQ)
      COMMON/STORE/AO(7000)
      EQUIVALENCE (AO,IAO)
      DIMENSION IAO(7000)
      COMMON/PFILE/IPOINT(314),JPOINT(314),LUM,LUN
      IF(IDF.EQ.1)GO TO 10
      IF(IDF.EQ.2)GO TO 20
      IF(IDF.EQ.3)GO TO 30
      WRITE(6,3000)
 3000 FORMAT(1X, 27H****ERROR IN DUMP CALL ****)
      RETURN
C CONTACT DATA
 10   WRITE(6,2008)MCYCLE
 2008 FORMAT(1X,26H CURRENT CYCLE NUMBER IS =,I4)
      WRITE(6,2007)
 2007 FORMAT(1X,13H CONTACT DATA,10(1H-)/8X,3HNBE,7X,3HNPE,7X,
     *       3HNPC,7X,3HNBC,/10X,3HFYE,8X,3HFXE,8X,3HFYC,8X,
     *       3HFXC,8X,2HFN,8X,2HSN,7X,3HSIN,7X,3HCOS,7X,3HXCP,7X,3HYCP)
      LENG=LREC*NPREC
      LREC1=1
      LREC2=LREC
      DO 701 KK=1,NPREC
      READ(LUMO (AO(I),I=LREC1,LREC2)
      LREC1=LREC1+LREC
      LREC2=LREC2+LREC
 701  CONTINUE
      NR=NPREC
      NBCHEK=LENG+1
 710  I6=1
 700  IF(I6.LT.NBCHEK)GO TO 510
C----------I6 IS GE NBCHEK----------
      IF(NR.GE.JCOO)GO TO 650
      JCOONR=JCOO-NR
      IF(JCOONR.GE.NPREC)GO TO 730
      LREC1=1
      LREC2=LREC
      DO 703 KK=1,JCOONR
      READ(LUMO (AO(I),I=LREC1,LREC2)
      LREC1=LREC1+LREC
      LREC2=LREC2+LREC
 703  CONTINUE
      NR=NR+JCOONR
      NBCHEK=(JCOONR*LREC)+1
      GO TO 710
 730  LREC1=1
      LREC2=LREC
      DO 702 KK=1,NPREC
      READ(LUMO (AO(I),I=LREC1,LREC2)
      LREC1=LREC1+LREC
      LREC2=LREC2+LREC
 702  CONTINUE
      NR=NR+NPREC
      NBCHEK=LENG+1
      GO TO 710
 510  IF(IAO(I6).GE.1.AND.IAO(I6).LE.NBLOKS)GO TO 511
      GO TO 650
 511  IF(NBCODD.EQ.0)GO TO 653
```

```
C
C BLOCK NUMBERS FOR WHICH CONTACT DATA TO BE PRINTED OUT
C CONTAINED IN ARRAY NOCON
C
      DO 654 K=1,NBCOO
      IF(IAO(I6).EQ.NOCON(K))GO TO 653
 654  CONTINUE
      GO TO 655
 653  CONTINUE
      I63=I6+3
      I64=I6+4
      I613=I6+13
      WRITE(6,2004)(IAO(I),I=I6,I63),
     *(AO(I),I=I64,I613)
 2004 FORMAT(/1X,4I10/1X,10E10.4)
 655  I6=I6+LBL
      GO TO 700
 650  CONTINUE
      REWIND LUM
      WRITE(6,2000)
 2000 FORMAT(1X,130(1H-))
      RETURN
C BLOCK DATA
 20   WRITE(6,2006)NBLOKS,NCYC,MCYCLE
 2006 FORMAT(1X,  6HNBLOKS,6X,4HNCYC,5X,6HMCYCLE/1X,I4,2I10)
      WRITE(6,2003)
 2003 FORMAT(1X,11H BLOCK DATA,10(1H-)/1X,9H NB IF NC,8X,2HXC,8X,2HYC,
     *       5X,5HTHETA,6X,4HCOST,6X,4HSINT,6X,2HDX,
     *       8X,2HDY,8X,4HDTHE,4X,4HMASS,3X,5HTOTLX/
     *       15X,5HTOTLY,5X,5HTOTLM,6X,5HBFLAG,6X,5HIFLAG)
      DO 930 NB=1,NBLOKS
C
C CHECK IF BLOCK REMOVED
C
      IF(NREM.EQ.0)GO TO 931
      DO 932 K=1,NREM
      IF(NB.EQ.NBNREM(K))GO TO 930
 932  CONTINUE
 931  CONTINUE
      IF=IQ(NB)
      IF(Q(IF+14).EQ.0.0.AND.Q(IF+15).EQ.0.0)GO TO 952
      IF(Q(IF+14).EQ.1.0.AND.Q(IF+15).EQ.1.0)GO TO 951
      IL=IF+15+10*IQ(IF+1)
      GO TO 954
 951  IL=IF+15+14*IQ(IF+1)
      GO TO 954
 952  IL=IF+15+6*IQ(IF+1)
 954  CONTINUE
      IF2=IF+2
      WRITE(6,2005)NB,IQ(IF),IQ(IF+1),(Q(I),I=IF2,IL)
 2005 FORMAT(/1X,3I3,1P10E10.2/(10X,1P11E10.2))
 930  CONTINUE
      RETURN
C BOX DATA
 30   WRITE(6,2002)
 2002 FORMAT(10X,3HBOX,7X,5HBLOCK,6X,6HCORNER)
      DO 120 NBOX =1,NBOXES
      I3=IQ(M3+NBOX-1)
 110  IF(I3.EQ.0)GO TO 120
      WRITE(6,2009)NBOX,IQ(I3+1),IQ(I3)
 2009 FORMAT(1X,3I12)
      I3=IQ(I3+2)
      GO TO 110
 120  CONTINUE
      RETURN
      END
C
C
      FUNCTION GLX(B,IC)
C
C  LOCAL - GLOBAL X-COORDINATE TRANSFORMATION
C
      COMMON Q(17435)
      DIMENSION IQ(17435)
      EQUIVALENCE(Q,IQ)
      DIMENSION B(10)
C
       GLX=B(3)+Q(IC)*B(6)-Q(IC+1)*B(7)
      RETURN
      END
C
C
      FUNCTION GLY(B,IC)
C
C  LOCAL - GLOBAL Y-COORDINATE TRANSFORMATION
C
      COMMON Q(17435)
      DIMENSION IQ(17435)
      EQUIVALENCE(Q,IQ)
      DIMENSION B(10)
C
      GLY=B(4)+Q(IC)*B(7)+Q(IC+1)*B(6)
      RETURN
      END
      SUBROUTINE PTIME (JA)
C     SIMULTANEOUS TIMING OF UP TO LSEC SEGMENTS OF CODE
      COMMON/CLOCK/SEC(30),ISEC(30)
      DATA LSEC/30/
C     INITIALISATION
      CALL PZERO (SEC,LSEC)
      CALL PZERI (ISEC,LSEC)
      RETURN
      ENTRY PTICK
C     START CLOCK JA
      CALL SECOND (ELT)
      SEC(JA)=SEC(JA)-ELT
      RETURN
      ENTRY PTOCK
C     STOP CLOCK JA
      CALL SECOND (ELT)
      SEC(JA)=SEC(JA)+ELT
      ENTRY PCALL
C     COUNT HOW MANY TIMES SEGMENT JA IS EXECUTED
      ISEC(JA)=ISEC(JA)+1
      RETURN
      END
      SUBROUTINE PZERI(KA,JA)
C ZEROISES JA ELEMENTS OF KA
      DIMENSION KA(1)
      DO 1 IA=1,JA
      KA(IA)=0
 1    CONTINUE
      RETURN
      END
      SUBROUTINE PZERO(XA,JA)
C ZEROISES JA ELEMENTS OF XA
      DIMENSION XA(1)
      DO 1 IA=1,JA
```

```
      XA(IA)=0.0
 1    CONTINUE
      RETURN
      END
      SUBROUTINE BLPLOT
C ROUTINE FOR PLOTTING THE BLOCK GEOMETRY
      COMMON/CBLOCK/HED(8),NBLOKM,NBOXES,M1,M2,M3,M4,M5,M6,M7,
     *                NBLOKS,NCYC,MCYCLE,NEMPT,RFLAG,UFLAG,EFLAG,NBCODD,
     *                IBOXES,JBOXES,BSIZE,XSIZE,YSIZE,GRAVY,NDCON(39),
     *                NUPDAT,UMOST,THMOST,SCREEN,FORCL,DISPL,NREM,
     *                NBNREM(60),IBPLT,IFPLT,IDPLT,ICONDA,IBLKDA,
     *                IBOXDA,XYL,THL,RESTFL,XBLD,YBLD,RMBLD,XBLDF,YBLDF,
     *                RMBLDF,LUMB,LUNB,NBL,LBL,LREC,LGNEIB,NPREC,
     *                JCOB,FB,ITDPLT,IRFPB,COMES,LPFILE,LBLOCK
      LOGICAL RFLAG,UFLAG,EFLAG
      COMMON Q(17435)
      DIMENSION IQ(17435)
      EQUIVALENCE (Q,IQ)
      FACT=SCREEN/AMAX1(XSIZE,YSIZE)
      FACTIV=1./FACT
      CALL TITLES(1,FACTIV)
      DO 100 NB=1,NBLOKS
C
C CHECK IF BLOCK REMOVED
C
      IF(NREM.EQ.0)GO TO 200
      DO 210 K=1,NREM
      IF(NB.EQ.NBNREM(K))GO TO 100
 210  CONTINUE
 200  CONTINUE
      I2=IQ(NB)
      NC=IQ(I2+1)
      XC=FACT*Q(I2+2)
      YC=FACT*Q(I2+3)
C IS BLOCK FIXED
      IF(IQ(I2).EQ.0)GO TO 20
      CALL SYMBOL(XC,YC,0.2,1HF,0.0,1)
C
C BLOCK NOT FIXED
 20   IC=I2+16
      X=FACT*GLX(Q(I2),IC)
      Y=FACT*GLY(Q(I2),IC)
      CALL PLOT(X,Y,3)
      DO 50 NP=2,NC
      IC=IC+6
      IF(Q(I2+14).EQ.1.0)IC=IC+4
      IF(Q(I2+15).EQ.1.0)IC=IC+4
      X=FACT*GLX(Q(I2),IC)
      Y=FACT*GLY(Q(I2),IC)
      CALL PLOT(X,Y,2)
 50   CONTINUE
      X=FACT*GLX(Q(I2),I2+16)
      Y=FACT*GLY(Q(I2),I2+16)
      CALL PLOT(X,Y,2)
 100  CONTINUE
      CALL PLOT(X,Y,3)
      CALL PLOT(0.0,0.0,3)
      CALL NEWPAGE
      RETURN
      END
      SUBROUTINE FORPLT
      COMMON/CBLOCK/HED(8),NBLOKM,NBOXES,M1,M2,M3,M4,M5,M6,M7,
     *                NBLOKS,NCYC,MCYCLE,NEMPT,RFLAG,UFLAG,EFLAG,NBCODD,
     *                IBOXES,JBOXES,BSIZE,XSIZE,YSIZE,GRAVY,NDCON(39),
     *                NUPDAT,UMOST,THMOST,SCREEN,FORCL,DISPL,NREM,
     *                NBNREM(60),IBPLT,IFPLT,IDPLT,ICONDA,IBLKDA,
     *                IBOXDA,XYL,THL,RESTFL,XBLD,YBLD,RMBLD,XBLDF,YBLDF,
     *                RMBLDF,LUMB,LUNB,NBL,LBL,LREC,LGNEIB,NPREC,
     *                JCOB,FB,ITDPLT,IRFPB,COMES,LPFILE,LBLOCK
      LOGICAL RFLAG,UFLAG,EFLAG
      COMMON/STORE/A(7000)
      EQUIVALENCE (A,IA)
      DIMENSION IA(7000)
      COMMON/PFILE/IPOINT(314),JPOINT(314),LUM,LUN
C FB IS MAXIMUM RESULTANT FORCE
      IF(FB.EQ.0.0)FB=1.E-05
      FG=FORCL/FB
      GG=1./FG
      FACT=SCREEN/AMAX1(XSIZE,YSIZE)
      CALL TITLES(2,GG)
      LENG=LREC*NPREC
      LREC1=1
      LREC2=LREC
      DO 701 KK=1,NPREC
      READ(LUM) (A(I),I=LREC1,LREC2)
      LREC1=LREC1+LREC
      LREC2=LREC2+LREC
 701  CONTINUE
      NR=NPREC
      NBCHEK=LENG-LREC+1
 710  I6=1
 700  IF(I6.LT.NBCHEK)GO TO 510
      IF(I6.GT.LENG)GO TO 500
      IF(NR.GE.JCOB)GO TO 510
      DO 520 KK=1,LREC
      A(KK)=A(KK+LENG-LREC)
 520  CONTINUE
      NPREC1=NPREC-1
      JCOBNR=JCOB-NR
      IF(JCOBNR.GE.NPREC1)GO TO 730
      LREC1=LREC+1
      LREC2=2*LREC
      DO 703 KK=1,JCOBNR
      READ(LUM) (A(I),I=LREC1,LREC2)
      LREC1=LREC1+LREC
      LREC2=LREC2+LREC
 703  CONTINUE
      NR=NR+JCOBNR
      LENG=LREC+JCOBNR*LREC
      NBCHEK=LENG-LBL+1
      GO TO 710
 730  LREC1=LREC+1
      LREC2=2*LREC
      DO 702 KK=1,NPREC1
      READ(LUM) (A(I),I=LREC1,LREC2)
      LREC1=LREC1+LREC
      LREC2=LREC2+LREC
 702  CONTINUE
      NR=NR+NPREC-1
      NBCHEK=LENG-LREC+1
      GO TO 710
 510  IF(IA0(I6).GE.1.AND.IA0(I6).LE.NBLOKS)GO TO 511
      GO TO 500
 511  CONTINUE
      X=A0(I6+12)*FACT
      Y=A0(I6+13)*FACT
      FX=A0(I6+5)*FG
      FY=A0(I6+4)*FG
```

```
      CALL PLOT(X,Y,3)
      X=X+FX
      Y=Y+FY
      CALL PLOT(X,Y,2)
      I6=I6+LBL
      GO TO 700
  500 CONTINUE
      REWIND LUM
      CALL NEWPAGE
      RETURN
      END
      SUBROUTINE DISPLT
C
C ROUTINE FOR PLOTTING INCREMENTAL BLOCK DISPLACEMENTS
C
      COMMON/CBLOCK/HED(8),NBLOKM,NBOXES,M1,M2,M3,M4,M5,M6,M7,
     *              NBLOKS,NCYC,MCYCLE,NEMPT,RFLAG,UFLAG,EFLAG,NBCODD,
     *              IBOXES,JBOXES,BSIZE,XSIZE,YSIZE,GRAVY,NDCON(39),
     *              NUPDAT,UMOST,THMOST,SCREEN,FORCL,DISPL,NREM,
     *              NBNREM(60),IBPLT,IFPLT,IDPLT,ICONDA,IBLKDA,
     *              IBOXDA,XYL,THL,RESTFL,XOLD,YOLD,RMOLD,XOLDF,YOLDF,
     *              RMOLDF,LUMO,LUNO,NBL,LBL,LREC,LGNEIB,NPREC,
     *              JCOD,FO,ITDPLT,IRFPO,COMES,LPFILE,LBLOCK
      LOGICAL RFLAG,UFLAG,EFLAG
      COMMON Q(17435)
      DIMENSION IQ(17435)
      EQUIVALENCE(Q,IQ)
      DO=0.
      DO 100 NB=1,NBLOKS
C
C CHECK IF BLOCK REMOVED
C
      IF(NREM.EQ.0)GO TO 110
      DO 120 K=1,NREM
      IF(NB.EQ.NBNREM(K))GO TO 100
  120 CONTINUE
  110 CONTINUE
      I2=IQ(NB)
      DN=SQRT(Q(I2+7)**2+Q(I2+8)**2)
      IF(DN.LE.DO)GO TO 100
      DO=DN
  100 CONTINUE
      IF(DO.EQ.0.0)DO=1.E-05
      DG=DISPL/DO
      GG=1./DG
      FACT=SCREEN/AMAX1(XSIZE,YSIZE)
      CALL TITLES(3,GG)
      DO 200  NB=1,NBLOKS
C
C CHECK IF BLOCK REMOVED
C
      IF(NREM.EQ.0)GO TO 130
      DO 140 K=1,NREM
      IF(NB.EQ.NBNREM(K))GO TO 200
  140 CONTINUE
  130 CONTINUE
      I2=IQ(NB)
      X=Q(I2+2)*FACT
      Y=Q(I2+3)*FACT
      DX=Q(I2+7)*DG
      DY=Q(I2+8)*DG
      CALL VECTOR(X,Y,DX,DY)
  200 CONTINUE
      CALL NEWPAGE
      RETURN
      END
      SUBROUTINE TDISPL
C
C ROUTINE FOR PLOTTING TOTAL BLOCK DISPLACEMENTS
C
      COMMON/CBLOCK/HED(8),NBLOKM,NBOXES,M1,M2,M3,M4,M5,M6,M7,
     *              NBLOKS,NCYC,MCYCLE,NEMPT,RFLAG,UFLAG,EFLAG,NBCODD,
     *              IBOXES,JBOXES,BSIZE,XSIZE,YSIZE,GRAVY,NDCON(39),
     *              NUPDAT,UMOST,THMOST,SCREEN,FORCL,DISPL,NREM,
     *              NBNREM(60),IBPLT,IFPLT,IDPLT,ICONDA,IBLKDA,
     *              IBOXDA,XYL,THL,RESTFL,XOLD,YOLD,RMOLD,XOLDF,YOLDF,
     *              RMOLDF,LUMO,LUNO,NBL,LBL,LREC,LGNEIB,NPREC,
     *              JCOD,FO,ITDPLT,IRFPO,COMES,LPFILE,LBLOCK
      LOGICAL RFLAG,UFLAG,EFLAG
      COMMON Q(17435)
      DIMENSION IQ(17435)
      EQUIVALENCE(Q,IQ)
      DT=0.0
      DO 100 NB=1,NBLOKS
C
C CHECK IF BLOCK REMOVED
C
      IF(NREM.EQ.0)GO TO 110
      DO 120 K=1,NREM
      IF(NB.EQ.NBNREM(K))GO TO 100
  120 CONTINUE
  110 CONTINUE
      I2=IQ(NB)
      DN=SQRT(Q(I2+11)**2+Q(I2+12)**2)
      IF(DN.LE.DT)GO TO 100
      DT=DN
  100 CONTINUE
      IF(DT.EQ.0.0)DT=1.E-05
      DG=DISPL/DT
      GG=1./DG
      FACT=SCREEN/AMAX1(XSIZE,YSIZE)
      CALL TITLES(4,GG)
      DO 200 NB=1,NBLOKS
C
C CHECK IF BLOCK REMOVED
C
      IF(NREM.EQ.0)GO TO 130
      DO 140 K=1,NREM
      IF(NB.EQ.NBNREM(K))GO TO 200
  140 CONTINUE
  130 CONTINUE
      I2=IQ(NB)
      X=Q(I2+2)*FACT
      Y=Q(I2+3)*FACT
      DX=Q(I2+11)*DG
      DY=Q(I2+12)*DG
      CALL VECTOR(X,Y,DX,DY)
  200 CONTINUE
      CALL NEWPAGE
      RETURN
      END
      SUBROUTINE HSTIFF
C
C SUBROUTINE TO CALCULATE DISPLACEMENTS ON BOUNDARY BLOCKS CARRYING EXTERNAL
C LOADS DUE TO EXTERNAL HALF-SPRINGS OF DOUBLE STIFFNESS
C
      COMMON/CBLOCK/HED(8),NBLOKM,NBOXES,M1,M2,M3,M4,M5,M6,M7,
     *              NBLOKS,NCYC,MCYCLE,NEMPT,RFLAG,UFLAG,EFLAG,NBCODD,
```

```
     *               IBOXES,JBOXES,BSIZE,XSIZE,YSIZE,GRAVY,NDCON(39),
     *               NUPDAT,UMOST,THMOST,SCREEN,FORCL,DISPL,NREM,
     *               NBNREM(60),IBPLT,IFPLT,IDPLT,ICONDA,IBLKDA,
     *               IBOXDA,XYL,THL,RESTFL,XOLD,YOLD,RMOLD,XOLDF,YOLDF,
     *               RMOLDF,LUNO,LUNO,NBL,LBL,LREC,LGNEIB,NPREC,
     *               JCOO,FO,ITDPLT,IRFPO,COMES,LPFILE,LBLOCK
      LOGICAL RFLAG,UFLAG,EFLAG
      COMMON Q(17435)
      DIMENSION IQ(17435)
      EQUIVALENCE (Q,IQ)
      WRITE(6,1000)
 1000 FORMAT(20X,43H TABLE OF X AND Z EXTERNAL FORCE COMPONENTS,
     *      /,19X,44(1H-),/)
      WRITE(6,1001)
 1001 FORMAT(2X,2HNB,2X,2HNP,5X,3HFXL,9X,3HFZL,9X,3HFXU,9X,3HFZU,
     *       8X,6HDSTIFN,6X,6HDSTIFS,/)
      DO 100 NB=1,NBLOKS
      IB=IQ(NB)
C-------IS BLOCK FIXED-------
      IF(IQ(IB).NE.0)GO TO 100
C-------NO-BLOCK NOT FIXED-------
      IF(Q(IB+14).NE.0.)GO TO 120
  110 IF(Q(IB+15).NE.0.)GO TO 130
      GO TO 100
C DISPLACEMENTS OF BOUNDARY BLOCKS UNDER EXTERNAL LOADS
  120 CONTINUE
      NC=IQ(IB+1)
      IC=IB+16
      DO 150 NP=1,NC
      IF(Q(IC+6).EQ.0..AND.Q(IC+8).EQ.0.)GO TO 140
C EXTERNAL FORCES PRESENT ALONG EDGE NP OF BLOCK NB
      FXL=Q(IC+6)*COS(Q(IC+7))
      FZL=Q(IC+6)*SIN(Q(IC+7))
      FXU=Q(IC+8)*COS(Q(IC+9))
      FZU=Q(IC+8)*SIN(Q(IC+9))
      DSTIFN=2.0*Q(IC+4)
      DSTIFS=2.0*Q(IC+5)
      WRITE(6,1002)NB,NP,FXL,FZL,FXU,FZU,DSTIFN,DSTIFS
 1002 FORMAT(1X,I3,I4,6E12.4)
  140 IC=IC+10
      IF(Q(IB+15).NE.0.)IC=IC+4
  150 CONTINUE
      GO TO 110
C CODE TO BE WRITTEN FOR DISPLACEMENTS DUE TO INTERNAL LOADS
  130 CONTINUE
  100 CONTINUE
      RETURN
      END
      SUBROUTINE VECTOR(X,Y,DX,DY)
C
      PI=4.0*ATAN(1.0)
      CALL PLOT(X,Y,3)
      X=X+DX
      Y=Y+DY
      CALL PLOT(X,Y,2)
      DT=(SQRT(DX**2+DY**2))/5.
      GM=ABS(DX)
      IF(GM.LE.1.E-5)DX=1.E-5
      ABA=ATAN2(DY,DX)
      IF(ABA.LT.0.)ABA=2.*PI+ABA
      ABA1=PI+ABA-.25
      ABA2=ABA1+.5
      XA=X+DT*(COS(ABA1))
      YA=Y+DT*(SIN(ABA1))
      CALL PLOT(XA,YA,2)
      CALL PLOT(X,Y,3)
      XA=X+DT*(COS(ABA2))
      YA=Y+DT*(SIN(ABA2))
      CALL PLOT(XA,YA,2)
      RETURN
      END
      SUBROUTINE TITLES(IPLOT,DIS)
      COMMON/CBLOCK/HED(8),NBLOKM,NBOXES,M1,M2,M3,M4,M5,M6,M7,
     *              NBLOKS,NCYC,MCYCLE,NEMPT,RFLAG,UFLAG,EFLAG,NBCODD,
     *              IBOXES,JBOXES,BSIZE,XSIZE,YSIZE,GRAVY,NDCON(39),
     *              NUPDAT,UMOST,THMOST,SCREEN,FORCL,DISPL,NREM,
     *              NBNREM(60),IBPLT,IFPLT,IDPLT,ICONDA,IBLKDA,
     *              IBOXDA,XYL,THL,RESTFL,XOLD,YOLD,RMOLD,XOLDF,YOLDF,
     *              RMOLDF,LUNO,LUNO,NBL,LBL,LREC,LGNEIB,NPREC,
     *              JCOO,FO,ITDPLT,IRFPO,COMES,LPFILE,LBLOCK
      LOGICAL RFLAG,UFLAG,EFLAG
      CALL SYMBOL(0.5,15.0,0.21,HED,0.,80)
      GO TO (100,200,250,260) IPLOT
  100 CONTINUE
C THIS IS A BLOCK GEOMETRY PLOT
      CALL SYMBOL(0.5,14.5,0.21,10HBLOCK PLOT,0.,10)
      GO TO 300
  200 CONTINUE
C THIS IS A EDGE-CORNER CONTACT FORCE PLOT
      CALL SYMBOL(0.5,14.5,0.21,17HCORNER FORCE PLOT,0.,17)
      GO TO 400
  250 CONTINUE
C THIS IS A INCREMENTAL DISPLACEMENT PLOT
      CALL SYMBOL(0.5,14.5,0.21,17HINCREM.DISPL PLOT,0.,17)
      GO TO 400
  260 CONTINUE
C THIS IS A TOTAL DISPLACEMENT PLOT
      CALL SYMBOL(0.5,14.5,0.21,16HTOTAL DISPL PLOT,0.,16)
      GO TO 400
  300 CONTINUE
      CALL SYMBOL(5.0,14.5,0.21,34HNUMBER OF PROBLEM UNITS PER INCH =,
     *  0.,34)
      CALL NUMBER(12.4,14.5,0.21,DIS,0.,2)
      GO TO 500
  400 CONTINUE
      CALL SYMBOL(5.0,14.5,0.21,34HNUMBER OF PROBLEM UNITS PER INCH =,
     *            0.,34)
      CALL NUMBER(12.4,14.5,0.21,DIS,0.,8)
  500 FL=MCYCLE
      CALL SYMBOL(0.5,14.0,0.21,18HITERATION NUMBER =,0.,18)
      CALL NUMBER(4.5,14.0,0.21,FL,0.,-1)
      CALL SYMBOL(7.5,14.0,0.21,16HSCALE . 1 INCH =,0.,16)
      CALL PLOT(11.0,14.0,3)
      CALL PLOT(12.0,14.0,2)
      RETURN
      END
      SUBROUTINE PL(IPCON)
      GO TO (10,20) IPCON
   10 CALL START(2)
      CALL PEN(1)
      RETURN
   20 CALL ENPLOT
      RETURN
      END
      SUBROUTINE FINISH
      COMMON/CBLOCK/HED(8),NBLOKM,NBOXES,M1,M2,M3,M4,M5,M6,M7,
     *              NBLOKS,NCYC,MCYCLE,NEMPT,RFLAG,UFLAG,EFLAG,NBCODD,
     *              IBOXES,JBOXES,BSIZE,XSIZE,YSIZE,GRAVY,NDCON(39),
```

```
     *              NUPDAT,UMBST,THMBST,SCREEN,FBRCL,DISPL,NREM,
     *              NBNREM(60),IBPLT,IFPLT,IDPLT,ICBNDA,IBLKDA,
     *              IBBXDA,XYL,THL,RESTFL,XBLD,YBLD,RMBLD,XBLDF,YBLDF,
     *              RMBLDF,LUMB,LUNB,NBL,LBL,LREC,LGNEIB,NPREC,
     *              JCBB,FB,ITDPLT,IRFPB,CBNES,LPFILE,LBLBCK
      LBGICAL RFLAG,UFLAG,EFLAG
      CBMMBN Q(17435)
      DIMENSIBN IQ(17435)
      EQUIVALENCE(Q,IQ)
      CBMMBN/STBRE/AB(7000)
      EQUIVALENCE (AB,IAB)
      DIMENSIBN IAB(7000)
      CBMMBN/PFILE/IPBINT(314),JPBINT(314),LUM,LUN
      CBMMBN/INEIG/IN(314),NEIGHB(314,8)
      DIMENSIBN INEI(2826)
      EQUIVALENCE(IN,INEI)
      CBMMBN/CLBCK/SEC(30),ISEC(30)
C
      CALL BLPLBT
      CALL FBRPLT
      CALL DISPLT
      CALL TDISPL
      WRITE(6,1000)SEC(1),SEC(2),SEC(3),ISEC(1),ISEC(2),ISEC(3)
 1000 FBRMAT(1X,17H TIME IN UPDATE =,F10.5/
     *       1X,17H TIME IN MBTIBN =,F10.5/
     *       1X,16H TIME IN REBBX =,F10.5/
     *       1X,18H CALLS TB UPDATE =,I10/
     *       1X,18H CALLS TB MBTIBN =,I10/
     *       1X,17H CALLS TB REBBX =,I10/)
      IPCBN=2
      CALL PL(IPCBN)
      WRITE(6,1001)MCYCLE,NUPDAT
 1001 FBRMAT(30X,15H TBTAL CYCLES =,I10/
     *       30X,17H NB. BF UPDATES =,I10)
C
C WRITE RESTART FILE IF NB ERRBRS
C
      IF(EFLAG)GB TB 100
      REWIND 2
      WRITE(2)(HED(I),I=1,LBLBCK)
      WRITE(2)(INEI(I),I=1,LGNEIB)
      WRITE(2)(IPBINT(I),I=1,LPFILE)
      MB1=MB-1
      WRITE(2)(Q(I),I=1,MB1)
      IF(LUN.EQ.3)GB TB 200
      DB 210 JA=1,JCBB
      READ(LUMB)(AB(I),I=1,LREC)
      WRITE(LUN)(AB(I),I=1,LREC)
  210 CBNTINUE
      REWIND LUN
  200 CBNTINUE
C----------CBPY INFB BN SCRATCH FILE TAPE4 BNTB TAPE2----------
      DB 300 KK=1,JCBB
      READ(4)(AB(I),I=1,LREC)
      WRITE(2)(AB(I),I=1,LREC)
  300 CBNTINUE
      WRITE(6,1002)
 1002 FBRMAT(30X,43H A RESTART FILE HAS BEEN WRITTEN BNTB TAPE2)
  100 CBNTINUE
      STBP
      END
```